

**The Expeditions ANTARKTIS XXI/3-4-5
of the Research Vessel „Polarstern“ in 2004**

**Die Expeditionen ANTARKTIS XXI/3-4-5
des Forschungsschiffes „Polarstern“ 2004**

**Edited by / Herausgegeben von
Victor Smetacek, Ulrich Bathmann, Elisabeth Helmke
with contributions of the participants /
unter Mitarbeit der Fahrteilnehmer**

Ber. Polarforsch. Meeresforsch. 500 (2005)
ISSN 1618 - 3193

ANTARKTIS XXI/3-4-5

21. Januar 2004 – 2. Juni 2004

• KOORDINATOR/COORDINATOR

Hans-Otto Pörtner

ANT XXI/3: Cape Town - Cape Town
FAHRTLEITER/CHIEF SCIENTIST
Victor Smetacek

ANT XXI/4: Cape Town – Cape Town
FAHRTLEITER/CHIEF SCIENTIST
Ulrich Bathmann

ANT XXI/5: Cape Town – Bremerhaven
FAHRTLEITER/CHIEF SCIENTIST
Elisabeth Helmke

INHALTSVERZEICHNIS / CONTENTS

FAHRTABSCHNITT ANT XXI/3 KAPSTADT – KAPSTADT

Fahrtleiter / Chief Scientist: Victor Smetacek 1-134

FAHRTABSCHNITT ANT XXI/4 KAPSTADT – KAPSTADT

Fahrtleiter / Chief Scientist: Ulrich Bathmann 135-268

FAHRTABSCHNITT ANT XXI/5 KAPSTADT –

BREMERHAVEN

Fahrtleiter / Chief Scientist: Elisabeth Helmke 269-302

FAHRTABSCHNITT ANT XXI/3 KAPSTADT – KAPSTADT

Fahrtleiter / Chief Scientist: Victor Smetacek

1. Introduction	3
Reiseroute/ Cruise track	7
2. Wetter	8
3. The physical setting of the european iron fertilization experiment 'Eifex' in the southern ocean	15
4. H ₂ O ₂ dynamics during a mesoscale iron enrichment in the southern ocean	46
5. Temporal changes in iron speciation during a mesoscale iron enrichment experiment	50
6. Changes in the speciation and biogeochemical cycling of other trace metals during eifex	55
7. Surface-active organic matter in the upper water column during EIFEX, a mesoscale open ocean iron enrichment experiment in the Southern Ocean	59
8. Progression of transparent exopolymer particles (tep) and potential of iron binding to tep during Eifex	61
9. CO ₂ -system measurements during Eifex	66
10. Chlorophyll <i>a</i> , particulate and dissolved carbon, nitrogen	70
11. Dissolved carbon, nitrogen and phosphorus as well as particulate phosphorus	74
12. Nutrient measurements during Eifex	75
13. Export production and mesopelagic remineralization during Eifex	78
14. Particulate and dissolved material and nucleic acid content during the iron fertilization experiment Eifex	81
15. Algal physiology and biooptics	82
16. The wax and wane of an iron-induced diatom bloom in the Southern Ocean	88

17. Flow-cytometry of phytoplankton during the Eifex cruise	101
18. Stable silicon isotopes in dissolved and biogenic silica	105
19. Primary production, phytoplankton biomass and distribution, and size fractionated bulk variables of the chlorophyll maximum during an iron fertilization experiment in the region of the antarctic polar frontal zone	106
20. Prokaryotic response to iron fertilization	115
21. Microzooplankton	117
22. Mezozooplankton	121
23. DMS, DMSP, DMSO and DMSP-lyase	127
24. Teilnehmer / Participants ANT XXI/3	131
25. Participating Institutes / Beteiligte Institute	131
26. Ship's Crew / Schiffsbesatzung ANT XXI/3	134

**FAHRTABSCHNITT ANT XXI/3 KAPTTSTADT -
KAPSTADT
(21.01.04 - 25.03.04)**

1. INTRODUCTION

V. Smetacek (AWI)

Rationale

The aim of cruise ANT XXI/3 – the European Iron Fertilisation Experiment (EIFEX) - was to study the growth and demise of a phytoplankton bloom induced by fertilising an area in the core of a mesoscale eddy with an appropriate amount of iron sulphate. Our experiment was the eighth in a series of similar experiments - 2 in the Equatorial Pacific, 3 in the Southern Ocean and 2 in the Subarctic Pacific – that have been carried out so far. Phytoplankton blooms were induced in all these experiments but in contrast to most earlier experiments including EisenEx carried out in November 2000 that only had 3 – 4 weeks at their disposal, EIFEX had 9 weeks to study the fate of the bloom adequately.

The overarching goal of this interdisciplinary cruise was to further our understanding of how open ocean ecosystems function and how the organisms of the plankton interact with one another and with the environment to drive biogeochemical cycles. Artificial iron fertilisation simulates natural processes that introduce iron to iron-limited, land-remote ocean waters. The phytoplankton respond by increasing growth rates but accumulation of biomass is dependent on a range of physical and chemical factors that together determine the characteristics of the growth environment. However, accumulation rate of biomass is the balance between growth and loss rates due to mortality of algal cells and eventual breakdown of organic matter by pelagic heterotrophs: bacteria, protozoal- and metazooplankton. We intended studying the relationship between growth of the phytoplankton and the concomitant effects of grazing and breakdown on the inventories of biogenic elements.

A major aim of the cruise was to find out the fate of iron fertilised blooms in the ACC: is their biomass retained in the surface layer and converted back into CO₂ by bacteria and zooplankton or does at least a part of it sink out, thereby removing significant amounts of CO₂ from the atmosphere and storing it in the deep ocean. The answer to this question is of relevance to understanding past climate cycles but also to the feasibility of using artificial iron fertilisation of the ACC as a technique to mitigate global warming caused by anthropogenic accumulation of atmospheric CO₂.

Itinerary

RV „Polarstern“ departed from Cape Town on the 21st January with 96 persons on board of which 43 were crew members and 53 were involved with carrying

out the scientific mission of this research cruise. The latter represented 14 institutes and 3 companies from 7 European countries and South Africa.

Our first task was to locate a promising eddy and map it in order to ascertain its suitability for the experiment. Satellite-based altimeters reveal the presence and characteristics of eddies in images of sea surface height and our observations of the eddy field south of Africa showed there were several to choose from. We picked the closest one due south of Africa at about 51°S; 18° E. We chose to conduct the experiment in an eddy south of the Antarctic Polar Front, located at about 50°S, because silicic acid is depleted to its north by mid-summer.

In order to gain an overview of the hydrographical field we commenced measurements at the position of the Subantarctic Front at 46°S which we reached on Jan. 24. After completing the first trial station with CTD casts and nets, we deployed the towed undulating instrument Scanfish and steamed south at about 15 km an hour. After a day of satisfactory performance in calm seas Scanfish was lost when the wire snapped suddenly for unknown reasons. Scanfish is buoyant so we searched for it by helicopter but without success. The wire had snapped some 150 m from the instrument so its weight apparently dragged Scanfish down to the bottom.

The last week of January was spent mapping the eddy, finding its centre, measuring the initial conditions of the experiment and finally on 2nd February the patch was fertilised. The same procedure that had proved successful during EisenEx was used: Polarstern steamed at 8 km/hr along an outward spiralling track from the eddy centre while a weakly acidified, strong solution of ferrous (iron) sulphate was released into the ship's propellor wash. The spiral was 250 km long and its circles 1 km apart. By Tuesday morning we had fertilised a circular patch of 150 km² area and 14 km diameter. The amount of iron sulphate released was calculated to raise iron concentrations in the 80 m deep mixed layer from the very low values characteristic of the ACC to values typical for productive coastal regions (from 0.1 to 1 nmol/litre). This was achieved with 6 tonnes of iron sulphate equivalent to 1 kg for 2 million cubic metres.

ADCP profiles indicated that this was a young eddy with an ellipsoid-shaped cold core 130 x 50 km in dimension extending well below 300m depth, clearly isolated from its surroundings and bounded to the north by the Polar Frontal jet. Silicic acid concentrations were very high in the cold core indicating that this water mass originated from south of the southern Polar Front. A cause for concern was the ellipsoidal shape which would gradually become rounded with time. What this would do to the fertilized patch was uncertain. One possibility was that the patch would be pulled out into a spiral and some of it might be lost to the surroundings. High CO₂ and nutrient concentrations in the core indicated that not much biological activity had taken place in it. Iron and phytoplankton concentrations in the cold core were very low (chlorophyll concentrations <0.2 mg Chl./m³) and contrasted strongly with the much higher values in the Polar Front (1.2 mg Chl/m³). In addition, salps were abundant in the eddy and their

heavy grazing pressure would have retarded the accumulation rate of phytoplankton biomass.

The alternative eddy in the West, close to the Greenwich meridian at 2° E, was circular and had formed in early December. It resembled the altimeter images of the EisenEx eddy which had been such a success, because it stayed in position for at least 6 months and retained the rounded patch nicely in its centre. Since the phytoplankton in the fertilised patch would require 3 weeks to reach bloom proportions, we decided to steam to the 2° E eddy, examine its suitability with a few transects and, if it proved to be more promising, fertilise it and stay there. If it did not, we would steam back to the first eddy and find our patch by using the FRRF. We did not expect to miss any fundamental insights in the first week or two of growth. The main incentive to shift eddies came from satellite images of chlorophyll in the ACC which clearly showed that the entire sector of the ACC to the west had concentrations similar to those present only along the Polar Front in our sector. The southern region from where our eddy core originated were barren in the same images. If the eddy centre in the 2° E eddy was as green as indicated by the satellite, we would gain 2 weeks by conducting our experiment there, even if we fertilised a week later.

On Feb. 3 we steamed due west to the alternative eddy, some 2 1/2 days away. We encountered two strong storms in short succession on the way which we decided to avoid by steaming 350 km north to calmer waters and let the storms pass along the latitude of our eddies. The storms also crossed the first eddy two days later, so we would have had to escape north there as well. The storms cost us three days and on Feb 9 we approached the eddy on a course aimed through its centre. Mapping the eddy and determining its centre was completed on Feb 12 and since the eddy strcuture and its phytoplankton population were more promising than the first eddy, we decided to fertilise this one as well which we completed on Feb 13. A drifting buoy was deployed in the centre of the patch and the fertilisation spiral carroied out around it.

On Feb 14 we commenced mapping the hydrography of the eddy with a grid of 8 north-south transects between 48° 48'S and 50° 36'S each with 10 stations 20 km apart. Three of the middle transects, also 20 km apart, cut through the core of the eddy. The transects on either side crossed the loop of fast currents enclosing it and maintaining its identity. The grid was completed by Feb 20 after which we steamed to the buoy and found that it had drifted out of the fertilised patch reflected in high chlorophyll values. We spent a night searching for the centre of the fertilised patch and the first in-patch station was carried out on Feb 22 followed by a reference station in outside water the next day. Chlorophyll concentrations were a uniform 1.6 mg/m³ down to 90 m, well above the 0.7 mg/m³ recorded in the surroundings, including the reference station. Values as high as 2.1 mg/m³ were recorded during the surface mapping of the patch which was evidence of remarkably high growth rates in the week following fertilisation.

The next week was spent carrying out long stations within and outside the fertilised patch with attempts to map its extent in between. The patch was found to cover an area of about 20 x 30 km slightly off the core centre but including it. The patch had two regions with chlorophyll concentrations above 2 mg/m³. Values in the rest of the patch were lower but more than double those in the surrounding water. After the first mapping the buoy was equipped with a range of instruments recording various parameters and two sediment traps and replaced in the larger area of higher productivity.

Because of dilution of the patch by areal extension and the fact that the phytoplankton had already consumed much of the iron, we decided to refertilise the entire patch. We did this by starting at the southern rim and zigzagging northward at intervals of 2 km. Each time we stopped fertilising when the eastern and western borders of the patch were reached signalled by the CO₂ concentration of surface water. We released another 7 tonnes of iron sulfate, this time over an area of about 400 km² two weeks after the first fertilisation of the initial 150 km² area.

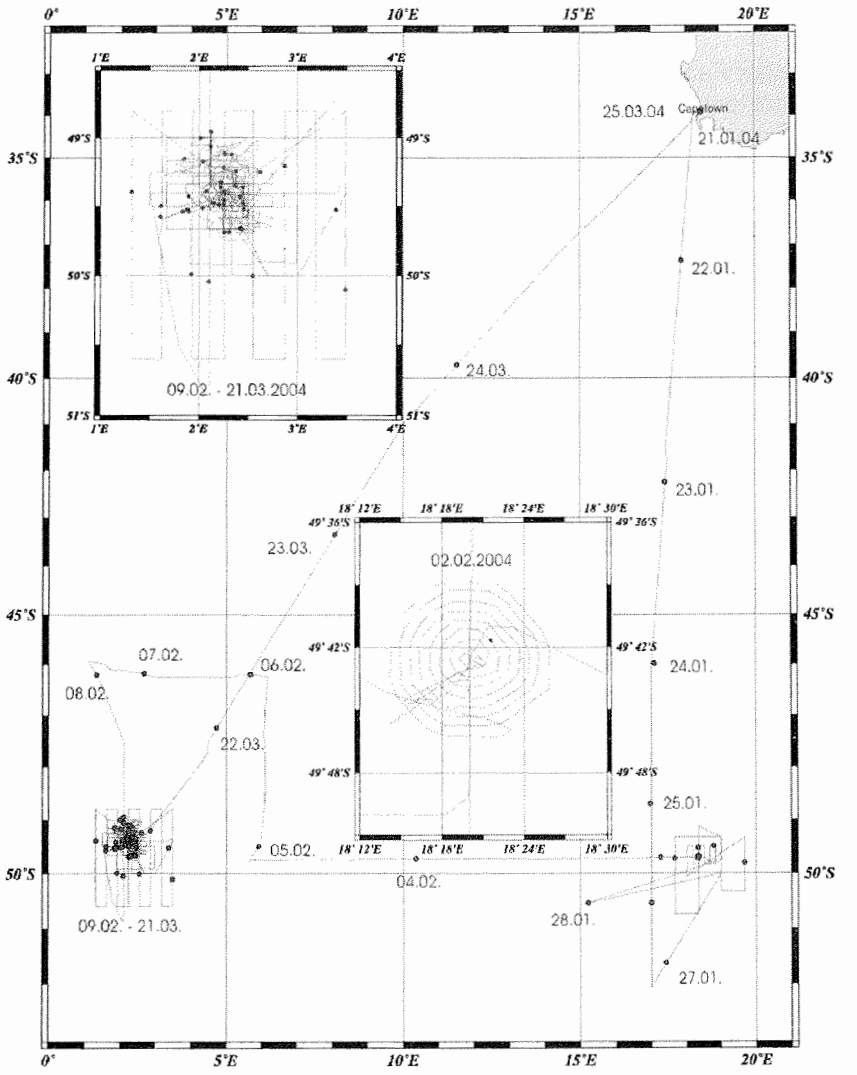
Chlorophyll concentrations above 2.5 mg/m³ extended down to 100 m depth and even at 150 m the values in some CTD casts were as high as in the unfertilised surface water around the patch (0.5 mg/m³). The highest chlorophyll value recorded was 2.9 mg/m³. By about the middle of the first week of March the buoy had completed another closed oval within the eddy, almost identical to the first. The buoy was retrieved, the instruments serviced and it was replaced in the centre of high chlorophyll concentrations.

March 4 and 5 were spent mapping the hot-spot by steaming back and forth along the same track with short CTD stations and letting the current carry it through our line of interception. The hot-spot with chlorophyll values above 2 mg/m³ was about 260 km² but around it was a much vaster area where values were about double those recorded prior to fertilisation and still characteristic of unfertilised water. A 60-hour station was carried out over the first March weekend to study temporal changes in the physical environment and diurnal rhythms in the plankton and chemistry of the water column.

The bloom reached its peak in the first week of March and its demise, signalled by sinking out of several of the dominant species, commenced in the second week. Iron and nutrient concentrations in the bloom were still fairly high, so iron or nutrient limitation was not responsible. Besides, other species continued to grow healthily, so what happened was a replacement of the dominant species by others. But the causes of the species succession were not apparent. The last outside station, carried out on March 17, indicated that the same succession pattern occurred in outside water as well.

Since the sinking particles were recorded by transmissometer profiles we carried out a number of deep casts down to the bottom to determine the areal extent of the mass sinking. An increase in spikes in these profiles in the bottom 200 m of the profiles indicated rapid sinking of what were presumably aggregates of whole phytoplankton. This was confirmed by microscopic examination of the samples from this layer.

The last station inside the patch was carried out on 20th March after which Polarstern left the eddy and arrived in Cape Town on 25th March.



PFS Polarstern
ANT XXI - 3
Capetown - Capetown
Jan, 21th 2004 til Mar, 25th 2004



Fig. 1 Cruise track of POLARSTERN ANT 21/3 EIFEX from 21.01.-25.03.2004

2. WETTER

J. Lentes, K. Buldt (DWD)

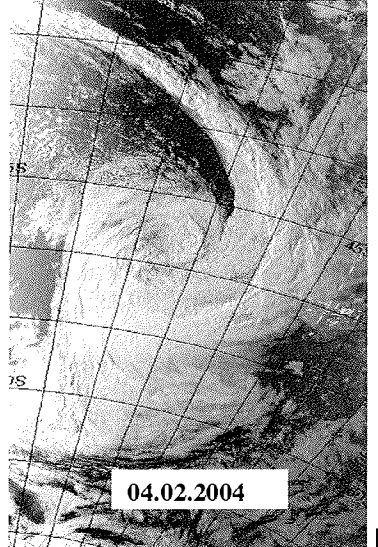
Wissenschaftliches Programm:
Eisendüngungsexperiment (European Iron Fertilisation Experiment EIFEX).

Das Ziel der Fahrt war die Untersuchung des Auf- und Abbaus einer Phytoplanktonblüte, die dann in einem Fleck von mehreren hundert Kilometern durch Düngung mit ca. 20 Tonnen Eisensulfatpulver erzeugt werden sollte. Es war beabsichtigt, das Experiment in einem Wirbel südlich der Antarktischen Polarfront, die bei ca. 50° Süd liegt, durchzuführen. Zuerst musste ein Wirbel ausfindig gemacht werden und dann wurde dessen Eignung mit Messungen vor Ort überprüft. Nach der Düngung mit Eisensulfatpulver sollte dann in einem Zeitraum von 9 Wochen das Schicksal der Blüte verfolgt werden.

Fahrtverlauf und Wetter:

Am 21. Januar 2004 abends verließ die FS Polarstern Kapstadt in Richtung Süden zum Arbeitsgebiet bei 45 bis 55 ° Süd und 17 bis 20° Ost. Ein Keil des Subtropenhochs bestimmte das Wetter auf dem Kurs der Polarstern bis zum 45. Breitengrad Süd mit meist nur geringer Bewölkung, leichtem bis mäßigen Wind und See bei 2 bis 3 Meter.

Am 25.1. zog ein flaches Tief mit wellender Kaltfront in der westlichen Höhenströmung nach Osten und beeinflusste das Wettergeschehen bei der Polarstern, zeitweise leichte Schneeschauer. Ab 26.1. erstreckte sich eine Zone flacher Druckverteilung entlang des 50. Breitengrades mit meist aufgelockerter Bewölkung und mäßigem Wind, See um 2,5 Meter. Nachdem ein weiteres flaches Tief die Polarstern überquert hatte, brachte am 28.1. ein Hochkeil wieder kurzzeitig freundliches Wetter, leichter bis mäßiger Wind und See um 2 Meter. Nachmittags fuhren wir in ein Nebelgebiet. Es folgte Bewölkungsverdichtung von Westen her. Ein Tiefdruckgebiet südwestlich von Bouvet Island zog rasch ostwärts und sein Frontensystem erreichte die Polarstern gegen Mitternacht. Am 29.1. in der Frühe lagen wir im Bereich der Kaltfront, der Wind hatte in der Nacht Stärke 6 bis 7 erreicht und so blieb es auch tagsüber, See um 3 Meter. Im weiteren Verlauf bestimmte ein umfangreiches steuerndes Tief mit Kerndruck 975 hPa zwischen dem 20. Grad Ost und dem 20. Grad West südlich des 55. Breitengrades bis Anfang Februar das Wettergeschehen. An seiner Nordflanke wurden immer wieder Frontensysteme ostwärts geführt und überquerten das Fahrtgebiet der Polarstern im zeitlichen Abstand von 24 Stunden. Es herrschte meist Westnordwestwind mit 6 bis 7 Bft und See um 3,5 Meter. Am 4.2. kam dann ein Sturmtief von Westen heran und zog in der Nacht zum 5.2. über das Einsatzgebiet der Polarstern hinweg.

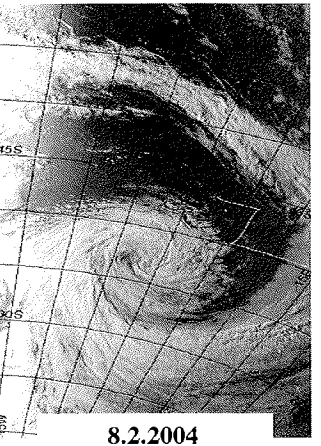


Der Kerndruck des Tiefs betrug 965 hPa

und die Wolkenstruktur war auf dem Satellitenbild vom 04.02.04 deutlich zu erkennen

Windstärke auf der Polarstern war 9 bis 10 Bft in der Nacht mit Wellenhöhe um 7 Meter. Nach Rückseitenwetter folgte im Bereich eines schwach ausgeprägten Hochkeils kurzzeitig Wetterberuhigung.

Über ein weiteres Sturmtief, das uns in der Nacht zum Sonntag (8.2.04) erreichen würde, wurde der Kapitän und der wissenschaftliche Fahrtleiter informiert. Daraufhin erfolgte eine Kursänderung und wir dampften nach Norden zur Position $46,2^{\circ}$ S $2,0^{\circ}$ E. In der Nacht zum 8. Februar erlebten wir dann den Sturm an der Ausweichposition immerhin noch mit Bft 9 und Wellen mit 8 bis 10 Meter. Weiter südlich gab es 15 Meter hohe Wellen und Windstärke um 11 Bft und somit wurde dann deutlich wie wichtig die Entscheidung zur Kursänderung aufgrund der rechtzeitigen Wetterwarnung gewesen ist.



Am 8.2. abends machten wir wieder Fahrt in Richtung Süden, um den gewünschten 2. Wirbel zu lokalisieren. Unser Einsatzgebiet lag weiterhin in einer kräftigen Westströmung, und in einem zeitlichen Abstand von 1 bis 2 Tagen zogen immer wieder Frontensysteme über uns hinweg und bestimmten das Wettergeschehen. Am 11.2./Mittwoch trat dann Wetterberuhigung ein, wir hatten Warmsektorbedingungen mit Nebel.

Danach bis zum 17.Februar wurden erneut in der kräftigen Westströmung immer wieder kleinere Tiefs mit den dazu gehörigen Frontensystemen über das Arbeitsgebiet der Polarstern hinweg geführt. Die Windstärke betrug hierbei 7 bis 8 Bft und Wellenhöhen um 5 Meter.

Ab 17. Februar verlagerte sich dann am Südrand des Subtropenhochs zunächst ein Keil hoher Druckes zu uns und es trat eine merkliche Wetterbesserung ein. Dies war jedoch nicht von langer Dauer, denn bei geringen Druckunterschieden zogen flache Tiefe über das Einsatzgebiet der Polarstern hinweg. Wir befanden uns meist im nördlichen Bereich der wärmeren Luftmassen und hatten als Folge davon 4 Tage lang überwiegend Nebel oder Hochnebel und somit auch keine Flugwetterbedingungen.

Die Hubschrauber blieben im Hangar.

In der Nacht zum 21.Februar überquerte uns dann wieder eine Kaltfront ostwärts. Bei Frontdurchgang und am Vormittag hatte der Wind Sturmstärke erreicht. Aufgrund der Wettervorhersage konnte der geplante Flugbetrieb um 0600 UTC trotz des stürmischen Windes und einzelner Schnee- und Graupelschauer zunächst durchgeführt werden, wurde dann aber für den weiteren Tagesverlauf wegen des zu hohen Seegangs eingestellt. Nach kurzer Wetterberuhigung kam dann bei erneuter Gradient-verschärfung und Kaltfrontdurchgang wieder Sturm auf, Bft 9 in der Nacht zum 24.Februar, ebenso in der Nacht zum 25.2. Ab mittags befanden wir uns dann auf der Kaltfrontrückseite und der Wind schwächte sich auf 7 Bft ab und in der Nacht zum Donnerstag weiter auf 5 Bft. Tagsüber am 26.2. hatten wir meist CAVOK, viel Sonne und Wind nur 3 bis 4 Bft.

Am Freitag nahm der Wind wieder erwartungsgemäß zu und in der Nacht zum 28.2. überquerte uns dann das Frontensystem eines Teiltiefs mit Windstärke 7 Bft.

Am 28.2. brachte Rückseitenwetter Schnee- und Graupelschauer und abends Wind mit 8 bis 9 Bft.

Beim Bergfest schlügen dann die Wellen aufs Achterdeck und löschen das Grillfeuer.

Nach nur kurzer Wetterberuhigung am 29.2. mit einigen sonnigen Abschnitten und schwächerem Wind ging es dann mit dem unbeständigen Wetter weiter, es folgte ein Tief aufs andere und immer auf der Rückseite folgte kalte Luft aus südlichen Richtungen mit Schnee- und Graupelschauern. Die Windstärke war meist zwischen 6 und 8 Bft, fast jede Woche erreichte er mal Sturmstärke 9 wie in der Nacht zum 2.3. mit Wellen um 7 Meter. Bei einigen Tiefs mit ausgedehntem Warmsektor war infolge Zufuhr warmer und feuchter Luft aus Norden lang anhaltender Nebel, oft über mehrere Tage hinweg. Nur am 9. und 10 März erstreckte sich der Einfluss des Subtropenhochs bis zum Einsatzgebiet der Polarstern. Druckanstieg und gleichzeitig schwacher Druckgradient brachten uns fast 2 Tage besseres Wetter mit CAVOK-Bedingungen und nur Windstärke 5.

Danach waren wir in einer Nordwestströmung mit erneut Zufuhr milder Luftmassen. Die Lufttemperatur betrug 6° C, und die Wassertemperatur nur

etwas über 4° C . Die Folge davon waren 3 Tage lang Nebel / Stratus um 100 FT. Die Windgeschwindigkeit lag meist bei 25 bis 30 Knoten.

Am 14. März nachmittags gelangten wir auf die Frontrückseite in den Bereich trockenerer Kaltluft und Flugbetrieb konnte wieder stattfinden. In den Folgetagen bis zum Ende der Woche wurden an der Südflanke des Subtropenhochs in einer kräftigen Westströmung immer wieder kleinere Frontensysteme über das Einsatzgebiet der Polarstern ostwärts geführt. Im jeweiligen Warmsektor dieser Frontensysteme hatte wir Nebel und bei Kaltfrontdurchgang am 18.3. wieder mal Windstärke 9 Bft und Wellen um 7 Meter.

Am 19. März schwächte sich dann nachmittags der Wind auf 6 bis 5 Bft ab und die Driftboje konnte bei ruhigerer See an Bord geholt werden.

Am 20.3. überquerte uns dann nachmittags noch mal ein kleines Frontensystem zum Abschied, wobei der Wind im Bereich der Kaltfront wieder 8 bis 9 Bft erreichte.

Ab 18 Uhr UTC begann die Rückreise nach Kapstadt und wir gelangten zunehmend unter den Einfluss des Subtropenhochs bei anfangs noch frischen, später schwachen bis mäßigen westlichen Winden und milden Temperaturen.

Tätigkeiten der Bordwetterwarte:

Meteorologische Beratung von Fahrt- und Schiffsleitung, der vom Schiff aus operierenden Hubschrauberpiloten sowie der verschiedenen wissenschaftlichen Gruppen und Fahrteilnehmer aus 7 europäischen Ländern und Südafrika.

Es wurden täglich 2 Wetterberichte erstellt und an die Brücke sowie an den Fahrtleiter verteilt. Morgens und abends fand jeweils ein Wetter-Update auf der Brücke statt.

Abends um 19:15 BZ täglich: Wetter-Briefing in englischer Sprache mit anschließend wissenschaftlichen Vorträgen der Meeresbiologen unter Leitung des Fahrtleiters Professor Smetacek .

Flugwetterberatungen wurden für die Hubschraubereinsätze jeweils auf Anforderung erstellt.

Täglich wurde 1 Ballonaufstieg durchgeführt, je nach Bedarf zusätzlich ein weiterer.

Von 06 bis 21 UTC alle 3 Stunden Augenbeobachtungen in Ergänzung zu den stündlichen Obsen der Automatischen Wetterstation .

Auskünfte und mündliche Wetterberatungen an alle wissenschaftlichen Fachgruppen wurden je nach Anforderung erteilt.

Funkempfang, IT, meteorologische Instrumente:

4.1 Datenversorgung und Funkempfang:

Die Arbeitsgebiete von FS Polarstern lagen während des gesamten Fahrtabschnitts innerhalb des Ausleuchtungsbereichs der Kommunikationssatelliten. Wie üblich bezogen wir daher täglich per E-Mail über das GF SF in Hamburg die mittels des DWD-Programms „Request“

angeforderten EZMW-Vorhersagekarten, Gitterpunktvorhersagen für Wind, Seegangsdaten des gleichen Modells, aktuelle Wettermeldungen aus dem Fahrtgebiet sowie den Heimatorten der Fahrtteilnehmer.

Zusätzlich nutzen wir die vom Sender Cape Naval des südafrikanischen Wetterdienstes in Pretoria auf den Frequenzen 7508 kHz, 13538 kHz sowie 18238 kHz ausgestrahlten Analyse- und Vorhersagekarten. Leider entsprach die Ausstrahlung nicht immer dem Sendeplan, weshalb eine ständige Überwachung der Frequenzen erforderlich war.

Vereinzelt, besonders in den Abend- wie auch in den frühen Morgenstunden, gelang der FAX Empfang (F1C) des DWD Senders Pinneberg auf der Frequenz 13882,5 kHz. So war es möglich hin und wieder auch genauere Aussagen über die Wetterlage zuhause bereitzustellen.

4.2 Nachrichtengeräte und Informationstechnologie IT:

Beim Betrieb der Allwellenempfänger von Telefunken gab es keinerlei Probleme. Die zum Communication Receivers AR5000 gehörende Antenne wurde bereits beim ersten Sturm dieser Reise beschädigt, so dass dieses Gerät im weiteren Verlauf nicht mehr nutzbar war.

Die PC's an den Arbeitsplätzen des Bordmeteorologen sowie des Wetterfunktechnikers arbeiteten nebst zugehöriger Peripheriegeräte einwandfrei.

Die wenigen vom Sender Cape Naval ausgestahlten F1C Sendungen zeichneten wir mittels der auf mehreren Rechnern installierten Software JVComm.32 auf.

Die SUN2 zur Visualisierung sämtlicher gemessenen meteorologischen Parameter bleibt weiterhin bei normaler Nutzung alle 33 bis 35 Stunden stehen. Somit musste diese Maschine auch weiterhin einmal täglich zu einem festen Zeitpunkt von Hand gebootet werden.

Die Datenerfassung mittels PODAS funktionierte einwandfrei. Die täglichen Wetterberichte der Bordwetterwarte sowie die laufend aktualisierten Heimatwetter standen allen Interessierten im bordeigenen Intranet schnell und optisch ansprechend zur Verfügung.

4.3 Satellitenbildempfang:

Die Tecnavia-Anlage lieferte während der gesamten Reise einwandfreie APT-Bilder von NOAA12. NOAA15 konnte nur bis zum 14. März empfangen werden. Ob die Einstellung der Übertragung von APT Bildern endgültiger oder nur vorübergehender Natur ist, konnte bis zum Ende der Reise nicht festgestellt werden.

Auch die TeraScan –Anlage funktionierte auf dieser Reise weitgehend störungsfrei, sieht man von weingen Ungereimtheiten in der Ausführung des

Flugplanes ab. Vereinzelt wurden in diesem Plan als aktiv geschaltete Überflüge nicht erkannt, oder nicht vollständig aufgezeichnet. Erst gegen Ende der Reise, beim Verlassen des letzten Operationsgebietes versagte sie Ihren Dienst. Nach intensiver Fehlersuche in Zusammenarbeit mit dem zuständigen Laborelektroniker stellte sich ein „teilweise festgefahrener“ Rechner als Ursache heraus. An diesen Tagen ließ sich für die Beratung jeweils nur ein jeweils morgens bzw. abends empfangenes APT Bild von NOAA12 nutzen.

4.4 Radiosondenaufstiege:

Die Durchführung der Radiosondenaufstiege sowie deren Auswertung mittels DigiCora und der DWD-Software (Metwatch) bereite wiederum keine Probleme. Mit Hilfe des auf dem Arbeitsrechner des Bordmeteorologen installierten Vaisala-Programms Metgraph konnten die laufenden Sondierungen online dargestellt und erforderlichenfalls für Flugwetterberatungen sofort ausgewertet werden.

4.5 ABWST

Zu Reisebeginn wurde die neue Version 1.5.0 installiert. Alle im vorangegangenen Reisebericht beschriebenen Fehler sind nun nicht mehr aufgetreten. Einzig der Export der in der AWST Datenbank enthaltenen Werte in eine Excel – Datei funktioniert nur bedingt. Ein Update, welches diesen Fehler beheben soll, wurde in Aussicht gestellt.

4.6 Data Collection Platform (DCP):

Sämtliche durch das Programm ABWST erstellten Obse sowie die von der DigiCora übermittelten Daten der 12 Uhr-UTC-Radiosondenaufstiege wurden in der DCP zwischengespeichert und von dort in das GTS befördert. Diese Prozedur funktionierte störungsfrei.

Das automatische Überspielen der codierten Radiosondendaten musste wie üblich überwacht werden. Gleichermaßen galt für die DCP-Zeit, welche regelmäßig zu kontrollieren und gegebenenfalls zu justieren war.

4.7 Meteorologische Instrumente:

Die meisten meteorologischen Messinstrumente arbeiteten weitgehend störungsfrei und erforderten lediglich die übliche routinemäßige Kontrolle und Pflege.

Eine Ausnahme bildete auf dieser Reise der Regenmesser. Das zugehörige Anemometer versagte bereits kurz nach Auslaufen zeitweise den Dienst. Das Schalenkreuz blieb stehen. Da kein Ersatz an Bord war konnte nur mittels geeigneter Schmierstoffe versucht werden, das Gerät wieder gangbar zu machen. Wie sich später zeigte, war offensichtlich ein Lagerschaden für den Ausfall verantwortlich. Nach dem ersten größeren Sturm der Reise klemmte die Achse des Schalenkreuzes endgültig fest. Zudem brach eine Schale ab. Da die Windgeschwindigkeit ab 9m/s in die Berechnung des Niederschlag eingeht und

diese auf der ganzen Reise so gut wie nie unterschritten wurde, mussten der Windmesser wie auch der Regenmesser Ende Februar komplett abgeschaltet werden. Somit stehen für diese Reise keine Niederschlagsdaten zur Verfügung.

Die elektronisch ermittelten Werte von Lufttemperatur und Luftfeuchtigkeit sowie des Taupunktes wurden durch regelmäßige Kontrollmessungen überprüft und bestätigt. Während einer länger andauernden Nebelphase fielen die Sensoren jedoch komplett aus. Sie waren vollständig mit Wasser gefüllt, welches auch nach Nebelauflösung nicht mehr aus dem Sensorkopf entweichen konnte. Nur durch wiederholtes Entwässern und Trocknen von Hand ließen sie sich reaktivieren. Letztlich musste ein Sensor (Stb) komplett gewechselt werden.

Die Gelegenheit zu Vergleichsmessungen des Luftdrucks ergaben sich während der Liegezeit in Kapstadt sowie im Verlauf der Reise, als die „Agulas“ in knapp 40 km Entfernung das zweite Arbeitsgebiet dieser Reise durchfuhr. Die jeweils nur geringen Differenzen lagen innerhalb der Toleranz.

4.8 Sonstiges

Als routinemäßigen Service für das AWI erstellten wir täglich Ausdrucke mit den Diagrammen sämtlicher meteorologischer Parameter aus PODAS sowie am Reiseende eine entsprechende Aufbereitung der 10-Minuten-Mittelwerte vom gesamten Teilabschnitt. Letztere wurden zusammen mit einer Auswahl repräsentativer Satellitenbilder, unseren 3-stündigen ABWST-Obsen sowie den Radiosondendaten von der DigiCora auf CD gebrannt und mitsamt den erwähnten Papierausdrucken zur Weiterleitung an die zuständige Sektion auf den Weg gebracht.

Im Rahmen eines langfristigen Fernerkundungsprojekts des „Center for Ocean Atmospheric Prediction Studies“ in Tallahassee/Florida fertigten wir auf entsprechende Bitte auch während dieses Reiseabschnitts einmal wöchentlich eine Zusammenfassung von Wind- und Navigationsdaten mit einer Auflösung von einer Minute an und leiteten die extrahierten Datensätze per E-Mail direkt an den zuständigen Sachbearbeiter weiter. Die von Polarstern übermittelten Werte sind dort zum Validieren eines neuen Satelliten (Quicksat) höchst willkommen und werden von Zeit zu Zeit auch in entsprechenden Fachorganen publiziert.

Beteiligte Institutionen, denen Dienstleistungen der Bordwetterwarte zur Verfügung standen:

- AWI Alfred Wegener Institut für Polar- und Meeresforschung, Bremerhaven
- DWD Deutscher Wetterdienst, Geschäftsfeld Seeschifffahrt, Hamburg
- VUB Vrije Universiteit Brussel, Belgien
- LOV Laboratoire d'Oceanographie de Villefranche-sur-mer, France
- GKSS Forschungszentrum Geesthacht
- HTA Heli Transair GmbH
- IFM-K Institut für Meereskunde
- ISW ISW Wassermesstechnik
- LAEISZ Reederei F. Laeisz
- OPTIM. OPTIMARE GmbH
- TU-HH Technische Universität Hamburg-Harburg
- UNI-HB Universität Bremen
- SZN Stazione Zoologica „A.Dohrn“ Italia
- NIOZ NIOZ Dept.Biol.Oceanog. Nederland
- ICMB INSTITUT DE CIENCIAS DEL MAR, Spain
- NTNU Norwegian University of Science & Tech.TBS, Norway
- UiB University of Bergen, Norway
- UCT University of Cape Town, South Africa
- UEA University of East Anglia, UK
- UNI-L Oceanography Laboratories, UK

3. THE PHYSICAL SETTING OF THE EUROPEAN IRON FERTILIZATION EXPERIMENT 'EIFEX' IN THE SOUTHERN OCEAN

V. Strass (AWI), B. Cisewski (AWI), S. Gonzalez (NIOZ), H. Leach (Univ. Liverpool), K.-D. Loquay (Optimare), H. Prandke (ISW), H. Rohr (Optimare) and M. Thomas (TU HH)

It has been hypothesized that the supply of iron to the open ocean affects the global climate development because it exerts a control on phytoplankton primary production and hence the exchange of carbon dioxide between the atmosphere and the ocean. The key role would be with the Southern Ocean where the surface euphotic zone in the present climate state is extremely rich in macro-nutrients. Excess plant nutrients, which are supplied by upwelling in the Antarctic Divergence but are not completely utilised by phytoplankton primary production, are subducted again at fronts within the Antarctic Circumpolar Current (ACC). Possible reasons for the limitation of primary production include

insufficient availability of light for the phytoplankton growing in the mixed layer when the mixing is deep due to wind stirring and convection, zooplankton grazing, and notably lack of trace nutrients such as iron.

Testing the iron hypothesis by performing an open ocean *in situ* experiment was the overarching goal of 'EIFEX'. The test was planned to consist of fertilizing a patch of water in the ACC with dissolved iron, pumped from the ship into the sea, and of monitoring the biological response to the addition of iron for as long as possible.

Prerequisite for conducting an open ocean *in situ* experiment is information about the physical setting. For that purpose, a suite of oceanographic measurements had to be carried out during Polarstern cruise ANT-XXI/3 'EIFEX'. These measurements were aimed at three particular objectives.

Objective 1: To identify a suitable site for the iron fertilization experiment. That site had to satisfy two differing conditions. Firstly, and ideally, it should be close to the Antarctic Polar Front where the silica-rich Antarctic Surface Water subducts, i.e. as close as possible to the region of potentially strongest impact on carbon draw-down. Secondly, on the other hand, the site had to be away from vigorous frontal jets to avoid the injected dissolved iron dispersing too rapidly. As a solution to this problem we planned to conduct the experiment within a mesoscale eddy, a strategy that proved successful during the previous iron fertilization experiment of Polarstern, EisenEx.

The measurements aimed at identifying a stable eddy were made by use of an instrument package combining the vessel-mounted acoustic Doppler current profiler (VM-ADCP) with either a towed undulator (Scanfish) or a CTD (Conductivity Temperature Depth sonde) operated in closely spaced station work. The ADCP+Scanfish/CTD package allowed the mesoscale density and velocity fields being mapped simultaneously with other physical and biological variables down to 200 - 300 m depth at sufficient horizontal resolution in quasi-synoptic manner.

Using this instrument package guided by information on sea surface height variability obtained from satellite altimetry before and during the cruise, we succeeded after 10 days of surveying since departure from Cape Town to identify and map a hydrographic structure which appeared ideal for conducting the experiment. That structure consisted of a cyclonic eddy of 50 - 130 km width, centered at 49°45'S 18°20'E, which obviously was in the process of being shed by the Southern Polar Front (SPF) due to detachment of a northward protruding meander. Due to its origin, the eddy contained in its centre the high concentrations of macro-nutrients typical of the SPF. The center of this eddy, named Eddy-1, was fertilized with iron between the 2nd and 3rd of February. Because Eddy-1 was however extremely poor in phytoplankton, it was left after fertilization in order to investigate another eddy-like structure that showed up in satellite altimeter images further west. That investigation, using the ADCP+CTD instrument package, was completed by the 11th of February with the identification of a cyclonic eddy centered at 49°24'S 02°15'E and

extending over 60 km x 100 km. This eddy, Eddy-2, was embedded in a meander of the APF. It also was rich in macro-nutrients but, in contrast to Eddy-1, contained a higher phytoplankton concentration that was more typical for the frontal band of the ACC in summer. Fertilization in Eddy-2, of a circular patch of 16 km diameter within its core, was performed February 12 - 13 and later repeated February 26 - 27. Eddy-2 provided the open-ocean laboratory for our experiment until the end of the cruise.

Objective 2: To monitor the displacement and spreading of the fertilized water body under the action of advection and diffusion.

For that purpose, different measuring techniques were used in combination. A surface buoy drogued at 18 – 26 m depth, equipped with GPS (Global Positioning System) receivers and radio as well as ARGOS satellite transmitters, was deployed in the centre of the eddy to aid the ship navigating in a Lagrangian manner while pumping the iron solution into the sea along a spiral-shaped track around the buoy in order to produce a fertilized patch as homogeneous as possible. After iron injection, the drift of the buoy as monitored via radio and ARGOS provided the primary source of information about the movement of the fertilized patch of water.

For mapping the full extend of the moving patch a helicopter flown LIDAR system was employed.

Numerous casts of a CTD sonde, attached to a rosette water sampler, were done for hydrographic profiling from the surface to intermediate and occasionally full ocean depths. The CTD rosette sampler also was the major tool for supplying the various scientific disciplines on board with water samples. By performing repeated CTD surveys in the area at fine horizontal resolution of a few kilometres it was possible to map the three-dimensional distribution of those variables and their change in time.

Measurements of currents by the vessel-mounted acoustic Doppler current profiler (VM-ADCP) were continuously made throughout the cruise and processed aboard to monitor the mesoscale circulation.

A tethered free-falling microstructure probe (MSS) was used for profiling small-scale turbulent motions down to 300 m depth. From these data the vertical distributions of turbulence parameters like overturning scales and energy dissipation rates can be estimated.

To continue to monitor the fertilized patch after the end of the cruise, autonomous floats (VS-APEX) were deployed just prior to departure. By using the combined information from measurements (a) through (d) we were able to follow the fertilized patch until we had to depart from our experimental site at the end of the cruise.

Objective 3: To provide a detailed description of the physical environment of the phytoplankton and zooplankton at the experimental site, and to provide the basic measurements needed for estimating fluxes of particulate and dissolved matter.

A detailed description of the physical environment can be obtained from combined analysis of the various measurements made. That description

consists of the three dimensional distributions of temperature, salinity, density, currents and turbulence parameters as well as of the horizontal distribution of integral or bulk characteristics like the mixed layer depth, including a discrimination between just homogeneously mixed and actively mixing turbulent layers, and their variation in time. Further, by combining vertical profiles of the turbulent kinetic energy derived from the ADCP current measurements with the vertical distribution of various microstructure data from the MSS, vertical eddy diffusivity profiles can be estimated.

However, providing a detailed description of the physical environment is to large extent left to post-cruise analysis work.

In seven sections following below the made measurements are described in more detail.

3.1 Underway Measurements of Currents with the Vessel-Mounted Acoustic Doppler Current Profiler

B. Cisewski and V. Strass (AWI)

Vertical profiles of ocean currents down to roughly 300 m depth were measured with a Vessel Mounted Acoustic Doppler Current Profiler (VM-ADCP, 150 kHz nominal frequency, manufactured by RDI,), installed at the ship's hull behind an acoustically transparent plastic window for ice protection. The ADCP has four transducer heads, arranged in a square formation, which point diagonally outwards at an angle of 30° relative to the vertical. The transducer heads simultaneously emit a sound pulse approximately every second, and record echoes returned from discontinuities in the water or from suspended particles. The echoes are range-gated into a series of vertical bins and analysed for their Doppler frequency shift which is related to the water velocity. Determination of the velocity components in geographical coordinates, however, requires that the attitude of the ADCP transducer head, its tilt, heading, motion and geographic position is also known. Attitude variables of the VM-ADCP were taken from the ship's navigation system. In addition, the ADCP can be used as a detector for zooplankton abundance by evaluating the echo amplitude.

The instrument settings were chosen to give a vertical resolution of current measurements of 4 m in 80 depth bins, and a temporal resolution of 2 min after ensemble averaging over individual profiles taken at a rate of roughly 1 Hz. Calibration data for the ADCP velocity measurements were obtained during the cruise, during approach to and departure from stations. Processing of the VM-ADCP data was done using the CODAS software package (developed by E. Firing and colleagues, SOEST, Hawaii).

The VM-ADCP data were collected continuously during the cruise whenever outside of exclusive economic zone waters.

ADCP grid 5

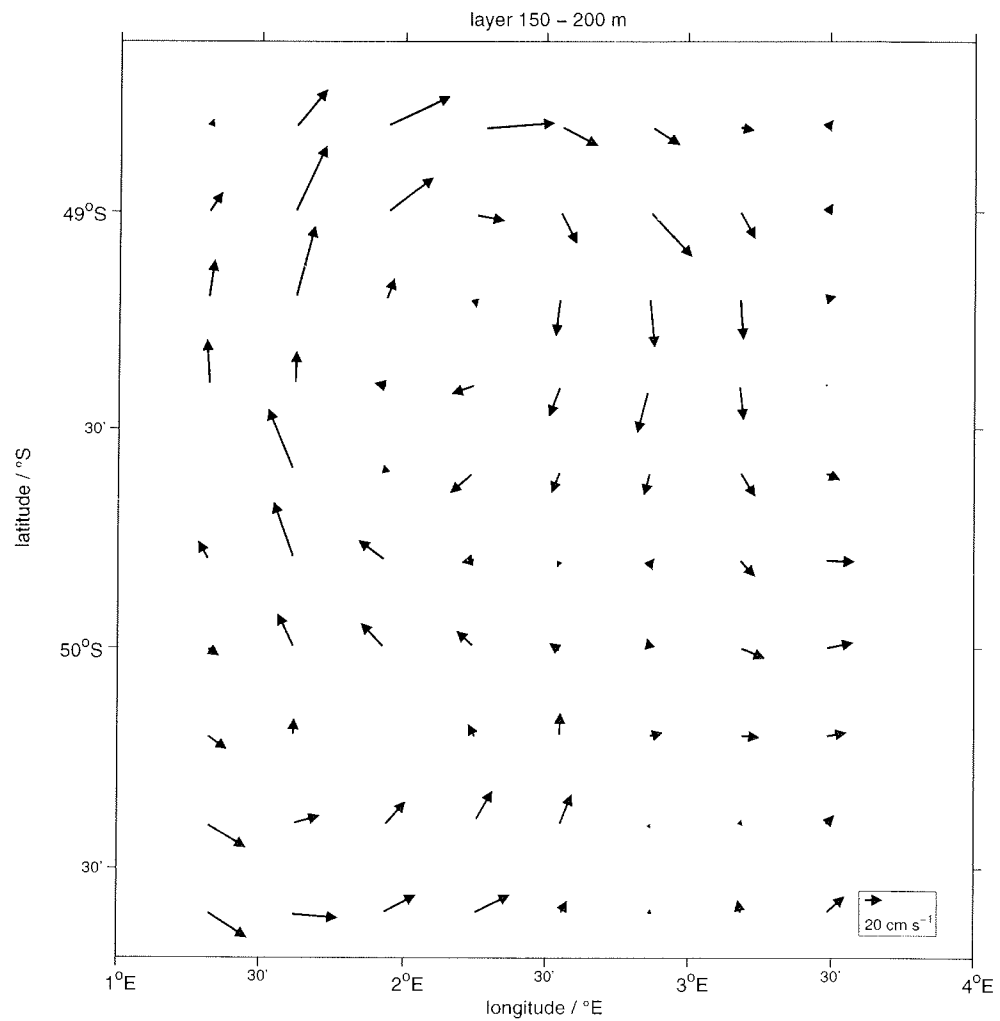


Fig. 3.1.1: Horizontal currents in the depth range 150 - 200 m measured between the 14th and 20th of February with the VM-ADCP at regularly spaced CTD station grid points. The pattern of current vectors reveals a cyclonic eddy (Eddy-2) centered at roughly 49°15'S 02°15'E, and the Polar Front that winds around it.

3.2 Underway Measurements of Hydrographic and Biological Variables with the Towed Undulating Vehicle 'Scanfish'

S. Gonzalez (NIOZ), H. Leach (Univ.Liverpool) and V. Strass (AWI)

The Scanfish (GMI Scanfish MK II) is a streamlined, wing-shaped body towed behind the steaming ship. By electrically adjustable flaps at its rear end the Scanfish can be made to undulate vertically through the upper water column according to the parameter settings entered at the control unit on deck. The depth range is enhanced by use of an active winch (Type Cormac 1500 assembled by Svendborg Skibshydraulik A/S) holding 2500 metres of 8.3 mm thick unfaired COAX towing cable, cable which is paid out during dive of the Scanfish and retrieved during climb. The Scanfish was mostly towed at speeds that varied between 7 and 8 knots. Combined with a dive/climb rate of 0.4 m/s, the Scanfish profiled through a depth range from roughly 5 to 230 m. These towing parameters resulted in a nominal horizontal resolution (half wavelength) of about 2 km along-track. Scanfish attitude while being towed, as well as the scientific data, were monitored and recorded in real-time on deck.

The scientific payload of the Scanfish consisted of a CTD (Sea-Bird Electronics SBE 911*p/us*), a light meter for PAR (photosynthetic active radiation), a fluorometer (Chelsea Instruments) and a turbidity meter (Seapoint Sensors, Inc.). From the CTD measurements the hydrographic variables of state, pressure (depth), temperature, salinity and density were determined, while the fluorometer readings were used to derive the chlorophyll concentration as an indicator of phytoplankton biomass. The CTD temperature measurements are assumed accurate to 0.001 °C according to the manufacturers specifications. Salinity needs to be calibrated later after the cruise when the post-cruise calibration of the ships lowered rosette-CTD will be also available. The Scanfish fluorometer readings (F) were converted into concentrations of chlorophyll *a* (Chl) using a model in which the yield ($Y = F/Chl$) changes with ambient light as measured by the PAR sensor. This enabled to reasonably remove the light-dependent quenching effect. Horizontal changes of yield were taken into account by comparison with Chl determined from underway surface samples by C. Klaas and co-workers.

Measurements with the Scanfish were made at the begin of the cruise, prior to fertilization in Eddy-1, during a meridional transect (trans01) running along 17°E from 46°00'S to 48°42'S. At this latest position, the Scanfish unfortunately was lost due to breakage of the cable. The reason of the breakage is yet unclear. However, as it occurred while the Scanfish was roughly halfway on its upward track, i.e. when the cable load is usually minimal, a likely reason is that the Scanfish hit an object in the water. Hadn't we lost the Scanfish that early, we certainly would have employed it much more during the cruise.

3.3 Hydrographic Station Work with CTD and Water Bottle Sampling

V. Strass (AWI), H. Rohr (Optimare), H. Leach (Univ. Liverpool), B. Cisewski (AWI), S. Gonzalez (NIOZ), H. Prandke (ISW), and M. Thomas (TU HH)

The CTD used for conventional deployments at hydrographic stations was, as the one in the Scanfish, of type Sea-Bird Electronics SBE 911*plus*. The CTD was supplemented by a transmissometer (Wet Labs C-Star, 660 nm wavelength), a chlorophyll-sensitive fluorometer (Dr. Haardt BackScat), and an altimeter (Benthos) to measure the distance to the sea floor. Also attached was a Fast Repetition Rate Fluorometer (FRRF) together with a light sensor, which was supplied by R. Röttgers.

The CTD and peripheral instruments were attached to a multi-bottle water sampler type Sea-Bird SBE 32 Carousel holding nominally 24 12-liter bottles. One of the bottles was however removed to give space for the FRRF. The performance of the water sampler was controlled by use of a laboratory standards thermometer of type SBE 35. Salinity derived from the CTD measurements will be calibrated by comparison to salinity samples, taken from the water bottles, which were analysed by use of a Guildline-Autosal-8400A salinometer that was adjusted to IAPSO Standard Seawater.

Altogether, 332 CTD casts were made at a total of 222 hydrographic stations. Most casts were limited to intermediate depths of 500 m. 20 casts however extended to full ocean depth, of which most were performed close to the end of the cruise. Many CTD stations were arranged in fine-meshed horizontal grids (see Figures o.3.1-5), either in fixed geographic coordinates or in Lagrangian coordinates relative to the buoy that was drifting with the patch. In an attempt to achieve a fast synoptic mapping of the eddy and the patch, several CTD casts, especially at the begin of the cruise, were made without closure of bottles. All CTD casts are listed in Table 3.3.1.

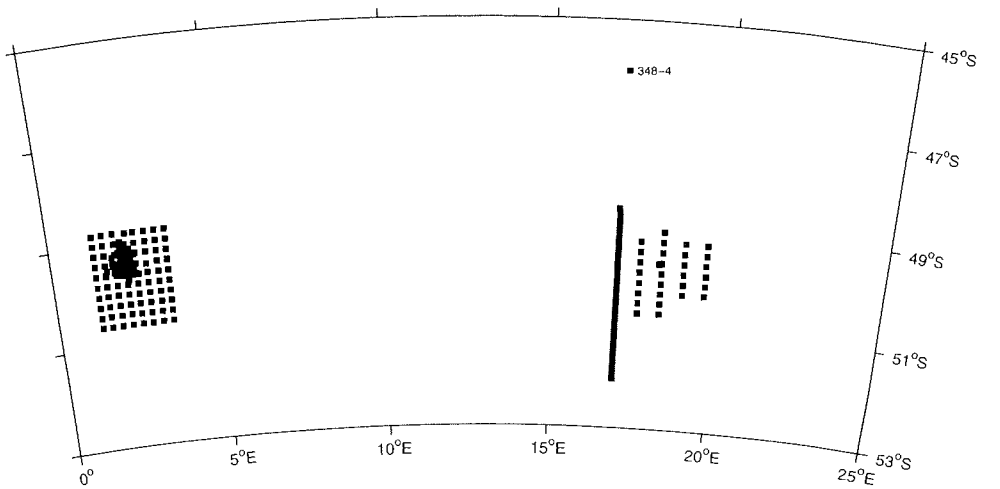


Fig. 3.3.1: Overview of all CTD station positions occupied during the cruise. Station positions grouped in transects and grids are displayed in more detail below in Figures 3.3.2 through 3.3.5.

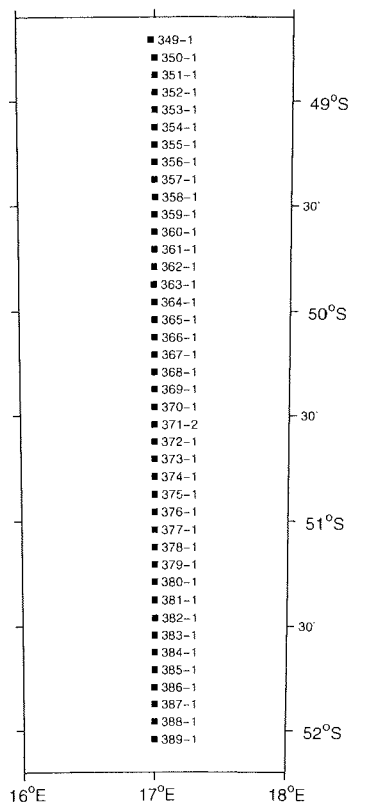


Fig. 3.3.2: Positions of CTD stations along Transect 2.

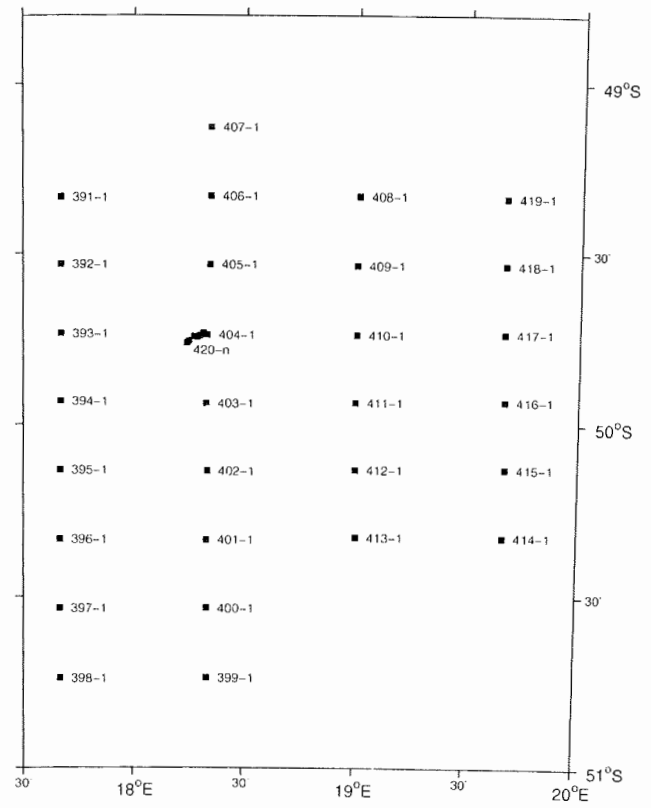


Fig. 3.3.3: Positions of CTD stations covering Eddy-1.

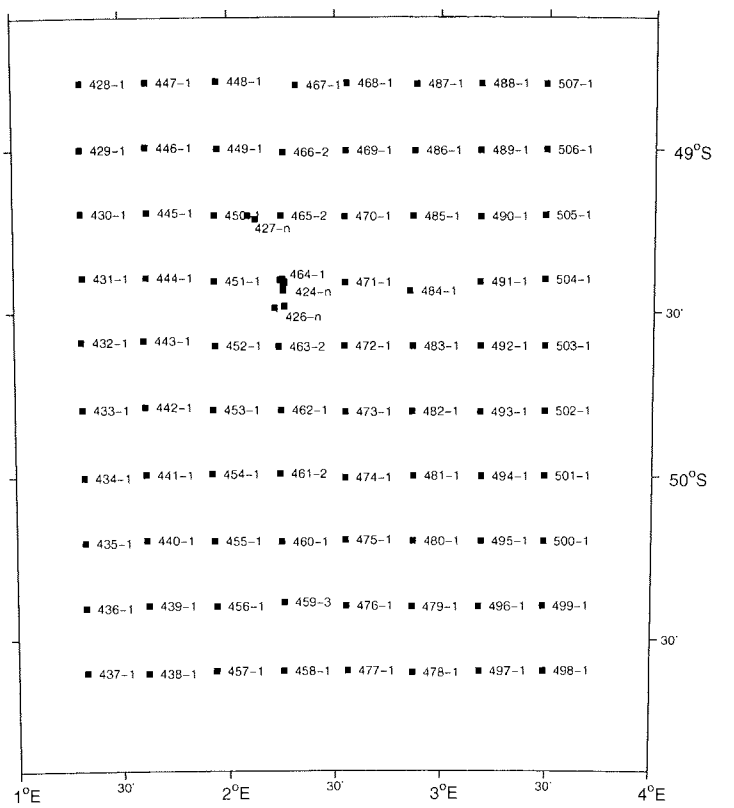


Fig. 3.3.4: Positions of CTD stations covering Eddy-2.

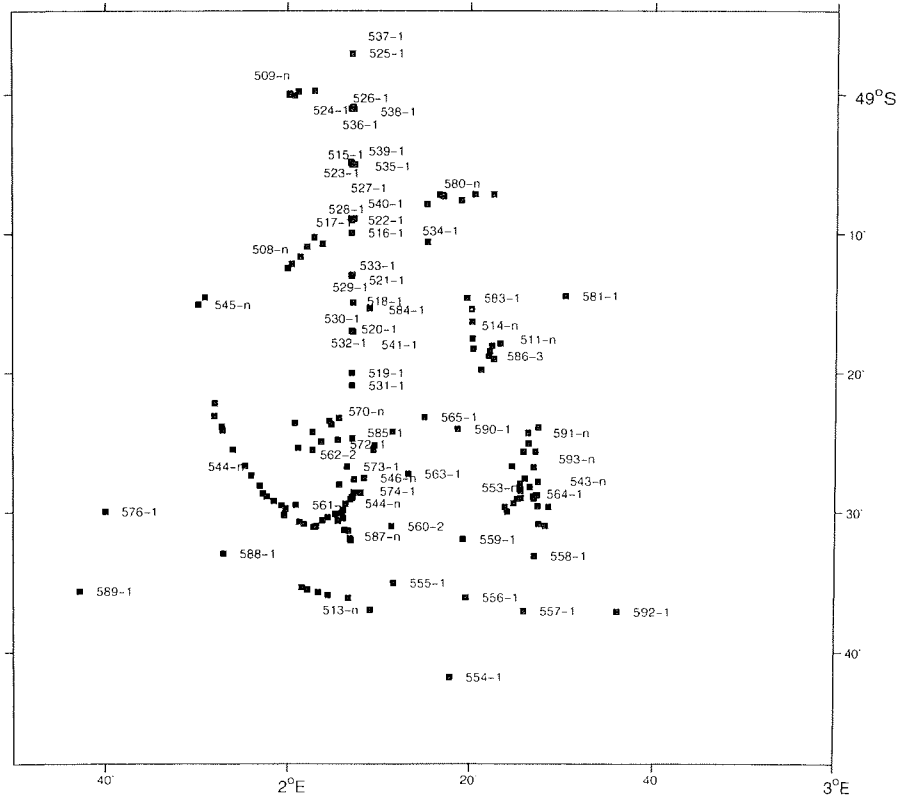


Fig. 3.3.5: Positions of CTD stations occupied during the run of the experiment in Eddy-2.

Tab. 3.3.1: ANTXXI/3 CTD Casts

Station	Date	Time	PositionLat	PositionLon	Water Depth	Profile Depth	Bottle Sampling	Type	Relation	Rem: Initi: na
PS65/348-4	24.01.04	09:09	45° 59.88' S	17° 02.92' E	4606	4644	Deep		Trans 02	348-1
PS65/349-1	25.01.04	11:29	48° 42.40' S	16° 58.30' E	4650	500	Misc		Trans 02	
PS65/350-1	25.01.04	13:07	48° 47.52' S	16° 59.95' E	4492	500	0		Trans 02	
PS65/351-1	25.01.04	14:07	48° 52.48' S	17° 00.05' E	4323	500	0		Trans 02	
PS65/352-1	25.01.04	15:09	48° 57.49' S	17° 00.06' E	4488	500	0		Trans 02	
PS65/353-1	25.01.04	16:15	49° 02.45' S	17° 00.04' E	4600	500	0		Trans 02	
PS65/354-1	25.01.04	17:13	49° 07.46' S	17° 00.07' E	4600	500	0		Trans 02	
PS65/355-1	25.01.04	18:13	49° 12.47' S	17° 00.04' E	4580	500	0		Trans 02	
PS65/356-1	25.01.04	19:12	49° 17.47' S	17° 00.01' E	4600	500	0		Trans 02	
PS65/357-1	25.01.04	20:15	49° 22.46' S	16° 59.95' E	4493	497	0		Trans 02	
PS65/358-1	25.01.04	21:27	49° 27.54' S	17° 00.30' E	4490	499	0		Trans 02	
PS65/359-1	25.01.04	22:34	49° 32.47' S	16° 59.94' E	4489	497	0		Trans 02	
PS65/360-1	25.01.04	23:43	49° 37.46' S	16° 59.94' E		501	0		Trans 02	
PS65/361-1	26.01.04	00:47	49° 42.41' S	17° 00.09' E	4492	500	0		Trans 02	
PS65/362-1	26.01.04	01:47	49° 47.35' S	16° 59.92' E	4492	496	0		Trans 02	
PS65/363-1	26.01.04	02:51	49° 52.44' S	16° 59.76' E	4235	503	0		Trans 02	
PS65/364-1	26.01.04	03:50	49° 57.44' S	16° 59.93' E	4200	500	0		Trans 02	
PS65/365-1	26.01.04	04:50	50° 02.46' S	17° 00.04' E	4169	496	0		Trans 02	
PS65/366-1	26.01.04	05:49	50° 07.47' S	17° 00.14' E	4143	497	0		Trans 02	
PS65/367-1	26.01.04	06:50	50° 12.44' S	17° 00.13' E	3960	500	0		Trans 02	
PS65/368-1	26.01.04	07:53	50° 17.47' S	16° 59.97' E	3645	507	0		Trans 02	
PS65/369-1	26.01.04	09:05	50° 22.42' S	17° 00.05' E	3604	499	0		Trans 02	
PS65/370-1	26.01.04	10:22	50° 27.51' S	17° 00.13' E	3208	502	0		Trans 02	
PS65/371-2	26.01.04	11:36	50° 32.58' S	17° 00.11' E	2578	501	0		Trans 02	
PS65/372-1	26.01.04	12:42	50° 37.49' S	17° 00.05' E	3668	497	0		Trans 02	
PS65/373-1	26.01.04	13:37	50° 42.41' S	17° 00.03' E	3624	500	Tep test		Trans 02	
PS65/374-1	26.01.04	14:35	50° 47.43' S	17° 00.01' E	3535	496	0		Trans 02	
PS65/375-1	26.01.04	15:28	50° 52.45' S	17° 00.12' E	3534	496	0		Trans 02	
PS65/376-1	26.01.04	16:25	50° 57.49' S	17° 00.05' E	3200	502	0		Trans 02	
PS65/377-1	26.01.04	17:23	51° 02.50' S	17° 00.03' E	3150	501	0		Trans 02	
PS65/378-1	26.01.04	18:26	51° 07.49' S	17° 00.07' E	3100	497	0		Trans 02	
PS65/379-1	26.01.04	19:22	51° 12.50' S	17° 00.10' E	3050	500	0		Trans 02	
PS65/380-1	26.01.04	20:19	51° 17.38' S	17° 00.05' E	3100	496	0		Trans 02	
PS65/381-1	26.01.04	21:21	51° 22.48' S	17° 00.11' E	2866	503	0		Trans 02	
PS65/382-1	26.01.04	22:22	51° 27.63' S	17° 00.21' E	2348	503	0		Trans 02	
PS65/383-1	26.01.04	23:21	51° 32.59' S	17° 00.03' E	2435	501	0		Trans 02	
PS65/384-1	27.01.04	00:17	51° 37.40' S	17° 00.02' E	2626	496	0		Trans 02	
PS65/385-1	27.01.04	01:10	51° 42.39' S	17° 00.03' E	2525	495	0		Trans 02	
PS65/386-1	27.01.04	02:06	51° 47.47' S	16° 59.98' E	2424	496	0		Trans 02	
PS65/387-1	27.01.04	02:59	51° 52.41' S	17° 00.03' E	2525	496	0		Trans 02	
PS65/388-1	27.01.04	03:54	51° 57.44' S	17° 00.02' E	2250	496	0		Trans 02	
PS65/389-1	27.01.04	04:48	52° 02.50' S	17° 00.10' E	2200	496	0		Trans 02	
PS65/389-4	27.01.04	06:38	52° 02.31' S	17° 00.61' E	2610	2510	Misc			
PS65/391-1	29.01.04	07:35	49° 20.02' S	17° 40.18' E	4560	496	Misc		Grid 01	
PS65/392-1	29.01.04	09:52	49° 31.87' S	17° 40.14' E	4600	500	0		Grid 01	
PS65/393-1	29.01.04	11:58	49° 43.92' S	17° 40.19' E	4444	495	0		Grid 01	
PS65/394-1	29.01.04	13:56	49° 55.88' S	17° 40.11' E	3223	496	Misc		Grid 01	
PS65/395-1	29.01.04	16:45	50° 07.98' S	17° 40.02' E	3320	503	0		Grid 01	
PS65/396-1	29.01.04	18:28	50° 20.05' S	17° 40.01' E	3320	495	0		Grid 01	
PS65/397-1	29.01.04	20:04	50° 31.99' S	17° 39.94' E	4560	500	0		Grid 01	
PS65/398-1	29.01.04	21:47	50° 44.13' S	17° 40.03' E	4650	495	Misc		Grid 01	
PS65/399-1	30.01.04	01:04	50° 44.17' S	18° 20.09' E	4444	497	0		Grid 01	
PS65/400-1	30.01.04	02:45	50° 32.07' S	18° 20.01' E	3972	497	0		Grid 01	

PS65/401-1	30.01.04	04:27	50° 20.03' S	18° 19.97' E	3972	496	0	Grid 01
PS65/402-1	30.01.04	06:13	50° 08.01' S	18° 20.02' E	3972	502	0	Grid 01
PS65/403-1	30.01.04	07:58	49° 56.01' S	18° 19.97' E	4360	499	0	Grid 01
PS65/404-1	30.01.04	09:51	49° 44.02' S	18° 19.98' E	4680	503	0	Grid 01
PS65/405-1	30.01.04	11:41	49° 31.92' S	18° 20.17' E	4545	501	Misc	Grid 01
PS65/406-1	30.01.04	14:39	49° 19.96' S	18° 20.24' E	4044	495	0	Grid 01
PS65/407-1	30.01.04	16:25	49° 07.96' S	18° 20.25' E	4044	504	0	Grid 01
PS65/408-1	30.01.04	19:30	49° 19.93' S	19° 00.13' E	4500	499	0	Grid 01
PS65/409-1	30.01.04	21:08	49° 32.02' S	19° 00.08' E	4700	497	0	Grid 01
PS65/410-1	30.01.04	22:47	49° 44.11' S	19° 00.07' E	4670	501	0	Grid 01
PS65/411-1	31.01.04	00:33	49° 56.08' S	18° 59.92' E	4567	494	0	Grid 01
PS65/412-1	31.01.04	02:16	50° 07.97' S	19° 00.00' E	4567	500	0	Grid 01
PS65/413-1	31.01.04	04:01	50° 19.75' S	19° 00.00' E	4350	494	0	Grid 01
PS65/414-1	31.01.04	06:50	50° 19.96' S	19° 40.02' E	4500	497	0	Grid 01
PS65/415-1	31.01.04	08:38	50° 07.95' S	19° 40.17' E	4560	502	0	Grid 01
PS65/416-1	31.01.04	10:37	49° 55.95' S	19° 40.07' E	4560	503	0	Grid 01
PS65/417-1	31.01.04	12:24	49° 44.02' S	19° 40.00' E	4444	498	0	Grid 01
PS65/418-1	31.01.04	14:08	49° 32.06' S	19° 39.99' E	4444	497	0	Grid 01
PS65/419-1	31.01.04	15:53	49° 20.07' S	19° 40.01' E	4000	497	0	Grid 01
PS65/420-3	01.02.04	18:05	49° 43.41' S	18° 19.50' E	4600	503	Type I	Centre eddy 1
PS65/420-6	01.02.04	20:02	49° 44.33' S	18° 18.10' E	4680	299	Type II	Centre eddy 1 420-5
PS65/420-8	01.02.04	21:33	49° 44.65' S	18° 17.33' E	4610	97	Type III	Centre eddy 1 420-7
PS65/420-11	01.02.04	22:42	49° 44.48' S	18° 17.01' E	4600	20	Zooplankton	Centre eddy 1 420-9
PS65/420-13	01.02.04	23:28	49° 44.50' S	18° 16.68' E	4650	442	Misc	Centre eddy 1 420-11
PS65/420-17	02.02.04	01:49	49° 44.94' S	18° 15.44' E	4567	995	Thorium	Centre eddy 1 420-15
PS65/420-19	02.02.04	03:29	49° 45.44' S	18° 14.55' E	4567	348	Henjes	Centre eddy 1 420-17
PS65/424-3	11.02.04	18:43	49° 23.99' S	2° 15.07' E	4090	498	Type I	T 0 eddy 2 424-2
PS65/424-8	11.02.04	21:04	49° 24.30' S	2° 15.56' E	4450	201	Type II	T 0 eddy 2
PS65/424-13	11.02.04	23:46	49° 24.43' S	2° 15.92' E	3888	142	Type III	T 0 eddy 2
PS65/424-17	12.02.04	01:25	49° 24.96' S	2° 15.64' E	3888	994	Thorium	T 0 eddy 2
PS65/424-20	12.02.04	03:17	49° 25.53' S	2° 15.46' E	4090	3858	Deep	T 0 eddy 2
PS65/424-22	12.02.04	06:38	49° 25.94' S	2° 15.43' E	4093	363	Henjes	T 0 eddy 2
PS65/426-1	13.02.04	12:27	49° 28.88' S	2° 15.95' E	3993	500	Type I	T 1 In patch
PS65/426-4	13.02.04	14:37	49° 28.82' S	2° 15.87' E	3993	200	Type II	T 1 In patch
PS65/426-7	13.02.04	16:27	49° 29.10' S	2° 13.25' E	3993	448	Klaas	T 1 In patch
PS65/427-1	13.02.04	19:05	49° 12.01' S	2° 04.99' E	3900	496	Type I	T 1 In patch
PS65/427-6	13.02.04	21:14	49° 12.53' S	2° 06.98' E	3670	353	Henjes	T 1 In patch
PS65/428-1	14.02.04	05:45	48° 47.90' S	1° 19.13' E	3850	497	0	Grid 5
PS65/429-1	14.02.04	07:34	48° 59.94' S	1° 19.01' E	3900	497	0	Grid 5
PS65/430-1	14.02.04	09:36	49° 11.88' S	1° 19.01' E	4006	504	0	Grid 5
PS65/431-1	14.02.04	11:47	49° 23.81' S	1° 19.09' E	4004	522	0	Grid 5
PS65/432-1	14.02.04	14:08	49° 35.70' S	1° 19.05' E	3795	499	0	Grid 5
PS65/433-1	14.02.04	16:21	49° 47.96' S	1° 19.02' E	3795	503	0	Grid 5
PS65/434-1	14.02.04	18:27	50° 00.04' S	1° 19.18' E	3690	506	0	Grid 5
PS65/435-1	14.02.04	20:38	50° 12.02' S	1° 19.11' E	4280	501	0	Grid 5
PS65/436-1	14.02.04	22:56	50° 24.10' S	1° 19.12' E	4160	502	0	Grid 5
PS65/437-1	15.02.04	01:08	50° 35.96' S	1° 19.29' E	3443	496	0	Grid 5
PS65/438-1	15.02.04	02:44	50° 36.11' S	1° 36.86' E	3443	493	0	Grid 5
PS65/439-1	15.02.04	04:30	50° 23.85' S	1° 37.30' E	2970	493	0	Grid 5
PS65/440-1	15.02.04	06:07	50° 11.86' S	1° 37.05' E	2970	496	0	Grid 5
PS65/441-1	15.02.04	07:45	49° 59.79' S	1° 37.00' E	3250	495	0	Grid 5
PS65/442-1	15.02.04	09:29	49° 47.63' S	1° 36.89' E	4120	505	0	Grid 5
PS65/443-1	15.02.04	11:17	49° 35.66' S	1° 36.82' E	4080	520	0	Grid 5
PS65/444-1	15.02.04	13:01	49° 23.64' S	1° 37.32' E	3993	3968	Deep	Grid 5
PS65/445-1	15.02.04	16:43	49° 11.81' S	1° 37.18' E	3791	498	0	Grid 5
PS65/446-1	15.02.04	18:18	48° 59.95' S	1° 37.13' E	3791	504	0	Grid 5
PS65/447-1	15.02.04	20:05	48° 47.94' S	1° 37.17' E	3970	508	0	Grid 5
PS65/448-1	15.02.04	21:46	48° 47.75' S	1° 56.30' E	3760	505	0	Grid 5
PS65/449-1	16.02.04	00:10	48° 59.88' S	1° 56.30' E	3883	501	0	Grid 5

PS65/450-1	16.02.04	02:26	49° 11.92' S	1° 56.20' E	3791	504	0	Grid 5
PS65/451-1	16.02.04	04:29	49° 23.94' S	1° 56.04' E	3790	502	Misc	Grid 5
PS65/452-1	16.02.04	06:38	49° 35.92' S	1° 56.09' E	3790	509	Type I	Grid 5
PS65/453-1	16.02.04	09:06	49° 47.97' S	1° 55.91' E	4120	501	0	Grid 5
PS65/454-1	16.02.04	11:25	49° 59.77' S	1° 55.77' E	4020	506	0	Grid 5
PS65/455-1	16.02.04	13:38	50° 11.90' S	1° 56.06' E	3253	512	0	Grid 5
PS65/456-1	16.02.04	15:44	50° 23.94' S	1° 56.28' E	3300	504	0	Grid 5
PS65/457-1	16.02.04	17:47	50° 35.84' S	1° 56.09' E	3500	479	0	Grid 5
PS65/458-1	16.02.04	19:24	50° 35.92' S	2° 15.17' E	3500	501	0	Grid 5
PS65/459-3	16.02.04	23:14	50° 23.34' S	2° 15.43' E	3870	505	0	Grid 5
PS65/460-1	17.02.04	00:51	50° 11.98' S	2° 15.10' E	3113	3062	Deep	Grid 5
PS65/461-2	17.02.04	05:08	49° 59.63' S	2° 14.57' E	3400	495	0	Grid 5
PS65/462-1	17.02.04	06:50	49° 48.03' S	2° 15.00' E	3800	500	Misc	Grid 5
PS65/463-2	17.02.04	10:41	49° 36.20' S	2° 14.48' E	3650	506	0	Grid 5
PS65/464-1	17.02.04	12:32	49° 24.02' S	2° 14.91' E	3883	497	Type I	Grid 5
PS65/465-2	17.02.04	16:16	49° 12.08' S	2° 14.93' E	4000	499	0	Grid 5
PS65/466-2	17.02.04	19:08	49° 00.37' S	2° 15.34' E	4000	490	Type I	Grid 5
PS65/467-1	17.02.04	21:23	48° 47.98' S	2° 15.26' E	4118	4168	Deep	Grid 5
PS65/468-1	18.02.04	00:47	48° 47.98' S	2° 33.30' E	4053	502	0	Grid 5
PS65/469-1	18.02.04	02:36	49° 00.06' S	2° 33.18' E	4114	497	0	Grid 5
PS65/470-1	18.02.04	04:16	49° 12.03' S	2° 32.98' E	4000	501	Type I	Grid 5
PS65/471-1	18.02.04	05:58	49° 24.08' S	2° 32.99' E	3900	501	Misc	Grid 5
PS65/472-1	18.02.04	07:40	49° 35.96' S	2° 32.96' E	4350	500	Type I	Grid 5
PS65/473-1	18.02.04	09:41	49° 48.09' S	2° 32.99' E	4120	506	0	Grid 5
PS65/474-1	18.02.04	11:25	50° 00.10' S	2° 32.90' E	4030	511	Type I	Grid 5
PS65/475-1	18.02.04	13:27	50° 11.85' S	2° 32.92' E	3333	497	0	Grid 5
PS65/476-1	18.02.04	15:18	50° 23.89' S	2° 33.02' E	3333	499	0	Grid 5
PS65/477-1	18.02.04	17:08	50° 35.88' S	2° 33.18' E	3000	501	0	Grid 5
PS65/478-1	18.02.04	18:42	50° 35.97' S	2° 52.05' E	2700	499	0	Grid 5
PS65/479-1	18.02.04	20:24	50° 24.01' S	2° 51.94' E	4070	500	0	Grid 5
PS65/480-1	18.02.04	22:10	50° 11.95' S	2° 52.05' E	3870	499	0	Grid 5
PS65/481-1	18.02.04	23:51	49° 59.99' S	2° 52.07' E	3333	499	0	Grid 5
PS65/482-1	19.02.04	01:38	49° 48.08' S	2° 52.03' E	3443	501	Zooplankton	Grid 5
PS65/483-1	19.02.04	05:11	49° 36.09' S	2° 51.97' E	3860	500	0	Grid 5
PS65/484-1	19.02.04	07:01	49° 24.05' S	2° 51.94' E	3670	3737	Deep	Grid 5
PS65/485-1	19.02.04	11:25	49° 12.04' S	2° 52.06' E	3780	504	0	Grid 5
PS65/486-1	19.02.04	13:17	49° 00.13' S	2° 52.17' E	4321	501	0	Grid 5
PS65/487-1	19.02.04	14:58	48° 48.12' S	2° 52.37' E	4321	505	0	Grid 5
PS65/488-1	19.02.04	16:29	48° 48.03' S	3° 11.07' E	4321	497	0	Grid 5
PS65/489-1	19.02.04	18:03	48° 59.95' S	3° 11.01' E	3200	496	0	Grid 5
PS65/490-1	19.02.04	19:30	49° 12.04' S	3° 10.97' E	2900	496	0	Grid 5
PS65/491-1	19.02.04	20:57	49° 24.06' S	3° 10.93' E	4090	506	0	Grid 5
PS65/492-1	19.02.04	22:24	49° 36.05' S	3° 11.07' E	4370	505	0	Grid 5
PS65/493-1	19.02.04	23:54	49° 48.03' S	3° 11.04' E	3456	505	0	Grid 5
PS65/494-1	20.02.04	01:28	49° 59.99' S	3° 11.10' E	3456	503	0	Grid 5
PS65/495-1	20.02.04	03:01	50° 11.91' S	3° 11.09' E	3333	504	0	Grid 5
PS65/496-1	20.02.04	04:36	50° 24.00' S	3° 10.94' E	3553	495	0	Grid 5
PS65/497-1	20.02.04	06:14	50° 35.93' S	3° 11.03' E	3550	500	0	Grid 5
PS65/498-1	20.02.04	07:43	50° 35.94' S	3° 29.05' E	4230	499	0	Grid 5
PS65/499-1	20.02.04	09:15	50° 23.97' S	3° 29.01' E	4230	500	0	Grid 5
PS65/500-1	20.02.04	10:53	50° 11.97' S	3° 29.11' E	4210	502	0	Grid 5
PS65/501-1	20.02.04	12:31	49° 60.00' S	3° 29.18' E	2323	500	0	Grid 5
PS65/502-1	20.02.04	14:15	49° 48.12' S	3° 29.05' E	3210	501	0	Grid 5
PS65/503-1	20.02.04	16:00	49° 36.12' S	3° 29.16' E	3213	498	0	Grid 5
PS65/504-1	20.02.04	17:40	49° 24.00' S	3° 28.94' E	3824	502	0	Grid 5
PS65/505-1	20.02.04	19:21	49° 12.06' S	3° 28.97' E	2900	498	0	Grid 5
PS65/506-1	20.02.04	20:57	49° 00.02' S	3° 29.14' E	4210	502	0	Grid 5
PS65/507-1	20.02.04	22:35	48° 48.01' S	3° 29.08' E	4120	504	0	Grid 5
PS65/508-2	22.02.04	07:53	49° 12.14' S	2° 00.44' E	3765	510	Type I	In patch

PS65/508-5	22.02.04	11:03	49° 10.90' S	2° 02.12' E	3650	202	Type III	In patch
PS65/508-11	22.02.04	14:03	49° 10.26' S	2° 02.93' E	3760	17	Zooplankton	In patch
PS65/508-16	22.02.04	16:36	49° 10.70' S	2° 03.83' E	3870	993	Type III	In patch
PS65/508-18	22.02.04	20:21	49° 12.44' S	2° 00.01' E	3650	447	Klaas	In patch
PS65/508-22	22.02.04	22:10	49° 11.64' S	2° 01.35' E	3650	346	Henjes	In patch
PS65/509-1	23.02.04	06:02	49° 00.03' S	2° 00.13' E	3800	500	Type I	Out patch
PS65/509-4	23.02.04	07:42	48° 59.96' S	2° 00.19' E	3800	198	Type II	Out patch
PS65/509-7	23.02.04	09:30	48° 59.80' S	2° 01.18' E	3870	50	Type III	Out patch
PS65/509-13	23.02.04	11:44	49° 00.09' S	2° 00.78' E	3765	1004	Thorium	Out patch
PS65/509-16	23.02.04	13:58	48° 59.76' S	2° 02.96' E	3765	349	Henjes	Out patch
PS65/511-1	24.02.04	18:47	49° 18.06' S	2° 22.33' E	3950	499	Type I	In patch ??
PS65/511-5	24.02.04	20:04	49° 18.47' S	2° 22.11' E	4120	199	Type II	In patch ??
PS65/511-9	24.02.04	21:22	49° 19.01' S	2° 22.58' E	3650	994	Thorium	In patch ??
PS65/511-12	24.02.04	23:29	49° 17.89' S	2° 23.25' E	3760	349	Henjes	In patch ??
PS65/513-3	27.02.04	18:57	49° 36.97' S	2° 09.09' E	3860	498	Type I	In patch
PS65/513-5	27.02.04	20:53	49° 36.11' S	2° 06.67' E	3870	199	Type II	In patch
PS65/513-9	27.02.04	23:21	49° 35.89' S	2° 04.45' E	3650	50	Type III	In patch
PS65/513-12	28.02.04	00:51	49° 35.68' S	2° 03.39' E	3876	1003	Thorium	In patch
PS65/513-16	28.02.04	02:36	49° 35.49' S	2° 02.19' E	3876	501	Misc	In patch
PS65/513-18	28.02.04	03:39	49° 35.33' S	2° 01.56' E	3876	350	Henjes	In patch
PS65/514-10	29.02.04	21:07	49° 17.55' S	2° 20.23' E	3650	12	Type III	Out patch
PS65/514-13	29.02.04	22:01	49° 18.26' S	2° 20.31' E	3550	990	Thorium	Out patch
PS65/514-18	29.02.04	23:53	49° 19.78' S	2° 21.18' E	3883	342	Henjes	Out patch
PS65/514-2	29.02.04	17:53	49° 15.42' S	2° 20.14' E	3824	499	Type I	Out patch
PS65/514-6	29.02.04	19:11	49° 16.33' S	2° 20.19' E	3824	197	Type II	Out patch
PS65/515-1	01.03.04	15:13	49° 05.05' S	2° 07.36' E	3883	503	Misc	Grid 11
PS65/516-1	01.03.04	16:38	49° 09.94' S	2° 06.98' E	4000	492	Misc	Grid 11
PS65/517-1	01.03.04	17:50	49° 10.57' S	2° 15.33' E	4000	497	Misc	Grid 11
PS65/518-1	01.03.04	19:34	49° 14.93' S	2° 07.16' E	3760	496	Misc	Grid 11
PS65/519-1	01.03.04	21:11	49° 20.02' S	2° 07.03' E	3560	510	Misc	Grid 11
PS65/520-1	01.03.04	22:39	49° 17.04' S	2° 07.15' E	3450	497	Misc	Grid 11
PS65/521-1	02.03.04	16:27	49° 12.93' S	2° 07.05' E	4000	497	Misc	Grid 11
PS65/522-1	02.03.04	17:30	49° 09.03' S	2° 06.97' E	3804	497	Type I	Grid 11
PS65/523-1	02.03.04	18:49	49° 05.07' S	2° 07.06' E	4050	501	Misc	Grid 11
PS65/524-1	02.03.04	19:49	49° 01.05' S	2° 06.96' E	3560	495	Misc	Grid 11
PS65/525-1	02.03.04	21:08	48° 57.07' S	2° 07.07' E	3760	497	Misc	Grid 11
PS65/526-1	02.03.04	22:14	49° 01.09' S	2° 07.27' E	3650	497	Misc	Grid 11
PS65/527-1	02.03.04	23:22	49° 05.05' S	2° 07.05' E	3450	496	Misc	Grid 11
PS65/528-1	03.03.04	00:34	49° 08.92' S	2° 07.33' E	3456	501	Type I	Grid 11
PS65/529-1	03.03.04	01:55	49° 13.02' S	2° 07.01' E	3456	499	Misc	Grid 11
PS65/530-1	03.03.04	03:06	49° 16.96' S	2° 07.00' E	3456	504	Misc	Grid 11
PS65/531-1	03.03.04	04:19	49° 20.92' S	2° 07.07' E	4000	499	Misc	Grid 11
PS65/532-1	03.03.04	05:18	49° 16.95' S	2° 07.01' E	4000	497	Misc	Grid 11
PS65/533-1	03.03.04	06:16	49° 12.96' S	2° 06.96' E	4000	500	Misc	Grid 11
PS65/534-1	03.03.04	07:23	49° 09.00' S	2° 07.02' E	3900	498	Type I	Grid 11
PS65/535-1	03.03.04	08:40	49° 04.97' S	2° 06.95' E	3760	502	Misc	Grid 11
PS65/536-1	03.03.04	10:09	49° 00.92' S	2° 07.16' E	3660	504	Misc	Grid 11
PS65/537-1	03.03.04	11:43	48° 57.12' S	2° 07.08' E	3456	502	Misc	Grid 11
PS65/538-1	03.03.04	13:03	49° 00.97' S	2° 07.08' E	3456	501	Misc	Grid 11
PS65/539-1	03.03.04	14:24	49° 04.88' S	2° 06.88' E	3456	502	Misc	Grid 11
PS65/540-1	03.03.04	15:45	49° 08.93' S	2° 06.92' E	3456	503	Type I	Grid 11
PS65/541-1	03.03.04	17:33	49° 16.97' S	2° 06.97' E	3780	498	Misc	Grid 11
PS65/543-1	04.03.04	01:45	49° 25.65' S	2° 27.14' E	3456	16	Zooplankon	In patch
PS65/543-10	04.03.04	06:54	49° 28.76' S	2° 27.32' E	3860	508	Type I	In patch
PS65/543-15	04.03.04	10:40	49° 30.81' S	2° 27.46' E	3560	497	Type II	In patch
PS65/543-18	04.03.04	13:27	49° 30.94' S	2° 28.21' E	3456	19	Type III	In patch
PS65/543-5	04.03.04	03:26	49° 26.80' S	2° 26.90' E	3456	348	Henjes	In patch
PS65/543-8	04.03.04	05:14	49° 27.82' S	2° 27.39' E	3860	990	Thorium	In patch
PS65/544-3	05.03.04	16:06	49° 28.59' S	2° 07.27' E	3456	503	Type B	In patch

PS65/544-5	05.03.04	18:04	49° 28.96' S	2° 07.16' E	3900	100	Type A	In patch
PS65/544-6	05.03.04	18:51	49° 28.92' S	2° 07.10' E	3900	349	Henjes	In patch
PS65/544-7	05.03.04	20:20	49° 29.06' S	2° 06.88' E	3660	98	Type B	In patch
PS65/544-9	05.03.04	22:09	49° 29.40' S	2° 06.35' E	3660	149	Type A	In patch
PS65/544-10	05.03.04	23:33	49° 29.84' S	2° 06.11' E	3456	350	Henjes	In patch
PS65/544-11	06.03.04	02:02	49° 30.14' S	2° 05.25' E	3456	100	Type B	In patch
PS65/544-12	06.03.04	04:30	49° 30.37' S	2° 04.42' E	3900	349	Henjes	In patch
PS65/544-14	06.03.04	06:00	49° 30.57' S	2° 03.82' E	3900	153	Type A	In patch
PS65/544-15	06.03.04	08:03	49° 30.97' S	2° 03.14' E	3670	100	Type B	In patch
PS65/544-16	06.03.04	08:37	49° 31.04' S	2° 03.01' E	3450	353	Henjes	In patch
PS65/544-18	06.03.04	10:13	49° 31.03' S	2° 02.83' E	3450	502	Type A	In patch
PS65/544-20	06.03.04	12:26	49° 30.82' S	2° 01.82' E	3456	100	Type B	In patch
PS65/544-24	06.03.04	14:22	49° 30.67' S	2° 01.27' E	3345	151	Type A	In patch
PS65/544-26	06.03.04	16:11	49° 30.18' S	1° 59.63' E	3900	249	Type B	In patch
PS65/544-29	06.03.04	18:02	49° 29.72' S	1° 59.78' E	3900	147	Type A	In patch
PS65/544-30	06.03.04	18:49	49° 29.50' S	1° 59.33' E	3456	371	Henjes	In patch
PS65/544-32	06.03.04	20:06	49° 29.19' S	1° 58.48' E	3880	98	Type B	In patch
PS65/544-35	06.03.04	22:04	49° 28.86' S	1° 57.72' E	3770	148	Type A	In patch
PS65/544-39	06.03.04	23:32	49° 28.65' S	1° 57.30' E	3456	347	Henjes	In patch
PS65/544-42	07.03.04	02:06	49° 28.09' S	1° 56.95' E	3456	150	Type A	In patch
PS65/544-46	07.03.04	04:33	49° 27.38' S	1° 56.03' E	3900	366	Henjes	In patch
PS65/544-48	07.03.04	06:09	49° 26.68' S	1° 55.36' E	3900	148	Type A	In patch
PS65/544-53	07.03.04	10:34	49° 25.52' S	1° 54.01' E	3660	502	Type I A	In patch
PS65/544-56	07.03.04	14:32	49° 24.15' S	1° 52.86' E	3456	151	Type A	In patch
PS65/544-58	07.03.04	15:27	49° 23.87' S	1° 52.80' E	3456	354	Henjes	In patch
PS65/544-60	07.03.04	18:27	49° 23.11' S	1° 51.96' E	3567	998	Thorium	In patch
PS65/544-63	07.03.04	20:21	49° 22.20' S	1° 52.02' E	4014	3983	Deep	In patch
PS65/545-1	08.03.04	06:30	49° 15.06' S	1° 50.20' E	3700	500	Type I A	In patch
PS65/545-4	08.03.04	09:47	49° 14.55' S	1° 50.95' E		19	Type III	In patch
PS65/546-2	09.03.04	12:41	49° 24.18' S	2° 11.65' E	3456	501	Type I	In patch
PS65/546-5	09.03.04	15:31	49° 25.20' S	2° 09.57' E	3456	201	Type II	In patch
PS65/546-7	09.03.04	16:35	49° 25.48' S	2° 09.43' E	3900	497	Type III	In patch
PS65/546-14	09.03.04	20:34	49° 27.44' S	2° 08.56' E	3780	993	Thorium	In patch
PS65/546-19	09.03.04	23:22	49° 27.65' S	2° 07.36' E	3870	347	Henjes	In patch
PS65/546-22	10.03.04	01:15	49° 27.98' S	2° 06.30' E	3888	3864	Deep	In patch
PS65/553-3	11.03.04	19:17	49° 27.85' S	2° 25.34' E	3560	497	Type I	In patch
PS65/553-5	11.03.04	21:07	49° 28.43' S	2° 25.49' E	3670	198	Type II	In patch
PS65/553-9	11.03.04	22:50	49° 28.96' S	2° 25.14' E	3560	238	Type III	In patch
PS65/553-10	11.03.04	23:51	49° 29.24' S	2° 24.98' E	3939	1005	Thorium	In patch
PS65/553-11	12.03.04	01:33	49° 29.89' S	2° 24.12' E	3939	350	Henjes	In patch
PS65/553-12	12.03.04	03:08	49° 29.54' S	2° 23.83' E	3939	552	Misc	In patch
PS65/554-1	12.03.04	12:17	49° 41.68' S	2° 17.93' E	3883	505	Misc	Grid 18
PS65/555-1	12.03.04	13:46	49° 34.94' S	2° 11.86' E	3993	503	Misc	Grid 18
PS65/556-1	12.03.04	14:58	49° 36.02' S	2° 19.54' E	3993	503	Misc	Grid 18
PS65/557-1	12.03.04	16:04	49° 36.97' S	2° 26.00' E	3993	497	Misc	Grid 18
PS65/558-1	12.03.04	17:10	49° 32.98' S	2° 26.88' E	3898	507	Misc	Grid 18
PS65/559-1	12.03.04	18:31	49° 31.92' S	2° 19.39' E	3900	735	Misc	Grid 18
PS65/560-2	12.03.04	20:52	49° 30.99' S	2° 11.53' E	3670	993	Misc	Grid 18
PS65/561-1	12.03.04	22:40	49° 29.53' S	2° 01.00' E	3770	497	Misc	Grid 18
PS65/562-2	13.03.04	00:23	49° 25.34' S	2° 01.37' E	3883	1005	Misc	Grid 18
PS65/563-1	13.03.04	02:18	49° 27.16' S	2° 13.46' E	3883	1004	Misc	Grid 18
PS65/564-1	13.03.04	04:16	49° 28.99' S	2° 25.57' E	3883	998	Misc	Grid 18
PS65/565-1	13.03.04	06:22	49° 23.26' S	2° 15.03' E	3900	995	Misc	Grid 18
PS65/570-2	14.03.04	02:17	49° 25.74' S	2° 03.17' E	3927	3898	Deep	Grid 20
PS65/570-4	14.03.04	05:50	49° 24.97' S	2° 03.74' E	3950	497	Type I	Grid 20
PS65/570-7	14.03.04	07:56	49° 24.28' S	2° 02.78' E	3950	198	Type II	Grid 20
PS65/570-9	14.03.04	09:25	49° 23.71' S	2° 00.93' E	3870	401	Type III	Grid 20
PS65/570-11	14.03.04	10:39	49° 23.76' S	2° 04.85' E	3670	992	Thorium	Grid 20
PS65/570-14	14.03.04	12:19	49° 23.50' S	2° 04.55' E	3883	552	Henjes	Grid 20

54

PS65/570-15	14.03.04	14:33	49° 23.37' S	2° 05.66' E	3883	754	Klaas	Grid 20		
PS65/572-1	14.03.04	16:15	49° 24.89' S	2° 05.44' E	3900	993	Misc	Grid 20	571-01	
PS65/573-1	14.03.04	17:29	49° 26.74' S	2° 06.60' E	3900	1011	Misc	Grid 20	572-01	
PS65/574-1	14.03.04	18:44	49° 28.55' S	2° 08.03' E	3900	994	Misc	Grid 20		
PS65/576-1	14.03.04	22:44	49° 29.95' S	1° 40.01' E	3870	20	Zooplankton	Out patch		
PS65/580-2	16.03.04	02:28	49° 07.88' S	2° 15.21' E	3883	501	Type I	In patch		
PS65/580-6	16.03.04	05:05	49° 07.27' S	2° 16.90' E	3900	238	Type II	In patch		
PS65/580-8	16.03.04	06:28	49° 07.24' S	2° 16.64' E	3900	20	Type III	In patch		
PS65/580-10	16.03.04	07:27	49° 07.29' S	2° 17.00' E	3780	993	Thorium	In patch		
PS65/580-12	16.03.04	09:48	49° 07.53' S	2° 18.73' E	3660	auf 549	Henjes	In patch		
PS65/580-14	16.03.04	12:16	49° 07.19' S	2° 20.35' E	3883	499	Klaas	In patch		
PS65/580-18	16.03.04	14:11	49° 06.94' S	2° 22.04' E	4033	4012	Deep	In patch		
PS65/581-1	16.03.04	18:12	49° 13.65' S	2° 29.91' E	3961	3920	Misc	Deep CTD grid		
PS65/583-1	17.03.04	00:08	49° 14.61' S	2° 19.63' E	3997	3959	Misc	Deep CTD grid		
PS65/584-1	17.03.04	03:47	49° 15.84' S	2° 09.05' E	3932	3911	Misc	Deep CTD grid		
PS65/585-1	17.03.04	07:34	49° 24.94' S	2° 07.02' E	4006	3988	Misc	Deep CTD grid		
PS65/586-3	17.03.04	14:11	49° 18.72' S	2° 21.98' E	3987	1510	Misc	In patch		
PS65/587-1	17.03.04	17:53	49° 31.88' S	2° 06.83' E	3950	498	Type I	Out patch		
PS65/587-3	17.03.04	19:09	49° 31.38' S	2° 06.65' E	3950	199	Type II	Out patch		
PS65/587-5	17.03.04	21:44	49° 32.01' S	2° 06.97' E	4000	19	Type III	Out patch		
PS65/587-10	17.03.04	23:41	49° 31.32' S	2° 06.35' E	3987	1007	Thorium	Out patch		
PS65/587-14	18.03.04	01:33	49° 30.67' S	2° 05.65' E	3883	552	Henjes	Out patch		
PS65/587-15	18.03.04	03:35	49° 30.35' S	2° 06.22' E	3950	755	Klaas	Out patch		
PS65/587-16	18.03.04	05:07	49° 30.23' S	2° 05.86' E	3930	3897	Deep	Out patch		
PS65/588-1	18.03.04	09:25	49° 32.98' S	1° 53.03' E	3780	504	Misc	Polar Front		
PS65/589-1	18.03.04	17:26	49° 35.78' S	1° 37.33' E	3884	499	Misc	Polar Front		
PS65/590-1	18.03.04	21:04	49° 23.80' S	2° 18.24' E	3823	3711	Misc	Eddy center		
PS65/591-1	19.03.04	06:33	49° 23.91' S	2° 27.29' E	3900	496	Type I	Out patch		
PS65/591-3	19.03.04	08:00	49° 24.31' S	2° 26.31' E	3880	196	Type II	Out patch		
PS65/591-5	19.03.04	09:22	49° 25.04' S	2° 26.40' E	3660	17	Type III	Out patch		
PS65/591-7	19.03.04	10:31	49° 25.54' S	2° 25.86' E	3450	500	Klaas	Out patch		
PS65/591-11	19.03.04	13:48	49° 26.27' S	2° 24.81' E	3941	3904	Deep	Out patch		
PS65/592-1	19.03.04	19:50	49° 36.99' S	2° 36.12' E	3760	494	Misc			
PS65/593-3	19.03.04	23:18	49° 27.51' S	2° 25.99' E	3660	494	Type I	In patch		
PS65/593-6	20.03.04	00:51	49° 28.11' S	2° 26.33' E	3456	998	Thorium	In patch		
PS65/593-9	20.03.04	03:05	49° 28.74' S	2° 27.16' E	3456	554	Henjes	In patch		
PS65/593-12	20.03.04	05:29	49° 28.71' S	2° 27.12' E	3900	1001	Thorium 2e	In patch		
PS65/593-14	20.03.04	08:06	49° 28.73' S	2° 27.38' E	3860	3829	Deep	In patch		
PS65/593-16	20.03.04	11:55	49° 28.85' S	2° 26.87' E	3883	199	Dieter	In patch		
PS65/593-17	20.03.04	12:43	49° 29.06' S	2° 27.53' E	3846	3800	Deep	In patch		
PS65/593-18	20.03.04	16:29	49° 29.52' S	2° 28.42' E	3842	1501	Misc	In patch		

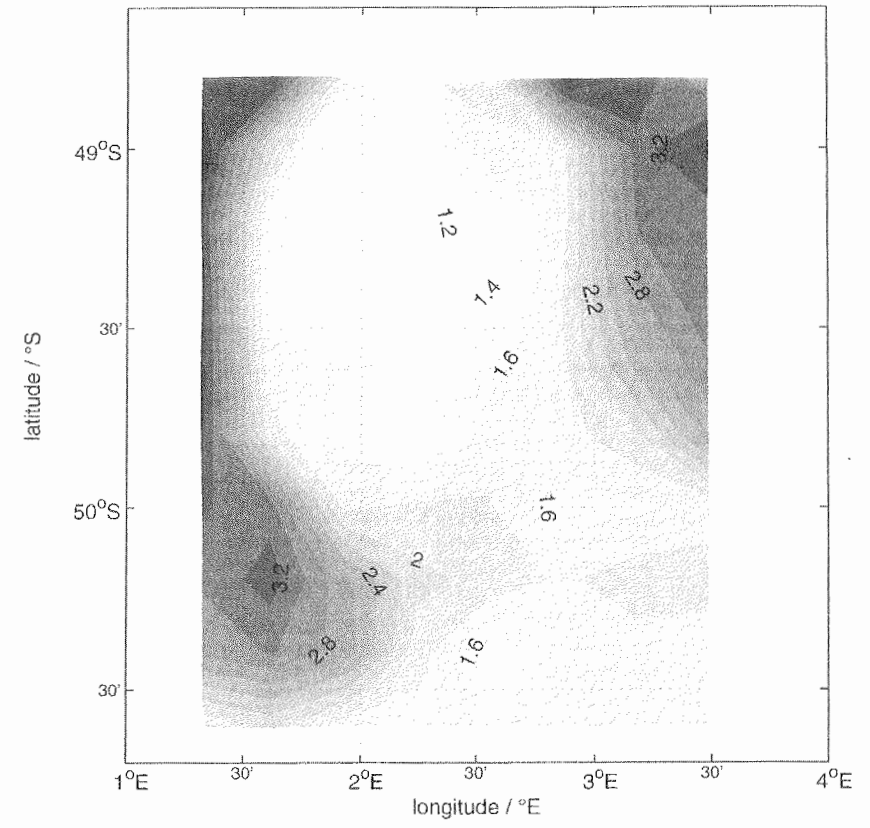


Fig. 3.3.6: Distribution of potential temperature at 200 m depth, the depth of the core of the cold Winter Water, as derived from the regularly spaced CTD stations of Grid 5. This temperature distribution correlates with that of currents shown in Fig. 3.1.1.

EIFEX inpatch versus outpatch stations

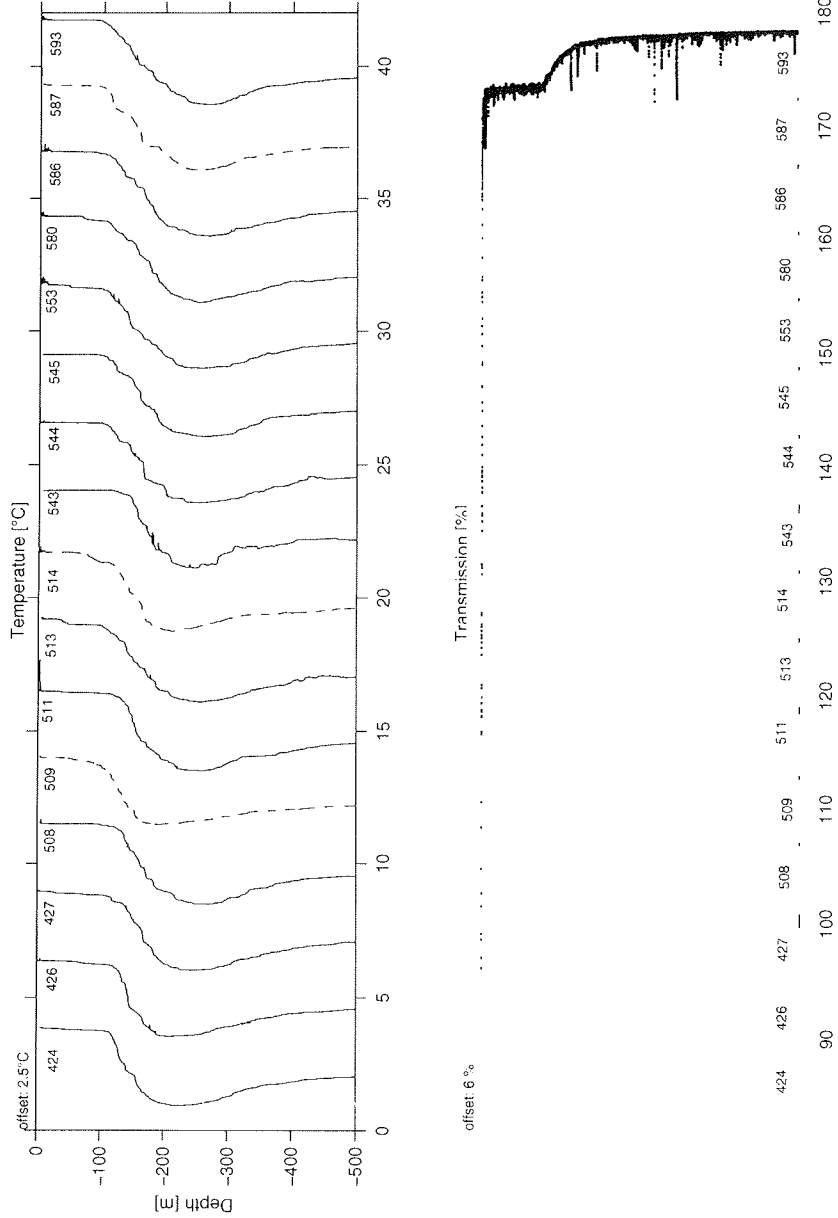


Fig. 3.3.7: CTD profiles of temperature and light transmission taken over the duration of the experiment in Eddy-2. Profiles plotted as continuous lines in the upper panel were taken inside the fertilized patch, dashed outside of the patch. The temperature profiles indicate that the mixed layer often extended down to 100 m depth. The decrease of light transmission in the mixed layer corresponds to the increase of the phytoplankton concentration that resulted from fertilization with iron. The increase of scatter in transmission below the mixed layer towards the end of the experiment indicates sinking particles.

3.4 Drift Buoys

V.Strass, B. Cisewski (AWI), H. Leach (Univ. Liverpool) and M. Thomas (TU HH)

Essential for conducting a Lagrangian experiment like EIFEX was to monitor continuously the motion of the fertilized patch. For that purpose buoy rigs, drogued at roughly mid-depth of the mixed layer, were used.

The rigs consisted of a surface spar buoy (manufactured by Fa. Behrens, Hamburg) that was equipped by Denkmanufaktur GmbH, Großenkneten, with 2 GPS receivers to record their geographic position. The GPS position was transmitted by radio (GPS/Radio module manufactured by Hydrosphere UK Ltd) as well as via satellite using ARGOS (GPS/ARGOS module from Denkmanufaktur GmbH). While the radio-transmitted position was sent and received nominally at 10 minute intervals by the ship-borne receiver station (also from Hydrosphere UK Ltd) when within a radius of a few nautical miles around the ship, ARGOS was used to get the buoy positions at irregular intervals of a few hours when outside the radio range. The raw ARGOS messages were recorded on board using the Terascan satellite receiving system; validated ARGOS positions were sent to the ship via email by OPTIMARE Sensorsysteme AG, Bremerhaven.

The surface buoy was connected to the drogue by a strong but elastic line in order to damp tension peaks and to allow the buoy to better follow the motion of the surface waves in high seas. The elastic line was made according to our specifications by Lippmann Tauwerk GmbH, Hamburg. The drogues, of basically cylindrical shape, 8 m long and 1.2 m wide, were made from heavy duty net garment according to our design (Pat.-Nr. DE 10149025 C1) by Engel-Netze, Bremerhaven.

Treibbojen-Rig „Bungee-Buoy“

AWI
Strass, Cisewski & Schütt

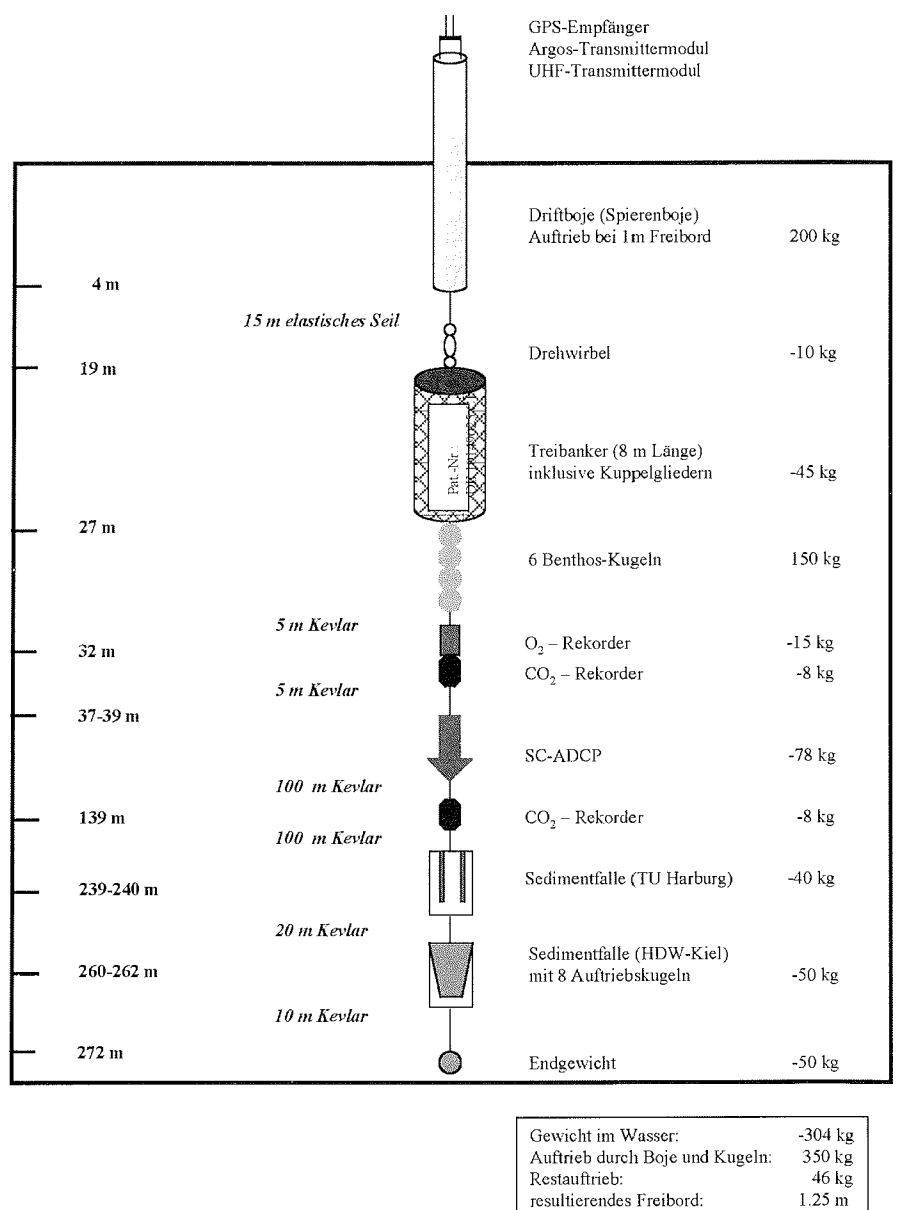


Fig. 3.4.1: Schematic drawing of the drift buoy rig.

From the 24th of February onwards, during drifts 05, 07 and 08 (see Table 3.4.1) until the end of the experiment, the buoys also carried a scientific payload. The payload consisted of one downward looking ADCP (RDI WH LongRanger), one Oxygen and two Carbon Dioxide Recorders (owned by R. Bellerby), one Sediment Trap type NTTA (from G. Gust and M. Thomas) and one Sediment Trap of the Kiel type (owned by U. Bathmann).

Tab. 3.4.1: Buoy Deployments

Name	Buoy ID	Start	Start	Start	End	End	End	Start	End	Notes
		dd.mm.yy	hh:mm	jday.dec	dd.mm.yy	hh:mm	jday.dec	stn	stn	
ARGOS										
drift01	8054	01/02/04	17:44	32,73889	03/02/04	08:09	34,33958			Eddy1
drift02	8054	11/02/04	19:00	42,79167	12/02/04	09:15	43,38542			Eddy2
drift03	9355	12/02/04	13:12	43,55000	24/02/04	14:27	55,60208			Eddy2
drift04	9354	22/02/04	08:51	53,36875	22/02/04	18:12	53,75833			Eddy2
drift05	9355	24/02/04	17:38	55,73472	04/03/04	08:25	64,35069	511ip	543ip	Eddy2
drift06	9354	04/03/04	09:51	64,41042	04/03/04	15:48	64,65833	543ip	543ip	Eddy2
drift07	9355	05/03/04	14:20	65,59722	11/03/04	08:30	71,35417	544ip48h	553	Eddy2
drift08	9355	11/03/04	18:29	71,77013	19/03/04	18:30	79,77083	553ip	592ip	Eddy2

The performance of the buoy rigs was rather good. Despite the passage of several storms and the rough seas, they followed the eddy circulation quite well (Figure 3.4.2) without obvious adrift by the wind. They also proved rather rugged in that no losses of drogues or instruments occurred during an overall drift time of 39 days. Unsatisfactory, however, was the recording of the buoy's GPS position and its transmission via radio and ARGOS. The likely reason of this problem was that the antennae frequently got drowned in the high seas.

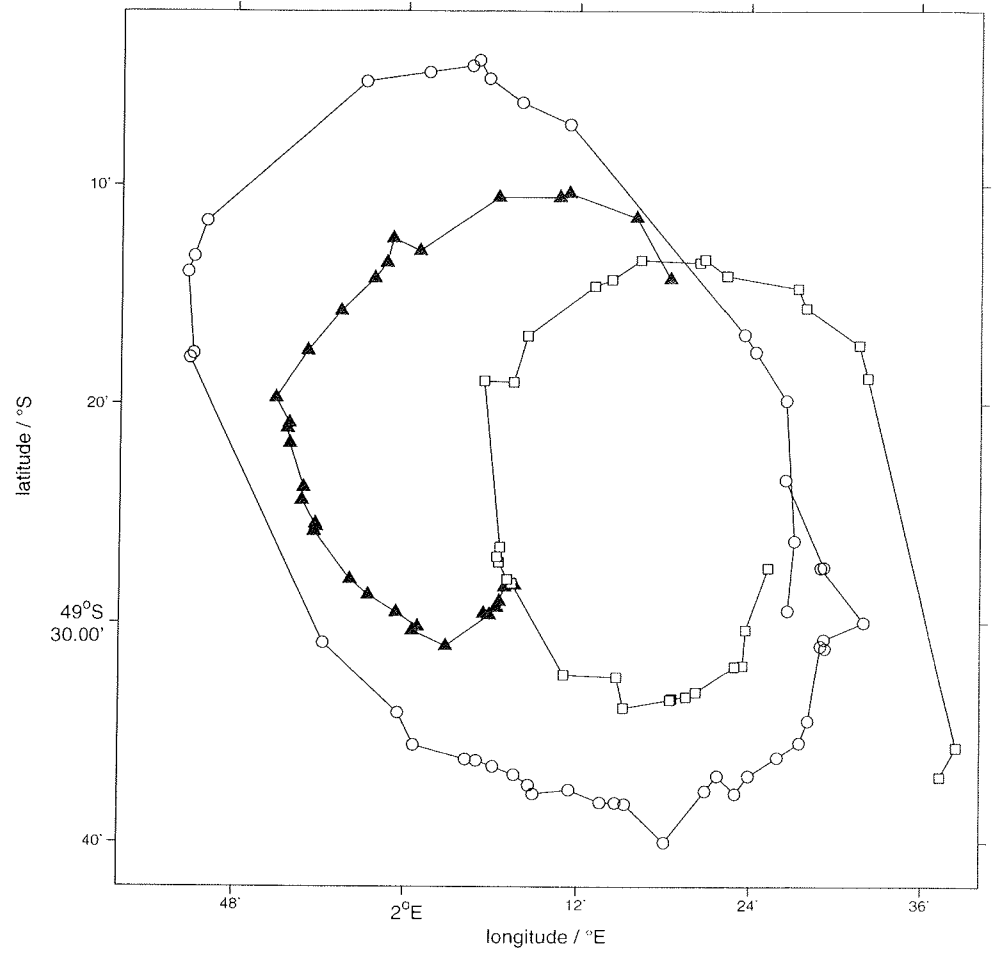


Fig. 3.4.2: Buoy tracks during drifts 05 (circles), 07 (triangles) and 08 (squares).

3.5 Mapping horizontal spreading of a developing phytoplankton bloom using an airborne chlorophyll *a* fluorescence LIDAR B. Cembella, H. Rohr, K. Loquay (Optimare), Volker Strass (AWI)

Introduction

The concentration of the broad-band (Figure 3.5.1) light harvesting pigment chlorophyll *a* (chl_{*a*}) is one of the key variables used for tracing phytoplankton bloom development and estimating phytoplankton biomass. *In vivo* chl_{*a*}

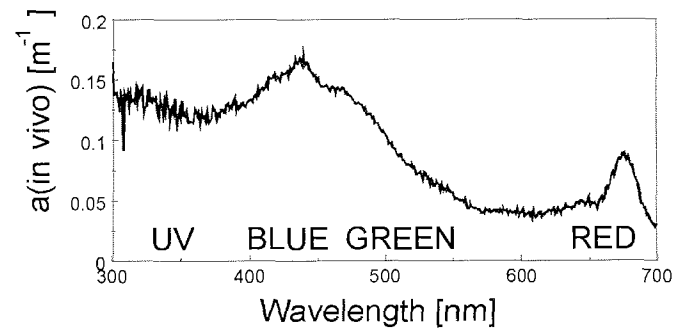


Figure 3.5.1: *In vivo* phytoplankton absorption spectrum of a natural phytoplankton assemblage.

fluorescence has been extensively used to study phytoplankton physiology and growth in both laboratory and field conditions (e.g. reviews of Lavorel and Etienne, 1977; Krause and Weis, 1984; Falkowski and Kiefer, 1985; Prézelin and Boczar, 1986; Krause and Weis, 1991; Owens, 1991). The *in vivo* fluorescence method to estimate chla concentrations was first introduced by Lorenzen (1966), however, *in vivo* fluorescence is not a conservative property of chla (Geider and Osborne, 1992). Fluorescence intensity per unit chla is a physiological variable which is strongly affected by variations in photosynthetic characteristics of phytoplankton in response to environmental conditions such as light or nutrient availability.

The rate of *in vivo* chla fluorescence F emitted by a seawater suspension of algae (Figure 3.5.2) can be described as:

$$F = E * \sigma_{\text{chl}} * \langle \text{chl} \rangle * \phi_F$$

where E is the radiation available for photosynthesis ($\mu\text{mol photon m}^{-2} \text{s}^{-1}$), σ_{chl} is the absorption cross section of algae per unit chla ($\text{m}^2 (\text{mg chla})^{-1}$), $\langle \text{chl} \rangle$ is the concentration of chlorophyll *a* (mg m^{-3}) and ϕ_F is the fluorescence quantum yield of chla ($\mu\text{mol photon emitted per } \mu\text{mol photon absorbed}$) (Falkowski and Kiefer, 1985).

The *in vivo* fluorescence of chla can now be monitored as an indicator parameter for phytoplankton biomass from space or airborne platforms, using either passive or active sensors (Kirk, 1994). Since the 1970s, active remote sensing using a laser fluorosensor system has been under development for measuring F. The active method (LIDAR or laser fluorosensor system) relies on a pulsed laser, which induces chla fluorescence, and a detection unit with a

telescope for the recording of fluorescence signals from the water surface (e.g. Measures and Bristow, 1971; Kim, 1973; Measures et al., 1973; Mumola et al., 1973; Chekalyuk et al., 1995). With this method, one can use (1) a narrow band excitation energy and (2) a set of beam-splitter with an array of different filters for high spectral resolution, revealing additional spectral characteristics of natural water seawater such as Raman scattering of water (Figure 3.5.2).

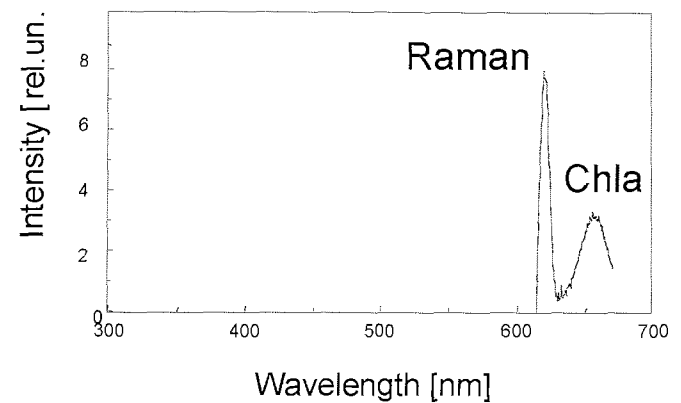


Figure 3.5.2: Fluorescence emission spectrum using 532 nm excitation wavelength (Raman at 649 nm; Chla at 685 nm).

A typical fluorescence LIDAR consists of a high power laser, emitting at near-UV or visible wavelengths, and a gated signal receiver for the detection of laser-induced radiation from the upper meters of the water column. A pulsed laser and a gated signal detector are used to discriminate the laser-induced water column return from the daylight background. LIDAR measurements offer the possibility of obtaining data at any time of the day or night. Night-time measurements of F have the advantage that E is entirely controlled by the LIDAR system, i.e. independent of ambient light conditions. A LIDAR system can be mounted on an aircraft or helicopter, which allows investigation of spatial and temporal sampling scales between those of ship and satellite data. Furthermore, LIDAR remote sensing of the upper water column can provide information on subsurface phenomena down to one attenuation length of the laser beam (see also Abroskin et al., 1987; Diebel Langohr et al., 1986; Hoge et al., 1988), which is especially important for biological variables such as $\langle \text{chl}a \rangle$ since these usually exhibit strong vertical heterogeneity.

The objective of the chla LIDAR application during this experiment was the detection and monitoring of relative phytoplankton biomass in an iron-fertilized eddy within the southern polar frontal region (49° S, 2° E), and to use this information for finding the optimum positions for *in situ* sampling of the bloom. For this purpose, helicopter-borne LIDAR surveys were conducted throughout the fertilization area and data were immediately reduced in order to obtain a quick-look of relative phytoplankton biomass distribution in the sampling area.

Material and Methods

On January 29th, 2004 testing and data acquisition was initiated and after completing a total of 25 mission days, phytoplankton bloom monitoring activities using the fluorescence lidar method were terminated on March 20th, 2004 (Table 3.5.1).

Table 3.5.1: Lidar deployment during the EIFEX experiment

Flight ID	Date [dd,mm,yy]	Mission	Region	Weather Conditions
flug04012901	29.01.04	Test system installation	Eddy 1	haze to clear
flug04013001	30.01.04	Test determination of system parameters	Eddy 1	clear to haze
flug04013101	31.01.04	Test determination of system parameters	Eddy 1	sunny to cloudy
flug04020101	01.02.04	Test passing front	Eddy 2	cloudy, sunny spells, later cloudy with shower
flug04021001	10.02.04	Patch search Part 1	Eddy 2	cloudy, sunny spells, beginning of dusk
flug04021002	10.02.04	Patch search Part 2	Eddy 2	cloudy, sunny spells, beginning of dusk
flug04021101	11.02.04	Test, photoquenching (noon)	Eddy 2	cloudy, sunny spells, later cloudy with shower
flug04021102	11.02.04	Test, photoquenching (dusk)	Eddy 2	later haze
flug04021301	13.02.04	Patch mapping, Flight over fertilisation area	Eddy 2	snow shower
flug04022101	21.02.04	Patch mapping	Eddy 2	rain
flug04022201	22.02.04	Patch mapping	Eddy 2	rain
flug04022601	26.02.04	Patch mapping	Eddy 2	rain
flug04022801	28.02.04	Patch mapping	Eddy 2	rain
flug04022901	29.02.04	Patch mapping	Eddy 2	rain
flug04030101	01.03.04	Patch mapping Part 1	Eddy 2	rain
flug04030102	01.03.04	Patch mapping Part 2	Eddy 2	rain
flug04030103	01.03.04	Patch mapping Part 3	Eddy 2	rain
flug04030301	03.03.04	Patch mapping	Eddy 2	cloudy with haze, later sunny spells
flug04030401	04.03.04	Patch mapping Part 1	Eddy 2	cloudy with haze, later sunny spells
flug04030402	04.03.04	Patch mapping Part 2	Eddy 2	cloudy with haze, later sunny spells
flug04030501a	05.03.04	Patch mapping Part 1	Eddy 2	cloudy with haze
flug04030501b	05.03.04	Patch mapping Part 2	Eddy 2	haze with fog
flug04030701	07.03.04	Patch mapping Part 1	Eddy 2	haze with fog
flug04030702	07.03.04	Patch mapping Part 2	Eddy 2	sunny
flug04030901	09.03.04	Patch mapping Part 1	Eddy 2	sunny
flug04030902	09.03.04	Patch mapping Part 2	Eddy 2	cloudy to haze
flug04031001	10.03.04	Patch mapping Part 1	Eddy 2	cloudy to haze
flug04031002	10.03.04	Patch mapping Part 2	Eddy 2	cloudy, clear view
flug04031401	14.03.04	Patch mapping Part 1	Eddy 2	cloudy, sunny spells
flug04031402	14.03.04	Patch mapping Part 2	Eddy 2	cloudy, clear view
flug04031501	15.03.04	Patch mapping Part 1	Eddy 2	cloudy, clear view
flug04031502	15.03.04	Patch mapping Part 2	Eddy 2	cloudy, clear view
flug04031601	16.03.04	Patch mapping Part 1	Eddy 2	cloudy, clear view
flug04031602	16.03.04	Patch mapping Part 2	Eddy 2	cloudy, clear view
flug04031801	18.03.04	Patch mapping Part 1	Eddy 2	cloudy, clear view, later fog and rain
flug04031802	18.03.04	Patch mapping Part 2	Eddy 2	sunny with snow, fair view, strong sun glint
flug04031901	19.03.04	Patch mapping Part 1	Eddy 2	cloudy, clear view
flug04031902	19.03.04	Patch mapping Part 2	Eddy 2	sunny
flug04032001	20.03.04	Patch mapping Part 1	Eddy 2	cloudy with fog and snow shower, flight cancelled because of ice
flug04032002	20.03.04	Patch mapping Part 2	Eddy 2	cloudy with rain shower, partly foggy, sunny spells

The excitation wavelength of this lidar system was selected at 532 nm, located at the decreasing slope in the absorption spectrum of a natural *in vivo* phytoplankton assemblage (Figure 3.5.1). The detection unit of this LIDAR system measures Rayleigh and Raman scattering in water at 532 and 649 nm, respectively, using a 10 nm band-width. Four 20 nm wide channels detect chla fluorescence at 685 and 730 nm and possible background signals are detected at 600 and 700 nm (Figure 3.5.2).

Helicopter-mounted LIDAR surveys require a minimum field of view and fair visibility. Furthermore, coverage of the sampling area required about 4 to 5 h of flying time. It was therefore impossible to fly at night or early in the morning before the expected photo-quenching from daylight affects the chla fluorescence intensity. Therefore, on February 10th, 2004 two test flights were conducted to obtain data for a later quantification of photo-quenching during the experiment. During the remainder of the experiments, flights were conducted around solar noon, when effects of photo-quenching were expected to be strongest but unaffected by diurnal changes.

The maximum flight time was limited to two and a half hours; therefore it was attempted to conduct two consecutive flights, weather permitting, to obtain complete coverage of the sampling area. Data were processed immediately

upon arrival. Raman normalized Chla fluorescence, which gives the fluorescence return signal of the first optical depth, was computed as a relative phytoplankton biomass indicator of the upper water column (Figure 3.5.3). In order to obtain a better comparison between the individual sampling days all data were normalized to a scale between 0 and 10. For an improved overview of the sampling area, the Raman-normalized chla fluorescence [rel.un] was plotted using Voronoi tessellations (Figure 3.5.3). The so-produced quick-look of Raman-normalized relative chla fluorescence intensity was available an hour after the end of the flight(s) latest.

Preliminary Results

The instrument performed very reliably throughout the experiment. All channels performed well and it was possible to normalize the chla fluorescence intensities to the water Raman scattering signal (Figure 3.5.3). A first view at the data revealed that photo-quenching occurred. Normalization of chla fluorescence intensities per flight to a fixed scale of 0 to 10 does not give any information on the actual quality and quantity of the phytoplankton bloom, but

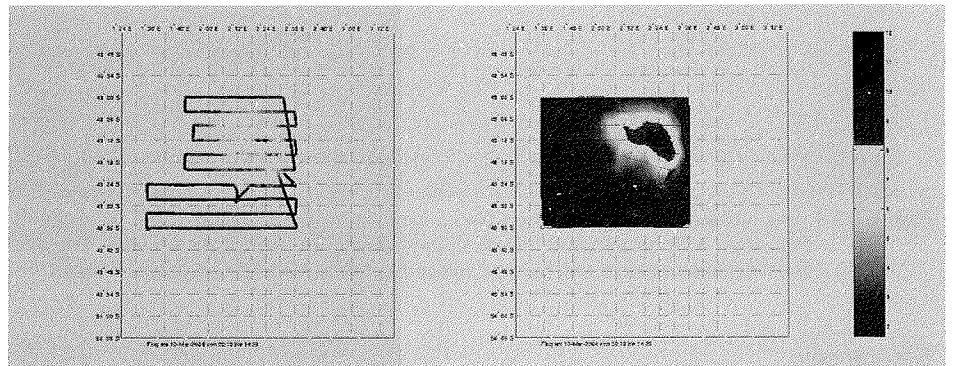


Figure 3.5.3: Relative chla fluorescence intensities along the track and as a map using Voronoi tesselations on 10-Mar-2004.

rather allows tracking of the very distinctive pattern of chla fluorescence, and therefore the location of the related phytoplankton bloom, with very little delay after the end of the monitoring flight.

The application of a chla fluorescence LIDAR made it possible to identify the location of the phytoplankton bloom and obtain through data reduction and interpolation of the relative chla fluorescence intensities maps (Figure 3.5.4). These maps help to visualize the bloom location and development in the sampling area. We present four exemplary plots that were obtained during the EIFEX experiment using such a quick-view approach in Figure 3.5.4. These plots demonstrate well the capacity of applied method.

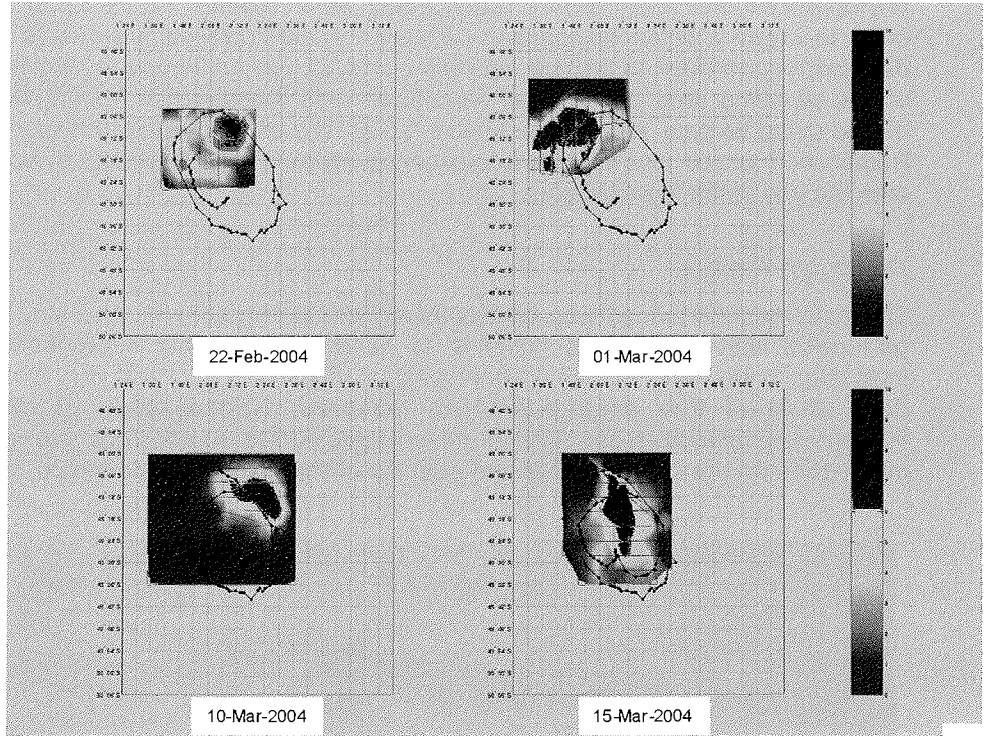


Figure 3.5.4: Examples of the phytoplankton bloom location based on relative chla fluorescence measured with an airborne LIDAR system during the EIFEX experiment. The thick lines indicate tracks of drift buoys deployed to follow the fertilised patch of water.

References

- Abroskin, A. G., A. F. Bunkin, D. V. Vlasov, A. L. Gorvunov, and D. M. Mirkamilov, 1987: Laser airborne sensing field experiments using the "Chaika" assembly. Proceedings of the Institute of General Physics of the Academy of Sciences of the USSR, Nova Science Publishers ed. F. V. Bunkin, Ed., Nova Science Publishers, 27-48.
- Chekalyuk, A. M., A. A. Demidov, and M. Y. Gorbunov, 1995: Lidar monitoring of phytoplankton and organic matter in the inner seas of Europe. EARSel, 3, 131-139.
- Diebel-Langohr, D., T. Hengstermann, and R. Reuter, 1986: Water depth-resolved determination of hydrographic parameters from airborne lidar measurements. Dynamic biological processes at marine physical interfaces, J. C. J. Nihoul, Ed., Elsevier, 591-602.
- Falkowski, P. and D. A. Kiefer, 1985: Chlorophyll a fluorescence in phytoplankton: Relationship to photosynthesis and biomass. Journal of Plankton Research, 7, 715-731.

- Geider, R. J. and B. A. Osborne, 1992: Algal Photosynthesis. Vol. 2, Current Phycology, Chapman and Hall, 255 pp.
- Hoge, F. E., C. W. Wright, W. B. Krabill, R. R. Buntzen, G. D. Gilbert, R. N. Swift, J. K. Yungel, and R. E. Berry, 1988: Airborne lidar detection of subsurface oceanic scattering layers. *Applied Optics*, 27, 3969-3977.
- Kim, H. H., 1973: New algae mapping technique by the use of an airborne laser fluorosensor. *Applied Optics*, 12, 1454-1459.
- Kirk, J. T. O., 1994: Light and photosynthesis in aquatic ecosystems. Cambridge University Press, 509 pp.
- Krause, G. H. and E. Weis, 1984: Chlorophyll fluorescence as a tool in plant physiology: II. Interpretation of fluorescence signals. *Photosynthesis Research*, 5, 139-157.
- , 1991: Chlorophyll fluorescence and photosynthesis: The basics. Annual Review in Plant Physiology and Plant Molecular Biology, 42, 313-349.
- Lavorel, J. and A.-L. Etienne, 1977: In vivo chlorophyll fluorescence. Primary processes of photosynthesis, J. Barber, Ed., Elsevier, 203-268.
- Lorenzen, C. J., 1966: A method for the continuous measurement of in vivo chlorophyll concentration. *Deep-Sea Research*, 13, 223-227.
- Measures, R. M. and M. Bristow, 1971: The development of a laser fluorosensor for remote environmental probing. *Canadian Aeronautics and Space Journal*, 17, 421-422.
- Measures, R. M., W. Houston, and M. Bristow, 1973: Development and field tests of a laser fluorosensor for environmental monitoring. *Canadian Aeronautics and Space Journal*, 19, 501-506.
- Mumola, P. B., O. J. Jarett, and C. A. J. Brown, 1973: Multiwavelength lidar for remote sensing of chlorophyll a in algae and phytoplankton. Conference on the use of laser for hydrographic studies, Wallops Island, VI, USA, NASA, 137-145.
- Owens, T. G., 1991: Energy transformation and fluorescence in photosynthesis. Particle Analysis in Oceanography, NATO ASI Series, Vol. G27, S. Demers, Ed., Springer-Verlag, 101-137.
- Prézelin, B. B. and B. A. Boczar, 1986: Molecular bases of cell absorption and fluorescence in phytoplankton: Potential applications to studies in oceanography. *Progress in Phycological Research*, 4, 349-464.

3.6 Micro Structure Turbulence Profiling with the MSS- Probe H. Prandke (ISW) and V. Strass (AWI)

The MSS is a tethered free-falling profiler for simultaneous microstructure and precision measurements of physical parameters in marine and limnic waters. It is produced by *Sea & Sun Technology GmbH* in co-operation with *ISW Wassermesstechnik*. During ANTXXI/3 'EIFEX' two profilers, the MSS90L (long version, serial No. MSS15, owned by AWI) and the MSS90 (serial No. MSS09, owned by ISW) were used.

The MSS is equipped with microstructure shear sensors (for turbulence measurements), a microstructure temperature sensor, standard CTD sensors, a Seapoint turbidity sensor, and vibration control sensor (ACC). The MSS15 in addition was equipped with an conductivity microstructure sensor. The sampling rate for all sensors is 1024 samples per second, the resolution is 16 bit. The data are transmitted via electrical cable to an on board unit and further to a PC for data acquisition.

The MSS is designed for vertical profiling within the upper 400 m. For measurements in free sinking mode, the profiler was balanced with negative buoyancy which gave it a sinking velocity of about 0.7 m/s. The MSS was operated using a special winch for microstructure profilers (SWM2000, produced by *ISW Wassermesstechnik*). Effects caused by cable tension (vibrations) and the ship's movement are excluded by a slack in the cable. The aim of the measurements was to study vertical mixing due to small scale turbulence and stratification in the top layer and the intermediate cold winter water in the ACC. This required an operation of the profiler from the surface to approximately 300m depth. With respect to the intermittence of marine turbulence, a burst sampling strategy was applied at each station. Typically, a burst of 5 profiles was taken.

During EIFEX, microstructure measurements were made at 34 stations. In total, 191 profiles were measured in a depth range between approx. 10 and 350 m. The size of the data set collected with the MSS profiler (condensed binary raw data) is about 3.3 Gbyte.

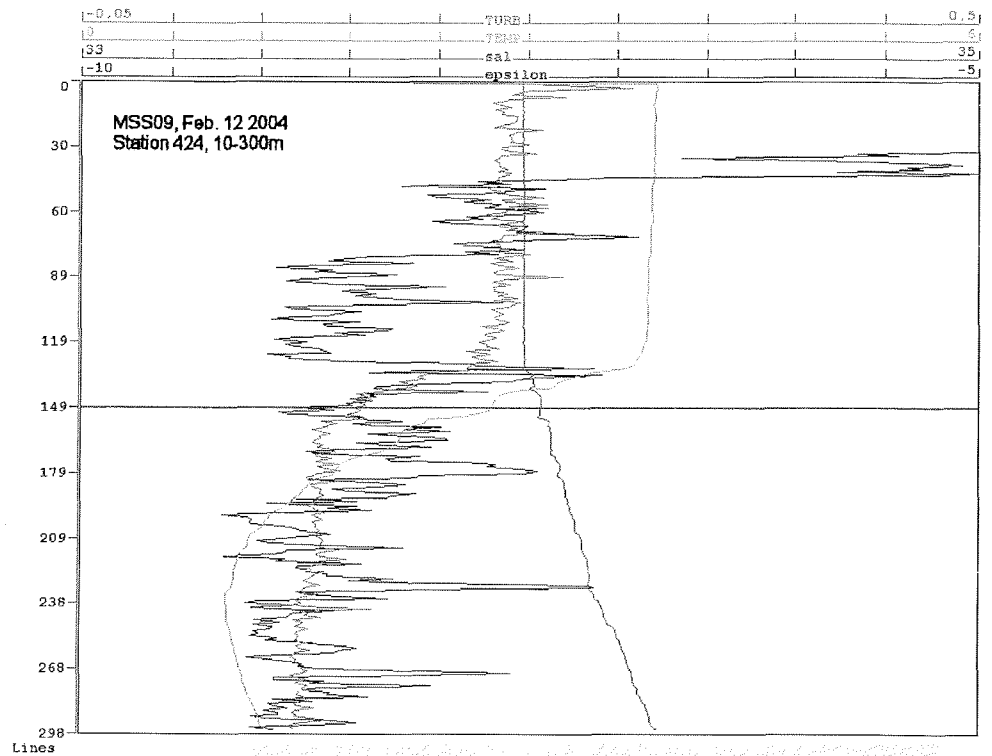


Fig. 3.6: Example profiles of turbidity (TURB), temperature (TEMP), salinity (sal) and the energy dissipation rate (ϵ) obtained from a MSS deployment.

3.7 Monitoring the bloom beyond the end of the cruise with VS-APEX floats

V.Strass (AWI) and H. Rohr (Optimare)

In order to receive data from the stimulated bloom even after departure from the experimental site, four autonomous profiling floats were deployed in the fertilized patch at the end of the cruise. These floats, termed VS-APEX (Versatile Sensor - Autonomous Profiling EXplorer), were newly designed and built by Webb Research Corp. after special request from the AWI. In addition to the standard APEX floats equipped with CTD and optional oxygen sensor, the VS-APEX also carry a transmissometer (WetLabs C-Rover) and a turbidity meter (Seapoint Sensors). The CTD in case of the VS-APEX is of type SBE-41 (Sea-Bird Electronics) and the oxygen sensor of type Aanderaa Oxygen Optode.

The VS-APEX are programmed for park-and-profile mission. The parking depth, at which they rest and drift with the currents, differs among the individual floats

(see Tab. 3.7.1). Once every two days the floats perform a vertical profile. Profiling starts with sinking to their common maximum depth, 1500 m. From there the floats ascend towards the surface, taking measurements at preset intervals of 50 m in the depth range below 250 m and of 10 m above. Once they reach the surface, they stay there for about 10 hours to completely transfer their data. Afterwards they sink again to their parking depth. At the time of writing this report, mid June 2004, each of the four floats has collected about 45 profiles of data, and continues to operate.

Tab. 3.7.1: VS-APEX Float Deployments

AWI Float ID	Park Depth [m]	Deployment			
		Day [dd.mm.yy]	Time [hh:mm]	Latitude S	Longitude E
50	200	14.03.04	11:30	49° 23.63'	02° 04.72'
53	300	17.03.04	14:00	49° 18.72'	02° 21.94'
51	500	14.03.04	11:30	49° 23.63'	02° 04.72'
52	1000	17.03.04	14:00	49° 18.72'	02° 21.94'

4. H₂O₂ DYNAMICS DURING A MESOSCALE IRON ENRICHMENT IN THE SOUTHERN OCEAN

P.L. Croot and K. Bluhm (IfM-K)

Introduction and Overview

Hydrogen peroxide (H₂O₂) is the most stable intermediate in the four-electron reduction of O₂ to H₂O and may function as an oxidant or a reductant. H₂O₂ is principally produced in the water column by photochemical reactions involving dissolved organic matter (DOM) and O₂ [Cooper *et al.*, 1988; Scully *et al.*, 1996; Yocis *et al.*, 2000; Yuan and Shiller, 2001]. Open ocean H₂O₂ concentrations show a distinct exponential profile with a maximum at the surface consistent with the photochemical flux. Concentrations can reach up to 300 nmol L⁻¹ in Equatorial and Tropical regions with high DOM concentrations such as in the Amazon plume in the Atlantic [Yuan and Shiller, 2001]. In regions with low DOM and low sunlight, surface H₂O₂ levels are much lower with values in the Southern Ocean of 10-20 nmol L⁻¹ [Sarthou *et al.*, 1997]. Rainwater is a major potential source for H₂O₂ to surface seawater as it is preferentially removed from the atmosphere, relative to other peroxides, during convective events [Croot *et al.*, 2004b]. Due to its high solubility in water, scavenging of H₂O₂ in deep convection is around 55-70% [Cohan *et al.*, 1999]. Mixing ratios of H₂O₂ in the marine troposphere show a strong latitude dependence with a maximum over the equator, suggesting that the air to surface flux at the equator should be high [Weller and Schrems, 1993].

H_2O_2 can also be produced by biological processes in the ocean and dark production has been observed in the Sargasso Sea [Palenik and Morel, 1988] and in phytoplankton cultures [Palenik *et al.*, 1987]. However studies to date have shown that the major production pathway in the water column is from photochemical production. In a few cases in the Southern Ocean, distinct H_2O_2 maximums at depth, corresponding to the chlorophyll maximum, suggest a significant biological source of H_2O_2 [Croot *et al.*, 2004a]. The 'dark decay lifetime' of H_2O_2 can vary from hours to weeks in the ocean [Petasne and Zika, 1997], but typically may be around 4 days in the open ocean [Plane *et al.*, 1987]. Overall the decay rate of H_2O_2 is apparently controlled by several factors: H_2O_2 concentration, colloid concentration, bacteria/cyanobacteria numbers and temperature [Wong *et al.*, 2003; Yuan and Shiller, 2001].

During EIFeX measurements of H_2O_2 in the upper 200 m of the water column were taken throughout the course of the experiment to examine: (i) Rates of formation and decay of H_2O_2 in Southern Ocean waters during a phytoplankton bloom. (ii) H_2O_2 controls on the kinetics of Fe(II) oxidation in seawater. (iii) Allow estimation of vertical mixing rates from H_2O_2 profiles.

Methods

H_2O_2 measurements in surface waters

Seawater samples were obtained either using Niskin bottles on a standard CTD rosette or from modified Teflon coated PVC General Oceanics (Miami, FL, USA) GoFlo (8 L) bottles. Samples were drawn into 100 mL low density brown polyethylene bottles which were impervious to light. Samples were analyzed within 1-2 hours of collection where possible and were not filtered. In the present work H_2O_2 was measured using a flow injection chemiluminescence (FIA-CL) reagent injection method [Yuan and Shiller, 1999]. In brief, the chemiluminescence of luminol is catalysed by the reaction of H_2O_2 present in the sample with Co^{2+} at alkaline pH. H_2O_2 standards were made by serial dilution from a primary stock solution (30% Fluka - Trace Select). The concentration of the primary standard was determined by direct spectrophotometry of the solution ($\text{A} = 40.9 \text{ mol L}^{-1} \text{ cm}^{-1}$, [Hwang and Dasgupta, 1985]). Secondary standards were analysed with a spectrophotometric method using Cu(II) and 2,9-dimethyl-1,10-phenanthroline [Kosaka *et al.*, 1998]. Seawater samples were measured directly by FIA-CL, while rainwaters were diluted, up to 1:100, with ultrapure water (18 M_Ω). Sample concentrations were corrected daily for the reagent blank [Yuan and Shiller, 1999] and for H_2O_2 in the ultrapure water (20-60 nmol L⁻¹). Samples were analyzed using 5 replicates: typical precision was 2-3% through the concentration range 1-100 nM, the detection limit (3σ) was typically 0.6 nmol L⁻¹.

Preliminary results and discussion

H_2O_2 profiles were measured at 28 stations during the course of EIFeX. The initial conditions encountered during EIFeX was typical for H_2O_2 in the Southern Ocean with relatively low surface concentrations (~ 30 nmol L⁻¹), which is relatively constant throughout the mixed layer and decreases exponentially to deeper waters. There was some evidence also for enhanced H_2O_2 levels in the

vicinity of the chlorophyll maximum (Figure 4.1 – at approximately 100 m) at both initial eddy pre-fertilization stations. During the course of EIFeX, overall H₂O₂ concentrations apparently increased presumably from the effects of increased photoactive DOC newly produced by the phytoplankton bloom. Changes in vertical mixing rates were also found to play a major role in controlling the H₂O₂ concentrations.

An intensive diel study in the iron fertilised patch was conducted on the 6th of March 2004 with sampling throughout the upper 150 m of the water column taking place every 4 hours during the day, allowing the natural cycle of H₂O₂ formation and decay to be studied. At a few selected stations, deep water H₂O₂ profiles were obtained with samples from below 500 m depth. Other shipboard experiments were also conducted to examine the decay rate of deep water H₂O₂ in the dark in order to provide better estimates of the decay rate for H₂O₂ in waters with low biological activity.

Acknowledgments

The authors would like to show their deep thanks and appreciation to the crew of the R.V. Polarstern, for all their efforts in helping us throughout ANTXXI-3. Thanks also to the Chief Scientist, Dr Victor Smetacek and to the AWI for making this cruise possible.

References

- Cohan, D.S., M.G. Schultz, D.J. Jacob, B.G. Heikes, and D.R. Blake, Convective injection and photochemical decay of peroxides in the tropical upper troposphere: Methyl iodide as a tracer of marine convection, *Journal of Geophysical Research-Atmospheres*, 104 (D5), 5717-5724, 1999.
- Cooper, W.J., R.G. Zika, R.G. Petasne, and J.M.C. Plane, Photochemical Formation of H₂O₂ in Natural Waters Exposed to Sunlight, *Environmental Science and Technology*, 22, 1156-1160, 1988.
- Croot, P.L., P. Laan, J. Nishioka, V. Strass, B. Cisewski, M. Boye, K. Timmermans, R. Bellerby, L. Goldson, and H.J.W. de Baar, Spatial and Temporal distribution of Fe(II) and H₂O₂ during EISENEX, an open ocean mesoscale iron enrichment, *submitted to Marine Chemistry*, 2004a.
- Croot, P.L., P. Streu, I. Peeken, K. Lochte, and A.R. Baker, Influence of ITCZ on H₂O₂ in near surface waters in the equatorial Atlantic Ocean, *Geophysical Research Letters (accepted)*, 2004b.
- Hwang, H., and P.K. Dasgupta, Thermodynamics of the Hydrogen Peroxide-Water System, *Environmental Science and Technology*, 19, 255-258, 1985.
- Kosaka, K., H. Yamada, S. Matsui, S. Echigo, and K. Shishida, Comparison among the methods for hydrogen peroxide measurements to evaluate advanced oxidation processes: Application of a spectrophotometric method using copper(II) ion and 2,9 dimethyl-1,10-phenanthroline, *Environmental Science & Technology*, 32 (23), 3821-3824, 1998.
- Palenik, B., and F.M.M. Morel, Dark production of H₂O₂ in the Sargasso Sea, *Limnology and Oceanography*, 33, 1606-1611, 1988.

- Palenik, B., O.C. Zafiriou, and F.M.M. Morel, Hydrogen peroxide production by a marine phytoplankter, *Limnology and Oceanography*, 32, 1365-1369, 1987.
- Petasne, R.G., and R.G. Zika, Hydrogen peroxide lifetimes in south Florida coastal and offshore waters, *Marine Chemistry*, 56 (3-4), 215-225, 1997.
- Plane, J.M.C., R.G. Zika, R.C. Zepp, and L.A. Burns, Photochemical modeling applied to natural waters, in *Photochemistry of environmental aquatic systems*, edited by R.G. Zika, and W.J. Cooper, pp. 215-224, American Chemical Society, Washington D.C., 1987.
- Sarthou, G., C. Jeandel, L. Brisset, D. Amouroux, T. Besson, and O.F.X. Donard, Fe and H₂O₂ distributions in the upper water column in the Indian sector of the Southern Ocean, *Earth and Planetary Science Letters*, 147, 83-92, 1997.
- Scully, N.M., D.J. McQueen, D.R.S. Lean, and W.J. Cooper, Hydrogen peroxide formation: The interaction of ultraviolet radiation and dissolved organic carbon in lake waters along a 43-75 degrees N gradient, *Limnology and Oceanography*, 41 (3), 540-548, 1996.
- Weller, R., and O. Schrems, H₂O₂ in the Marine Troposphere and Seawater of the Atlantic Ocean, *Geophysical Research Letters*, 20, 125-128, 1993.
- Wong, G.T.F., W.M. Dunstan, and D.B. Kim, The decomposition of hydrogen peroxide by marine phytoplankton, *Oceanologica Acta*, 26 (2), 191-198, 2003.
- Yocis, B.H., D.J. Kieber, and K. Mopper, Photochemical production of hydrogen peroxide in Antarctic Waters, *Deep Sea Research Part I : Oceanographic Research*, 47(6), 1077-1099, 2000.
- Yuan, J., and A.M. Shiller, Determination of Subnanomolar Levels of Hydrogen Peroxide in Seawater by Reagent-Injection Chemiluminescence Detection, *Analytical Chemistry*, 71, 1975-1980, 1999.
- Yuan, J., and A.M. Shiller, The distribution of hydrogen peroxide in the southern and central Atlantic ocean, *Deep-Sea Research II*, 48, 2947-2970, 2001.

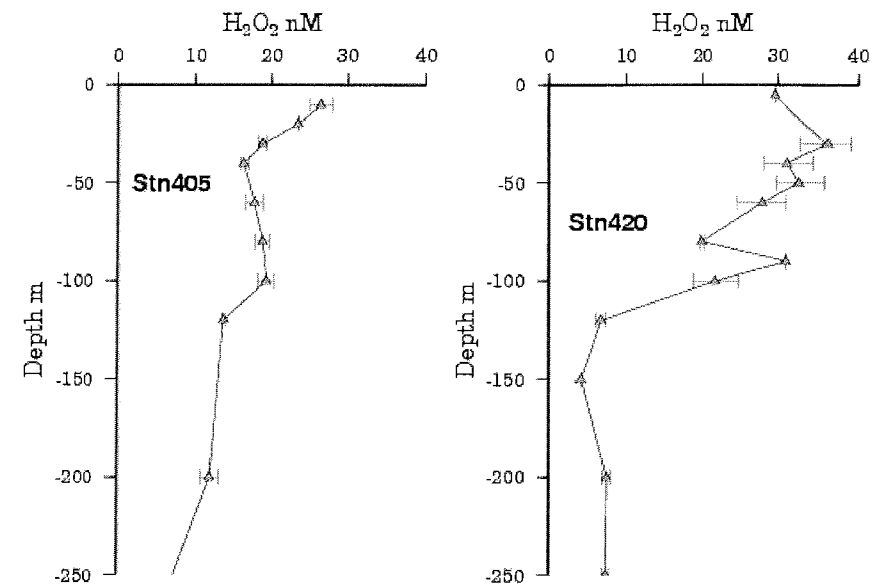


Figure 4.1: The vertical distribution of H_2O_2 at the $t = 0$ stations for Eddy 1 and Eddy 2 during EIFeX.

5. TEMPORAL CHANGES IN IRON SPECIATION DURING A MESOSCALE IRON ENRICHMENT EXPERIMENT

P.L. Croot, K. Bluhm, E. Breitbarth (IfM-K) and M. Öztürk (NTNU)

Introduction and Overview

The role of iron in limiting primary production in the oceans is now well established through *in situ* iron enrichment experiments including those conducted previously in the Southern Ocean such as SOIREE, EisenEx and SOFeX. Yet the processes by which iron is retained and recycled in the water column are still poorly understood, in particular with regard to the longer term effects of post bloom collapse after the effects of iron fertilization have subsided. An iron enrichment experiment such as has been carried out during ANTXXI-3 (EIFeX), there arises an opportunity to examine several of the key processes concerning iron biogeochemistry on both larger spatial and temporal scales. During EIFeX we aimed to examine several key aspects of iron biogeochemistry:

Fe(II): Recent studies have shown the importance of Fe(II) in cold waters in maintaining high concentrations of dissolved iron [Croot *et al.*, 2001; Croot and Laan, 2001; Croot and Laan, 2002]. It is also a useful way to follow the released iron as the signal from the added Fe(II) can last for several hours and the surface waters can be sampled rapidly (90s or less) [Croot and Laan, 2002].

Colloidal iron: The Fe(II) is oxidised with time to Fe(III) which rapidly forms colloidal particles, this colloidal iron is not as bioavailable to phytoplankton as that in the dissolved phase [Kuma and Matsunaga, 1995; Nishioka and Takeda, 2000], but can be accessed by mixotrophic species [Nodwell and Price, 2001]. The colloidal iron pool may be very important for maintaining a steady flux of iron to the dissolved phase as it is also can be converted to the dissolved phase by grazing[Barbeau and Moffett, 2000]. Measurement of colloidal iron was performed by ultrafiltration routinely on hydrocast samples.

Iron speciation: In seawater the speciation of iron is dominated by organic complexation [Rue and Bruland, 1995; van den Berg, 1995]. In previous iron fertilization experiments there have been dramatic changes in the concentration of these iron binding ligands but the responses have been at different stages of the iron induced bloom [Croot *et al.*, 2001; Rue and Bruland, 1997]. In SOIREE the increase in iron complexing ligands did not occur until 8-10 days after the first iron infusion and it is suggested that the main source was bacterial production. For EIFEX we measured the speciation of iron throughout the course of the experiment and undertook some biological measurements in collaboration with AWI colleagues to try and pinpoint which species and why these iron ligands are being produced.

Iron solubility: Iron is poorly soluble in seawater and this is the main reason why its concentration is so low in seawater. During EIFEX we propose to measure the solubility of iron using a simple radiotracer technique developed by Kuma and coworkers [Kuma *et al.*, 1998; Kuma *et al.*, 2000; Kuma *et al.*, 1996; Nakabayashi *et al.*, 2002]. Measurements of iron solubility combined with iron speciation data (above) will provide us with the data necessary to model the key processes in iron cycling during this experiment. During this cruise, we undertook over 1000 analyses for dissolved and total iron in order to examine some of the processes that affected the bioavailability and absolute concentrations of Fe in the enriched patch. It is hoped that from this data we will be better able to understand the processes involved.

Methods

During cruise ANT XXI/3 the fate of the iron added to the seawater was studied using a variety of state of the art analytical techniques. The work was characterized by high density sampling and profiling both inside and outside the patch. This was accomplished by using GO-FLO samplers on a Kevlar wire for the vertical distribution of iron at each station.

Spatial distribution of iron: Measurement of iron

To prevent sample contamination, trace metal clean techniques were applied and all sample manipulations were carried out in the laminar flow hood of the IfM-Geomar Class 100 Clean Container. Typically at each station samples were obtained for total dissolved iron (0.2 µm Sartorius cartridge filter) and total iron (unfiltered sample). Samples were also collected for ultrafiltration using either PALL FILTRON 1kD tangential flow cartridges or Vivaflow 10kD ultrafiltration cartridges. On occasion samples were size fractionated using 5 or 10 µm polycarbonate filters (Osmonics or Nuclepore) with a Savillex Teflon filtration unit. All samples for total metal analysis were acidified to pH < 2 with ultraclean quartz distilled concentrated hydrochloric acid.

Iron was measured on-board using a flow injection technique with in-line pre-concentration on a chelating resin followed by chemiluminescence detection (FIA-CL) [Bowie *et al.*, 1998]. Samples were acidified for at least 24 hours prior to addition of ammonium acetate buffer (pH 4.5) and sodium sulfite to reduce Fe(III) to Fe(II), the sample was then allowed to react for at least 1 hour before analysis. Fe(II) from the buffered sample is preconcentrated onto a column of immobilized 8-hydroxyquinoline [Dierssen *et al.*, 2001]. After a loading time of 1 to 4 minutes, the column is washed with deionised water and the iron is eluted with dilute hydrochloric acid. The iron mixes with luminol, and buffer to produce chemiluminescence in the flow cell of a photomultiplier tube connected to a photon counter. The chemiluminescence occurs as a result of the iron catalyzed oxidation of luminol (3-aminophthalhydrazide) by hydrogen peroxide, producing blue light (424 nm). The accuracy of the method was checked and confirmed using NASS-5 reference sea water. Throughout the cruise, the blank and detection limit (3x standard deviation of blank) remained constant at 0.021 and 0.004 nM respectively. Reproducibility was typically 2% at the 0.3 nM concentration and better than 10% at the 0.06 nM level.

Fe(II) measurements

Fe(II) was measured continuously during underway sampling using a method developed early during EisenEx [Croot and Laan, 2002]. The rapid reaction between Fe(II) and luminol was utilized to make rapid (90-112s per measurement) analyses of the Fe(II) concentration in the seawater. Vertical profiles for Fe(II) and H₂O₂ were also obtained were possible, in order to examine the redox kinetics of Fe during the experiment.

Preliminary results and discussion

Opportunities for iron sampling during EIFeX were much reduced in comparison to EisenEx because of the decision to locate the container with the bags of ferrous sulfate for the infusions directly above the IfM-Geomar clean container. This meant no sampling for iron could be conducted 24 hours before or after an iron infusion (effectively a period of 3 days) as the area around the clean container was covered with ferrous sulfate dust or high concentrations of iron saturated solutions. A further day was normally lost when the ferrous sulfate bags were moved into the container from the storage areas in the hold. A

further problem arose during the first iron infusion when one of the iron tanks was released onto the deck rather than being pumped over the stern and this resulted in a continual release of iron slowly to surface waters surrounding the ship over several days. For this reason samples taken with the GO-FLOs over the first week after the infusion at the 2nd eddy were confined to below 40 m depth. Luckily despite the high concentrations of iron outside the clean container, the precautions made during infusions and loading of the iron storage container, by covering the intakes and the door seals with tape and switching the container off, meant that there was no contamination inside the clean container.

Unfortunately during the first 2 weeks of the experiment there was little opportunity for sampling of the iron patch due to the problems outlined above and the decision to undertake an eddy wide survey of a week's duration. Thus we have little information on the iron loss rates during the critical formation of the bloom and can not compare EIFeX with early experiments such as EisenEx and SOFeX. Additionally the lack of a transient tracer for the patch, like SF₆ as used in early iron fertilizations, meant it was more difficult to separate the effects of possible shipboard contamination from real iron patch waters during the initial phases of the experiment. However the longer duration of EIFeX allowed a better view into the long term processes that shape iron recycling and bloom dynamics and results from stations occupied later in the cruise show a remarkable retention of dissolved iron throughout the mixed layer.

Measurements of Fe(II) were performed on a few occasions, mostly however several days after the iron infusions (see above for details) when Fe(II) levels were very low but the presence of Fe(II) was very significant. Fe(II) concentrations were monitored during a diel cycle on one occasion and showed a strong diel cycle consistent with photochemical production. Several experiments were run to determine *in situ* Fe(II) oxidation rates and preliminary results suggested that they were in good agreement with that expected for the given temperature and H₂O₂ concentrations.

Over 200 frozen samples were collected for iron solubility and iron speciation studies to be performed in Kiel over the coming months after the cruise. These measurements will be accomplished by a series of radiotracer, voltammetric and ultrafiltration studies.

Acknowledgments

The authors would like to show their deep thanks and appreciation to the crew of the R.V. Polarstern, for all their efforts in helping us throughout ANTXXI-3. Particular thanks needs to be expressed to the Chief Engineer Volker Schulz for keeping our new clean container running despite everything the Southern Ocean threw at it (literally in most cases). Anna Farrenkopf (Ecochemie) kindly loaned us the use of an extra voltammeter for use during EIFeX. This work was funded directly by the IfM-Geomar and thanks to Professor Doug Wallace for securing funds for the construction of the clean container which was used extensively during this cruise. Thanks also to the Chief Scientist, Dr Victor Smetacek and to the AWI for making our participation in this cruise possible.

References

- Barbeau, K., and J.W. Moffett, Laboratory and field studies of colloidal iron oxide dissolution as mediated by phagotrophy and photolysis, *Limnology and Oceanography*, 45, 827-835, 2000.
- Bowie, A.R., E.P. Achterberg, R.F.C. Mantoura, and P.J. Worsfold, Determination of sub-nanomolar levels of iron in seawater using flow injection with chemiluminescence detection, *Analytica Chimica Acta*, 361, 189-200, 1998.
- Croot, P.L., A.R. Bowie, R.D. Frew, M. Maldonado, J.A. Hall, K.A. Safi, J. La Roche, P.W. Boyd, and C.S. Law, Retention of dissolved iron and Fe^{II} in an iron induced Southern Ocean phytoplankton bloom, *Geophysical Research Letters*, 28, 3425-3428, 2001.
- Croot, P.L., and P. Laan, Ferrous Wheels in the Ocean: The Southern Ocean Fairground, *Berichte zur Polarforschung, Alfred-Wegener-Institut für Polar- und Meeresforschung*, 400, 149-158, 2001.
- Croot, P.L., and P. Laan, Continuous shipboard determination of Fe(II) in Polar waters using flow injection analysis with chemiluminescence detection., *Analytica Chimica Acta*, 466, 261-273, 2002.
- Dierssen, H., W. Balzer, and W.M. Landing, Simplified synthesis of an 8-hydroxyquinoline chelating resin and a study of trace metal profiles from Jellyfish Lake, Palau, *Marine Chemistry*, 73, 173-192, 2001.
- Kuma, K., A. Katsumoto, H. Kawakami, F. Takatori, and K. Matsunaga, Spatial variability of Fe(III) hydroxide solubility in the water column of the northern North Pacific Ocean, *Deep-Sea Research*, 45, 91-113, 1998.
- Kuma, K., A. Katsumoto, N. Shiga, T. Sawabe, and K. Matsunaga, Variation of size-fractionated Fe concentrations and Fe(III) hydroxide solubilities during a spring phytoplankton bloom in Funka Bay (Japan), *Marine Chemistry*, 71, 111-123, 2000.
- Kuma, K., and K. Matsunaga, Availability of colloidal ferric oxides to coastal marine phytoplankton, *Marine Biology*, 122, 1-11, 1995.
- Kuma, K., J. Nishioka, and K. Matsunaga, Controls on iron(III) hydroxide solubility in seawater: The influence of pH and natural organic chelators, *Limnology and Oceanography*, 41, 396-407, 1996.
- Nakabayashi, S., K. Kuma, K. Sasaoka, S. Saitoh, M. Mochizuki, N. Shiga, and M. Kusakabe, Variation in iron(III) solubility and iron concentration in the northwestern North Pacific Ocean, *Limnology and Oceanography*, 47 (3), 885-892, 2002.
- Nishioka, J., and S. Takeda, Change in the concentrations of iron in different size fractions during growth of the oceanic diatom *Chaetoceros* sp.: importance of small colloidal iron, *Marine Biology*, 137, 231-238, 2000.
- Nodwell, L.M., and N.M. Price, Direct use of inorganic colloidal iron by marine mixotrophic phytoplankton, *Limnology and Oceanography*, 46, 765-777, 2001.
- Rue, E.L., and K.W. Bruland, Complexation of Iron(III) by Natural Organic Ligands in the Central North Pacific as Determined by a New Competitive Ligand Equilibration/Adsorptive Cathodic Stripping Voltammetric Method, *Marine Chemistry*, 50, 117-138, 1995.

Rue, E.L., and K.W. Bruland, The role of organic complexation on ambient iron chemistry in the equatorial Pacific Ocean and the response of a mesoscale iron addition experiment, *Limnology and Oceanography*, 42, 901-910, 1997.

van den Berg, C.M.G., Evidence for organic complexation of iron in seawater, *Marine Chemistry*, 50, 139-157, 1995.

Table 5.1: Summary of stations sampled for iron during ANTXXI-3

Station #	Depths	Comment
420	40, 50 , 60, 70, 80, 90, 100, 100 m	Deck covered in Fe solution
427	30, 40, 50, 60, 75, 85, 95, 105 m	Deck still with Fe waste
466	35, 55, 75, 95 m	
508	40, 50, 60, 70, 80, 90, 100, 110 m	
513	25, 35, 45, 55, 60, 80, 100, 120 m	
514	25, 35, 45, 55, 60, 80, 100, 120 m	
543	25, 35, 45, 55, 60, 80, 100, 120 m	
544	20, 40 , 60 m	Every 4 hours sampling
553	30, 40, 50, 60, 80, 100, 120, 150 m	
570	20, 30, 40, 50, 60, 80, 100, 120, 150, 200, 250, 300 m	
580	20, 30, 40, 50, 60, 80, 100, 120, 150, 200, 250, 300 m	

6. CHANGES IN THE SPECIATION AND BIOGEOCHEMICAL CYCLING OF OTHER TRACE METALS DURING EIFEX

P.L. Croat (IfM-K) and M. Özturk (NTNU)

¹FB2 Marine Biogeochemistry, Leibniz-Institut für Meereswissenschaften (IfM-Geomar), Dienstgebäude Westufer, Düsternbrooker Weg 20, 24105 Kiel, Germany.

²Norwegian University of Science and Technology (NTNU), TBS- NO- 7491-Trondheim, Norway.

Introduction and Overview

Phytoplankton blooms arising from iron fertilization will also have effects on the biogeochemical cycling of other trace metals. Particle reactive metals such as Mn, Pb, Ti and Al may be more effectively scavenged from the water column

due to the increased particle loading from the added iron forming colloids and ultimately particles, similarly the increased phytoplankton growth will also provide an increase in scavenging. Increases in the production of dissolved organic complexing agents may also change the speciation of bio active metals such as Cu, Cd?, Co, Ni and Zn, which will also be transferred from the dissolved to the particulate phase as they are taken up by growing phytoplankton cells.

Little emphasis has been paid so far to the effects of iron enrichment on the biogeochemical cycling of other trace metals. Some data has been published on total metal concentrations for a few elements from the short lived Iron-Ex I experiment [Gordon, 1998 #1623]. While for the first Southern Ocean iron enrichment experiment, SOIREE, there was little change seen for Ni and Cu, though changes were seen in the labile Zn and dissolved Cd during the course of the bloom [Frew et al., 2001]. The changes in the Cd:P ratio in the seawater seen during SOIREE is important as this ratio in marine sediments is often used as a paleotracer for deep water oceanic phosphate and productivity via preserved foraminifera [Boyle, 1988 #722]. Incubation experiments in the Southern Ocean [Cullen et al., 2003] have indicated that iron limitation causes phytoplankton to have enhanced Cd:P in their cells because of reduced growth rate, resulting in a reduced Cd:P ratio in seawater.

For the EIFeX experiment we collected over 400 samples for trace metal analysis to examine the fate of other biogeochemically important trace metals during an iron enrichment experiment.

Methods

During cruise ANT XXI/3 changes in the speciation of other important metals (Al, Mn, Co, Ti, Ni, Cu, Zn, Cd and Pb) in seawater was studied during the course of the iron enriched phytoplankton bloom. The work was characterized by high density sampling and profiling both inside and outside the patch. This was accomplished by using GO-FLO samplers on a Kevlar wire for obtaining vertical distributions of each element at each station. Onboard speciation measurements were performed for dissolved Cd and Zn. Samples were also collected and acidified for measurements of the dissolved and total metal concentrations – these samples will be analyzed back in the laboratory in Kiel. Frozen samples were also collected for further speciation studies back in the Kiel.

Speciation of Cadmium and Zinc:

Determination of the speciation of cadmium and zinc was accomplished using a rotating disk thin film mercury electrode (RD-TFME) with a Metrohm VA757 Voltammeter. The electrode substrate was glassy carbon and mercury was deposited for 15 minutes prior to use at -1.2 V with a rotation speed of 1600 rpm [Elwood, 2004]. The speciation determinations were carried out according to established protocols for both cadmium [Bruland, 1992] and zinc [Bruland, 1989].

Preliminary results and discussion

Zinc and cadmium speciation data was collected during the course of EIFeX and both showed the presence of organic chelators in these waters (Figures 1 and 2). In general higher concentrations of Zn binding ligands were found than for Cd. Consistent with other studies in the Southern Ocean, there were however detectable amounts ($\sim \text{pmol L}^{-1}$) of free Cd^{2+} and free Zn^{2+} in the surface waters. No evidence was seen for any possible conditions of Zn limitation for phytoplankton during the Fe enrichment experiment. Temporal changes in the speciation of Cd and Zn can not yet be assessed as the total metal concentrations are still to be measured in the laboratory in Kiel. Further work in the laboratory will examine Zn, Cd and Co speciation in stored samples (frozen for storage and then thawed immediately prior to analysis). The total concentrations of trace metals in archived samples from EIFeX will be measured in the laboratory in Kiel using a combination of solvent extraction and voltammetric techniques.

Acknowledgments

The authors would like to show their deep thanks and appreciation to the crew of the R.V. Polarstern, for all their efforts in helping us throughout ANTXXI-3. Thanks also to the Chief Scientist, Dr Victor Smetacek and to the AWI for making this cruise possible.

References

- Bruland, K.W., Complexation of zinc by natural organic ligands in the central North Pacific, *Limnology and Oceanography*, 34, 269-285, 1989.
- Bruland, K.W., Complexation of cadmium by natural organic ligands in the central North Pacific, *Limnology and Oceanography*, 37, 1008-1017, 1992.
- Cullen, J.T., Z. Chase, K.H. Coale, S.E. Fitzwater, and R.M. Sherrell, Effect of iron limitation on the cadmium to phosphorous ratio of natural phytoplankton assemblages from the Southern Ocean, *Limnology and Oceanography*, 48, 1079-1087, 2003.
- Ellwood, M.J., Zinc and cadmium speciation in subantarctic waters east of New Zealand, *Marine Chemistry*, 87, 37-58, 2004.
- Frew, R.D., A.R. Bowie, P.L. Croot, and S. Pickemere, Macronutrient and trace-metal geochemistry of an in situ iron-induced Southern Ocean bloom, *Deep-Sea Research II*, 48, 2467-2481, 2001.

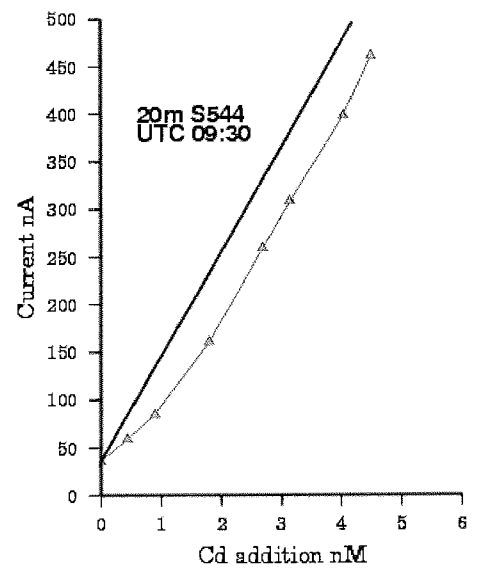


Figure 6.1: Example of Cadmium Speciation Titration obtained during EIFeX. The upper line shows the expected response in organic free seawater, the real data (green triangles) shows curvature indicating organic complexation of cadmium.

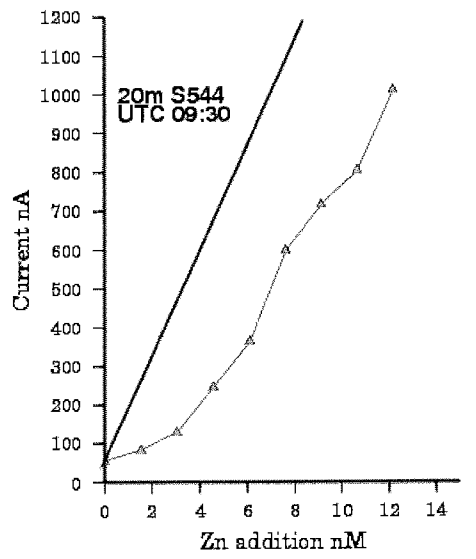


Figure 6.2: Example of Zinc Speciation Titration obtained during EIFeX. The upper line shows the expected response in organic free seawater, the real data (green triangles) shows curvature indicating organic complexation of zinc.

7. SURFACE-ACTIVE ORGANIC MATTER IN THE UPPER WATER COLUMN DURING EIFEX, A MESOSCALE OPEN OCEAN IRON ENRICHMENT EXPERIMENT IN THE SOUTHERN OCEAN

P.L. Croot (IfM-K)

Introduction and Overview

Surface-active organic matter is an important influence on numerous geochemical and physical processes in the ocean. The air-sea exchange rates of dissolved gases can be significantly decreased from the presence of surface-active material in the sea surface micro-layer (Frew et al., 1990). Surfactants can also alter the equilibrium between the dissolved and particulate phases for many trace metals (Shine and Wallace, 1996) and enhancing the aggregation of small colloids and particles, resulting in increased fluxes from the surface ocean (Mopper et al., 1995; Zhou et al., 1998). The source of these surfactants is presumed to be primarily from phytoplankton exudates and their degradation products either by direct production (Zutic et al., 1981) or from zooplankton grazing (Kujawinski et al., 2002) with large concentrations of surfactants often being observed during phytoplankton blooms in coastal waters. The composition of the surface-active material has been shown to be dominated by polysaccharide compounds (Passow et al., 1994) but also includes biologically derived lipids and proteins.

In the present work samples from the upper water column were measured for surfactant activity using an established sensitive electrochemical method. This work represents the first measurements of surfactant activity during an open ocean iron induced phytoplankton bloom. This work complements other data collected during EIFeX on:

Transparent exopolymer particles (TEP), in which the surfactants may be precursor compounds.

Trace metal data, where surfactants may affect the removal rates and speciation of certain metals.

Methods

Measurements of surfactants

Samples were collected from GO-FLO sampling bottles deployed on a Kevlar wire so as to avoid contamination from surfactants present in the sea surface microlayer. Filtered (pre-cleaned 0.2 µm Sartorius cartridge filter) samples were drawn into ethanol rinsed polyethylene vials and kept at 4° C in the dark until analysis. A limited number of unfiltered samples were also analysed during the course of the cruise.

Surfactant concentrations were measured using AC-Voltammetry with a Metrohm VA 757 voltammeter using o-nitrophenol as a probe compound (Gasparovic et al., 1998). Standards were run in samples of deep seawater (low surfactants) or UV oxidized seawater using Triton X-100 as an external standard. Aliquots (20 mL) of the seawater samples were spiked with o-

nitrophenol in solvent cleaned Quartz or Teflon cell cups. The samples were purged with N₂ gas for 3 minutes and pre-concentrated on the Hg drop for deposition times of 0, 60, 180 and 300 s.

Preliminary results and discussion

Samples were collected and analysed onboard during EIFeX from 6 stations during the course of the phytoplankton bloom. Further samples were collected and immediately frozen for later analysis in the laboratory to examine whether freezing and storage has an effect on the surfactant activity of the samples. In general surfactant activity was extremely low initially throughout the water column (< 0.02 mg L⁻¹ Triton X-100 equivalents) as expected for an open ocean, deep mixed layer, low chlorophyll location. In the last few days of EIFeX enhanced levels (~ 0.04 mg L⁻¹ Triton X-100 eq) of surfactant activity were found in the water column immediately below the mixed layer, similarly enhanced levels were also found at deeper depths (100-200 m) consistent with the sinking of organic material occurring at this time. A small scale grazing experiment to examine the effects of copepod grazing on surfactant activity was also conducted with Sandra Jansen (AWI) at this time.

Future work will involve examining the possible sources of the increased surfactant activity during EIFeX: production by iron or light stressed diatoms, grazing of diatoms by zooplankton

Acknowledgments

The authors would like to show their deep thanks and appreciation to the crew of the R.V. Polarstern, for all their efforts in helping us throughout ANTXXI-3. Thanks also to the Chief Scientist, Dr Victor Smetacek and to the AWI for making this cruise possible. This work was in part supported by DFG CR145/4 awarded to P Croot and U Passow (AWI).

References

- Frew, N.M., Goldman, J.C., Dennett, M.R. and Johnson, A.S., 1990. Impact of phytoplankton-generated surfactants on air-sea gas exchange. *Journal of Geophysical Research*, 95: 3337-3352.
- Gasparovic, B., Vojvodic, V. and Cosovic, B., 1998. Excretion of organic matter during an experimental phytoplankton bloom followed using o-nitrophenol as an electrochemical probe. *Croatica Chemica Acta*, 71(2): 271-284.
- Kujawinski, E.B., Farrington, J.W. and Moffett, J.W., 2002. Evidence for grazing-mediated production of dissolved surface-active material by marine protists. *Marine Chemistry*, 77: 133-142.
- Mopper, K. et al., 1995. The Role of Surface-Active Carbohydrates in the Flocculation of a Diatom Bloom in a Mesocosm. *Deep-Sea Research Part II-Topical Studies in Oceanography*, 42(1): 47-73.
- Passow, U., Alldredge, A.L. and Logan, B.E., 1994. The role of particulate carbohydrate exudates in the flocculation of diatom blooms. *Deep-Sea Research*, 41: 335-357.

- Shine, J.P. and Wallace, G.T., 1996. Flux of surface-active organic complexes of copper to the air-sea interface in coastal marine waters. *Journal of Geophysical Research-Oceans*, 101(C5): 12017-12026.
- Zhou, J., Mopper, K. and Passow, U., 1998. The role of surface-active carbohydrates in the formation of transparent exopolymer particles by bubble adsorption of seawater. *Limnology and Oceanography*, 43(8): 1860-1871.
- Zutic, V., Cosovic, B., Marcenko, E. and Bihari, N., 1981. Surfactant Production by Marine Phytoplankton. *Marine Chemistry*, 10: 505-520.

8. PROGRESSION OF TRANSPARENT EXOPOLYMER PARTICLES (TEP) AND POTENTIAL OF IRON BINDING TO TEP DURING EIFEX

E. Breitbarth, U. Passow, A. Terbrüggen (AWI) and P.L. Croot (IfM-K)

Introduction and Overview

The goal of this project was to examine the production of transparent exopolymer particles (TEP) by phytoplankton, the potential of iron binding to TEP and how this may affect the bioavailability of iron during the EIFEX cruise. Unchelated iron added to seawater, as in an iron enrichment experiment rapidly form colloidal hydroxides which precipitate and are lost from surface waters. However marine phytoplankton has evolved various mechanisms to retain iron in surface waters. Ligands of bacterial (siderophore) or phytoplankton (possibly porphyrin like compounds) origin have been suggested to play a major role in trace metal cycling in the euphotic layer (i.e. Hutchins 1999). Trace metals also bind to acidic polysaccharides, which are believed to be the major components of TEP. The production processes and importance of TEP in marine systems has been well described (Passow 2002). The exudation of polysaccharides by phytoplankton and formation of TEP could have a significant impact on iron chemistry in seawater. The exudation of large amounts of acidic polysaccharides may be triggered either by iron deplete conditions or alternatively by phytoplankton responses to sudden increase of iron in the water. Thus production of TEP and TEP-precursors under iron limitation could represent an adaptation of phytoplankton to the iron conditions in seawater. In this sub-project we investigated the total and dissolved polysaccharide concentrations and the amount of TEP in seawater as the iron induced phytoplankton bloom progressed. During EIFeX, incubation experiments were also performed to test the hypothesis that marine phytoplankton increase the formation of TEP by producing dissolved polysaccharides in response to the removal of iron limitation.

Methods

During the progression of the iron induced phytoplankton bloom of ANT XXI/3 the concentrations of TEP in seawater were monitored. Samples were taken routinely using CTD casts from stations inside and outside the iron fertilized patch. Additionally incubation experiments were carried out, following the development of TEP and the effect on iron bioavailability in the incubation bottles as a response to various iron and chelating agent additions. Trace metal clean techniques (all sample manipulations in laminar flow hoods) were applied throughout the incubation experiments with the exception of water for the first incubation which was collected from the CTD rosette. GO-FLO bottles on a Kevlar wire were used for the remaining three incubations.

Temporal distribution of TEP and carbohydrates sampling and measurement of TEP

Over the course of the bloom seawater was routinely sampled from the CTD rosette at depths 10 – 250 m from in- and out-patch stations. For each depth three replicate samples were filtered on 0.4 µm polycarbonate filters using 250 – 500 ml seawater depending on biomass and a vacuum \leq 150 mbar. Filters were stained with 0.5 ml Alcian-Blue solution for 5 seconds, flushed with 2-3 ml MilliQ-H₂O and frozen at -20°C until later analysis. To analyze the TEP content filters were acidified for 2-4h in 5 ml 80% (v:v) H₂SO₄. The absorbance of this solution was measured at 787 nm in a spectrophotometer (Passow and Allredge 1995). The accurate performance of the spectrophotometer was verified in the beginning of the cruise using Perkin Elmer gray glass secondary calibration standards. The TEP content was determined by a similar method for the incubation experiments. The analysis differed in using 0.2 µm pore-size filters and lower filtrations volumes according to higher biomass towards the end of the incubation periods.

sampling for carbohydrates

Carbohydrate samples were sampled for total (CHO) and dissolved carbohydrates (DCHO, filtered via 0.4 µm polycarbonate filter for CTD casts and 0.2 µm for incubation experiments). Seawater for CHO/DCHO analysis was collected parallel to the TEP samples from the CTD rosette. 20 ml aliquots of either filtered or unfiltered seawater were poured into pre-combusted borosilicate glass vials and stored at -20°C for later analysis at the AWI, Bremerhaven.

Treatments of the incubation experiments

In general, all treatments were incubated in triplicates. Additionally, 3 untreated bottles served as controls. The complete suite of experimental parameters was also sampled from another three untreated bottles at the onset of the experiment (T_0). For each time-point individual incubation bottles were used, to exclude a contamination risk if bottles had to be opened and closed repeatedly for sampling. Water sampled from GoFlo Bottles was combined from several bottles over a depth range within the mixed layer as the volume of a single bottle was not sufficient to supply the amount of water required for each incubation.

Incubation I: Additions of 0.5, 1 and 2.3 nM Fe(III) to seawater collected from the chl-a maximum at station 420 in 1 liter polycarbonate bottles were made using a 1.79 μ M standard. All treatments were applied in 3 replicates. Additionally, three untreated bottles served as controls. Bottles were then incubated at 4°C and 35 μ mol quanta m⁻² s⁻¹ during a 12h light:dark cycle. Time steps for measurements were 0, 2, 4 and 7 days. Parameters of measurements were TEP, CHO/DCHO, chl-a, total dissolved Fe and total Fe concentration, glucosidase activity (measured by J. M. Arrieta), flow cytometry (measured by M. Dibbern) and PAM fluorometry. Additionally, water was sampled for later phytoplankton counts using Utermöhl techniques.

Incubation II: Seawater was collected at station 427 from 30 and 40m depth. Additions of 0.5 and 1 nM Fe(III) were made and bottles were incubated under similar conditions as described for incubation I. Additionally to the parameters of incubation I, samples for Fe speciation were taken and frozen at -20°C until later analysis.

Incubation III: A combination of iron and ligand additions was made to water originating from 20-50m depth at station 546. Glucaric acid 1,4-lactone was added to a final concentration of 1.3 μ M. As a second treatment 1.3 μ M additions of Glucaric acid 1,4-lactone were combined with 1.0 nM additions of Fe(III). Parameters of measurements were TEP, CHO/DCHO, chl-a, Fe speciation, total dissolved Fe and total Fe concentration. The incubation time was 24h.

Incubation IV: Seawater was sampled at station 553 from 20-60m depth. Glucaric acid 1,4-lactone and Desferrioxamine-B (a trihydroxamate siderophore) were added to final concentrations of 1.3 μ M and 1.0 μ M respectively. After the T₀ samples, TEP, CHO/DCHO, chl-a, Fe speciation, total dissolved Fe and total Fe concentration samples were taken after an incubation time of 48h.

Fe measurements of incubation samples

Total dissolved iron (0.2 μ m filtered) and total iron values (unfiltered) were determined on board using a flow injection technique with in-line pre-concentration on a chelating resin followed by chemiluminescence detection (FIA-CL) as described in the previous section by Croot et al.. Further, iron speciation samples were taken and immediately frozen at -20°C for later analysis using cathodic stripping voltammetry (Croot and Johansson 2000) in the trace metal laboratory at IFM-GEOMAR, Kiel.

chlorophyll-a measurements

Chlorophyll-a content of incubation samples was determined fluorometrically after acetone extraction of the material collected on a GF/F filter. For a detailed description see Claas et al, this issue. The filtration volume varied from 200 to 600 ml depending on the time steps during the incubations and thus according to biomass.

Utermöhl samples

For phytoplankton enumeration 90ml of sample was mixed with 10 ml Formalin (20%) and stored at 4°C in light shaded bottles. Samples will be processed at the AWI, Bremerhaven, applying traditional Utermöhl techniques. Preliminary results and discussion The depth profiles of TEP samples analyzed from CTD casts during ANT XXI-3, are summarized in Table 8.1. The data presented in this report are considered preliminary and are subject to modification after further analysis.

The total TEP concentrations in seawater progressively increased with the developing phytoplankton bloom over the course of the iron fertilization experiment. To examine the effect of iron fertilization on polysaccharide exudation and TEP formation by phytoplankton we examined the TEP:chl-a ratio. Shown as an example from 60m depth the TEP:chl-a ratio is plotted over time in Figure 1. As a response to fertilization the ratio first increases for 2 days and then gradually decreases over the course of the experiment until the bloom diminishes and thus the dying cells again release increased amounts of TEP forming polysaccharides into the water. This trend needs to be checked later after the analysis of the CHO/DCHO samples for the influence of the potential TEP precursors. The data suggest that TEP formation could be influenced by the concentration or bioavailability of iron in seawater. The increase of the TEP:chl-a ratio after the first infusion may be interpreted as a result of an immediate phytoplankton response to the sudden availability of iron. This may result in increased TEP as initially cells increase their photosynthesis rates with the addition of the iron but still leak considerable newly fixed carbon back to the seawater as DOC. As trace metals bind to gel like structures such as TEP, it is hypothesized that the bioavailability of iron in seawater may be enhanced by this process. Later on fresh healthy cells from the developing phytoplankton bloom will be less leaky and thus the production of the TEP precursor compounds per unit biomass will decrease. The increase in the TEP:Chl-a ratio near the end of the experiment may be from a combination of processes such as cell death, resumption of iron limitation and/or grazing by zooplankton as the bloom declines, all of which may increase the concentration of TEP precursor compounds. Total iron and total dissolved iron measurement results are preliminary at this stage and measurements of iron speciation, which are particularly important for this analysis, will be carried out at the IFM-GEOMAR upon return of the frozen samples from the cruise.

Interpretation of the results from incubation experiments is awaiting further laboratory analysis. These results will be used to verify the observations from the field sampling and will enhance our understanding of the iron binding capacity of TEP. The final assessment will be completed within the following months at the IFM-GEOMAR Kiel and the AWI, Bremerhaven.

Acknowledgments

The authors express their thanks and appreciation to M. Öztürk, K. Bluhm and M. Schmidt for their help and discussions during the cruise. Special thanks also to the chief scientist V. Smetacek as well as to the crew of the R.V. Polarstern.

References

- Croot, P.L., Johansson, M., 2000. Determination of iron speciation by cathodic stripping voltammetry in seawater using the competing ligand 2-(2-thiazolylazo)-p-cresol (TAC). *Electroanalysis* 12, 565-576.
- Passow, U., 2002. Transparent exopolymer particles (TEP) in aquatic environments. *Progress in Oceanography* 55, 287-333.
- Passow, U., Alldredge, A.L., 1995. A dye-binding assay for the spectrophotometric measurement of transparent exopolymer particles (TEP). *Limnology and Oceanography* 40, 1326-1335.

Summary of stations sampled for TEP and CHO/DCHO during ANT XXI-3

Station #	Depths (m)	Comment
420	5, 30, 40, 50, 60, 80, 90, 100, 120, 150, 200	eddy 1, T_0 station, Incubation Experiment I
424	20, 30, 40, 60, 80, 90, 100, 120, 150, 200	eddy 2, T_0 station
426	10, 20, 40, 60, 80, 110, 150	Inc. Exp. II at subsequent station 427
452	30, 65, 100, 150	
464	10, 20, 60, 100, 150	
466	10, 20, 50, 60, 90	
474	10, 20, 40, 60, 80, 100, 150	
508	10, 20, 40, 60, 80, 100, 120, 150, 200	
509	10, 20, 40, 60, 80, 100, 120, 200	
511	10, 20, 40, 60, 80, 100, 120, 150, 200	
513	10, 20, 40, 60, 80, 100, 120, 150, 200	
514	10, 20, 40, 60, 80, 100, 120, 150, 200	
543	20, 40, 60, 80, 100, 120, 150, 200	
544-56	10, 20, 40, 60, 80, 100, 120, 150	cast 56 of 48h drift station
546	10, 20, 40, 60, 80, 100, 120, 150, 200	Incubation Experiment III
553	10, 20, 40, 60, 80, 100, 120, 150, 200	Incubation Experiment IV
570	10, 20, 40, 60, 80, 100, 120, 150, 200	
591	10, 20, 40, 60, 80, 100, 120, 150, 200	

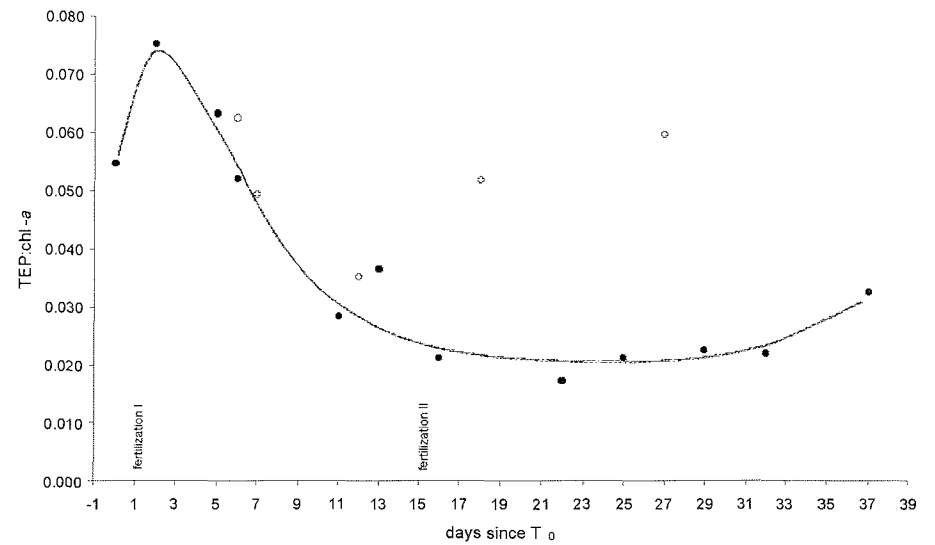


Figure 8.1: The progression of the TEP : chl-a ratio at 60m depth over the course of the iron induced phytoplankton bloom (plotted in days since the first infusion, T_0). TEP values used are arbitrary units (absorption). The closed circles represent samples from stations within the fertilized patch. Open circles symbolize data originating from stations outside the fertilized patch. The outside stations from days 7 and 12 are likely influenced by the iron fertilization. They possessed elevated iron and chlorophyll values which were more representative of the water-mass within the fertilized patch. The dashed line illustrates the trend of the TEP : chl-a ratio, being elevated shortly after infusion, clearly decreasing over the course of the developing bloom and rising again with the decay of the phytoplankton biomass.

9. CO₂-SYSTEM MEASUREMENTS DURING EIFEX

R. Bellerby, C. Neill (UIB), L. Mkatshwa, C. Balt (UCT)

Objectives

Micronutrient supplementation experiments have shown that the addition of iron to the surface ocean can, especially in HNLC regions, increase the CO₂ uptake of phytoplankton. A limited number of iron addition experiments have been conducted in the Southern Ocean and these have all induced a significant carbon drawdown from the atmosphere. However, uncertainty remains on the long term efficiency of such a carbon pumping mechanism. Short term carbon atmospheric carbon uptake has not categorically been shown to equate to sustained export production and thus be an efficient conduit for long term sequestration of atmospheric carbon to the deep ocean.

In light of the uncertainty in the fate of the increased atmospheric carbon uptake, it was the aim of this study to further knowledge into the rates, transports and fates of iron induced carbon uptake. This study not only studied the "traditional" picture of the CO₂ system – surface carbon exchange from ship based fCO₂ measurements and the carbonate system from discrete measurements, but monitored, for the first time, the CO₂ and O₂ characteristics *in situ* from moored instrumentation to provide high density information on the diurnal and short term CO₂ uptake ecosystem response.

Work at Sea

Total carbon dioxide (C_T) analyses were made in both discrete and underway mode by the coulometric titration method using a SOMMA system with gas loop calibration and comparison against certified reference materials (CRM) from Prof. Andrew Dickson. The TCO₂ measurements of CRM material generally agreed to better than 3µmol.kg⁻¹.

Total alkalinity was determined from discrete samples by potentiometric titration using the VINDTA instrument (Versatile Instrument for the Determination of Titration Alkalinity). The standardization is done the same way as the TCO₂ samples, running a CRM in the beginning and two duplicates per station and finishing with a CRM.

The fugacity of carbon dioxide (fCO₂) was measured on-line from the ship's seawater supply and air-intake from the crow's nest using a Li-Cor based method every 1 minute with calibration against 4 standard gases which in turn have been calibrated against NOAA/CMDL standard gases.

In situ pCO₂ was determined using SAMI-CO₂ instruments at 35 and 150m. The instruments were deployed on the patch mooring with appropriate re-deployments to maintain the quasi-centrality of the buoy in the fertilised patch.

Oxygen optodes were used both in underway laboratory mode in parallel with fCO₂ measurements and with complimentary CTD sensors on the central mooring in conjunction with the pCO₂ sensor at 35m. Winkler calibrations were performed on samples from the ships underway seawater supply and from discrete rosette samples when the CTD was taken close to the buoy.

Preliminary results

Fugacity of carbon dioxide

A comprehensive data set was obtained for surface seawater fCO₂ from the subtropics to the Antarctic Zone with emphasis on the Polar Frontal Zone. Included in the data set is a very detailed study of two eddies south of the Polar Front. Central to the EIFEX study was the continuous monitoring of the fCO₂ during the iron fertilisation study. Once the iron induced bloom had started and CO₂ drawdown had exceeded the very small ($\pm 2\text{ atm}$) natural variation within the fertilised eddy, real-time fCO₂ measurements were used to steer the cruise track in and out of the eddy. In total over 41,000 seawater fCO₂ measurements

were taken. Figure 9a shows the drawdown of CO₂ in the eddy compared to the unfertilised background corresponding to a change from ambient of about 30_atm (360 to 330_atm).

Total inorganic carbon and Total Alkalinity

Discrete measurements of C_T were taken regularly from samples from the CTD casts. Measurements were made within 24 hours of collection. The addition of iron was followed by a significant drawdown in mixed layer CT. Figure 9b shows the temporal development of the C_T profile over the first 16 days following fertilisation. No significant change in nitrate normalised total alkalinity was observed suggesting that none or very little calcification took place throughout the study.

Oxygen and in situ pCO₂ measurements

No data has as yet been processed from these systems.

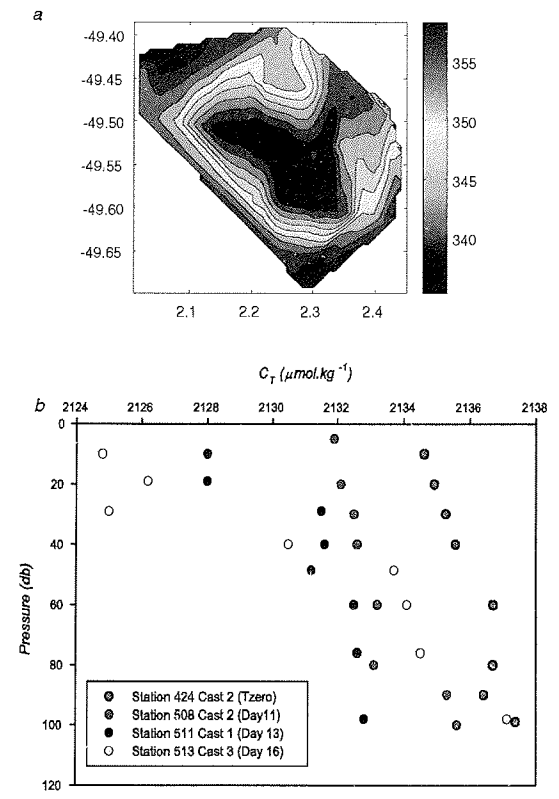


Figure 9a shows the drawdown of CO₂ in the eddy compared to the unfertilised background corresponding to a change from ambient of about 30 μatm (360 to 330 μatm). Figure 9b shows the temporal development of the CT profile over the first 16 days following fertilisation.

10. CHLOROPHYLL A, PARTICULATE AND DISSOLVED CARBON, NITROGEN

C. Klaas, M. Schmidt, A. Terbrüggen, D. Wolf-Gladrow (AWI)

1. Introduction:

The purpose of this study is to establish the evolution of the plankton community following the iron fertilization in the mixed layer. Measurements of Chlorophyll a (Chla) was carried out at discrete depth intervals ranging from 5 to 250 m at stations inside and outside the fertilized patch from the beginning to the end of the experiment. Chla concentrations were also determined at 15 minutes to 3 hour intervals in surface water collected from the ship's pump. In addition, the fate (export and remineralization) of particulate organic matter and biominerals will be determined by following the time evolution of deep profiles (100 m to 3000 m depth) of POC, PON, Biogenic silica (BSi) and calcium carbonate (CaCO_3) combined with heterotrophic activity measurements (O_2 evolution in incubation experiments carried out by G. Herndl).

2. Material and Methods:

Water samples for Chla determination were filtered onto 25 mm diameter GF/F filters at pressures not exceeding 200 mbar. Filters were immediately transferred to centrifuge tubes with 10 ml 90% acetone and 1ccm of glass beads. The tubes were sealed and stored at -20°C for at least 30 min and up to 24 hours. Chla was extracted by placing the centrifuge tubes in a grinder for 3 min followed by centrifugation at 0°C . The supernatant was poured in quartz tubes and measured for Chla content in a Turner 10-AU fluorometer. Calibration of the fluorometer was carried out at the beginning and at the end of the cruise following the JGOFS protocol procedure [Knap et al., 1996]. Results of the fluorometer calibration diverged by 5% between beginning and end of the cruise. Chla content was calculated using the equation given in Knap et al. [1996] using average parameter values from the two calibrations. Measurement uncertainty was estimated from triplicate water samples taken from depths ranging between 10 and 100 m depth and averaged 5% of measured values. 5 to 30 L seawater samples were filtered onto 25 mm diameter pre-combusted GF/F filters and onto 47 mm diameter polycarbonate filters for POC and PON analysis and BSi and CaCO_3 analysis, respectively. After filtration filters were dried overnight at 50°C and stored into pre-combusted glass petri dishes and HCL-cleaned plastic (PP) eppendorf tubes, respectively. Filter samples were stored frozen (-20°C) for further analysis on land.

3. Results:

Horizontal and vertical evolution of Chla distribution measured on board during the experiment is given in figures 10.1 and 10.2. At the beginning of fertilization strong patchiness in Chla distribution was found, with values ranging from 0.5 up to $1.2 \mu\text{g Chla l}^{-1}$, indicating a spring-summer bloom in the region (Fig. 10.1a). Larger phytoplankton ($> 20 \mu\text{m}$) constituted an important fraction (43 %) of the Chla standing stocks at the beginning of the experiment (Fig. 10.2c).

Because of the patchy distribution of Chla in the area, significant differences between in patch and out patch were observed from about day 10 after fertilization (Fig. 10.1 and 10.2). During the experiment a decrease in Chla concentrations outside the fertilized patch was observed (Fig. 10.2b) together with a decrease in size composition of the phytoplankton community (Fig. 10.2c). The opposite trend was found inside the fertilized patch (as determined from photosynthetic efficiency measurements) with an increase of Chla concentrations up to $3.16 \mu\text{g l}^{-1}$ and values over $2 \mu\text{g l}^{-1}$ extending down to 100 m depth on day 23 after fertilization (Fig. 10.2a). The size composition of the assemblage inside the patch did not show a significant trend during the experiment (Fig. 10.2c) and large cells constituted an important fraction of total Chla standing stocks.

4. References:

Knap, A., A. Michaels, A. Close, H. Ducklow and A. Dickson (eds.). 1996. Protocols for the Joint Global Ocean Flux Study (JGOFS) Core Measurements. JGOFS Report Nr. 19, vi+170 pp. Reprint of the IOC Manuals and Guides No. 29, UNESCO 1994.

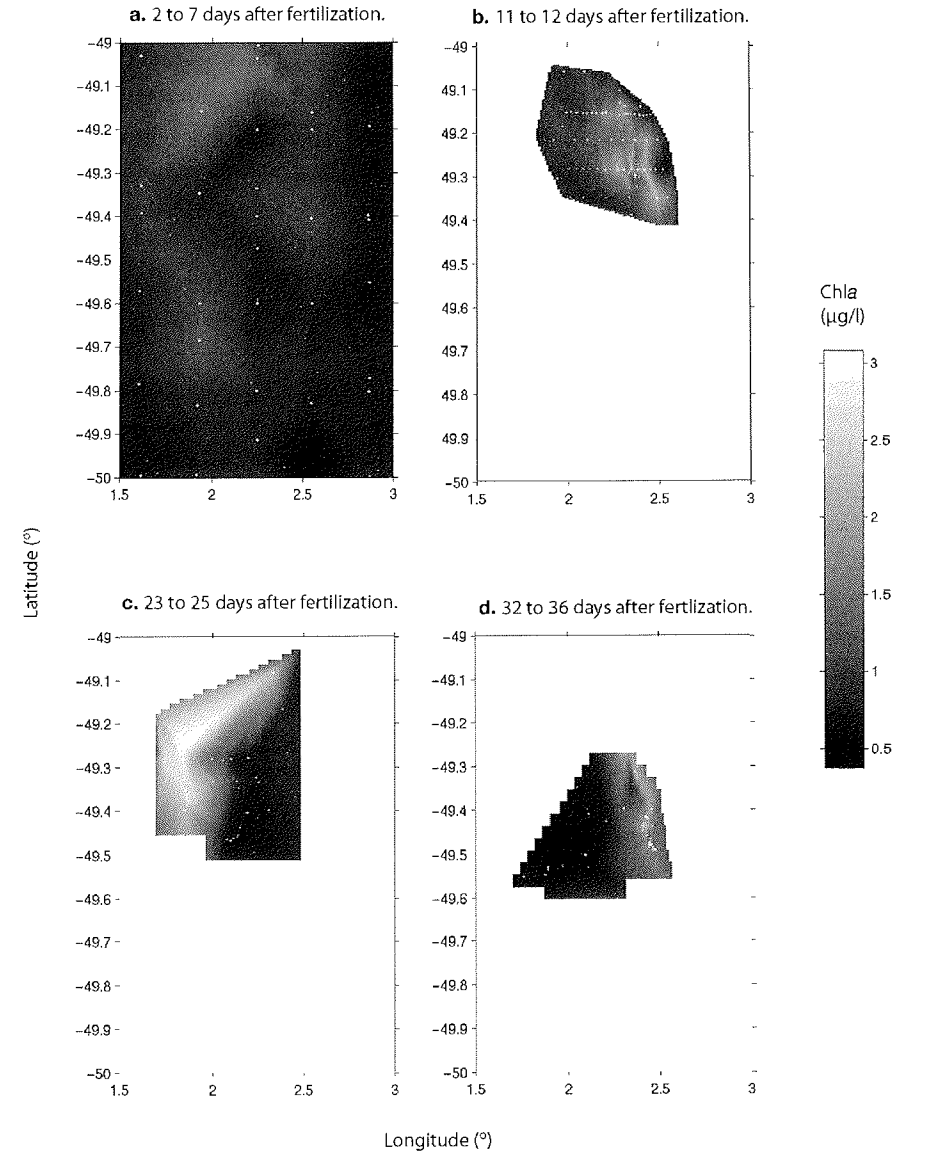


Figure 1. Evolution of surface Chla distribution from day 2 to day 36 after fertilization.

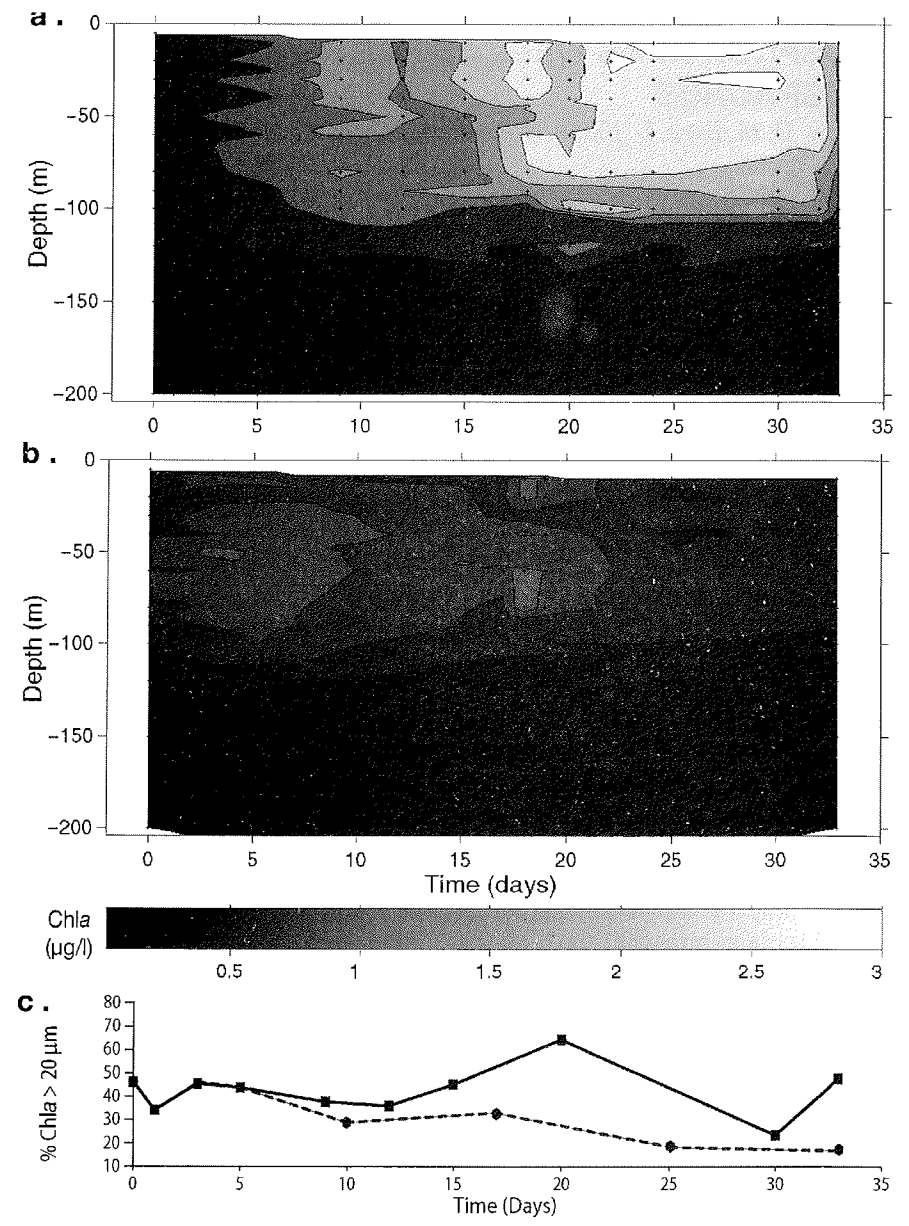


Figure 2. Temporal evolution of vertical profiles of Chla. **a:** inside the fertilized patch, **b:** outside the fertilized patch. **c:** % fraction of Chla larger than 20 μm (squares and full line indicate in-patch station, hexagons and dotted-line indicate out-patch stations).

11. DISSOLVED CARBON, NITROGEN AND PHOSPHORUS AS WELL AS PARTICULATE PHOSPHORUS

Passow, U; M. Berg; C. Klaas; M. Schmidt; A. Terbrüggen; (AWI)

1. Introduction:

The goal of these measurements was to contribute to an elemental budget and describe the cycling of the various elements in the dissolved organic phase. Sampling for particulate organic phosphorus (POP), dissolved organic carbon (DOC), nitrogen (DON) and phosphorus (DOP) determination were carried out at discrete depth intervals ranging from 5 to 250 m at stations inside and outside the fertilized patch during the whole experiment. Samples were filtered from the same depths as the POC/PON samples. Towards the end of the fertilization time course, particulate matter started to sink out of the surface layer. Several deep profiles going down to the bottom (3000-4000 m) were sampled for particulate organic matter including POP and processed as described above.

2. Material and Methods:

One to two liters of seawater samples were filtered onto 25 mm diameter GFF filters and stored in plastic (PE) petri dishes for POP analysis. About 100 ml samples for DOC, DON and DOP were filtered at low pressure through 25 mm diameter pre-combusted GFF filters using a pre-cleaned all-glass filtration unit. Pre-cleaning of glassware consisted of acid washing (10% HCl and copious rinsing with deionized water) followed by combustion at 450°C for 1 h. The filtrate was collected directly into pre-combusted glass ampoules for DOC determination and into plastic (PE) vials for DON and DOP determinations. The procedure was repeated 3 times in order to rinse the vials and the filtration unit, keeping only the last 100 ml filtrate for analysis. Samples were stored frozen (-20°C) for later analysis.

DOC will be determined by high temperature combustion (Sharp 1973, Mar. Chem. 1, 211-229). DON and DOP will be measured simultaneously using a nutrient analyser (Valderrama 1981, Mar. Chem. 10, 109-122). A potassium persulfate, boric acid and sodium hydroxide mix is used as the oxidizing reagent for the digestion of both nitrogen and phosphorus. Both organic ((-)-Adenosine 3',5'-cyclic monophosphate hydrate, AMP) and inorganic standards will be run daily to provide a constant check, and the organic standards will be used for the calibration. The onboard digestion of nitrogen and phosphorus was not successful due to the incomplete closure of a significant proportion of the sample vessels prior to oxidation under high temperature and pressure

References

- Sharp, J. H. 1973 Total organic carbon in seawater-comparison of measurements using persulphate oxidation and high temperature combustion. Mar. Chem. 1:211-229

Valderrama, J. 1981, The simultaneous analysis of total nitrogen and total phosphorus in natural waters. Mar. Chem. 10, 109-122

12. NUTRIENT MEASUREMENTS DURING EIFEX

M. Jäger, A.M. Webb, L. Hoppe (AWI)

The concentrations of the nutrients ammonium, nitrate, nitrite, phosphate and silicate in seawater were determined using a Technicon II autonanalyzer. Samples were taken of seawater pumped to the lab while the ship was underway. The pump's inlet was at about 8 meters below the surface. The underway samples were collected at a rate of about one every 30 minutes. Sub-samples were also taken from samples collected with the CTD, GOFLO and Snatcher. Results of the underway gridding were initially used to find a suitable eddy. It was planned to fertilise an eddy which had its origin south of the Polar front and had spun off to a position north of the Polar front. Such an eddy would have relatively high silicate concentrations, which would be necessary for the growth of the phytoplankton diatoms. The first eddy investigated had been seen on satellite altimetry. This eddy was found to have a surface silicate concentration of around 28 $\mu\text{mol/l}$. This value was relatively high and deemed more than adequate for unlimited growth of the diatoms for the size of bloom expected. Unfortunately, this eddy did not have a large enough seeding stock of diatoms. After fertilising the eddy the experiment moved to the next eddy, which had been seen further east in the altimetry.

In order to find the core of the second eddy, several long transects were executed and nutrients were measured in the surface waters. Then a better overall picture of the surface waters of the eddy centre was achieved by adopting a tighter sampling pattern. Silicate concentrations for the initial long transects and of the compact pattern are displayed in figure 12.1. The higher concentrations in the south east ($50^\circ\text{S}, 3^\circ\text{E}$) show that the eddy was oval in shape. The assumed core of the second eddy had silicate concentration at the surface of around 19 $\mu\text{mol/l}$. Although this value was lower than the first eddy it was still relatively high. The eddy was north of the polar front, and the surface waters surrounding the eddy had silicate concentrations of between 4 and 10 $\mu\text{mol/l}$. The other nutrients measured at the surface of the core of the eddy were: nitrate 24.9 $\mu\text{mol/l}$; nitrite 0.2 $\mu\text{mol/l}$; phosphate 1.8 $\mu\text{mol/l}$ and ammonium 0.6 $\mu\text{mol/l}$. The seeding stock of phytoplankton in the second eddy was more suitable to the experiment. This eddy was fertilised with iron sulphate and the focus of the experiment remained on this second eddy.

The iron fertilization created a significant bloom in the phytoplankton. A bloom needs nutrients to grow and survive. Comparing the nutrient concentrations before fertilisation with the concentration of the last station 5 weeks later we saw that there was a significant uptake of nutrients. The total decrease in silicate concentration in the mixed layer was about 10 $\mu\text{mol/l}$. Nitrate concentration decreased by about 1.5 $\mu\text{mol/l}$, and phosphate by about 0.1 $\mu\text{mol/l}$.

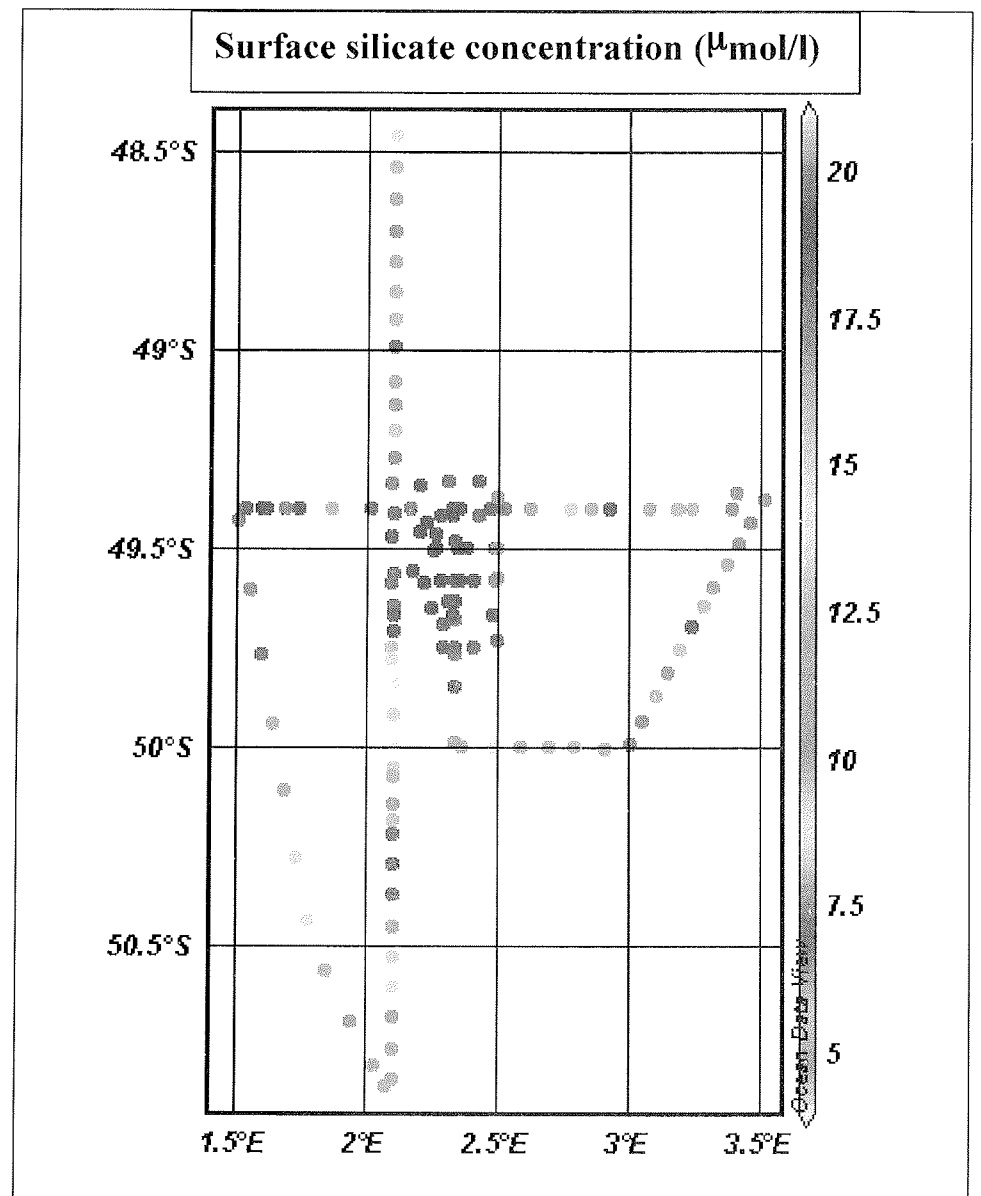


Figure 12.1: silicate concentrations at surface of second eddy before fertilisation

13. EXPORT PRODUCTION AND MESOPELAGIC REMINERALIZATION DURING EIFEX

N. Savoye (VUB), I. Vöge and J. Friedrich (AWI)

Export production

^{234}Th deficit is classically used to estimate particulate organic carbon (POC) and biogenic silica (BSi) export. During Eifex, a peculiar effort has been given to vertical and time resolution sampling for total (i.e. particulate + dissolved) ^{234}Th using two methods and to the determination of POC: ^{234}Th and BSi: ^{234}Th ratios on 'sinking' particles using several approaches. Total ^{234}Th has been sampled every 2 to 5 days within the Fe-fertilized patch and every 10 days out of the patch, with a vertical resolution of 15 samples between surface and 800-1000m. In order to assess POC: ^{234}Th and BSi: ^{234}Th ratios, particles have been caught using (1) regular Niskin bottles, (2) plankton nets, (3) Marine Snow Catcher, (4) flow through centrifuge, and (5) sediment traps. Part of the sampling and of the analyses was and will be done in collaboration with U. Bathmann, M. Berg, J. Henjes, P. Assmy, M. Rutgers van der Loeff, C. Hanfland and W. Geibert (AWI, Germany), and J. Navez and F. Dehairs (VUB, Belgium). ^{234}Th activity was measured on board. The results presented here (Fig. 13.1 to 13.3) are preliminary will be refined after beta background counting and ^{234}Th recovery calculation at home lab.

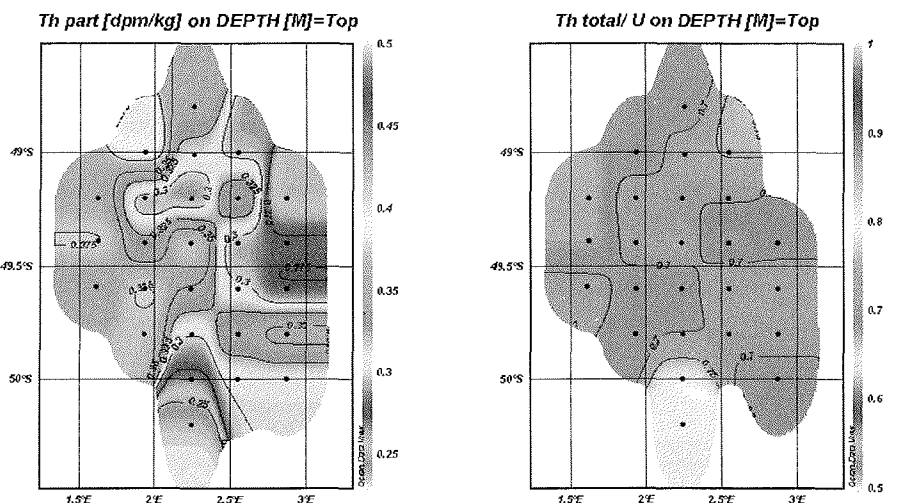


Figure 13.1: mapping the eddy: particulate ^{234}Th activity (left panel) and ^{234}Th deficit (right panel) in surface waters.

The study area was mapped just after the first Fe-infusion. From the ^{234}Th point of view it appears that the initial conditions were rather stable with ^{234}Th deficit of ca 70% and particulate ^{234}Th activity accounting for ca 20% of total activity

(Fig. 13.1). ^{234}Th activity profiles in the course of the experiment are reported on Fig. 13.2. Results indicate that in the patch ^{234}Th activity in the upper 100m first increased between day -1 (i.e. 1 day before Fe-infusion) and day 9 (i.e. 9 days after Fe-infusion), stayed stable between day 9 and day 23, increased again until day 28, but then decreased between day 30 and day 36. Out of the patch, ^{234}Th activity stayed roughly constant between day -1 and day 25 and then decreased between day 25 and day 34. Note that the high ^{234}Th activity of day 10 out-patch may be due to a sampling in a different water mass compared to other days.

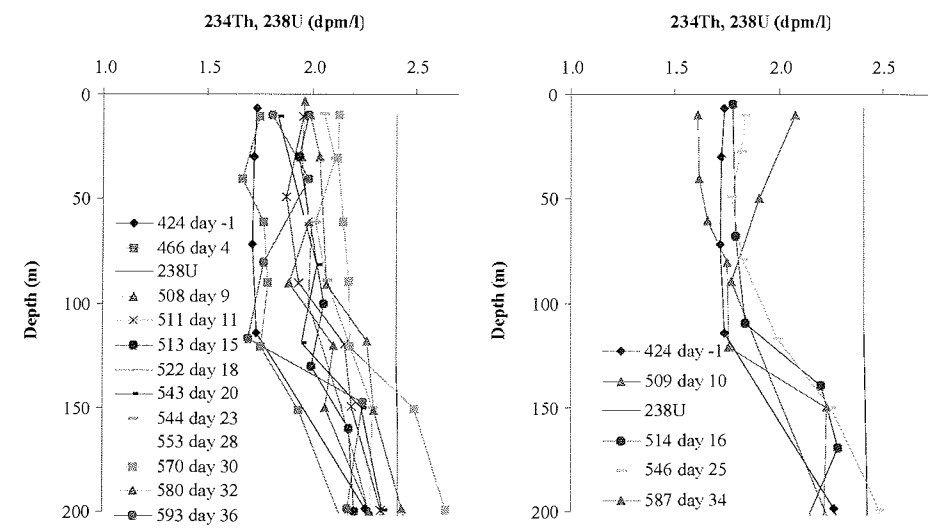


Figure 13.2: ^{234}Th and ^{238}U activities in (left panel) and out of (right panel) the Fe-fertilized patch.

^{234}Th fluxes (Fig. 13.3) have been calculated using a non-steady state model. These estimates indicate that the ^{234}Th fluxes were usually low or moderate (< 2000 dpm/m²/d), except (1) between ~day 10 and day 20 where values of ca 4000 dpm/m²/d were calculated for 100m and/or 200m in and out patch, and (2) at the end of the experiment with values of 4200 and 6500 dpm/m²/d out-patch at 100 and 200m, respectively, and with values of 10300 and 15400 dpm/m²/d in-patch at 100 and 200m, respectively.

The comparison of ^{234}Th activity and fluxes between in- and out-patch seems to indicate that the addition of Fe first reduced the vertical flux of particles by feeding surviving phytoplankton, and then strongly increased this flux because of the increase of phytoplankton biomass.

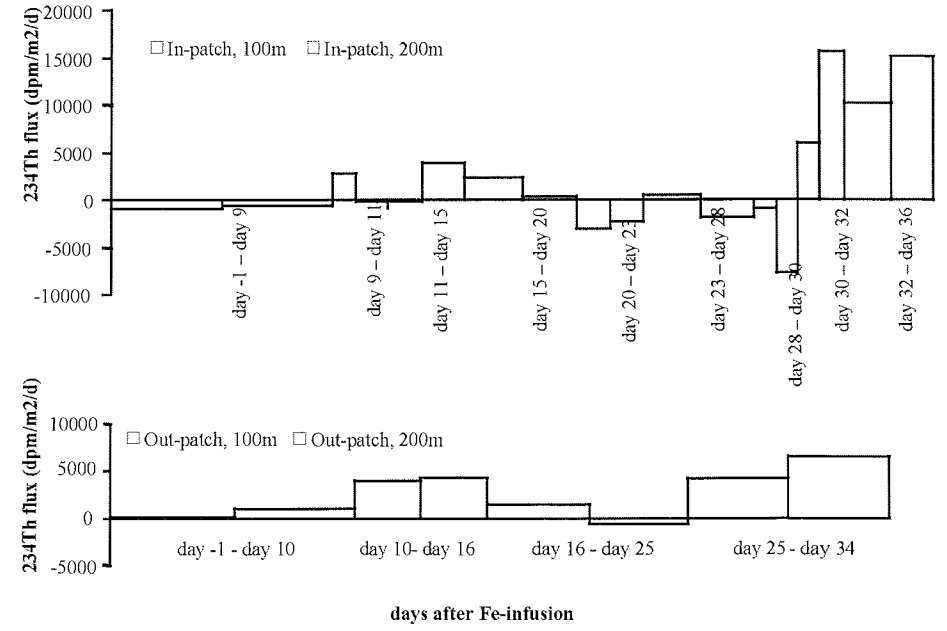


Figure 13.3: ^{234}Th fluxes at 100 and 200m in- and out-patch.

Remineralization in the twilight zone

Biogenic particulate Ba (Ba_{xs}) can be used to estimate organic carbon mineralization in the twilight zone (~100-500m) using a transfer function that involves Ba_{xs} stock, O_2 consumption and C mineralization. The Ba cycle has been studied during Eifex: dissolved and particulate Ba were sampled from surface to 1000m depth and acantharians from the mixed layer were isolated. The estimation of mesopelagic C remineralization from Ba_{xs} data will be compared with the results of O_2 consumption experiments (collaboration with G. Herndl, NIOZ, Netherlands) and the role of acantharians in the Ba cycle assessed (collaboration with J. Henjes, AWI, Germany). Ba analyzes will be performed in collaboration with D. Cardinal (RMCA, Belgium), and with S. Jacquet and F. Dehairs (VUB, Belgium).

^{234}Th excess in the mesopelagic layer has been described recently as a proxy of particle remineralization. ^{234}Th has been sampled and counted during Eifex as described above. Data need to be refined (see above) before being interpreted.

Silicon stable isotopes

Filtered seawater has been sampled for silicon stable isotope analysis of silicate, complementary to particulate biogenic silica sampled for silicon isotope (D. Wolf-Gladrow, AWI, Germany). Silicate stable isotopes will be analyzed by D. Cardinal (RMCA, Belgium).

14. PARTICULATE AND DISSOLVED MATERIAL AND NUCLEIC ACID CONTENT DURING THE IRON FERTILIZATION EXPERIMENT EIFEX

G. M. Berg, M. Mills, A. Terbrüggen, I. Benner (AWI)

Introduction

The goal of this work is 1) to trace the fraction of upwelled nutrients in the Southern Ocean that is consumed by phytoplankton upon relief of Fe limitation, and 2) to trace the fraction of phytoplankton biomass with newly incorporated nutrients that subsequently sinks out of the water column and is entrained in deeper water masses. Our approach is to combine nitrogen and carbon stable isotope measurements to identify nutrient sources and sinks in dissolved and particulate pools and to mass balance nutrient flows. In addition, nutrient utilization by diatoms is examined through quantification of nucleic acids coding for nutrient transporter genes. The combination of stable isotope measurements, which are time-integrated, with measurements of gene expression, which is instantaneous, will provide a context for the examination of the physiological mechanisms responsible for the nutrient utilization during the Fe fertilization experiment.

Materials and Methods

Particulate samples:

Samples for analysis of particulate organic carbon (POC) and nitrogen (PON) content and stable isotopes ($d^{13}\text{C}$) and ($d^{15}\text{N}$) were filtered at discrete depth intervals between 5-200 m at in-patch and out-patch stations. Depending on the water column biomass ($0.7\text{-}3.0 \mu\text{g Chl a l}^{-1}$), between 5 and 2 liters were filtered through a pre-combusted Whatman GF/F glass fiber filter. The filters were dried overnight at 50°C and stored dry in combusted glass Petri dishes until mass spectrometric analysis. Duplicate samples were taken for calculation of sampling precision at regular intervals. All four parameters were measured on the same filter. Samples for determination of $d^{15}\text{NH}_4^+$ and $d^{15}\text{NO}_3^-$ were filtered through pre-combusted GF/F filters at low pressure using an acid pre-cleaned teflon and glass system. Duplicate samples were taken at regular intervals for precision analysis. The $d^{15}\text{NO}_3^-$ samples were acidified to $\text{pH} < 2$ with $5 \mu\text{l ml}^{-1}$ 50% phosphoric acid and stored refrigerated in the dark until analysis using the ammonia diffusion method (Sigman et al. 1999). The $d^{15}\text{NH}_4^+$ samples were stored frozen until analysis (Holmes et al. 1998). Samples for $d^{15}\text{N-DON}$ were filtered through $0.2 \mu\text{m}$ polycarbonate filters and stored frozen until ultrafiltration using a 1kDa membrane prior to analysis.

Nucleic acids:

Samples for nucleic acids (RNA extraction) were filtered onto precombusted GF/F and/or Durapore (Millipore) membranes and stored frozen at -80°C in RNAlater (Ambion) nucleic acid preservation solution according to manufacturer's recommendations.

Results

Particulate samples:

A subset of the particulate samples have been analyzed at the time of this report. The $d^{15}\text{N}$ values are low (0 to $-1\text{\textperthousand}$) indicative of either a high fractionation factor for NO_3^- uptake or a reliance on NH_4^+ uptake by the community.

Gene expression:

The quantification of specific RNA transcripts will be performed in conjunction with monoculture growth experiments of diatoms isolated during the EIFEX cruise to isolate and sequence the NO_3^- transporter genes.

References

- Holmes, R. M. et al. 1998. Measuring $^{15}\text{N}-\text{NH}_4^+$ in marine, estuarine and fresh waters: An adaptation of the ammonia diffusion method for samples with low ammonium concentrations. Mar. Chem. 60:235-243
- Sigman, D. M. et al. 1999. The $d^{15}\text{N}$ of nitrate in the Southern Ocean: consumption of nitrate in surface waters. Glob. Biogeochem. Cycles 13:1149-1166
- Valderrama J.C. 1981. The simultaneous analysis of total nitrogen and total phosphorus in natural waters. Mar. Chem. 10:109-122

15. ALGAL PHYSIOLOGY AND BIOOPTICS

Rüdiger Röttgers, Franciscus Colijn & Meike Dibbern (GKSS)

Introduction

It is well known that iron-limited planktonic algae are responding physiologically to iron addition considerably fast on times scales of only a few day or even hours. Variable chlorophyll fluorescence techniques has been used to investigate these physiological changes as well as to simply distinguish iron-replete from iron-depleted cells. A simple goal of our measurements was to track the iron-enriched water patch by a surface water flow-trough system using Fast-Repetition-Rate-Fluorescence (FRRF) techniques.

Beyond it different techniques were used to follow the photo-physiological changes of the phytoplankton occurring after iron addition and to estimate photosynthesis and primary production. This includes photoacclimation, i.e. effects of solar irradiance, vertical mixing of the water column and water transparency. In addition we were interested in the comparison of different variable chlorophyll fluorescence techniques and in using these different techniques to estimate primary production.

Methods and Sampling

All variable chlorophyll fluorescence techniques (PAM, Pump & Probe, FRRF) can be used to determine the quantum efficiency of photochemical energy

conversion in photosystem II (PSII). The maximum efficiency (F_v/F_m) is determined in the dark, after prolonged "dark adaptation", whereas the effective quantum efficiency ($(F_m' - F)/F_m'$) is determined under a constant irradiance levels. The FRRF techniques determines additional parameters, e.g. the functional absorption cross-section of PSII, which can not be determined by the other techniques. We used two FRRF instruments (FastTracka, Chelsea, UK). One instrument was set up as a flow-trough system measuring surface water taken from about 11m below the ship. The second instrument was connected to the CTD system on a water sampling rosette and was measuring depth-profile of the first 250m,. It was equipped with a PAR sensor which provides in situ irradiance data. We measured about 120 depth profiles during the whole cruise. Two Xe-PAM instruments (Walz, Germany) were located in a 4°C cooling container. One was used to measure with the Pulse-Amplitude Modulated (PAM) Fluorescence technique, the other one to measure with the Pump and Probe Fluorescence technique. At each station both instruments were used to determine F_v/F_m of samples taken from up to 10 different water depths, and to determine photosynthesis vs. irradiance curves from samples of up to six different water depths, by measuring $(F_m' - F)/F_m'$ at 10 different irradiances levels.

The radiocarbon (C-14) method and a photosynthetron was used to determine carbon-based photosynthesis vs. irradiance curves from six different samples at each station. At some station we determine total and dissolved photosynthetic production by filtering the incubated samples through 0.2 μm filter cartridges. We measured about 200 carbon-based P vs. E curves and about 300 P vs. E curve using the different variable fluorescence techniques.

To calculated carbon-based photosynthetic rates from variable-fluorescence-based rates we need information of the light absorption by the algae and about the in-situ irradiance conditions. Therefor about 200 samples were taken from the respective water depth, filtered and frozen to determine the particulate absorption spectra of the phytoplankton community. The in situ irradiance field was measured during a few station using a profiling spectral radiometer (Satlantic Instr.).

Results and Discussion

The flow-trough FRRF instrument was started three days after we left Cape Town (24. Jan 2004). F_v/F_m values were low from the beginning and between 0.25 and 0.38 during the whole cruise until we were approaching Cape Town again (22.–24. Mar 2004) these values were never exceeded, except in those waters where we added iron before (Figure 15.1). There were no clear differences in F_v/F_m between the different water masses (subtropical to polar). Hence, the whole Southern Atlantic seemed to be iron-limited during the late austral summer, a clear difference to the former EisenEx cruise which took place in the austral spring and showed low values only south of the Subantarctic Front. F_v/F_m values north of it were between 0.35 and 0.45 (Ber. Polarforschg. 400).

After the first iron release on 3rd of February we could observed slightly increased F_v/F_m values (~0.40) shortly after finishing the fertilisation when we

were heading west and probably crossed water which was fertilised a few hours before (see Figure 15.1).

The second time we found increased values a few days after fertilising the second patch at February the 14th (see Figure 15.1). Afterwards it was possible to find the fertilised patch by looking at the actual Fv/Fm values. The values were steadily increasing to up to 0.57 at March the 8th and then slightly decreasing again until the end of the cruise to about 0.49 (Figure 15.1).

We observed typical daily cycles of the quantum efficiency (Figure 15.2). The value increased from previous lower but constant night values to the highest value shortly after sun rise at surface irradiance level still below a few $\mu\text{mol photons m}^{-2} \text{s}^{-1}$, then the quantum efficiency decreased by non-photochemical quenching during the day following mainly the actual irradiance values and thereby reaching higher values again after sun set. This low-irradiance induced increase of Fv/Fm just before sun rise can be observed with all photoautotrophic organisms.

The in situ depth profiles showed higher values inside the fertilised patch, reaching values of up to 0.55 regularly and occasionally of up to 0.60, quite near the maximum values of ~0.65 (Figure 15.3). The values were considerably constant over the whole water column, showing that the observed mixed layer, which extended to a depth of about 100m was mixed rapidly since no fast photoacclimative response was visible. Two times during the cruise the wind speed slowed down and the surface mixed layer decreased to less than 50m. This had strong effects on the photo-physiology of the phytoplankton, which will be investigated further when all in situ data are analysed.

The determined chlorophyll a-specific maximum photosynthetic capacity (P^*_{\max}) was not observed to change significantly during the whole experiment and was similar inside and outside of the fertilised patch, perhaps because of a strong irradiance-dependent daily cycle which covers possible changes due to iron addition. P^*_{\max} varied between 0.9 and 3.8 $\mu\text{gC } \mu\text{gChl } a^{-1} h^{-1}$. During a daily cycle measured inside the fertilised patch (Figure 15.4), P^*_{\max} was low at the beginning of the first evening (2.0 – 2.4 $\mu\text{gC } \mu\text{gChl } a^{-1} h^{-1}$), then constant during the night and increased steadily during the following day, reaching higher values than at the day before (3.4 – 3.8 $\mu\text{gC } \mu\text{gChl } a^{-1} h^{-1}$). At the same time the surface irradiance was about 30% lower at the second day and has been more than 2 times higher on the day before. The photo-physiological response to the ambient irradiance is much more pronounced than that to iron addition.

DOC production at saturating irradiance was low and between 0.02 and 0.11 $\mu\text{gC } \mu\text{gChl } a^{-1} h^{-1}$, reaching only occasionally higher values of 0.14–0.22 $\mu\text{gC } \mu\text{gChl } a^{-1} h^{-1}$ (Figure 15.5). It was always lower than 10% (mean 4%) of the total production and near the detection limit.

We will further calculate primary production by modelling the in situ light conditions and using production data from the P vs. E measurements. Secondly day time FRRF depth profiles will be used to calculate primary production from variable fluorescence data alone. Both derived values of primary production will be compared to the results from on-deck incubations conducted by Ilka Peeken.

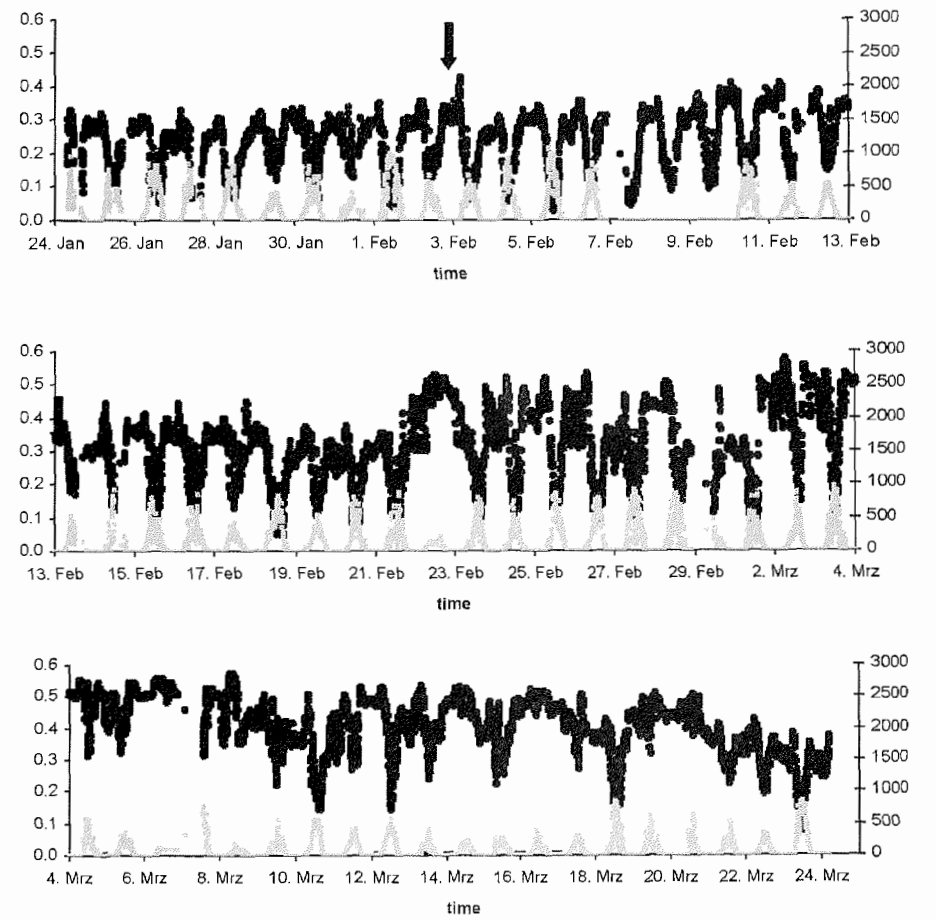


Figure 15.1. Time series of the quantum efficiency of PSII photochemistry (F_v/F_m , black dots) from the flow-trough FRRF system and the global radiation (grey dots) during ANT XXI/3. The first eddy fertilisation took place on February 2nd, the second one on February 12th. The black arrows mark the first time after the fertilisation when higher F_v/F_m values were observed.

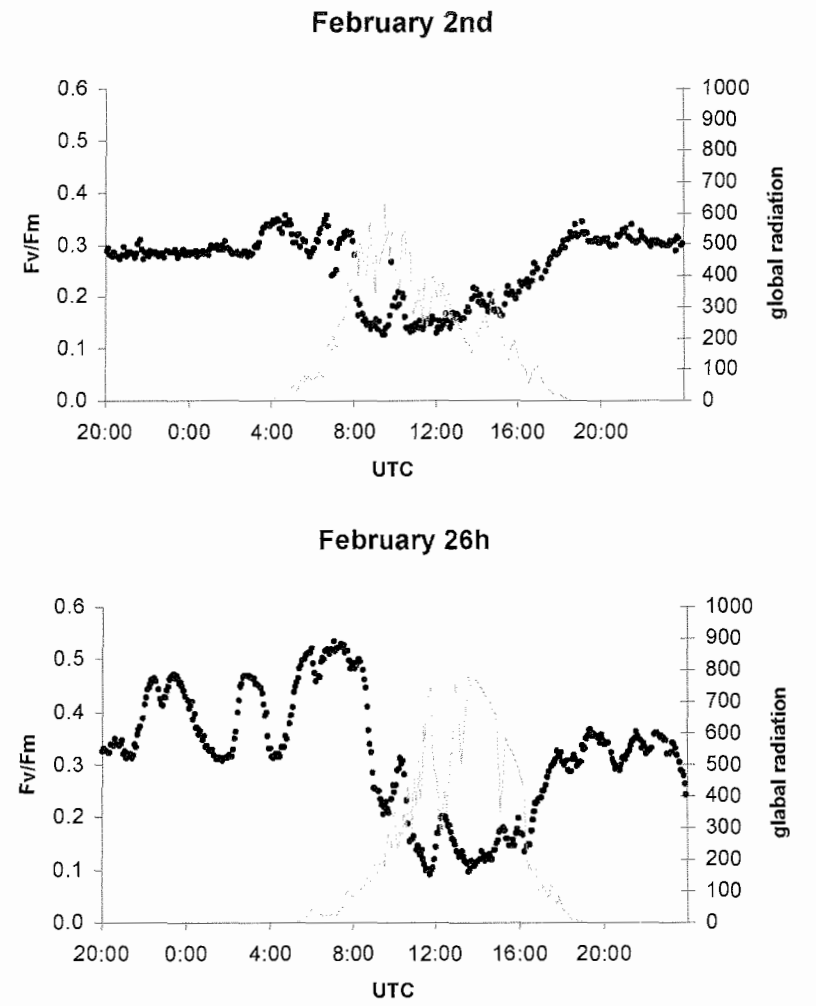


Figure 15.2. Two single day measurements of F_v/F_m (black dots) from the flow-trough FRRF system and the appropriate global radiation (grey) on days when the ship was steaming continuously. February 2nd was when the first iron fertilisation took place. A typical daily variation in F_v/F_m is visible with highest values shortly before sun rise and the decrease by non-photochemical quenching with increasing irradiance during the day. During February the 25th and 26th the ship was mapping the iron-fertilised patch. The typical daily cycle is superimposed by periodic changes of F_v/F_m when the ship was moving from outside into the patch and vice versa.

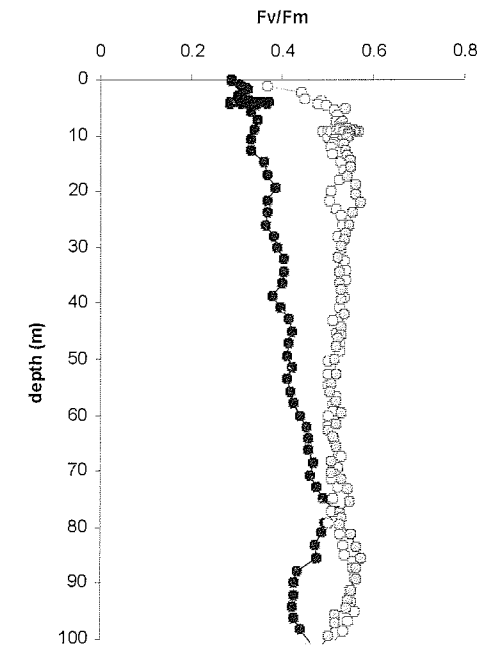


Figure 15.3. Vertical profile of the quantum efficiency (F_v/F_m) from three different cast. One outside of the fertilised patch (black dots) and two profile inside the patch (grey and open dots).

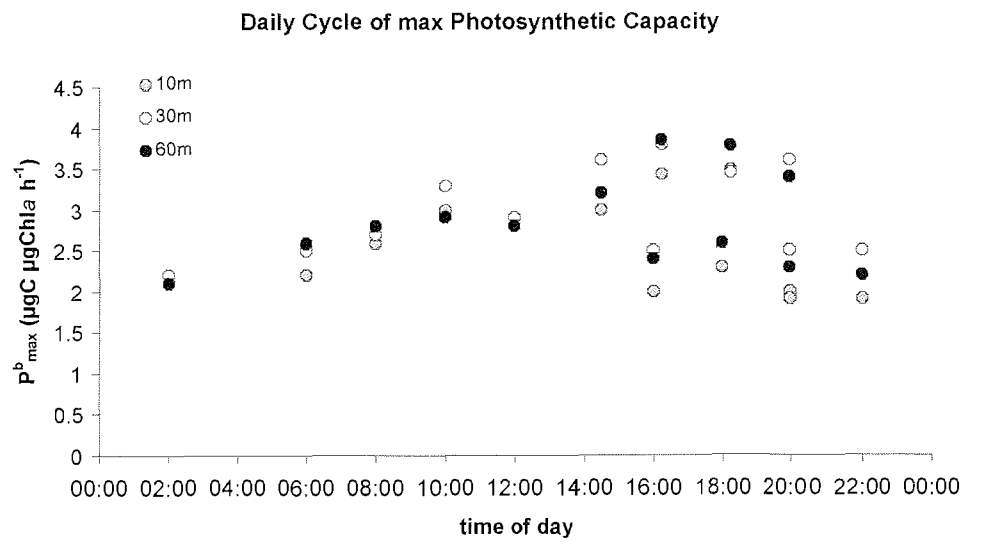


Figure 15.4. Measurements of the maximum photosynthetic capacity (P_{\max}^b) from different depths during 28 hours inside the iron-fertilised patch. The measurement started with low values at 16:00h and continued until 20:00h of the following day showing an increase in P_{\max}^b during this day until 16:00h.

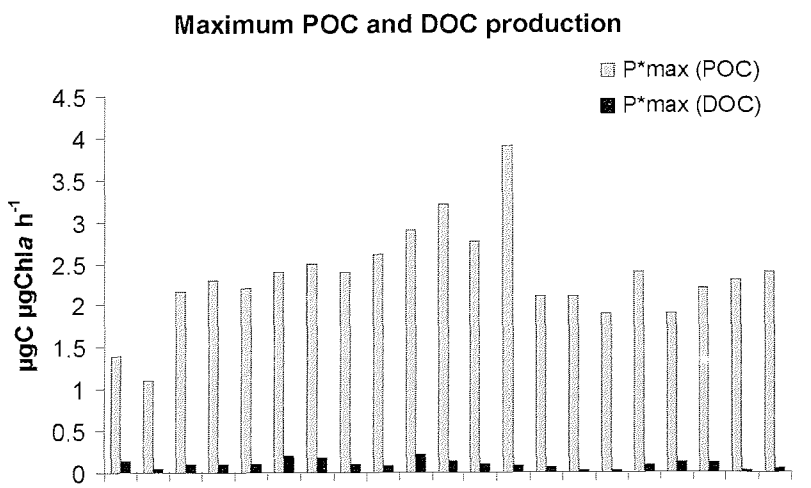


Figure 15.5. Summary of all DOC production measurements. Shown are the maximum particulate carbon production ($P_{\max}^*(\text{POC})$, grey bars) and the maximum dissolved carbon production ($P_{\max}^*(\text{DOC})$, black bars).

16. THE WAX AND WANE OF AN IRON-INDUCED DIATOM BLOOM IN THE SOUTHERN OCEAN

P. Assmy, J. Henjes, K. Schmidt, V. Smetacek (AWI) and M. Montresor (SZN)

Introduction

All mesoscale *in situ* iron fertilization experiments have resulted in the build-up of phytoplankton biomass and established, beyond doubt, that iron availability is the key factor limiting growth rates of oceanic phytoplankton in "high-nutrient, low-chlorophyll" (HNLC) regimes (Coale et al. 1996; Boyd et al. 2000; Gervais et al. 2002; Tsuda et al. 2003). With the exception of the iron-experiment carried out offshore Alaska (SERIES in Boyd et al. 2004) the termination of the iron-induced blooms could not be monitored. All iron-induced blooms were dominated by diatoms, however species dominance and succession have only been marginally addressed. The detailed analysis of the diatom community during the iron-fertilization experiment "EisenEx" showed a major shift in species composition due to iron addition. Species dominance changed from slow-growing, heavily silicified diatoms at the initial stage of the bloom to fast-growing, weakly silicified ones at end of the experiment, leading to a four-fold increase in diatom biomass despite heavy grazing pressure by metazoa (Assmy and Henjes, in preparation). Moreover, the dominant protozoans (ciliates and dinoflagellates) and shell-bearing and non-shell-bearing sarcodines (e.g. foraminifera, acantharia, heliozoa) showed a positive response to this iron-induced phytoplankton bloom. These results clearly stress the importance of key species/groups for the interpretation of biogeochemical cycles and food web interactions. The aim of EIFEX was to follow an iron-induced bloom in the Southern Ocean over a longer period of time in order to investigate the fate of the carbon fixed by phytoplankton and to study the principles underlying bloom formation and species succession.

Methods

Mesoscale survey

Three days after the first iron addition a mesoscale grid survey was conducted (between 48°48' S and 50°36' S, 01°19' E and 03°29' E) over one week to map the eddy and the variability of plankton assemblage. During the grid 5 L of surface seawater were collected from the ship water intake (moon pool) at 8 m depth every 12 nautical miles. Samples were immediately concentrated down to 50 ml by pouring the water gently through a 10 µm-mesh net and then fixed with hexamine-buffered formaline at a final concentration of 2%. The concentrating system (cylinders with the plankton mesh and polycarbonate tubes) was thoroughly washed with high-pressure tap water and subsequently rinsed with filtered seawater after processing every single sample. Two-ml subsamples were settled in Hydrobios sedimentation chambers. Microscopical analyses were performed onboard on inverted Zeiss microscopes (Axiovert 135 and Axiovert 25). Large and less abundant organisms were counted in the whole chamber whereas smaller organisms were enumerated over two mid transects.

Iron-induced bloom development

At the major in- and out-patch stations, duplicate 200 ml water samples were collected at 12 discrete depths, between 5 and 250 m, for quantitative and qualitative estimation of phyto- and small protozooplankton concentration back in the home laboratory. One set of samples was preserved with hexamine-buffered formaline and one with Lugol's iodine. One-two L of seawater collected at the same depths were filtered through 0.8 µm-pore-size cellulose acetate filters for the quantification of biogenic silica (BSi). Samples were stored at -20 °C and will be analysed following wet alkaline digestion method (Müller and Schneider, 1993). For the assessment of larger and less abundant protozoa as well as juvenile and small-sized adult copepods, the whole content of two Niskin bottles (24 L) was sampled at 11 depths, between 10 and 550 m, and concentrated down to 50 ml by pouring the water gently through a 20 µm mesh net. In order to get a preliminary evaluation of the temporal development of the plankton community, 2 L of seawater from 20 m depth were concentrated over a 10 µm-mesh net at all the major in- and out-patch station and immediately counted. The decline of the bloom towards the end of the experiment was followed by a series of deep CTD casts down to the bottom, at around 4000 m depth. Samples were taken at discrete depths, based on the transmissometer profile. The content of a whole Niskin bottle (12 L) was concentrated down to 50 ml by pouring the water gently through a 10 µm-mesh net. Special care was taken not to contaminate the deep sample with surface water by thoroughly washing the nets and tubes after each sample collection.

Serial dilution cultures (SDC) were established at six stations in the fertilized eddy during bloom development. This method, based on the successive dilution of a small volume of water sample into a suitable growth medium, allows for an estimate of the phytoplankton fraction that is not preserved by fixatives and provides material for further ultrastructural examination (Thronsen, 1995). A 20 µm-mesh hand phytoplankton net was towed in the surface water layer (ca. 2-3 m) at all major stations throughout the experiment to collect live plankton for establishing unicellular isolates and material for scanning electron microscopy (SEM) investigations. A large number of monoclonal strains, especially of *Fragilariaopsis kerguelensis*, were established to test intraspecific genetic variability. Different genetic markers will be used to test the existence of one or multiple populations within the target species and to follow the population structure at the genetic level at different stages of the bloom (pre-bloom, peak phase and bloom decline).

In order to achieve a quantitative visual impression of the bloom development pictures of a standardized subsample were taken with a Zeiss digital camera (AxioCam MRc 5). Pictures were randomly taken at low magnification (100*) to get an overview of the plankton assemblage.

Preliminary results and discussion

Mesoscale distribution

The initial distribution of total diatoms in the survey area was characterised by highest abundances within the eddy, whereas cell numbers in surrounding waters were considerably lower. The two large *Chaetoceros* species of the

Phaeoceros group, *C. dichaeta* and *C. atlanticus* (Figs 16.1A+B), contributed to the high abundances within the eddy whereas cell concentrations in surrounding waters were low. These species form long chains connected by long and hollow spines filled with chloroplasts. Other diatom species of numerical importance within the eddy included *Pseudo-nitzschia lineola*, *Corethron pennatum* and *C. inerme*, *Fragilaropsis kerguelensis*, *Thalassionema nitzschiooides* and *Thalassiothrix antarctica*. Furthermore, the heterogenous group of discoid diatoms (including *Thalassiosira* spp., *Asteromphalus* spp. and other centric diatoms) contributed a considerable fraction to the total diatom abundance. The phototrophic dinoflagellate *Ceratium* sp. (Fig. 16.C) and the diatom species, *Lioloma* sp. and *Trichotoxon* sp. (Fig. 16.1D), deserve special consideration since their distribution patterns were inversely correlated with total diatom abundance. These species showed low abundances within the eddy and highest cell numbers in surrounding waters. The hydrographical regime was likely the primary determinant of phytoplankton distribution and species composition at the beginning of the experiment. The eddy had detached from the southern Polar Front Zone (SPFZ) and the dominance of large *Chaetoceros* species within the eddy was likely a characteristic feature of more southerly water masses. *Lioloma* sp. and *Trichotoxon* sp. and *Ceratium* sp. on the other hand were clearly associated with water masses surrounding the eddy, which probably originated from the northern Polar Front Zone (NPFZ) and formed a meander around the eddy. Our results indicate that certain plankton species might be used as indicator species for certain water masses. However, next to physical factors other mechanisms might influence the phytoplankton distribution. These include chemical and biological factors, such as macro- and micronutrient concentrations and grazing pressure. Macronutrients were in abundant supply within the eddy but also in the surrounding water masses and it is therefore unlikely that their concentrations had a strong impact on the abundance and distribution of phytoplankton species. The iron-enriched patch within the eddy matched quite well with the distribution map of large *Chaetoceros* species, however a marked iron-induced accumulation of these species is unlikely to have occurred within the first days of the experiment. Grazing is another important biological factor shaping pelagic ecosystems. Not only growth rates determine phytoplankton biomass build up but also the mortality environment. Most of the dominant diatom species in the eddy were large cells or formed long chains and were protected against grazers by either long spines, bristles or heavily silicified frustules. These "giant diatoms" are therefore less susceptible to grazing than smaller, faster-growing species that are kept in check by the grazer community.

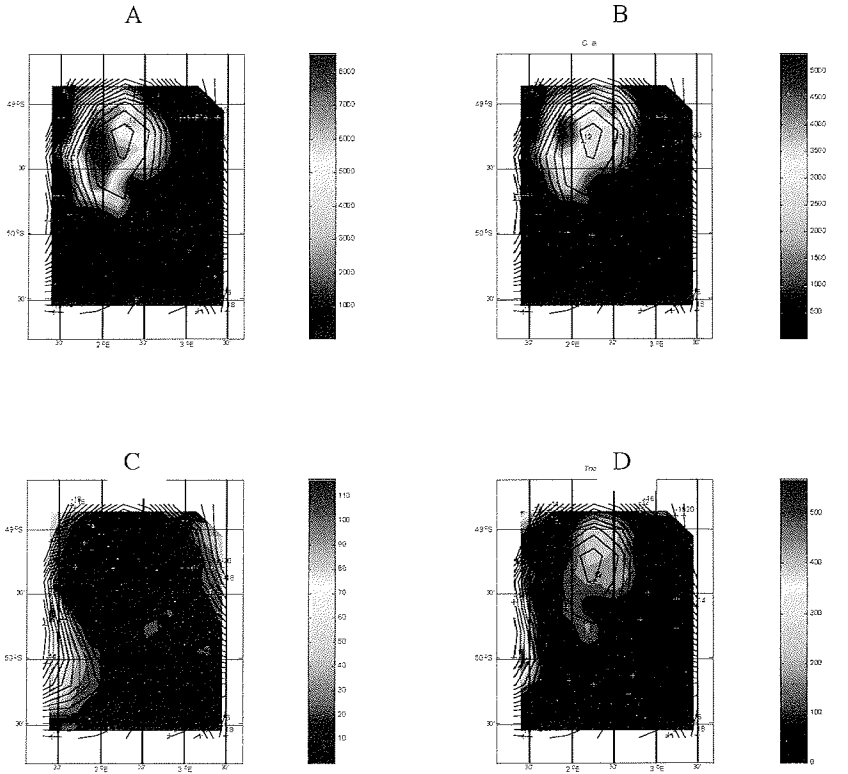


Fig. 16.1: Abundance distributions (cells l^{-1}) of A) *Chaetoceros dichaeta*, B) *Chaetoceros atlanticus*, C) *Ceratium* sp. and D) *Lioloma* sp. and *Trichotoxon* sp. during the CTD-grid of the fertilized eddy (day 1-3 after fertilization). Species abundances are represented with a colour scale superimposed to a stream function map of the eddy.

Temporal development

The total diatom abundance had tripled from initially 72×10^3 cells l^{-1} to 234×10^3 cells l^{-1} inside the fertilized patch after three weeks and declined to 120×10^3 cells l^{-1} at the end of the experiment (Fig. 16.2A). The collapse of the diatom bloom was partly due to the decline of the large *Chaetoceros* species, *C. dichaeta* and *C. atlanticus*, during the second half of the experiment (Figs. 16.2B+C). This is illustrated by pictures of the plankton assemblage taken during the peak phase of the bloom (day 26) and the decline of the bloom (day 37) (Fig. 16.3). Also less abundant species like *Lioloma* sp. showed a marked decrease in cell numbers inside the patch during the second half of the experiment (Fig. 16.1D). Some species, like *F. kerguelensis* and *Corethron inerne*, were still increasing by the end of the experiment (Figs. 16.2E+F). Hence only some species collapsed and sank out of the surface mixed layer whereas others continued to

grow. Outside the patch phytoplankton concentration did not increase and abundances remained low throughout the experiment. The relatively high abundances of *F. kerguelensis* and some other species not shown here (e.g. *Corethron pennatum* and *Pseudo-nitzschia lineola*) recorded outside the patch on day 12 might be due to sampling of different water masses probably associated with the NPFZ. Also the exact position of in-patch stations relative to the core of the fertilized patch need to be precisely evaluated to get a better picture of the temporal development of the bloom. The decline of some diatom species was probably associated with selective grazing or in the case of *Chaetoceros* species with the life history of these species. Grazing played a decisive role in structuring the evolution of the bloom as indicated by the strong increase of fecal pellets by the end of the experiment. However, zooplankton grazing pressure was unlikely to account for the rapid decline and sinking of the large *Chaetoceros* species inside, as well as outside the patch. No clear signs of mechanical breakage associated with crustacean grazing were in fact observed. *C. dichaeta* and *C. atlanticus* cells appeared senescent and chains with many empty cells or cells with disintegrating cytoplasm, which showed no autofluorescence under epifluorescence microscopy, were recorded. The rapid decline and sinking of these species to greater depths and the sea floor as illustrated in Figure 16.4 could only be explained by a sudden event like an epidemic or programmed cell death and a subsequent aggregation of senescent and dead cells that led to their rapid transport out of the surface mixed layer. These results clearly stress the importance of species-specific information for the interpretation of bloom formation and decline, and successional patterns.

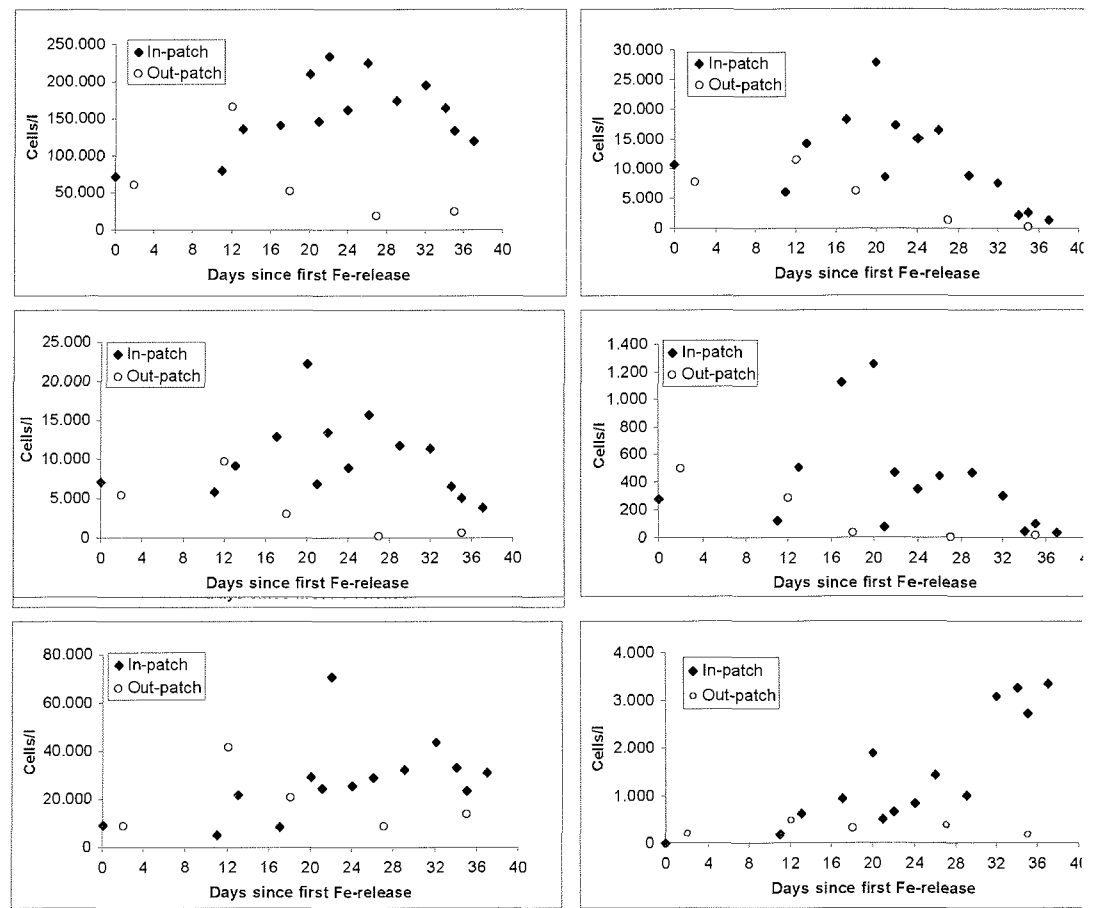


Fig. 16. 2: Temporal development of diatom abundance (cells l⁻¹) at 20 m depth of A) total diatoms, B) *Chaetoceros dichaeta*, C) *Chaetoceros atlanticus*, D) *Liołoma* sp., E) *Fragilaropsis kerguelensis* and F) *Corethron inerme* inside and outside the fertilized patch.

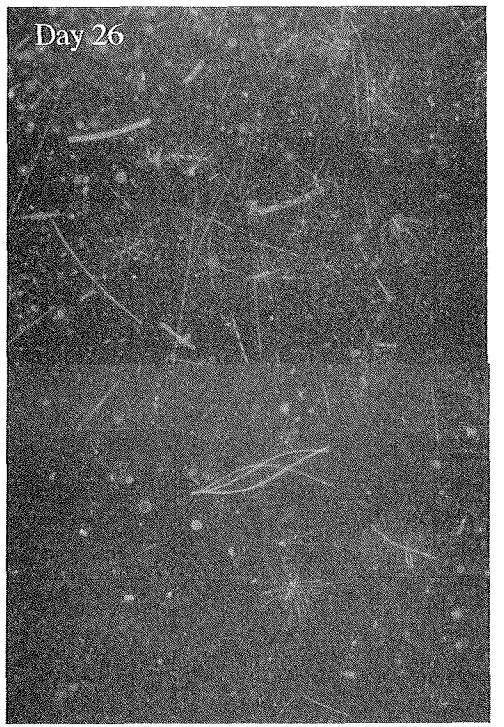


Fig. 16.3: Light micrographs of the surface plankton community on day 26 and day 37 of the experiment inside the fertilized patch.

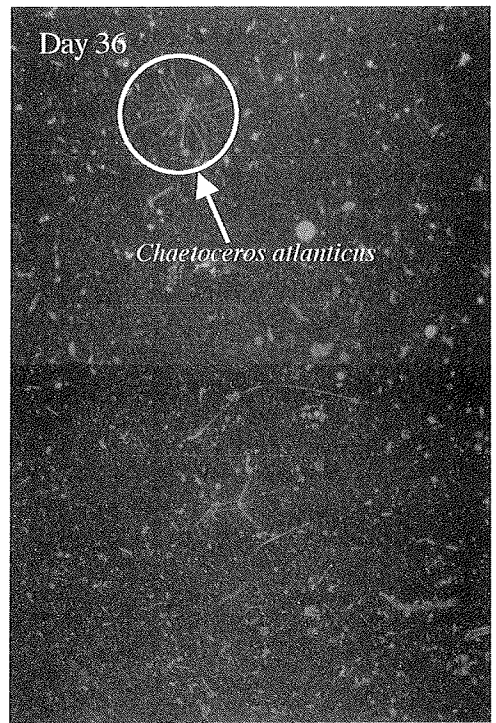


Fig. 16.4: Light micrographs of exported plankton material 15 m above the sea floor at nearly 4000 m depth. Note the fine diatom debris most likely derived from disintegrated fecal material. Intact empty frustules of for example *Chaetoceros atlanticus* and *Corethron pennatum*, as highlighted, were also found at these depths.

Protozooplankton

The abundance of acantharia ($50,454 \text{ ind. m}^{-3}$) recorded at the beginning of this experiment was the highest ever observed in the Southern Ocean and one of the highest ever recorded in the open ocean (Fig. 16.5A). Compared to results from other studies, acantharian abundances seem to follow a seasonal pattern with lowest values during winter and fall (Gowing, 1989; Gowing and Garrison, 1992) and highest concentrations during spring and summer (Henjes and Assmy, in preparation; this study). Acantharia increased in numbers by a factor of three in fertilized waters until day 24, but decreased thereafter to two times the initial value at the end of the experiment. In unfertilised waters abundance increased in the first half of the experiment, but declined afterwards to a value below the initial values after 36 days (Fig. 16.5A). These results show that acantharia responded to iron fertilization. We can hypothesize either an advantage deriving from more favourable food concentrations or from the increased carbon fixation rates induced by iron addition of the photosynthetic symbionts living in acantharia. The increased carbon fixation is likely to exceed the inferred daily metabolic requirements of the host for carbon and hence can lead to higher reproduction rates. During EIFEX all observed acantharia

contained autotrophic symbionts. In general, the notably high abundances recorded so far during this study emphasise that fact that acantharia can be as numerous as other protozoan groups (e.g. large dinoflagellates; Fig. 16.6A) and thus might play a significant role in food web dynamics, carbon export and vertical flux of trace elements (especially strontium and barium) incorporated in their celestite than previously thought.

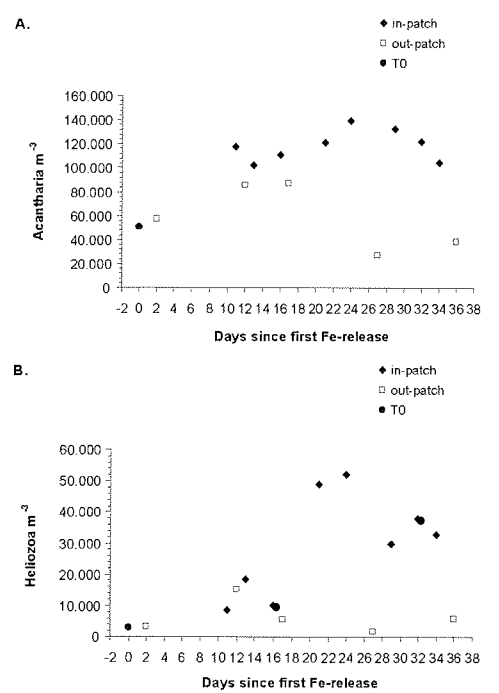


Fig. 16.5. Temporal development of sarcodine abundance in 20 m depth inside and outside the fertilized patch. (A) acantharia; (B) heliozoa.

The temporal development of the heliozoa (most likely *Sticholonche* spp.) showed a similar trend as that recorded for acantharia. However, the increase in abundance observed until day 26 was six times higher (Fig. 16.5B). Although the abundance decreased afterwards it was still notably higher at the end of the experiment as compared to the initial value. Outside the fertilized patch, numbers doubled in the course of the experiment. The increased concentration of heliozoa during this experiment are in contrast to the results of the previous iron-enrichment experiment (EisenEx), which showed a clear decline in abundance.

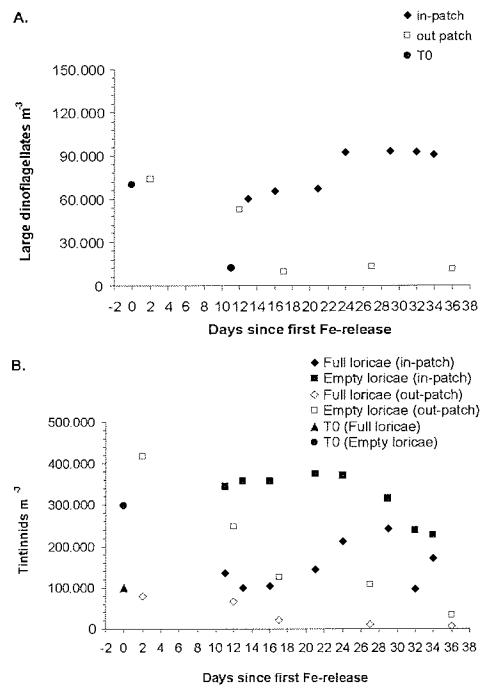


Fig. 16.6. Temporal development of protozoan abundance inside and outside the fertilized patch. (A) Large dinoflagellates; (B) tintinnid ciliates. From 20 m depth.

Within the other protozoa, larger thecate dinoflagellates ($>50 \mu\text{m}$) showed only a slight increase in fertilized waters, whereas a strong decline could be observed in surrounding waters in the course of the experiment (Fig. 16.6A). Most likely grazing pressure by metazoa regulated population growth of larger dinoflagellates during EIFEX.

Tintinnid ciliate abundance more than doubled until day 29, and decreased subsequently until the end of the experiment. Outpatch values, however, showed a very strong decline by more than an order of magnitude until day 36 (Fig. 16.6B). Empty tintinnid loricae, indicators of grazing pressure by other protozoa and metazoa, showed three times higher abundances than alive tintinnids in the first half of the experiment and subsequently declined suggesting a reduction in grazing pressure on this protozoan group. These preliminary findings are in strong contrast to results from EisenEx, where grazing pressure on tintinnid ciliates increased in the course of the experiment.

Metazooplankton

During EIFEX copepod nauplii showed only a slight increase in abundance. However, the trend was not as distinct, which could be caused by a rather uneven distribution of the copepod nauplii within the fertilized patch. In surrounding waters no change in abundance could be observed (Fig. 16.7A).

Initial abundance (16,818 ind. m^{-3}) of small copepods <1.5 mm (mainly consisting of copepodites stages CI-CV) were one of the highest ever recorded for Polar Frontal waters during summer. However, small copepods showed no consistent trend inside the patch during the experiment, whereas outside fertilized waters they declined slightly (Fig. 16.7A). In contrast to copepod abundances, metazoan faecal pellet numbers increased significantly (30 times) in the course of the experiment (Fig. 16.7B) indicating an extremely high faecal pellet production due to intensified grazing on the phytoplankton bloom by metazoa.

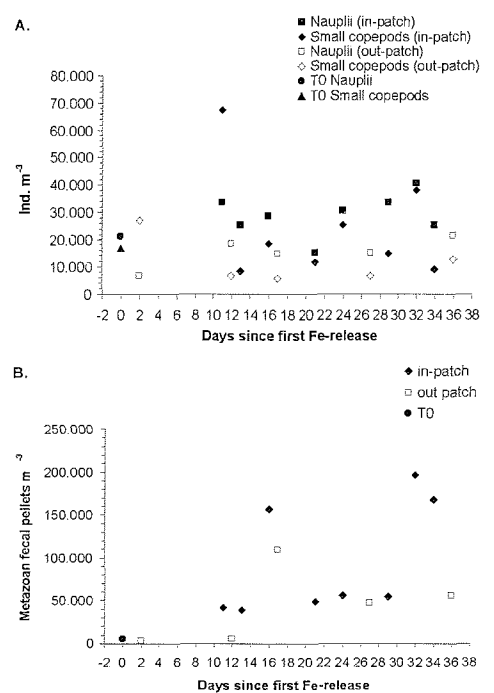


Fig. 16.7. Temporal development of (A) copepod nauplii, small copepod (< 1.5 mm) abundance and (B) metazoan faecal pellet numbers. From 20 m depth.

References

- Boyd PW, Watson AJ, Law CS, Abraham ER, Trull T, Murdoch R, Bakker DCE, Bowie AR,
 Buesseler KO, Chang H, Charette M, Croot P, Downing K, Frew R, Gall M,
 Hadfield M, Hall JA, Harvey M, Jameson G, LaRoche J, Liddicoat M, Ling
 R, Maldonado MT, McKay RM, Nodder SD, Pickmere S, Pridmore R,
 Rintoul S, Safi KA, Sutton P, Strzepek R, Tanneberger K, Turner S, Waite
 A, Zeldies J (2000) A mesoscale phytoplankton bloom in the polar
 Southern Ocean stimulated by iron fertilization. *Nature* 407: 695-702.

Boyd PW, Law CS, Wong CS, Nojiri Y, Tsuda A, Levasseur M, Takeda S, Rivkin R, Harrison PJ, Strzepek R, Gower J, McKay M, Abraham ER, Arychuk M, Barwell-Clarke J, Crawford W, Crawford D, Hale M, Harada K, Johnson K, Kiyosawa H, Kudo I, Marchetti A, Miller W, Needoba J, Nishioka J, Ogawa H, Page J, Robert M, Saito H, Sastri A, Sherry N, Soutar T, Sutherland N, Taira Y, Whitney F, Wong S-KE, Yoshimura T (2004) The decline and fate of an iron-induced subarctic phytoplankton bloom. *Nature* 428: 549-552.

Coale KH, Johnson KS, Fitzwater SE, Gordon MR, Tanner S, Chavez FP, Ferioli L,

Sakamoto C, Rogers P, Millero F, Steinberg P, Nightingale P, Cooper D, Cochlan WP, Landry MR, Constantinou J, Rollwagen G, Trasvina A, Kudela R (1996) A massive phytoplankton bloom induced by an ecosystem-scale iron fertilization experiment in the equatorial Pacific Ocean. *Nature* 383: 495-501.

Gervais F, Riebesell U, Gorbunov MY (2002) Changes in primary productivity and chlorophyll a in response to iron fertilization in the Southern Polar Frontal Zone. *Limnol Oceanogr* 47: 1324-1335.

Gowing MM (1989) Abundance and feeding ecology of Antarctic phaeodarian radiolarians. *Marine Biology* 103: 107-118.

Gowing MM, Garrison DL (1992) Abundance and feeding ecology of larger protozooplankton in the ice edge zone of the Weddell and Scotia Seas during the austral winter. *Deep-Sea Research* 39: 893-919.

Müller PJ, Schneider R (1993) An automated method for the determination of opal in sediments and particulate matter. *Deep-Sea Research* 40, 425-44.

Thronsen J (1995) Estimating cell numbers. In Hallegraeff, G. M., Anderson, D. M. & Cembella, A. D. [Eds.] *Manual on Harmful Marine Microalgae*. UNESCO, Paris, pp. 63-80.

Tsuda A, Takeda S, Saito H, Nishioka J, Nojiri Y, Kudo I, Kiyosawa H, Shiomoto A, Imai K,

Ono T, Shimamoto A, Tsumune D, Yoshimura T, Aono T, Hinuma A, Kinugasa M, Suzuki K, Sohrin Y, Noiri Y, Tani H, Deguchi Y, Tsurushima N, Ogawa H, Fukami K, Kuma K, Saino T (2003) A Mesoscale Iron Enrichment in the Western Subarctic Pacific Induces a Large Centric Diatom Bloom. *Science* 300: 958-961

17. FLOW-CYTOMETRY OF PHYTOPLANKTON DURING THE EIFEX CRUISE

Franciscus Colijn, Meike Dibbern (GKSS-IfK)

To document the phytoplankton composition and to observe changes in the phytoplankton composition a newly developed flowcytometer (fcm) has been used (Cytobuoy). This analytical instrument enables the on-line measurement of phytoplankton composition in terms of cell numbers, size class distribution and fluorescence parameters (red, orange and yellow), as well as cell form and structure related parameters (forward and side scatter). The principle of this instrument is shortly described. Water samples are pumped into the fcm by a precision pump. The phytoplankton cells are flowing through a measuring cuvette where all the particles go through a laser beam with blue laser light. During the illumination of a single particle or colony the optical characteristics (red, orange and yellow-green fluorescence, and forward and side-scatter) are measured and the data collected. The current fcm also makes an optical scan of every particle (see Fig. 17.1), which gives information on e.g. the distribution of fluorescing particles (chloroplasts) in the cells. This enables identification of cell types if fingerprints of the dominant species are available. Depending on the composition of the sample a few hundred (if many large particles are present) to 1000 to 2000 particles are counted and analysed. This procedure takes less than a minute to up to 10 minutes in very dilute samples.

The instrument has been successfully used in two different modes: on-line during transects and grids, as well as manual (specific CTD samples from different depths). Both modes were applied whereas at the end of the cruise a long transect between the experimental area (49° South, 1° East) and Cape Town was sampled at one hour intervals to test the applicability during on-line measurements. Every 4 hours additionally a water sample has been collected to compare the fcm measurements with the phytoplankton composition based on light microscopy.

Specific measurements were made on net samples collected by the phytoplankton group to obtain so-called fingerprints (Fig. 17.1) of the dominant species occurring in the surface samples. Apart from these net-samples cultures obtained during the cruise were measured because they give the ultimate proof how the finger prints of a species look like. This information was needed to be able to interpret the dot plots obtained during the regular measurements. Because of the large size of the cells during the intensive growth phase of the phytoplankton community problems arose which led to clogging of the fcm inlet tube. A major obstruction was once detected and the machine had to be cleaned up thoroughly. Apart from this problem with very large colonial cells (more than 1 mm in length) the fcm worked extremely reliable.

The primary data treatment shows that cell numbers could be easily measured in surface as well as deep water samples. Surprisingly, the deep CTD casts at the end of the cruise revealed fluorescent particles till the bottom at a number of about 10-20 cells per ml. Because cells can not live at that depth they must

have been settled rather quickly probably in the form of major aggregates because single small cells would not reach the bottom so fast, without being dissolved or digested. This observation was a further proof that a large part of the bloom was sinking to the bottom at the end of the bloom period.

The distribution of cell numbers and total fluorescence for all cells measured ($>5\mu\text{m}$) and for larger cells ($>20\mu\text{m}$) was correlated with other parameters during the cruise: a good relation has been observed between these parameters and the fluorescence measured with a Fast Tracka FRRF machine (see for details the report section by R. Roettgers). (Fig. 17.2).

We will further analyse the relations with chlorophyll-a and with the cell numbers determined by the phytoplankton group.

Several observations were made on the depth distribution of phytoplankton during the in – and out – patch samplings at a whole series of stations. Here we will try to relate our observations to the ones made by others. An example of the depth distribution of cells in the upper mixed layer is given in Fig. 17.3. We will look for correlations with e.g. the chlorophyll-a distribution.

The fcm was used by several other groups as an important measuring device: thus sedimentation rates could be estimated for the 'snatcher' samples by the group working on the sedimentation of thorium from the surface layer, and cell number estimates could be made successfully for the dilution experiments to estimate growth rates and microzooplankton grazing. Estimates of grazing rates of mesozooplankton were not successful, because the cell density changes during the measuring intervals were too small, or the grazing pressure of single animals was not high enough to document changes in cell numbers. However, the machine has been exploited in several ways which shows the capabilities of fcm in experimental designs.

Technical limitations occurred (see above) with the size of very large cells: ordinary fcm's developed for medical applications with small cell sizes can not cope with particles of more than $100\text{ }\mu\text{m}$'s whereas we could easily measure particles of several hundreds of μm 's.

However the number of events of such large particles is restricted unless one accepts very long counting times. We preferred to analyse more samples instead of applying longer measuring times. Nevertheless the capability of the fcm to measure large particles is extremely good because the measuring cell has a diameter of 1mm (!) and colonies of several hundreds of μm 's were regularly detected.

Whether physiological changes in the plankton can be measured, has to be analysed later on. Fluorescence per particle, increase of amount of chlorophyll per particle, and maybe other relevant parameters have to be analysed and evaluated before conclusions can be drawn.

Comparison will be made with intensive FRRF measurements (see next section).

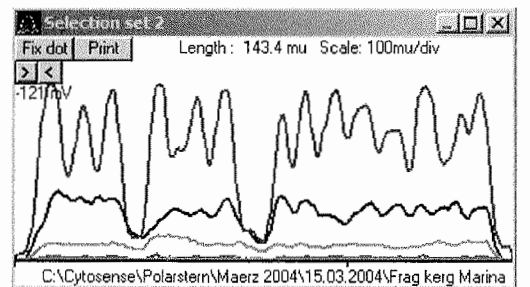


Fig. 17.1.a. *Fragilariaopsis kerguelensis*

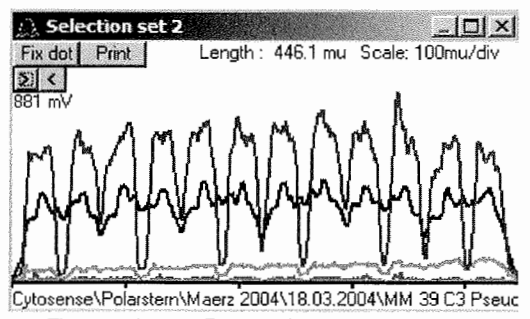
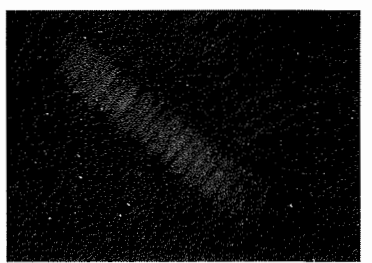


Fig. 17.1.b. *Pseudonitzschia* sp.

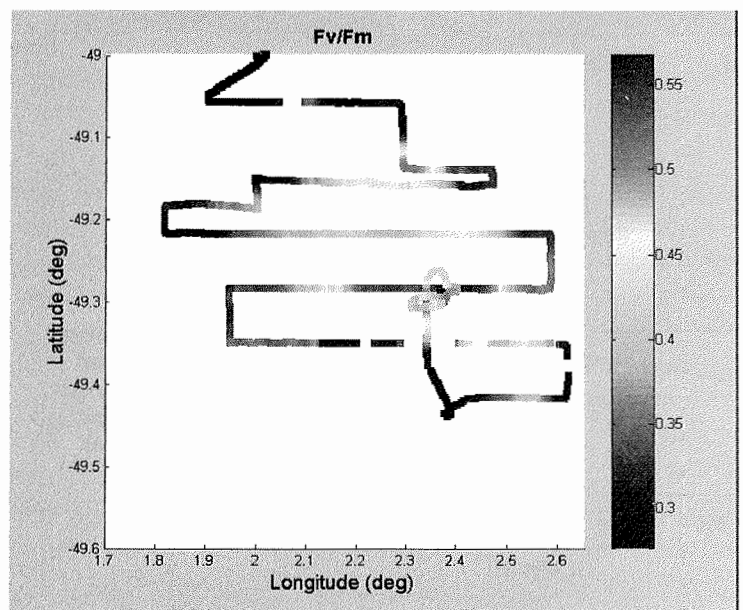
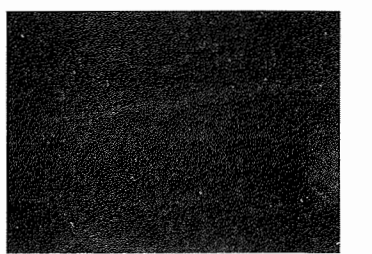


Fig. 17.2.a. FRRF Grid of 23-24 February

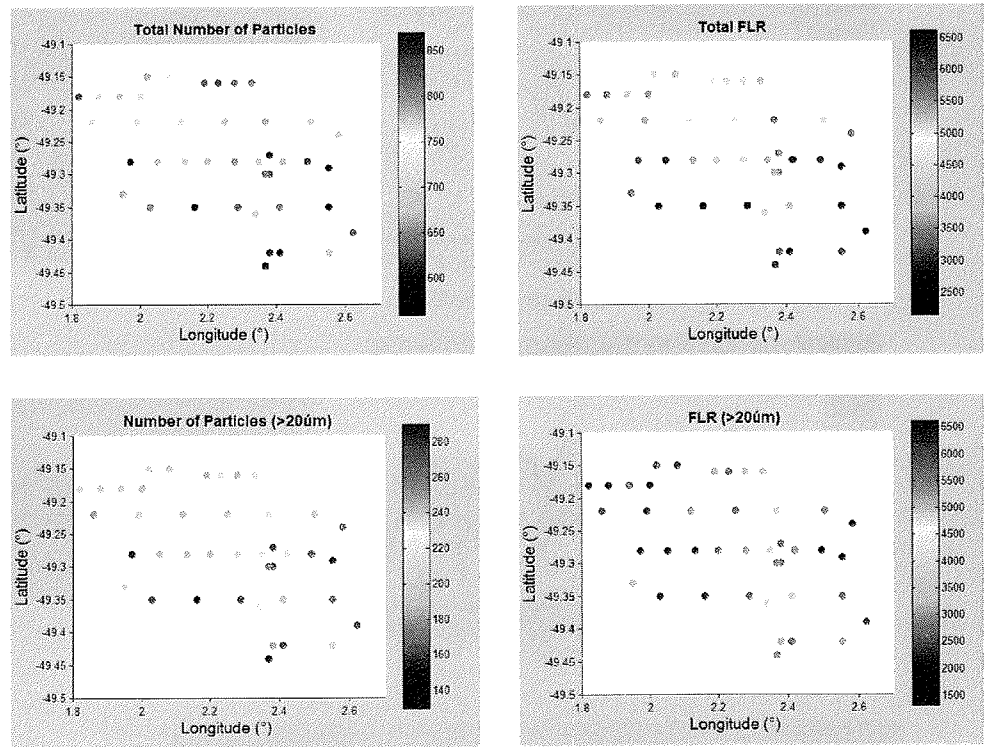


Fig. 17.2.b. FCM Grid of 23-24 February

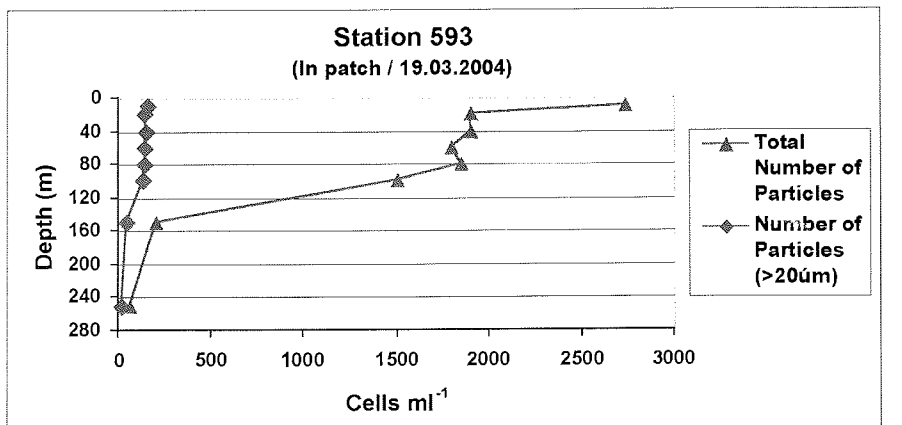


Fig. 17.3. a. Depth distribution of cells in the upper mixed layer at station 593 (in patch) at the end of the bloom period.

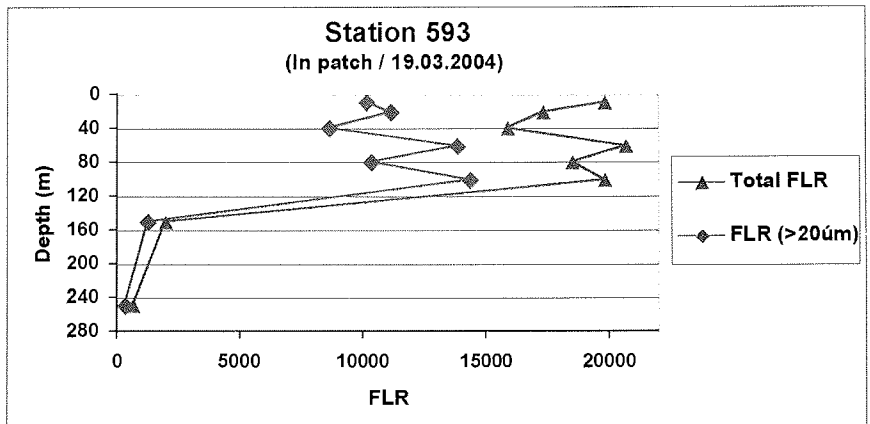


Fig. 17.3. b.

18. STABLE SILICON ISOTOPES IN DISSOLVED AND BIOGENIC SILICA.

D. Wolf-Gladrow, C. Klaas (AWI)

Introduction and objectives

In natural environments, three stable isotopes of silicon are present with masses 28, 29, and 30. ^{28}Si is the most abundant of the three with 92.2% followed by ^{29}Si with 4.7% and ^{30}Si with 3.1%.

Measurements of the isotopic composition from culture experiments using three marine diatom species have shown that the silicon isotope composition, $\delta^{30}\text{Si}$, of biogenic silica (BSi) is 1.1‰ lighter than that of dissolved silica (DSi, silicate) in seawater (De La Rocha et al., 1997). These results also indicate that the fractionation of Si isotopes should be independent of species composition and temperature? Based on these findings, stable silicon isotope composition of diatomic silica deposited in marine sediments has been proposed as an ideal proxy for silicon utilization due to Rayleigh distillation (De La Rocha et al., 1998). The iron fertilization experiment EIFEX in the Southern ACC provides an ideal opportunity to study the silicon isotopic fractionation under controlled conditions but on natural diatom assemblages. The iron-induced algal bloom was dominated by large diatoms, mainly, *Chaetoceros spp.*, *Pseudonitzschia lineola*, *Corethron pennatum*, *Thalassiothrix antarctica* and *Fragilaropsis kerguelensis* (see contribution by Assmy et al.). These diatoms are common in the opaline sediment girdle around the Antarctic continent. Measurements of the isotopic composition of the BSi and DSi samples collected during EISENEX will provide information on the fractionation factor and on the validity of a simple

Rayleigh distillation model in the open ocean. This will help establish the link between water column process and the isotopic signal found in the sediments.

Work at sea

During EIFEX, 20 to 50 L seawater (depending on biomass present in the water column) were collected at discrete depths using 12 L bottles attached to a CTD rosette. Water samples were filtered onto 0.4 μm pore size polycarbonate filters at pressure of 200 mbar. Filters were dried at 50°C overnight and stored at -20°C for analysis $d^{30}\text{Si}$ in the biogenic fraction. Three litres of the filtrate were also collected in acid cleaned PE bottles for analysis of $d^{30}\text{Si}$ of the dissolved silica and stored in the dark at 4°C.

Samples collected using a multinet were also filtered in polycarbonate 0.4 μm pore size for the analysis of whatever in the organic matter of diatom frustules.

Future work/outlook

The $d^{30}\text{Si}$ of the collected material will be analysed by Christina De La Rocha in Cambridge, England. DSi and BSi has to be quantitatively converted to SiF_4 before the isotope composition can be measured on a mass spectrometer. The preparation of samples before mass spectroscopy is quite demanding. Results can be expected beginning 2005.

19. PRIMARY PRODUCTION, PHYTOPLANKTON BIOMASS AND DISTRIBUTION, AND SIZE FRACTIONATED BULK VARIABLES OF THE CHLOROPHYLL MAXIMUM DURING AN IRON FERTILIZATION EXPERIMENT IN THE REGION OF THE ANTARCTIC POLAR FRONTAL ZONE

I. Peeken, L. Hoffmann (IfM-K)

1 Introduction:

The objectives of our work were:

- To measure ^{14}C primary production in different phytoplankton size classes and to quantify the primary production inside and outside the iron fertilised waters
- To monitor the spatial and temporal distribution of phytoplankton biomass and distribution during EIFEX
- To determine the Redfield ratio (C:N:P), bPSi and pigments in different size fractions of the chlorophyll maximum in response to iron fertilisation
- To measure the stability of silica shells in response to iron limitation
- To find out, if the pigment phaeophytin can function as a chelator for iron uptake
- To collect cultures for future experiments
- To take samples for N_2O -measurements

2 Primary production:

2.1 Introduction:

In order to determine carbon budgets for iron fertilization experiments, it is essential to estimate the primary production of the phytoplankton inside and outside the fertilized patch. Size fractionated ^{14}C uptake was carried out to study the shifts in the community structure of the phytoplankton during the iron fertilization in austral fall.

2.2 Methods:

Primary production was determined from incorporation of the radioisotope ^{14}C . Water samples from various depth (10 – 80 m) were incubated for 24 hours in deck incubators using neutral density screenings for the appropriate light depth (50%, 25%, 12,5%, 6%, 1%, 0,1%). The incubators were cooled by a flow of surface water. For correction of bacteria radio labelled uptake, dark bottles were incubated. ^{14}C uptake in each sample was analysed in the different size fractions <2 μm , 2 – 20 μm and >20 μm using 0,2 cellulose acetate filters and 2 and 20 μm polycarbonate filters. Occasionally additional a 10 μm polycarbonate filter was analysed. ^{14}C was analysed by liquid scintillation counting (Tricarb 1900 TR).

2.3 Preliminary results:

Size fractionated primary production showed the clearest response to iron fertilisation in the >20 μm fraction inside the patch with maximum of 28 mg C $\text{m}^{-3} \text{ d}^{-1}$ (fig. 19.1). In contrast, outside the patch all fractions had a decreasing primary production during the course of the experiment. Towards the end of the EIFEX experiment the primary production of the >20 μm fraction decreased again dramatically reaching almost the pre fertilisation values. Compared to the outside stations, there was also an increase of primary production in the < 2 μm and 2 – 20 μm fraction, but the overall signal was less pronounced with shifting contribution of these size classes to primary production.

3 Phytoplankton biomass and distribution:

3.1 Introduction:

To investigate the full impact of iron fertilization on the ecosystem, it is essential to study the reaction of all phytoplankton classes. The monitoring of phytoplankton distribution by marker pigments can be used to get a broad overview of the phytoplankton response, particular the nano- and picophytoplankton, to iron fertilisation in the fertilised patch and the surrounding waters. The measurements will be replenished by additional monitoring of the pico- and nanophytoplankton by flow cytometry. Pigment samples can further be used to monitor a potential grazing impact of mesozooplankton by the detection of different phaeopigments.

3.2 Methods:

Seawater samples were filtered onto 25 mm Whatman GF/F filters and stored in 1,5 ml cryo tubes at -80°C until analysis. In total 530 samples from CTD casts

and 200 surface samples during transects have been carried out. The pigments were analysed using the method described by Barlow et al. [1997]. Eluting pigments were detected by absorbance (440 nm) and fluorescence (Ex: 410 nm, Em: > 600 nm). Pigment distribution was calculated based on marker pigments using the CHEMTAX program with the ratio matrix for the southern ocean [Mackey et al., 1996].

For the major in- and outstations flow cytometry samples were taken from the CTD casts. 4 ml of seawater were filled in cryo vials (Nalgene) and preserved with Formaldehyde. The samples were immediately frozen at -80°C and thereafter stored at -20°C prior to analysis. The samples will be analysed by Marcel Veldhuis (NIOZ)

3.3 Preliminary results:

During the EIFEX experiment the following phytoplankton groups were observed: diatoms, Phaeocystis-type and Emiliana huxleyi-type haptophytes, chlorophytes, autotroph dinoflagellates, pelagophytes, and cyanobacteria. The main beneficiary during EIFEX were diatoms who increased 5-fold to almost 2000 ng chl a l⁻¹ in 20 m water depth (fig. 19.2). The second important group were Phaeocystis-type haptophytes, which increased but did not peak like the diatoms. Both groups decreased again towards the end of the experiment, when iron got limited again (Croot, pers. com.). All other phytoplankton showed a slight decrease during the course of the iron fertilisation experiment. Outside the fertilised patch all phytoplankton groups decreased over time indicating the natural end of the phytoplankton growing season in this region of the Southern Ocean.

4 Size fractionation of phytoplankton biomass and distribution:

4.1 Introduction:

Changes in the elemental composition of phytoplankton due to iron fertilization would affect biogeochemical models assuming constant ratios. To investigate differences in the elemental composition between different size fractions and the possible changes of the elemental ratios we took size fractionated POC, PON, POP, and bPSI samples in and outside the iron-fertilized patch. Size fractionated HPLC measurements were performed to get information on species composition and size dependent phytoplankton growth.

4.2 Methods:

Samples for fractionated POC, PON, POP, bPSI, flow cytometry, and pigment measurements were taken in- and outside the iron fertilized patch. Fractionated filtration with a 20 µm gaze, 2 µm polycarbonate filters, and GF/F filters allowed us to determine the size fractions of total, >20 µm, 2-20 µm, and <2 µm for these parameters. The volume of water filtered was dependent on the amount of biomass in the water. After filtration, all filters were rinsed with filtered seawater to avoid a loss of biogenic material sticking on the filter cups. For POC and PON pre-combusted GFF filters and for POP normal GFF filters were used.

The filtration of bPSi was done on cellulose acetate filters. All filters were dried for at least 48 hours in a drying oven and then stored in eppendorf caps.

Before the POC/PON measurement, the filters were acid fumed over night with 32 % HCl to remove the inorganic carbon. The carbon and nitrogen content of the particulate, organic material was analysed the C/N Analyser (Euro EA Elemental Analyzer) after Ehrhard and Koeve [1999]. The POP content was determined using the method after Hansen and Koroleff [1999]. Particulate organic silicate was determined after Puch [1990].

For pigment samples additional size fractionated filtrations with 8 μm and 1 μm polycarbonate filters were carried out. Immediately after filtration the pigment filters were stored in 1,5 ml cryo vials at -80°C until analysis. Sub samples from these fractions (4 ml of each) were used for flow cytometry. These samples were filled in cryo vials (Nalgene), preserved with formaldehyde, immediately frozen at -80°C and stored at -20°C thereafter. The samples will be analysed by Marcel Veldhuis (NIOZ).

4.3 Preliminary results:

First results show that the total POC, PON, POP, and bPSi values from the chlorophyll maximum at the in-stations were higher than at the out-stations (fig. 19.3). The POC, PON, and POP values increased at the in-stations during the iron fertilisation experiment with a noticeable dip at day 22 (26 for POP) and decreased towards the end of the experiment. In contrast to this the total bPSi values showed a constant increase at the in-stations during the whole time of the experiment. At the out-stations the POC, PON, POP, and bPSi values declined slightly over time in comparison with the first station. These results, and the very similar increase of total chlorophyll a (data not shown) indicate a clear response of phytoplankton to iron fertilisation. The constant increase of the bPSi concentration indicated a strong diatom growth, which is supported by the pigment data (fig. 19.2).

The percentage of total chlorophyll a showed big differences between the three size fractions <2 μm , 2-20 μm , and >20 μm (fig. 19.4) in the chlorophyll maximum at 20 m depth. Before iron fertilisation, the 2-20 μm fraction dominated the phytoplankton community with more than 60 %. This size fraction stayed dominant during the whole experiment, but during the first 26 days the >20 μm fraction increased its contribution to total chlorophyll a at the expense of the smaller fractions. Towards the end of the experiment, when iron concentrations decreased (Croot pers. com.), the values indicated a return to pre-fertilisation conditions with a decreasing contribution of the > 20 μm fraction and an increasing contribution of the 2-20 μm fraction.

The >20 μm fraction was the main beneficiary of iron fertilisation while the smaller fractions showed no or a negative response to iron fertilisation. This results implicate, that larger cells suffer more during iron deplete conditions and are able to increase their growth rates after fertilisation. In contrary to that, smaller cells, with a higher surface to volume ratio, are obviously better adapted to low iron concentrations and can not benefit from higher iron concentrations in the same way than the larger ones.

5 Stability of silica shells:

5.1 Introduction:

Iron dependent changes in the nutrient uptake ratios effect also the silica cycle. Hutchins and Bruland [1998] and Takeda [1998] have shown that diatoms establish higher Si:cell, Si:C, Si:N, and Si:P ratios under iron limited conditions. These findings suggest more silicified, faster sinking cells under iron limited conditions. According to this iron fertilisation would lead to thinner diatom shells. This could effect the sinking speed and remineralisation time of the frustules. If thinner shells have less stability it would have great implications on grazing pressure of mesozooplankton.

5.2 Methods:

To determine the shell thickness and stability of diatom frustules 20 μm hand nets were taken at each station. The samples were fixed with 1% Lugol's iodine solution, stored at 4 °C in the cooling room on board, and will be analysed in the following months. Shell thickness will be determined with Scanning Electron Microscopy (SEM) after removal of organic cell material with hydrogen peroxide. Frustule stability will be determined in collaboration with Christian Hamm (AWI) as described in Hamm et al. [2003].

6 Grazing experiments:

6.1 Introduction:

Phaeophytin a, the degradation product of chlorophyll a, may be a natural chelator for iron uptake of phytoplankton. Major pathways of this pigment are still under debate, since it occurs during zooplankton grazing but is also known to be a product of decaying phytoplankton blooms. Phaeophytin is part of the Light Harvesting Complex LHC-II and part of the electron transport chain to photosystem I. Phaeophytin can be released either by zooplankton grazing or by decay of phytoplankton. Since these processes occur at different times of the phytoplankton bloom, it is of relevance to understand pathways that liberate this pigment.

6.2 Methods:

Grazing experiments with copepods and salps were carried out on board. Seawater from 20 m depth was filtered through a 100 μm net to avoid large grazers and filled into 2,5 l bottles. For the copepod grazing experiments ten copepods were transferred into six bottles and six bottles remained as controls. For iron, pigments, and cell counting T_0 samples were taken. Three bottles each were transferred to incubators with and without light (see table 19.1). After 24 hours the experiment was stopped and samples for iron, pigments, and cell counts were taken. The grazing experiments with salps were carried out with one salp per bottle and only performed in the dark. In order to circumvent damage of the animals these experiments lasted only 8 hours.

7 Phytoplankton cultures:

7.1 Introduction:

Controlled lab experiments can be used to investigate the impact of iron on Redfield ratios, silica shell stability and thickness. Additional investigation regarding the ability of diatoms to perform luxury uptake of iron and general iron cell quotas can be addressed with this type of experiments. To supplement the current diatom collection in Kiel additional phytoplankton was isolated during EIFEX and maintained under iron depleted conditions.

7.2 Methods:

Phytoplankton, especially diatoms, was isolated from water samples of different stations. We carefully transferred single cells or colonies from the concentrated water sample and rinsed them three times in drops of sterile filtered natural seawater. These isolates were cultivated in 0,2 µm filtered Southern Ocean seawater to keep the growing conditions as natural as possible.

8 N₂O-profiles:

8.1 Introduction:

N₂O is a climate relevant gas. Previous studies have shown elevated N₂O concentrations at the pycnocline during an iron fertilisation experiment (SOIREE). In order to investigate the conflicting effect of iron fertilisation experiments N₂O gas was investigated inside and outside the iron fertilised patch

8.2 Methods:

Seawater samples were taken from 8 CTD casts in 15 – 20 depth (3 replicates each) inside and outside the fertilised patch. The samples were preserved with HgCl₂ and stored at 4°C. The samples will be measured by S.Walter and H. Bange (IfM-Geomar, Kiel).

References:

- Barlow, R.G., D.G. Cummings, and S.W. Gibb, Improved resolution of mono- and divinyl chlorophylls a and b and zeaxanthin and lutein in phytoplankton extracts using reverse phase C-8 HPLC., Mar. Ecol. Prog. Ser., 161, 303-307, 1997.
- Ehrhard, M., and W. Koeve, Determination of particulate organic carbon and nitrogen: In Methods of Seawater Analysis (Editor: Grasshoff, K., Kremling, K., Ehrhard, M.), Wiley -VCH, Weinheim, New York, 437-444, 1999.
- Hamm, C.E., R. Merkel, O. Springer, P. Jurkojc, C. Maier, K. Prechtel, and V. Smetacek, Architecture and material properties of diatom shells provide effective mechanical protection, Nature, 421, 841-843, 2003.
- Hansen, H.P., and F. Koroleff, Determination of nutrients: In Methods of Seawater Analysis (Editor: Grasshoff, K., Kremling, K., Ehrhard, M.), Wiley -VCH, Weinheim, New York, 159-228, 1999.
- Hutchins, D.A., and K.W. Bruland, Iron-limited diatom growth and Si:N uptake ratios in a coastal upwelling regime, Nature, 393, 561-564, 1998.

- Mackey, M.D., D.J. Mackey, H.W. Higgins, and S.W. Wright, 'CHEMTAX'- a program for estimating class abundances from chemical markers: application to HPLC measurements of phytoplankton, Mar. Ecol. Prog. Ser., 144, 265-283, 1996.
- Puch, M., Zum Silikathaushalt des Pelagials im Europäischen Nordmeer, Diplom thesis, University Kiel, Kiel, 1990.
- Takeda, S., Influence of iron availability on nutrient consumption ratio of diatoms in oceanic waters, Nature, 393, 774-777, 1998.

Table 19.1: Set up of grazing experiments

treatment	light/dark	volume	replicates	incubation time
copepods	light	2,5 l	3	24 h
control	light	2,5 l	3	24 h
copepods	dark	2,5 l	3	24 h
control	dark	2,5 l	3	24 h
salp	dark	2,5 l	3	8 h
control	dark	2,5 l	3	8 h

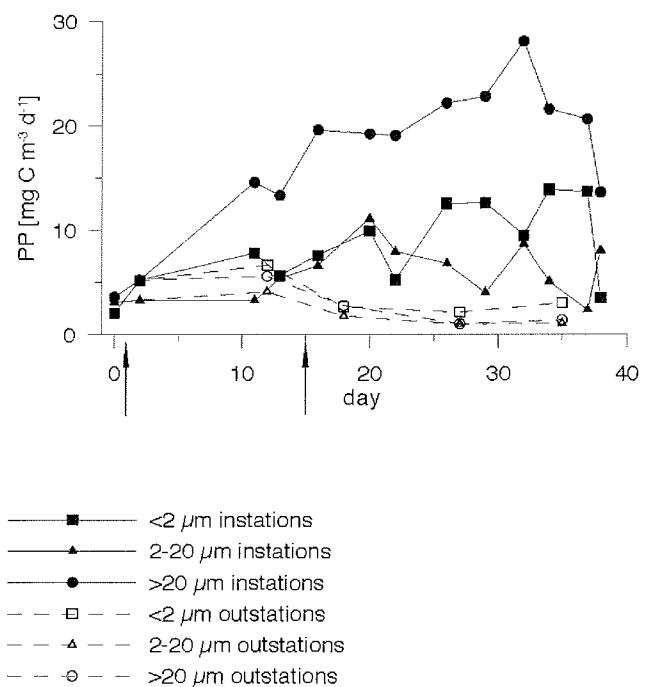


Fig. 19.1: Primary production in $\text{mg C m}^{-3} \text{d}^{-1}$ of the three size fractions $<2 \mu\text{m}$, $2-20 \mu\text{m}$, and $>20 \mu\text{m}$ inside and outside the iron fertilised patch (20m water depth). Arrows indicate days of iron fertilisation.



Fig. 19.2: Phytoplankton distribution expressed in chlorophyll a concentration in ng l^{-1} of diatoms, Phaeocystis-type haptophytes and other phytoplankton (including Chlorophytes, autotroph Dinoflagellates, Pelagophytes, *Emiliania huxleyi*-type haptophytes and Cyanobacteria) at in- and out-stations during the iron fertilisation experiment (20m water depth). Arrows indicate days of iron fertilisation.

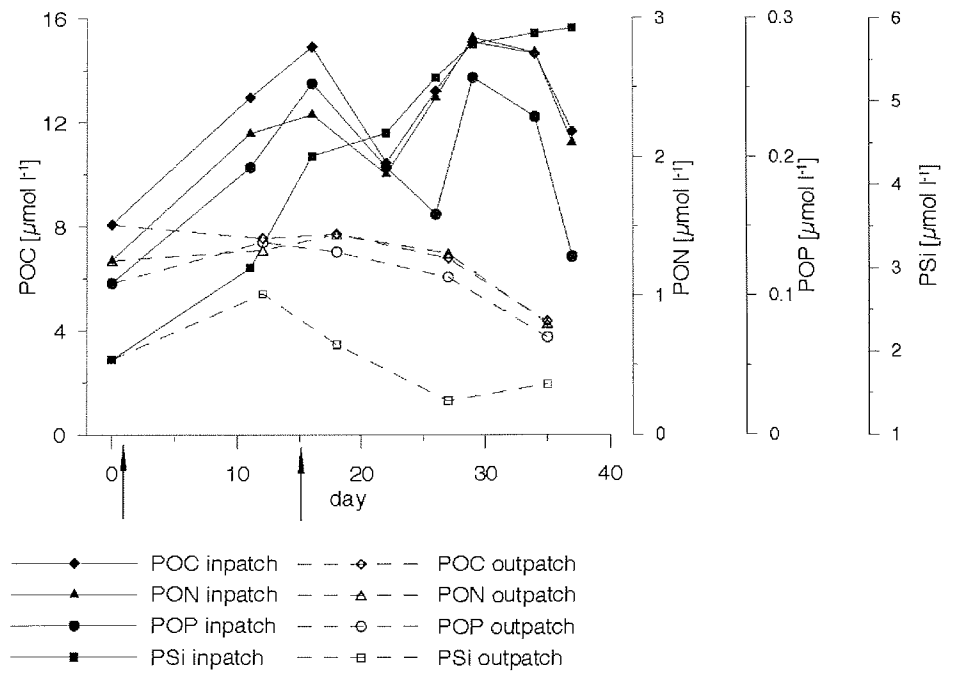


Fig. 19.3: Total POC, PON, POP, and bPSi in $\mu\text{mol l}^{-1}$ from 20m water depth at the in- and out-stations during the iron fertilisation experiment. Arrows indicate days of iron fertilisation.

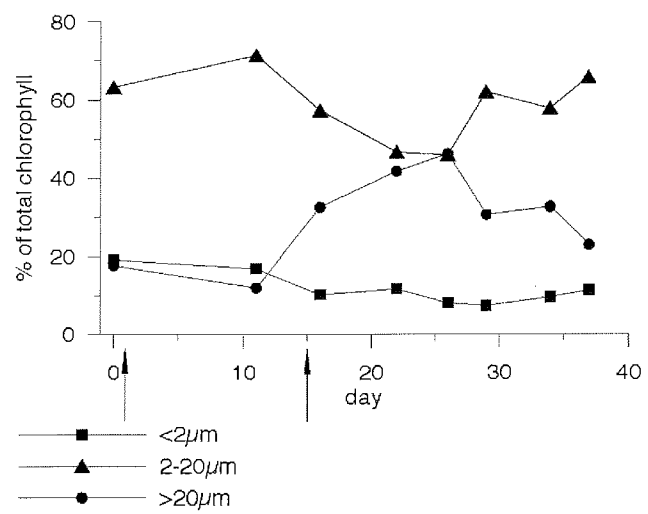


Fig. 19.4: Percentage of total chlorophyll a of the three size fractions <2 μm , 2-20 μm , and >20 μm from stations inside the iron fertilised patch (20m water depth). Arrows indicate days of iron fertilisation.

20. PROKARYOTIC RESPONSE TO IRON FERTILIZATION

J.M. Arrieta and G.J. Herndl (NIOZ)

Previous studies have shown that iron fertilization can produce phytoplankton blooms in the Southern Ocean. It is hypothesized that stimulation of primary production by iron fertilization leads to export of significant amounts of this newly produced organic carbon into deeper layers of the ocean. However, little is known about the fate and export rates of iron induced blooms. Marine prokaryotes play an essential role in both the remineralization and the transfer of organic materials to higher trophic levels [1] in marine systems. Additionally, prokaryotic enzymes can rapidly solubilize the organic coating of sinking particles, preventing carbon sinking [2]. Therefore, any serious attempt to quantify the fluxes of organic materials in the oceanic water column must take prokaryotic activity into account.

Previous work (Eisenex) showed that both bacterial biomass and hydrolytic activity were enhanced in the Fe-fertilized patch [3]. However, the decay and ultimate fate of the bloom could not be measured during Eisenex and a number of questions were left unsolved.

In order to answer these questions we measured a number of parameters during EIFEX:

Prokaryotic abundance, production, respiration and activity of the electron transfer system (ETS). These will allow us to estimate the total carbon demand of prokaryotes, and constrain the fraction of the primary production available for particle flux. Additionally any shifts in the prokaryotic growth efficiency (production / production + respiration), together with the ETS measurements can offer important clues to determine whether prokaryotic activity is directly limited by iron availability in the Southern Ocean.

Prokaryotic hydrolytic activity. Two enzymes involved in the breakdown of carbohydrates (α - and β -glucosidase) and one responsible for the hydrolysis of peptides and proteins (aminopeptidase) were measured. Although the concentrations of inorganic phosphate at the site of the experiment were high, prokaryotes also use these enzymes to split phosphate-containing organic molecules, especially when carbon limited. Samples have been collected to conduct a capillary electrophoresis zymography analysis in the same fashion as it was done for during Eisenex. We are confident that we will be able to extend this analysis to other enzyme activities other than β -glucosidase this time. Shifts in the patterns of enzyme activity can offer important clues about the quality of the available organic materials and to the general physiological state of the prokaryotic community.

Prokaryotic diversity. No changes were detectable in the species richness of the prokaryotic community during Eisenex, using rapid fingerprinting techniques [3]. However, it is possible that we missed more subtle changes in the relative

abundance of certain groups of prokaryotes or changes that could have taken place at later stages in the development of the bloom. We will use the same rapid fingerprinting techniques for EIFEX, combined with the recently improved MICRO-CARD-FISH [4]. This technique combines the detection of microbial activity by microautoradiography with a highly sensitive version of FISH (fluorescence in situ hybridization) and allows to link the measurements of microbial activity to certain taxonomic groups.

Although not all the previously described measurements are available yet, our preliminary results (see Figs. 20.1, 20.2, 20.3) show an enhancement of prokaryotic activity inside the Fe-fertilized patch, similar to that observed during Eisenex. Moreover, our preliminary calculations show that about 50% of the estimated primary production in the patch could be channeled through planktonic prokaryotes.

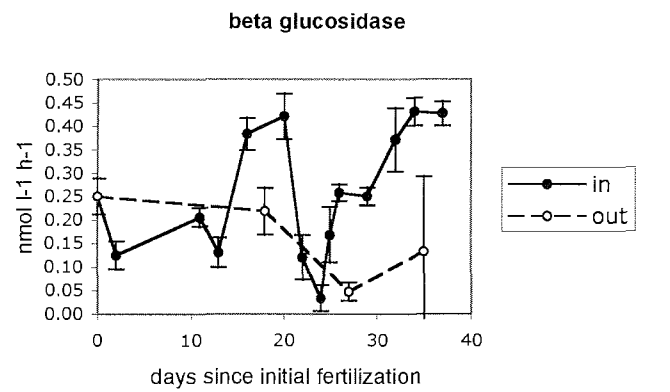


Fig 20.1. b-glucosidase activity inside and outside the Fe fertilized patch

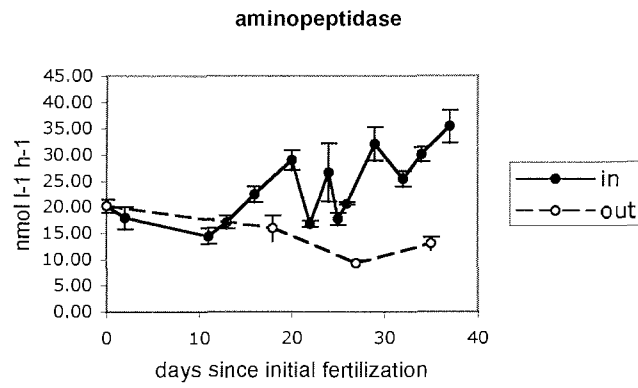


Fig 20.2. Aminopeptidase activity inside and outside the Fe fertilized patch

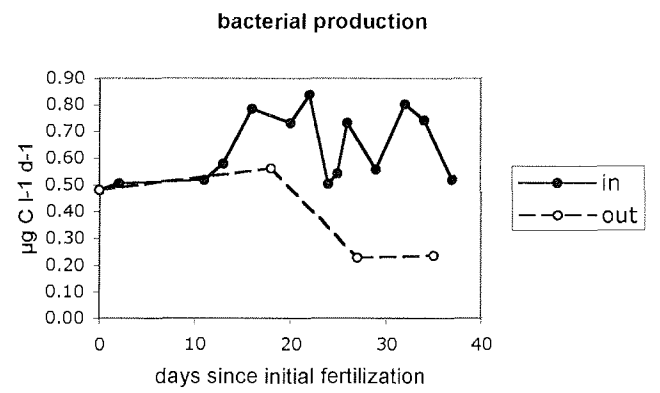


Fig 20.3. Bacterial production inside and outside the Fe fertilized patch

- Cho, B.C. and F. Azam, Major role of bacteria in biogeochemical fluxes in the ocean's interior. *Nature*, 1988. 332: p. 441-443.
 Bidle, K.D., M. Manganelli, and F. Azam, Regulation of oceanic silicon and carbon preservation by temperature control on bacteria. *Science*, 2002. 298(5600): p. 1980-1984.
 Arrieta, J.M., et al., Response of bacterioplankton to iron fertilization in the Southern Ocean. *Limnol. Oceanogr.*, 2004. 49(3): p. 799-808.
 Teira, E., et al., Combining catalyzed reporter deposition-fluorescence in situ hybridization and microautoradiography to detect substrate utilization by Bacteria and Archaea in the deep ocean. *Appl. Environ. Microbiol.*, 2004. 70: in press.

21. MICROZOOPLANKTON

M. Latasa (CSIC)

Introduction

Evidence from experimental and field investigations indicates that the structure and species composition of phyto- and protozooplankton assemblages play a decisive role in the response of the system to an iron enrichment. Grazing-controlled phytoplankton populations are usually composed by organisms of small size. The reason for the existence of blooms, mostly composed of large cells, is usually attributed to long generation times (weeks) of the metazoan zooplankton responsible for grazing the microphytoplankton ($>20 \mu\text{m}$). It has been observed, however, that protists can also be important grazers of large cells such as diatoms. For instance, protistan grazing had a very significant role in the fate of a Fe-induced diatom bloom in the Equatorial Pacific. In the

Southern Ocean, Fe-induced blooms can occur naturally (e.g., by input of Fe from melting icebergs) or artificially.

Objectives

- 1.- To quantify the grazing activity of microzooplankton on phytoplankton in Fe-enriched and Fe-poor waters of the Southern Ocean especially at both short-(<few days) and long time-scales (1-4 weeks).
- 2.- Estimate the dynamics of growth and grazing of key species of phytoplankton.

Material and Methods

The methodology used comprises dilution experiments in adequate size bottles, where grazing pressure is decreased by increasing the dilution of whole seawater with filtered seawater. This method allows the simultaneous quantification of phytoplankton growth and mortality.

Microscopy and HPLC pigment analyses of these experiments reveal the grazing pressure by the protist population on main phytoplankton groups (pigment markers), size classes and key species (microscopy).

In some occasions incubations were performed in parallel. One of them on deck, thermostatized with surface seawater and shaded to receive 20% of the incident irradiance. The on-board analysis of cell pigment concentration (with the Cytosense, see below) from the initial experiment showed that this irradiance did not induce a photoacclimation response in terms of pigment content. The second incubation was performed in a cool room set at 2 °C, under 85 $\mu\text{mol m}^{-2} \text{s}^{-1}$ irradiance and with a L:D cycle of 14.5:9.5 h to mimic the natural light rhythm. Experiments were performed over 48 h (most) or 24 h periods (Table 21.1).

Water from the CTD cast was directly filtered from the sampling bottle by gravity pressure through an acid-clean Suporcap 0.2 μm capsule (Gelman) and used to setup the serial dilutions to 10, 20, 30, 40, 50 and 60% of the whole seawater. Nutrients from K medium were added to this diluted samples plus three bottles containing whole seawater. Because of the impossibility of getting Fe-free seawater from the CTD cast (P. Croot pers. comm.) an additional cast was performed with Go-Flo bottles deployed on a Kevlar cable. Three additional acid-clean bottles were incubated with whole seawater from this cast. However, Fe analysis after incubation did not allow discarding a slight Fe contamination (1-2 nM, M. Öztürk, pers. comm.). It was not possible to determine the origin of such contamination.

Samples were taken to estimate the apparent growth rates for pigment HPLC, bacteria (flowcytometry), picophytoplankton (cytosense in collaboration with F. Colijn) and microphytoplankton (microscopy). For HPLC a maximum of 2 L were filtered with positive pressure (< 0.3 bars) in a cold room set at 5 °C. In some experiments a 5 μm in-line size fractionation was performed with Poretics 5 μm polycarbonate filters followed by Whatman GFF fiber filters. In the rest of the

experiments only GFF filters were used. After filtration filters were folded, wrapped in aluminum foil and frozen and stored at -80 °C. Glass fiber filters were previously blotted dry with absorbent paper.

Table 21.1. Log data of the dilution experiments (Dilfex) performed during Eifex. T_0 and T_f indicate hour of beginning and end of the experiment.

	IN / OUT	T_0	Day ₀	T_f	Day _f	Comments
DILFEX01	OUT t_0 . ST 420	01 30	02-02-04	02 30	03-02-04	SZFX. Patch 1. Fe-clean from Go-Flo but t^o high
DILFEX02	OUT t_0 . ST 424	03 30	12-02-04	03 30	14-02-04	From CTD IV. Patch 2
DILFEX03	OUT t_0 . ST 464	03 30	12-02-04	05 15	14-02-04	Same as above. Cool room. Small bottles
DILFEX04	OUT of patch 1. Station number?	01 00	14-02-04	00 15	16-02-04	From Go-Flo, grow out bottles 32, 33 and 34
DILFEX05	IN. ST 508	18 30	22-02-04	17 00	24-02-04	From CTD IV- Thorium. Probes
DILFEX06	IN. ST 508	18 30	22-02-04	21 00	24-02-04	Same as above. Probes
DILFEX07	OUT. ST 509	14 00	23-02-04	14 30	25-02-04	From Go-Flo. Probes
DILFEX08	IN. ST 513	23 40	27-02-04	01 00	01-03-04	From CTD III
DILFEX09	IN. ST 513	23 40	27-02-04	04 30	01-03-04	From CTD III
DILFEX10	OUT. ST 514	21 00	29-02-04	21 45	02-03-04	Mix CTD/Go-Flo
DILFEX11	IN. ST 543	14 00	04-03-04			
DILFEX12	IN. ST 544 Hot Spot	18 30	05-03-04	18 30	07-03-04	From CTD III diel cycle
DILFEX13	IN. ST 544	20 30	06-03-04	22 00	07-03-04	From CTD. Small bottles
DILFEX14	OUT. ST 546	17 30	09-03-04	18 45	10-03-04	From CTD III and Go-Flo
DILFEX15	IN. ST 553	23 00	11-03-04	23 00	13-03-04	From CTD III
DILFEX16	IN. ST 556	15 45	12-03-04	15 45	13-03-04	From CTD III
DILFEX17	OUT. ST 576	23 30	14-03-04	23 30	16-03-04	From CTD III
DILFEX18	IN. ST 580	07 00	16-03-04	07 15	17-03-04	From CTD III
DILFEX19	OUT. ST 587	22 00	17-03-04	24 00	18-03-04	From CTD III
DILFEX20	IN. ST 591	10 00	19-03-04	10 00	20-03-04	From CTD III
DILFEX21	IN. ST 591	10 00	19-03-04	08 30	21-03-04	From CTD III

For bacterial observation at the flowcytometer, 4 mL of sample were fixed with a solution of paraformaldehyde/glutaraldehyde to a final concentration of 1%. For the cytosense analysis fresh samples were run immediately "in vivo". The volume counted went from 0.5 mL to 5 mL depending on the concentration of the samples. Cells were classified according to their length, as measured by the cytosense, in 7 size classes: less than 2 μm , 2-5 μm , 5-10 μm , 10-20 μm , 20-50 μm , 50-100 μm , 100-200 μm and more than 200 μm .

Preliminary results

Pigments, bacteria and microphytoplankton samples will be analyzed on land.

Cytosense

The results from few experiments have been processed and only some selected examples are shown. Comparing the cell fluorescence at the beginning and at the end of the experiments allowed testing for photoacclimation during the experiment in the different size fractions. For Dilfex02 there was a significant increase of red fluorescence (chlorophyll) at the end of the experiment for the larger than 20 μm fraction (Figure 21.1). The absence of this same change in other fractions precludes concluding that the observed change was due to differences in irradiance conditions between incubation and nature.

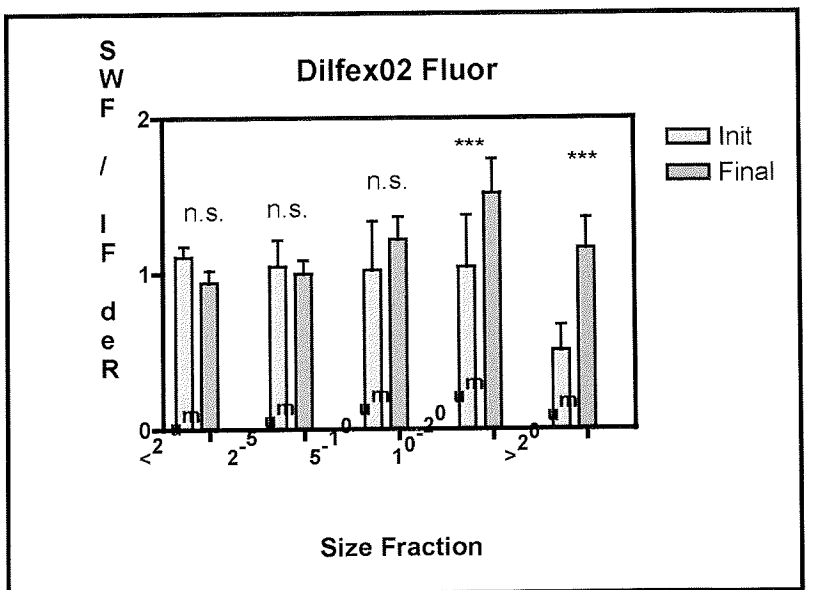


Figure 21.1. Fluorescence per cell biovolume (estimated as forward scattering) at time initial and final for different size fractions. Asterisks indicate significant differences ($p<0.05$, t-test).

As expected, apparent growth rates increased at higher dilutions which allowed estimating grazing and growth rates. Surprisingly size fractionation in Dilfex04

did not show significant differences in grazing pressure on the different size classes. However, this result should be looked at with caution since the fraction larger than 20 μm was not very well sampled under the conditions used for the Cytosense analysis. As it is mentioned above, the dynamics of microphytoplankton will be better determined under microscopic examination.

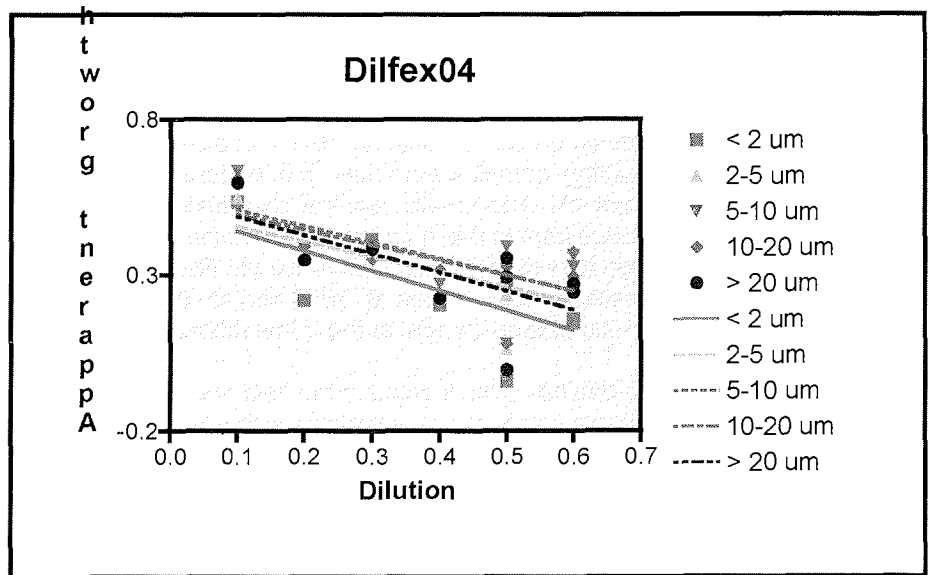


Fig. 21.2. Apparent growth rates at different dilutions (grazing pressure) for the different size classes. No significant changes of the slopes could be found.

22. MEZOZOOPLANKTON

U. Bathmann, L.von Harbou, S. Jansen, S. Krägesky, T. Stadtlander (AWI)

During the first iron fertilization experiment in the Southern Polar Frontal Zone conducted by Polarstern (EisenEx), migration behavior and composition of the zooplankton community inside the fertilized patch changed in comparison to the unfertilized waters, with the net result of higher concentrations of zooplankton biomass in waters with higher chlorophyll concentrations. This experiment has also shown the great grazing impact of the mesozooplankton on the Fe-bloom and on the vertical flux of matter via faecal pellets.

The main objectives for the zooplankton work during EIFEx and our preliminary results obtained during the cruise are stated in the following, accompanied by a brief description of the methods that have been used to address them.

Determination of...

...the zooplankton biomass distribution inside and outside the Fe-fertilized patch and the dominance in species composition contribution to this biomass
For qualitative and quantitative estimate of ind per m² and m³, the water column down to 400 m was sampled at 5 standard depths (25, 50, 100, 160 and 400 m) with a Multi-Net (55 µm and 100 µm mesh size) on a regular basis inside and outside the fertilized patch during night and day. Maximum sampling depth of the Multi-net for one night- and one day-catch at an in-patch station was 1000 m. The estimation of the biomass of larger and of faster swimming animals such as krill will be based on samples from several hauls from the rectangular midwater trawl (RMT, mouth openings 8 and 1 m², mesh-size 2000 and 200 µm) which was towed behind the ship for 10 min at distinct depths. For later identification and counting, samples were fixed with buffered formaldehyde up to a final concentration of 4%. Additionally, several individuals of the most abundant zooplankton groups from in patch and out patch stations were carefully caught with Bongo nets (see below), kept in 0.2 µm filtered seawater for 24 h at 4°C and subsequently deep-frozen at -20°C and at -80°C for later determination of biomass and carbon content at the home laboratory.

Furthermore, zooplankton patches were located in the field and migration behavior followed by continuous acoustic observations with a SIMRAD EK 60 echo sounder system for the upper 300 m of the water column. Calibrations of the acoustic data for biomass estimation, distribution and species composition will be carried out by means of Multi-Net and RMT catches.

Preliminary data analysis based on net catches and acoustic data indicate that the zooplankton biomass increased in the fertilized patch compared to unfertilized water masses as we have seen in previous fertilization experiments. In contrast, comparable to the EisenEx results, high chlorophyll concentrations seems to be unfavorable for salps, which were abundant at the beginning of the cruise but were absent at the end in the center of the fertilized eddy. Although their abundance also decreased over time in the non-fertilized waters following the typical seasonal cycle in autumn in the Polar Frontal Zone, the salp population declined earlier in water masses with high chlorophyll concentrations.

...the impact of zooplankton grazing within and outside the Fe-fertilized patch and estimation of the impact on the carbon flux and fate of the phytoplankton bloom

Zooplankter for experiments were collected outside and inside the patch during night and day with a Bongo net (100 µm and 300 µm) towed vertically from depth between 150 and 20 m to the surface at a maximum speed of 0.3 ms⁻¹. The content of the cod ends were immediately diluted with surface water and brought to the laboratory for further handling.

First results showed, that the grazing impact of the dominant mesozooplankton groups on the phytoplankton community was very high. Most of the data still

need to be determined from stored samples and linked to the abundance data from the acoustics and the net samples, therefore no precise rates can be specified at this stage.

Gut fluorescence

The gut fluorescence technique was carried out routinely during the cruise. For determination of the *in situ* gut fluorescence and gut clearance rates of copepods, other zooplankton including krill, sub samples from the diluted net catch were collected on a piece of mesh immediately after the net was on deck (t0) and at t2, t5, t10, t15, t25 and t40 min. The mesh for each time step was immediately frozen down to -80°C by putting the net with the zooplankton sample into a pre-cooled metal block. Animals were sorted as well as pigments extracted and measured later the day by keeping them frozen as long as possible. Ingestion rates derived with the gut fluorescence method indicate the high grazing rates combined with rather fast gut passage times for nearly all species investigated. However, results need to be compared and discussed within the frame of the results of the other methods applied to estimate the grazing rates and connected to the abundance data before it is possible to evaluate the zooplankton grazing impact on the phytoplankton bloom.

The filter feeding salps were analyzed for gut pigment contents as described for the copepods, while instead of whole animals only the guts were extracted to compensate for the clogging of salps with phyto- and smaller zooplankton during their capture in the nets. Results of all sampled stations combined show that the pigment content in the salp guts was slightly different in t0 and out patch stations (3.4 µg Chl a equivalents/ Ind of 3 cm standard body length) from in patch stations (4.3 µg Chl a eq./ Ind of 3 cm standard body length), indicating a strong grazing impact of salps in both areas. Interestingly, the chlorophyll a to phaeopigment ratio was higher in animals from in patch stations. For a more detailed picture, samples from different depths inside and outside the patch were preserved for later HPLC analysis to compare the uptake and digestion under different food conditions. As a consequence of the so far stated differences in grazing behavior and in regard to their diurnal vertical migration, the overall grazing impact of salps on the plankton community during EIFEx has to be calculated including their residence time in the surface layers which will be determined by means of net catches and acoustic data.

In addition to gut fluorescence analysis of copepods and salps, samples of Bongo net catches were frozen in liquid nitrogen immediately after the net was on deck (no later than 10 min) and stored at -80°C for later analysis of the gut content.

Fecal pellet production

Fecal pellet production experiments have been carried out to estimate the grazing rates and the impact of the zooplankton for the carbon flux of the phytoplankton bloom as well as for content analysis of the fecal pellets. Furthermore the experiments should give an idea about size and shape of the

fecal pellets of the different abundant zooplankton species for later classification of the fecal pellets from the sediment traps.

Experiments with the abundant copepod species were carried out for 24 hours with water from the chlorophyll maximum. Animals were placed in 1 or 2 liter bottles on a slowly rotating plankton wheel at *in situ* temperature and dim light. After 24 hours, the content of the bottles were carefully sieved over 30 µm mesh and fixed with buffered formaldehyde for later enumeration, size measurements and content analysis of the fecal pellets.

Additionally, fecal pellets from freshly caught copepods were collected in order to get "*in situ*" fecal pellets for content and size analysis. Samples need to be obtained and results need to be discussed with regard to the analysis of the sediment traps samples and the vertical distribution of copepods and fecal pellets.

Fecal pellet production experiments with salps were carried out over 8 to 24 h. Animals were kept according to their size in 3 to 15 L containers in surface seawater with ambient phytoplankton concentrations at 4°C. The salps produced between 0.5 and 1.0 FP/ Ind /hour, rates did not change distinctively with high or low chlorophyll concentrations. Fecal pellets produced during the experiment and *in situ* fecal pellets of salps were collected for later analysis (Chl a, carbon content, microscopy) to compare the content and the characteristics of the pellets produced under different food conditions and to estimate their contribution to the carbon flux.

...the influence of a diatom dominated bloom on the grazing and reproduction of copepods

During the whole cruise, egg production experiments were carried out with the abundant calanoid copepod species *Rhincalanus gigas*, *Calanus simillimus* and *Pleuromamma* sp. The three different species showed different responses to the induced phytoplankton bloom. *C. simillimus* produced around 18 eggs female⁻¹ day⁻¹ during the whole cruise with no differences between the in and out patch stations. *Pleuromamma* sp. produced almost no eggs, as well with no differences between the in and out patch stations. This two results were standing in contrast to the response of *R. gigas*, who produced no eggs in the beginning of the cruise and on all out patch stations, while the production rate in patch increased until day 30 after the fertilization up to 50 eggs female⁻¹ day⁻¹. The maximal production rate of 154 eggs female⁻¹ day⁻¹ was found for one female, which is very high for *R. gigas* and is not known to be observed before during this time of the year. Results will be linked to microscopic analysis of the net samples and the samples from the CTD were nauplia and eggs should be enumerated and assigned to the corresponding copepod species.

Frozen samples for determination of changes in the biochemical composition will be analyzed back home in the institute (e.g. C/N and DNA/RNA ratio). Egg production should also give a background for the grazing impact and the development of the zooplankton population in and outside the patch.

...the influence of the food conditions on the tunicate *Salpa thompsoni*

In addition to the samples mentioned above, the biometry and elemental composition of salps (frozen at -20°C and -80°C) will be analyzed in detail (dry weight, C/N ratio, carbohydrates, proteins, lipids and fatty acids as trophic markers) to examine the impact of bloom conditions on salps on one hand and to get a more detailed picture of the salps life cycle on the other hand. Samples from this cruise in late summer/ autumn in the ACC will be compared with samples from other cruises to learn more about the life strategies of salps and their significance in the food chain. The latter seems of special interest with regard to their increasing presence in Antarctic waters. During EIFEx, several hyperiid amphipods species were observed regularly in the salps cavity and sampled for biometrical analysis as well.

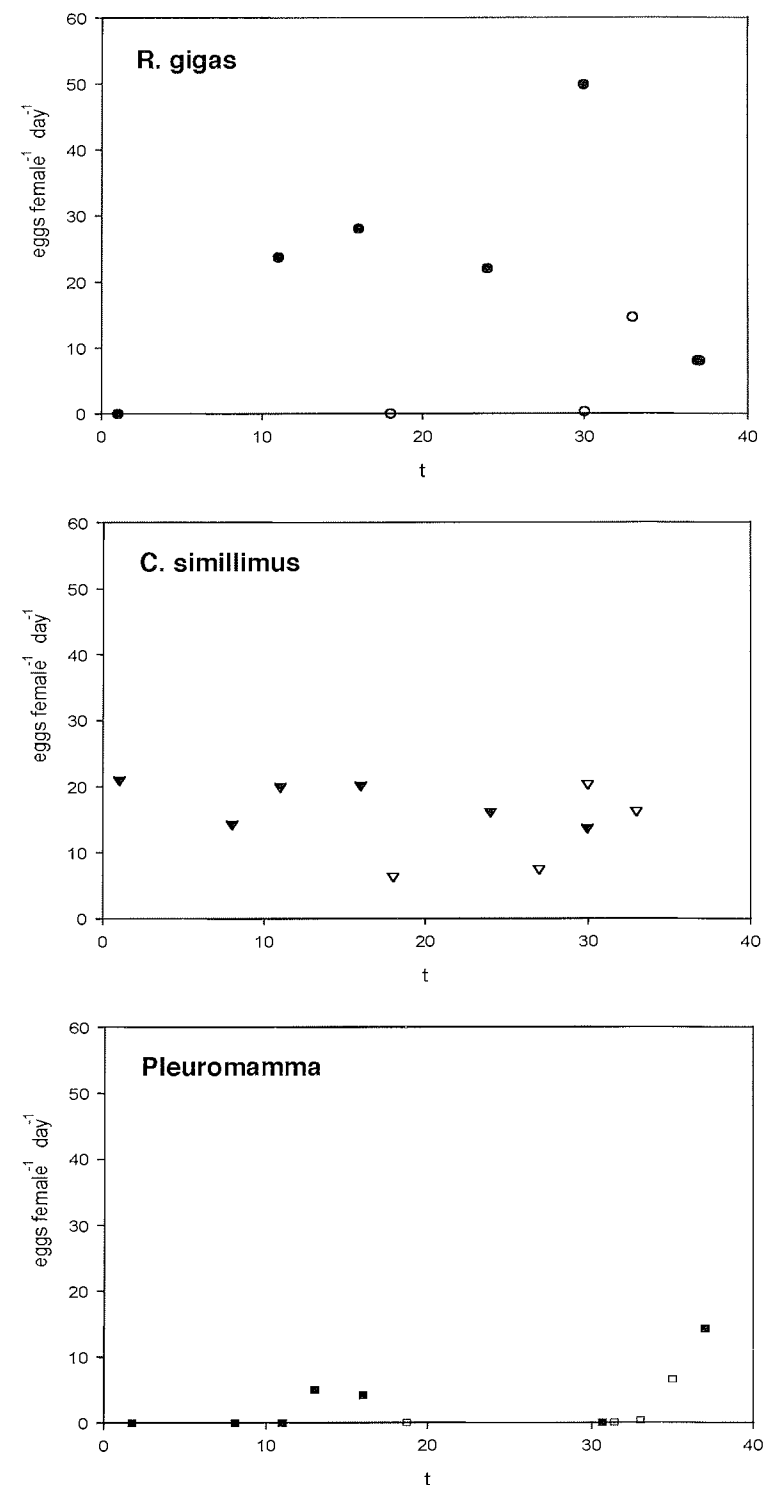


Fig.22.1 : Egg production rates of the abundant larger copepods *Rhincalanus gigas*, *Calanus simillimus* and *Pleuromamma* sp. Filled symbols show the rates on the in patch stations, empty symbols show the values from the out patch stations.

23. DMS, DMSP, DMSO AND DMSP-LYASE

Louise Darroch (UEA)

Introduction

Dimethylsulphide (DMS) is the major marine source of reduced sulphur released into the atmosphere. Not only does DMS represent the gaseous link between the oceans and the atmosphere in the global cycle of sulphur, but it is also a source of non-sea salt sulphate aerosols. These particles can contribute to the acidity of the atmosphere, and in turn the acidity of rain. In addition, they can form cloud condensation nuclei (CCN) and lead to the accumulation of clouds. The resulting cloud albedo is particularly important for climate, especially in remote marine regions, since it will reflect incoming solar radiation and subsequently lower the temperature of the atmosphere. Previous model studies have suggested that the albedo of the Antarctic region is particularly susceptible to changes in aerosol concentration and that a doubling of DMS emissions could lead to an average 1°C cooling of the global climate. Furthermore, Antarctic ice cores suggest that DMS emissions were significantly higher during glacial periods than in warm interglacials.

The major source of DMS in seawater is thought to be through the algal and bacterial enzymatic cleavage of dimethylsulphoniopropionate (DMSP), which is biosynthesised by specific groups of marine micro-algae in varying amounts. The breakdown of DMSP to DMS is catalysed by DMSP-lyase enzymes and is greatly enhanced during microbial processes such as zooplankton grazing and viral- and auto-lysis. Dimethylsulphoxide (DMSO) is an oxidised form of DMS and is found within micro-algal cells and free in the water. It has recently been suggested that algal DMSP, DMSP-lyase, DMS and DMSO are all involved in the protection of cells against the damaging effects of oxidative stress. Oxidative stressors, such as solar ultraviolet radiation and iron limitation have been shown to substantially increase cellular DMSP/or its lysis to DMS in marine algal cultures.

Previous studies of *in situ* iron addition in HNLC regions of the equatorial Pacific and Southern Ocean have shown that DMSP-producing phytoplankton respond rapidly to the new iron, with an approximate three-fold increase in DMSP over a few days. However, the net production and emission of DMS to the atmosphere were variable. In order to better inform mathematical models of past and future climate change, it is important to assess the variability of net DMS production. Therefore, samples for DMS, DMSP-lyase and particulate and dissolved DMSP and DMSO were taken from different depths in the water column, inside and outside the iron enriched patch. In addition to iron enrichment, further investigations were performed to assess the effect of oxidative stress on DMS, DMSP, DMSO and DMSP-lyase. These included artificial and natural light incubations, a diel experiment, fluorescent staining of stressed cells and the collection of samples for the iron isoform of superoxide dismutase (SOD: an anti-oxidant enzyme found in phytoplankton).

Methods and materials

DMS was purged from GF/F seawater filtrates using oxygen-free nitrogen and the resultant gas stream cryo-trapped at -20°C on Tenax resin. These pre-concentrated samples were then injected onto a Chromosil 330 packed column and analysed using a gas chromatograph with flame photometric detector. The same aliquot was then analysed for DMSO following the reduction of DMSO to DMS via the addition of purified DMSO reductase. Alkali hydrolysed GF/F filters for the analysis of particulate DMSO (Tris 50 mmol l⁻¹ buffered) and particulate DMSP were stored in gas tight, crimp-sealed vials for analysis back at UEA via gas chromatography with flame photometric detection. DMSP dissolved samples were stored in the same way but using GF/F filtrates that were pre-purged of DMS. Samples for DMSP lyase were concentrated onto 2 µm polycarbonate Nuclepore filters and stored at -80°C for analysis back at UEA. This will be achieved via the time course of DMS production following the addition of excess DMSP substrate to sonicated or unprocessed filters. Samples for SOD were also concentrated onto 2 µm polycarbonate Nuclepore filters and stored at -80°C for analysis back at UEA. SOD will be resolved via non-denaturing polyacrylamide gel electrophoresis. Samples for iodine speciation were also collected during the cruise from either CTD casts or the non-toxic supply. Whole seawater samples were collected in 50 ml corning tubes and stored at -20°C before analysis by Alex Baker at UEA.

Sample collection and preliminary results

A. Depth profiles

Samples were taken for DMS, particulate & dissolved DMSP and DMSO, and DMSP-lyase for all stations listed below.

Station no.	Cast	Date	Depths (m)
420	05	01/02/04	10, 30, 40, 50, 60, 80, 90, 120
424	08	11/02/04	10, 20, 30, 40, 60, 80, 90, 100, 120
426	04	13/02/04	10, 20, 30, 40, 60, 80, 100, 110, 120
452	01	16/02/04	10, 30, 50, 65, 80, 100
464	01	17/02/04	10, 20, 40, 60, 80, 100, 120
474	01	18/02/04	10, 20, 40, 65, 80, 100
508	05	22/02/04	10, 20, 30, 40, 60, 80, 90, 100, 120
509	03	23/02/04	10, 20, 30, 40, 50, 60, 80, 100, 120
511	05	24/02/04	10, 20, 30, 40, 50, 60, 80, 100, 120
513	05	27/02/04	10, 20, 30, 40, 50, 60, 80, 100, 120
514	06	29/02/04	10, 20, 30, 40, 60, 80, 90, 100, 120
522	01	02/03/04	10, 20, 30, 40, 60, 80, 90, 100, 120
543	15	04/03/04	10, 20, 30, 40, 60, 80, 90, 100, 120
546	05	09/03/04	10, 20, 40, 60, 80, 100, 110, 120
553	05	11/03/04	10, 20, 25, 40, 50, 80, 90, 100, 120
570	07	14/03/04	10, 20, 30, 40, 60, 80, 90, 100, 120
580	06	16/03/04	10, 20, 30, 40, 60, 80, 90, 100, 120
587	03	17/03/04	10, 20, 30, 40, 60, 80, 100, 110, 120
591	03	18/03/04	10, 20, 30, 40, 60, 80, 100, 110, 120

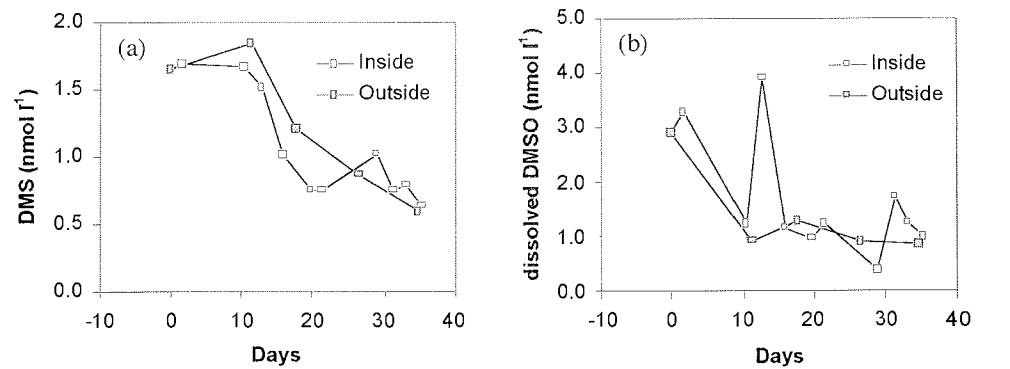


Figure 23.1 shows the concentrations of (a) DMS and (b) dissolved DMSO at 10 m depth inside and outside of the patch throughout the course of the experiment.

Surface DMS concentrations declined during the course of the experiment both inside and outside the patch (Fig. 23.1). Concentrations declined from 1.64 to 0.63 and 0.59 nmol l⁻¹ respectively. Surface dissolved DMSO concentrations were also lower towards the end of the experiment, declining from 2.90 to 1.00 & 0.85 nmol l⁻¹ inside and outside the patch respectively (Fig. 23.2). Iron enrichment did not appear to impact on surface DMS concentrations greatly. A large increase in dissolved DMSO was measured on day 13 (Station 511) inside the patch, reaching 3.92 nmol l⁻¹. Further analysis of data may be required to explain this.

B. Diel cycle

Water was collected from CTD A for 36 hrs during the experiment. Samples for DMS, particulate and dissolved DMSP and DMSO, and DMSP-lyase were collected from 10 m for all casts listed below.

Date	Cast	Approx. Time
05/03/04	05	18:00
05/03/04	09	22:00
06/03/04	11	02:00
06/03/04	14	06:00
06/03/04	18	10:00
06/03/04	24	14:25
06/03/04	29	18:00
06/03/04	35	22:00
07/03/04	42	02:00
07/03/04	48	06:00

Figure 23.2 shows the changes in both DMS and dissolved DMSO over 36 hrs within the patch. Concentrations ranged from 0.56 – 0.82 nmol l⁻¹ and 0.99 - 1.31 nmol l⁻¹ over the course of the experiment for each compound respectively. However, no clear diel cycles for either compound could be seen.

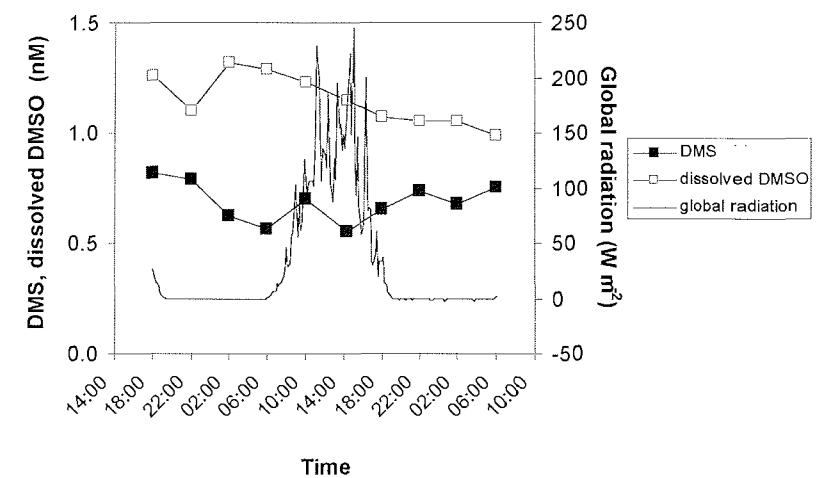


Figure 23.3. The changes in DMS and dissolved DMSO concentrations over 36 hrs in the patch centre

B. SOD

Samples for particulate DMSP and DMSO, DMSP-lyase and SOD were collected from 20 m depth from stations inside or outside the patch as follows.

Station No.	Cast	Date	Approx. Time
555	01	12/03/04	13:45
557	01	12/03/04	16:00
559	01	12/03/04	18:50
561	01	12/03/04	23:40
562	01	13/03/04	00:20
563	01	13/03/04	02:15
564	01	13/03/04	04:15
565	01	13/03/04	06:25

Future Work

Samples for particulate DMSP and DMSO, dissolved DMSP, DMSP lyase and SOD are still to be analysed. Samples will then be compared to other factors such as light, temperature, wind speed, phytoplankton variability and iron.

24. TEILNEHMER / PARTICIPANTS ANT XXI/3

1. Arrieta, J.M.	NIOZ	28. Krägesky, S.	AWI
2. Assmy, P.	AWI	29. Latasa	CSIC
3. Balt, C.	UCT	30. Leach, H.	UNI-L
4. Bathmann, U.	AWI	31. Lentes, J.	DWD
5. Bellaby, R.	UiB	32. Loquay, K.-D.	OPTIM
6. Benner, I.	AWI	33. Mkatshwa, S.	UCT
7. Berg, G.M.	AWI	34. Montresor, M.	SZN
8. Bluhm, K.	IFM-K	35. Nasis, Ilias	Fielax
9. Breitbarth, E.	IFM-K	36. Neill, C.	UiB
10. Büchner	HTA	37. Öztürk, M.	NTNU
11. Buldt, K.	DWD	38. Peeken, I.	IFM-K
12. Cisewski, B.	AWI	39. Prandke, H.	ISW
13. Colijn, F.	GKSS	40. Rohr, H.	OPTIM
14. Croot, P.	IfM-K	41. Röttgers, R.	GKSS
15. Darroch, L.	UEA	42. Savoye, N.	VUB
16. Dibbern, M.	GKSS	43. Schmidt, K.	AWI
17. Federowitz	HTA	44. Schmidt, M.	AWI
18. Feldt	HTA	45. Smetacek, V.	AWI
19. Gonzales, S.	NIOZ	(chief scientist)	
20. Harbou, v., L.	AWI	46. Stadtlander, T.	AWI
21. Henjes, J.	AWI	47. Stimac	HTA
22. Herndl, G.J.	NIOZ	48. Strass, V.	AWI
23. Hoffmann, L.	IFM-K	49. Terbrüggen, A.	AWI
24. Hoppe, L.	AWI	50. Thomas, M.	TU-HH
25. Jäger, M.	AWI	51. Vöge, I.	AWI
26. Jansen, S.	AWI	52. Webb, A.	UCT
27. Klaas, C.	AWI	53. Wolf-Gladrow, D.	AWI

25. PARTICIPATING INSTITUTES / BETEILIGTE INSTITUTE

VUB Belgium
Vrije Universiteit Brussel
Department of Analytical
and Environmental Chemistry
Pleinlaan 2
B-1050 Brussels

LOV	<u>France</u> Laboratoire d'Océanographie de Villefranche-sur-mer (LOV) Diversity, Biogeochemistry and Microbial Ecology Group CNRS-UPMC, UMR 7093 BP 28 06234 Villefranche-sur-mer
AWI	<u>Germany</u> Alfred-Wegener-Institut für Polar- und Meeresforschung (AWI) Columbusstrasse 27515 Bremerhaven
DWD	Deutscher Wetterdienst Geschäftsfeld Seeschiffahrt Jenfelder Allee 70 A D-22043 Hamburg
LAEISZ	Reederei F. Laeisz Barkhausenstr. 37 27568 Bremerhaven
IFM-K	Institut für Meereskunde an der Universität Kiel Düsternbrooker Weg 20 24105 Kiel
TU-HH	Technische Universität Hamburg-Harburg Schwarzenbergstrasse 95 21073 Hamburg
HSW	Helicopterservice Wasserthal GmbH Kätnerweg 43 22393 Hamburg
UNI HB	Universität Bremen Postfach 33 04 40 28334 Bremen
GKSS	Forschungszentrum Geesthacht Institut für Küstenforschung, GFE, Fernerkundung Max-Planck-Str. D-21502 Geesthacht
OPTIM.	OPTIMARE GmbH Jadestraße 59 26382 Wilhelmshaven

ISW	ISW Wassermesstechnik Lenzer Str. 5 17213 Petersdorf
SZN	<u>Italy</u> Stazione Zoologica 'A. Dohrn' Villa Comunale 80121 - Napoli (Italy)
NIOZ	<u>Netherlands</u> NIOZ Dept. Biol. Oceanog. Postbox 59 NL-1790 AB Den Burg/Texel
CSIC	<u>Spain</u> INSTITUT DE CIENCIAS DEL MAR (CSIC) Passeig Marítim de la Barceloneta, 37-49 E-08003 BARCELONA
UiB	<u>Norway</u> University of Bergen Allégaten 55 5007 Bergen
NTNU	Norwegian University of Science & Tech. TBS Bynes veien 46 7491 Trondheim
UCT	<u>South Africa</u> University of Cape Town Oceanography Dept. Rondebosch 7701
UEA	<u>UK</u> University of East Anglia School of Environmental Sciences University of East Anglia Norwich NR4 7TJ
UNI-L	Oceanography Laboratories The University of Liverpool Liverpool, L69 3BX

26. SHIP'S CREW / SCHIFFSBESATZUNG ANT XXI/3

01. Pahl, Uwe	Master	German
02. Schwarze, Stefan	1.Offc.	German
03. Schulz, Volker	Ch.Eng.	German
04. Fallei, Holger	2.Offc.	German
05. Grimm, Sebastian	2.Offc.	German
06. Jahn, Thomas	2.Offc.	German
07. Schneider, Claus	Doctor	German
08. Hecht, Andreas	R.Offc.	German
09. Erreth, Monostori, G.	1.Eng.	German
10. Hoffmann, Bernd	2.Eng.	German
11. Simon, Wolfgang	2.Eng.	German
12. Fröb, Martin	Fielax-Elo	German
13. Gerchow, Peter	Fielax-Elo	German
14. Holtz, Harmut	ElecTech.	German
15. Piskorzynski, Andreas	Fielax-Elo	German
16. Schulz, Harry	Fielax-Elo	German
17. Clasen, Burkhard	Boatsw.	German
18. Neisner, Winfried	Carpenter	German
19. Burzan, G.-Ekkehard	A.B	German
20. Hartwig-Labahn, Andreas	A.B.	German
21. Kreis, Reinhard	A.B.	German
22. Leisner, Bert	A.B.	German
23. Moser, Siegfried	A.B.	German
24. Schröder, Norbert	A.B.	German
25. Schultz, Ottomar	A.B.	German
26. Völker, Frank	A.B.	German
27. Beth, Detlef	Storekeep.	German
28. Arias Iglesias,Enr.	Mot-man	Chile
29. Dinse, Horst	Mot-man	German
30. Fritz, Günter	Mot-man	Austria
31. Krösche, Eckard	Mot-man	German
32. Toeltl, Siegfried	Mot.-man	German
33. Fischer, Matthias	Cook	German
34. Martens, Michael	Cooksmate	German
35. Tupy,Mario	Cooksmate	German
36. Dinse, Petra	1.Stwdess	German
37. Schöndorfer, Ottilie	Stwdss/KS	German
38. Deuß, Stefanie	2.Stwdess	German
39. Schmidt,Maria	2.Stwdess	German
40. Streit, Christina	2.Stwdess	German
41. Tu, Jian Min	2.Steward	China
42. Wu, Chi Lung	2.Steward	German
43. Yu, Chung Leung	Laundrym.	Hongk.

FAHRTABSCHNITT ANT XXI/4 KAPSTADT – KAPSTADT

Fahrtleiter / Chief Scientist: Ulrich Bathmann

INHALTSVERZEICHNIS / CONTENTS

1.	Introduction	135
	Reiseroute/ Cruise track	140
2.1	Demography of antarctic krill and other euphausiacea in the Lazarev Sea	141
2.2	Distribution and abundance of krill larvae	154
2.3	Acoustic krill observations	157
2.4	Survival strategies of <i>euphausia superba</i> in autumn	166
3	Circulation, ice and zooplankton-abundances	169
4.	Zooplankton- Biovolume	190
5.	Biology of pelagic tunicates in the Lazarev Sea during April 2004	196
6.	Distribution of surface zooplankton and mikronekton as potential prey for antarctic top predators – a suit experience	200
7.	Spatial patterns in food requirements of marine birds and mammals in the lazarev sea, april 2004 (polarstern ant-xxi-4, so-globec)	206
8.	Sampling of larval and juvenile fish in the Lazarev Sea for molecular identification – observed autumnal distribution patterns	212
9.	Cetaceans and sea ice	214
10.	Max-doas messung atmosphärischer spurengase	217
11.	Benthic fluxes around the antarctic polar front during the austral fall season	218
12.	Acoustic seafloor investigations with parasound	227
13.	Oxygen and nutrients in the globec area	229
14.	Continuous Plankton Recorder (CPR): Australian Antarctic Division Project 472	232
15.	Bojenausbringung	234
15.a)	Sea-Ice Buoy Deployments	234
16.	Meteorological conditions during cruise	235
17.	Journalistische Dokumentation	238
18.	Liste der Staionen ANT XXI/4	240
19.	Ship's Crew / Schiffsbesatzung Ant XXI/4	266
20.	Participants / Fahrteilnehmer Ant XXI/4	267
21.	Participating Institutes / Teilnehmende Institute	268

**FAHRTABSCHNITT ANT XXI/4 KAPTSTADT -
KAPSTADT**
(27.03.04 - 06.05.04)

1. INTRODUCTION

U. Bathmann (AWI)

The krill expedition ANT 21_4 was a major contribution to the international GLOBEC and CCMLAR research programmes that focus on krill survival mechanisms within the life cycle biology of this Antarctic key species. The international science programme „Global Ocean Ecosystem Dynamics“ (GLOBEC), that was started 4 years ago „to advance our understanding of the structure and functioning of the global ocean ecosystem, its major subsystems, and its response to physical forcing so that a capability can be developed to forecast the response of the marine ecosystem to global change“. In the Southern Ocean the target organism is krill (*Euphausia superba*), its fluctuations in biomass standing stock in relation to ocean circulation and sea ice dynamics, krill physiology and its role in the Antarctic ecosystem. One of the mysteries still to be explained is how krill survives the long periods of the Antarctic winter where food is sparse. Part of our work also will contribute to another large international monitoring and management programme run by the Convention for the Conservation of Antarctic Marine Living Resources (CCAMLR). Founded in 1982 CCAMLR nations including Germany carry out research in Antarctica to advance the scientific knowledge for protection and fishery management in the Southern Ocean. The scientific council advises the nations in research strategies and the Commission is the political arm of CCAMLR.

In April 2004 the krill spawning period was over for at least several weeks. Organisms had already started to reduce their metabolism, and were in a transition phase from high summer to low winter conditions. The relatively high oxygen consumption of larvae and juveniles – a measure of their metabolic activity - indicated that the specimens still found sufficient food in the water and between ice. Adult krill, however, had already reduced the summer values in daily carbon consumption (30% of the body carbon) down to only a few percent typical for food intake in winter. Ingested food comprised in 2/3 of phytoplankton and the remaining 1/3 in microzooplankton. The trigger that induces the reduction in body metabolism and the reduction in feeding is still unknown but we will perform enzymatic measurements in the home laboratory on frozen samples to gain some insight into the underlying mechanisms. Growth experiments with different larval stages of krill show that they were very fit with a daily mortality of less than 2%. We assume that krill larvae did feed on ice algae to fulfil their energy demand, but it is still unclear to which degree krill larvae also feed on microzooplankton. In first experiments performed during our cruise it became evident that the amount of microzooplankton as food items

increases with the age of the krill larvae. But krill larvae are still mysterious in many respects. They do not carry sufficient lipid reserves, as do the adults, to account for hunger periods during winter. And they do not show any mechanisms like the reduction in metabolic activity to save body energy. Thus, it still remains unclear how krill larvae survive during the strong long winter and we have to perform more experiments to construct a proper energy budget for the different growing seasons. The deep frozen krill will be analysed for biochemical and pharmaceutical substances back in home laboratories.

The krill in the Lazarev Sea were concentrated in two areas: the northeast corner between 61°S and 64°S and the marginal ice edge zone (MIZ) between 67°S and 69°S. In the MIZ the largest krill with body length up to 54 mm and an age of more than 3 years was found. Krill in the north were considerably smaller, younger and did not spawn in the previous season. Ice krill were found only in the very proximity of the continental ice shelf. Krill distribution was monitored down to 600m water depth by means of the echo sounder. The krill swarms were rather small and did migrate vertically on a diurnal cycle. Juveniles of the age class 1 (year) – the recruits – were virtually absent, with one exception on a single northern station, which indicates that the breeding success of krill in the previous year was rather low. Very young larvae, i.e. larvae from the current year, were rather abundant. These larvae have to feed continuously to survive and this might become a problem in the coming winter months. Spawning must have taken place rather late this year and we assume that the survival rate of these late spawners are rather low despite the fact that most young larvae were in excellent physiological condition. Krill larvae in the age between 30 and 60 days were very abundant in the central area (65-67°S), a fact that contradicts published findings that in turn show maximum larvae abundance on the continental shelf in the south of the Lazarev Sea. We have to closely examine the oceanographic current regime to solve this mystery. We also have to analyse the frozen samples at home to determine whether the krill here are genetically similar to the krill of the other Antarctic areas e.g. from the Antarctic Peninsula region.

The surface under ice trawl (SUIT) net caught krill larvae in the close vicinity of sea ice floes, an indication that the organisms were feeding on the ice biota and were hiding between floes against their predators. The biomass obtained from the SUIT net hauls of the upper metres in the ocean ranged between 10 and 1000 grams with one exceptional catch of 30 kg. This also indicates, that krill occurred - if at all - in locally concentrated swarms, and that krill was only present at sea surface and under the ice during night time and that its distribution was rather patchy. On the contrary, the guts of sea birds, attracted by the ships light and landing on deck, did contain many krill, fish larvae and squid - the latter not being caught in considerable numbers by the nets. Besides krill, the salps (tunicates) were surprisingly abundant in the ice-covered areas. Whether this exceptional occurrence of the so-called "warm water species" in the Coastal Current indicate an intrusion of advecting water masses from the north, or is an indicator for climate shifts, has still to be determined.

Zooplankton in the Lazarev Sea comprised of copepods, tunicates, arrow worms, polychaetes, amphipods, pteropods and jellyfish and was concentrated in the upper hundreds metres of the water column. Copepods dominated in abundance and very often also in biomass. Whereas the smaller 2 mm copepods were concentrated in the surface layers, the 4mm *Calanoides acutus* already had started to migrate down for hibernation in 500 to 1000m. The other large *Calanus propinquus* remained in surface layers as it contains special storage and anti freeze lipids that help the organisms to be active in winter. Both groups of copepods were preyed upon by chaetognaths that slime transparent body helps them to grab the prey with the setae equipped with hooks and attached on either side of the head. In the upper 100m of the -1.86°C super cool waters of the coastal current, the zooplankton was somewhat reduced and was dominated by appendicularia and salps. Most of the zooplankton in the coastal current was found in the slightly warmer waters that intruded onto the shelf between 400 and 150m. These layers were inhibited by polychaetes, hunting copepods well known from the Weddell Gyre.

The whale observations from the International Whaling Commission collaborated with other Antarctic research programs and examined variability in baleen whale distribution and movements in southern waters in relation to their prey, Antarctic krill and sea ice concentrations. On transit between Cape Town and the cruise survey area, only one whale sighting was made but in the survey area 16 sightings of 22 whales including humpback and minke whales, a single sperm whale and some unidentified species were seen. In summary, the low numbers of top predators in the area indicate that the central Lazarev Sea seems to be a low production area for krill.

During the previous cruise of Polarstern – the European Iron Fertilization Experiment (EIFEX) – scientists fertilized a 10 km^2 wide patch in the centre of an ocean eddy with iron and stimulated a considerable phytoplankton bloom composed mainly of diatoms. During the experiment biomass and productivity of bacteria and zooplankton also increased. At the end of EIFEX, some diatom species sank out of the productive surface layer to water depths close to the sea floor. Especially the geochemists sampled the sea floor underneath the EIFEX location to learn whether the bloom had sunken to the sea floor and if so, to what degree this input of fresh organic carbon has changed geochemical profiles in the sediments.

The 9 stations where sediment surface layers were sampled and analysed by the geochemical group on board ship. These stations included those at the Polar front where the previous iron experiment EIFEX had been performed. First results indicate that the phytoplankton growing at sea surface did sink through the water column and had reached the sea floor in about 4000m water depth within a few weeks. This input of rather fresh organic material induced biological degradation at and in the surface sediments. On one core retrieved from the sediments of the Polar front, a 10cm thick, fluffy layer of fresh organic matter showed remarkable biological degradation that caused oxygen reduction in about 5cm sediment depth followed by oxygen rich layers underneath. This

exciting finding just illustrates how tightly the biological processes at ocean surface are coupled with biogeochemical reactions in the sediments. If we can fully understand these mechanisms we are in a better position to use the sediment record as history books to reconstruct upper ocean processes that in turn are related to global processes in general.

Icy winds and heavy sea did not prevent the able crew to perfectly operate Polarstern on 102 stations in autumn 2004 in the Lazarev Sea that was more than anticipated. Krill was fished in open water and under the ice, we measured it's physiology, collected zooplankton and nekton, counted birds and observed whales. We characterised the physical, chemical and biological properties of the water column from ocean surface to the deep-sea and penetrated the sea floor to interpret past ocean processes encrypted in it's sediments. Many thanks to all companies that provided help for this hard work. All members on board endowed an excellent human spirit and a fine humour and helped to keep a pleasant working atmosphere even during long nights of work. Polarstern arrived in Cape Town as scheduled on 6 May 2004.

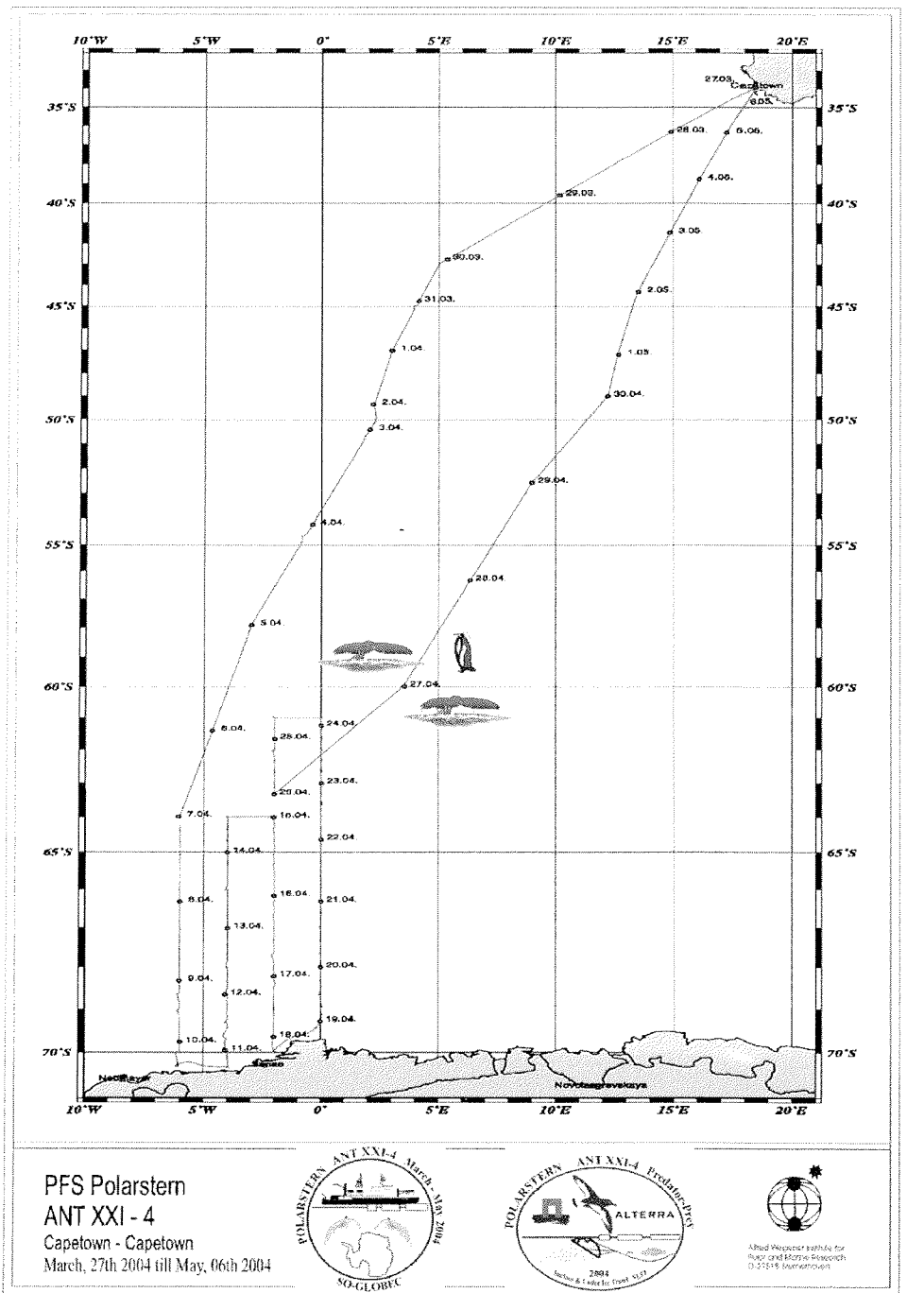


Fig. 1 Cruise track of POLARSTERN ANT 21/4 from 27.03.-06.05.2004

2.1 DEMOGRAPHY OF ANTARCTIC KRILL AND OTHER EUPHAUSIACEA IN THE LAZAREV SEA

V. Siegel, B. Bergström, S. Schöling, M. Vortkamp (BfF)

Introduction

Investigations on Antarctic krill have a long history starting with the early Discovery studies in the 1920/30ies. These historic studies concentrated on krill distribution and basic biology. Although these studies covered most of the Antarctic Ocean, data are spread over a time period of several years and research effort was not spread evenly across the Southern Ocean. Especially regions with severe sea-ice conditions were less adequately sampled. Recent studies concentrate more on quantitative aspects of krill stock abundance, with the aim to develop a proper management of this living resource. Research effort concentrated in the Southwest Atlantic and Prydz Bay area of the Indian Ocean, probably because of the remoteness and the difficult sea-ice conditions in the Lazarev Sea. Despite the collection of some krill data in the Lazarev Sea by the Discovery research this region of the Southeast Atlantic hardly ever studied in great detail. Even the Russian study from March 1982 (Makarov and Sysoyeva, 1985) concentrated on the distribution of krill in this area and paid less attention to quantitative aspects.

However, the Lazarev Sea is thought to be the doorway to the Weddell Sea and possibly the entrance of the krill population into the Weddell Gyre. Few results of recent (1980ies to 90ies) indicated variable conditions for the krill and salp population, but a standardized survey has not yet been carried out in this area to lead to quantitative results on krill abundance and demographic parameters of this population. Even less information are available on other euphausiid species. Since the analysis of the latitudinal distribution of Antarctic euphausiids by Baker (1965) only a few local studies paid attention to these other species, Siegel (1988) studied growth of euphausiids, Nordhausen (1992, 1994) described *Thysanoessa macrura* distribution, and several authors investigated distribution of *E. crystallorophias* in the, Prydz Bay, Lazarev Sea or Ross Sea (Thomas and Green, 1988; Pakhomov et al., 1998; Sala et al., 2002).

The description of krill demographic parameters and the investigation of population dynamics of the stock were the major focus of the krill net sampling programme to the Lazarev Sea in austral autumn 2004. Recruitment indices as well as other parameters, such as length-at-maturity and growth parameters are fundamental building stones for the Krill Yield Model. This model is used by CCAMLR to calculate the potential yield of krill that does neither harm the krill population nor the populations of dependant krill predator species. The outcome of the model serves to set regional precautionary catch limits for a rational use of the resource.

Material and Methods

Experience gained through participation in other international programmes like BIOMASS has shown that standardization of equipment and methods is one of the most crucial steps for any successful work during the field sampling period and later analytical work. The following net sampling protocols set out the procedures so that carrying out the Lazarev Krill Survey 2004 could collect comparable high quality data sets that will facilitate the establishment of a uniform and valuable database.

There are two primary objectives for the net sampling programme: to validate and identify acoustic targets, confirming which targets can be considered as krill and obtaining krill length frequency data for Target Strength estimation to describe krill demography and large scale distribution patterns of size groups and maturity stages as well as larval distribution and abundance.. The CCAMLR Convention on the Conservation of Antarctic Marine Living Resources) Working Group recommended the use of a standard type of net to avoid potential variation in catchability and selectivity of nets during krill centred survey activities. The most appropriate type of net presently available is the RMT8+1 (Rectangular Midwater Trawl). This net was used as the standard net for target and random hauls.

At each station a quantitative standard double oblique tow was conducted from the surface down to 200 m. Such a depth range is considered to be the best compromise between the time available for sampling and the likely vertical depth range of krill. During the hauls ship's speed was maintained at 2.5 ± 0.5 knots. A constant wire speed of 0.5 m/sec was maintained during paying out and 0.3 m/sec during hauling. The net mouth angle is remarkably constant during hauling within the speed ranges given above. When the net reached maximum depth, the winch was stopped for about 30 seconds to allow the net to stabilize before starting to retrieve the net. The total time of the net haul from surface to bottom to surface was approximately 40 minutes.

The use of a real-time time-depth-recorder (TDR) is essential to maintain a smooth net trajectory and control the track of the net and the maximum fishing depth. Calibrated flowmeters were used to give a measure of net speed during the haul as well as the total distance travelled. The flowmeter was mounted outside the net opening to avoid clogging which may reduce the efficiency. The dependence of mouth angle to the vertical of net speed has been investigated for the RMT system.

The quantitative study of the krill population was carried out along four parallel meridional transects which extended from the continental coast into oceanic waters (see Figure 2.1.1). The transects were located along 6° , 4° , 2° and 0° W. Additional standard tows were carried out on transect 3 and 4 between 64° and 61° S. Net samples were taken every 20 nautical miles along each transect. A total of 93 RMT stations was carried out during the cruise. A double oblique net tow was carried out routinely at all stations. Immediately after the tow displacement volume of the RMT sample was measured and krill and salps

were removed from the RMT8 sample. Samples were sorted immediately after the haul. Antarctic krill and other Euphausiid species as well as salp species were sorted quantitatively from the RMT 8. However, if the sample size was larger than one litre then a representative subsample was analysed. Krill was stored in 4 % formalin-seawater solution for later length measurements and maturity stage analyses. From larger krill samples a number of 50 to 100 krill specimens was preserved in 96% ethanol for later molecular genetic studies.

Length measurements were taken from representative sub-samples with a minimum of 150 specimens. Length measurements and detailed maturity stages were identified from 6974 krill specimens. We used the 'Discovery' method for *E. superba* (total length from the anterior margin of the eye to the tip of the telson) and the 'standard 1 total length' between the tip of the rostrum and the posterior end of the uropods for all other euphausiids (Mauchline 1980). Additional information were collected for sex and maturity stages of euphausiids according to the classification established by Makarov and Denys (1981). These measurements served the interpretation of the success of the current reproductive season and the status of the spawning stock, but as well give us some indication on the survival rate of recruits in the population spawned in the previous year.

All relevant station data as well as all counts and measurements were recorded onto computer before the end of the cruise in the data base format established by the Institut für Seefischerei in Hamburg. Samples for genetic studies will be analysed by Kristineberg Marine Research Station (Sweden). Data and samples will be available on request according to the rules of access set out by CCAMLR in the relevant Scientific Committee documents.

Preliminary results

The Lazarev Sea is located in the high-latitude part of *E. superba*'s range, directly adjacent to the Antarctic continent. 64 samples out of a total of 93 contained krill in varying quantities. The largest krill catch yielded 30 kg or 94000 specimens in a standard haul at one of the northern stations of the 2°W transect. Major krill concentrations occurred in the northern part between 61° and 64°S (Figure 2.1.2a). Another patch of relatively high krill concentration was found across the survey area just outside the marginal ice-zone. Another small local spot with higher krill abundance was observed inside the pack-ice on the western transect south of 69°S.

Stations with zero krill catches were scattered all over the entire study area. A day-night comparison was carried out using krill abundance data grouped into non-linear abundance classes (Figure 2.1.3a). The results clearly indicate that all zero catches and most of the catches with only single krill specimens were taken during daytime. All samples with more than 10 specimens were collected during night. Only some of the very large catches were also obtained during daytime. This result on distinct differences between day and night is surprising. From similar surveys in the Antarctic Peninsula area and Scotia Sea we know that krill is usually caught in great numbers during daylight in the upper 200 m

water column. For the present survey net avoidance cannot be the reason for such a substantial difference in catchability during the day, because the net operation was carried out in a standardized way and similar effects should have been observed in other surveys. A second possible explanation could be a different behaviour of krill during this late autumn period in these high latitudes.

Maybe vertical migration behaviour could be responsible for the low day catches. Vertical migration has been reported from the summer period and occurs generally within the upper 140 m water column, and in more northern latitudes like South Georgia it may occur over the upper 200 m water column. This was the reason for our standard oblique tows down to 200 m to cover the entire known vertical migration range. If, however, this migration pattern changes seasonally and krill migrates over greater vertical distances beyond 200 m depth during autumn, then we might have missed these deep concentrations during our day sampling. A final conclusion cannot be drawn from the present data without further studies on vertical distribution and additional sampling beneath the 200 m depth layer.

The second environmental feature which can influence krill distribution and abundance is the seasonal ice-cover. During the survey period the area south of 68°S was covered by pack-ice. A comparison between the open water survey area and the pack-ice zone showed some differences in krill abundance for these two areas (Figure 2.1.3b). Inside the pack-ice the number of stations with no or few krill was generally higher than in the open water area. On the other hand, those samples with more than 100 or 1000 krill per standard tow were found more frequently in ice-free areas. However, this difference is much less pronounced than the day-night difference between samples. It has to be tested whether the difference will be significant after adjusting krill abundance data to a standardized filtered water volume.

The composite length frequency distribution of krill showed that the population was dominated by the modal size class of 36 mm (Figure 2.1.4). This represents the average length-at-age of age-class 2. This age-class usually consists of immature specimens that have not yet participated in the spawning process, but will mature until the next summer spawning event. Age-class 1 is usually characterized by juvenile krill with a mean length-at-age of approximately 27-28 mm. This age class was almost completely missing during our investigation and was only found in greater numbers at a single station (1106) on transect 4 north of 64°S. Adult age-classes 3 and 4 (length-at-age 44 and 50 mm, respectively) did occur in small quantities, while the oldest age-class 5+ (>54 mm) was missing from our samples. It could have been that this age-class was represented by a poor year-class or these oldest animals had already died off after the end of the current spawning season.

The spatial distribution of krill size and developmental stages showed some geographical differences (Fig. 2.1.5). Most of the krill between 61° and 68°S showed a unimodal size frequency distribution. These were juveniles or immature stages of 34 mm modal length.. As mentioned above, higher concentrations of one-year-old juveniles of 27 mm on average were only found

at station 1106 in the north. However, south of the ice edge the size composition of krill changed. Here we still observed a broad mode between 27 and 35 mm, which represented the immature components of the northern stations, but also included some of the younger juveniles. However, the overall length frequency distribution was bimodal with a distinct peak of larger animals around 47 mm belonging mostly to adult developmental stages.

Analyses of the maturity stage composition verified that the spawning season in the Lazarev Sea had completely ended before April. No more females were found with spermatophores attached, but adult females showed clearly empty ovaries so that they could be identified as "spent" females (stage 3E) (Figure 2.1.6). In some cases a "re-maturation" had already taken place, i.e. the ovaries had recovered to a "pre-spawning" stage 3A, but because of the large size of these animals (> 45 mm) it had to be considered that these animals had spawned during the current season. Females larger than 40 mm are generally mature and participate in the spawning event. During our study we found quite a few females beyond this size which were definitely of immature stage according to their external sexual characteristics. The same happened to quite a number of males, which according to their large size should have been adults, but showed immature characteristics of stages 2A3 (advanced petasma) or even the earlier stage 2A2 (petasma split into two fingers). In these cases a "rejuvenation" could have occurred after the end of the spawning season, i.e. mature males and females regressed in their external sexual characteristics to immature forms. This phenomenon was already described from very few individual krill maintained in an aquarium experiment (Poleck and Denys, 1982), but was not yet reported from field studies of natural populations.

Thysanoessa macrura was the second most common euphausiid species in the Lazarev Sea (Fig. 2.1.2b). This species was encountered at 72 stations out of 93. Distribution was more homogeneous than for krill, and abundance was relatively low compared to other areas in the Southwest-Atlantic sector. Maximum numbers per tow did hardly exceed 150 specimens. Although *Thysanoessa macrura* is known from the southern Weddell Sea and spread across our entire survey area well into the pack-ice zone, it was not found on the narrow continental shelf.

The length frequency distribution showed a distinct modal size of 25 mm, indicating a mixture of two and three-year old animals in the population (length-at-age approx. 22 and 27 mm, respectively) (Fig. 2.1.7). Age-class 1 is expected to have grown to a mean of 17 to 19 mm at this time of the year, but as the length frequency distribution indicates, this age group was not very abundant in our samples. Maximum age of *Thysanoessa macrura* is supposed to be 3+ with an infinite length of 37 mm. However, there are indications from our length data that there may be an additional age class beyond 30 mm size, because we regularly found large adults between 30 and 40 mm, even if their total number was not very high.

Baker (1965) described the latitudinal distribution of Antarctic euphausiid species and found *E. crystallorophias* as the southernmost species inhabiting the neritic zone of the continent. This has since then been confirmed for all parts of the Southern Ocean. Therefore, the restricted distribution of this species was of no surprise during our survey. *E. crystallorophias* was clearly confined to five stations on the narrow shelf and the steep continental slope. Published length-at-age data indicate one-year-old animals to be of 18 to 19 mm mean size. This fits fairly well with our data which show a first mode at 17 mm (Fig. 2.1.8). This size class consisted almost exclusively of juvenile specimens. The population was clearly dominated by two-year old immature males and females, peaking at 28 mm modal size. Older and adult age classes were missing from our samples, although *E. crystallorophias* is known to grow larger than 40 mm and live at least until age-class 4+.

E. triacantha and *E. frigida* are species of the mesopelagic depth layer, but regularly occur in night samples in the upper 200 m from the Antarctic Peninsula and Scotia Sea waters. Their main distribution centre lies just south of the Polar Front, but may extend to the northern boundary of the seasonal pack-ice. However, these species are not recorded from the Weddell Sea. *E. triacantha* was completely absent from our samples in the Lazarev Sea. Low numbers of *E. frigida* were caught at 8 stations north of 64°S, while this species was completely missing south of 64°S. From an earlier cruise to the southern Weddell Sea in summer 1980, *E. frigida* was reported only from stations located north of 60°S (Hempel et al. 1983). During the present study distribution of *E. frigida* obviously extended 240 miles further south than in 1980. *E. frigida* is supposed to live for little more than one year. Mean length-at-age for the Southwest Atlantic population is 17-18 mm at the end of the summer season, which fits well with the observed 16-17 mm in the northern Lazarev Sea, indicating similar growth patterns of this species for the entire Atlantic sector..

References

- Baker A. de C. (1965) The latitudinal distribution of Euphausia species in the surface waters of the Indian Ocean. Discovery Reports 33: 309-334
Hempel I., Hubold G., Kaczmaruk B., Keller, R., Weigmann-Haass, R. (1983)
Distribution of some groups of zooplankton in the inner Weddell Sea in summer 1979/80. Ber. Polarforschung 9: 1-36
Makarov R.R. and Denys C.J. (1981) Stages of sexual maturity of Euphausia superba. BIOMASS Handbook 11: 1-13
Makarov, R.R. and Sysoyeva , M.V. (1985) Biology and distribution of Euphausia superba in the Lazarev Sea and adjacent waters.
Mauchline J (1980) Measurement of body length of Euphausia superba Dana. BIOMASS Handbook 4: 1-9
Nordhausen W (1992) Distribution and growth of larval and adult Thysanoessa macrura (Euphausiacea) in the Bransfield Strait Region, Antarctica. Marine Ecology - Progress Series 83: 185-196
Nordhausen W (1994) Winter abundance and distribution of Euphausia superba, *E. crystallorophias*, and Thysanoessa macrura in Gerlache Strait

- and Crystal Sound, Antarctica. *Marine Ecology - Progress Series* 109: 131-142
- Pakhomov EA, Perissinotto R, Froneman PW (1998) Abundance and trophodynamics of Euphausia crystallorophias in the shelf region of the Lazarev Sea during austral spring and summer. *Journal of Marine Systems*. 31:3-324
- Poleck, T.P., Denys, C.J. (1982) Effect of temperature on the moulting, growth and maturation of the Antarctic krill *Euphausia superba* (Crustacea: Euphausiaceae) under laboratory conditions. *Marine Biology* 70: 255-265.
- Sala A, Azzali M, Russo A (2002) Krill of the Ross Sea : distribution, abundance and demography of *Euphausia superba* and *Euphausia crystallorophias* during the Italian Antarctic Expedition (January-February 2000). *Scientia Marina* 60: 123-133
- Siegel V (1987) Age and growth of Antarctic Euphausiacea (Crustacea) under natural conditions. *Marine Biology (Berlin)* 96: 483-495
- Thomas PG, Green K (1988) Distribution of *Euphausia crystallorophias* within Prydz Bay and its importance to the inshore marine ecosystem. *Polar Biology* 8: 327-331

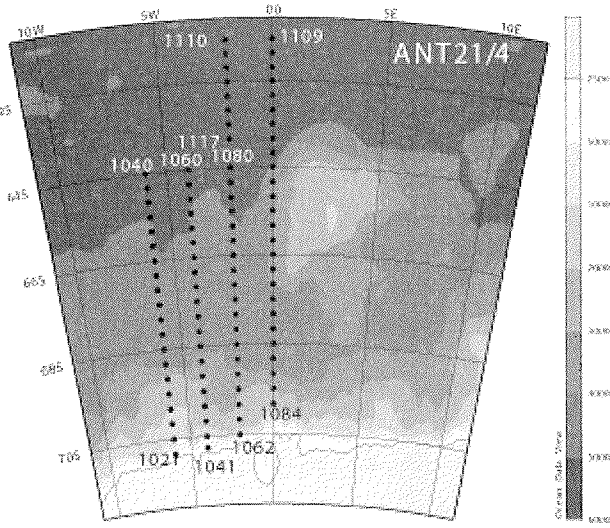


Figure 2.1.1: RMT station grid in the Lazarev Sea during April 2004 including bathymetric depth contours

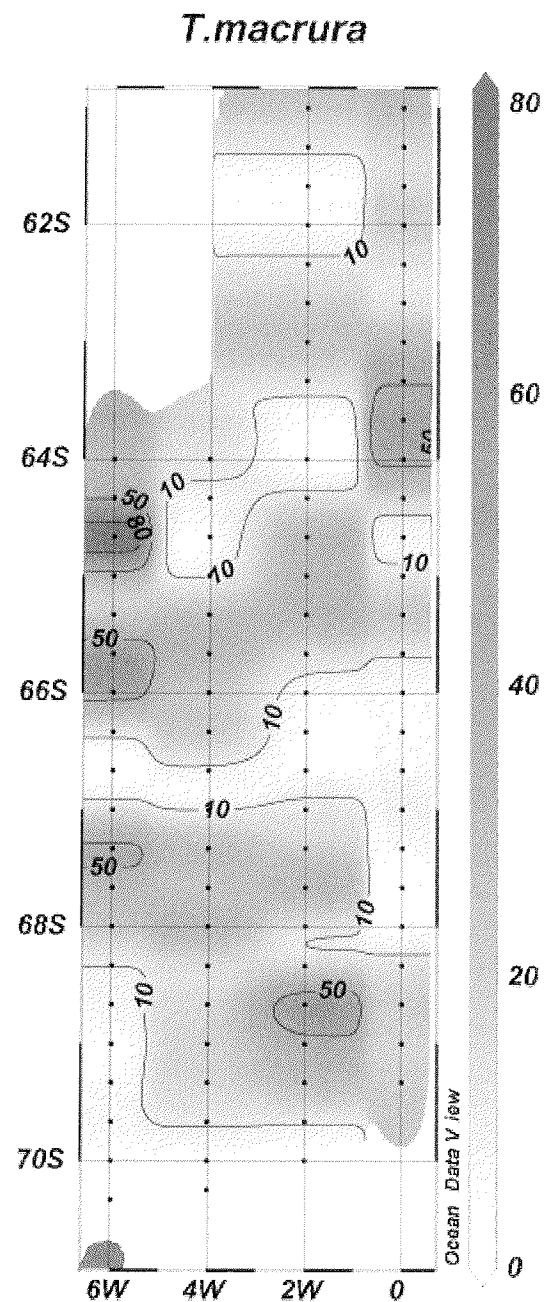


Figure 2.1.2: Spatial distribution of euphausiid species given as number per standard tow (double oblique haul from surface to 200 m depth, a. *Euphausia superba* b. *Thysanoessa macrura* c. *Euphausia crystallorophias* d. *Euphausia frigida*

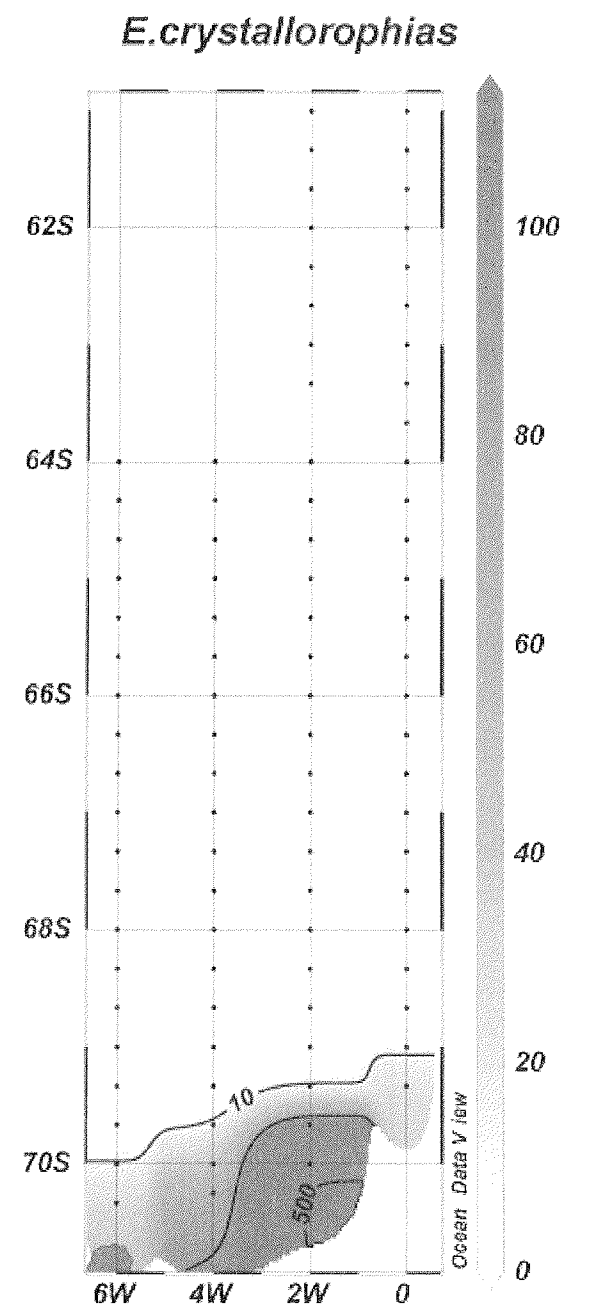


Figure 2.1.3: Comparisons of krill abundance between a. day and night samples b. samples from outside and inside the pack-ice zone

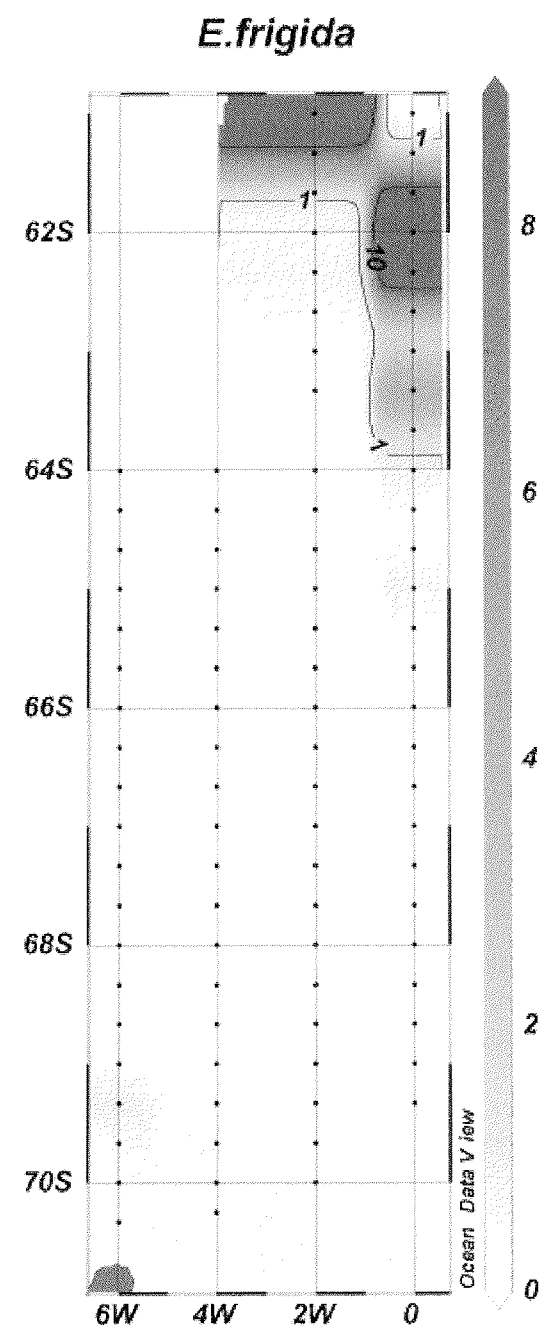
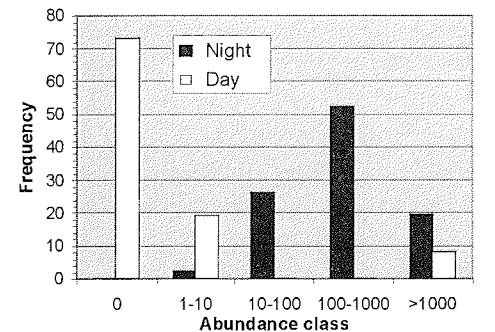


Figure 2.1.4: Composite length frequency distribution of Antarctic krill *Euphausia superba* for the study area

Euphausia superba day-night comparison



Euphausia superba in and outside pack-ice

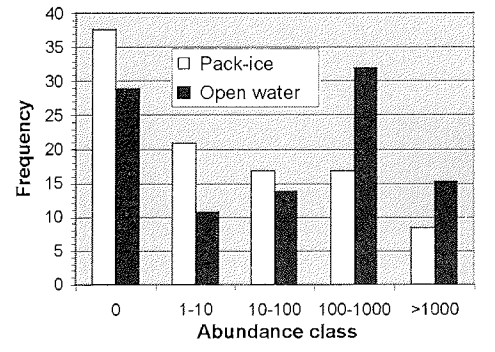


Figure 2.1.5: *E. superba* spatial distribution of regional length frequency distributions in the Lazarev Sea

Euphausia superba

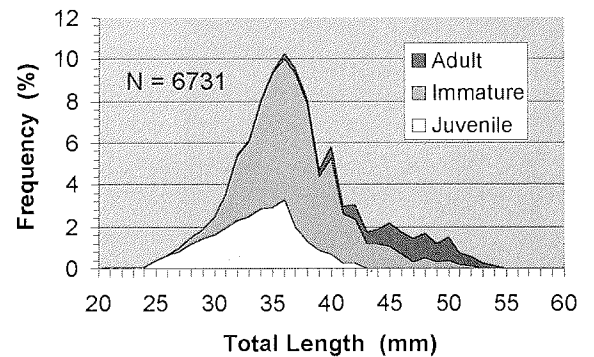


Figure 2.1.6: Overall maturity stage composition of *E. superba* in the Lazarev Sea during April 2004

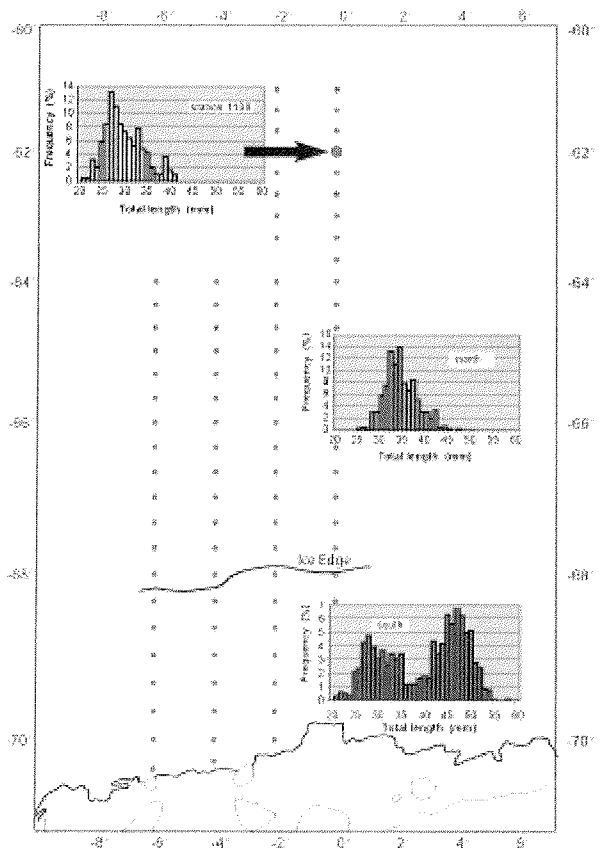


Figure 2.1.7 : Length frequency distribution of *Thysanoessa macrura* in the Lazarev Sea

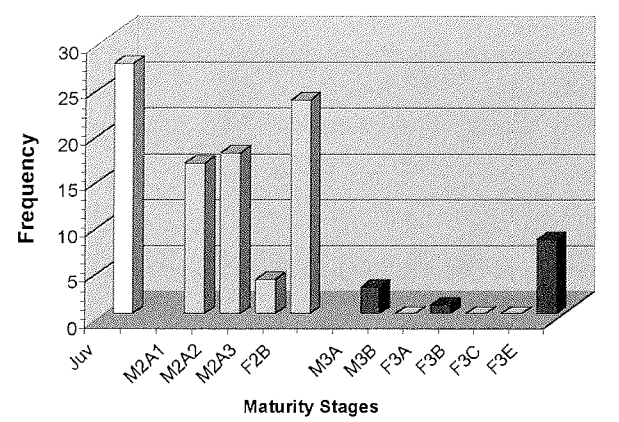
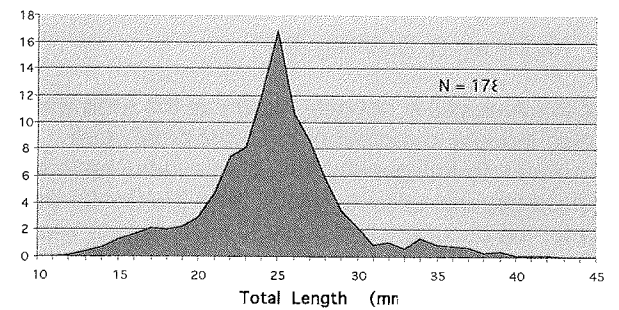
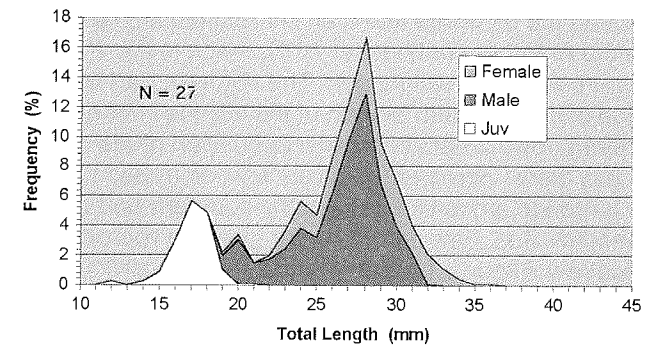


Figure 2.1.8 : Length frequency distribution of *E. crystallorophias* in the southern Lazarev Sea

Thysanoessa macrur



Euphausia crystallorophias



Euphausia frigida

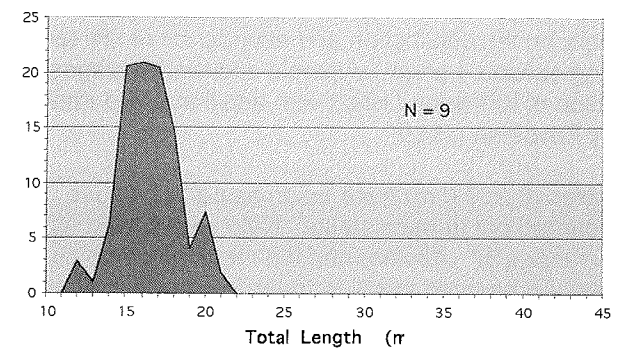


Figure 2.1.9: Length frequency distribution of *E. frigida* in the northern Lazarev Sea

2.2 DISTRIBUTION AND ABUNDANCE OF KRILL

LARVAE

V. Siegel, M. Haraldsson, J. Kitchener, S. Schöling (BfF)

The South Atlantic sector of the Antarctic is not only known as the area where krill is most abundant, it is also thought to represent the most productive spawning area of the circum-Antarctic krill populations. These ideas have been developed since the early Discovery expeditions, which show the Scotia Sea as a seasonally important area for the occurrence of krill larvae. This idea was in principle confirmed during the international FIBEX expedition in 1982 and the CCAMLR Survey 2000. These surveys showed a large amount of krill larvae in the western part of the Atlantic sector. On the other hand, a limited number of data from the Discovery expeditions indicate that these larval concentrations move further to the east with the season progressing. In autumn to early winter krill Furcilia larvae are spread as far as 20°E at latitudes from 50 to 60°S.

In the Southeast Atlantic around the 0-degree meridian krill distribution ranges from approximately 50°S to the Antarctic continent at 70°S, which is the widest latitudinal coverage in its circum-Antarctic distribution. The northern part north of 60°S is under the influence of the "northern branch of the Weddell Gyre" flowing to the east and therefore downstream of the krill population of the Scotia Sea and the spawning success there. However, only very few information on krill spawning and larvae occurrence are available from the southern part of this broad krill habitat, i.e. the Lazarev Sea. Few records were given on reproductive females or larvae in the Discovery Reports, probably because of the difficult access to this high latitude area, which also shows the widest extent of seasonal pack-ice around Antarctica.

If, however, the Weddell Gyre is the source of the high krill densities in the Scotia Sea, then the westward moving water masses of the Lazarev Sea should feed substantial amounts of krill larvae into the system to sustain the large population observed at the northern outflow of the Weddell Gyre. To test this hypothesis, we used the RMT station grid in the Lazarev Sea between 61 and 70°S to collect additional data on the distribution and abundance of krill larvae after the end of the spawning season. Larval calyptopis and furcilia stages were identified using the description of Kirkwood (1982) with additional information for *E. crystallorophias* given by Fevolden (1980).

Double oblique RMT1 samples (0-200-0 m) were taken as part of a suite of standard netting protocols carried out at each station. Nets were towed for an average of 39 min (quartile ranges 37 - 42 min) and the resulting samples, or in some cases subsamples, were preserved in 4% formalin in seawater. Samples were sorted for macroplankton and large species such as krill, salps and other gelatinous forms were removed. Samples were then split using a folsom plankton splitter into a series of aliquots. One to two, fractions of between a 1/2 to 1/32 of the preserved amount were usually counted to ascertain the numbers of euphausiid larvae. Data will finally be standardised to abundance 1000 m⁻³

based on flow rates determined from flowmeters attached next to the RMT 1 net. It is known that the RMT1 can fish independently of the RMT8 and presents a mouth area to the water which is very sensitive to ships speed (Pommeranz et al. 1983). We determined that the average speed of the net through the water for all deployments was 2.5 knots (quartile range 2.25- 2.90 knots) at which speeds the mouth area ranges from around 0.4-0.6 m² (mean ~ 0.5 m²). Data will be standardised accordingly.

An analysis of spatial mesozooplankton krill larvae in the Lazarev Sea has been carried out, based on 93 RMT 1 double oblique hauls (0 -200 m) taken during the 'Lazarev Krill Study 2004' synoptic survey. Since we lost two net buckets during net operations, we could use quantitative data from only 91 samples.

Larvae of *E. superba* consisted mostly of calyptopis larvae (88.2 %) with C2 being the most common stage. Furcilia larvae occurred as F1 to F3 stages during the study period. Calculating backwards from the day of their first or last occurrence, we can make some estimations about the onset and end of the spawning event of the current season. Assuming that C1 larvae are generally 30 days old, then the latest spawning probably occurred in the last week of March. Highest densities were observed for C2 (Table 2.2.1), which are thought to be approximately 45 days old. This would date the main spawning event back to the last week of February. Furcilia 3 larvae were still rare in our samples. Their estimated age is around 85 days, which brings us to an onset of the krill spawning season around 15 January. Compared to other regions of the South Atlantic this is a relatively late onset and late peak of the spawning season, which may start in mid December and peak in early to mid January. These dates may, however, vary by year and location. For the Lazarev Sea Spiridonov (1985) speculated that spawning may show a delayed start but at the same time a very short duration of 1.5 months and less, because of the peculiarities in the sea-ice regime. Our data indicate that spawning did occur late, but the duration of the spawning event was definitely longer than hypothesized.

Highest abundances of krill larvae were found south of 65°S. However, there was a clear difference between the occurrence of calyptopis and furcilia larvae. Highest concentrations of calyptopis were found between 65° and 68° S (Fig. 2.2.1) mainly on the two western transects (4° to 6°W). This area was located just outside the sea-ice covered region. On the other hand, furcilia larvae concentrated inside the pack-ice covered area south of 68°S. This spatial segregation of larval stages is difficult to explain, especially because most of the adult spent females had been observed in the area of furcilia occurrence, while the younger stages were found further to the north. These distribution patterns warrant a further close examination of the oceanographic environmental conditions of the study area. Concentrations of furcilia larvae were by one order of magnitude smaller than those for calyptopis, however, this can be explained by high mortality rates for krill larvae in general, which might occur over a two month period.

Thysanoessa macrura larvae were distributed across the entire survey area. No clear preference for local concentrations was obvious from our data. Distribution of larvae was relatively uniform inside the pack-ice zone as well as outside in open water. There were only a few specimens in late calyptopis or early furcilia larval stages, which did not belong to F6. More than 97 % of all larvae had already developed into this oldest larval stage (Table 2.2.1). Developmental times are unknown for *T. macrura* larvae. However, due to first occurrence of larvae the birthdate of the species is thought to be early in September, which is winter. This would mean that developmental times for *T. macrura* larvae during winter are much longer than known for the summer-spawner *E. superba*.

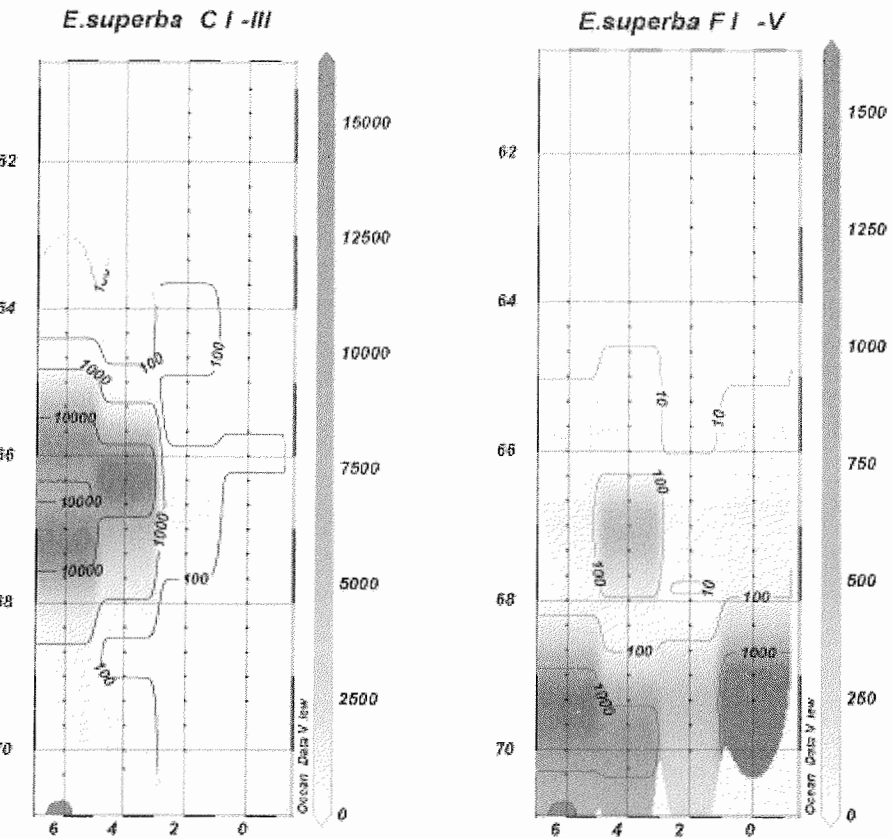
Larvae of *E. crystallorophias* were only found in samples from stations on the continental shelf or along the shelf break. There were no calyptopis larvae in the samples, all animals had already developed into F1 to F3 stages. F2 was the most frequent stage with more than 91 % (Table 2.2.1). Regarding developmental times of 90 days for F1 and at least 125 days for F3, this would narrow down the spawning period of this species to early December till mid January. This is consistent with observations from the Weddell Sea, where the main spawning period is generally December.

Table 2.2.1. Frequency of occurrence of euphausiid larval stages in the Lazarev Sea in April 2004 ; C = calyptopis, F = furcilia stages

Larval stage	<i>E. superba</i>	<i>E. crystallorophias</i>	<i>T. macrura</i>
C1	21.1	0	0
C2	46.9	0	0
C3	20.2	0	0.1
F1	10.3	6.2	0.4
F2	0.9	91.9	0.8
F3	0.5	2.0	0.6
F4	0	0	0.3
F5	0	0	0.2
F6	0	0	97.5

References

- Fevolden, S. (1980) Krill off Bouvetöya in the southern Weddell Sea with a description of larval stages of *Euphausia crystallorophias*. *Sarsia* 65: 149-162.
- Kirkwood JM (1982) A guide to the Euphausiacea of the Southern Ocean. Australian National Antarctic Research Expeditions. Research Notes 1: 1-45.
- Pommeranz, T, Herrmann, C., Kühn, A. (1983) Mouth angles of the Rectangular Midwater Trawl (RMT1+8) during paying out and hauling. *Meeresforschung* 29:267-274.
- Spiridonov, V.A. (1985) Spatial and temporal variability in reproductive timing of Antarctic krill (*Euphausia superba* Dana). *Polar Biology* 15: 161-174.



2.3 Acoustic krill observations

B. Bergström (Sweden), J. Franeker (ALTERRA), U. Bathmann (AWI),
J.Rogenhagen (FIELAX)

The scientific echosounder EK 60 is one of the fixed sounding systems onboard Polarstern. It provides an acoustic image of the water column and is normally used to detect fish shoals and other species in the water column. On this cruise our main aim was to achieve a continuous mapping of the zooplankton in the water column along the entire krill survey area and along the stations. The data will be used to calculate the biomass estimate for CCAMLR and will be put in conjunction with the abundance of krill that is seen in the RMT stations.

The EK 60 provides four operating frequencies, ranging from 38 kHz to 210 kHz, with different penetration depths, ranging from ca. 400 m to ca. 1000 m. The data is displayed online and recorded in digital format. All frequencies were operated regularly. The EK60 interferes very much with other sounding devices of Polarstern. To achieve high quality data, the EK60 was used as a stand

alone sounding device with Hydrosweep and Parasound switched off. In total, the EK 60 was in operation for nearly 32 days with a total data volume of 50 GByte, which as a first step were on board processed to ca. 30 GByte of data. South of 60°S, the measurements mainly had to be carried out by the Swedish and Dutch project partners. The final postprocessing will be done later on. Additional acoustic measurements were carried out in situ onboard. Here, a new sounding system was tested and for the first time used with living species. The SonoKrill system is designed to measure the velocity and density contrast (reflectivity) of zooplankton in water. A small, waterfilled chamber with the species inside is transduced with a variable high frequency in the ultra sound range. To provide additional control on the target, a camera system is installed, that allows referencing the target area of the species with the acoustic measurement. With this system, more than 700 measurements were performed, mainly on krill, but as well with other species, most of them fresh caught.

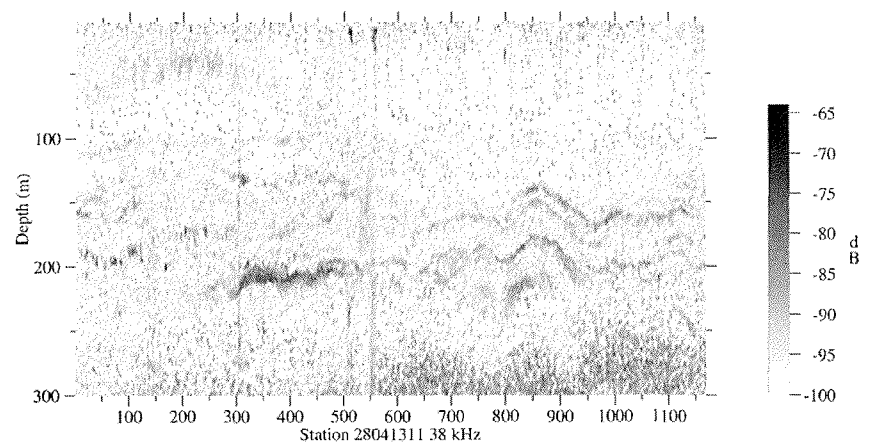
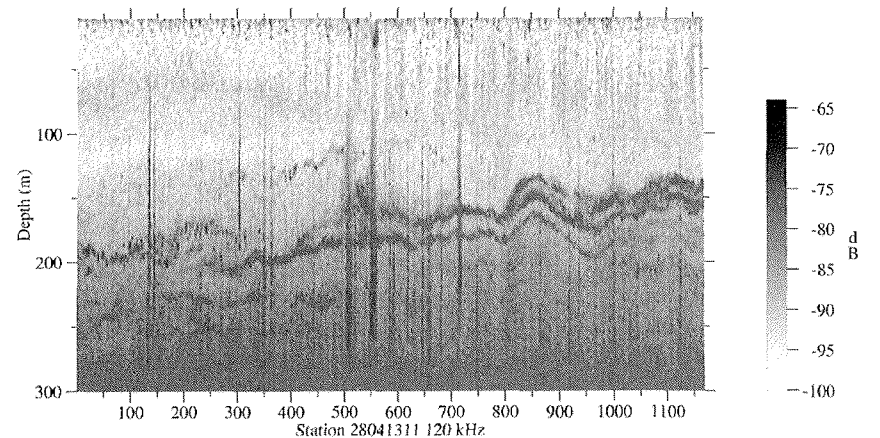


Fig. 2.3.1 Non-processed echosounder Profile (here only 38 kHz and 120 kHz displayed)
showing stratified layers in the depth range of 140 m to 200 m in the water column.

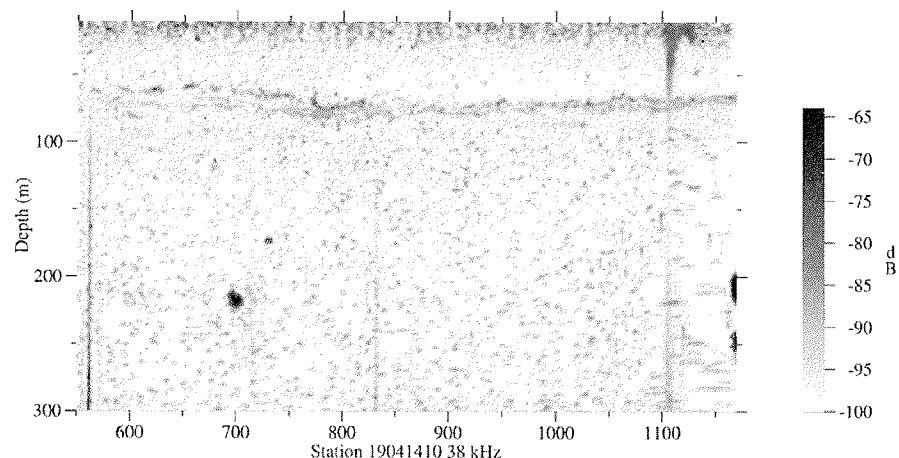
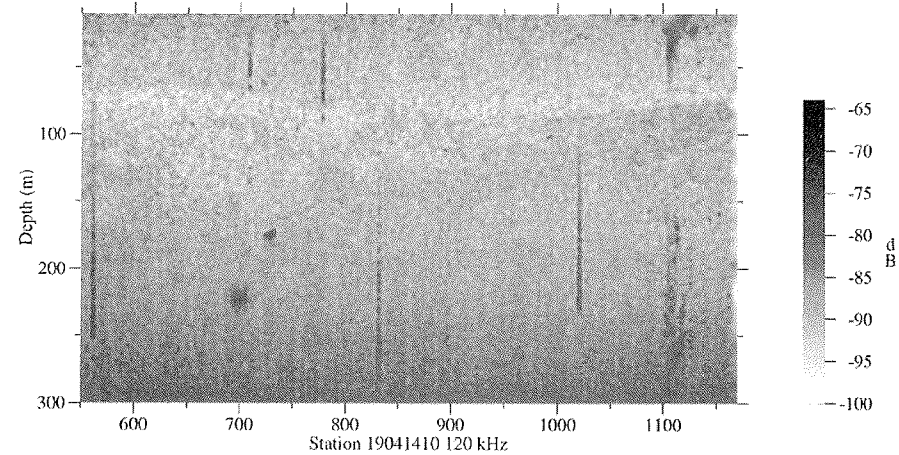


Fig. 2.3.2 Non-processed echosounder Profile (here only 38 kHz and 120 kHz displayed). Dark spots at a depth of 170 m and 230 m indicate the presence of probably smaller fish.

EK60 Protocol ANT XXI/4 south of 60° South

Operation	German Op. of Day	Visual Observation	Observation of Day	Sunrise-Sunset	Daylight of Day
7.4.04 10:26			07.04.2004 9:25		07.04.2004 7:17
7.4.04 11:32	0,05				
7.4.04 12:33					
7.4.04 17:04	0,19		07.04.2004 17:04	0,32	07.04.2004 17:34
					08.04.2004 7:24
8.4.04 10:01			08.04.2004 9:00		
8.4.04 17:08	0,30		08.04.2004 17:08	0,34	08.04.2004 17:27
					09.04.2004 7:38
9.4.04 9:52			09.04.2004 8:52		
9.4.04 14:35	0,20				
9.4.04 15:47					
9.4.04 17:14	0,06		09.04.2004 17:14	0,35	10.04.2004 7:49

	10.04.2004 9:00		
	10.04.2004 17:00		
	11.04.2004 8:58		
0,29			
	11.04.2004 17:02		
	12.04.2004 9:00		
0,28			
	12.04.2004 17:00		
	13.04.2004 8:52		
0,29			
	13.04.2004 17:10		
	14.04.2004 8:58		
0,07			
	14.04.2004 17:00		
	10.04.2004 17:01	0,38	
	11.04.2004 7:48		
	11.04.2004 16:45	0,37	
	12.04.2004 7:48		
	12.04.2004 16:45	0,37	
	13.04.2004 7:41		
	13.04.2004 16:51	0,38	
	14.04.2004 7:37		
	14.04.2004 16:55	0,39	
0,33			

14.4.04 17:13
15.4.04 10:19
15.4.04 13:07
15.4.04 13:35
15.4.04 16:43

0,20

15.04.2004 9:20
0,12
0,13
15.04.2004 16:45

15.04.2004 7:29
0,31
15.04.2004 16:51
0,39
16.04.2004 7:37

16.4.04 10:12
16.4.04 16:50

16.04.2004 9:05
0,28

0,33

17.4.04 10:24
17.4.04 11:49
17.4.04 12:12
17.4.04 14:20
17.4.04 15:20
17.4.04 15:49

17.04.2004 9:17
0,06

0,09
0,02

0,31
0,36

17.04.2004 16:40

18.04.2004 9:15

18.04.2004 16:10

162

15.04.2004 7:29
0,31
15.04.2004 16:51
0,39
16.04.2004 7:37

16.04.2004 9:05
0,38

0,33

17.04.2004 9:17
0,06
0,09
0,02
0,31
17.04.2004 16:32
0,36

17.04.2004 16:40

18.04.2004 8:04

18.04.2004 16:10

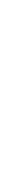
0,34

17.04.2004 7:52
0,31
17.04.2004 16:32
0,36

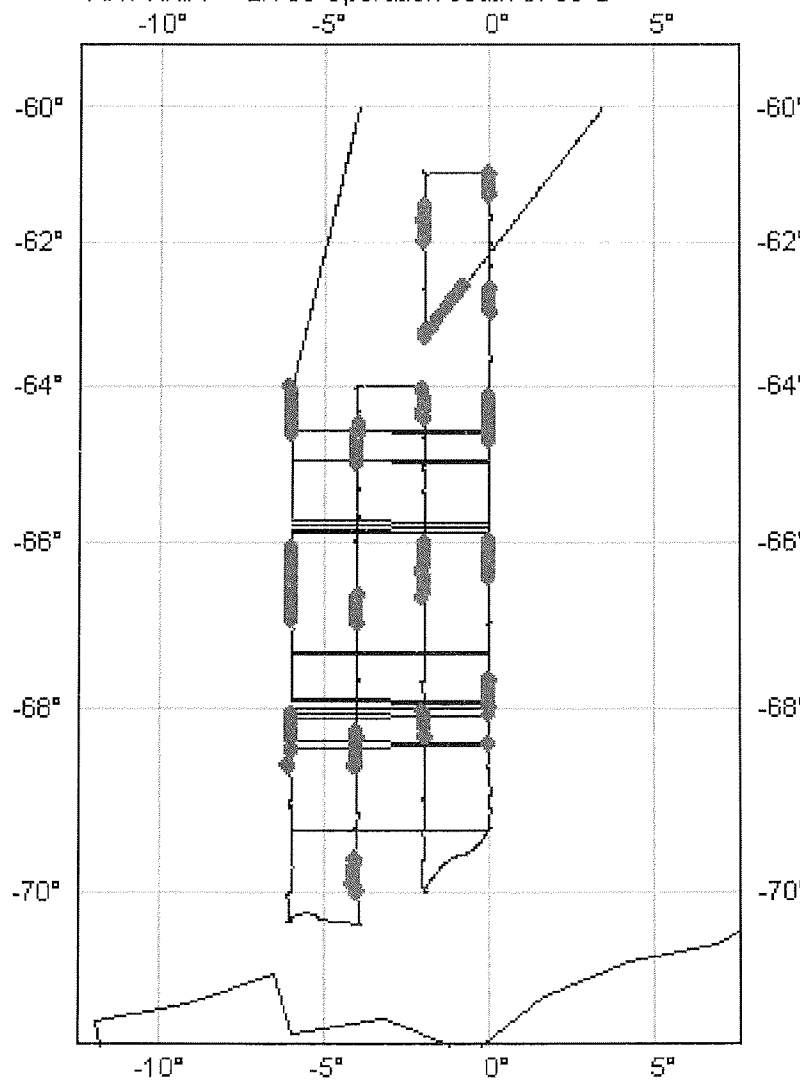
17.04.2004 9:15
0,34

162

	18.04.2004 16:45	0,31	19.04.2004 8:00	
	19.04.2004 9:20		19.04.2004 15:58	0,33
	19.04.2004 16:15	0,29	20.04.2004 7:55	
	20.04.2004 9:30		20.04.2004 16:03	0,34
20.4.04 10:35	20.04.2004 16:25	0,29	21.04.2004 7:52	
20.4.04 15:35	21.04.2004 9:00	0,32	21.04.2004 16:06	0,34
			22.04.2004 7:44	
21.4.04 10:28	21.04.2004 16:40	0,27	22.04.2004 16:12	0,35
	22.04.2004 9:05			
			23.04.2004 7:37	
21.4.04 16:55	22.04.2004 16:35	0,31	23.04.2004 16:19	0,36
	23.04.2004 8:56			
22.4.04 10:09				
22.4.04 16:31				
23.4.04 9:57		0,26		
23.4.04 16:17				

23.04.2004 16:30	0,32		24.04.2004 7:34	
24.04.2004 9:10			24.04.2004 16:22	0,37
24.04.2004 16:36			24.04.2004 16:22	0,37
24.04.2004 16:40	0,31		25.04.2004 7:43	
25.04.2004 9:15			25.04.2004 16:28	0,36
25.04.2004 16:41	0,27		25.04.2004 16:45	
26.04.2004 9:35			26.04.2004 16:17	0,35
26.04.2004 16:40	0,25		26.04.2004 16:40	0,30

ANT XXI/4 EK 60 Operation south of 60°S



Scale: 1:23693983 at Latitude 0°

◆ German Operation (18% of total time)

Fig. 2.3.3 Cruise track south of 60°S. Wide symbols indicate those part of the cruise track where the EK 60 was operated by the German programme.

2.4 SURVIVAL STRATEGIES OF *EUPHAUSIA SUPERBA* IN AUTUMN

B. Meyer, S. Spahic, V. Fuentes, C. Guerra, M. Teschke (AWI)

Sea ice extent and overwintering success are major factors dictating the condition, recruitment and population size of Antarctic krill. However, mechanisms of krill survival during wintering are still poorly known. This topic is characterised by much speculation, some controversy and limited site data. Because much of the krill habitat is ice-covered in winter, pelagic phytoplankton, the major food source in summer, is in short supply. Suggested survival mechanisms fall into two categories, firstly non-feeding strategies, and second, switching to alternative foods. The non-feeding strategies include utilisation of stored lipids, reduction in metabolic rate and shrinkage in size. Feeding strategies involve switching to ice algae, zooplankton or seabed detritus.

All of these overwintering mechanisms have been observed at different times and places, but their relative importance remains unclear. Also the mechanisms differ with ontogeny, with the furcilia having a greater requirement to feed than adults. Conflicting conclusions on overwintering probably reflect both the difficulty in assessing all potential strategies simultaneously and the flexibility of krill in a variable environment.

Metabolic rates, grazing and growth of larval krill and adults

The aims of the cruise were to measure on freshly caught krill:

Feeding

Metabolic rates (oxygen consumption and ammonium production) and metabolic enzyme activity

Growth and mortality rates

Melatonin concentration

DNA/RNA ratio

a) Feeding rates

The incubation technique was used and the animals were incubated for 24h in natural seawater added with phytoplankton and microzooplankton. 5 to 10 larval krill were incubated in 2.5 L bottles, whereas 5 adult krill were incubated in 65 L container. The chl a concentration in all experiments ranged between 0.2 and 7.3 $\mu\text{g L}^{-1}$.

For a provisional calculation of clearance rate on a carbon basis we used a C:chl a ratio of 50 and a literature derived length mass regression and C conversion factors from a former cruise in this area 1999 (ANTXIII/3).

The clearance rates (CR) of the larvae were between 4.3 and 27 ml mg $^{-1}$ C. h $^{-1}$ and in a similar range to values than in autumn 1999 and derived for early furcilia in a summer bloom at Rothera 2000. The clearance rate on microzooplankton is higher in furcilia II (FII, 11-14 ml mg $^{-1}$ C. h $^{-1}$) than in FI (5 ml mg $^{-1}$ C. h $^{-1}$), but in general lower than on phytoplankton (see above). Their daily ration (DR) ranged from 0.2 to 16 % body C d $^{-1}$ depending on the available food concentration.

Adult krill showed a DR between 0.02 and 3 % body C d $^{-1}$. These values a

higher than the DR measured on a former cruise in a similar area in autumn 1999 but the most of the estimated rations were still lower than summer values (Fig. 2.4.1), suggesting that the adults were in a phase between summer activity and winter close down. This is underlined by the metabolic rates measured on this cruise (see Fig. 2.4.2).

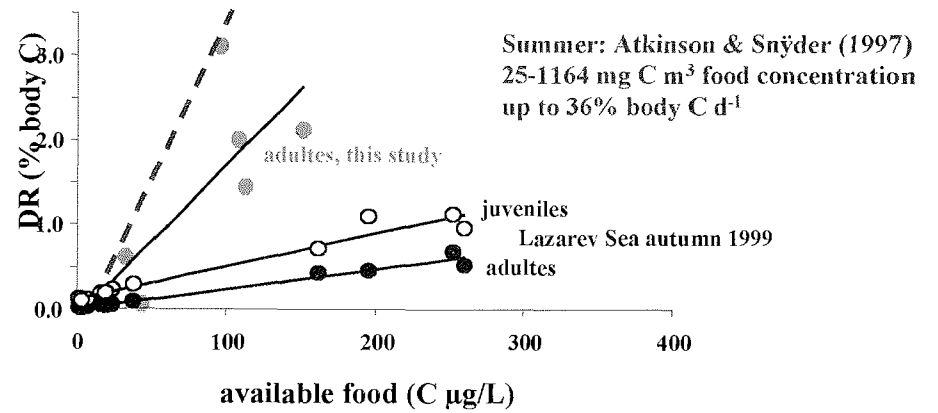


Fig.2.4.1 Daily ration (DR) as a function of food availability in adult krill from this study (green) compared with summer values (red) and from the Lazarev Sea 1999 (blue)

b) Metabolic rates

Different stages of freshly caught larval krill (calyptopes, furcilia I and II) were incubated for 24h in sealed 120ml bottles and, whereas the adults were incubated in 400ml chambers. Oxygen uptake rates were measured using the Winkler technique and Micro Optodes. The ammonium excretion rates were measured photometrically using the method of Solarzano. By this we like to thank Ludmilla Baumann, a member of the geochemistry group of Eberhard Sauter, who analysed our samples on board for oxygen and ammonia concentration.

The respiration rates of the larvae were in a range of well fed animals from 0.7 to $1.3 \mu\text{l O}_2 \text{ mg DM}^{-1} \text{ h}^{-1}$ for calyptopes and from 0.6 to $1.4 \mu\text{l O}_2 \text{ mg DM}^{-1} \text{ h}^{-1}$ for furcilia stages. The adults showed values close to autumn values measured 1999 (ANT XIII/3) and were mostly lower than summer rates (Fig. 2). The O/N ratios showed a high variability in adult krill (13-63), demonstrating a high variability in the metabolic substrate used by the animals (< 20 protein -, > 20 lipid dominated metabolism). The O/N ratio in the calyptope stages was 16 and in the furcilia stages between 18 and 42. The metabolic rates of larval krill were comparable to those of larvae incubated for 7 days in high food conditions during cruise ANT XIII/3 (1999) and to those during a summer bloom at Rothera (2000), indicating that they were in optimal physiological condition. This was also indicated by their low mortality rates and intermoult periods (see below). The metabolic enzymes, Citralsynthases and Pyruvat-dehydrogenases will be

analysed in freshly caught krill frozen at -80°C at AWI.

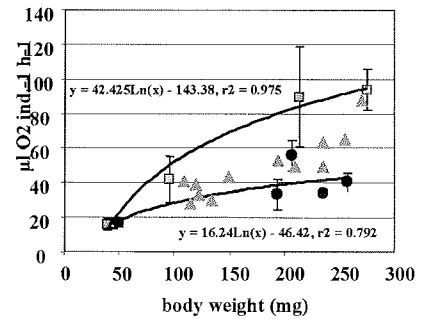


Figure 2.4.2: Oxygen uptake rates of freshly caught adult krill from this study (triangles) compare to summer data from Ishii 1989 (squares) and a former autumn cruise near the Lazarev Sea 1999 (ANTXIII/3).

c) Moulting and growth rates of larval krill.

We conducted 7 moulting experiments one with calyptopes and 3 with F1 and 3 with FII. Experiments were run for 2 days, with animals placed individually in 100 ml beakers of surface seawater. At the end, moulters were counted and all animals and moult frozen. The intermoult period (IMP) were similar to those derived by autumn furcilia in the SW Lazarev Sea (ANTXIII/3), 12 to 15 days per stage. In the calyptope stages it was up to 40 days. To further determine growth rates, we aim to measure uropod length in the moult and the new animal to get the length increment on moult. When combined with the moulting frequency this will provide an estimate of growth rates of calyptopes and furcilia in our working area.

d) Melatonin concentration

It has now been documented that among autumn the metabolic rates and feeding activity of adult krill is reduced compared to summer values. Our working hypothesis was that the melatonin production in the animal may change seasonally and may correlate with its metabolic and feeding activities. Melatonin has been identified in a number of crustaceans but its roles and mechanisms of action in crustacean physiology are still unclear.

Therefore freshly caught adult krill were immediately frozen in liquid nitrogen and stored at -80°C for analysing melatonin concentration and the activity of the related enzyme N-acetyltransferase in krill at AWI. Our aim is to estimate if melatonin is in general present in krill and if it has a seasonal and/or daily circadian rhythm in its concentration measured. The latter question was tested by conducting a short term experiment with adult krill reared under 3 different photoperiods at 0°C (24 h darkness, 12:12 h light/dark, 24 h light). 21 krill were reared under each condition in two 65 L container filtered with filtered sea water ($0.5\mu\text{m}$ filtered). After 4 days adaptation to these conditions it was started to

subsample 3 krill every 4 h from each experimental set up during 24 hours by freezing the animals in liquid nitrogen and store them in a -80°C freezer. Samples during darkness were collected under dim red light.

e) DNA/RNA ratio

The DNA/RNA ratio has proven to be a valid fitness indicator for the development of fish larvae, enabling calculations of recruitment success in fish populations. On the last cruise, we started to develop this approach for larval krill by measuring their DNA/RNA ratios during long term experiments with controlled diets. The variability of the data was high and our number of samples analysed was too small to give a solid interpretation of the values in freshly caught animals, so that we started a similar experiment again to get more data points.

Starvation experiments:

210 animals (FII-FIII) were held individually in 100ml beakers of 0.2 μ m filtered seawater.

Experiments with high food concentrations:

210 animals (FII-FIII) were held individually in 100ml beakers with high or saturating phytoplankton concentrations (2-4 μ g Chl a l⁻¹)

The two set-ups are needed to allow comparison of the DNA/RNA ratios of animals in optimal nutritional condition with those under starvation stress to get a better interpretation of field data. The experiment was running for 16 days and subsamples of larvae for measuring the DNA/RNA ratio was taken every 4th day.

3. CIRCULATION, ICE AND ZOOPLANKTON-ABUNDANCES

B. Cembella, T. Witte, R. Graupner (OP), A. Engeler, U. Marx, V. Strass (AWI)

Introduction

As a preliminary study for the Lazarev Sea Krill Study (LAKRIS) the oceanographic programme concentrated on a section of the Lazarev Sea between the Greenwich meridian to 6° E and 64° to 70° S during the Antarctic fall (April). This multiyear project focuses on population dynamics of the Antarctic krill populations in the Lazarev Sea. The project is embedded in the international programme Global Ocean Ecosystem Dynamics (GLOBEC).

The area of investigation covers the most eastern section of the Weddell Sea where hydrographic and biological features are not well documented in earlier studies. In addition, complicated hydrographic features are expected since it is not clear whether or not the Weddell Gyre extends that far east. The force and direction of the currents in the area remain unknown. The spatial and temporal dynamics of the hydrographic features must be determined in order to answer

key questions concerning the krill biology in the area with respect to advection of krill or its food source..

General objectives of the oceanographic programme of LAKRIS are:

What spatial distribution pattern of krill can be retrieved from the ADCP-profiles?

What is the correlation of these distribution pattern of krill with the general circulation of water masses in the Lazarev Sea (eastern Weddell Gyre)?

What is the importance of mesoscale water mass dynamics on the distribution pattern of krill?

How does the dial vertical migration change throughout the year?

Which is the influence of seasonal ice coverage on the horizontal and vertical krill distribution?

Does advection of organisms with water masses and ice play a significant role for the population dynamics of krill in the Lazarev Sea?

The specific objectives of the oceanographic programme during this cruise were:

Estimation of water mass circulation pattern in the Lazarev Sea (eastern Weddell Gyre).

Estimation of the extent of mesoscale dynamics in water mass distribution.

Estimation of the extent of ice coverage during the Antarctic fall in the Lazarev Sea.

Estimation of krill-specific characteristics in the ADCP-profile.

Material and Methods

Station grid

On April 4th, 2004 CTD profiling was initiated on the most north-eastern station of the sampling grid on Transect 1 (Figure 3.1). Sampling continued along Transect 1 in southern direction and subsequently south to north along Transect 2 until the last station of the grid was completed on April 22nd, 2004. Following the grid, stations were added along the Greenwich meridian and 2° W up to 61° S (Figure 3.1). CTD casts were carried out on each full degree and on stations south of 68° S every 20 min. Time constraints lead to a reduction the regular cast depth to the upper 1000 m with some bottom casts at strategic locations (Figure 3.1; Table 3.1).

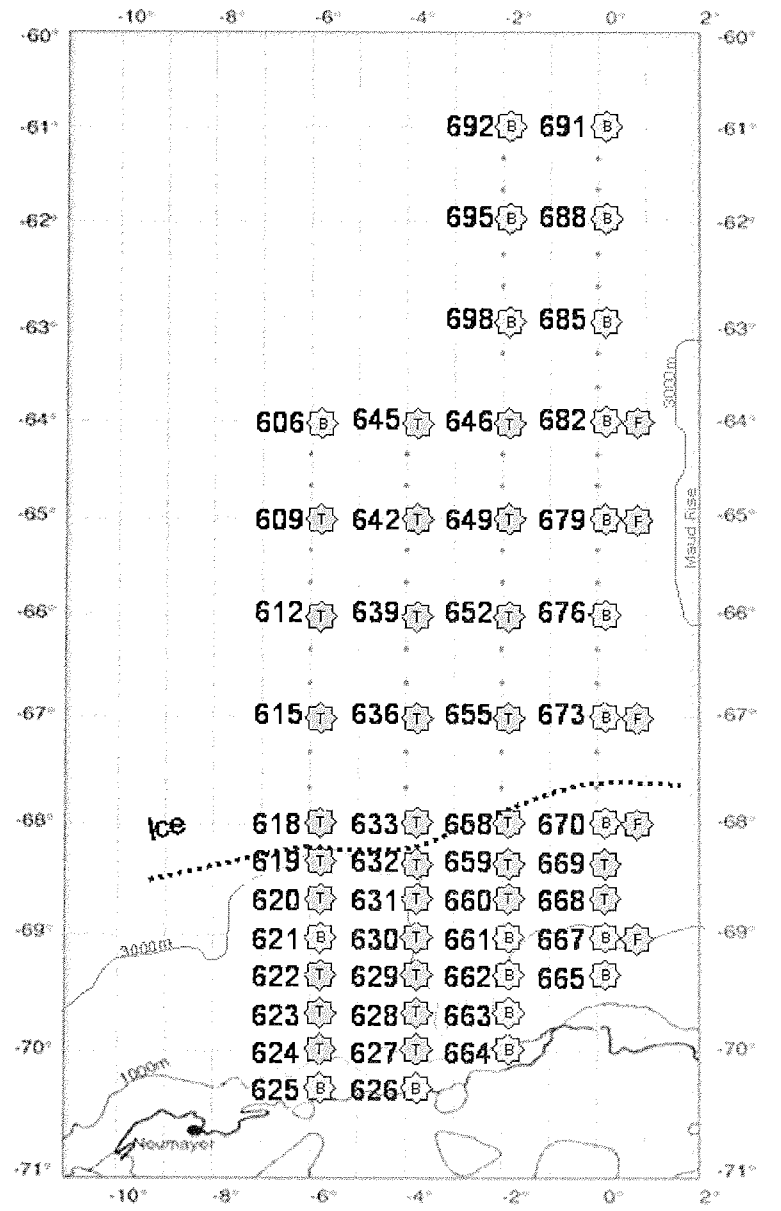


Figure 3.1: Krill sampling grid during ANT21-4. B are bottom and T represent positions of 1 to 1000m CTD casts. F are positions of APEX float deployment.

Table 3.1: CTD and float deployment in krill sampling grid

Station	Cast	CCAMLR	Instrument	SN	Latitude [deg]	Longitude [deg]	NBSdepth [m]	Start [dd.mm]
606	2	1040	SBE911plus	09P16392-0485	64 0.612 S	6 4.006 W	5230	07.04.04
609	2	1037	SBE911plus	09P16392-0485	65 1.872 S	5 59.612 W	5118	07.04.04
612	2	1034	SBE911plus	09P16392-0485	66 1.506 S	5 59.836 W	4935	08.04.04
615	2	1031	SBE911plus	09P16392-0485	67 2.044 S	5 59.046 W	4859	08.04.04
618	2	1028	SBE911plus	09P16392-0485	68 1.240 S	6 0.096 W	4743	09.04.04
619	1	1027	SBE911plus	09P16392-0485	68 20.169 S	6 0.412 W	4536	09.04.04
620	2	1026	SBE911plus	09P16392-0485	68 38.907 S	6 7.181 W	4071	09.04.04
621	4	1025	SBE911plus	09P16392-0485	69 5.433 S	6 2.338 W	2610	10.04.04
622	2	1024	SBE911plus	09P16392-0485	69 21.874 S	6 0.239 W	2259	10.04.04
623	2	1023	SBE911plus	09P16392-0485	69 42.362 S	5 59.600 W	2336	10.04.04
624	2	1022	SBE911plus	09P16392-0485	70 0.370 S	6 3.436 W	1876	10.04.04
625	2	1021	SBE911plus	09P16392-0485	70 18.270 S	6 3.581 W	227	10.04.04
626	2	1041	SBE911plus	09P16392-0485	70 20.308 S	3 59.381 W	504	11.04.04
628	2	1043	SBE911plus	09P16392-0485	69 39.789 S	4 6.623 W	2674	11.04.04
629	2	1044	SBE911plus	09P16392-0485	69 19.363 S	4 4.009 W	3053	12.04.04
630	2	1045	SBE911plus	09P16392-0485	68 58.087 S	4 1.050 W	3520	12.04.04
631	2	1046	SBE911plus	09P16392-0485	68 39.625 S	4 5.915 W	3594	12.04.04
632	2	1047	SBE911plus	09P16392-0485	68 20.572 S	4 2.282 W	4011	12.04.04
633	2	1048	SBE911plus	09P16392-0485	68 0.921 S	4 1.478 W	4259	12.04.04
636	2	1051	SBE911plus	09P16392-0485	67 0.842 S	4 0.230 W	4725	13.04.04
639	2	1054	SBE911plus	09P16392-0485	65 59.044 S	4 5.063 W	487	13.04.04
642	2	1057	SBE911plus	09P16392-0485	65 0.620 S	4 0.297 W	5104	14.04.04
645	3	1060	SBE911plus	09P16392-0485	63 59.746 S	3 59.994 W	5246	15.04.04
646	2	1080	SBE911plus	09P16392-0485	64 0.982 S	2 2.435 W	5169	15.04.04
649	2	1077	SBE911plus	09P16392-0485	65 1.130 S	159.886 W	5048	15.04.04
652	2	1074	SBE911plus	09P16392-0485	66 1.120 S	2 0.326 W	4972	16.04.04
655	2	1071	SBE911plus	09P16392-0485	67 1.407 S	2 0.180 W	4692	16.04.04
658	2	1068	SBE911plus	09P16392-0485	68 1.305 S	2 1.103 W	4421	17.04.04
659	1	1067	SBE911plus	09P16392-0485	68 19.890 S	2 0.911 W	4228	17.04.04
660	2	1066	SBE911plus	09P16392-0485	68 41.397 S	159.956 W	3662	17.04.04
661	2	1065	SBE911plus	09P16392-0485	69 0.689 S	2 2.494 W	3247	17.04.04
662	2	1064	SBE911plus	09P16392-0485	69 21.369 S	2 1.067 W	2980	18.04.04
663	2	1063	SBE911plus	09P16392-0485	69 40.200 S	159.810 W	2846	18.04.04
664	2	1062	SBE911plus	09P16392-0485	70 0.620 S	157.836 W	3480	18.04.04
665	2	1084	SBE911plus	09P16392-0485	69 19.305 S	0 0.100 E	2425	19.04.04
667	2	1085	SBE911plus	09P16392-0485	68 58.273 S	0 1.507 E	3381	19.04.04
667	5	1085	APEX Float	1366	68 57.570 S	0 3.430 E	3392	19.04.04
668	2	1086	SBE911plus	09P16392-0485	68 39.966 S	0 3.292 E	2460	19.04.04
669	2	1087	SBE911plus	09P16392-0485	68 20.433 S	0 2.619 W	3760	20.04.04
670	3	1088	SBE911plus	09P16392-0485	68 0.024 S	0 0.748 W	4516	20.04.04
670	4	1088	APEX Float	1364	67 57.820 S	0 1.184 E	4528	20.04.04
673	5	1091	SBE911plus	09P16392-0485	66 59.827 S	0 1.125 W	4711	21.04.04
673	5	1091	APEX Float	1365	66 59.870 S	0 2.177 E	4715	21.04.04
676	2	1094	SBE911plus	09P16392-0485	65 58.467 S	0 0.258 E	3518	21.04.04
679	3	1097	SBE911plus	09P16392-0485	64 59.992 S	0 0.241 E	3741	22.04.04
679	4	1097	APEX Float	1362	64 59.440 S	0 0.030 E	3736	22.04.04
682	2	1100	SBE911plus	09P16392-0485	63 59.017 S	0 0.924 W	5204	22.04.04
682	3	1100	APEX Float	1363	63 56.836 S	0 0.857 E	5206	22.04.04
685	2	1103	SBE911plus	09P16392-0485	63 0.425 S	0 1.594 E	5310	23.04.04
688	2	1106	SBE911plus	09P16392-0485	62 1.266 S	0 3.352 E	5370	24.04.04
691	2	1109	SBE911plus	09P16392-0485	61 0.552 S	0 1.730 E	5386	24.04.04
692	2	1110	SBE911plus	09P16392-0485	60 58.224 S	2 3.042 W	5360	25.04.04
695	2	1113	SBE911plus	09P16392-0485	62 1.247 S	2 3.907 W	5349	25.04.04
698	2	1116	SBE911plus	09P16392-0485	63 0.556 S	2 0.208 W	5285	26.04.04
703	2	n/a	SBE911plus	09P16392-0485	52 35.340 S	9 0.640 E	3328	29.04.04
703	4	n/a	NEMO	003	52 35.390 S	9 1.790 E	3333	29.04.04
705	2	n/a	SBE911plus	09P16392-0485	49 0.967 S	12 14.833 E	4324	30.04.04
705	6	n/a	NEMO	005	49 1.170 S	12 18.170 E	4572	30.04.04
709	3	n/a	SBE911plus	09P16392-0485	44 20.173 S	13 32.785 E	4684	02.05.04

CTD-Profiles

A Seabird-911plus (s/n 09P16392-0485) including temperature (s/n 03P2423), conductivity (s/n 2078) and pressure (s/n 68997) sensor was mounted to the Polarstern bio-rosette sampler. As additional sensors a BENTHOS altimeter (s/n 208), Dr. Haardt chlorophyll-a fluorometer (s/n 8060) and a Wetlab transmissometer (s/n CST-403-DR) were attached to the rosette sampler. Standard procedure after each station was to rinse and fill the conductivity sensor with Milli-Q water and thoroughly rinse the optical windows of the

fluorometer and transmissometer with Milli-Q water. Samples ($n=81 \times 3$ depths) for salinometer (Guildline 8400B) cross calibrations were taken from depths that corresponded to noise-free sections of the salinity profile during the down cast. Samples ($n=150 \times 3$) for chlorophyll-a cross calibration were taken at 10 m, maximum depth of chlorophyll-a fluorescence and 250 m.

APEX and NEMO Float deployment

Five APEX Floats were deployed along the 0° E longitude (Table 3.1) and three NEMO Floats were deployed between 52° and 44° S (Table 3.2).

Continuous Acoustic Doppler Current Profiler (ADCP)

Current velocities were measured continuously using a RDI ADCP. The instrument operated at a frequency of 153.6 kHz and was mounted to the keel of the vessel. The depth range varied between 250 and 400 m depending on the concentration of scattering material in the water column. The pulse and vertical bin length was 8 m and the sampling interval was 120 s. Data were rejected at an error $> 20\%$ and the reference layer was set between 6 and 15 bins in order to avoid surface effects and biases near bin 1. The absolute velocity of the ship was calculated through GPS referencing. Merging current and vessel velocity measurements yielded absolute ground-referenced vertical current profiles. The raw data were logged onto a hard-disk and post-processing of these data was conducted upon return to the laboratory.

Thermohaline System (THS)

Data of the two thermosalinographs that are located in the bow (surface) and keel (11 m) were extracted from the PODAS data server along the transfer to and from the krill grid and the krill transects with a resolution of one data point per minute (see general course plot for this leg). Continuous chlorophyll-a fluorescence at 11 m depth was also extracted from the PODAS data server with a resolution of one data point per minute.

Other data acquisition

In Support of the EIFEX2004 and geochemical experiments, bottom CTD casts, including the bio-rosette sampler and optical instruments were carried out on positions in and north of the polar frontal zone (Table 3.2). Autonomous drifters were also deployed during the krill experiment (Table 3.1) and within the polar frontal system (Table 3.2).

Table 3.2: CTD and float deployment during the geochemical stations

Station	Cast	Instrument	SN	Latitude [deg]	Longitude [deg]	NBSdepth [m]	Start [dd.mm.yy hh.mm]
598	2	SBE911plus	09P16392-0485	49° 20'12" S	2° 12'42" E	3952	02.04.04 09:09
600	4	NEMO Float	002	49° 59'74" S	2° 20'20" E	3595	03.04.04 06:33
703	2	SBE911plus	09P16392-0485	52° 35'340" S	9° 0'640" E	3328	29.04.04 09:08
703	4	NEMO Float	003	52° 35'390" S	9° 1'790" E	3333	29.04.04 13:31
705	2	SBE911plus	09P16392-0485	49° 0'967" S	12° 14'833" E	4324	30.04.04 14:10
705	6	NEMO Float	005	49° 1'170" S	12° 18'170" E	4572	30.04.04 21:59
709	3	SBE911plus	09P16392-0485	44° 20'173" S	13° 32'785" E	4684	02.05.04 13:06

Data and sample analyses were carried out according to the JGOFS, WOCE and SeaWiFS protocols ({ #1045}, {#1760}, {#1697}).

Preliminary Results

Surface water mass distribution between Cape Town, SA and Antarctica
 Surface temperature – salinity data show that several frontal systems were passed. The most northern system was the Subtropical Front (STF) with warmer, high salinity waters, followed by the Subantarctic Front (SAF) with warmer, lower salinity waters. Temperatures slowly decreased while passing the Polar Frontal Zone (PFZ), the Southern Polar Front (SPF) and the Weddell Front (WF). During passage through the Weddell Gyre, salinity increased toward the Continental Water Boundary (CWB) until the Coastal Current (CC), where lowest surface temperatures and relatively low salinities were encountered (Figures 3.2 and 3.3).

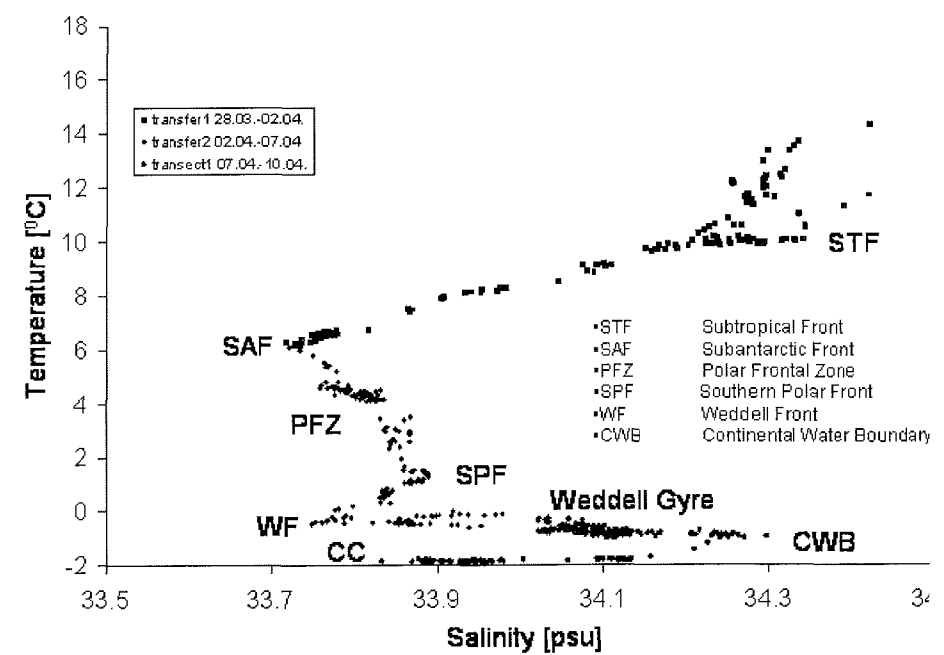


Figure 3.2: TS-diagram of online surface thermohaline data between Cape Town, SA and Antarctica.

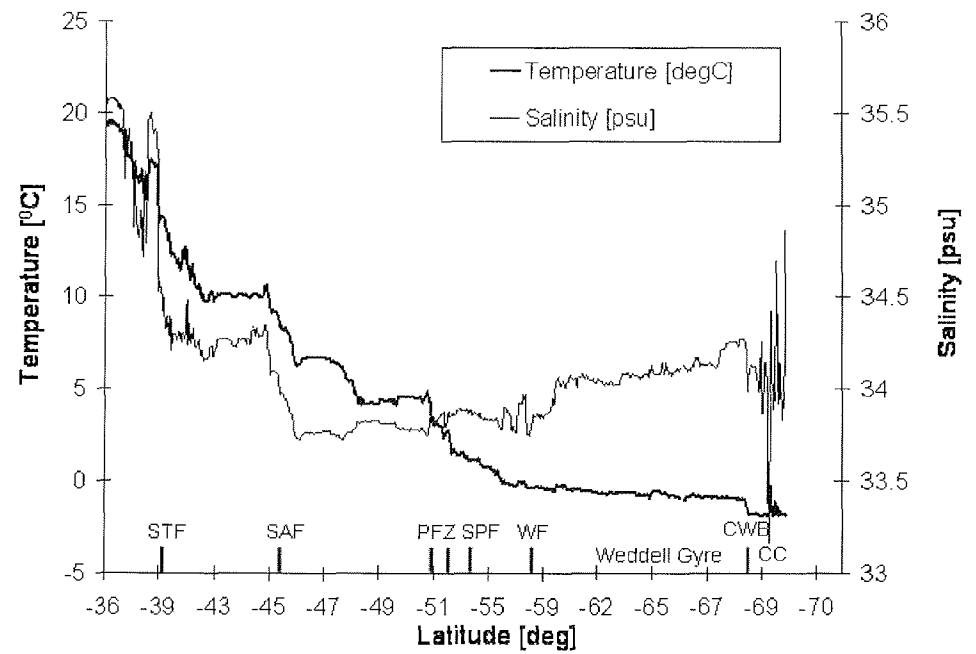


Figure 3.3: Surface temperature and salinity between Cape Town, SA and Antarctica.

Surface water mass distribution inside the krill sampling grid

An decreasing extent of the Coastal Current from west to east was found from of surface temperature and salinity data analyses. The Continental Water Boundary became predominant in the south-eastern section of the sampling grid. Ice extent was slightly greater in the south-western section of the sampling grid. At the time of this first transect, strong winds prevailed from the south (Figure 3.4).

Water mass distribution 0 to 1000 m

The salinity and temperature data from the upper 1000 m along the transects inside the GLOBEC/CCAMLR sampling grid allow identification and estimation of the distribution of water masses in this section of the Lazarev Sea during the Antarctic fall (Figures 3.5 to 3.12). On Transects 1 to 3 the warm deep water (WDW), winter water (WW), coastal current (CC), continental water boundary (CWB), and the Weddell Gyre can be identified. The CC was not found on Transect 4. The ice close to the shelf on Transect 4 was thick during the sampling period. Therefore it was not possible to sample closer to the Antarctic coast and information on water masses close to the coast is not available.

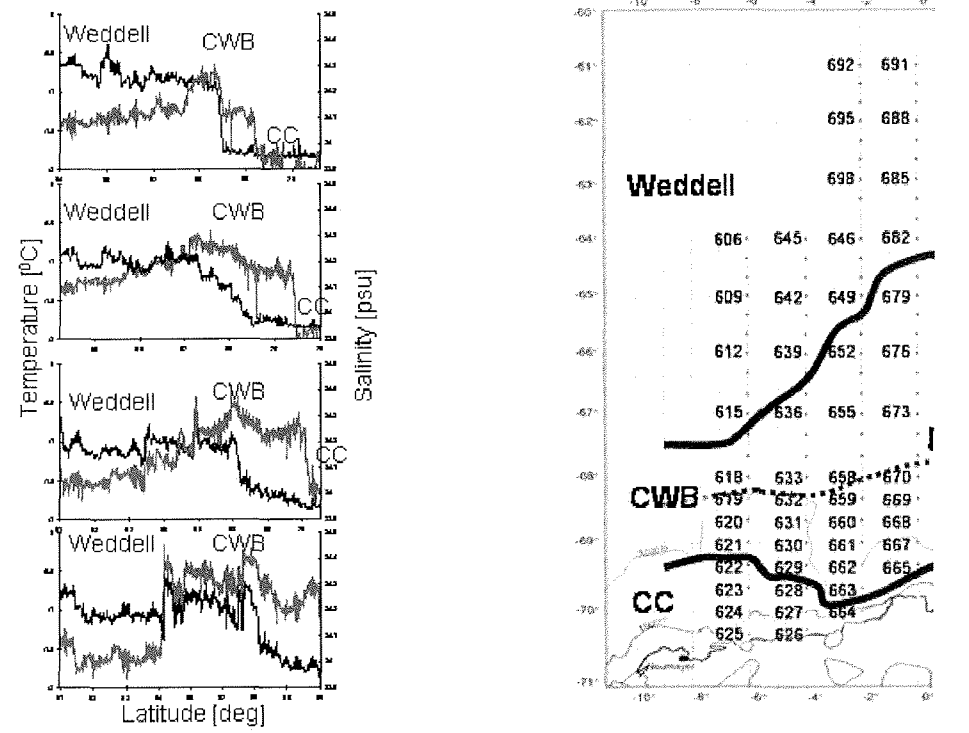


Figure 3.4: The right-hand panel shows surface temperature and salinity distribution along Transect 1 to 4 (top to bottom) inside the GLOBEC/CCAMLR sampling grid. Surface water masses and ice coverage is indicated in the left-hand panel.

The transition between WW and WDW, which is described by the 0.0 °C isotherm and the 34.6 isohaline, was found at a depth of 100 to 150 m, sloping down towards the shelf break to 500 to 700 m (Transects 1 and 2).

The coastal current had a horizontal extension of about 70 nautical miles on Transect 1, decreasing to 20 nautical miles on Transect 3. In contrast to the CC, a larger extension of the Continental Water Boundary (CWB) from west to east was observed. On Transect 1, the CWB spread over approximately 120 nautical miles whereas on Transect 4 the CWB was about 300 nautical miles wide.

The corresponding density distributions along Transects 1 to 4 are shown in Figures 3.13 and 3.14. The density distribution confirms the identification of water masses using temperature and salinity distribution.

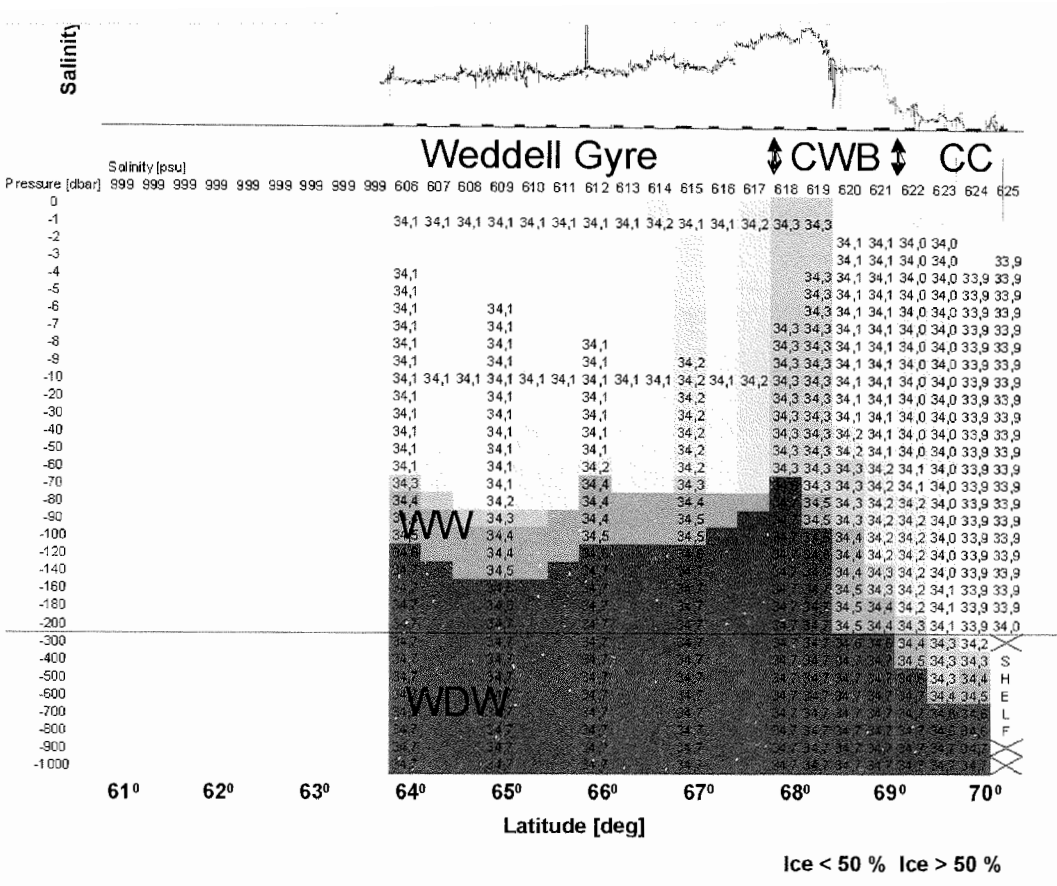
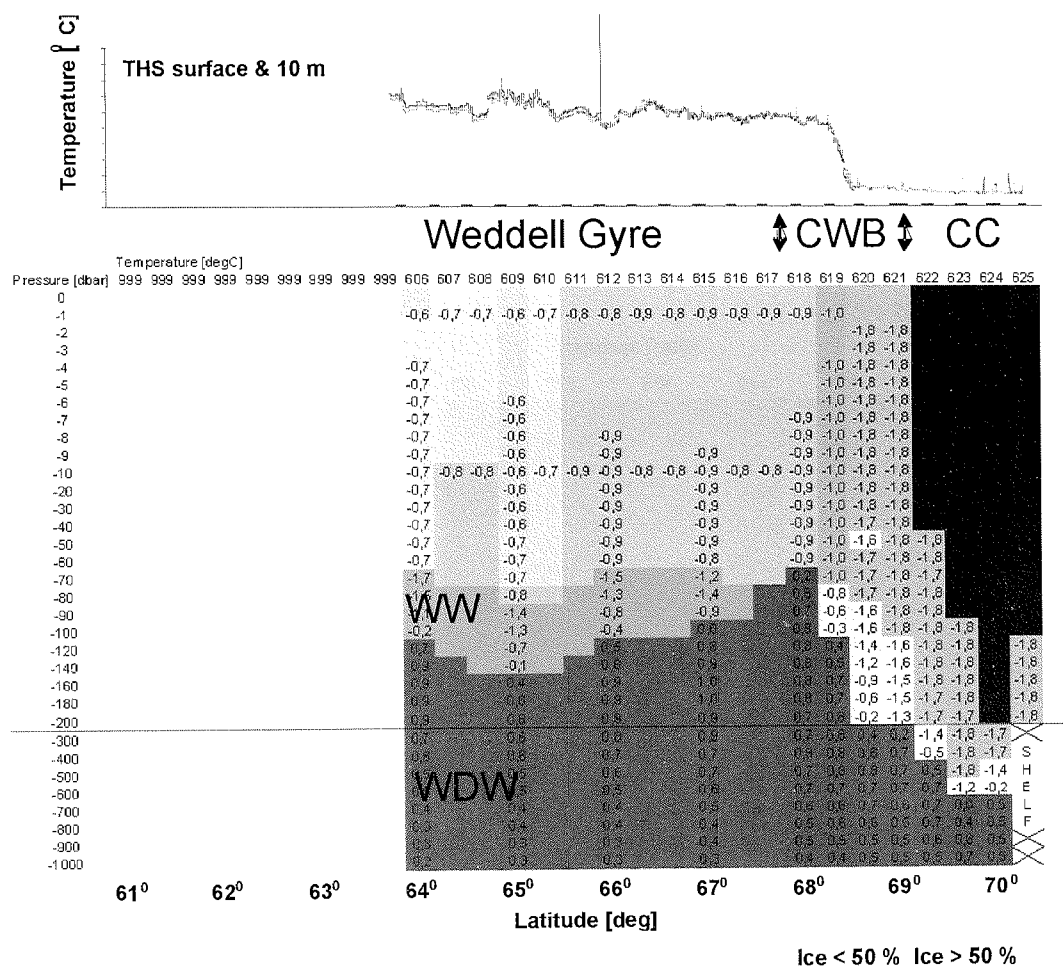


Figure 3.5: Salinity distribution on Transect 1; upper panel shows the data from the THS; lower panel data from CTD profiles (surface and 10 m values were extracted from THS).



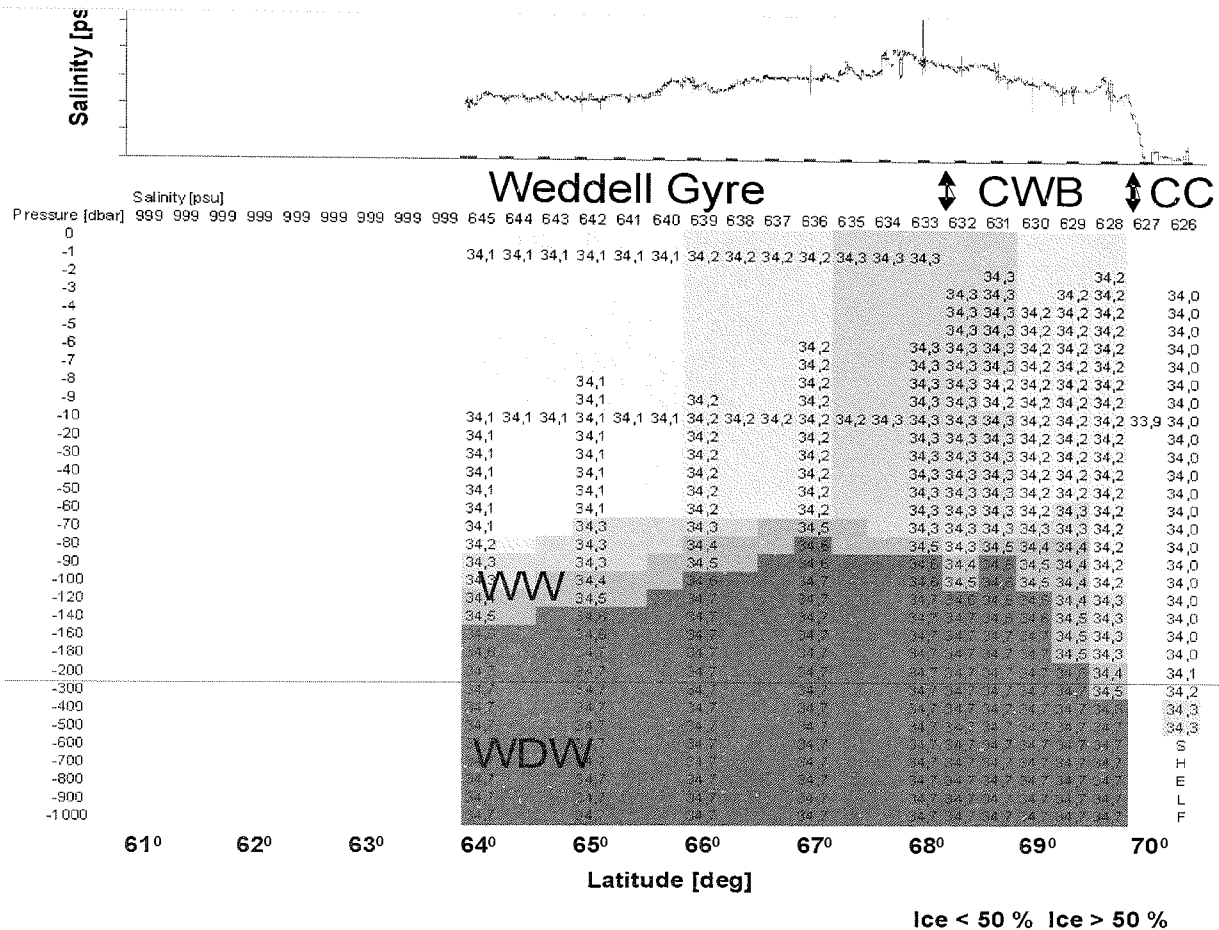


Figure 3.7: Salinity distribution on Transect 2; upper panel shows the data from the THS; lower panel data from CTD profiles (surface and 10 m values were extracted from THS).

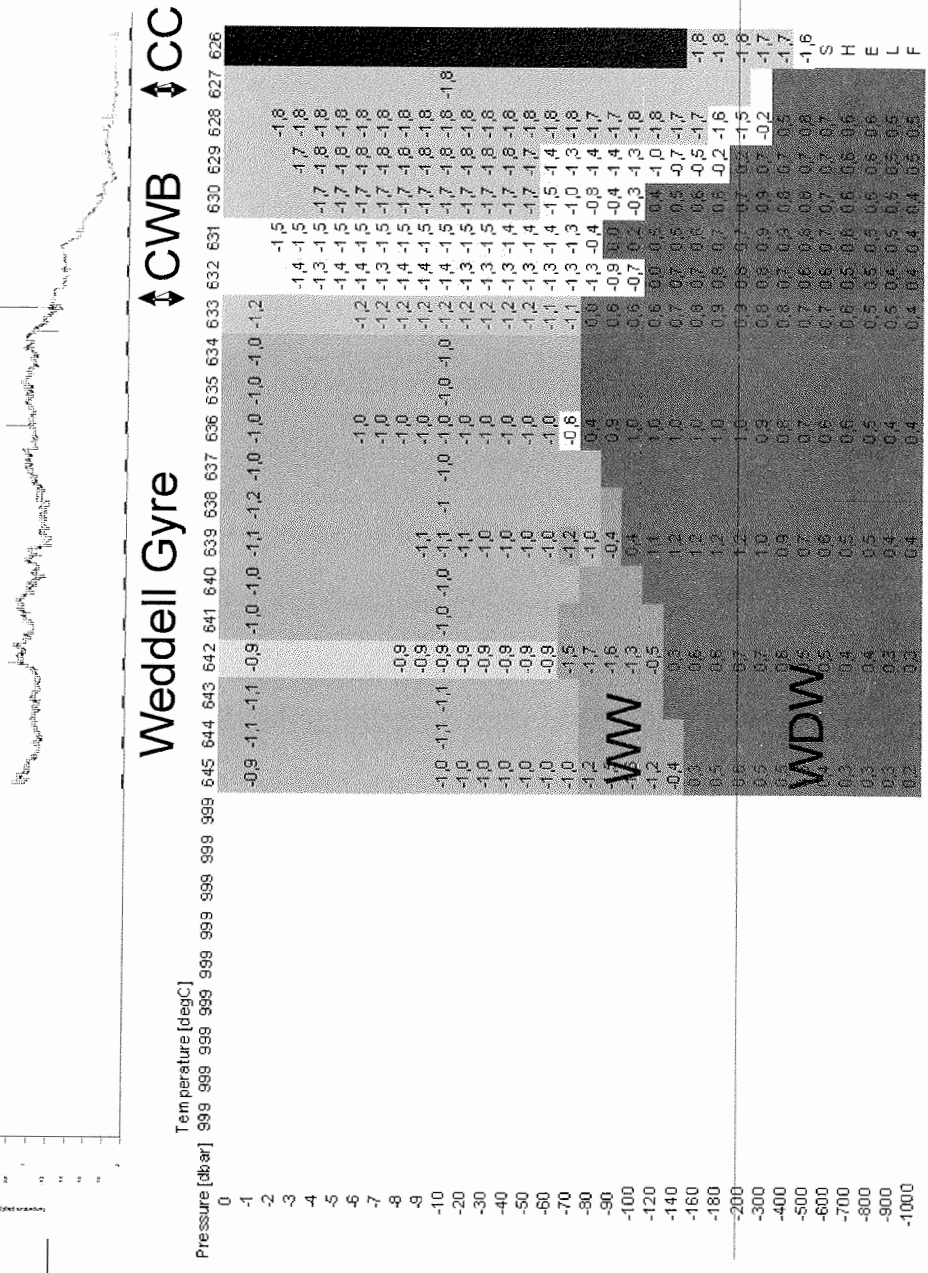


Figure 3.8: Temperature distribution on Transect 2; upper panel shows the data from the THS; lower panel shows CTD profiles (surface and 10 m values were subtracted from THS)

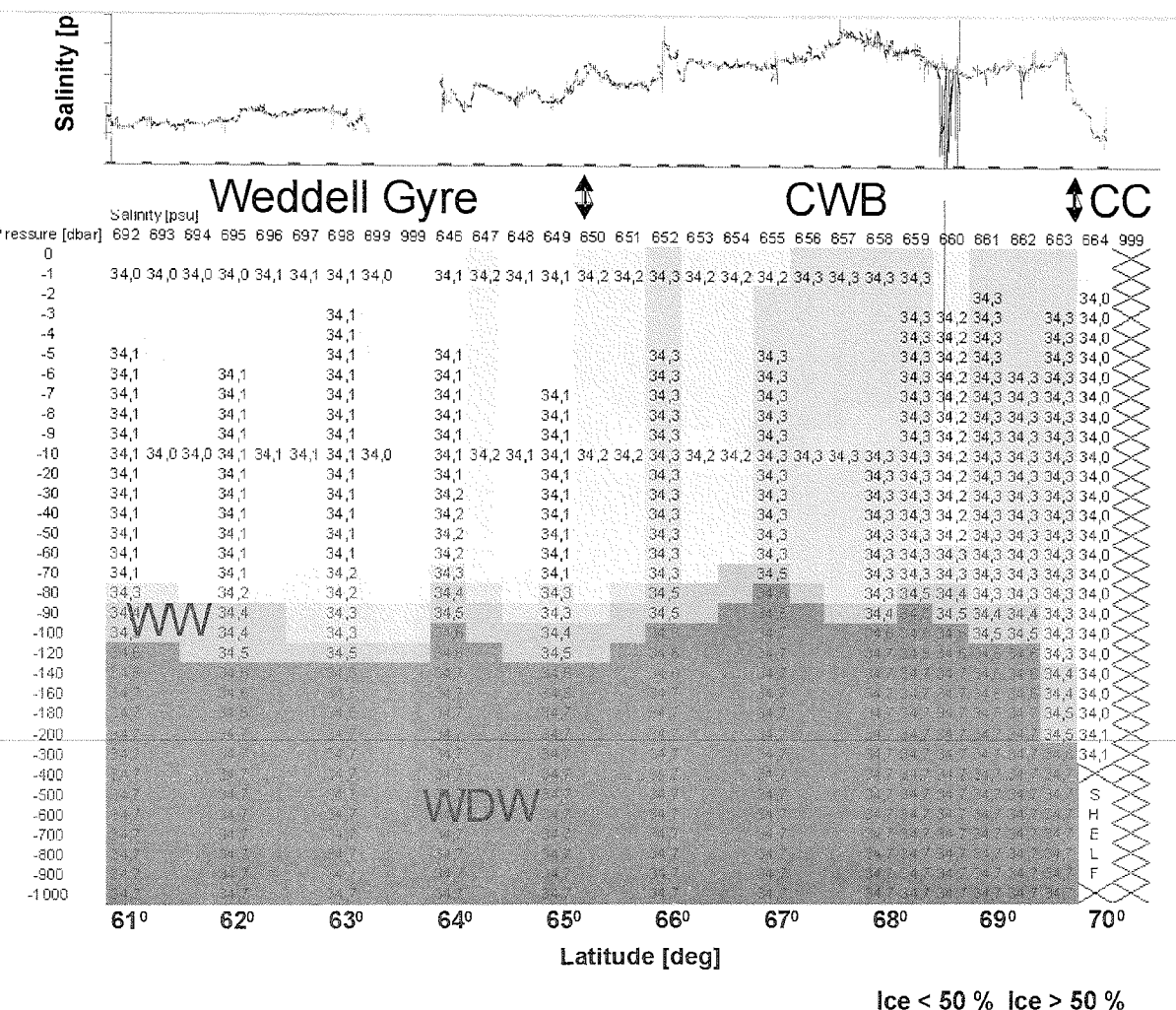
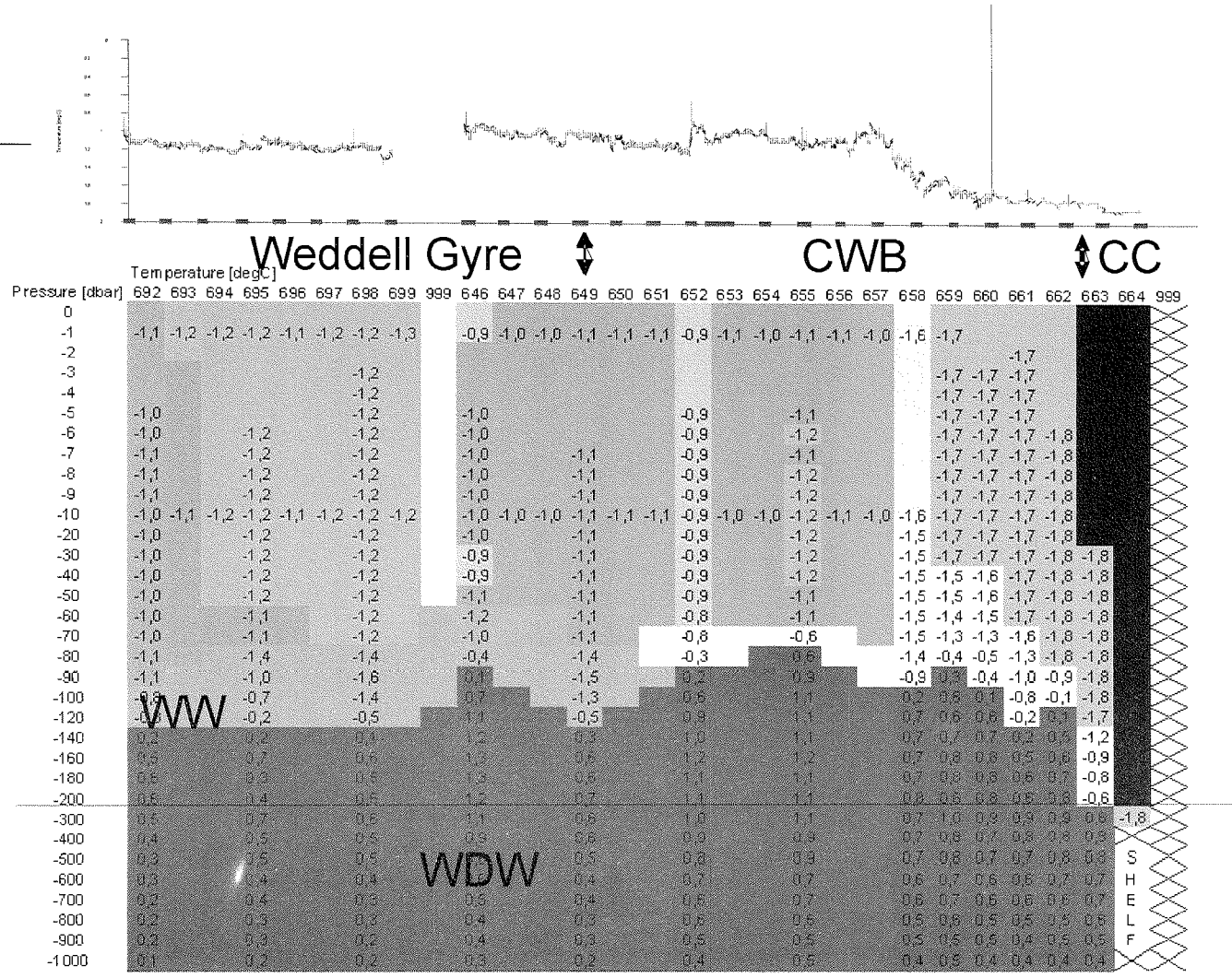


Figure 3.9: Salinity distribution on Transect 3; upper panel shows the data from the THS; lower panel data from CTD profiles (surface and 10 m values were extracted from THS).



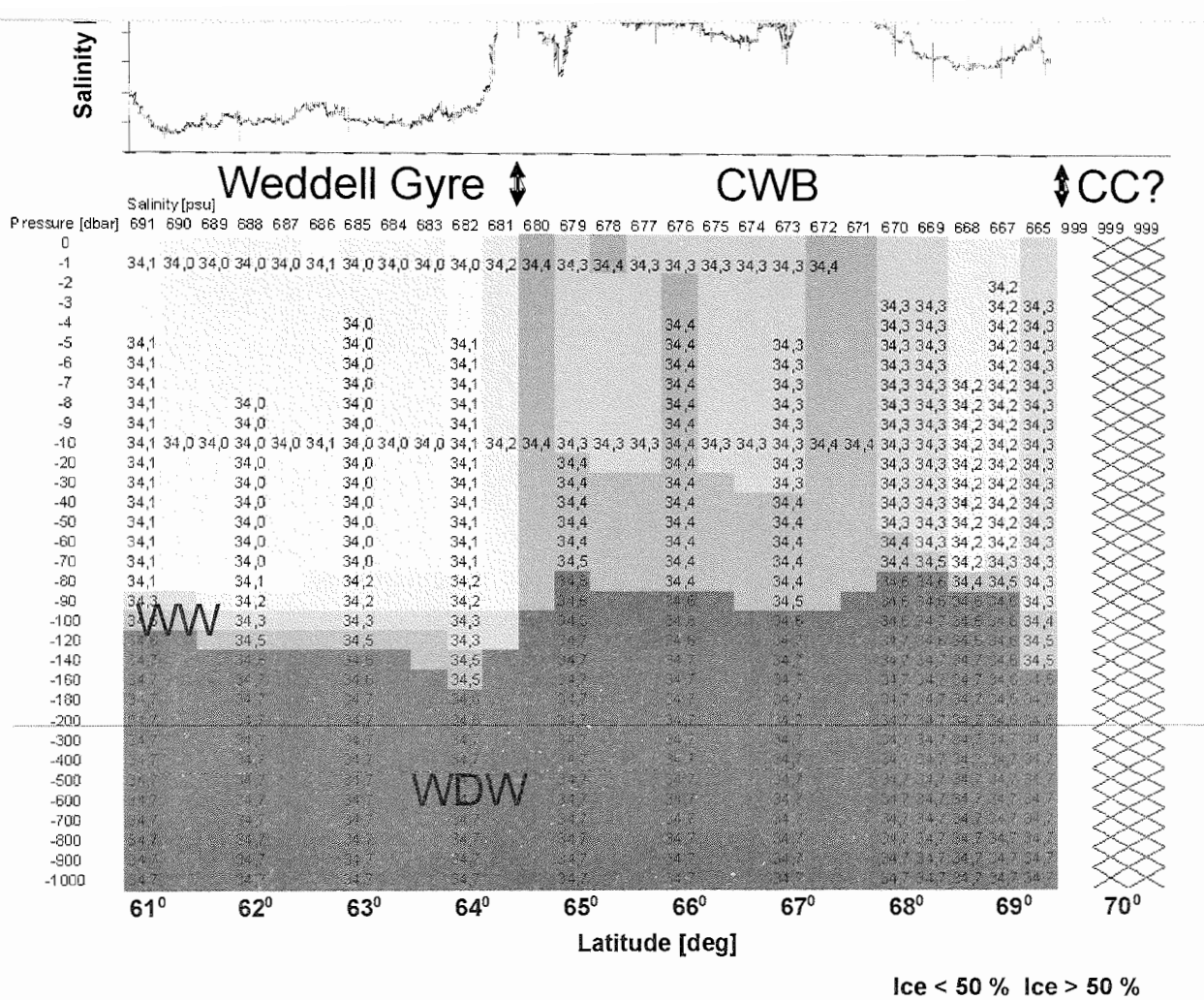


Figure 3.11: Salinity distribution on Transect 4; upper panel shows the data from the THS; lower panel data from CTD profiles (surface and 10 m values were extracted from THS).

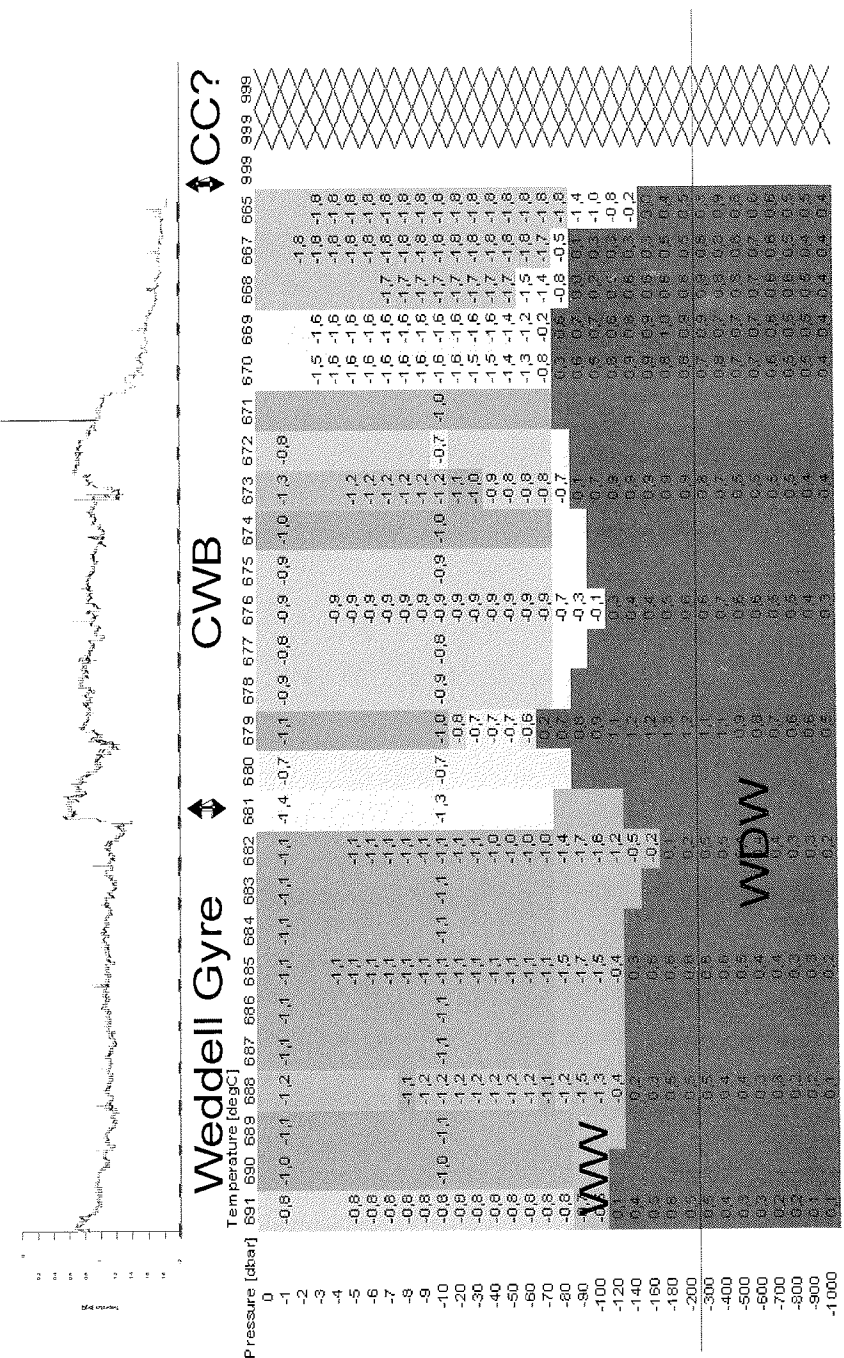


Figure 4.9. Temperature distribution on Transect 1. Upper panel shows the data from the THS; lower panel shows the data from the CTD profiles (surface and 10 m values).

↑

↓

↑

↓

↑

↓

↑

↓

↑

↓

↑

↓

↑

↓

↑

↓

↑

↓

↑

↓

↑

↓

↑

↓

↑

↓

↑

↓

↑

↓

↑

↓

↑

↓

↑

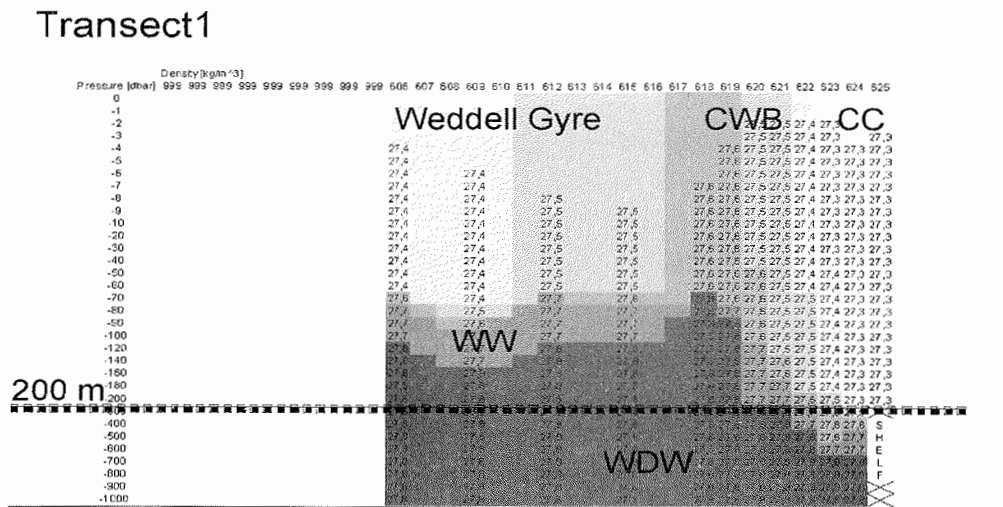
↓

↑

↓

↑

↓



Transect2

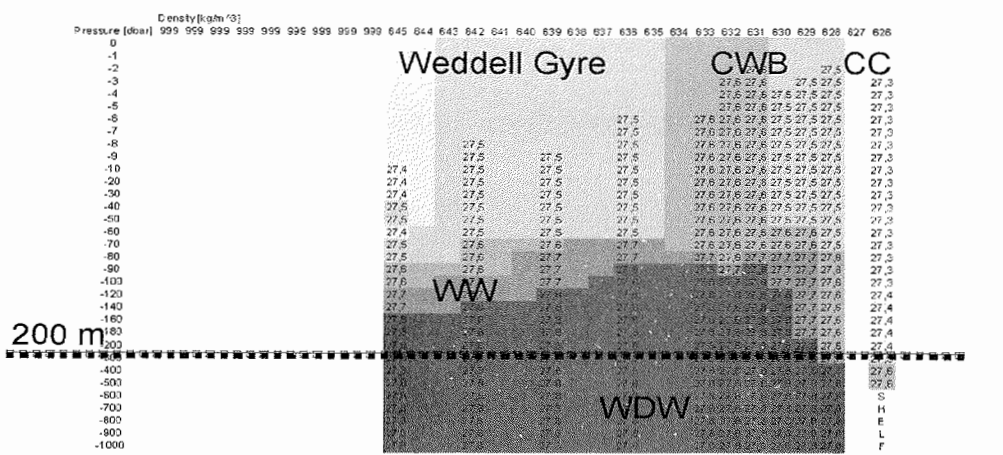
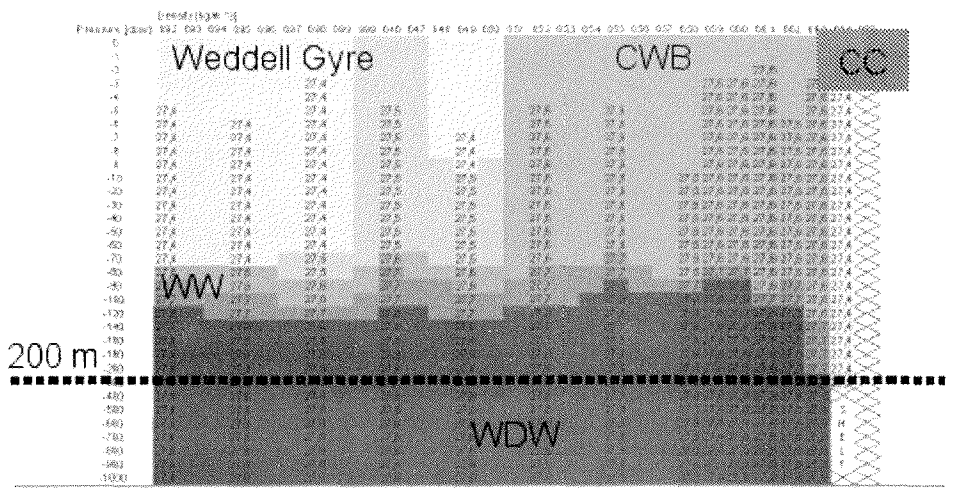


Figure 3.13: Density distribution on Transects 1 and 2 calculated from CTD profiles.

Temperature and salinity profiles during the geochemical stationsInside and north of the polar frontal region, CTD casts were conducted for geochemical research (Figures 3.15 and 3.16). Salinity-temperature gradients that allowed for clear vertical identification of the water masses were measured. The CTD profiles of the three stations that were located within the Polar Front (PF) were distinct from the station north of the PF in region of the Subtropical-Subantarctic Front (STF-SAF) (Figure 3.15). The station in the STF-SAF showed generally higher temperature, salinity, chlorophyll-a fluorescence, and a lower transmission in the surface water layer.

Transect3



Transect4

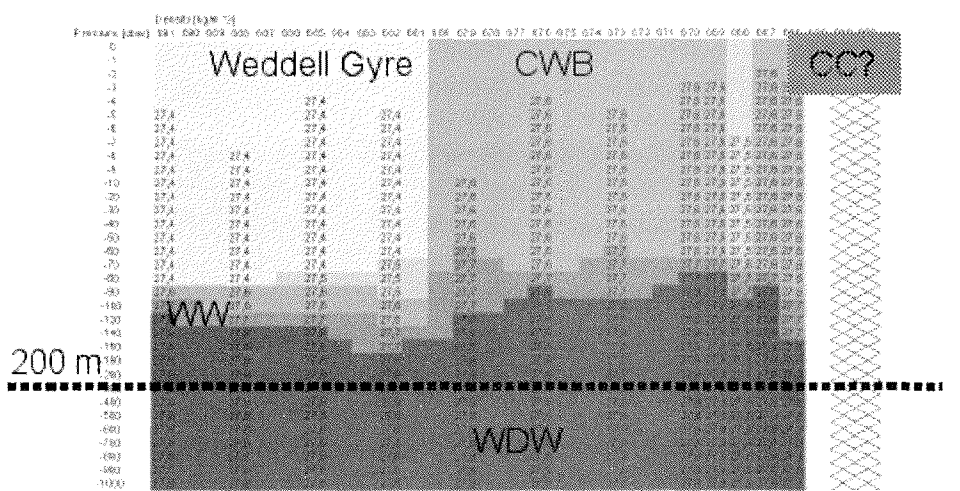


Figure 3.13: Density distribution on Transects 1 and 2 calculated from CTD profiles.

The T-S plot in Figure 3.17 shows the identification of the water masses that were encountered during the CTD cast. The surface layer in the polar frontal zone was separated from the Antarctic Intermediate Water (AAIW) through a thermocline at 250 m. North of the PF the surface layer and the AAIW were separated from each other through the Subantarctic Mode Water (SAMW). The Lower Cold Deep Water was located below the AAIW in the PF at 1500 m and north of the PF at 3000 m (Figure 3.17).

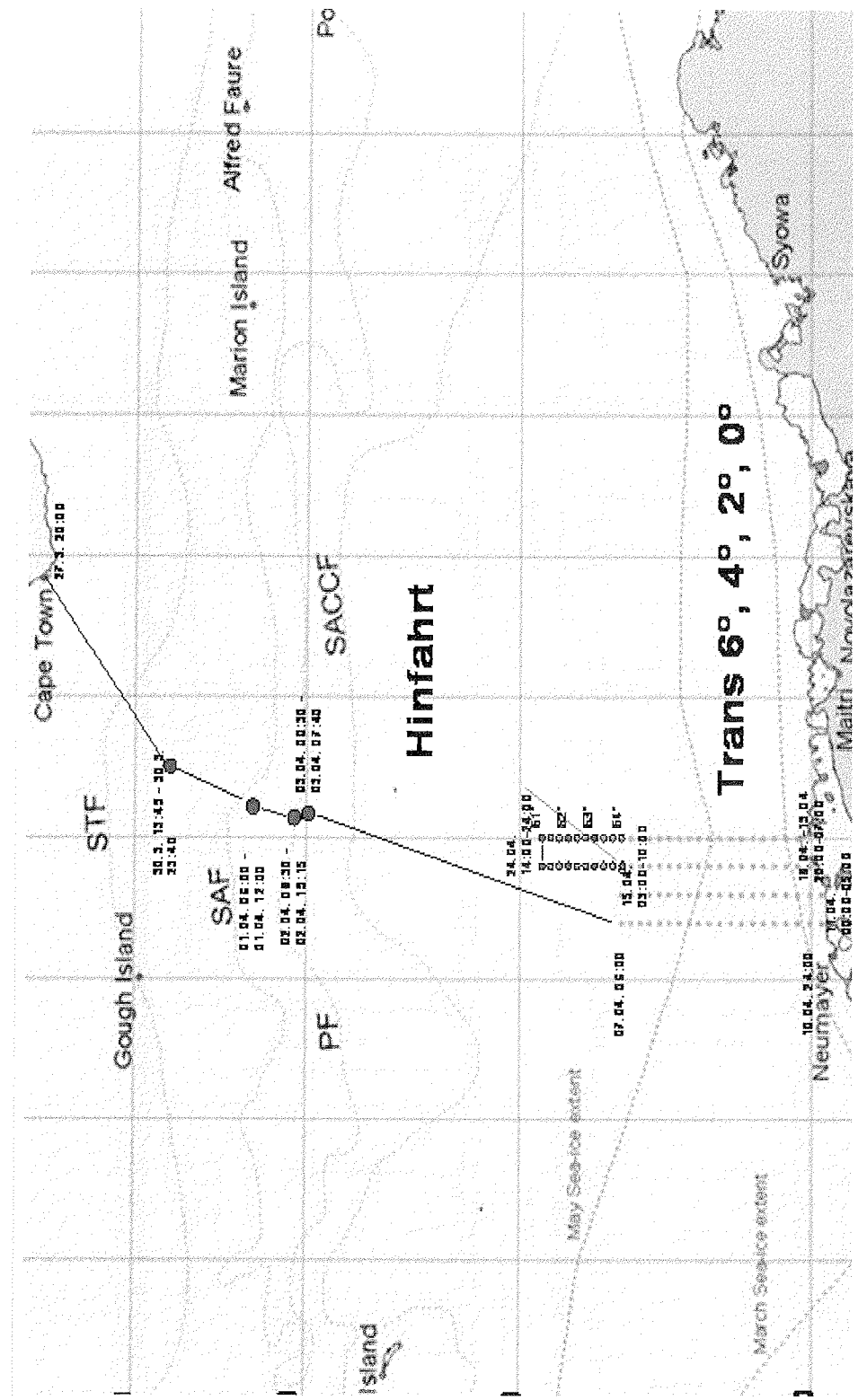


Figure 3.15: Sampling locations of geochemical stations.

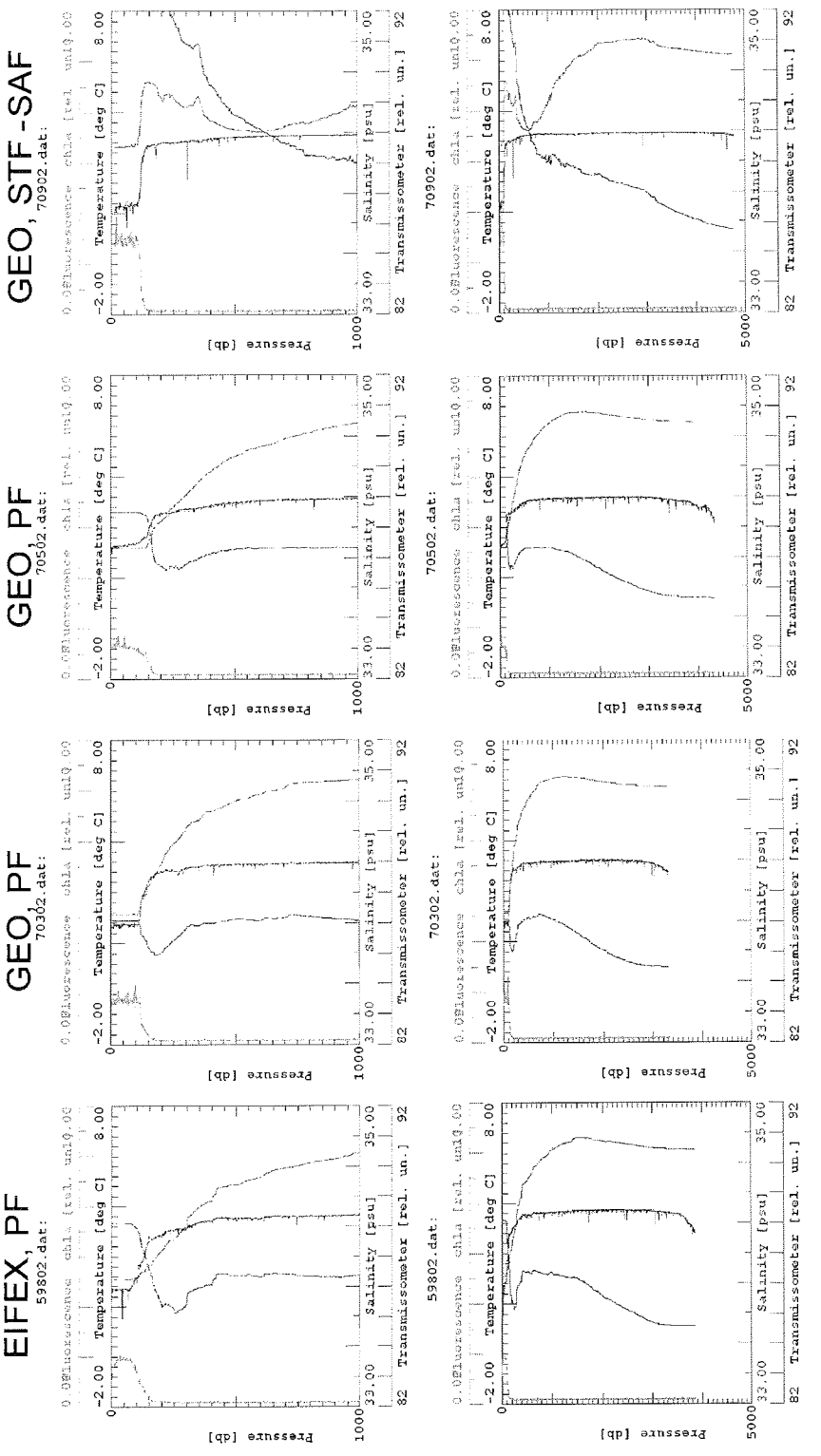


Figure 3.16: Representative CTD profiles at the geochemical stations in the polar, subtropical-subantarctic frontal region.

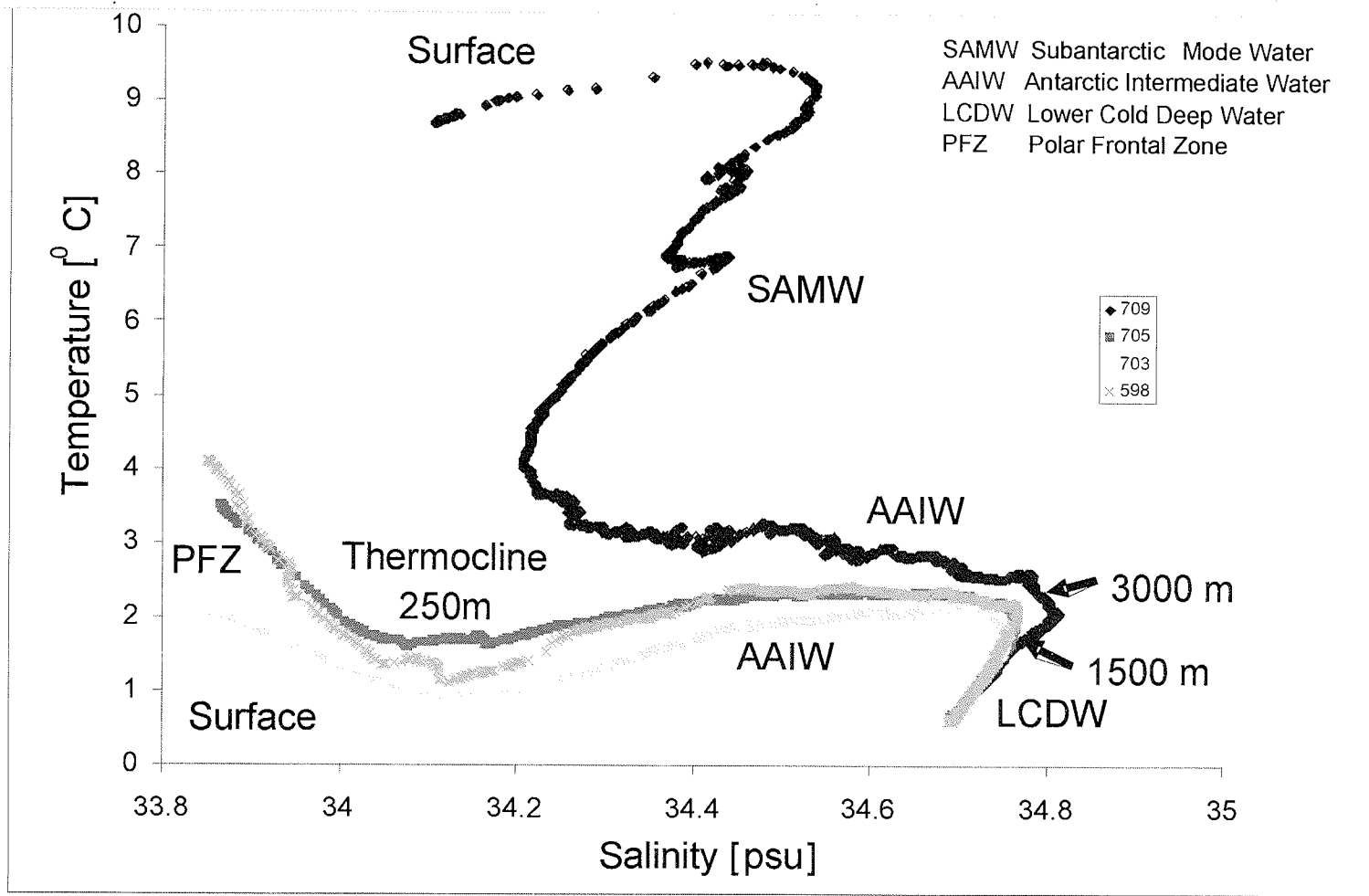


Figure 3.17: TS plot from the geochemical stations.

4. ZOOPLANKTON- BIOVOLUME

Svenja Kruse, Regine Herrmann (AWI)

1. Introduction

The aim of this cruise was to measure the biovolume of the zooplankton in the three different water masses "Weddell-Sea", "Boundary" and the "Antarctic Coastal Current". In addition to that we tried to identify and count all the species – or at least the different families we found in our samples.

We took the samples during the expedition "ANT XXI-4" on the research vessel "Polarstern" from the 26.03.04 until 06.05.05 during the antarctic autumn. After 13 days (8.4.04) we took the first multinet from the Lazarev-Sea and measured the zooplankton- biovolume. We took 15 samples (4 per transect) between 64°S and the Antarctic continent and between 0 and 6°E (see table 4.1).

Table 4.1.: The Stations of the cruise ANT XXI-4, were we took samples with the multinet. Also in this table are the date, time, position and the waterdepth.

Stationsno.	Date 2004	Time	Position °S	Position °W	Waterdepth [m]
615-5	08/04/2004	22:10	67°3,311S	5°57,746W	4860
618-3	09/04/2004	09:28	68°1,141S	6°0,505W	4744,4
623-3	10/04/2004	11:18	69°42,466S	5°59,306W	2346
625-4	10/04/2004	23:24	70°18,509S	6°9,181W	336,8
626-3	11/04/2004	07:36	70°19,834S	3°55,828W	495,6
628-4	11/04/2004	18:13	69°39,308S	4°7,156W	2738
633-4	12/04/2004	22:48	68°1,611S	4°3,881W	4500
636-3	13/04/2004	12:48	67°0,887S	3°59,572W	4723
655-3	16/04/2004	22:15	67°1,620S	2°0,397W	4689
661-4	17/04/2004	02:53	68°58,395S	1°57,975W	3556
664-3	18/04/2004	19:39	70°0,540S	1°58,536W	382
665-9	19/04/2004	11:35	69°18,853S	0°0,0191W	2427
666-4	19/04/2004	19:45	68°58,034S	0°2,919E	3354
670-	20/04/2004	09:32	67°58,778S	0°0,735W	3670
673-2	20/04/2004	00:22	66°58,018S	0°0,759E	4650

2. Material and Methods

We took 4 stations per transect – two in the Weddell-Sea, one in the Coastal Boundary and one in the Antarctic coastal current. In the Weddell-Sea and in the Boundary we took samples in 0-50m, 50-100m, 100-250m, 250-500m, and 500-1000m depth, whereas in the Coastal Current 0-50m, 50-100m, 100-150m, 150-200m, and in 200-250m. We used a multinet with a meshsize of 100µm with a speed of 0,5m/sec.

After bringing the samples on board we preserved them in 4% Formaline and washed them after 3 days. Afterwards we took out all the jelly fish, radiolarians, algea, chaetognaths, and appendicularia to measure their biovolume separately. Before we started to identify and count the species we poured the sample through a sieve with a meshsize of 1000µm so that we divided the sample into organisms < and > 1000µm and put them into test-tubes.

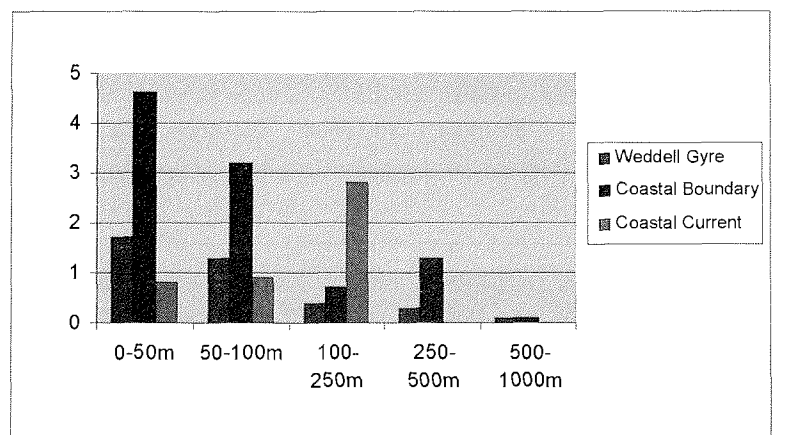
To reduce the water we pressed a hollow glass-rod – where we attached a gaze with $20\mu\text{m}$ meshsize at one ending and which fits exactly into the tube – carefully down, so that the water could run into the rod and wasn't included in the measured biovolume anymore.

After preparing the samples we identified the species or at least the families and counted them. Additionally we measured the length of the appendicularia and chaetognaths.

To compare the different water masses we calculated the number of species per litre.

3. Results and conclusions

1) Biovolume: Concerning the average biovolume (see graph 4.1), which was measured without chaetognaths and appendicularians, the zooplankton in the Lazarev-Sea was concentrated on the first 100m as well as in the coastal boundary. But the biovolume here was twice as much as in the Lazarev-Sea. In contrast to that, the zooplankton in the Antarctic Coastal Current preferred depths between 100 and 250m. This increase with depth was because of the WDW (warm deep water) underlying the CC (coastal current).



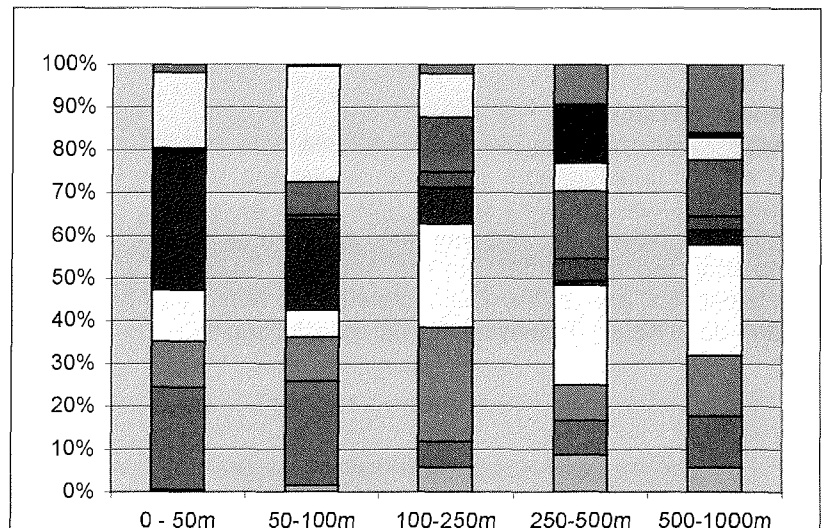
Graph 4.1: The average biovolume [ml/L] in the three different water masses "Weddell-Gyre", "Coastal Boundary", and "Coastal Current" in the five different depths.

2) The average vertical distribution: The average vertical distribution in numbers (see table 2) was regarded without the copepods, because they dominate the zooplankton with more than 90%.

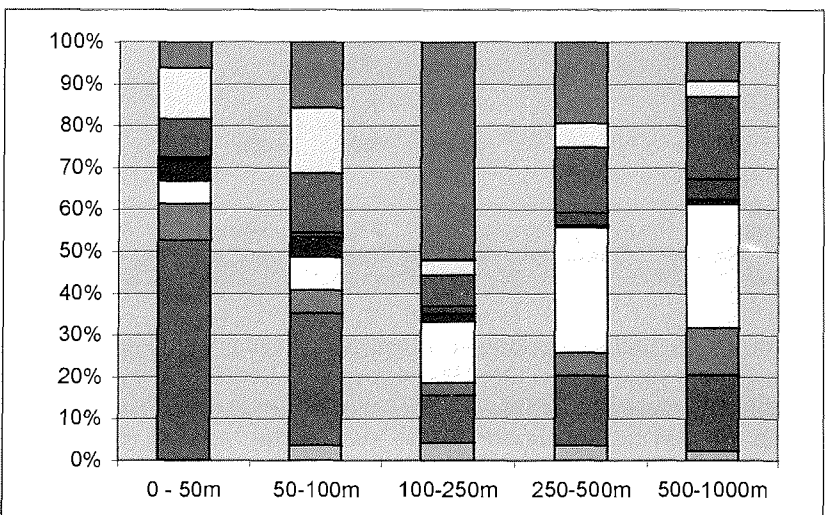
In general the vertical distribution in the three water masses (see graph 4.2-4.4) was rather similar, but they differed in the horizontal distribution. The Weddell-Gyre (see graph 4.3) was dominated by high numbers of pteropods, ostracods, chaetognaths and eggs (undefined, size of 1-2mm). The Coastal Current (see graph 4.4) contained in contrary higher numbers of appendicularia, euphausiids and polychaets.

The Coastal Boundary (see graph 4.2) in between stood under the influence of both water masses.

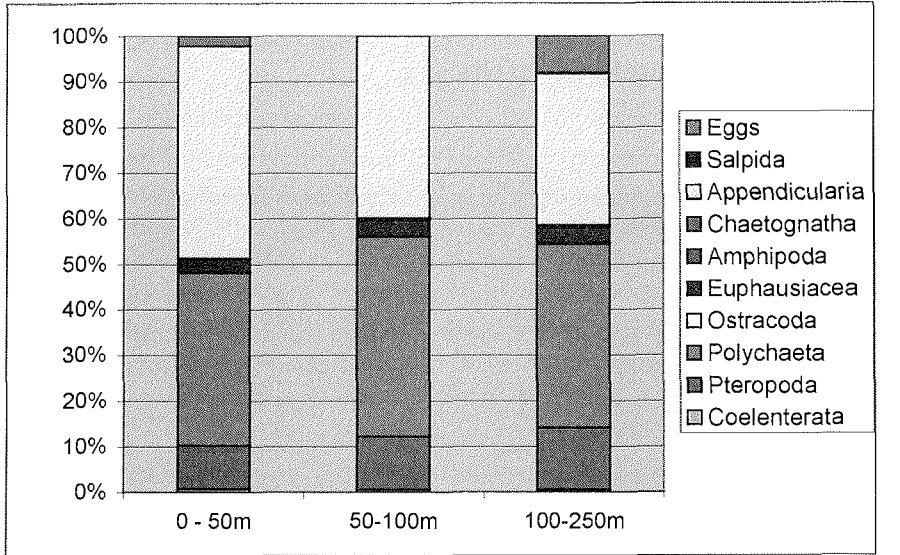
Alltogether euphausiids, pteropods and polychaets were concentrated on the upper 250m. Appendicularia dominated the upper 100m of the Coastal Current. Coelenterata, amphipods and ostracods were very rare in the surface layers, looking at the percentages. In numbers it was the other way round. The surprisingly high amount of eggs was remarkable as well.



Graph 4.2: The vertical depth distribution in the Coastal Boundary [%]



Graph 4.3: The vertical depth distribution in the Weddell-Gyre [%]



Graph 4.4: The vertical depth distribution in the Antarctic Coastal Current [%]

Table 4.2: The average amount in numbers of all found individuals [Ind./L] in the three different water masses "Weddel-Gyre", "Coastal Boundary", and "Antarctic Coastal Current" in different depths (without copepods)

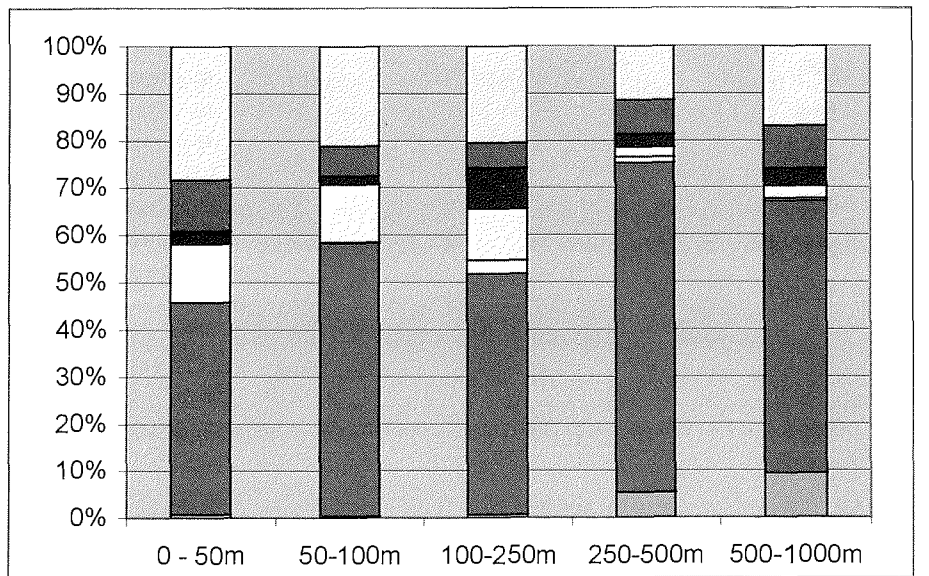
	0-50m	50-100m	100-250m	250-500m	500-1000m
Weddel-Gyre	33,975	25,213	20,925	8,564	2,560
Coastal boundary	31,884	11,961	7,102	4,402	1,260
Antarctic Coastal Current	25,548	34,765	45,364		

3) The copepods: High numbers of copepods of various species were found in the Southern Ocean (see table 4.3). The species smaller than 1mm were left out, because they take more than 80% of all copepods. This made it possible to have a closer look at the different species.

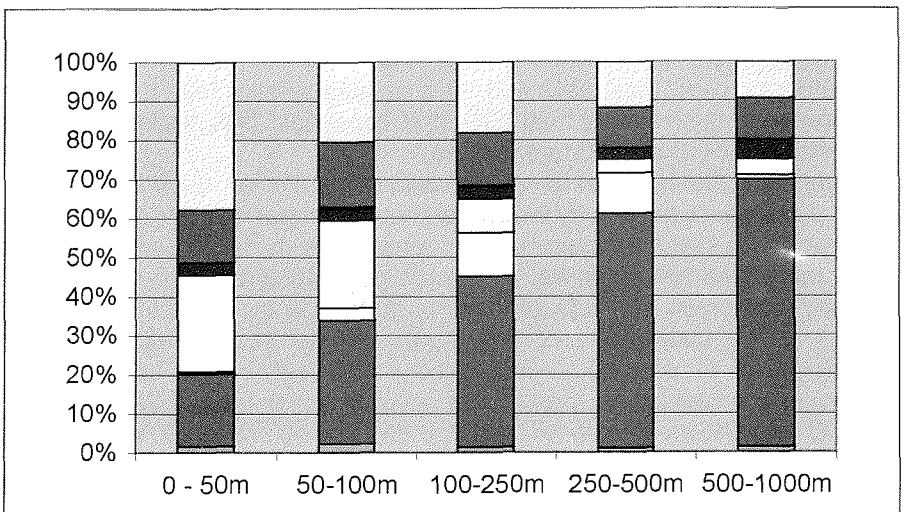
The horizontal distribution of all species was rather similar, but it differed in the vertical distribution, at least by looking at the percentages. In the Weddell-Gyre (see graph 4.6) *Calanus propinquus* decreased with depth and *Calanoides acutus* increases. In numbers *C. acutus* decreased as well. The Coastal Boundary (see graph 4.5) was quite similar to that. In the Coastal Current (see graph 3.7) the distribution of *C. acutus* did not really change, but the percentages of *C. propinquus* increased a little with depth. Looking at the numbers of the species, *C. propinquus* occurred rather frequently in the upper layers. *C. propinquus* has special storage and anti-freeze lipids, which make it possible to stay active at the supercooled surface. *C. acutus* was dominant in deeper layers, looking at the percentages.

But it still occurs in high numbers in the upper layers. It will migrate down to stay in the depth over winter (diapause). The numbers of *Euchaeta sp.* decreased in the Weddell-Gyre and increased in the Coastal Current.

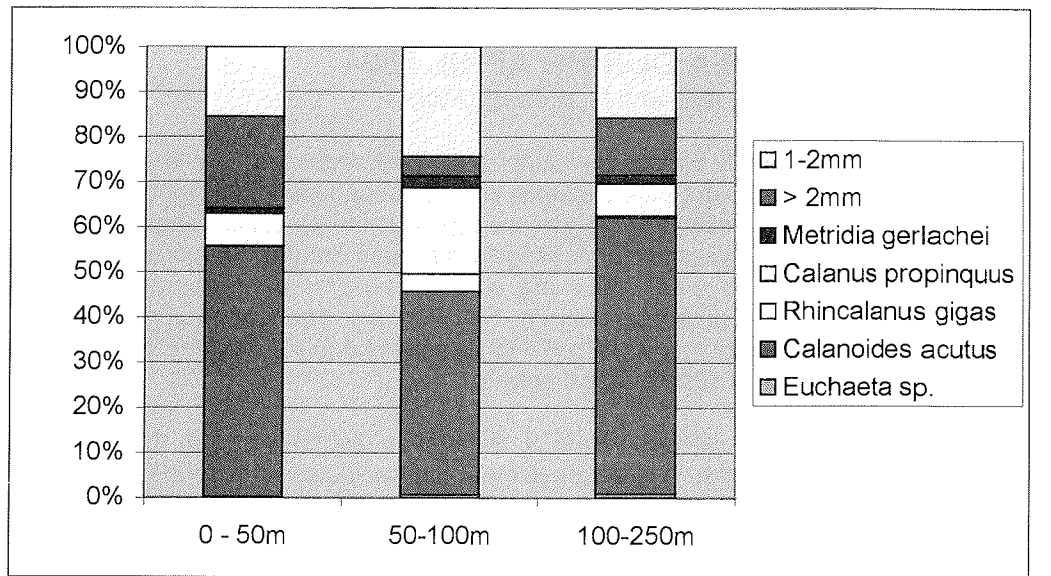
It was still at the surface layers and did not lay its eggs in the depth.
Smaller species (<2mm) were dominating the surface layers and fed here on
the last algae. The question is, for how long.



Graph 4.5: The copepod species >1mm [%] in the Coastal Boundary in different depths



Graph 4.6: The copepod species >1mm [%] in the Weddell-Gyre in different depths



Graph 4.7: The copepod species >1mm [%] in the Antarctic Coastal Current in different depths

Table 4.3: The average amount in numbers [Ind./L] of all copepod species (>1mm) in the three different water masses "Weddell-Gyre", "Coastal Boundary", and "Antarctic Coastal Current" in different depths.

	0 - 50m	50-100m	100-250m	250-500m	500-1000m
Weddell-Gyre	83,916	45,153	16,254	12,401	8,030
Boundary	242,278	129,411	25,786	19,74	8,026
Antarctic Coastal Current	44,130	71,287	69,017		

4. Special thanks

We would like to thank Uli Bathmann for his great support during the cruise.
Also thanks to Ulrike Marx for taking photos and the great crew on Polarstern!!!!

5. BIOLOGY OF PELAGIC TUNICATES IN THE LAZAREV SEA DURING APRIL 2004

E.A. Pakhomov (UBC) and M. Brenner (AWI)

Salps, particularly *Salpa thompsoni* and *Ihlea racovitzai*, are the third most important metazoans after Antarctic krill and copepods in the Southern Ocean. Due to their capacity of rapid asexual reproduction (budding), salps are known to form dense swarms dominating in different Antarctic regions. Salps are microphagous species, which are able to consume organic matter at rates exceeding daily primary productivity. Salps are also known as organisms able to channel surface biogenic carbon into long-living pools or into the deep sea via production of fast sinking faecal pellets.

The classical knowledge of the *S. thompsoni* distribution from the Discovery period indicates that it is very patchy and is restricted to latitudes between 45 and 60°S. However, during the last 20 years, salp swarms have been repeatedly reported in more southern regions, indicating that the salp distribution range may have shifted towards the south. The factors that caused this shift are still under discussion. However, southward shift may bring salps, which are strong competitors, to the regions traditionally occupied by Antarctic krill. Also, salps in the southern parts of the Southern Ocean may be exposed to environmental conditions close to their ecophysiological limits.

The major aims of this cruise were to investigate salp spatial distribution, their developmental stage composition and feeding intensity in the Lazarev Sea during austral autumn (April) 2004. At every grid station, salps were collected from the standard oblique 0-200 m RMT-8 catches, counted, sexed and measured (oral-atrial length). Immediately after capturing, stomachs of 3 to 15 salps of different size classes were dissected out and placed individually into plastic tubes filled with 10 ml of 90% acetone for gut pigment extraction in darkness at -18°C for at least 24 hours. Finally, developmental stages of aggregate and solitary forms of *S. thompsoni* only have been identified with the special attention to any abnormalities in the salp embryo development.

Composition and distribution. Two species of salps, namely *Salpa thompsoni* and *Ihlea racovitzai*, have been identified in RMT-8 tows in the top 200-m water layer of the Lazarev Sea during April 2004. Frequency of occurrence of *S. thompsoni* and *I. racovitzai* in samples was 57 and 54%, respectively. For both species, a strong correlation between salp appearance in catches and time of the day has been observed. Except the south most stations, both species were only occurring in catches during the time of darkness. The nighttime concentrations of *S. thompsoni* ranged from <0.1 to 33 ind.1000m⁻³ (Fig. 5.1). Generally, *S. thompsoni* concentrations were below 5 ind.1000m⁻³ north of the sea ice extent, while salp densities increased to 10-30 ind.1000m⁻³ in the stations occupied over the continental shelf and slope (Fig. 5.1). Densities of *I. racovitzai* were always very low varying between <0.1 and 4 ind.1000m⁻³ (Fig.5.1). This species was mainly caught north of the region covered by the

sea ice and only occasionally in the ice-covered area (Fig. 5.1).

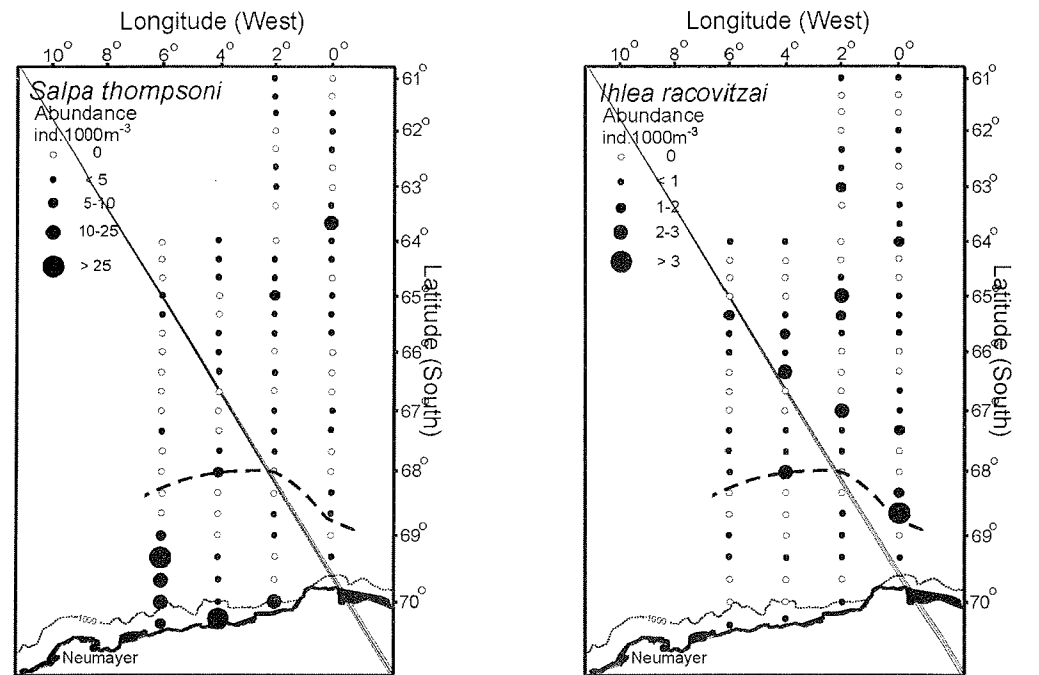


Figure 5.1. Spatial distribution of *Salpa thompsoni* and *Ileia racovitzai* in the Lazarev Sea during April 2004. Dashed line shows the sea ice extent.

Size structure and development. Population structure of *S. thompsoni* has been analyzed separately in two contrasting regions: open waters not covered by the sea ice and influenced by the Weddell Gyre water masses and coastal ice covered waters influenced by the Coastal Current water masses. Aggregate forms of *S. thompsoni* have been dominating south of 64° latitude and only a single solitary specimen has been caught in the coastal region. Open water samples were characterized by the presence of two distinct size cohorts between 20 and 30 mm (Fig. 5.2). This salp population was advanced in development with stages 3 and 5 (spent) dominating samples. Almost 20% of all aggregates have been identified as having some sort of embryo development disruption (stage X) (Fig. 5.2). Unlike open water population, the coastal grouping had at least 6 distinct size cohorts varying between 9 and 36 mm length. The specimens of this grouping have been at early, mainly 1 and 2, stages of development and only about 15% of specimens had embryo development deformations (Fig. 5.2).

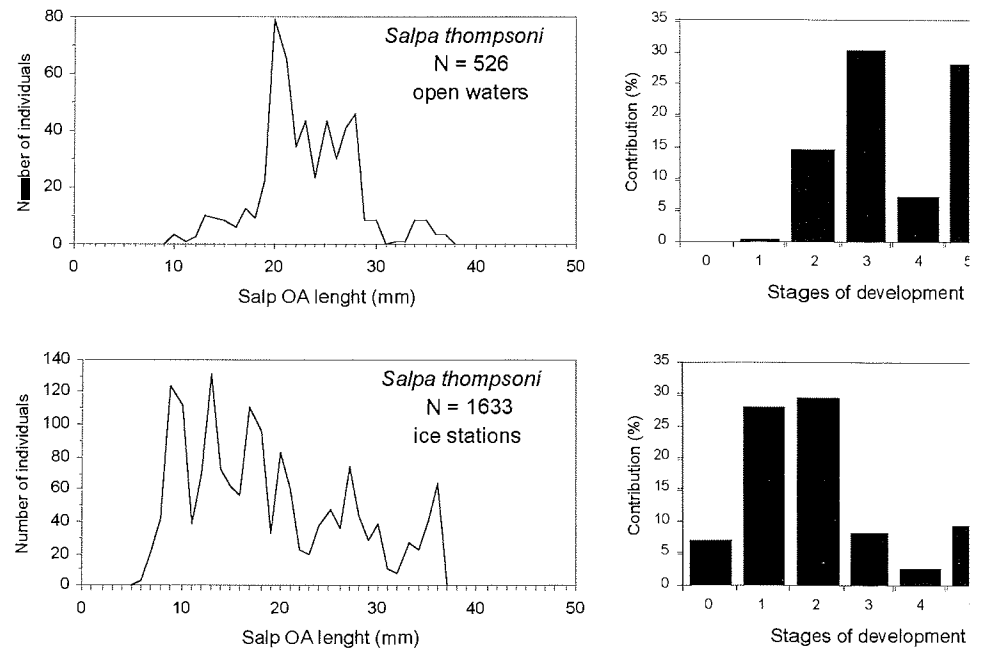


Figure 5.2. Length frequency distribution and development stage composition of *Salpa thompsoni* populations in open coastal waters of the Lazarev Sea during April 2004.

Length frequency distribution of *I. racovitzai* was not different across the grid with several distinct size cohorts visible between 20 and 50 mm (Fig. 5.3).

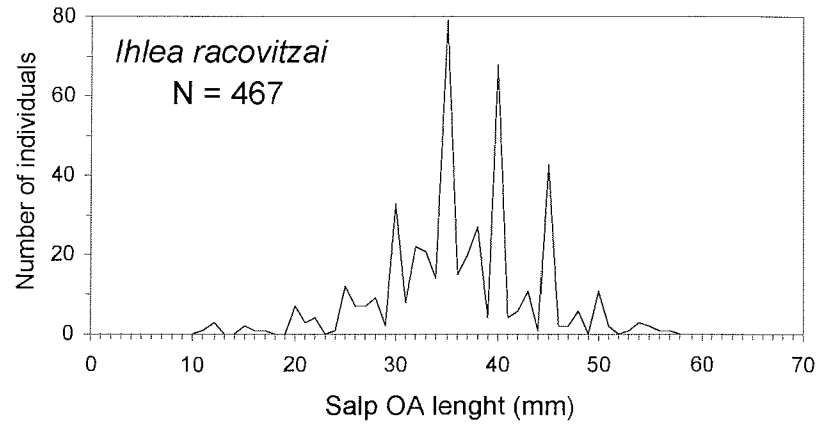


Figure 5.3. Length frequency distribution of *Ibla racovitzai* in the Lazarev Sea during April 2004.

Feeding dynamics. The feeding intensity of *S. thompsoni* has been different in day and nighttime samples and plotted separately (Fig. 5.4). The relationship between salp length and concentration of pigments in the salp stomach has been best fitted by the power function. Salps sampled in the south most stations had the highest gut pigment concentrations reaching values of ca 23000 ng(pigm).ind.⁻¹ for 36 mm salps (Fig. 5.4). The highest gut pigment contents of *S. thompsoni* (dashed line in Fig. 5.4, top left panel) corresponded to stations with surface chlorophyll-a concentrations exceeding 0.4 mg.m⁻³, while the majority of the population in open waters were feeding (solid line in Fig. 5.4) at chlorophyll-a concentrations < 0.2 mg.m⁻³.

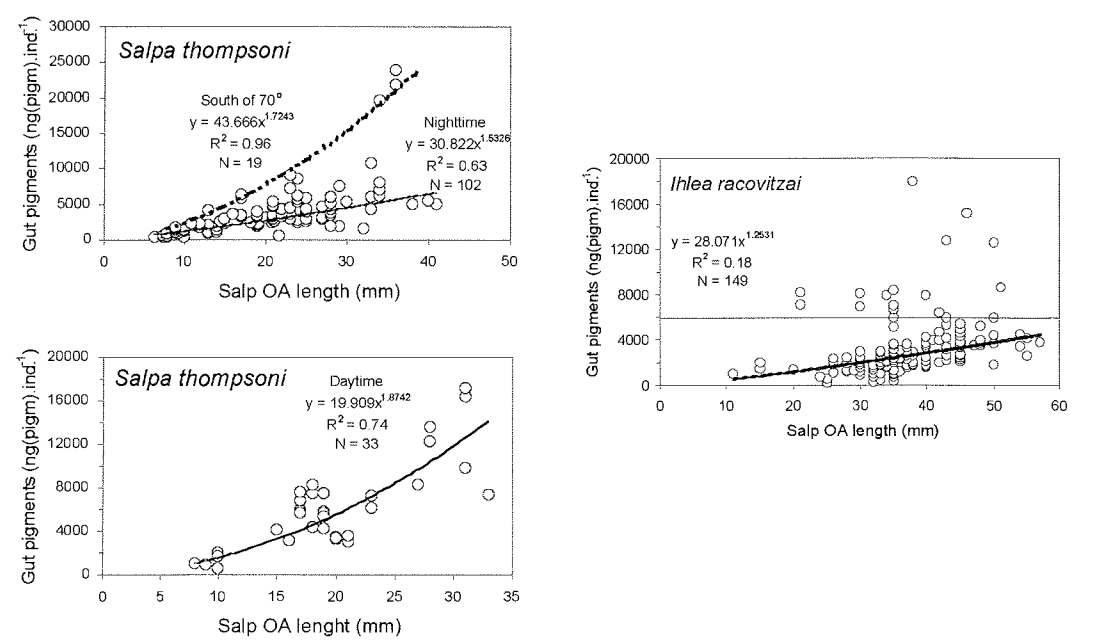


Figure 5.4. Gut pigment contents of *Salpa thompsoni* (left) and *Ileia racovitzai* (right) in the Lazarev Sea during April 2004.

The gut pigment values for *I. racovitzai* are reported for the first time. Similarly with *S. thompsoni*, pigment concentrations increased with the salp length. Also, the scattered, highest gut pigment values (values above dashed line on the right panel of Fig. 5.4) were obtained for specimens collected at stations with chlorophyll-a concentrations exceeding 0.4 mg.m⁻³ (Fig. 5.4).

Concluding remarks. Overall, populations of both salp species were not numerous in the area of investigation compared to summer values. For comparison, during December 1994 and January 1995 only *S. thompsoni* densities in the Lazarev Sea were as high as 100-1000 ind.1000 m⁻³.

Interestingly, the *S. thompsoni* population was more numerous than the population of *I. racovitzai*, despite the latter is considered to be a cold, coastal water species. There were distinct differences in the population structure of *S. thompsoni* sampled in waters influenced by the Weddell Gyre and Coastal Current water masses. The appearance of relatively numerous, younger, developing and actively feeding *S. thompsoni* grouping in the south most stations came as a surprise. The only plausible explanation for this phenomenon is that the Costal Current is responsible for advection of this grouping from the southeast region. It is likely that this grouping has been advected into the area recently, judging by the absence of solitary specimens and lower than to the north percentage of disrupted embryos. We do not know the fate of this grouping and perhaps detailed post-cruise analysis of oceanographic data will provide an explanation for the presence of *S. thompsoni* population in such extreme conditions. Finally, several hundreds salps have been frozen for elemental and biochemical analyses, which may also help in the interpretation of the salp behavior in the Lazarev Sea and their ability to cope with the cold waters during austral autumn.

Additional activities. In total, 26 macrozooplankton samples were collected along the Greenwich Meridian between 69°20' and 61°S. Samples were preserved in 4-6% formaldehyde seawater solution for the subsequent laboratory analyses to investigate seasonal and inter-annual variability in the macroplankton composition of the Lazarev Sea.

In addition, several hundreds specimens of lantern fish, mostly *Electrona antarctica*, were preserved across the survey for future stomach content analyses to understand their importance as zooplankton and Antarctic krill predators.

6. DISTRIBUTION OF SURFACE ZOOPLANKTON AND MIKRONEKTON AS POTENTIAL PREY FOR ANTARCTIC TOP PREDATORS – A SUIT EXPERIENCE

H. Flores, J.A. van Franeker, A. Meijboom, M.van Dorssen (ALTERRA)

Introduction

The Antarctic seasonal sea-ice zone provides a favourable habitat for the majority of Antarctic marine lifeforms. High primary production is a common feature not only at hydrographic frontal zones, but also at the ice edge. In summer, the retreating ice enhances primary production by releasing nutrients from the melting ice and stabilizing the surface layer through low salinity water (Arrigo et al. 1998). Considerable numbers of higher level predators - birds, seals and whales - are found throughout the seasonal sea-ice zone. They rely on the plankton and nekton available in the area, among which

Antarctic krill (*Euphausia superba*) is the most prominent organism. The pelagic community of the seasonal sea-ice zone has been described as a krill-dominated system (Smith & Schnack-Schiel 1990). However, in the diet of several abundant seabird species and some seals, krill occurs in a much lower proportion than previously estimated. Looking at the year-round provision of these animals, krill often turned out to be of only seasonal importance. Fish and squid seem to play an important role in the energy budget of Antarctic warm blooded predators. Jelly-type prey such as salps, ctenophores, doliodids etc. may also be important when they occur in high densities, but are hard to detect in diet investigations. On several cruises into the sea-ice zone, the food demand of higher level predators based on their abundances and species composition turned out to persist towards the inner pack-ice. These findings pose questions to the traditional assumption that productivity and, as a consequence, density of higher level predators are highest in the area close to the ice edge. Apparently, the role of the ice-covered habitat in the energy budget of the Southern Ocean needs to be investigated in more detail. The structure and capacity of the sea-ice system are not yet clearly understood. Larger scale investigations in and under the ice so far have been scarce due to the inaccessibility of this habitat. Major exchange with the pelagic community can occur through grazing at the water-ice boundary, or by feeding on algae and animals released during the melting process (Hempel 1991). Krill sometimes significantly relies on grazing on ice algae. Until now it is unknown to which extent fish or squid take advantage of the ice-associated community, which in turn can serve as prey for top level predators. Many bird species in the seasonal sea-ice zone rely on prey they find in the upper few meters of the water column (Ainley & DeMaster 1990). In order to understand feeding and food distribution of these abundant higher level predators, extensive sampling of surface layer plankton and nekton seems to be necessary, both in open water and under sea-ice. At Alterra, this interest led to the development of SUIT (Surface and Under Ice Trawl), a net which allows surface layer fishing both in open water and in ice. During ANT XXI/4, the net was operated for the first time. We hope that results from this cruise and future SUIT-based investigations will help to get a better understanding of the food web in the Antarctic seasonal sea-ice zone, especially in the ice-ladden areas.

Materials and Methods

Trawling of SUIT was performed during ANT XXI/4 on 24 stations on the regular CCAMLR grid between April 4 and April 25, 2004. The net system consists of a 2.25m x 2.25m steel frame with a commercial shrimp net attached to it (7mm half mesh). Large floaters at the top of the frame keep the net at the surface. To avoid sampling the mixed surface layer behind the ship's propeller, a special shearboard allows the net to shear to the side of the ship at an angle of ca. 30°. Wheels on top of the frame allow the net to 'roll' along the underside of icefloes during ice-fishing. Inside the shrimp net, a circular plankton net (diam. 50cm, 0.3mm mesh) was mounted to sample smaller sized zooplankton. A flashlight was attached to the frame in order to reduce escaping of animals by shock-blinding them. Fishing was done at nighttime, when most plankton species as well as

some pelagic fish species are known to approach the surface. Standard hauls lasted between 25 and 30 minutes at a towing speed of 3-4 knots in open water and 1.5-2.5 knots in ice. At 5 Stations, SUIT was operated during daylight to allow establishment of working procedures and visual surveillance of its behaviour in open water and ice. Catch data from these stations were excluded from the current analysis. Once on board, catches of the plankton and shrimp net were treated separately. Total water displacement volume of both samples was measured immediately after retrieval. The catch from the shrimp net was put on sorting trays and separated on species level in most cases. Only in samples >2 liter, subsamples were taken with the help of a plankton splitter. Volume and number of each fraction of the catch was noted. Afterwards, samples were quantitatively stored at -30°C. The plankton net sample was divided in 2 to 8 subsamples, depending on the size of the sample. At least 1 subsample was frozen at -30°C. Standard procedure with the second subsample included collection of krill and other zooplankton above the size of large copepods, their identification and count. It was then preserved in formaline (4% in seawater) to ensure proper identification of more and smaller species in the home laboratory. If more subsamples were taken, these were preserved in formaline or ethanol (70%). Total volume of the plankton catch and each fraction of it were expressed as ml per m² sea surface towed to allow comparability among stations. Relative catch composition was expressed as percentage of numbers per haul. In a parallel effort of our group, abundance counts of birds, seals and whales were conducted during daylight hours. After proper analysis, results of the predator counts will later be compared with the surface distribution of their potential prey.

Results

Among the 24 Stations covered in the area of investigation, 8 were completed in sea ice. Among these, data from 4 stations were excluded from analysis because they were done in daylight conditions, or heavy ice in the net indicated reduced catchability. In open water, 3 stations were excluded because of daylight operation or technical problems. On an overall view, the study area was broadly covered, distances between stations not exceeding 2 degrees of latitude. For the convenience of this report, data from both nets were combined. Total catches ranged over more than an order of magnitude. They reached from <0.1 ml·m⁻² in the sea ice to an exceptional haul of > 4.5 ml·m⁻² in the northeastern part of the study area (Figure 6.1). The composition of catches at each station is shown in Figure 6.2. In General, catch composition at the ice-free stations was considerably diverse. Apart from krill, the hyperiid *Cyllopus lucasi* was caught in considerable numbers at almost all stations. Siphonophores, most frequently *Diphyes antarctica*, occurred in abundance at some stations, as well as the pteropod *Clio pyramidata* and alciopid polychaetes. Single fish (*Electrona antarctica*) were caught at 4 stations in the open water. Fish larvae occurred scarcely, but regularly. A change in species composition was apparent from north to south. *Euphausia frigida* was caught only in the stations of the extended CCAMLR grid north of 64°S, as well as salps and tomopterid polychaetes.

Between 64°S and 66°S, diversity was low, krill and *C. lucasi* combined accounting for more than 90% by numbers of individuals. Towards the ice edge, species numbers increased again, and furciliae of krill and *Thysanoessa macrura* appeared in the catches. The composition of catches exhibited a pronounced difference between stations in ice and stations in open water. In the ice-free ocean, juvenile and adult krill dominated the catches by 95% in terms of biovolume at most stations. Single hauls yielded also significant volumes of coelenterates. In the small volumes obtained in the ice-covered areas, furcilia larvae of krill and *T. macrura* represented the major part of the catches, both in volume and numbers. The proportion of krill gradually increased towards north, with a mixed catch composition of furciliae and juvenile krill in the northernmost ice station, which included larger areas of open water in the trawl line. Only a single fish was caught under the ice. An item to be mentioned is the catch of an arm of an octopoid with a length of 20cm.

Discussion

On this expedition, a new gear was tested designed to sample the surface layer of the Antarctic Ocean, both in open water and under ice. As a matter of course, the interpretation of data obtained with a new method has some constraints. To our knowledge, no other similar methods have been applied in this region to allow direct comparison. Thus, little can be said about selectivity and catchability of the net. However, looking at the catch composition and the amount of biomass caught, SUIT seemed to be able to catch surface plankton in equal amount and diversity as other well standardized methods, such as the standard Rectangular Midwater Trawl (RMT). The eventually high amounts of krill indicate that SUIT was well able to catch fast swimming *E. superba*. Because of the above outlined constraints to our new gear, it is not clear if the low number of fish caught reflects low abundances in the upper 2m of the water column, or is due to their ability to actively avoid or escape the net. As a consequence, we note that biovolumes and numbers of individuals presented in this report were standardized to the m^2 towed to make catches comparable among each other, but actual densities *in situ* might be different depending on the species. In ice, trawling speed was significantly lower than in open water, which might have influenced the ability of SUIT to catch mobile organisms. Speed under ice however was comparable to that of the standard RMT in the deeper water layers. Incorporation of ice particles may negatively bias the catches by blocking parts of the entrance area of the net, or disrupting the catch. Highest amounts of biomass were obtained in the northern part of the area of investigation. This region is influenced by water masses originating from the Weddell Gyre. High abundances of krill were in line with the results of the RMT catches (see report in this volume). The incidental catch of $4.5 \text{ ml} \cdot \text{m}^{-2}$ indicates that a patch of dense krill aggregation was hit, which is a common feature in krill distribution. However, it should be noted that this high density patch occurred at the station closest to the bordering hydrographic region of the Maud Rise sea mount which is presumably much richer in marine life. The lowest catches were obtained in the ice-covered areas. Most of the ice was relatively young, its age ranging in the order of hours to days.

In this young sea-ice, the development of a rich biocenose had just begun. The numbers of furcilia larvae caught in these areas indicate that some primary production was already in place which they could feed on. During daytime monitoring, low numbers of birds, seals and whales were recorded in the ice. This suggests that the biologically 'young' community in the ice was not yet attractive for warm blooded predators. There seemed to be three different surface plankton communities which were distributed latitudinally throughout the open water area. A similar three-fold zonation was described by the multinet group on this cruise (see report in this volume). It is likely that the observed zonation reflects the distribution of different water masses, which were (from north to south) Weddell Gyre, boundary water and Antarctic coastal water. Our investigations concentrated on the surface layer as a major foraging area for top level predators. We could show that considerable amounts of krill and other zooplankton appear close to the surface during nighttime. This autumn, prey apparently concentrated in the northern part of the Lazarev Sea. Krill by far dominated all other prey types. However, many top predators depend at least partly on other prey than krill, such as fish and squid. These prey types may not be easily caught in a relatively small research net, but their densities are likely to follow zooplankton abundance (Hempel 1991). Incidental catches of myctophids and squid indicated that these prey types at least occasionally occur at the sea surface. A limited number of stomach samples from Antarctic Petrels showed a highly diverse and opportunistic diet, including krill, large crustaceans, squid, fish and jellyfish. The young sea-ice we encountered during the expedition apparently could not support large stocks of higher level predators. It is hypothesized that when the winter season progresses, the sea-ice will biologically 'mature' with continued growth of ice-algae gradually attracting higher food-levels, up to that of the top predators and their favoured types of prey. The next step in the seasonal SO-GLOBEC studies in the Lazarev Sea, planned for mid-winter 2006 will shed further light on such processes.

Literature cited

- AINLEY DG, DEMASTER DP (1990) The upper trophic levels in polar marine ecosystems. In: Smith I, Walker O (eds) *Polar oceanography*. Academic Press: 599
- ARRIGO KR et al. (1998) Primary production in Southern Ocean waters. *J Geophys Res* 103 No. C8: 15587-15600
- HEMPEL G (1991) Life in the Antarctic sea ice zone. *Polar Record* 27 (162): 249-254
- SMITH SL, SCHNACK-SCHIEL SB (1990) Polar zooplankton. In: Smith I, Walker O (eds) *Polar oceanography*. Academic Press: 527-598

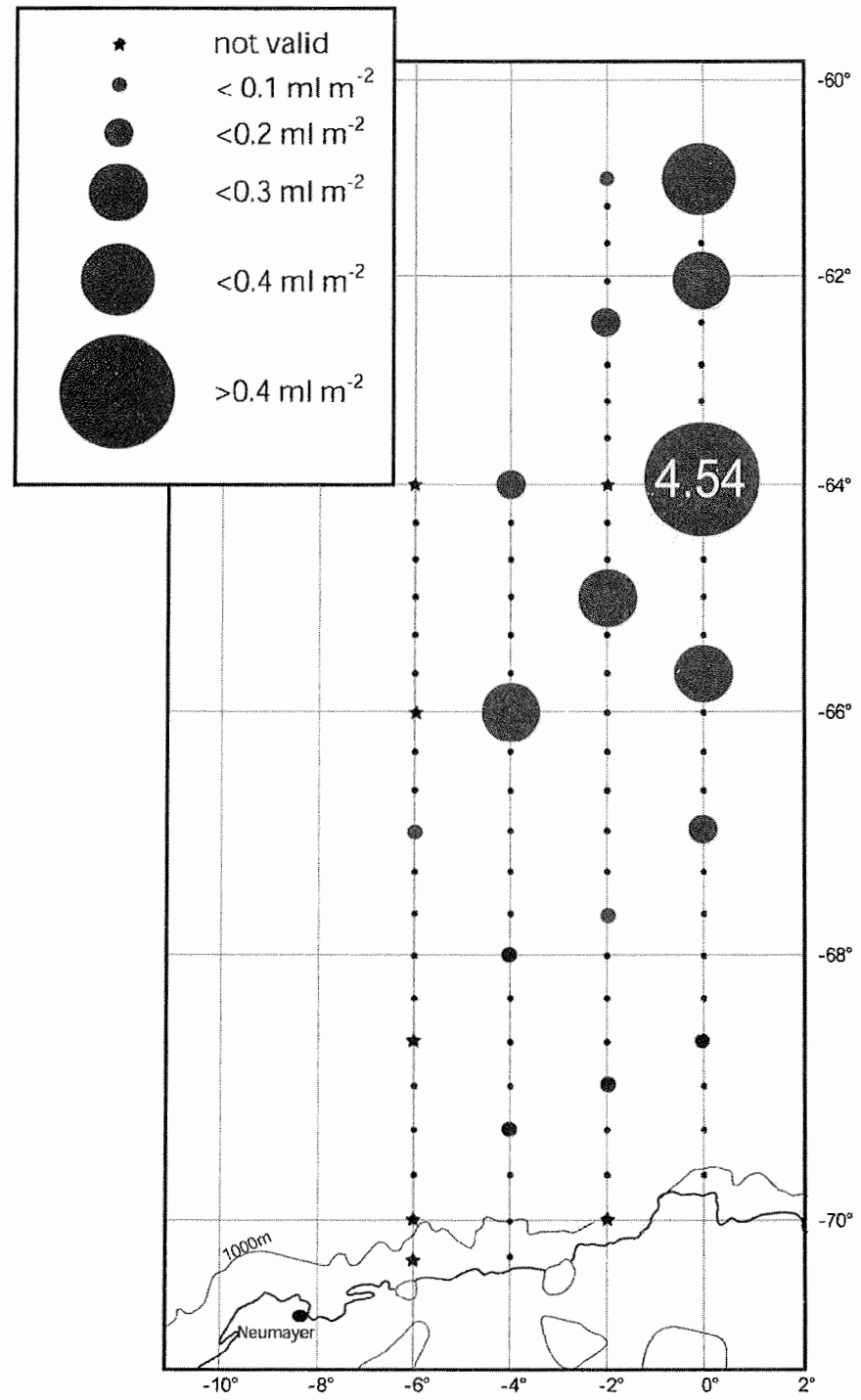


Figure 6.1. Total biovolumes caught at SUIT stations, indicated in ml m^{-2} towed seasurface

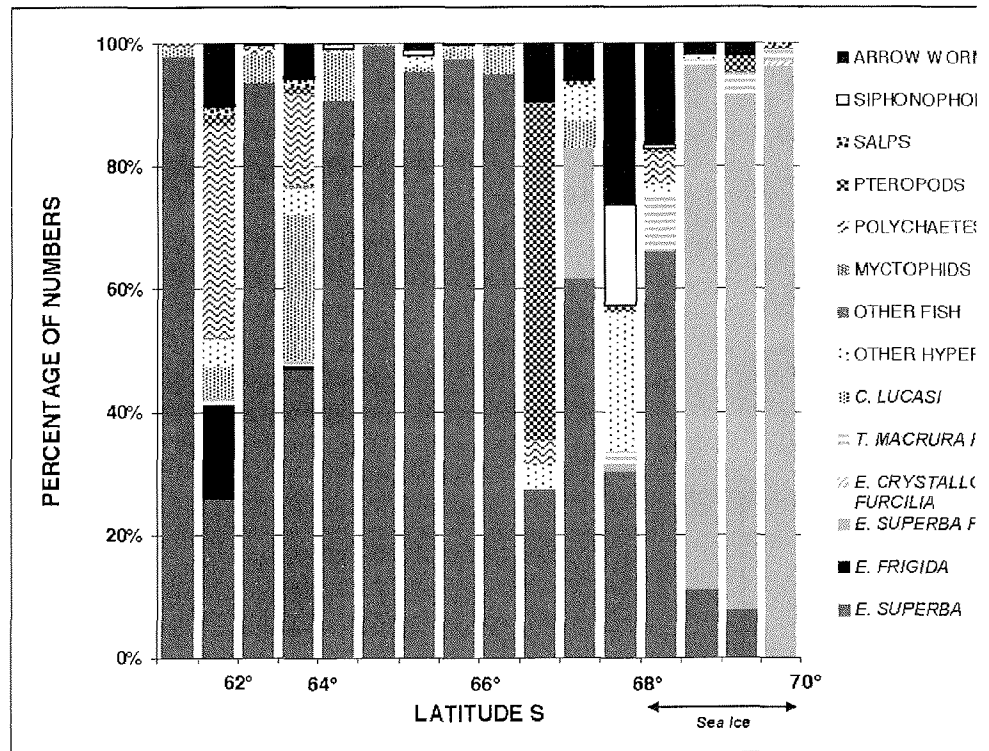


Figure 6.2. Composition of SUIT catches in latitudinal order. Each Column represents one station

7. SPATIAL PATTERNS IN FOOD REQUIREMENTS OF MARINE BIRDS AND MAMMALS IN THE LAZAREV SEA, APRIL 2004 (POLARSTERN ANT-XXI-4, SO-GLOBEC).

J. A. van Franeker, H. Flores, A. Meijboom, M. van Dorssen (ALTERRA)

INTRODUCTION

The ALTERRA project on Antarctic top predators and their prey aims to enhance knowledge on Southern Ocean foodwebs, in particular those related to the seasonal sea ice zone. Top predator abundances suggest that biological production in sea ice is a major driving force behind animal population sizes and biodiversity in the Antarctic ecosystem. The interdisciplinary approach and seasonal spread in Polarstern's SO-GLOBEC cruises offers an excellent framework to enhance the knowledge of marine Antarctic foodwebs.

Within the broad field of investigations in the ANT-XXI-4 autumn study in the Lazarev Sea, Alterra used a top down approach focusing on the upper levels in the foodweb.

For the first time, quantitative studies of distributions of top predators were directly combined with sampling prey in the upper surface layer of the ocean, whether in open water or under ice. For this purpose a new type of net was developed, the Surface and Under-Ice Trawl (SUIT). The net was successfully deployed in sampling the upper 2.5 meter of surface water (Flores *et al.*, this volume). This report gives an initial view on the results of the study of the distribution of top predators. As a first step towards comparison to other food-web levels, data are presented in spatial patterns of food requirements of the top predator community. Data analysis in relation to catches of the SUIT net and other studies on board will be conducted in a later phase. A dense grid of fishing with Rectangular Midwater Trawl (RMT) was completed in the framework of krill stock monitoring for CCAMLR (Siegel *et al.*, this volume). Prey abundance in subsurface layers was also monitored by use of SIMRAD echosounder and details were obtained by various types of vertical net hauls. All datasets will be linked in a later phase of data processing.

METHODS

Ship-based censuses of birds and mammals were made from an outdoor observation post installed on top of the bridge of Polarstern. The outdoor position allows unobstructed clear view to all sides, which amongst other is crucial to identify ship-associated birds that have to be omitted from density calculations.

Bird censuses use band-transect methodology based on the snapshot method which avoids density bias by bird movement (Tasker *et al.* 1984). Birds are counted from the moving ship, in a band transect during time blocks of ten minutes. Ship speed and transect width can be used to convert observed numbers of animals to densities per unit of surface area for each ten-minute period. The standard width of the transect band is 300m, taken as 150m to each side of the ship. Depending on viewing conditions such as seastate, light level and glare, the transect may be limited to one side of the ship and transect width may be adapted to a distance that maximizes detection of all individuals of different species.

Ice-seal censuses are based on the same band records as used for bird observations. Band-transect counts are considered adequate for seal censuses (Laws 1980), but the Antarctic Pack Ice Seal Program (APIS) more recently recommends line-transect methods where possible (SCAR Group of Specialists on Seals 1994). Therefore, for ship-based seal counts in ice areas, line transect data (Hiby and Hammond 1989) are collected in addition to band transect observations. For the time being however, data analysis uses only the band transect data. In the analyses observed seal numbers were corrected for diurnal patterns in haul-out behaviour.

Whale censuses are based on whale observations during the bird and seal counts, irrespective of distance. Since the focus of the observer is on the narrow band transect, chances for detection of whales at greater distances are reduced. Data records include angle and distance of first spotting, following line-transect methods. However, our current data analysis for whales is based on simple estimated 'effective detection ranges'. The limited number of observations does not yet allow calculation of more detailed detection curves.

During ANT XXI-4, a two person observer team of dedicated whale observers using line-transect methods operated from the inside bridge, and once processed, such data may assist in calibrating the 'effective whale detection ranges' to be used in association with the bird and seal censuses.

Analysis. Top predator density data may be used to calculate daily prey requirements. Calculations are based on published literature of field metabolic rates and energy contents of prey as described in Van Franeker *et al.* (1997). In addition to the quantitative counts, qualitative information was collected on the occurrence of species outside transect bands or during oceanographical stations. Such data are not used for density estimates. Environmental data are derived from the ship sensor system and visual observations (e.g. ice conditions).

Analyses in this paper are based on averages of all 10 minute counts conducted in between subsequent stations. Stations were spaced at each 20 minutes of latitude. At each station the Rectangular Midwater Trawl (RMT) was deployed for CCAMLR krill monitoring (Siegel *et al.*, this volume). Evidently, during hours of darkness no top predator censuses were possible, explaining the interrupted pattern of data points in figures 1 and 2. Due to intensive work on the SUIT net, predator counts at the start of the first transect (northern part along 6°W) are incomplete. For this report, only data collected south of 61°S are considered, that is those occurring in or very near the extended ANT-XXI-4 study grid.

Diet study

At an opportunity basis, stomach samples were obtained from individuals that accidentally landed on or collided with the ship. Birds were measured, weighed and stomach contents were collected by stomach flushing after which they were immediately released. Eight Antarctic Petrels were found dead, and these were collected and stored frozen. Some regurgitates were collected from deck.

RESULTS AND DISCUSSION

Within the study area, 323 ten-minute standard counts were completed, totalling to 255 km² of band-transect area surveyed.

Sea ice extended to about 68°S during our studies, and more or less followed the -1.4°C isotherm for sea-surface water temperatures as shown in figures 6.1 and 6.2. North of the ice, water temperatures did not steadily increase. Sea surface temperatures show an intrusion of cooler water in the northeastern part of the grid, probably related to currents generated by the seamount Maud Rise situated just northeast of our area of investigation.

Average densities of top predators were low (2.99 birds, 0.16 seals 0.003 whales per km²). Due to low abundance of penguins in the ice-covered zone, marine mammals dominate the spatial pattern of top predator food requirements, as seen in a comparison of Fig. 7.1 and Fig 7.2. Distributional patterns of all species were extremely patchy. The southern part of the study grid had an over 90% cover of very recently formed sea ice. This area was almost desert-like in terms of top predators, with only the odd Emperor Penguin and Snow Petrel around. Such an appearance is uncommon in sea ice. Somewhat older sea-ice is often characterized by higher numbers of penguins, petrels and mammals (van Franeker *et al.* 1997), but these conditions were hardly present

under the autumn conditions in our study grid. In the more northern part of the ice, near the ice-edge, we did encounter patchy concentrations of ice-seals (Crabeater and Leopard) and some Minke Whale and Adélie Penguins were observed.

The open waters just north of the ice were very poor in top predators. Only further north, birds like Snow- and Antarctic Petrels and Chinstrap Penguins became more numerous. Bird densities and encounters with whales increased towards the 64°S northern boundary, and seemed to peak in the extended grid sections between 64°S and 61°S. Remarkably, high numbers of Snow Petrels were seen in fully open water far north of the sea-ice, usually their preferred habitat. This indicates poor prey-availability in the young sea-ice. The relatively high predator densities in the more northern parts of the grid could well be related to enrichment of surface waters related to currents initiated by Maud Rise to the northeast.

An initial comparison of top predator distributions with catches from SUIT (Flores *et al.*, this volume) and RMT nets (Siegel *et al.*, this volume) suggests spatial similarity for enriched communities in the open water to the north, especially the northeast.

The RMT catches suggest some elevated zooplankton prey abundance north of the ice edge. This is not directly matched by top predators, unless it is assumed that seals resting on ice near the ice-edge, might move the relatively short distance to open water to feed. However, Crabeater Seals were only once observed north of the ice edge.

Within the sea-ice, catches by both RMT and SUIT nets were generally low, as were the densities of top predators. In the spatial pattern of fishing stations, there was no possibility for dedicated fishing effort around the isolated patches of higher top predator abundance. Low abundance of both predators and prey in the sea-ice during this autumn grid in the Lazarev Sea is explained from the fact that almost all of the sea-ice had formed only very recently, and lacked biological development attracting larger and higher level organisms. Our hypothesis is that when the season progresses, under-ice prey species and their predators will become increasingly abundant. The SO-GLOBEC winter cruise (2006) in the Lazarev Sea may shed further light on this, but eventually we aim to conduct similar work over the full annual cycle and in different regions.

Diet samples from stomach flushings, birds found dead and regurgitates virtually all originated from Antarctic Petrels, the dominant bird species in the open water zones of the grid. Samples will be analyzed later, but contents were clearly more variable than catches of either SUIT or RMT nets, and included not only krill, but also squid, fish and jellyfish type prey.

References cited

- Hiby A.R. and Hammond P.S. 1989. Survey techniques for estimating cetaceans. In: Donovan G.P.(ed). The comprehensive assessment of whale stocks: the early years. Rep.Int.Whal.Comn (Special Issue II). Cambridge. pp 47-80.
- Laws, R.M. (ed) 1980. Estimation of population sizes of seals. BIOMASS Handbook No. 2: 21 pp. SCAR, Cambridge.

SCAR Group of Specialists on Seals 1994. Antarctic Pack Ice Seals: indicators of environmental change and contributors to carbon flux. APIS Program, draft implementation plan, Aug. 1994. SCAR Group of Specialists on Seals, Seattle. 7 pp.

Tasker M.L., Hope Jones P, Dixon T, and Blake B.F. 1984. Counting seabirds at sea from ships: a review of methods employed and a suggestion fro a standardized approach. *Auk* 101:567-577.

Van Franeker, J.A., Bathmann, U.V., & Mathot, S. 1997. Carbon fluxes to Antarctic top predators. *Deep Sea Research II* 44(1/2): 435-455.

Food requirements birds (penguins and flying birds) in kg/km²

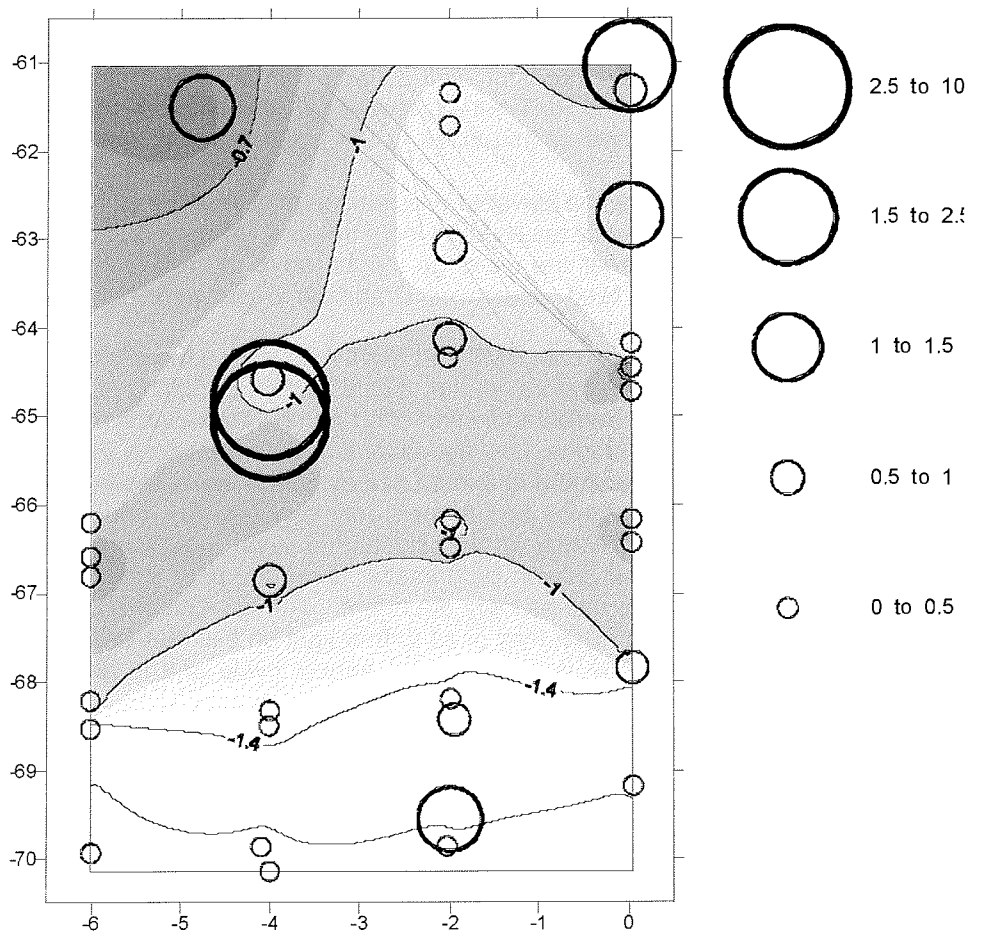


Figure 7.1
Average food requirements of marine birds in the ANT-XXI-4 study grid, April 2004. Averages were calculated for sections between stations (each 20 minutes of latitude). Interrupted pattern of datapoints caused by lack of observations during darkness. Note non-linear scale in symbol size for food requirements and different scaling in Figure 7.2. Shading shows surface water temperatures (SST) as measured at keel sensor. Ice-edge roughly followed the -1.4°C isotherm in SST.

Food requirements top predators (birds and mammals) in kg/kr

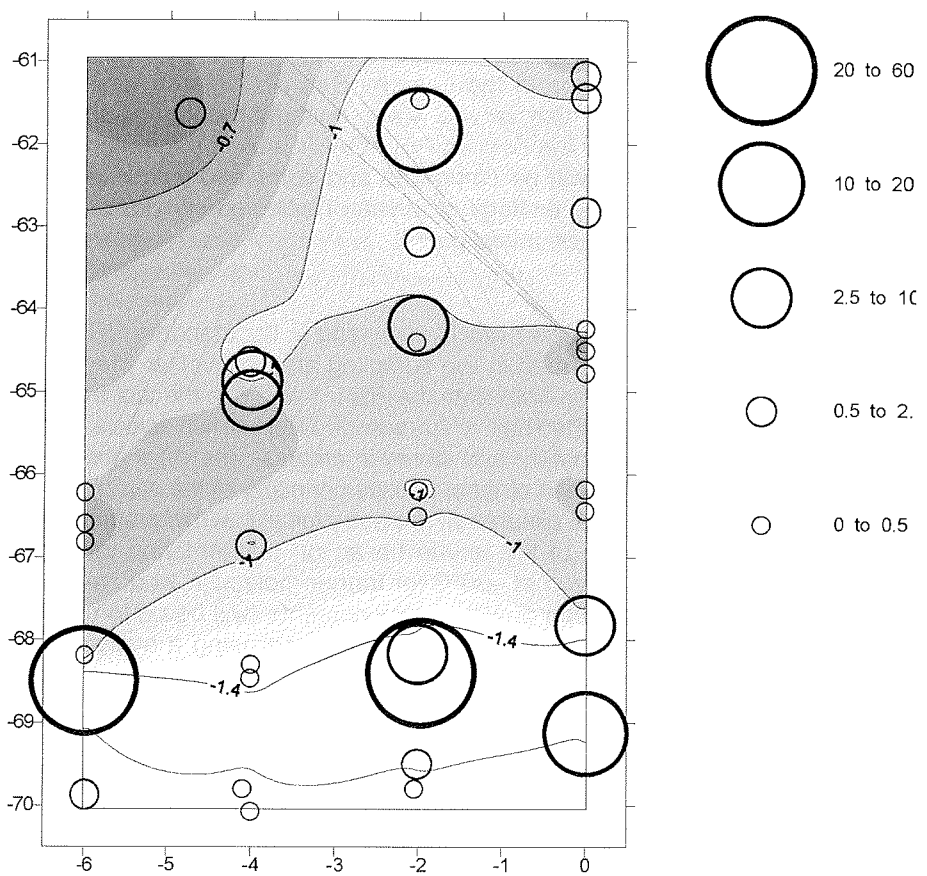


Figure 7.2.
Average food requirements of the toppredator community (birds, seals and whales) in the ANT-XXI-4 study grid, April 2004. Further explanation as in caption of Fig.7.1.

8. SAMPLING OF LARVAL AND JUVENILE FISH IN THE LAZAREV SEA FOR MOLECULAR IDENTIFICATION – OBSERVED AUTUMNAL DISTRIBUTION PATTERNS

A. Van de Putte (LAE)

Introduction

During of the GLOBEC 2 cruise in the Lazarev Sea (27th March to 6th May 2004), samples of fish and fish larvae were collected onboard the RV Polarstern. In the framework of the Belgian PELAGANT project the morphologic identification of these larvae will be compared and combined with molecular identification methods. Feeding ecology of larvae of selected species such as *Pleuragramma antarcticum* will be investigated.

Material and methods

Samples were taken using RMT 8+1 trawls according to the standard CCAMLR protocol for krill surveys (performed in the sampling area by Volker Siegel). In transect 1-3 samples were taken from both the RMT 1 and 8 in the last transect (4) samples were taken from the RMT 1. Larvae of different fish species were photographed using a digital camera and stored in ethanol (analytical grade) for molecular identification. Storage in ethanol causes shrinking of the samples and the loss of pigmentation. Digital pictures of the samples will allow quantification of shrinking and identification of the larvae based on pigmentation patterns. Some of the samples were frozen at -30°C for further molecular work, analysis of the otolithes and determination of fish energy contents (will be performed by Hauke Flores). Finally, part of the samples were stored using a buffered 4% formalin solution for further stomach content analysis.

Results

A total of 1338 fish were caught along the four transects in the sampling area. Catches had an average size of 19,144, with slightly higher catch numbers during night trawls and in the coastal zone (Figure 8.1).

Most specimens could be identified to the species level, but where this was not possible, identification was completed to family level (Figure 8.2). 7,55% of specimens remained unidentified, due to the fact that the appropriate keys were not available. These specimens were either small larval stages that were too small to be identified with the larval keys, or small juveniles that were too developed to be identified using the larval keys and not enough to use the adult keys.

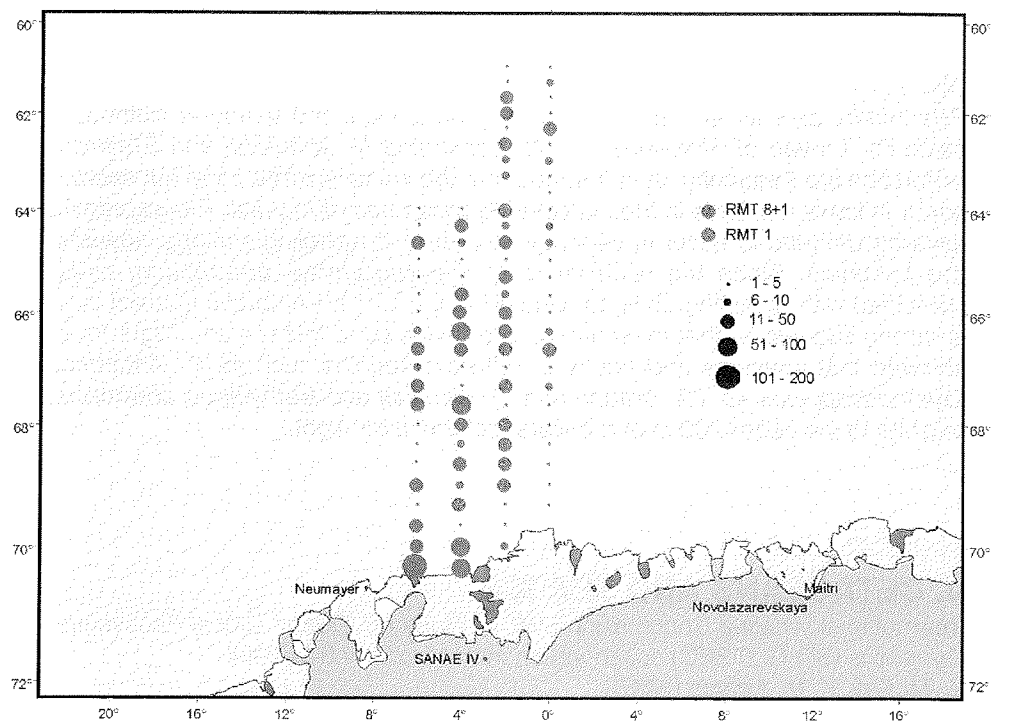


Figure 8.1. Samples collected in the Lazarev Sea

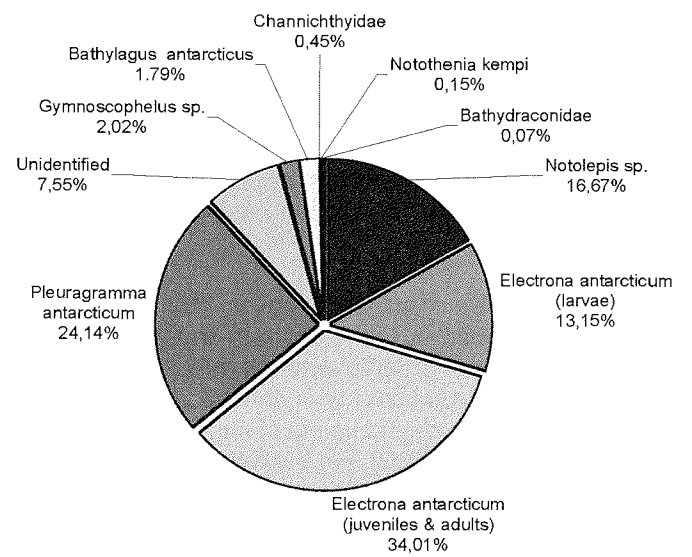


Figure 8.2. Species composition of total samples collected in the Lazarev Sea

Discussion

Preliminary data already showed some geographical and temporal distribution patterns. Larvae of *Notolepis* sp. (*N. coasti* and *N. annulata*) and *Electrona antarctica* are frequently caught throughout the whole ice free zone but seem to occur in lower numbers in the ice-covered areas near the coast. *Pleuragramma antarcticum* tend to occur in very high numbers in sampling stations closest to the continent. Since the occurrence of *Pleuragramma antarcticum* larvae coincided with sampling stations situated in the Circum-Antarctic Current there is strong suggestion that these larvae are restricted to this current. Night trawls showed that juveniles and adults of different species such as *E. Antarctica*, *Gymnophelus* sp. (*G. braueri* and *G. nicolsai*) and *BathyLAGUS antarcticus*, migrate to the upper 200 m of the water column over night.

9. CETACEANS AND SEA ICE

International Whaling Commission (IWC) – Southern Ocean Global Ecosystem Dynamics (SO GLOBEC) collaboration in the Lazarev Sea 2004
S. McKay, K. M. Asmus (IWC)

Introduction:

Until recently, few marine research cruises in the Southern Ocean have attempted to simultaneously collect data on both cetaceans and their prey with the objective of integrating these and other biological and physical data to investigate linkages at fine and large scales (pers. comm. D. Thiele). SO GLOBEC studies have provided the ideal platform for these long-term studies, where scientists from a range of disciplines can conduct intensive focussed studies, within the framework of international collaboration. Given the shared objectives among the IWC, GLOBEC and CCAMLR, the IWC has determined that the most effective means of investigating these ecological issues is to focus a considerable amount of cetacean research within the framework provided by these programs.

The main objective of the whale observation program is to 'define how spatial and temporal variability in the physical and biological environment influences cetacean species in order to determine those processes in the marine ecosystem which best predict long-term changes in cetacean distribution, abundance, stock structure, extent and timing of migrations and fitness' (from SOWER meeting, Edinburgh 2000). For the first time this season, extensive sea ice information will be recorded and analysis undertaken both on board and after the voyage to determine the patterns between sea ice and whale densities in Antarctic waters. Both of these objectives are being pursued aboard Polarstern through collaboration with GLOBEC and CCAMLR using the multidisciplinary ecosystem approach to data collection, analysis and modelling mentioned above. Involvement with the Polarstern voyage leg ANT XXI/4 this season focussing on the overwintering of Antarctic krill (*Euphausia superba*) in the

Lazarev Sea, has provided the opportunity to have whale observers on board, undertaking extensive data collection for the period of austral autumn and winter.

At this time of year a number of whale species migrating between the Antarctic continental feeding grounds and warmer breeding areas would be expected, especially humpback whales. A number of species would also be expected in the sea ice areas, including minke and killer whales.

Methods:

Visual survey for cetaceans was conducted aboard Polarstern using standard line transect protocols during daylight hours when weather conditions were appropriate (Beaufort sea state < 6). Sightings were recorded on a laptop-based program 'Logger', which also allowed recordings of seals, seabirds and sea ice concentrations. GPS position, ship course and speed were logged by the PODAS system, which was downloaded from the ship's database. Survey effort generally commenced after the morning meeting from inside the bridge wings and ceased at dark.

While steaming in ice, digital photos were collected every 5 minutes, always from the same point on the bridge for comparison. The sea ice concentrations and types within each photo were then classified out to 1 kilometer from the bow using the protocol outlined on the ASPeCt (Antarctic Sea ice Processes and Climate) CD.

Results:

On transit between Cape Town and the cruise survey area, only one whale sighting was made, but this was likely due to reduced effort due to weather and low sightability conditions. The survey area proved to be a different story with 16 sightings of 22 whales including humpback and minke whales, a single sperm whale and some unidentified species. Four sightings of 12 individual humpback whales were made on the 25th April in the extended survey leg north of the 4th transect. These whales were all travelling north, an indication of the ice cover extending and the whales starting on their northward migration.

One exceptional sighting occurred on the 27th April with four humpback whales choosing to spend over four hours with the vessel. A single blow was initially seen on the port side of the vessel at 11:00 UTC and was immediately recognised as a humpback whale. As it approached closer more blows were sighted and the group was identified as five individuals. There were also approximately 150 chinstrap penguins swimming around the vessel and as the whales approached closer to the vessel, they started chasing each other, possibly for play or seeking the same food source. At one point, the group of five whales split and two individuals swam around the bow to the starboard side while the other three remained on the port side. During this time, one of the whales from the port side disappeared out towards the horizon where another group of humpback whales was present. The remaining four then continued to surface around the vessel for the next four hours, blowing, snorting, pectoral fin slapping, spy-hopping and even breaching, giving everyone on board a spectacular show. It is possible that the whales were just as interested in us as we were in them.

Although the overall total of sightings during the voyage is not high at 26 sightings of 50 individuals, it is reasonable for this area at this time of year and the patchiness expected in whale distribution (Figure 9.1). The total distance travelled during the voyage until the end of data collection was 5921nm which provided an encounter rate of 0.0084 whales per nm or 1 whale every 118nm. Due to the amount of time spent at stations, time has to be taken into consideration as well as distance travelled. The total time spent on survey (both full effort and casual observations) was 272 hours, providing a figure of 0.184 whales per hour or 1 whale every 5.44 hours. Of course these figures are very general and further analysis is required to examine the effects of effort and the total sightings.

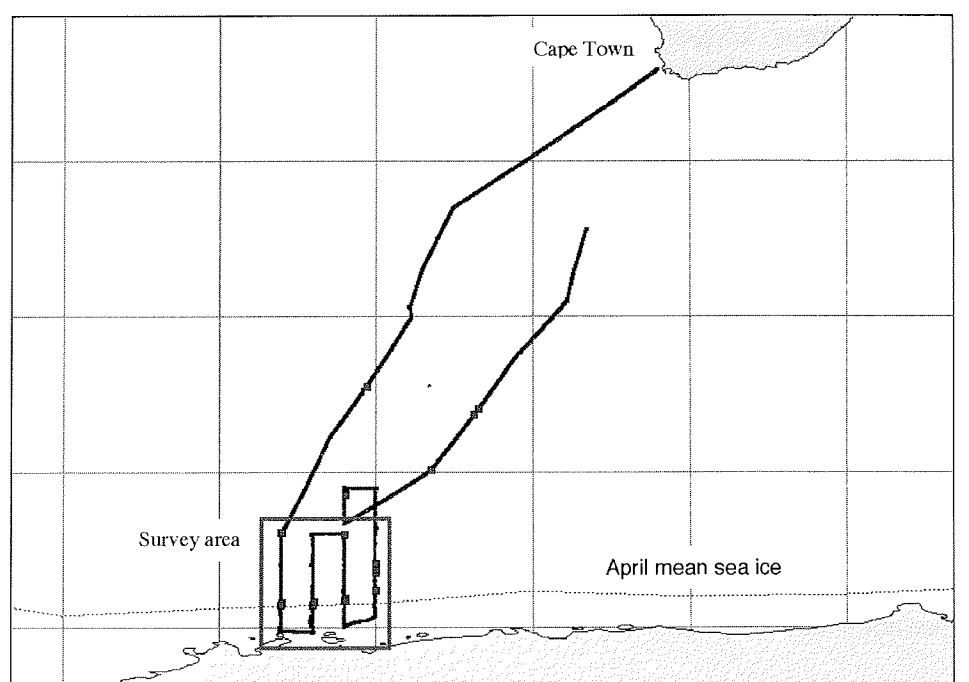


Figure 9.1. Map of transit and survey area with all cetacean sightings and April mean sea ice extent. Note apparent correlation with sightings and sea ice.

The majority of the sea ice encountered was first year ice in the form of cakes and small and medium floes, and brash and frazil. Both singular and cemented pancake ice were also quite common closer to the ice margin. Some multiyear floes in the form of growlers, icebergs and floes were sighted quite frequently but these made up a small percentage of the overall ice cover. More extensive analysis of the data will be conducted on return from the voyage to start making linkages between the sea ice extent and whale distribution.

Thank you to our fellow scientists and crew aboard Polarstern, who did an exceptional job in looking after us in every aspect of daily life, especially Captain Uwe Pahl and the bridge crew for providing us with a great working environment.

10. MAX-DOAS MESSUNG ATMOSPHÄRISCHER

SPURENGASE

U. Platt, T. Wagner, B. v. Harling

Während aller fünf Etappen der diesjährigen Expedition ANTARKTIS XXI werden Messungen atmosphärischer Spurengase mittels der Differentiellen Optischen Absorptions-Spektroskopie (DOAS) durchgeführt. Diese bewährte Methode benutzt das von den Spurengasen gestreute Sonnenlicht, um diese anhand ihrer charakteristischen Absorptionslinien zu identifizieren und ihre Konzentration zu bestimmen. Da einige Spurengase wie BrO, HCHO und SO₂ im UV-Bereich absorbieren, andere wie H₂O und IO im sichtbaren Bereich und wieder andere wie O₃, O₄, OCLO und NO₂ in beiden Bereichen, werden zwei Spektrographen verwendet. Das Streulicht wird mittels vierer Teleskope gesammelt, die an Deck in einem Rahmen frei schwingend angebracht sind, um die Bewegungen des Schiffs auszugleichen. Drei der Teleskope sind über Glasfaserkabel mit dem UV-Spektrographen verbunden, das vierte mit dem im sichtbaren Bereich arbeitenden Spektrographen. Die Spektren im UV-Bereich werden mittels einer CCD mit 1024*256 Pixeln aufgenommen, die im sichtbaren Bereich mit einer eindimensionalen CCD mit 2048 Pixeln. Die so gewonnenen Daten werden auf CD gebrannt und später in Heidelberg ausgewertet. Aus den Absorptionsspektren kann dort die Konzentration einzelner Spurengase berechnet werden. Da die Teleskope unter verschiedenen Elevationswinkeln messen, kann darüber hinaus auch auf die vertikale Verteilung geschlossen werden. Dies ist die sogenannte Multi-Axis-DOAS (MAX-DOAS).

Bis auf eine Unterbrechung von einigen Tagen, verursacht durch einen defekten Computer, wurden tagsüber kontinuierlich Spektren aufgenommen. In der Nacht lief ein Kalibrierungsprogramm, während dessen sowohl Eigenschaften der CCDs vermessen, als auch Spektren einer Hg-Ne-Lampe und einer Halogen-Lampe aufgenommen wurden. Die gesamte Messung läuft weitgehend automatisch, gesteuert durch eine spezielle Software. Obwohl die Daten einen brauchbaren Eindruck machen, kann eine endgültige Aussage darüber erst in Heidelberg gemacht werden. Die erhaltenen Ergebnisse können insbesondere dazu verwendet werden, Messungen des SCIAMACHY-Instruments an Bord des Satelliten ENVISAT zu validieren. Dieser befindet sich seit März 2002 in einem polaren Orbit, so dass Messungen an Bord der Polarstern auf den Expeditionen in die Antarktis dazu besonders geeignet sind.

11. BENTHIC FLUXES AROUND THE ANTARCTIC POLAR FRONT DURING THE AUSTRAL FALL SEASON

E. Sauter, O. Sachs, J. Wegner, L. Baumann, M. Gensheimer (AWI)

Introduction

Early diagenetic processes in surface sediments are closely linked to the sedimentation of particulate organic matter (POM) onto the seafloor. Remineralization and burial of organic carbon (C_{org}) determines the geochemical milieu and, thus, both affects the conditions of benthic life as well as the long-term fixation of carbon exported from surface waters. Therefore, the quantification of C_{org} fluxes is of major interest for benthic ecology, early diagenetic modeling and geochemical budgets, which, in turn, are an important aspect of a quantitative understanding of the carbon cycle at present and in the past. The sensitivity of the earth's polar regions in this respect has been recognized since many years. Although, the sediments of polar seas are hitherto rarely included in organic carbon flux budgets. For example, the global estimate of sedimentary C_{org} fluxes by Jahnke (1996) is limited to 60° latitude.

Most of the organic carbon arriving at meso and oligotrophic sediments is remineralized right below the sediment/water interface, consuming dissolved oxygen as a primary electron acceptor. In addition, oxygen functions as a final oxidant for anaerobic pathways. Thus, the measurement of pore-water oxygen microprofiles provides a suitable tool for the determination of C_{org} fluxes through the sediment/water interface and of C_{org} remineralization rates.

Beside the quantification of oxic respiration by *in situ* chamber or laboratory core incubation, O_2 microelectrodes have proven to be an appropriate tool to determine diffusive oxygen fluxes via the measurement of the pore water O_2 depth distribution in high resolution. According to Glud et al. (1994) and Sauter et al. (2001) it is highly desirable to measure these O_2 microprofiles *in situ*, i.e. at the sea floor, in order to avoid sampling and pressure artifacts during core retrieval.

Only little data, mostly measured *ex situ*, exist for high latitudes beyond 60° N or S, such as the areas near Svalbard (Hulth et al., 1994), the Greenland and Norwegian Seas (Sauter et al., 2001), the Arctic Ocean (Boetius and Damm, 1998), the Southern Ocean (Rabouille et al., 1998) and the Weddell Sea (Schlüter et al., 2001). Nevertheless, *in situ* O_2 data coverage is poor for the polar regions. Regarding the deep southern South Atlantic, there exist, to our knowledge, no *in situ* measured flux data at all. Especially due to the great water depths laboratory flux measurements on retrieved sediment cores generally lead to overestimation of flux values. Therefore little is known both about the total amount of organic carbon remineralized and fixed within surface sediments of the Southern Ocean.

Beside open questions in early diagenesis, there is a lack of knowledge about the sediment's reaction on seasonal and episodical food supply from above. Therefore emphasis was put on the investigation of seasonal signals at the end of the period of surface production.

During the previous cruise of Polarstern – the European Iron Fertilization

Experiment (EIFEX) – scientists fertilized a 10 km² wide patch in the center of an ocean eddy with iron and stimulated a considerable phytoplankton bloom composed mainly of diatoms. During this experiment biomass as well as bacterial and zooplankton productivity also increased (Cruise reports ANT XXI/3 and publications arising there from). At the end of EIFEX, some diatom species sank out of the productive surface layer to water depths close to the sea floor. Two weeks later, on the transfer from Cape Town to the GLOBEC area, the EIFEX region was re-visited in order to perform additional water sampling and to investigate the effect of the bloom on the benthic environment. The latter was not covered during the previous cruise.

Beside the association to the EIFEX experiment, one of the main geochemical tasks during ANT XXI/4 was to learn, to what degree this input of fresh organic carbon changed the geochemical milieu within the surface sediment. The Polar Front is in this respect of special interest, since the hydrographic and topographic settings found in the water column along the meandering front and at the seafloor, respectively, lead to a relatively high primary production compared to the otherwise poor Southern Ocean. Accordingly, a band of high chlorophyll concentration was observed by space born sensors along the Polar Front. Suggested by those satellite images, the EIFEX eddy still existed and kept its geographical position in the otherwise eastward flowing ACC. Nevertheless, the plankton bloom had disappeared in the meantime and the chlorophyll concentration decreased from 3 to about 0.5 µg L⁻¹.

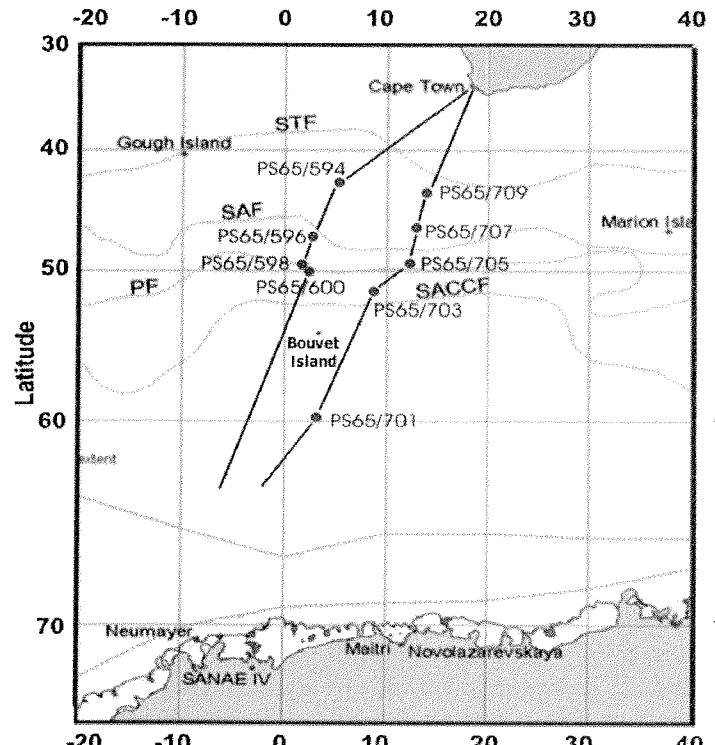


Fig. 11.1: Map of the GEO stations.
Depicted front systems are not determined during this cruise.

In order to assess and to compare the particularities of the Polar Front stations, additional locations, situated within the Sub Antarctic Zone, the Polar Frontal Zone, and south of the PF at the EIFEX reference station and in the Weddell Gyre have been investigated (Fig. GEO-11.1 and Tab.GEO-11.1).

Tab. GEO-11.1: Station List

Station	Date	Time	Latitude	Longitude	Depth, [m]	Gear	Region
PS65/594-1	30.03.04	13:49	42° 59,99' S	5° 00,08' E	4732,9	LANDER	SAZ
PS65/594-3	30.03.04	15:58	42° 59,91' S	4° 59,06' E	4908,5	MUC	
PS65/594-4	30.03.04	19:17	42° 59,61' S	4° 59,22' E	4747,1	BWS	
PS65/596-1	01.04.04	07:52	47° 0,39' S	2° 59,92' E	4317,3	BWS	PZ
PS65/596-2	01.04.04	10:46	47° 0,61' S	2° 59,93' E	4331,9	MUC	
PS65/598-1	02.04.04	08:30	49° 18,50' S	2° 11,68' E	3941,6	LANDER	PF,
PS65/598-2	02.04.04	10:25	49° 20,94' S	2° 11,94' E	3966,0	CTD/RO	ex EIFEX
PS65/598-3	02.04.04	12:41	49° 22,37' S	2° 10,85' E	3986,4	MUC*	
PS65/598-5	02.04.04	18:08	49° 19,74' S	2° 10,37' E	3961,2	MUC	
PS65/600-1	03.04.04	00:28	49° 59,88' S	2° 20,22' E	3588,8	LANDER	PF,
PS65/600-2	03.04.04	01:53	50° 0,20' S	2° 19,63' E	3564,4	MUC	EIFEX, ref.
PS65/600-3	03.04.04	04:36	50° 0,31' S	2° 18,99' E	3555,6	BWS	
PS65/701-1	27.04.04	08:19	59° 59,04' S	3° 30,26' E	5368,1	LANDER	WG
PS65/701-2	27.04.04	09:55	59° 59,27' S	3° 32,96' E	5341,0	MUC	
PS65/701-3	27.04.04	13:21	59° 59,11' S	3° 32,66' E	5399,4	BWS	
PS65/703-1	29.04.04	06:15	52° 35,12' S	9° 00,19' E	~3330	LANDER	
PS65/703-2	29.04.04	07:42	52° 34,86' S	8° 59,58' E	3314,0	MUC	PF
PS65/703-3	29.04.04	10:09	52° 35,34' S	9° 00,64' E	3337,5	CTD/RO	
PS65/705-1	30.04.04	10:55	49° 0,06' S	12° 15,32' E	4293,0	LANDER	PF
PS65/705-2	30.04.04	12:32	49° 0,82' S	12° 15,06' E	4317,0	MUC	
PS65/705-4	30.04.04	15:33	49° 0,97' S	12° 14,82' E	4326,0	CTD/RO	
PS65/705-5	30.04.04	20:23	49° 0,40' S	12° 17,13' E	4311,0	MUC	
PS65/707-1	01.05.04	10:08	47° 10,86' S	12° 41,70' E	4874,9	MUC*	PZ
PS65/709-1	02.05.04	11:22	44° 20,17' S	13° 31,48' E	4742,0	MUC*	SAZ
PS65/709-2	02.05.04	14:35	44° 20,17' S	13° 32,37' E	4638,1	CTD/RO	

Gear: LANDER = Free falling micro profiler; MUC = multiple corer; BWS = bottom water sampler; *) failure; Regions: SAZ = Sub Antarctic Zone, PZ = Polar Zone, PF = Polar Front, WG = Weddell Gyre

Instruments used

Using an UNISENSE™ *in situ* micro profiler built into a free falling lander (Fig. GEO-11.2) pore water oxygen concentrations were measured in a vertical resolution of 0.5 mm. This allows exact calculation of diffusive oxygen fluxes through the water-sediment interface, from which organic carbon fluxes to the seafloor can be derived. Fluxes quantified by microprofiles can be considered to be the basic O₂ turnover within an oxic sediment, mainly caused by micro fauna. Besides oxygen micro sensors the profiler was equipped with a special probe to measure the electrical resistivity of sediment and bottom water. From this parameter the sediment porosity can be derived in high vertical resolution.

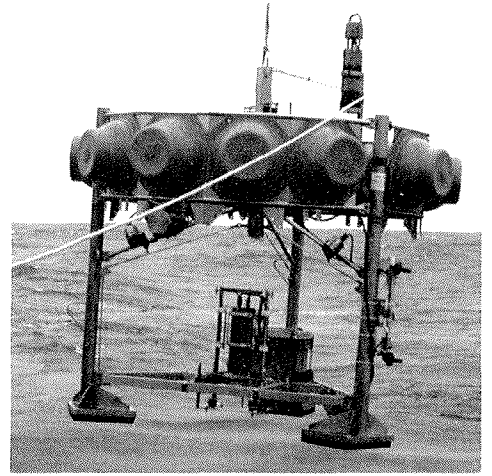


Fig. GEO-11.2: Benthic lander equipped with a deep-sea micro profiler for *in situ* flux measurements.

In addition, sediment samples were taken by a multiple corer (MUC). The cores were segmented into slices which were squeezed out to obtain pore water by means of a N₂-operated pore water squeezer. Pore water was used for nutrient analysis whereas porosity, C/N and bacteriological parameters will be determined subsequently from the sediment samples.

For each of the GEO stations it was foreseen to deploy the *in situ* micro profiler and, while the device is measuring autonomously, to deploy the multicorer and the bottom water sampler. As an option CTD casts were planned at the Polar Front stations.

The fact that there exist no *in situ* measurements of benthic diffusive fluxes in this region already reflects the potential difficulties to work there. Especially, rough weather conditions during the austral fall season make it difficult to closely follow sedimentation events in the deep Southern Ocean. Therefore we consider the five successful lander stations as a good yield. In addition, drop stones from melting icebergs make sediments in some areas difficult to penetrate by the hydraulically dampened MUC. Beside the rough sea, this is the reason for the gear's failure at some of the stations.

Nevertheless it was indeed possible to find freshly deposited material on some of the cores. In contrast to the sediment, in the water column molecular diffusion plays a minor role compared to other mixing processes. Solute concentrations are – to a first approximation – often taken to be constant in the near-bottom water column. Although, bottom water gradients of dissolved and particulate matter can be found to be even steep, depending on sediment activity and bottom water flow conditions.

For the purpose of coupling sedimentary biogeochemistry to the complex processes of the near-bottom water column, a special bottom water sampler was deployed at some of the stations (as time and weather permitted). The device allows a quick sampling of 6 variable heights over ground within the 2 meters above the seafloor. The device basically consists of 6 water collectors (similar to nisking bottles) which are mounted horizontally one above another on a vertically turnable pipe. A large current flag turns the bottles into luv-lee direction. A ground releaser activates a burn wire mechanism which closes the bottles several minutes after ground setting. The time delay ensures that the resuspension cloud is flushed away before the collectors are closed. Bottom water gradients are, of course strongly dependent on the flow regime in the near bottom zone. Therefore the lander was equipped with an acoustic current meter.

Preliminary results

The sediments in the Sub Antarctic Front and in the Polar Frontal Zone were found to be deeply oxygenated. Bioturbation tracks from Polychaeta and Malacostraca were observed in up to 22 cm sediment depth (Fig. GEO-11.3). From laboratory micro sensor measurements oxygen can be estimated to reach down to several decimeters (at 10 centimeter sediment depth the pore water concentration is still about $100 \mu\text{mol L}^{-1}$). The relatively steep surface gradient (Fig. GEO-11.4) most likely is caused by decompression phenomena during core retrieval and leads to overestimation of fluxes. However, it can be corrected by means of an empirical relation established from the relationship between laboratory and *in situ* measurements performed at the same location (Sauter et al., 2001).

At the Polar Front (Stations PS65/598 and 600), *in situ* microprofiles have been obtained from the lander deployment which revealed the pore water oxygen gradient to be steeper at the surface than suggested by the entire graph (e.g. fitted by an e-function). We ascribe this finding to the freshly settled fluff layer on top of the sediment (Fig. GEO-11.5) which enhances oxygen consumption due to increased bacterial activity. The non-harmonic shape of the O_2 profile indicates that the geochemical milieu is not in steady state but is still reacting on the fresh C_{org} supply from above. The *in situ* fluxes determined within the surface layer are several times higher than the basic diffusive flux from a fit to the entire profile. Herewith we were able to discriminate seasonal / episodical fluxes from basic turnover even for sediments in water depths around 4000 meters.

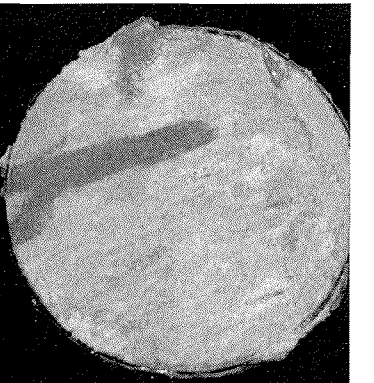


Fig. GEO-11.3: Dark brown horizon in a burrow in 22 cm sediment depth in a off core from Station PS65/594-3 (tube: 10 cm Ø).

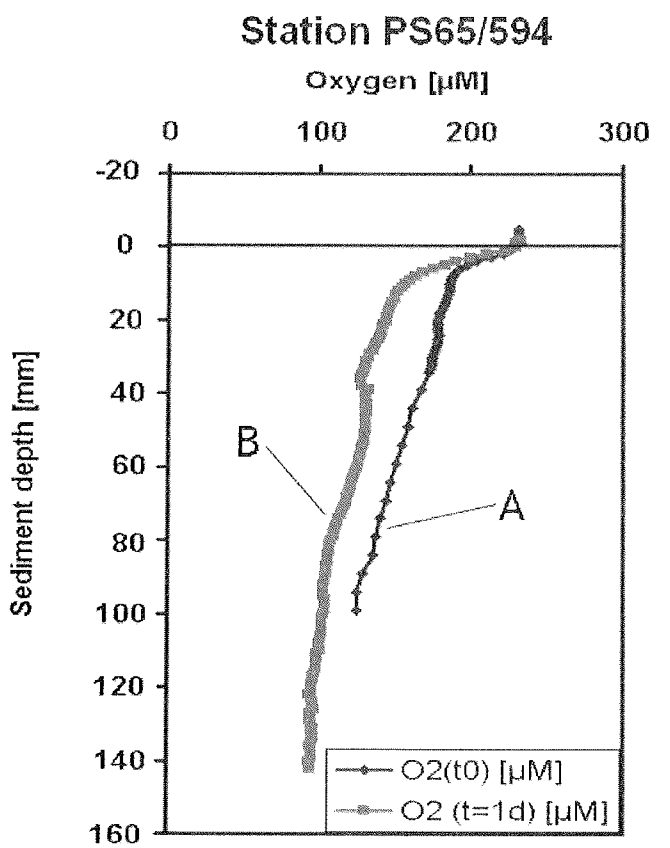


Fig. GEO-11.4: Oxygen microprofiles from the Sub Antarctic Zone. Profile A was measured immediately after core retrieval, profile B after 1 day.

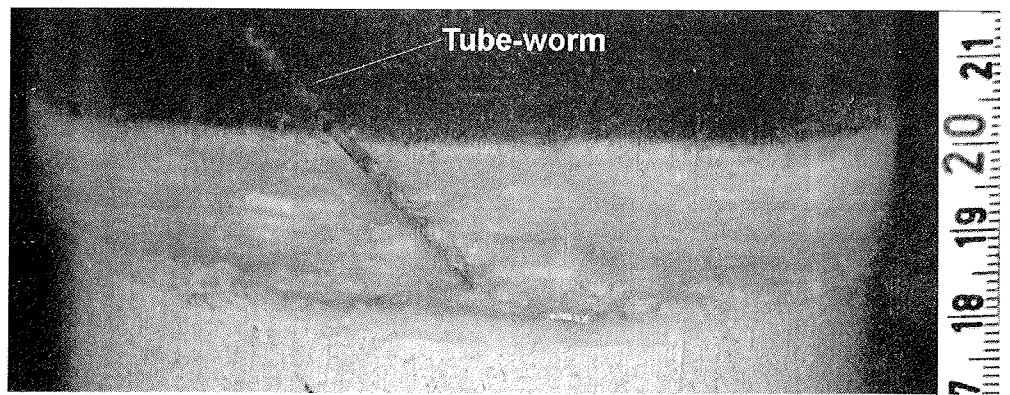


Fig. GEO-11.5: Sediment core retrieved from Station PS65/600 covered with freshly deposited fluff (thickness: ~5 mm). Photograph by U. Marx

Tab. GEO-11.2: Preliminary sediment description of the MUC samples

Cruise/Site	Sediment depth (cm)	Structure	Description
PS65/594-3	0-10	bioturbated	Foraminiferous mud, brown, homogenous, fora (0,1-0,2 mm), tube-worms, vertical tubes (2 mm long). The surface is covered with foraminiferal fecal pellets.
	10-24	bioturbated	Foraminiferous mud, light brown, homogenous, vertical tubes (2-3 mm Ø), 20-22 cm: horizontal brown (oxygenated) burrows (1cm Ø).
PS65/596-2	0-13	bioturbated	Foraminiferous mud, brown to grayish, homogeneous amounts of spherical (0,1-0,2 mm) and some dark spirally foraminifera, vertical and horizontal (~5 mm Ø).
	13-16	bioturbated	Foraminiferous mud, light brown, homogenous, fora (0,1-0,2 mm).
PS65/600-2	0-16	bioturbated	Diatomaceous mud, light brown to grayish, homogeneous small light gray and white spherical or fluffy components consist of needle-shaped diatoms (aggregates), radiolarians, spherical (0,1-0,2 mm) and some dark convoluted foraminifera, calcareous smooth (2-6 mm long) tube-worms, spheroidal segments worms (2-4mm Ø, 25 mm long), rare serpulid tube and chitinous tube worms (~3 mm Ø, 12 mm long) drop stones (1-6 mm Ø). Surface covered with light fluff-layer (4-5 mm) consisting of diatoms, radiolaria and fecal pellets (?).
PS65/701-2	0-41	no fabric recognizable	Mud, brown to dark brown, small black concretions (0,1 mm Ø), rare radiolarians, 10-14 cm: vertical 6 mm Ø.
PS65/703-2	0-20	no fabric recognizable	Diatomaceous mud, light brown, smaller light gray spherical or fluffy components (diatoms, radiolaria) small tube-worm remains (same species compared to PS65/600-2), small echinoderm (Fig. GEO-6) at surface



Fig. GEO-11.6: Opt.

Tab. GEO-11.2 ff.: Preliminary sediment description of the MUC samples

Cruise/Site	Sediment depth (cm)	Structure	Description
PS65/705-2	0-13	cloudy and flaky fabric	Diatomaceous fluffy sediment, brown, inhomogeneous, unconsolidated, large (6-8 cm Ø) and small (a few mm Ø) components. Some smaller light gray spherical or layered components consist of diatoms and radiolarians.
	13-21	cloudy fabric	Rough fluff-sediment-interface, diatomaceous mud, brown to dark brown, inhomogeneous, more consolidated than the upper layer, light gray and white spherical or layered, marbled components, radiolarians.
	21-28	no fabric recognizable	Mud, gray, homogenous, light gray and white.

On the transect back to Cape Town there was the opportunity to sample sediments at the Polar Front another 4 weeks later in the year. Whereas on the way south investigations were performed exactly at the EIFEX spot, we now

worked east of the EIFEX location but in accordance to remote sensing chlorophyll data, in an area of particular high summer production, even exceeding the amount of biomass produced during EIFEX (PS65/705), and in a low production area south of the PF (PS65/703). Unfortunately, coring turned out to be very difficult at these locations. The only core retrieved was covered by a fluff layer of several centimeters thickness which must have been deposited some days or weeks before sampling. As measured with laboratory (*ex situ*) micro profiles, anoxic conditions are reached within the fluff layer while the sediment underneath is still oxygenated (Fig. GEO-11.7). Repeated measurements revealed that oxygen is rapidly consumed and almost completely depleted within the sediment surface after 1 day core incubation under *in situ* temperature.

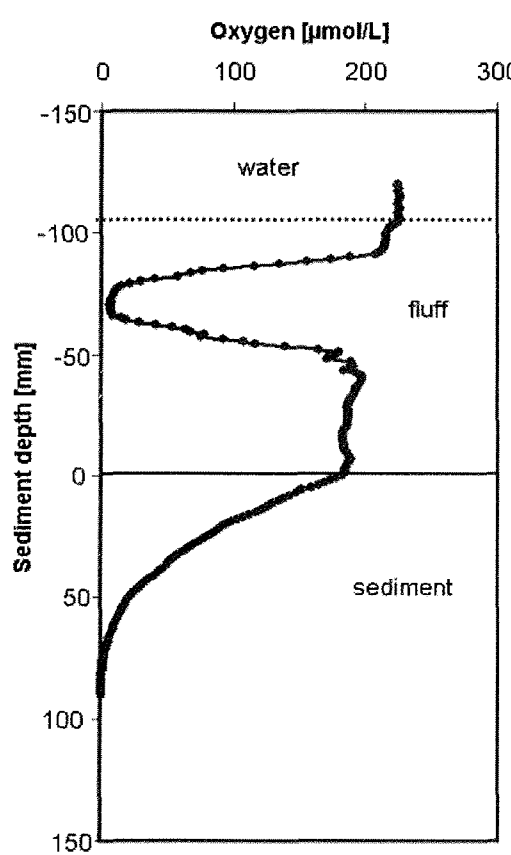


Fig. GEO-11.7: Oxygen micro profile measured at Station PS65/705-2 (*ex situ*). Oxygen within the thick fluff layer is partially depleted.

Conclusions

These findings show that episodical and seasonal C_{org} pulses even in remote deep-sea environments 1) can cause considerable short term changes in both the biogeochemical milieu and biological activity and 2) probably are the major contribution to the annual sedimentation. Quality and composition of the sedimented material has to be analyzed back home in order to assess the degradability of the material and to estimate the portion preserved in the sediment.

From our results it is also evident, that the Polar Front is of particular importance in terms of sedimentation in the otherwise poor Southern Ocean.

Since it is very difficult to meet time and location of such sedimentation events, field data are very rare. It therefore would be of great interest to continue this kind of research, especially in the different front systems of the ACC. On the other hand it is important to quantify benthic fluxes during other seasons and for other areas of the Southern Ocean in order to obtain basin-wide estimates for the basic turnover of organic matter.

At last, it shall be pointed out, that this investigation is considered to be of exceptional value since the investigations could be conducted at a site intensively investigated during the previous cruise leg ANT XXI/3 (EIFEX) which generated a broad data set at the same location. Herewith the entire succession of processes from the initial surface bloom to final sedimentation and benthic remineralization could be followed. We think, it would be of great benefit for the comprehension of interacting processes in the water column and at the sea floor, to further merge pelagic and benthic studies in the way performed here.

References

- Boetius, A., Damm, E. (1998). Benthic oxygen uptake, hydrolytic potentials and microbial biomass at the Arctic continental slope. *Deep-Sea Research I*, 45, 239-275.
- Glud, R.N., Gundersen, J.K., Jørgensen, B.B., Revsbech, N.P., Schulz, H.D. (1994). Diffusive and total oxygen uptake of deep-sea sediments in the eastern South Atlantic Ocean: in situ and laboratory measurements. *Deep-Sea Research I*, 41, 1767-1788.
- Hulth, S., Blackburn, T.H., Hall, P.O.J. (1994). Arctic sediments (Svalbard): consumption and microdistribution of oxygen. *Marine Chemistry*, 46, 293-316.
- Jahnke, R.A. (1996). The global ocean flux of particulate organic carbon: Areal distribution and magnitude. *Global Biochemical Cycles*, 10, 71-88.
- Rabouille, C., Gaillard, J.-F., Relexans, J.-C., Tréguer, P., Vincendeau, M.-A. (1998). Recycling of organic matter in Antarctic sediments: A transect through the polar front in the Southern Ocean (Indian sector). *Limnology and Oceanography*, 43, 420-432.
- Sauter, E.J., Schlüter, M., Suess, E. (2001). Organic carbon flux and remineralization in surface sediments from the northern North Atlantic derived from pore-water oxygen micropore profiles. *Deep Sea Research*, 48, 529-553.

12. ACOUSTIC SEAFLOOR INVESTIGATIONS WITH PARASOUND

J.Rogenhagen (FIELAX), E.Sauter, O.Sachs (AWI)

One of the fixed sensor installations onboard RV Polarstern is the sediment echosounder PARASOUND (Krupp Atlas Electronics, Bremen). The system provides digital, high resolution information on the sediment coverage and the internal structure of the sediments.

For this purpose the echosounder uses the so-called parametric effect: PARASOUND radiates two primary frequencies in the kilohertz range that generate a secondary pulse of lower frequency, which provides the signal. The secondary frequency can be chosen between 2.5 and 5.5 kHz and is adjusted by varying the variable primary frequency from 20.5-23.5 kHz while the next primary frequency is fixed to 18 kHz. Due to its low secondary frequency and a small emitting angle of 4 degrees, PARASOUND achieves high resolution of the sediment structures and penetrating depths of around 100 meters. Data recording is done by PC-based Software (Parastore3) that digitizes and processes the signal. Finally, data is stored on hard disks and transferred to CD-ROMs for further processing and visualization.

The secondary frequency of the sediment echosounder during the cruise has been 4 kHz with a recording length of mostly 665 ms and 266 ms (that corresponds to a depth range of 500 m and 200 m assuming sound velocity of water). The exceptional large recording length of 665 ms has been chosen to let the system run in a more or less remote mode, as there were no watch keepers available. During daytime, the recording window was adjusted to the topography on-the-fly, during night time the system recorded without adjustment. This lead to some loss of data, especially in regions with rough topography, e.g. Meteor Rise.

During our approach to the EIFEX region, some geochemical stations were carried out and accompanied with the PARASOUND system. Here, PARASOUND operated for about 90 hours and approx. 1.5 GByte of data were recorded, processed and stored on storage devices.

On the way back from the Krill Survey area in the Lazarev Sea to Cape Town several geochemical stations were performed and accompanied with PARASOUND measurements. To avoid disturbances of the in parallel operating SIMRAD Echosounder, the measurements were reduced to a minimum of one hour in advance and after the stations work.

In summary approx. 3 GByte of data were achieved. Due to the operational mode of the system during the cruise, the data is scattered along the route and therefore of reduced value to the scientific community.

The sediment echosounding of cruise ANT XXI/4 has been performed for the AWI marine geology working group (E.Sauter).

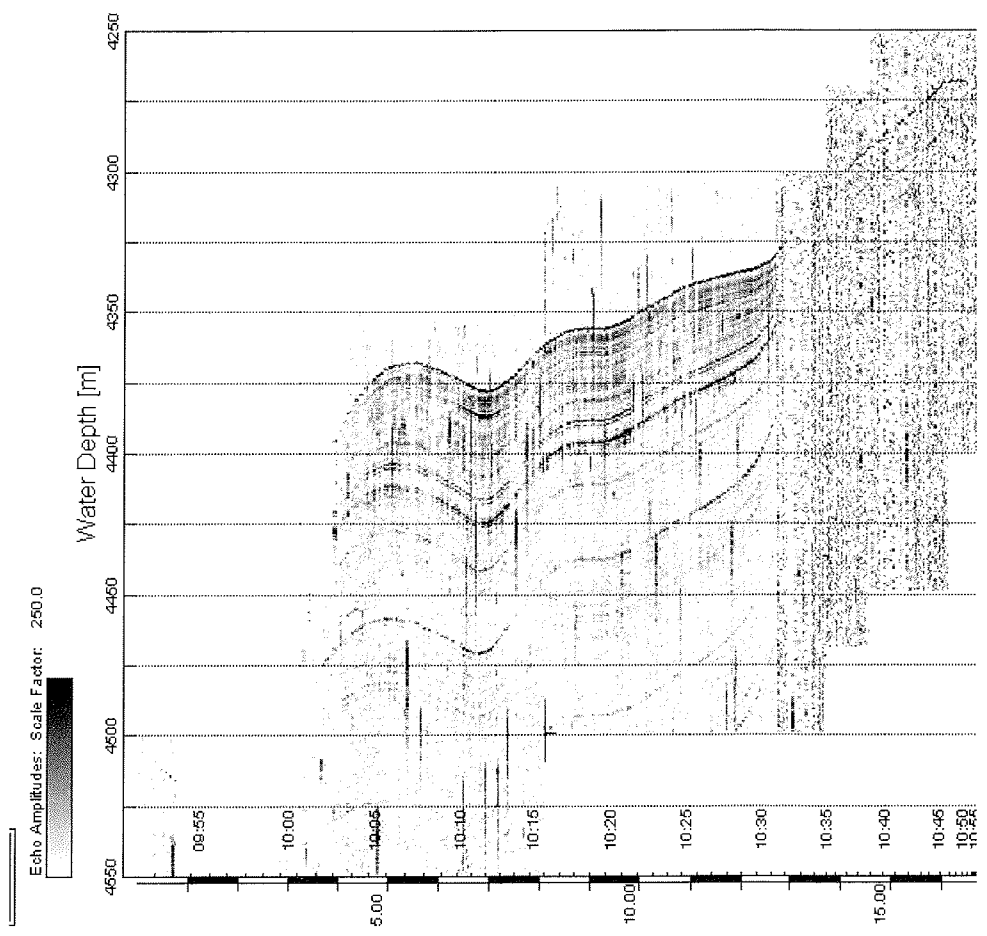


Fig. 12.1: Non-processed Parasound Profile while approaching Station PS65/705-2 along the polar front.

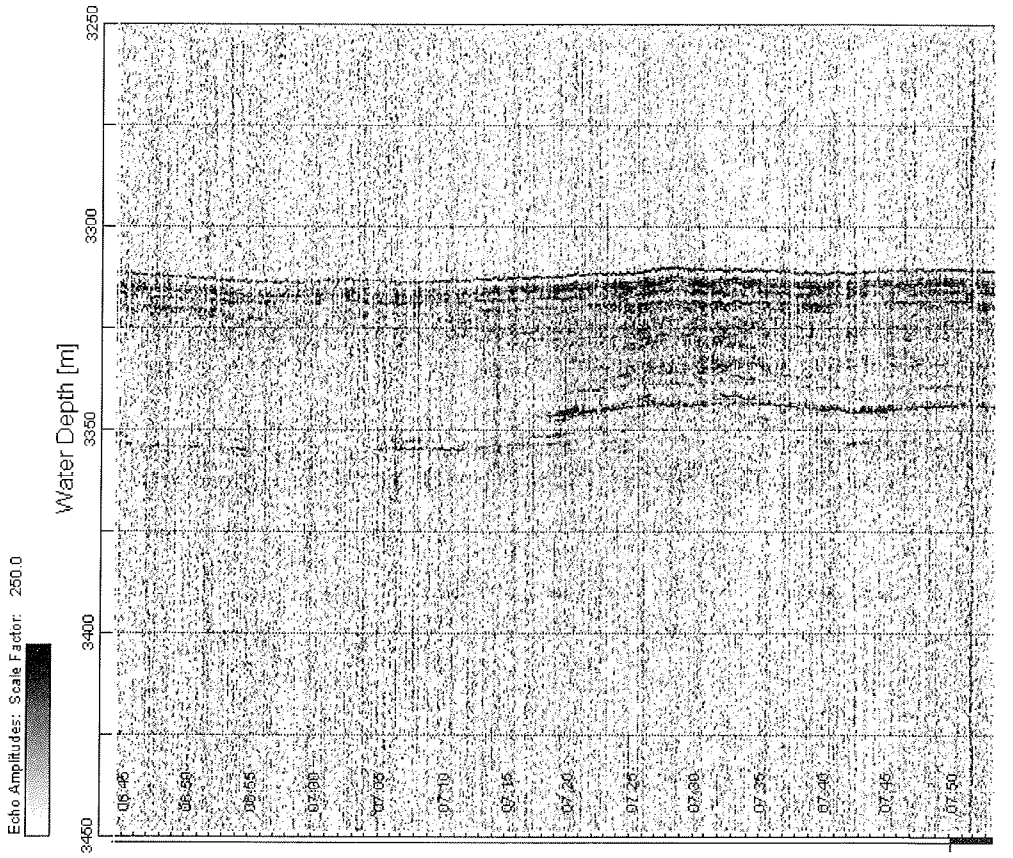


Fig. 12: Non-processed Parasound Profile while approaching Station PS65/703-2 in the Southern Antarctic Current (Southern Polar Front).

13. OXYGEN AND NUTRIENTS IN THE GLOBEC AREA

E. Sauter, L. Baumann, M. Gensheimer, U. Bathmann (AWI)

Water samples of 32 CTD stations on the 4 krill survey transects (Fig. 13.1) have been analyzed for the nutrients nitrate, nitrite, phosphate, and silicate as well as for dissolved oxygen. This contribution from the geochemistry to the Krill Survey was performed to support the hydrographic characterization of the different water masses found in the target area and to provide additional information on the environmental setting the surveyed organisms live in. For instance the depth distribution of nitrate and oxygen in the upper water column can help to explain migration phenomena and depth preferences of the zooplankton.

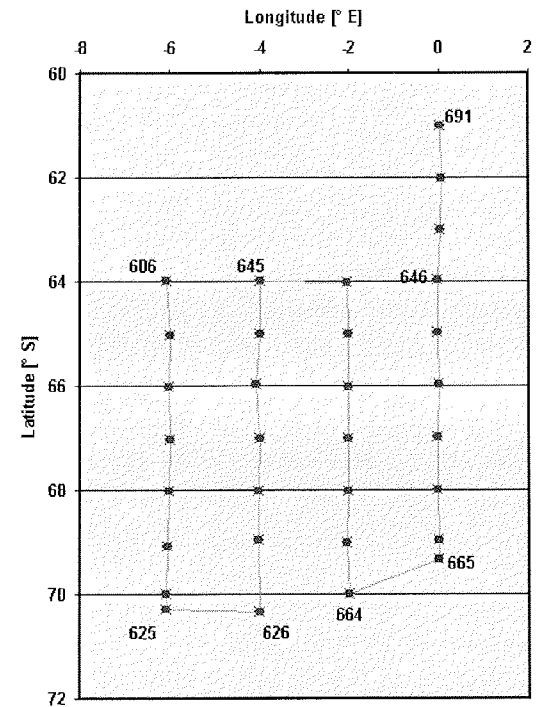


Fig. 13.1: Nutrient sampling positions in the Krill Survey area

Oxygen

The sea water oxygen concentration was determined by conventional Winkler titration (Grasshoff et al., 1983) using special glass flasks of ca. 60 ml volume. As expected, the oxygen concentration was found to decrease rapidly from saturation at the sea surface to the oxygenminimum depth between 200 and 500 m. Below, concentrations slightly increase towards the deep-sea to reach typical values of about 235-245 $\mu\text{mol/L}$. Most of the profiles are shaped like a question mark as exemplarily shown in Fig. 13.2. Compared to the deep Greenland Sea, where deep water renewal causes bottom water oxygen concentrations to be $>300 \mu\text{mol/L}$, an influence of freshly ventilated deep-water could not be observed in this area. As an exception of these findings the profiles taken at the southern most stations, in vicinity of the shelf ice edge, revealed oxygen to remain hight throughout the entire water column, reflecting the descending of surface water super-cooled at the front of the shelf ice edge (Fig. 13.3).

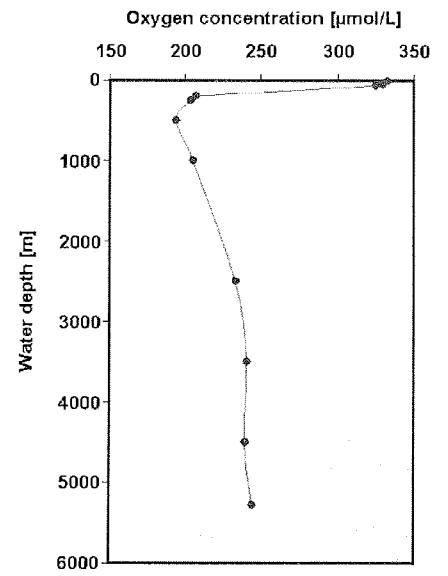


Fig. 13.2: Exemplaric oxygen profile over the entire water column at 64°S 0°E (Station PS 65/682).

Transect 3 Oxygen [µmol/L]

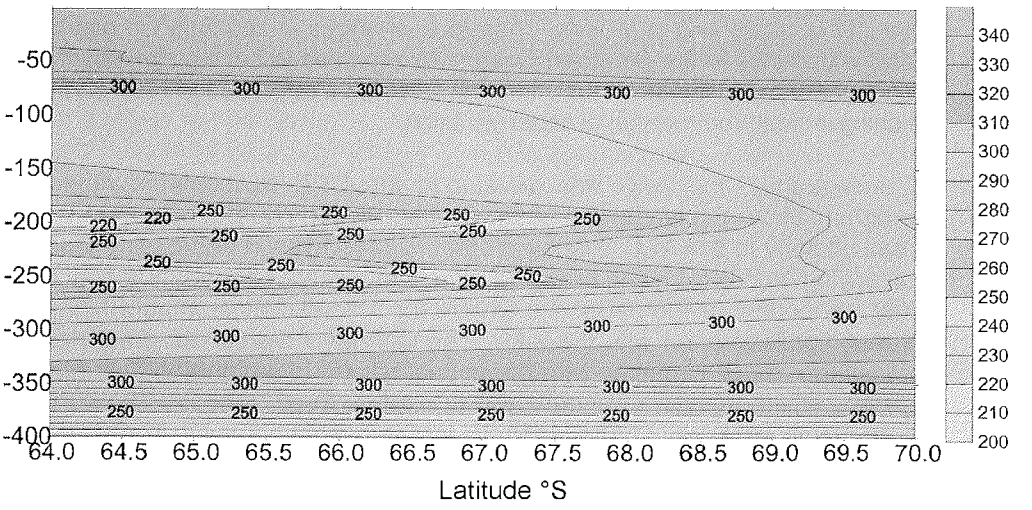


Fig. 13.3: Oxygen distribution along Transect 3. The oxygen minimum zone weakens towards the south due to super-cooled water descending in front of the shelf ice.

Literature cited

Grasshoff, K., Erhard, M., Kremling, K., 1983. Methods of Seawater Analysis.
Verlag Chemie, Weinheim, 417pp.

14. CONTINUOUS PLANKTON RECORDER (CPR): AUSTRALIAN ANTARCTIC DIVISION PROJECT 472

John Kitchener (AAD)

The Southern Ocean Continuous Plankton Recorder (SO-CPR) survey, which for the last 7 seasons or so had only involved Australia and Japan, now includes Germany from 2004. This serves to address AAD's Goal 1 of maintaining the Antarctic Treaty System and enhancing Australia's influence through cooperating with Antarctic Treaty partners in the involvement in setting the direction of international scientific programs and forums relating to Antarctic issues, e.g. international CPR survey, SCOR, SCAR, GOOS and GLOBEC.

The SO-CPR survey primarily addresses AAD's Goal 2 of protecting the Antarctic environment by providing information on the status or "health" of the Southern Ocean through the monitoring of zooplankton.

Zooplankton are sensitive to environmental parameters such as temperature, movement of currents and water quality. Due to their sensitivity, short life spans and fast growth rates plankton populations respond rapidly to environmental change, and consequently make excellent biological indicators.

The CPR program is expected to provide information on natural variation in zooplankton patterns as well as effects of global change. Zooplankton are also the principal dietary components of many higher vertebrates, including penguins, seals and sea-birds. Therefore, changes in zooplankton distribution and abundance in the Southern Ocean are expected to have a significant effect on higher trophic levels. In turn, this will serve as a reference to help distinguish fishing impact from natural or other variation.

Consequently, the AAD has developed the CPR zooplankton monitoring program, under the leadership of Dr. Graham Hosie. The CPR program is a key methodology in the AAD Biology program's objectives in addressing Goal 2 in surveying biodiversity and mapping effects of climate change. It is now also a key component of the Japanese Centre for Antarctic Environment Monitoring through collaboration with the AAD. The German Antarctic program has now joined the SO-CPR survey with the mutual benefit of supporting their plankton studies while providing the survey with another fixed transect. The survey to date mainly relies on *Aurora Australis* for the majority of tows. These voyages cover a large area which is ideal for mapping biodiversity, but they also have variable routes and schedules according to logistic and science program demands which can complicate attempts to assess temporal variation as distinct from spatial patterns. The Japanese icebreaker *Shirase* has provided tows along two fixed transects 110°E and 150°E at fixed times which provides useful references for the other data. The addition of the fixed transect between Cape Town and Georg von Neumayer station, sampled several times a year on *Polarstern*, will further improve our analyses, as well as improving our spatial coverage for studying patterns in the Antarctic Circumpolar Current.

By employing a CPR, surface or near-surface zooplankton can be collected at normal ship speed during a voyage. The unit is usually towed about 100 metres astern of the ship for approximately 450 nautical miles at a time. By splicing consecutive tows together one is able to produce an un-interrupted transect across the ocean, providing information on zooplankton distribution patterns, community structure, and abundance levels.

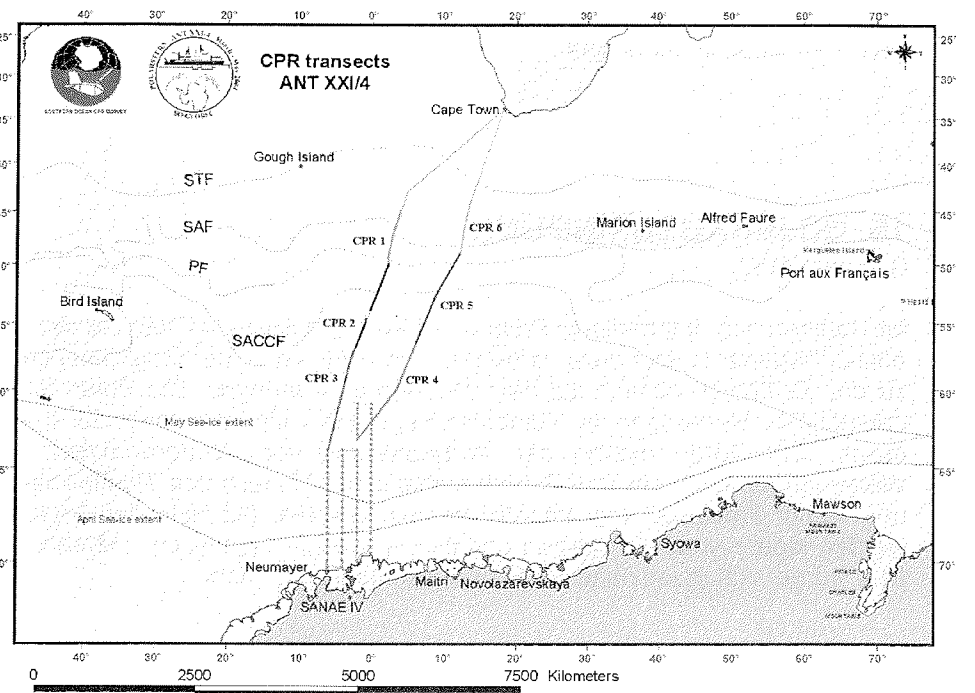


Figure 14.1. Map showing CPR deployments during ANT XXI/4.

The CPR component during ANT XXI/4 involved the collection of samples on the southward and northward legs of the Cape Town – Lazarev Sea krill survey area route (Fig. 14.1). The CPR was deployed 3 times from Cape Town en route to the krill survey area, and a further 3 deployments occurred en route from the krill box back to Cape Town. The resulting 6 samples, a combined total distance of 2422 nautical miles of continuous plankton recordings, will be analysed back at the laboratory at AAD headquarters in Kingston, Tasmania, Australia.

All six routine CPR tows were successfully undertaken onboard *Polarstern*. There were no problems encountered with the gear at any time.

Twenty-six routine CPR runs have been completed this last 2003/04 ANARE season on *Aurora Australis*, with a further 6 CPR tows undertaken during JARE 2003/04 onboard *Shirase*, and now the addition of 6 more from ANT XXI/4 on *Polarstern*.

Sincere thanks go to Uli Bathmann for his keen interest in furthering the SO-CPR program by incorporating CPR sampling into the voyage schedule, and of course to Master Uwe Pahl, boatswain Burkhardt Clasen and crew of *Polarstern*, for their willing assistance and faultless deployment and retrieval of gear in all weather conditions.

15. BOJENAUSBRINGUNG

C. Haas (AWI)

Im Rahmen des "International Program of Antarctic Buoys" (IPAB) hat sich das Alfred-Wegener-Institut dazu verpflichtet, im Rahmen seiner Möglichkeiten bis zu drei Driftbojen jährlich auf dem Meereis auszubringen. Die Bojen führen dreistündige Messungen der Temperatur und des Luftdrucks sowie der Eisdrift durch. Die Daten dienen der Verbesserung von Wetteranalysen und Wettervorhersagen, die zum Betrieb numerischer Modelle des Weddellmeeres und seiner Eisbedeckung am AWI benutzt werden. Mit Hilfe der Bojendrift werden Meereismodelle validiert und ihre Rheologie verbessert. Während Ant 21/4 wurde drei Bojen nahe der Schelfeiskante ausgebracht.

15.a) SEA-ICE BUOY DEPLOYMENTS

C. Haas (AWI)

In the framework of the "International Program of Antarctic Buoys" (IPAB) the Alfred-Wegener-Institute regularly deploys drifting buoys on ice floes. Every three hours, the buoys measure air temperature, air pressure as well as position. This data allow improvement of weather analysis, forecasts, and numeric models at AWI for the Weddell Sea and its ice coverage. With the help of drifting buoys sea ice models can be validated and their rheology can be improved. We have deployed three sea ice buoys as far south as possible and close to the sehla ice edge. The data from all three sensors are transmitted to AWI via the ARGOS satellite system.

16. METEOROLOGICAL CONDITIONS DURING CRUISE

R. Brauner, H. Sonnabend (DWD)

Wissenschaftliches Programm:

Die Forschungsfahrt war Teil des internationalen Programms „Global Ocean Ecosystem Dynamics“ (GLOBEC), das den Beziehungen zwischen umhertreibenden marinen Tieren des offenen Wassers (Zooplankton) und den physikalischen Umweltbedingungen im Meer gewidmet ist.

In der Antarktis konzentrierten sich die GLOBEC Forschungen auf den Krill, dessen Bestandsschwankungen, Biologie und Physiologie, sowie die Rolle von Krill im Nahrungsgefüge des eisfreien und eisbedeckten Antarktischen Ozeans. Diese Tiergruppe - die Leuchtgarnelen – wurden seit Jahrzehnten untersucht und noch immer verbergen sie einige Geheimnisse, z.B. wie sie den langen antarktischen Winter überdauern. Besondere Aufmerksamkeit galt den mit Meereis bedeckten Flächen des Lazarev Meeres, um dort Krill aufzuspüren, der sich gerne zwischen den Eisschollen vor seinen Fraßfeinden den Robben, Walen, Pinguinen und fliegenden Vögeln verbirgt.

Fahrtverlauf und Wetter:

Polarstern verließ am Abend des 27.03.2004 den Hafen von Kapstadt. Bereits kurz nach dessen Verlassen stellte sich die für die südlichen Breiten bekannte Dünung ein. Der Nordwestwind frischte weiter auf und nach Passage einer Kaltfront drehte der Wind auf Südwest und wehte mit etwa 7 Windstärken Bft. Die 4 bis 6 Meter hohe See war dem Schiffskurs entgegengesetzt, was zu heftigen Stampfbewegungen führte. Nach einigen Tagen Fahrzeit drehte der Wind auf Nordwest und vom 31.03 bis zum 02.4.04 wurden nahe der ozeanischen Polarfront bei etwa 50 Grad Süd einige Arbeitstationen angelaufen. Ab dem 02.04.2004 wurde 700 Seemeilen bis zum Hauptarbeitsgebiet gedampft. Ein Hochkeil brachte nur eine vorübergehende Wetterberuhigung. Ein nachfolgendes Tief wurde in Kernähe passiert, auf der Rückseite stellte sich eine Südwestströmung zwischen 6 und 8 Windstärken ein. Südlich der ozeanischen Polarfront wurden Lufttemperaturen um -3 °C gemessen. Diese führten zu einer Schiffsvereisung im Bugbereich.

Auf etwa 54 Grad südlicher Breite zeigten sich die ersten Eisberge. Erste Treibeisfelder traten kurz nach Erreichen des 68-sten Breitengrades auf.

Die südwestliche Luftströmung erwies sich aufgrund einer Omega-Lage als sehr beständig. Das belegt auch die Abbildung 16.2. Im Zeitraum vom 07.04 bis 27.04, als Polarstern im zentralen Arbeitsgebiet verweilte, dominierten infolge des blockierenden Hochgebietes Winde aus West bis Süd mit einer Häufigkeit von 70% und mit Windstärken zwischen 4 und 6 Bft. Aufgrund dieser Konstellation war daher die Eislage entspannt. Die Tiefdruckgebiete wurden nach Nordosten abgedrängt und die Forschungsarbeiten an den einzelnen Stationen des Hauptarbeitsgebietes konnten ohne Verzögerungen durchgeführt werden. Über 14 Tage dauerte die Omega Lage an. Oft wurde am Himmel die typische Stratocumulusbewölkung beobachtet, welche sich über dem relativen

warmen Wasser bildete. Besonders über dichtem Meereis und nahe der Schelfeiskante war es aufgrund der trockenen Luftmassen oft wolkenlos und die Temperaturen erreichten Werte bis -20.3°C . Selbst bei Lufttemperaturen um -10°C und 6 Windstärken wurde eine Windchill-Temperatur um -30°C erreicht.

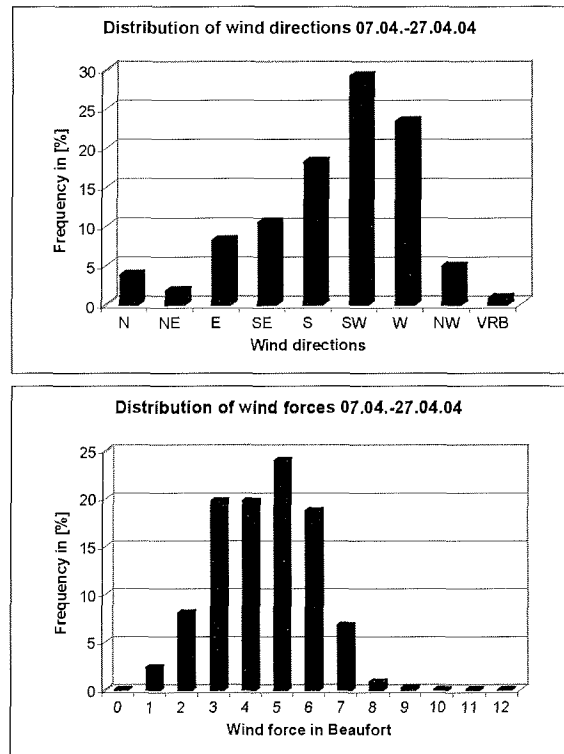


Abb.16.2 und 16.3: Häufigkeit der Windrichtungen und Windstärken im Hauptarbeitsgebiet

Am 18.04.04 näherten sich erstmals die Ausläufer eines Tiefdruckgebietes, welche entlang 55°Süd ostwärts zogen. Bis zum Verlassen des Arbeitsgebietes verweilte Polarstern im südlichen Quadranten der Tiefdruckgebiete. Es wehten Winde aus dem südöstlichen Sektor. Dabei herrschte leichter Frost und zeitweise führte Schnee zu einer Sichtverschlechterung. Schwache Zwischenhochkeile schoben sich zwischen die aufeinanderfolgenden Tiefdruckgebiete, sie brachten aber nur eine kurze Wetterberuhigung. Der Wind flautete vorübergehend ab, jedoch blieb eine konstante Dünung von ca. 2 Metern Höhe. Nur in meereisbedeckten Gebieten wurde die Dünung auf unter 0.5 Meter gedämpft.

Am 26.04.04 begann Polarstern die Rückfahrt nach Kapstadt. Unterwegs wurde an vier Stationen südlich und nördlich der ozeanischen Polarfront die Fahrt unterbrochen werden, um einige Messungen vorzunehmen.

Zum 28.04.04 näherte sich von Westen her ein erstes kräftiges Tiefdruckgebiet. Das Sturmtief brachte am 29./30.4. Winde aus dem westlichen Sektor mit 8 Windstärken Bft. und einer Wellenhöhe von 6 bis 7 Metern.

Da diese Sturmentwicklung der Fahrtleitung rechtzeitig angekündigt wurde, konnten die Messungen an den Stationen zufrieden stellend erledigt werden, bevor sich von Westen her das nächste Tiefdruckgebiet ankündigte. Zum 01.05 näherte sich von Westen ein Orkantief mit einem Kerndruck von 935 hPa. Es zog auf etwa 60 Grad südlicher Breite ostwärts. Da Polarstern eine Arbeitsstation auf etwa 45 Grad Süd bearbeitete, erreichte der Nordwestwind immerhin noch Windstärke 8 Bft. und die See erreichte eine signifikante Höhe von 6.5 Metern.

Am 02.05 nachmittags wurden die Forschungsarbeiten eingestellt und Polarstern nahm Kurs auf Kapstadt. Polarstern erreichte den Hafen von Kapstadt am Morgen des 06.05.2004.

Tätigkeiten der Bordwetterwarte:

3.1 Beobachtungsdienst

Während der Reise wurden von der automatischen Wetterstation synoptische Meldungen per Data Collecting Platform (DCP) dem internationalen Meldennetz GTS (Global Telecommunication System) zur Verfügung gestellt. Zwischen 06.00 UTC und 21.00 UTC wurden sie in 3-stündigem Abstand durch Augenbeobachtungen des Himmels, Seegang und Meereisbeobachtungen ergänzt. Der tägliche Radiosondenaufstieg zum 12.00 UTC Termin wurde ebenfalls über DCP versandt.

Beratungsdienst

3.2.1 Grundsätzliches

Die meteorologische Beratung für Schiff, Wissenschaft und Flugbetrieb ist die wichtigste Aufgabe des Bordwetterdienstes. Im Vordergrund stehen dabei Sicherheitsaspekte für das Schiff und den Einsatz von Fluggerät. Darüber hinaus ist jedoch für die Planung und effiziente Durchführung von wissenschaftlichen Programmen und logistischen Operationen eine detaillierte meteorologische Beratung in einer möglichst weitreichenden Zeitskala unverzichtbar.

Insbesondere unter diesem mittelfristigen Aspekt ist der beratende Meteorologe auf die Ergebnisse der numerischen Vorhersagemodelle angewiesen. Basierend auf den langjährigen guten Erfahrungen aller Meteorologen des Bordwetterdienstes diente auch während dieser Reise routinemäßig das Modell des ECMWF als Beratungsgrundlage.

3.2.2 Beratungen für Schiffs- und Fahrtleitung

Täglich wurde eine Bodenwetterkarte analysiert, um das verwendete Modell zu überprüfen. Eine Grundlage dafür sind auch die an Bord empfangenen aktuellen Satellitenbilder. Die Beratungstätigkeit wurde mit den Prognosekarten des ECMWF, sowie mit den durch das DWD-Programm MetMaster visualisierten Seegangs- und Winddatensätzen des ECMWF durchgeführt. Dieses Material wurde bei ausreichenden Empfangsbedingungen durch Faksimilekarten des Südafrikanischen Wetterdienstes (SAWB) ergänzt. Insbesondere für die kontinuierliche Wetterüberwachung und für Kurzfristprognosen sind die mit der TeraScan Anlage aufgezeichneten NOAA- und DMSP-Satellitenbilder eine unverzichtbare Hilfe.

Auf der Grundlage dieser Informationen wurde zweimal täglich ein Wetterbericht mit einem Prognosezeitraum von 24 Stunden für die Schiffführung und die wissenschaftliche Fahrtleitung erstellt. Die Wetterberichte wurden dem Fahrtleiter, Kapitän und dem Brückenoffizier unter Verwendung von Satellitenbildern und Prognosekarten, ggf. auch Eiskarten eingehend erläutert. Darüber hinaus fand routinemäßig ein morgendliches Briefing im Konferenzraum statt.

Zusätzlich wurden als Grundlage für weiterreichende Planungen Berichte mit mittelfristigen Aussichten ausgegeben sowie mit Antritt der Heimreise eine täglich aktualisierte Routenberatung an die Schiffführung gegeben.

3.2.3 Eisberatung

Die Entwicklung der Eissituation, insbesondere die Verlagerung der Eisfelder, wird maßgeblich von der synoptischen Entwicklung beeinflusst. Diesbezügliche Fragen waren daher fast immer auch Gegenstand der Beratungsgespräche. Neben den amerikanischen Eiskarten (National Ice Center) wurden als Beratungsunterlagen vom Bundesamt für Seeschifffahrt (BSH) u.a. die von der Universität Bremen aufbereiteten Eiskarten zur Verfügung gestellt.

Für detaillierte Informationen über die Eissituation im jeweiligen Einsatzgebiet „vor Ort“ wurden die hoch aufgelösten Satellitenbilder der TeraScan Anlage im sichtbaren Kanal (DMSP, NOAA) verwendet. Zur Übersicht wurden auch die in einer schlechteren Auflösung vorhandenen Bilder im Mikrowellenbereich (DMSP) benutzt.

17. JOURNALISTISCHE DOKUMENTATION

P. Demmler (München)

Als Journalistin der Fahrt war es zum einen mein Ziel, den besonderen Reiz der antarktischen Landschaften fotografisch einzufangen. Das andere Augenmerk galt den Forschungsaktivitäten an Bord und ihrer Bedeutung für Wissenschaft und Gesellschaft.

Meine Fotoausrüstung bestand hauptsächlich aus einer Canon EOS 1V mit zwei Zoomobjektiven (EF 16-35 mm f/2,8 L; EF 70-200 mm f/2,8 L IS), deren hohe Lichtstärke sich in der fortgeschrittenen Jahreszeit oft als Segen erwies. Gerade die oft unwirtlichen Wetter- und Lichtverhältnisse im antarktischen Herbst, die hohe Ansprüche an die Fotografin stellten, erbrachten im Resultat gut verwertbares Bildmaterial. Im Laufe der Fahrt entstanden rund 2500 Bilder, von denen wie vereinbart eine Auswahl dem AWI-Bildarchiv zur Verfügung gestellt wurde.

Zu den fotografischen Dokumentationen der verschiedenen Aktivitäten an Bord erhielt ich von den Forschern detaillierte Hintergrundinformationen über deren Forschungsziele, die zugrunde liegenden Hypothesen und über erste Resultate.

Eine wichtige Aufgabe war es hierbei, mich mit den jeweiligen Arbeitsdisziplinen und -methoden vertraut zu machen und die Informationen so aufzuarbeiten, dass sie einem breiten Publikum verständlich werden. Mein naturwissenschaftliches Studium war hierfür eine geeignete Grundlage, um in die zum Teil komplexe Thematik der verschiedenen Forschergruppen vorzudringen. Die Geduld der Wissenschaftler und ihre Bereitschaft ausführlich über ihre Arbeit zu reden haben mir dabei sehr geholfen. Dafür möchte ich Ihnen danken.

Die aufgearbeiteten Themen, die während ANT XXI_4 bearbeitet wurden, sollen über Zeitungen und populärwissenschaftliche Zeitschriften ihren Weg in die Öffentlichkeit finden, damit diese die übergeordnete Relevanz der Polar- und Meeresforschung besser verstehen lernt. Zwei Artikel, einen für eine überregionale Zeitung sowie einen in einer naturwissenschaftlich orientierten Zeitschrift, wurden jetzt schon publiziert. Weitere Beiträge sind in Vorbereitung. Die Expedition hat mir viele wertvolle und unvergessliche Eindrücke geschenkt und Anregungen zu weiteren, anknüpfenden Projekten gegeben.

18. LISTE DER STATIONEN ANT XXIV

Station	Date	Time	PositionLat	PositionLon	Depth [m]	Windstr. [m/s]	Gear Abbrev.	Action	Comment
PS65/594-1	30.03.04	13:49	42° 59,99' S	5° 0,08' E	4732,9	WNW 14	LANDER	surface	
PS65/594-2	30.03.04	14:07	42° 59,81' S	4° 59,33' E	4748,9	WNW 13	CTD/RO	surface	
PS65/594-2	30.03.04	14:13	42° 59,85' S	4° 59,36' E	4749,5	WNW 14	CTD/RO	at depth	EL31 100m ausgesteckt
PS65/594-2	30.03.04	14:19	42° 59,84' S	4° 59,31' E	4748,9	WNW 14	CTD/RO	on deck	
PS65/594-3	30.03.04	14:30	42° 59,85' S	4° 59,27' E	4750,4	NW 14	MUC	surface	
PS65/594-3	30.03.04	15:58	42° 59,91' S	4° 59,06' E	4908,5	WNW 15	MUC	at sea bottom	GE52.2 4766m ausgesteckt
PS65/594-3	30.03.04	17:27	42° 59,93' S	4° 59,19' E	4755,3	WNW 14	MUC	on deck	
PS65/594-4	30.03.04	17:34	42° 59,91' S	4° 59,18' E	4754,1	WNW 14	BWS	surface	
PS65/594-4	30.03.04	19:17	42° 59,61' S	4° 59,22' E	4747,1	NW 14	BWS	at sea bottom	4790m
PS65/594-4	30.03.04	19:24	42° 59,55' S	4° 59,21' E	4748,4	NW 14	BWS	off bottom	
PS65/594-4	30.03.04	21:03	42° 59,15' S	4° 58,90' E	4746,8	NW 15	BWS	on deck	
PS65/594-1	30.03.04	21:47	42° 59,92' S	5° 0,03' E	4736,4	NW 15	LANDER	released	
PS65/594-5	30.03.04	21:48	42° 59,92' S	5° 0,03' E	4734,3	NW 15	CTD/RO	surface	
PS65/594-5	30.03.04	21:55	42° 59,88' S	5° 0,03' E	4734,4	NW 15	CTD/RO	at depth	auf 203m
PS65/594-5	30.03.04	22:09	42° 59,82' S	4° 59,96' E	4730,8	NW 13	CTD/RO	on deck	
PS65/594-1	30.03.04	23:39	42° 59,72' S	4° 59,66' E	0,0	WNW 14	LANDER	on Deck	
PS65/595-1	31.03.04	13:14	44° 57,54' S	4° 0,33' E	2154,0	NW 17	CPR	into water	100m Draht ausgesteckt
PS65/595-1	01.04.04	05:57	46° 59,79' S	3° 0,13' E	4308,2	NNW 15	CPR	heave	
PS65/595-1	01.04.04	06:03	47° 0,01' S	2° 59,96' E	4313,3	NW 17	CPR	on deck	
PS65/596-1	01.04.04	06:19	47° 0,09' S	3° 0,16' E	4307,6	NW 16	BWS	surface	
PS65/596-1	01.04.04	07:52	47° 0,39' S	2° 59,92' E	4317,3	W 16	BWS	at sea bottom	4332m
PS65/596-1	01.04.04	08:02	47° 0,46' S	2° 59,97' E	4322,4	W 16	BWS	off bottom	
PS65/596-1	01.04.04	09:19	47° 0,68' S	2° 59,78' E	4548,4	WNW 15	BWS	on deck	
PS65/596-2	01.04.04	09:25	47° 0,64' S	2° 59,84' E	4335,2	WNW 14	MUC	surface	
PS65/596-2	01.04.04	10:46	47° 0,61' S	2° 59,93' E	4331,9	WNW 17	MUC	at sea bottom	auf 4321m
PS65/596-2	01.04.04	12:04	47° 0,70' S	2° 59,47' E	4335,5	WNW 19	MUC	on deck	
PS65/597-1	01.04.04	12:18	47° 0,13' S	2° 59,05' E	4322,6	WNW 20	CPR	into water	GE52.2 100m ausgesteckt
PS65/597-1	02.04.04	07:59	49° 18,07' S	2° 12,35' E	3920,4	WSW 11	CPR	heave	
PS65/597-1	02.04.04	08:04	49° 18,11' S	2° 12,19' E	3924,8	WSW 14	CPR	on deck	
PS65/598-1	02.04.04	08:30	49° 18,50' S	2° 11,68' E	3941,6	WSW 13	LANDER	surface	

PS65/598-2	02.04.04	09:09	49° 20,12' S	2° 12,42' E	3952,0	WSW 9	CTD/RO	surface	
PS65/598-2	02.04.04	10:25	49° 20,94' S	2° 11,94' E	3966,0	SW 10	CTD/RO	at depth	auf 3828m
PS65/598-2	02.04.04	11:39	49° 21,71' S	2° 11,64' E	3974,8	WSW 9	CTD/RO	on deck	
PS65/598-3	02.04.04	11:43	49° 21,74' S	2° 11,60' E	3976,0	WSW 9	MUC	surface	
PS65/598-3	02.04.04	12:41	49° 22,37' S	2° 10,85' E	3986,4	W 10	MUC	at sea bottom	GE52.2 3982m ausgesteckt
PS65/598-3	02.04.04	13:57	49° 22,74' S	2° 9,99' E	3979,6	W 7	MUC	on deck	
PS65/598-4	02.04.04	15:20	49° 18,95' S	2° 11,62' E	3947,2	WSW 10	MN	surface	
PS65/598-1	02.04.04	15:22	49° 18,96' S	2° 11,63' E	3948,0	W 11	LANDER	Information	Hydrophon zu Wasser
PS65/598-1	02.04.04	15:24	49° 18,97' S	2° 11,61' E	3948,0	W 11	LANDER	released	
PS65/598-4	02.04.04	15:36	49° 19,13' S	2° 11,56' E	3950,0	W 10	MN	at depth	EL30 436m ausgesteckt
PS65/598-4	02.04.04	15:54	49° 19,32' S	2° 11,42' E	3952,4	WSW 11	MN	on deck	
PS65/598-1	02.04.04	16:48	49° 19,00' S	2° 10,97' E	3951,6	WSW 8	LANDER	on Deck	
PS65/598-5	02.04.04	17:04	49° 19,03' S	2° 11,04' E	3951,6	W 10	MUC	surface	
PS65/598-5	02.04.04	18:08	49° 19,74' S	2° 10,37' E	3961,2	W 11	MUC	at sea bottom	3966m ausgesteckt
PS65/598-5	02.04.04	19:13	49° 20,45' S	2° 9,76' E	3966,8	WSW 12	MUC	on deck	
PS65/599-1	02.04.04	19:31	49° 20,86' S	2° 9,47' E	3970,8	W 12	CPR	into water	
PS65/599-1	03.04.04	00:05	49° 59,65' S	2° 19,97' E	3600,8	WSW 12	CPR	heave	
PS65/599-1	03.04.04	00:12	49° 59,99' S	2° 20,06' E	3573,6	WSW 11	CPR	on deck	
PS65/600-1	03.04.04	00:28	49° 59,88' S	2° 20,22' E	3588,8	SW 18	LANDER	surface	
PS65/600-2	03.04.04	00:47	50° 0,25' S	2° 19,70' E	3558,8	SW 13	MUC	surface	
PS65/600-2	03.04.04	01:53	50° 0,20' S	2° 19,63' E	3564,4	WSW 13	MUC	at sea bottom	GE52.2 3549m ausgesteckt
PS65/600-2	03.04.04	03:01	50° 0,16' S	2° 19,20' E	3573,2	WSW 11	MUC	on deck	
PS65/600-3	03.04.04	03:21	50° 0,21' S	2° 19,09' E	3567,6	WSW 10	BWS	surface	
PS65/600-3	03.04.04	04:36	50° 0,31' S	2° 18,99' E	3555,6	SW 13	BWS	at sea bottom	3566m
PS65/600-3	03.04.04	04:42	50° 0,33' S	2° 19,00' E	3554,0	WSW 11	BWS	off bottom	
PS65/600-3	03.04.04	06:05	50° 0,66' S	2° 19,11' E	3514,4	WSW 10	BWS	on deck	
PS65/600-1	03.04.04	06:24	49° 59,86' S	2° 20,20' E	3578,8	SW 8	LANDER	released	
PS65/600-4	03.04.04	06:33	49° 59,74' S	2° 20,20' E	3594,8	WSW 6	NFLOAT	surface	
PS65/600-1	03.04.04	07:36	49° 59,63' S	2° 20,46' E	3596,4	W 8	LANDER	on Deck	
PS65/601-1	03.04.04	08:48	49° 58,68' S	2° 19,08' E	3489,2	W 7	CPR	into water	
PS65/601-1	04.04.04	08:49	54° 0,53' S	0° 14,93' W	2663,6	NW 9	CPR	heave	
PS65/601-1	04.04.04	08:56	54° 1,10' S	0° 15,39' W	2812,0	NW 9	CPR	on deck	
PS65/602-1	04.04.04	09:45	54° 5,18' S	0° 17,76' W	2526,8	NW 8	SUIT	surface	

PS65/602-1	04.04.04	10:30	54° 6,01' S	0° 17,49' W	2530,0	NW 9	SUIT	on deck	
PS65/603-1	04.04.04	14:31	54° 37,21' S	0° 40,71' W	1606,4	W 9	RMT	surface	M-RMT
PS65/603-1	04.04.04	14:56	54° 37,05' S	0° 42,43' W	1635,6	W 8	RMT	on deck	
PS65/604-1	04.04.04	15:21	54° 39,37' S	0° 44,47' W	1835,6	W 9	RMT	surface	S-RMT
PS65/604-1	04.04.04	15:40	54° 39,39' S	0° 46,01' W	2028,4	W 10	RMT	heave	GE72.1 461m ausgesteckt
PS65/604-1	04.04.04	16:08	54° 39,47' S	0° 48,06' W	2315,6	W 9	RMT	on deck	
PS65/605-1	04.04.04	16:15	54° 39,55' S	0° 48,06' W	2323,6	W 9	CPR	into water	
PS65/605-1	05.04.04	06:10	56° 57,63' S	2° 18,60' W	3915,2	E 13	CPR	on deck	Filmwechsel
PS65/605-1	05.04.04	06:19	56° 58,25' S	2° 18,84' W	3970,4	E 14	CPR	into water	
PS65/605-1	07.04.04	06:07	63° 59,65' S	5° 59,67' W	5242,8	W 9	CPR	on deck	
PS65/606-1	07.04.04	06:19	63° 59,89' S	5° 59,97' W	5241,6	W 8	RMT	surface	
PS65/606-1	07.04.04	06:37	64° 0,12' S	6° 1,69' W	5230,4	WSW 8	RMT	heave	478m ausgesteckt
PS65/606-1	07.04.04	07:06	64° 0,44' S	6° 4,29' W	5230,4	W 7	RMT	on deck	
PS65/606-2	07.04.04	07:23	64° 0,37' S	6° 3,08' W	5228,8	WSW 8	CTD/RO	surface	
PS65/606-2	07.04.04	08:57	64° 0,62' S	6° 4,04' W	5230,8	W 4	CTD/RO	at depth	auf 4925m
PS65/606-2	07.04.04	10:02	64° 0,93' S	6° 4,31' W	5233,6	NNE 0	CTD/RO	Information	im Umkreis von 3 SM kein Eis vorhanden
PS65/606-2	07.04.04	10:27	64° 1,00' S	6° 4,40' W	5234,4	SSE 0	CTD/RO	on deck	
PS65/606-1	07.04.04	10:34	64° 0,96' S	6° 4,51' W	5234,8	N 0	SUIT	surface	
PS65/606-1	07.04.04	11:35	63° 59,46' S	6° 4,35' W	5237,2	NW 1	SUIT	on deck	
									Standard-RMT/Kein Eis/Keine Eisberge im 3 sm-Bereich
PS65/607-1	07.04.04	14:15	64° 19,72' S	6° 0,11' W	5215,0	WNW 5	RMT	surface	GE72.1 395m ausgesteckt
PS65/607-1	07.04.04	14:29	64° 20,22' S	6° 0,55' W	5213,6	W 7	RMT	heave	GE72.1 395m ausgesteckt
PS65/607-1	07.04.04	14:54	64° 21,10' S	6° 1,37' W	5212,0	WSW 6	RMT	on deck	
PS65/608-1	07.04.04	17:05	64° 39,62' S	5° 59,96' W	0,0	W 7	RMT	surface	
PS65/608-1	07.04.04	17:22	64° 40,34' S	6° 0,06' W	0,0	WSW 6	RMT	heave	456m ausgesteckt
PS65/608-1	07.04.04	17:50	64° 41,48' S	6° 0,00' W	5200,0	WSW 6	RMT	on deck	Eisberge: 0 , Eisbedeckung: 0
PS65/609-1	07.04.04	19:55	64° 59,58' S	5° 59,94' W	5120,4	W 4	RMT	surface	
PS65/609-1	07.04.04	20:12	65° 0,30' S	6° 0,03' W	5118,8	SW 5	RMT	heave	
PS65/609-1	07.04.04	20:41	65° 1,48' S	6° 0,00' W	5117,2	WSW 4	RMT	on deck	
PS65/609-2	07.04.04	21:02	65° 1,64' S	5° 59,76' W	5117,6	SW 4	CTD/RO	surface	
PS65/609-3	07.04.04	21:04	65° 1,65' S	5° 59,74' W	5118,0	SW 4	HN	surface	
PS65/609-3	07.04.04	21:11	65° 1,72' S	5° 59,70' W	5117,6	NNW 1	HN	on deck	
PS65/609-2	07.04.04	21:28	65° 1,87' S	5° 59,62' W	5117,6	SW 4	CTD/RO	at depth	auf 994m

PS65/609-2	07.04.04	21:52	65° 1,98' S	5° 59,36' W	5117,6	SSW 6	CTD/RO	on deck	
PS65/609-4	07.04.04	21:55	65° 2,01' S	5° 59,35' W	5116,4	SSW 6	BONGO	surface	
PS65/609-4	07.04.04	22:04	65° 2,11' S	5° 59,31' W	5116,4	SSW 6	BONGO	at depth	auf 200m
PS65/609-4	07.04.04	22:29	65° 2,28' S	5° 59,07' W	5115,2	SSW 6	BONGO	on deck	
PS65/610-1	08.04.04	00:32	65° 19,78' S	6° 0,06' W	5069,0	SSW 4	RMT	surface	Standard-RMT/Kein Eis/Keine Eisberge im 3 sm-Bereich
PS65/610-1	08.04.04	00:48	65° 20,46' S	5° 59,92' W	5066,4	SSW 4	RMT	heave	GE72.1 422m ausgesteckt
PS65/610-1	08.04.04	01:15	65° 21,63' S	5° 59,95' W	5055,2	S 6	RMT	on deck	
PS65/611-1	08.04.04	03:23	65° 39,79' S	5° 59,90' W	4978,8	SW 4	RMT	surface	Standard-RMT/Kein Eis/Keine Eisberge im 3 sm-Bereich
PS65/611-1	08.04.04	03:37	65° 40,33' S	5° 59,74' W	4977,2	SW 4	RMT	heave	GE72.1 396m ausgesteckt
PS65/611-1	08.04.04	04:03	65° 41,25' S	5° 59,68' W	4973,6	SW 3	RMT	on deck	Eisbedeckung: 0 / Eisberge: 0
PS65/612-1	08.04.04	06:07	65° 59,55' S	6° 0,02' W	0,0	W 8	RMT	surface	
PS65/612-1	08.04.04	06:24	66° 0,30' S	0° 0,06' W	4932,4	W 7	RMT	heave	GE 72.1 auf 442m ausgesteckt
PS65/612-1	08.04.04	06:51	66° 1,45' S	6° 0,18' W	4934,0	W 7	RMT	on deck	
PS65/612-2	08.04.04	07:11	66° 1,50' S	5° 59,82' W	4934,4	WSW 8	CTD/RO	surface	
PS65/612-2	08.04.04	07:32	66° 1,54' S	5° 59,84' W	4934,8	WSW 8	CTD/RO	at depth	991m
PS65/612-2	08.04.04	07:56	66° 1,61' S	5° 59,90' W	4933,6	WSW 6	CTD/RO	on deck	
PS65/612-3	08.04.04	08:04	66° 1,64' S	5° 59,93' W	4934,4	WSW 7	BONGO	surface	
PS65/612-3	08.04.04	08:11	66° 1,67' S	5° 59,98' W	4934,4	WSW 8	BONGO	at depth	auf 200m
PS65/612-3	08.04.04	08:30	66° 1,72' S	6° 0,06' W	4933,6	WSW 6	BONGO	on deck	
PS65/612-4	08.04.04	08:40	66° 1,64' S	6° 0,04' W	4934,0	WSW 7	SUIT	surface	
PS65/612-4	08.04.04	09:26	66° 1,62' S	6° 1,64' W	4935,6	WSW 5	SUIT	on deck	
PS65/613-1	08.04.04	11:41	66° 19,69' S	6° 0,13' W	4889,2	W 6	RMT	surface	
PS65/613-1	08.04.04	11:55	66° 20,22' S	5° 59,98' W	4888,0	W 5	RMT	heave	
PS65/613-1	08.04.04	12:19	66° 21,15' S	6° 0,00' W	4888,8	WSW 8	RMT	on deck	
PS65/614-1	08.04.04	14:28	66° 39,61' S	6° 0,00' W	4852,8	W 4	RMT	surface	Standard-RMT/Kein Eis/Keine Eisberge im 3 sm-Bereich
PS65/614-1	08.04.04	14:44	66° 40,25' S	5° 59,82' W	4854,8	SW 6	RMT	heave	GE72.1 425m ausgesteckt
PS65/614-1	08.04.04	15:10	66° 41,33' S	5° 59,70' W	4857,2	SW 4	RMT	on deck	
PS65/615-1	08.04.04	17:21	66° 59,64' S	6° 0,02' W	0,0	SSW 10	RMT	surface	
PS65/615-1	08.04.04	17:38	67° 0,45' S	6° 0,01' W	4864,0	SSW 9	RMT	heave	GE 72.1 451m ausgesteckt
PS65/615-1	08.04.04	18:08	67° 1,69' S	5° 59,88' W	4860,4	SSW 10	RMT	on deck	

PS65/615-2	08.04.04	18:19	67° 1,83' S	5° 59,67' W	4859,6	SSW 9	CTD/RO	surface	
PS65/615-2	08.04.04	18:48	67° 2,05' S	5° 59,04' W	4858,8	SSW 9	CTD/RO	at depth	1000m
PS65/615-2	08.04.04	19:13	67° 2,07' S	5° 58,36' W	4858,8	SW 10	CTD/RO	on deck	
PS65/615-3	08.04.04	19:20	67° 2,07' S	5° 58,19' W	4858,8	SSW 10	SUIT	surface	
PS65/615-3	08.04.04	19:22	67° 2,06' S	5° 58,14' W	4858,4	SSW 11	SUIT	slipped	
PS65/615-3	08.04.04	19:27	67° 2,20' S	5° 58,16' W	4858,4	SW 10	SUIT	start trawl	
PS65/615-3	08.04.04	19:53	67° 3,02' S	5° 58,54' W	4858,4	SSW 9	SUIT	stop trawl	
PS65/615-3	08.04.04	20:01	67° 3,04' S	5° 58,30' W	4858,4	SW 10	SUIT	on deck	
PS65/615-4	08.04.04	20:20	67° 3,08' S	5° 58,07' W	4858,4	SSW 9	BONGO	surface	
PS65/615-4	08.04.04	20:32	67° 3,14' S	5° 57,94' W	4858,4	SSW 11	BONGO	at depth	
PS65/615-4	08.04.04	20:44	67° 3,24' S	5° 57,84' W	4858,0	SSW 10	BONGO	on deck	
PS65/615-5	08.04.04	20:52	67° 3,28' S	5° 57,78' W	4856,8	SSW 10	MN	surface	
PS65/615-5	08.04.04	21:32	67° 3,43' S	5° 57,52' W	4858,0	SSW 12	MN	at depth	auf 1036m
PS65/615-5	08.04.04	22:10	67° 3,72' S	5° 57,47' W	4857,6	SSW 9	MN	on deck	
PS65/616-1	09.04.04	00:21	67° 19,60' S	6° 0,07' W	4854,8	SSW 13	RMT	surface	Standard-RMT/Kein Eis/Keine Eisberge im 3 sm-Bereich
PS65/616-1	09.04.04	00:37	67° 20,27' S	6° 0,15' W	4854,8	SSW 13	RMT	heave	GE72.1 404m ausgesteckt
PS65/616-1	09.04.04	01:05	67° 21,42' S	5° 59,99' W	4855,2	SSW 12	RMT	on deck	
PS65/617-1	09.04.04	03:16	67° 39,59' S	6° 0,03' W	4793,2	S 6	RMT	surface	Standard-RMT/Kein Eis/Keine Eisberge im 3 sm-Bereich
PS65/617-1	09.04.04	03:31	67° 40,20' S	5° 59,74' W	4791,2	S 6	RMT	heave	GE72.1 409m ausgesteckt
PS65/617-1	09.04.04	03:59	67° 41,33' S	5° 59,66' W	4791,2	S 7	RMT	on deck	
PS65/618-1	09.04.04	06:16	67° 59,62' S	6° 0,17' W	0,0	S 11	RMT	surface	
PS65/618-1	09.04.04	06:32	68° 0,23' S	6° 0,01' W	4742,0	S 12	RMT	heave	GE 72.1 404m ausgesteckt
PS65/618-1	09.04.04	07:01	68° 1,19' S	6° 0,05' W	4742,8	S 12	RMT	on deck	
PS65/618-2	09.04.04	07:19	68° 1,24' S	6° 0,06' W	4743,2	S 12	CTD/RO	surface	
PS65/618-2	09.04.04	07:41	68° 1,24' S	6° 0,09' W	4743,6	S 13	CTD/RO	at depth	994m
PS65/618-2	09.04.04	08:06	68° 1,14' S	6° 0,33' W	4744,4	S 13	CTD/RO	on deck	
PS65/618-3	09.04.04	08:15	68° 1,14' S	6° 0,48' W	4744,4	S 12	MN	surface	
PS65/618-3	09.04.04	08:55	68° 1,16' S	6° 0,57' W	4744,8	S 12	MN	at depth	auf 1063m
PS65/618-3	09.04.04	09:28	68° 1,23' S	6° 0,35' W	4054,0	S 13	MN	on deck	
PS65/619-1	09.04.04	11:51	68° 20,06' S	6° 0,10' W	4539,0	S 15	CTD/RO	surface	Neueisbildung/Keine Eisberge im 3 sm-Bereich

PS65/619-1	09.04.04	12:16	68° 20,17' S	6° 0,41' W	4535,6	S 14	CTD/RO	at depth	EL31 993m ausgesteckt
PS65/619-1	09.04.04	12:43	68° 20,28' S	6° 0,49' W	4526,0	S 12	CTD/RO	on deck	
PS65/619-2	09.04.04	12:53	68° 20,35' S	6° 0,49' W	4522,0	S 13	RMT	surface	Standard-RMT
PS65/619-2	09.04.04	13:05	68° 20,87' S	6° 0,30' W	4492,0	S 13	RMT	heave	GE52.2 362m ausgesteckt
PS65/619-2	09.04.04	13:29	68° 21,73' S	0° 0,02' W	4435,6	S 12	RMT	on deck	
PS65/620-1	09.04.04	15:38	68° 38,35' S	6° 2,18' W	0,0	SSW 12	RMT	surface	Standard-RMT 6/10 Pancake ice/Keine Eisb. im 3 sm-Bereich
PS65/620-1	09.04.04	15:53	68° 38,81' S	6° 3,49' W	0,0	SSW 12	RMT	heave	GE52.2 382m ausgesteckt
PS65/620-1	09.04.04	16:20	68° 39,13' S	6° 6,52' W	4100,0	S 12	RMT	on deck	
PS65/620-2	09.04.04	16:30	68° 39,05' S	6° 6,75' W	0,0	S 12	CTD/RO	surface	
PS65/620-2	09.04.04	16:53	68° 38,92' S	6° 7,16' W	0,0	SSW 10	CTD/RO	at depth	996m
PS65/620-2	09.04.04	17:22	68° 38,61' S	6° 7,39' W	4100,0	SSW 10	CTD/RO	on deck	
PS65/620-3	09.04.04	17:34	68° 38,41' S	6° 7,34' W	0,0	SSW 11	SUIT	surface	
PS65/620-3	09.04.04	17:36	68° 38,37' S	6° 7,32' W	0,0	SSW 11	SUIT	slipped	
PS65/620-3	09.04.04	17:47	68° 38,31' S	6° 6,76' W	0,0	SSW 11	SUIT	start trawl	
PS65/620-3	09.04.04	17:58	68° 38,33' S	6° 5,90' W	0,0	SSW 12	SUIT	stop trawl	
PS65/620-3	09.04.04	18:21	68° 38,06' S	6° 5,77' W	4100,0	S 10	SUIT	on deck	
PS65/620-4	09.04.04	18:30	68° 37,88' S	6° 5,69' W	0,0	SSW 11	BONGO	surface	
PS65/620-4	09.04.04	18:42	68° 37,91' S	6° 5,78' W	0,0	S 10	BONGO	at depth	200m
PS65/620-4	09.04.04	18:55	68° 37,87' S	6° 5,77' W	4100,0	S 11	BONGO	on deck	Eisbedeckung: 6/10, Eisberge: 1
PS65/621-1	09.04.04	22:03	69° 0,43' S	6° 1,26' W	0,0	S 7	RMT	surface	
PS65/621-1	09.04.04	22:26	69° 1,49' S	6° 2,40' W	0,0	S 6	RMT	heave	
PS65/621-1	09.04.04	23:01	69° 3,08' S	6° 5,12' W	2650,0	S 7	RMT	on deck	
PS65/621-2	09.04.04	23:27	69° 4,13' S	6° 4,58' W	2635,2	SSW 6	RMT	surface	Standard-RMT 9/10 Pancake ice/Keine Eisb. im 3 sm-Bereich
PS65/621-2	09.04.04	23:35	69° 4,31' S	6° 3,87' W	2628,4	SSW 6	RMT	heave	GE72.1 255m ausgesteckt
PS65/621-2	09.04.04	23:57	69° 4,81' S	6° 1,95' W	2616,0	SSW 7	RMT	on deck	
PS65/621-3	10.04.04	00:08	69° 5,06' S	6° 1,34' W	2609,6	S 4	BONGO	surface	
PS65/621-3	10.04.04	00:15	69° 5,11' S	6° 1,46' W	2609,6	SSE 6	BONGO	at depth	SE32.2 100m ausgesteckt
PS65/621-3	10.04.04	00:22	69° 5,13' S	6° 1,61' W	2610,0	SSW 6	BONGO	on deck	
PS65/621-4	10.04.04	00:30	69° 5,15' S	6° 1,75' W	2610,4	SSW 6	CTD/RO	surface	
PS65/621-4	10.04.04	01:21	69° 5,43' S	6° 2,33' W	2609,2	S 6	CTD/RO	at depth	EL31 2569m ausgesteckt
PS65/621-4	10.04.04	02:17	69° 5,66' S	6° 2,59' W	2604,0	S 7	CTD/RO	on deck	

PS65/622-1	10.04.04	04:02	69° 19,69' S	5° 59,98' W	0,0	S 5	RMT	surface	
PS65/622-1	10.04.04	04:19	69° 20,46' S	6° 0,00' W	0,0	SSW 6	RMT	heave	GE 72.1 auf 434m ausgesteckt
PS65/622-1	10.04.04	04:46	69° 21,65' S	6° 0,15' W	2260,0	SSW 4	RMT	on deck	
PS65/622-2	10.04.04	04:54	69° 21,79' S	6° 0,17' W	0,0	SSW 4	CTD/RO	surface	
PS65/622-2	10.04.04	05:17	69° 21,87' S	6° 0,23' W	0,0	SSW 4	CTD/RO	at depth	991m
PS65/622-2	10.04.04	05:43	69° 21,88' S	6° 0,31' W	2260,0	SW 7	CTD/RO	on deck	Eisbedeckung: 9/10, Eisberge: 0
PS65/623-1	10.04.04	08:01	69° 39,64' S	6° 0,32' W	0,0	WSW 6	RMT	surface	
PS65/623-1	10.04.04	08:19	69° 40,56' S	6° 0,54' W	0,0	W 6	RMT	heave	
PS65/623-1	10.04.04	08:48	69° 41,91' S	5° 59,94' W	2306,4	W 8	RMT	on deck	
PS65/623-2	10.04.04	09:03	69° 42,31' S	5° 59,75' W	2333,2	WSW 8	CTD/RO	surface	
PS65/623-2	10.04.04	09:17	69° 42,35' S	5° 59,64' W	2335,6	WSW 9	CTD/RO	Information	Eisbedeckung 8/10, 5 Eisberge
PS65/623-2	10.04.04	09:25	69° 42,36' S	5° 59,59' W	2336,4	WSW 8	CTD/RO	at depth	auf 998m
PS65/623-2	10.04.04	09:55	69° 42,44' S	5° 59,39' W	2342,4	WSW 7	CTD/RO	on deck	
PS65/623-3	10.04.04	10:04	69° 42,46' S	5° 59,33' W	2344,0	WSW 8	MN	surface	
PS65/623-3	10.04.04	10:41	69° 42,54' S	5° 59,07' W	2370,0	WSW 9	MN	at depth	auf 1078m
PS65/623-3	10.04.04	11:18	69° 42,59' S	5° 58,73' W	2378,4	WSW 9	MN	on deck	
PS65/624-1	10.04.04	13:28	69° 59,23' S	5° 58,95' W	0,0	WSW 15	RMT	surface	Standard-RMT 5/10 Neueis/Keine Eisb. im 3sm-Bereich
PS65/624-1	10.04.04	13:44	69° 59,68' S	6° 0,68' W	0,0	WSW 14	RMT	heave	GE72.1 436m ausgesteckt
PS65/624-1	10.04.04	14:12	70° 0,52' S	6° 3,55' W	1,0	WSW 13	RMT	on deck	
PS65/624-2	10.04.04	14:24	70° 0,54' S	6° 3,67' W	0,0	WSW 13	CTD/RO	surface	
PS65/624-2	10.04.04	14:48	70° 0,38' S	6° 3,45' W	1883,6	WSW 12	CTD/RO	at depth	EL31 1000m ausgesteckt
PS65/624-2	10.04.04	15:15	70° 0,19' S	6° 3,14' W	1884,4	WSW 15	CTD/RO	on deck	
PS65/624-3	10.04.04	15:38	70° 1,75' S	6° 6,27' W	1831,6	WSW 14	SUIT	surface	
PS65/624-3	10.04.04	15:51	70° 2,02' S	6° 6,65' W	0,0	WSW 15	SUIT	start trawl	GE52.2 120m ausgesteckt
PS65/624-3	10.04.04	16:03	70° 2,18' S	6° 8,23' W	0,0	WSW 15	SUIT	stop trawl	
PS65/624-3	10.04.04	16:20	70° 2,10' S	6° 8,22' W	1830,0	WSW 15	SUIT	on deck	
PS65/625-1	10.04.04	19:42	70° 18,58' S	6° 1,18' W	0,0	WSW 16	SUIT	surface	
PS65/625-1	10.04.04	20:09	70° 18,49' S	6° 2,73' W	0,0	WSW 17	SUIT	stop trawl	
PS65/625-1	10.04.04	20:34	70° 18,30' S	6° 3,49' W	238,0	WSW 15	SUIT	on deck	
PS65/625-2	10.04.04	21:09	70° 18,27' S	6° 3,65' W	226,8	WSW 15	CTD/RO	surface	
PS65/625-2	10.04.04	21:19	70° 18,27' S	6° 3,58' W	227,2	W 16	CTD/RO	at depth	auf 207m
PS65/625-2	10.04.04	21:28	70° 18,24' S	6° 3,57' W	226,8	WSW 16	CTD/RO	on deck	

PS65/625-3	10.04.04	21:57	70° 18,17' S	6° 5,15' W	0,0	WSW 17	RMT	surface	
PS65/625-3	10.04.04	22:09	70° 18,42' S	6° 6,37' W	0,0	WSW 17	RMT	heave	
PS65/625-3	10.04.04	22:36	70° 18,52' S	6° 9,23' W	230,0	WSW 18	RMT	on deck	Eisbedeckung 9/10 4 eisberge im 3sm umkreis
PS65/625-4	10.04.04	23:00	70° 18,51' S	6° 9,17' W	0,0	WSW 18	MN	surface	
PS65/625-4	10.04.04	23:11	70° 18,53' S	6° 9,14' W	336,8	WSW 17	MN	at depth	auf 286m
PS65/625-4	10.04.04	23:26	70° 18,55' S	6° 8,87' W	327,6	WSW 18	MN	on deck	
PS65/625-5	10.04.04	23:38	70° 18,41' S	6° 9,00' W	338,8	WSW 21	BONGO	surface	
PS65/625-5	10.04.04	23:48	70° 18,43' S	6° 8,90' W	336,4	WSW 20	BONGO	at depth	auf 200m
PS65/625-5	11.04.04	00:01	70° 18,48' S	6° 8,74' W	328,4	WSW 21	BONGO	on deck	
PS65/626-1	11.04.04	05:02	70° 19,74' S	3° 57,88' W	0,0	WSW 16	RMT	surface	
PS65/626-1	11.04.04	05:19	70° 19,86' S	3° 58,90' W	0,0	WSW 15	RMT	heave	GE 72.1 auf 467m ausgesteckt
PS65/626-1	11.04.04	05:48	70° 20,11' S	4° 0,82' W	495,0	SW 14	RMT	on deck	
PS65/626-2	11.04.04	06:01	70° 20,31' S	4° 0,48' W	493,6	SW 11	CTD/RO	surface	
PS65/626-2	11.04.04	06:15	70° 20,27' S	3° 59,40' W	503,2	SW 10	CTD/RO	at depth	495m
PS65/626-2	11.04.04	06:36	70° 20,18' S	3° 58,05' W	499,2	SSW 8	CTD/RO	on deck	
PS65/626-3	11.04.04	06:49	70° 19,98' S	3° 57,23' W	498,8	SSW 8	MN	surface	Eisbedeckung: 9/10 Pfannkucheneis/Eisschlamm, Eisb.: 0
PS65/626-3	11.04.04	06:59	70° 19,94' S	3° 56,69' W	498,8	S 7	MN	at depth	267m
PS65/626-3	11.04.04	07:10	70° 19,87' S	3° 56,14' W	496,8	S 6	MN	on deck	
PS65/626-4	11.04.04	07:14	70° 19,85' S	3° 55,95' W	492,4	SSE 6	MN	surface	
PS65/626-4	11.04.04	07:23	70° 19,80' S	3° 55,56' W	495,6	SSE 5	MN	at depth	271m
PS65/626-4	11.04.04	07:36	70° 19,71' S	3° 55,03' W	500,0	S 4	MN	on deck	
PS65/627-1	11.04.04	10:19	69° 59,92' S	3° 59,21' W	0,0	WSW 7	RMT	surface	
PS65/627-1	11.04.04	10:37	69° 59,11' S	4° 0,02' W	0,0	SW 8	RMT	heave	Eisbedeckung 7/10 2 Eisberge im Umkreis
PS65/627-1	11.04.04	11:09	69° 57,66' S	4° 1,79' W	43,0	SW 8	RMT	on deck	
PS65/627-2	11.04.04	11:39	69° 57,08' S	4° 3,45' W	1100,0	SW 9	LD	surface	Eisdrift boje auf einer 20m_Scholle ausgebracht
PS65/627-3	11.04.04	12:15	69° 57,20' S	4° 4,88' W	2106,4	WSW 9	CTD/RO	surface	
PS65/627-3	11.04.04	12:21	69° 57,17' S	4° 5,27' W	2104,4	SW 10	CTD/RO	on deck	Abbruch wegen Sensorvereisung
PS65/627-4	11.04.04	12:30	69° 57,11' S	4° 5,84' W	2114,8	WSW 10	CTD/RO	surface	
PS65/627-4	11.04.04	12:33	69° 57,10' S	4° 6,05' W	2118,8	SW 10	CTD/RO	on deck	2. Abbruch wegen Vereisung
PS65/628-1	11.04.04	15:00	69° 39,30' S	4° 0,24' W	0,0	SW 10	RMT	surface	RMT-Standard 9/10 Neueisbildung./Keine Eisb. im 3 sm-Bereich

PS65/628-1	11.04.04	15:16	69° 39,63' S	4° 2,06' W	0,0	SW 10	RMT	heave	GE72.1 469m ausgesteckt
PS65/628-1	11.04.04	15:46	69° 40,17' S	4° 5,61' W	1,0	SW 8	RMT	on deck	
PS65/628-2	11.04.04	16:01	69° 40,03' S	4° 6,08' W	0,0	SW 7	CTD/RO	surface	
PS65/628-2	11.04.04	16:23	69° 39,80' S	4° 6,51' W	2673,6	S 7	CTD/RO	at depth	999m
PS65/628-2	11.04.04	16:48	69° 39,47' S	4° 6,94' W	2728,0	SSW 8	CTD/RO	on deck	
PS65/628-3	11.04.04	16:51	69° 39,43' S	4° 7,00' W	2730,4	SSW 7	NFLOAT	surface	Test
PS65/628-4	11.04.04	16:58	69° 39,32' S	4° 7,14' W	2738,0	SSW 7	MN	surface	
PS65/628-4	11.04.04	17:34	69° 38,93' S	4° 7,28' W	2694,4	SW 9	MN	at depth	1081m
PS65/628-4	11.04.04	18:13	69° 38,41' S	4° 7,95' W	2667,2	SW 8	MN	on deck	
PS65/628-5	11.04.04	18:23	69° 38,27' S	4° 8,24' W	2657,2	SW 8	BONGO	surface	
PS65/628-5	11.04.04	18:35	69° 38,11' S	4° 8,57' W	2660,4	SW 8	BONGO	at depth	200m
PS65/628-5	11.04.04	18:48	69° 37,94' S	4° 8,88' W	2692,8	SW 8	BONGO	on deck	
PS65/628-6	11.04.04	18:52	69° 37,87' S	4° 8,98' W	0,0	SW 8	BONGO	surface	
PS65/628-6	11.04.04	19:05	69° 37,69' S	4° 9,33' W	0,0	SSW 8	BONGO	at depth	200m
PS65/628-6	11.04.04	19:19	69° 37,48' S	4° 9,71' W	2690,0	SSW 7	BONGO	on deck	
PS65/628-7	11.04.04	19:21	69° 37,45' S	4° 9,77' W	0,0	SSW 7	BONGO	surface	
PS65/628-7	11.04.04	19:32	69° 37,29' S	4° 10,07' W	0,0	SW 6	BONGO	at depth	200m
PS65/628-7	11.04.04	19:43	69° 37,14' S	4° 10,36' W	2690,0	SW 6	BONGO	on deck	
PS65/629-1	11.04.04	22:14	69° 19,28' S	4° 1,86' W	0,0	WSW 13	SUIT	surface	
PS65/629-1	11.04.04	23:28	69° 19,16' S	4° 2,97' W	3045,0	SW 13	SUIT	on deck	
PS65/629-2	12.04.04	00:03	69° 19,42' S	4° 4,05' W	3061,6	WSW 11	CTD/RO	surface	
PS65/629-2	12.04.04	00:26	69° 19,36' S	4° 4,01' W	3052,8	SW 13	CTD/RO	at depth	EL31 995m ausgesteckt
PS65/629-2	12.04.04	00:50	69° 19,30' S	4° 3,69' W	3038,0	SW 10	CTD/RO	on deck	
PS65/629-3	12.04.04	01:01	69° 19,23' S	4° 3,44' W	0,0	WSW 11	RMT	surface	Standard-RMT 4/10 Treibeis/Keine Eisb. im 3sm-Bereich
PS65/629-3	12.04.04	01:21	69° 19,78' S	4° 5,35' W	0,0	SW 11	RMT	heave	GE72.1 498m ausgesteckt
PS65/629-3	12.04.04	01:50	69° 20,53' S	4° 7,88' W	1,0	WSW 12	RMT	on deck	
PS65/629-4	12.04.04	02:12	69° 20,53' S	4° 7,88' W	0,0	WSW 10	BONGO	surface	
PS65/629-4	12.04.04	02:24	69° 20,48' S	4° 7,74' W	0,0	SW 13	BONGO	at depth	SE32.2 219m ausgesteckt
PS65/629-4	12.04.04	02:38	69° 20,41' S	4° 7,43' W	1,0	WSW 10	BONGO	on deck	
PS65/630-1	12.04.04	05:44	69° 0,36' S	4° 0,05' W	0,0	SW 12	RMT	surface	
PS65/630-1	12.04.04	06:01	68° 59,59' S	4° 0,04' W	0,0	WSW 13	RMT	heave	GE 72.1 auf 462m ausgesteckt
PS65/630-1	12.04.04	06:29	68° 58,39' S	4° 0,75' W	3230,0	SW 10	RMT	on deck	

PS65/630-2	12.04.04	07:03	68° 58,11' S	4° 1,23' W	3505,6	SW 14	CTD/RO	surface	
PS65/630-2	12.04.04	07:25	68° 58,09' S	4° 1,05' W	3520,8	WSW 12	CTD/RO	at depth	992m
PS65/630-2	12.04.04	07:51	68° 58,03' S	4° 0,42' W	3504,4	SW 13	CTD/RO	on deck	Eisbedeckung: 6/10, Eisberge: 2
PS65/631-1	12.04.04	10:15	68° 39,32' S	4° 2,14' W	0,0	WSW 12	RMT	surface	
PS65/631-1	12.04.04	10:27	68° 39,56' S	4° 3,29' W	0,0	WSW 12	RMT	heave	Eisbedeckung 6/10 Keine Eisberge
PS65/631-1	12.04.04	10:54	68° 40,00' S	4° 5,79' W	3500,0	WSW 13	RMT	on deck	
PS65/631-2	12.04.04	11:23	68° 39,84' S	4° 6,35' W	3582,8	W 12	CTD/RO	surface	
PS65/631-3	12.04.04	11:29	68° 39,78' S	4° 6,22' W	3585,2	WSW 12	HN	surface	
PS65/631-2	12.04.04	11:43	68° 39,63' S	4° 5,92' W	3593,2	WSW 12	CTD/RO	at depth	auf 1005m
PS65/631-3	12.04.04	11:46	68° 39,59' S	4° 5,87' W	3596,0	WSW 14	HN	on deck	
PS65/631-2	12.04.04	12:09	68° 39,32' S	4° 5,39' W	3619,2	WSW 13	CTD/RO	on deck	
PS65/632-1	12.04.04	14:30	68° 19,36' S	3° 59,17' W	0,0	SW 13	RMT	surface	Standard-RMT 2-3/10 Treibeis/Keine Eisb. im 3 sm-Bereich
PS65/632-1	12.04.04	14:48	68° 19,96' S	4° 0,68' W	0,0	WSW 14	RMT	heave	GE72.1 469m ausgesteckt
PS65/632-1	12.04.04	15:19	68° 20,80' S	4° 2,88' W	4007,0	SW 14	RMT	on deck	
PS65/632-2	12.04.04	15:30	68° 20,71' S	4° 2,65' W	0,0	WSW 14	CTD/RO	surface	
PS65/632-2	12.04.04	15:52	68° 20,57' S	4° 2,29' W	4010,8	SW 16	CTD/RO	at depth	EL31 1026m ausgesteckt
PS65/632-2	12.04.04	16:19	68° 20,46' S	4° 1,55' W	4014,0	SW 13	CTD/RO	on deck	
PS65/633-1	12.04.04	18:46	67° 59,71' S	3° 59,60' W	0,0	SW 14	RMT	surface	
PS65/633-1	12.04.04	19:03	68° 0,30' S	4° 0,67' W	0,0	SW 15	RMT	heave	GE 72.1 423m ausgesteckt
PS65/633-1	12.04.04	19:31	68° 1,17' S	4° 2,25' W	4250,0	SW 16	RMT	on deck	Eisbedeckung: Treibeisfelder, Eisberge: 0
PS65/633-2	12.04.04	19:45	68° 0,95' S	4° 1,64' W	4259,6	SSW 15	CTD/RO	surface	
PS65/633-2	12.04.04	20:10	68° 0,91' S	4° 1,46' W	4259,6	SW 15	CTD/RO	at depth	auf 993m
PS65/633-2	12.04.04	20:35	68° 0,94' S	4° 1,51' W	4259,6	SW 15	CTD/RO	on deck	
PS65/633-3	12.04.04	20:42	68° 0,91' S	4° 1,42' W	4259,2	SW 14	SUIT	surface	
PS65/633-3	12.04.04	21:15	68° 1,52' S	4° 3,40' W	4500,0	SSW 12	SUIT	on deck	
PS65/633-4	12.04.04	21:35	68° 1,60' S	4° 3,86' W	0,0	SSW 14	MN	surface	
PS65/633-4	12.04.04	22:11	68° 1,68' S	4° 3,68' W	0,0	SW 13	MN	at depth	auf 1061m
PS65/633-4	12.04.04	22:48	68° 1,27' S	4° 2,92' W	4500,0	SW 13	MN	on deck	
PS65/633-5	12.04.04	22:55	68° 1,16' S	4° 2,64' W	0,0	SSW 14	BONGO	surface	
PS65/633-5	12.04.04	23:02	68° 1,15' S	4° 2,69' W	0,0	SW 13	BONGO	at depth	auf 150m
PS65/633-5	12.04.04	23:15	68° 1,07' S	4° 2,33' W	4560,0	SW 14	BONGO	on deck	
PS65/633-6	12.04.04	23:17	68° 1,08' S	4° 2,34' W	0,0	SSW 14	BONGO	surface	

PS65/633-6	12.04.04	23:21	68° 1,02' S	4° 2,27' W	0,0	SW 14	BONGO	at depth	auf 150m
PS65/633-6	12.04.04	23:31	68° 0,85' S	4° 2,13' W	4650,0	SW 14	BONGO	on deck	
PS65/634-1	13.04.04	02:05	67° 39,73' S	3° 59,06' W	0,0	SW 15	RMT	surface	Standard-RMT/Kein Eis/Keine Eisberge im 3 sm-Bereich
PS65/634-1	13.04.04	02:22	67° 40,37' S	3° 59,90' W	0,0	SW 14	RMT	heave	GE72.1 447m ausgesteckt
PS65/634-1	13.04.04	02:50	67° 41,37' S	4° 1,32' W	1,0	SSW 14	RMT	on deck	
PS65/634-2	13.04.04	03:16	67° 39,74' S	3° 59,54' W	0,0	SW 14	RMT	surface	Standard-RMT
PS65/634-2	13.04.04	03:33	67° 40,31' S	4° 0,46' W	0,0	SW 13	RMT	heave	GE72.1 238m ausgesteckt
PS65/634-2	13.04.04	03:50	67° 40,80' S	4° 1,36' W	1,0	SW 15	RMT	on deck	
PS65/635-1	13.04.04	06:25	67° 19,64' S	3° 59,53' W	0,0	SW 15	RMT	surface	
PS65/635-1	13.04.04	06:38	67° 20,08' S	3° 59,94' W	0,0	SSW 15	RMT	heave	Ge 72.1 auf 379m ausgesteckt
PS65/635-1	13.04.04	07:03	67° 20,92' S	4° 0,96' W	4500,0	SSW 14	RMT	on deck	Eisbedeckung: 0 , Eisberge: 0
PS65/636-1	13.04.04	09:49	66° 59,73' S	3° 59,21' W	0,0	SSW 12	RMT	surface	
PS65/636-1	13.04.04	10:02	67° 0,19' S	3° 59,51' W	0,0	SW 12	RMT	heave	Kein Eis
PS65/636-1	13.04.04	10:22	67° 0,76' S	4° 0,56' W	4726,0	SSW 12	RMT	on deck	
PS65/636-2	13.04.04	10:34	67° 0,79' S	4° 0,53' W	4725,6	SSW 11	CTD/RO	surface	
PS65/636-2	13.04.04	10:56	67° 0,84' S	4° 0,24' W	4724,8	SSW 11	CTD/RO	at depth	auf 991m
PS65/636-2	13.04.04	11:22	67° 0,94' S	3° 59,79' W	4725,2	SW 10	CTD/RO	on deck	
PS65/636-3	13.04.04	11:32	67° 0,89' S	3° 59,60' W	4723,6	SSW 9	MN	surface	
PS65/636-3	13.04.04	12:07	67° 1,04' S	3° 58,95' W	0,0	SW 9	MN	at depth	EL30 1087m ausgesteckt
PS65/636-3	13.04.04	12:48	67° 1,12' S	3° 58,71' W	1,0	SW 10	MN	on deck	
PS65/636-4	13.04.04	12:56	67° 1,13' S	3° 58,63' W	0,0	SW 10	BONGO	surface	
PS65/636-4	13.04.04	13:09	67° 1,14' S	3° 58,56' W	0,0	SW 6	BONGO	at depth	SE32.2 200m ausgesteckt
PS65/636-4	13.04.04	13:22	67° 1,23' S	3° 58,51' W	1,0	SSW 9	BONGO	on deck	
PS65/637-1	13.04.04	16:03	66° 39,94' S	4° 0,04' W	0,0	S 4	RMT	surface	Standard-RMT/Kein Eis/Keine Eisberge im 3 sm-Bereich
PS65/637-1	13.04.04	16:20	66° 40,67' S	3° 59,54' W	0,0	S 5	RMT	heave	GE 72.1 auf 460m ausgesteckt
PS65/637-1	13.04.04	16:48	66° 41,65' S	3° 58,73' W	4500,0	SSE 4	RMT	on deck	Kein Eis/Eisberge
PS65/638-1	13.04.04	19:26	66° 20,38' S	4° 0,14' W	0,0	SE 5	RMT	surface	Kein Eis/Eisberge
PS65/638-1	13.04.04	19:42	66° 19,70' S	3° 59,96' W	0,0	SE 4	RMT	heave	GE 72.1 auf 460m ausgesteckt
PS65/638-1	13.04.04	20:10	66° 18,53' S	3° 59,82' W	4340,0	ESE 4	RMT	on deck	
PS65/639-1	13.04.04	22:24	65° 59,87' S	3° 59,94' W	0,0	SSE 3	SUIT	surface	
PS65/639-1	13.04.04	23:02	65° 58,94' S	4° 4,29' W	4871,6	SSE 4	SUIT	stop trawl	Keine Eisbedeckung/Eisberge

PS65/639-1	13.04.04	23:16	65° 58,77' S	4° 5,19' W	4871,6	SSE 4	SUIT	on deck	
PS65/639-2	13.04.04	23:38	65° 58,97' S	4° 5,24' W	4871,2	S 5	CTD/RO	surface	
PS65/639-2	14.04.04	00:02	65° 59,04' S	4° 5,06' W	4870,8	S 6	CTD/RO	at depth	EL31 997m ausgesteckt
PS65/639-2	14.04.04	00:26	65° 59,27' S	4° 4,96' W	4870,8	S 7	CTD/RO	on deck	
PS65/639-3	14.04.04	00:34	65° 59,37' S	4° 4,93' W	4870,4	SSW 6	RMT	surface	Standard-RMT
PS65/639-3	14.04.04	00:50	66° 0,06' S	4° 5,20' W	4864,8	SSW 6	RMT	heave	GE72.1 417m ausgesteckt
PS65/639-3	14.04.04	01:17	66° 1,16' S	4° 5,64' W	4860,0	SSW 6	RMT	on deck	
PS65/640-1	14.04.04	03:58	65° 39,90' S	3° 59,28' W	0,0	SW 9	RMT	surface	Standard-RMT/Kein Eis/Keine Eisberge im 3 sm-Bereich
PS65/640-1	14.04.04	04:12	65° 40,43' S	4° 0,06' W	0,0	WSW 9	RMT	heave	GE 72.1 auf 394m ausgesteckt
PS65/640-1	14.04.04	04:37	65° 41,35' S	4° 1,33' W	4860,0	SW 8	RMT	on deck	Kein Eis/Eisberge
PS65/641-1	14.04.04	07:19	65° 19,52' S	3° 59,50' W	0,0	SSW 13	RMT	surface	Kein Eis/Eisberge
PS65/641-1	14.04.04	07:35	65° 20,13' S	4° 0,11' W	0,0	SSW 12	RMT	heave	GE 72.1 auf 449m ausgesteckt
PS65/641-1	14.04.04	08:04	65° 21,08' S	4° 0,88' W	4700,0	SSW 15	RMT	on deck	
PS65/642-1	14.04.04	10:44	64° 59,39' S	4° 0,47' W	0,0	S 19	RMT	surface	
PS65/642-1	14.04.04	10:53	64° 59,76' S	4° 0,52' W	0,0	SSW 17	RMT	heave	
PS65/642-1	14.04.04	11:19	65° 0,59' S	4° 0,75' W	4650,0	SSW 19	RMT	on deck	Kein Eis/Eisberge
PS65/642-2	14.04.04	11:29	65° 0,66' S	4° 0,64' W	0,0	SSW 18	CTD/RO	surface	
PS65/642-2	14.04.04	11:50	65° 0,62' S	4° 0,30' W	0,0	SSW 17	CTD/RO	at depth	auf 1004m
PS65/642-2	14.04.04	12:19	65° 0,82' S	4° 0,15' W	5104,0	S 14	CTD/RO	on deck	
PS65/643-1	14.04.04	14:57	64° 39,77' S	3° 59,51' W	0,0	SSW 17	RMT	surface	Standard-RMT/Kein Eis/Keine Eisberge im 3 sm-Bereich
PS65/643-1	14.04.04	15:14	64° 40,45' S	4° 0,54' W	0,0	SSW 14	RMT	heave	GE72.1 436m ausgesteckt
PS65/643-1	14.04.04	15:43	64° 41,58' S	4° 2,22' W	1,0	SSW 15	RMT	on deck	
PS65/644-1	14.04.04	18:32	64° 19,66' S	3° 59,79' W	0,0	SW 17	RMT	surface	
PS65/644-1	14.04.04	18:51	64° 20,20' S	4° 0,43' W	0,0	SW 14	RMT	on deck	Auf Grund von Windenproblemen abgebrochen
PS65/644-1	14.04.04	19:20	64° 19,96' S	3° 59,83' W	0,0	SSW 15	RMT	surface	Kein Eis/Eisberge
PS65/644-1	14.04.04	19:36	64° 20,49' S	4° 0,45' W	0,0	SW 13	RMT	heave	GE 72.1 auf 432m ausgesteckt
PS65/644-1	14.04.04	20:01	64° 21,42' S	4° 1,49' W	4560,0	SW 13	RMT	on deck	
PS65/645-1	14.04.04	22:42	63° 59,59' S	4° 0,09' W	0,0	SW 12	RMT	surface	
PS65/645-1	14.04.04	22:57	63° 59,86' S	4° 0,95' W	0,0	SW 14	RMT	heave	Kein EIS/Eisberge
PS65/645-1	14.04.04	23:26	64° 0,44' S	4° 2,54' W	4560,0	SW 15	RMT	on deck	

PS65/645-2	14.04.04	23:45	64° 0,64' S	4° 3,05' W	5244,4	SW 15	RMT	surface	Standard-RMT
PS65/645-2	15.04.04	00:02	64° 1,11' S	4° 3,89' W	5246,8	SSW 16	RMT	heave	GE52.2 450m ausgesteckt
PS65/645-2	15.04.04	00:31	64° 1,96' S	4° 5,27' W	5245,2	SW 14	RMT	on deck	
PS65/645-3	15.04.04	01:16	63° 59,88' S	3° 59,82' W	5246,8	SSW 14	CTD/RO	surface	
PS65/645-3	15.04.04	01:42	63° 59,76' S	3° 59,99' W	5244,4	SSW 15	CTD/RO	at depth	EL31 983m ausgesteckt
PS65/645-3	15.04.04	02:11	63° 59,61' S	4° 0,39' W	5245,6	SSW 12	CTD/RO	on deck	
PS65/645-4	15.04.04	02:20	63° 59,62' S	4° 0,43' W	0,0	SW 14	SUIT	surface	
PS65/645-4	15.04.04	02:27	63° 59,77' S	4° 0,83' W	0,0	SSW 14	SUIT	start trawl	GE52.2 150m ausgesteckt
PS65/645-4	15.04.04	02:48	64° 0,51' S	4° 2,63' W	0,0	SSW 13	SUIT	stop trawl	
PS65/645-4	15.04.04	03:00	64° 0,44' S	4° 3,35' W	1,0	SSW 14	SUIT	on deck	
PS65/646-1	15.04.04	09:59	64° 0,03' S	1° 59,82' W	0,0	SW 11	SUIT	surface	
PS65/646-1	15.04.04	10:30	64° 0,95' S	2° 2,16' W	0,0	SW 12	SUIT	stop trawl	Kein Eis/Eisberge
PS65/646-1	15.04.04	10:43	64° 0,97' S	2° 2,62' W	5230,0	SW 12	SUIT	on deck	
PS65/646-2	15.04.04	11:00	64° 0,97' S	2° 2,74' W	5189,2	SW 11	CTD/RO	surface	
PS65/646-2	15.04.04	11:22	64° 0,98' S	2° 2,44' W	5188,0	SSW 14	CTD/RO	at depth	auf 991m
PS65/646-2	15.04.04	11:47	64° 1,03' S	2° 2,09' W	5188,0	SW 13	CTD/RO	on deck	
PS65/646-3	15.04.04	11:53	64° 1,04' S	2° 2,05' W	0,0	SW 14	RMT	surface	
PS65/646-3	15.04.04	12:09	64° 1,62' S	2° 2,69' W	0,0	SW 13	RMT	heave	GE52.2 401m ausgesteckt
PS65/646-3	15.04.04	12:32	64° 2,46' S	2° 3,80' W	1,0	SW 12	RMT	on deck	
									Standard-RMT/Kein Eis/Keine Eisberge im 3sm-Bereich
PS65/647-1	15.04.04	15:05	64° 19,42' S	2° 0,51' W	0,0	SW 13	RMT	surface	
PS65/647-1	15.04.04	15:20	64° 19,80' S	2° 1,66' W	0,0	WSW 11	RMT	heave	GE52.2 408m ausgesteckt
PS65/647-1	15.04.04	15:43	64° 20,46' S	2° 2,94' W	1,0	S 10	RMT	on deck	
PS65/648-1	15.04.04	18:24	64° 39,64' S	1° 59,70' W	0,0	SSW 10	RMT	surface	
PS65/648-1	15.04.04	18:39	64° 40,13' S	2° 0,37' W	0,0	SSW 12	RMT	heave	GE 52.2 auf 402m ausgesteckt
PS65/648-1	15.04.04	19:04	64° 40,96' S	2° 1,52' W	5200,0	SSW 11	RMT	on deck	Kein Eis/Eisberge
PS65/649-1	15.04.04	21:38	64° 59,46' S	2° 0,04' W	0,0	S 7	RMT	surface	
PS65/649-1	15.04.04	21:52	65° 0,05' S	1° 59,95' W	0,0	S 8	RMT	heave	Kein Eis/Eisberg
PS65/649-1	15.04.04	22:14	65° 0,96' S	1° 59,97' W	5046,0	SSW 8	RMT	on deck	
PS65/649-2	15.04.04	22:26	65° 1,01' S	1° 59,85' W	5049,2	SSW 9	CTD/RO	surface	
PS65/649-3	15.04.04	22:34	65° 1,05' S	1° 59,82' W	5048,8	SSW 8	HN	surface	
PS65/649-2	15.04.04	22:46	65° 1,10' S	1° 59,84' W	5047,6	SW 3	CTD/RO	at depth	auf 991m
PS65/649-3	15.04.04	22:52	65° 1,14' S	1° 59,89' W	5046,8	SW 8	HN	on deck	

PS65/649-2	15.04.04	23:12	65° 1,21' S	1° 59,96' W	5046,8	SSW 7	CTD/RO	on deck	
PS65/649-4	15.04.04	23:16	65° 1,22' S	1° 59,98' W	5046,8	SSW 8	SUIT	surface	
PS65/649-4	15.04.04	23:32	65° 1,66' S	2° 0,43' W	5037,2	SW 7	SUIT	start trawl	
PS65/649-4	15.04.04	23:56	65° 2,80' S	2° 1,34' W	0,0	SSW 8	SUIT	stop trawl	
PS65/649-4	16.04.04	00:08	65° 2,85' S	2° 1,74' W	1,0	SW 8	SUIT	on deck	
PS65/650-1	16.04.04	02:37	65° 19,55' S	1° 59,29' W	0,0	SW 6	RMT	surface	Standard-RMT/Kein Eis/Keine Eisberge im 3 sm-Bereich
PS65/650-1	16.04.04	02:52	65° 20,00' S	2° 0,30' W	0,0	WSW 4	RMT	heave	GE52.2 401m ausgesteckt
PS65/650-1	16.04.04	03:18	65° 20,77' S	2° 2,08' W	1,0	SSW 5	RMT	on deck	
PS65/651-1	16.04.04	05:50	65° 39,49' S	2° 0,15' W	0,0	WSW 5	RMT	surface	
PS65/651-1	16.04.04	06:04	65° 40,03' S	2° 0,26' W	0,0	WSW 6	RMT	heave	GE 52.2 auf 401m ausgesteckt
PS65/651-1	16.04.04	06:30	65° 41,11' S	2° 0,04' W	5000,0	WNW 2	RMT	on deck	Kein Eis/Eisberge
PS65/652-1	16.04.04	08:51	65° 59,61' S	2° 0,02' W	0,0	WNW 5	RMT	surface	
PS65/652-1	16.04.04	09:08	66° 0,18' S	1° 59,97' W	0,0	WNW 4	RMT	heave	Kein Eis/Eisberge
PS65/652-1	16.04.04	09:35	66° 1,18' S	2° 0,25' W	4971,6	WNW 2	RMT	on deck	
PS65/652-2	16.04.04	09:50	66° 1,20' S	2° 0,30' W	4971,2	WNW 4	CTD/RO	surface	
PS65/652-3	16.04.04	09:51	66° 1,20' S	2° 0,30' W	4971,2	WNW 3	HN	surface	
PS65/652-3	16.04.04	10:01	66° 1,24' S	2° 0,35' W	4971,2	WSW 8	HN	on deck	
PS65/652-2	16.04.04	10:15	66° 1,19' S	2° 0,32' W	4970,8	WSW 6	CTD/RO	at depth	auf 996m
PS65/652-2	16.04.04	10:40	66° 1,34' S	2° 0,29' W	4970,4	W 5	CTD/RO	on deck	
PS65/653-1	16.04.04	12:51	66° 19,57' S	2° 0,26' W	0,0	WSW 7	RMT	surface	Standard-RMT/Kein Eis/Keine Eisberge im 3 sm-Bereich
PS65/653-1	16.04.04	13:07	66° 20,03' S	2° 1,53' W	0,0	WSW 7	RMT	heave	GE52.2 403m ausgesteckt
PS65/653-1	16.04.04	13:30	66° 20,65' S	2° 3,40' W	1,0	W 7	RMT	on deck	
PS65/654-1	16.04.04	15:47	66° 39,76' S	1° 59,17' W	0,0	WSW 5	RMT	surface	Standard-RMT/Kein Eis/Keine Eisberge im 3 sm-Bereich
PS65/654-1	16.04.04	16:03	66° 39,89' S	2° 0,79' W	0,0	W 6	RMT	heave	GE52.2 402m ausgesteckt
PS65/654-1	16.04.04	16:27	66° 40,08' S	2° 2,93' W	5000,0	WSW 7	RMT	on deck	Kein Eis/Eisberge
PS65/655-1	16.04.04	19:12	66° 59,58' S	1° 59,94' W	0,0	W 5	RMT	surface	
PS65/655-1	16.04.04	19:27	67° 0,20' S	2° 0,02' W	0,0	W 6	RMT	heave	GE 52.2 auf 401m ausgesteckt
PS65/655-1	16.04.04	19:53	67° 1,22' S	2° 0,08' W	4694,0	W 7	RMT	on deck	Kein Eis/Eisberge
PS65/655-2	16.04.04	20:03	67° 1,31' S	2° 0,07' W	4692,8	W 7	CTD/RO	surface	
PS65/655-2	16.04.04	20:26	67° 1,40' S	2° 0,17' W	4693,6	WSW 5	CTD/RO	at depth	auf 994 m

PS65/655-2	16.04.04	20:55	67° 1,57' S	2° 0,21' W	4689,6	W 4	CTD/RO	on deck	
PS65/655-3	16.04.04	21:08	67° 1,61' S	2° 0,35' W	4689,2	W 7	MN	surface	
PS65/655-3	16.04.04	21:37	67° 1,73' S	2° 0,44' W	4688,4	W 6	MN	at depth	auf 1083m
PS65/655-3	16.04.04	22:15	67° 1,99' S	2° 0,46' W	4687,2	WNW 9	MN	on deck	
PS65/656-1	17.04.04	00:22	67° 19,79' S	1° 58,64' W	0,0	W 6	RMT	surface	Standard-RMT/Kein Eis/Keine Eisberge im 3 sm-Bereich
PS65/656-1	17.04.04	00:37	67° 19,77' S	2° 0,08' W	0,0	W 6	RMT	heave	GE52.2 402m ausgesteckt
PS65/656-1	17.04.04	01:00	67° 19,71' S	2° 2,30' W	1,0	WNW 7	RMT	on deck	
PS65/657-1	17.04.04	03:23	67° 39,67' S	1° 58,58' W	0,0	WSW 5	RMT	surface	Standard-RMT/Treibeis/Keine Eisberge im 3 sm-Bereich
PS65/657-1	17.04.04	03:36	67° 39,81' S	1° 59,94' W	0,0	W 8	RMT	heave	GE52.2 402m ausgesteckt
PS65/657-1	17.04.04	04:00	67° 40,12' S	2° 2,36' W	4700,0	W 7	RMT	on deck	
PS65/657-2	17.04.04	04:17	67° 40,08' S	2° 1,94' W	0,0	W 7	SUIT	surface	
PS65/657-2	17.04.04	04:24	67° 40,17' S	2° 2,64' W	0,0	W 5	SUIT	start trawl	
PS65/657-2	17.04.04	04:54	67° 40,61' S	2° 6,25' W	0,0	WSW 5	SUIT	stop trawl	
PS65/657-2	17.04.04	05:07	67° 40,61' S	2° 6,99' W	4700,0	WSW 6	SUIT	on deck	
PS65/658-1	17.04.04	07:25	67° 59,47' S	2° 0,16' W	0,0	WSW 5	RMT	surface	
PS65/658-1	17.04.04	07:41	68° 0,07' S	2° 0,51' W	0,0	WSW 5	RMT	heave	GE 52.2 auf 403m ausgesteckt/ Treibeisfelder, keine Eisb.
PS65/658-1	17.04.04	08:05	68° 0,98' S	2° 0,10' W	4418,4	WSW 4	RMT	on deck	
PS65/658-2	17.04.04	08:19	68° 1,26' S	2° 0,64' W	4416,4	WSW 4	CTD/RO	surface	
PS65/658-2	17.04.04	08:40	68° 1,30' S	2° 1,08' W	4420,0	WSW 4	CTD/RO	at depth	auf 996m
PS65/658-2	17.04.04	09:03	68° 1,31' S	2° 1,28' W	4420,8	WSW 4	CTD/RO	on deck	
PS65/658-3	17.04.04	09:16	68° 1,33' S	2° 1,54' W	4418,4	WSW 3	MN	surface	
PS65/658-3	17.04.04	09:48	68° 1,32' S	2° 1,76' W	4418,8	WSW 4	MN	at depth	auf 1064m
PS65/658-3	17.04.04	10:27	68° 1,30' S	2° 1,97' W	4421,6	WSW 4	MN	on deck	
PS65/659-1	17.04.04	12:41	68° 19,91' S	2° 0,27' W	4233,2	W 2	CTD/RO	surface	1/10 Treibeis/Keine Eisberge im 3 sm-Bereich
PS65/659-1	17.04.04	13:08	68° 19,89' S	2° 0,90' W	4228,8	W 3	CTD/RO	at depth	EL31 996m ausgesteckt
PS65/659-1	17.04.04	13:37	68° 19,92' S	2° 1,18' W	4227,6	W 3	CTD/RO	on deck	
PS65/659-2	17.04.04	13:50	68° 19,92' S	2° 0,98' W	4228,4	WNW 3	RMT	surface	Standard-RMT
PS65/659-2	17.04.04	14:04	68° 19,94' S	1° 59,27' W	4236,4	W 3	RMT	heave	GE52.2 402m ausgesteckt
PS65/659-2	17.04.04	14:31	68° 19,96' S	1° 56,38' W	4253,6	WNW 3	RMT	on deck	
PS65/659-3	17.04.04	14:49	68° 19,97' S	1° 56,54' W	0,0	W 3	MN	surface	

PS65/659-3	17.04.04	15:24	68° 20,04' S	1° 56,63' W	0,0	W 3	MN	at depth	EL30 1078m ausgesteckt
PS65/659-3	17.04.04	16:02	68° 20,08' S	1° 56,65' W	1,0	WSW 4	MN	on deck	
PS65/660-1	17.04.04	18:25	68° 39,72' S	2° 0,18' W	0,0	WNW 3	RMT	surface	
PS65/660-1	17.04.04	18:39	68° 40,30' S	2° 0,18' W	0,0	W 4	RMT	heave	GE 52.2 auf 407m ausgesteckt
PS65/660-1	17.04.04	19:03	68° 41,27' S	2° 0,15' W	3645,6	WNW 3	RMT	on deck	
PS65/660-2	17.04.04	19:16	68° 41,41' S	2° 0,08' W	3658,8	WNW 2	CTD	surface	
PS65/660-2	17.04.04	19:37	68° 41,41' S	1° 59,96' W	3664,0	W 1	CTD	at depth	991m
PS65/660-2	17.04.04	20:04	68° 41,40' S	1° 59,86' W	3666,4	W 1	CTD	on deck	Eisbedeckung: 9/10, Eisberge: 0
PS65/661-1	17.04.04	22:30	68° 59,36' S	2° 1,68' W	0,0	NW 1	SUIT	surface	10/10 Eisbedeckung/ 1 Eisberg
PS65/661-1	17.04.04	22:42	68° 59,63' S	2° 2,04' W	0,0	WNW 3	SUIT	start trawl	
PS65/661-1	17.04.04	23:07	69° 0,51' S	2° 2,87' W	0,0	WNW 3	SUIT	stop trawl	
PS65/661-1	17.04.04	23:20	69° 0,60' S	2° 2,86' W	0,0	W 1	SUIT	on deck	
PS65/661-2	17.04.04	23:36	69° 0,66' S	2° 2,71' W	3247,2	W 2	CTD/RO	surface	
PS65/661-2	17.04.04	23:58	69° 0,69' S	2° 2,50' W	3246,4	W 1	CTD/RO	at depth	EL31 991m ausgesteckt
PS65/661-2	18.04.04	00:25	69° 0,74' S	2° 2,26' W	3244,0	SSW 0	CTD/RO	on deck	
PS65/661-3	18.04.04	00:37	69° 0,58' S	2° 1,69' W	3256,4	W 0	RMT	surface	Standard-RMT 9/10 Pfannkucheneis/Keine Eisb. im 3 sm-Bereich
PS65/661-3	18.04.04	00:51	69° 0,27' S	2° 0,28' W	0,0	W 1	RMT	heave	GE52.2 404m ausgesteckt
PS65/661-3	18.04.04	01:16	68° 59,61' S	1° 57,99' W	1,0	SSE 0	RMT	on deck	
PS65/661-4	18.04.04	01:37	68° 59,38' S	1° 58,03' W	0,0	SE 1	MN	surface	
PS65/661-4	18.04.04	02:14	68° 59,48' S	1° 58,11' W	0,0	NE 1	MN	at depth	EL30 1073m ausgesteckt
PS65/661-4	18.04.04	02:53	68° 59,54' S	1° 58,29' W	1,0	NE 1	MN	on deck	
PS65/661-5	18.04.04	03:05	68° 59,55' S	1° 58,40' W	0,0	E 1	BONGO	surface	
PS65/661-5	18.04.04	03:18	68° 59,56' S	1° 58,46' W	0,0	NNE 2	BONGO	at depth	SE32.2 200m ausgesteckt
PS65/661-5	18.04.04	03:30	68° 59,56' S	1° 58,44' W	1,0	NNE 1	BONGO	on deck	
PS65/661-6	18.04.04	03:36	68° 59,57' S	1° 58,49' W	0,0	NNE 2	BONGO	surface	
PS65/661-6	18.04.04	03:47	68° 59,58' S	1° 58,56' W	0,0	NNE 2	BONGO	at depth	SE32.2 200m ausgesteckt
PS65/661-6	18.04.04	04:00	68° 59,60' S	1° 58,57' W	3260,0	NNE 2	BONGO	on deck	
PS65/662-1	18.04.04	07:23	69° 19,54' S	2° 0,24' W	0,0	SE 6	RMT	surface	Eisbedeckung: 9/10, Eisberge: 3
PS65/662-1	18.04.04	07:38	69° 20,13' S	2° 0,25' W	0,0	SE 6	RMT	heave	GE 52.2 auf 403m ausgesteckt
PS65/662-1	18.04.04	08:02	69° 21,07' S	2° 0,42' W	2982,8	SE 6	RMT	on deck	
PS65/662-2	18.04.04	08:21	69° 21,41' S	2° 0,53' W	2976,4	SE 6	CTD/RO	surface	
PS65/662-2	18.04.04	08:43	69° 21,37' S	2° 1,05' W	2980,0	SE 6	CTD/RO	at depth	

PS65/662-2	18.04.04	09:10	69° 21,35' S	2° 1,67' W	2984,4	SE 6	CTD/RO	on deck	
PS65/663-1	18.04.04	11:49	69° 38,77' S	2° 0,44' W	0,0	SE 6	RMT	surface	9/10 Eisbedeckung, 3 Eisberge im 3 nm Range
PS65/663-1	18.04.04	12:03	69° 39,23' S	1° 59,54' W	0,0	SE 6	RMT	heave	GE52.2 403m ausgesteckt
PS65/663-1	18.04.04	12:25	69° 39,85' S	1° 57,69' W	1,0	SE 6	RMT	on deck	
PS65/663-2	18.04.04	12:47	69° 40,02' S	1° 57,97' W	2838,4	ESE 5	CTD/RO	surface	
PS65/663-2	18.04.04	13:41	69° 40,20' S	1° 59,80' W	2845,6	SE 5	CTD/RO	at depth	EL31 2826m ausgesteckt
PS65/663-2	18.04.04	14:42	69° 40,36' S	2° 2,01' W	2844,8	SE 6	CTD/RO	on deck	
PS65/664-1	18.04.04	17:14	69° 59,69' S	2° 0,42' W	0,0	ESE 6	RMT	surface	
PS65/664-1	18.04.04	17:28	70° 0,28' S	1° 59,61' W	0,0	SE 6	RMT	heave	auf 403m ausgesteckt
PS65/664-1	18.04.04	17:55	70° 0,72' S	1° 57,15' W	3447,2	ESE 6	RMT	on deck	
PS65/664-2	18.04.04	18:14	70° 0,66' S	1° 57,41' W	3416,0	SE 6	CTD/RO	surface	
PS65/664-2	18.04.04	18:38	70° 0,62' S	1° 57,83' W	3396,0	SE 5	CTD/RO	at depth	335m
PS65/664-2	18.04.04	19:10	70° 0,55' S	1° 58,39' W	3474,4	SE 6	CTD/RO	on deck	
PS65/664-3	18.04.04	19:17	70° 0,54' S	1° 58,51' W	381,6	SE 5	MN	surface	
PS65/664-3	18.04.04	19:26	70° 0,53' S	1° 58,67' W	395,6	SE 5	MN	at depth	266m
PS65/664-3	18.04.04	19:39	70° 0,50' S	1° 58,86' W	407,6	SE 5	MN	on deck	
PS65/664-4	18.04.04	19:53	70° 0,48' S	1° 58,87' W	415,6	SE 5	SUIT	surface	Eisbedeckung: 10/10, Eisberge: 0
PS65/664-4	18.04.04	21:03	69° 59,43' S	1° 57,35' W	686,4	SE 4	SUIT	on deck	
PS65/665-1	19.04.04	06:51	69° 20,38' S	0° 0,95' W	0,0	S 1	RMT	surface	
PS65/665-1	19.04.04	07:04	69° 20,04' S	0° 0,42' W	0,0	SW 1	RMT	heave	auf 402m ausgesteckt
PS65/665-1	19.04.04	07:37	69° 19,44' S	0° 1,08' E	2437,2	SSE 2	RMT	on deck	
PS65/665-2	19.04.04	07:50	69° 19,42' S	0° 0,83' E	2450,8	SSE 2	CTD/RO	surface	Eisbedeckung: 9/10, Eisberge 3
PS65/665-3	19.04.04	08:29	69° 19,32' S	0° 0,21' E	2453,6	SW 2	HN	surface	
PS65/665-2	19.04.04	08:40	69° 19,30' S	0° 0,09' E	2425,2	SW 2	CTD/RO	at depth	auf 2403m
PS65/665-3	19.04.04	08:41	69° 19,30' S	0° 0,07' E	2424,4	WSW 2	HN	on deck	
PS65/665-4	19.04.04	09:08	69° 19,19' S	0° 0,23' W	2417,2	SW 2	HN	surface	
PS65/665-4	19.04.04	09:17	69° 19,16' S	0° 0,33' W	2414,4	SSW 2	HN	on deck	
PS65/665-2	19.04.04	09:30	69° 19,10' S	0° 0,44' W	2410,8	WSW 2	CTD/RO	on deck	
PS65/665-5	19.04.04	09:36	69° 19,08' S	0° 0,50' W	2408,4	SSW 3	BONGO	surface	
PS65/665-5	19.04.04	09:42	69° 19,05' S	0° 0,56' W	2406,0	SW 3	BONGO	at depth	auf 100m
PS65/665-5	19.04.04	09:49	69° 19,03' S	0° 0,63' W	2398,8	SW 2	BONGO	on deck	
PS65/665-6	19.04.04	09:52	69° 19,01' S	0° 0,66' W	2397,2	SW 3	BONGO	surface	

PS65/665-6	19.04.04	09:53	69° 19,01' S	0° 0,67' W	2403,2	SW 3	BONGO	at depth	auf 50m
PS65/665-6	19.04.04	10:02	0° 0,00' N	0° 0,00' E	2450,0	N 0	BONGO	on deck	
PS65/665-7	19.04.04	10:03	69° 18,96' S	0° 0,74' W	2394,0	SW 2	BONGO	surface	
PS65/665-7	19.04.04	10:06	69° 18,94' S	0° 0,77' W	2392,8	WSW 2	BONGO	at depth	auf 50m
PS65/665-7	19.04.04	10:10	69° 18,93' S	0° 0,80' W	2392,8	WSW 2	BONGO	on deck	
PS65/665-8	19.04.04	10:20	69° 18,88' S	0° 0,88' W	2407,6	WSW 2	HN	surface	
PS65/665-9	19.04.04	10:21	69° 18,87' S	0° 0,89' W	2398,0	SW 3	MN	surface	
PS65/665-8	19.04.04	10:27	69° 18,84' S	0° 0,93' W	2428,0	SW 3	HN	on deck	
PS65/665-9	19.04.04	10:55	69° 18,69' S	0° 1,14' W	2435,2	WSW 2	MN	at depth	auf 1072m
PS65/665-9	19.04.04	11:35	69° 18,48' S	0° 1,51' W	2450,0	SW 2	MN	on deck	
PS65/665-10	19.04.04	12:25	69° 16,07' S	0° 0,97' W	0,0	SW 2	LD	surface	
PS65/666-1	19.04.04	14:20	69° 5,84' S	0° 0,60' E	0,0	W 5	LD	surface	
PS65/667-1	19.04.04	15:15	69° 0,20' S	0° 0,08' W	0,0	WSW 4	RMT	surface	Standard-RMT 10/10 FY-Ice/2 Eisberge im 3sm-Bereich
PS65/667-1	19.04.04	15:30	68° 59,53' S	0° 0,07' W	0,0	WSW 4	RMT	heave	GE52.2 402m ausgesteckt
PS65/667-1	19.04.04	15:53	68° 58,58' S	0° 0,06' W	1,0	WSW 5	RMT	on deck	
PS65/667-2	19.04.04	16:03	68° 58,46' S	0° 0,70' E	3392,8	WSW 5	CTD/RO	surface	
PS65/667-3	19.04.04	16:05	68° 58,45' S	0° 0,73' E	3392,0	WSW 4	HN	surface	
PS65/667-3	19.04.04	16:21	68° 58,38' S	0° 0,85' E	3393,6	WSW 3	HN	on deck	
PS65/667-2	19.04.04	17:05	68° 58,27' S	0° 1,49' E	3381,6	WSW 7	CTD/RO	at depth	3355m
PS65/667-2	19.04.04	18:15	68° 58,10' S	0° 2,76' E	3355,6	WSW 6	CTD/RO	on deck	
PS65/667-4	19.04.04	18:29	68° 58,06' S	0° 2,87' E	3354,8	WSW 7	MN	surface	
PS65/667-4	19.04.04	19:04	68° 57,94' S	0° 3,35' E	3346,4	WSW 8	MN	at depth	1086m
PS65/667-4	19.04.04	19:45	68° 57,76' S	0° 4,01' E	3333,2	WSW 8	MN	on deck	
PS65/667-5	19.04.04	19:55	68° 57,75' S	0° 3,55' E	3333,0	SW 8	AFLOAT	surface	
PS65/668-1	19.04.04	22:15	68° 39,37' S	0° 2,41' W	0,0	WSW 11	SUIT	surface	
PS65/668-1	19.04.04	22:56	68° 39,95' S	0° 4,41' W	3440,4	WSW 10	SUIT	on deck	4/10 Eisbedeckung, kein Eisberg in 3sm Range
PS65/668-2	19.04.04	23:23	68° 39,99' S	0° 3,87' W	3013,2	SW 10	CTD/RO	surface	
PS65/668-2	19.04.04	23:45	68° 39,97' S	0° 3,30' W	0,0	WSW 8	CTD/RO	at depth	auf 993m
PS65/668-2	20.04.04	00:12	68° 39,83' S	0° 2,81' W	3687,2	WSW 9	CTD/RO	on deck	
PS65/668-3	20.04.04	00:19	68° 39,85' S	0° 2,94' W	3673,6	WSW 11	RMT	surface	Standard-RMT
PS65/668-3	20.04.04	00:32	68° 40,17' S	0° 4,01' W	0,0	WSW 9	RMT	heave	GE52.2 403m ausgesteckt

PS65/668-3	20.04.04	00:55	68° 40,68' S	0° 5,95' W	1,0	WSW 9	RMT	on deck	
PS65/669-1	20.04.04	03:26	68° 19,63' S	0° 1,14' E	0,0	WSW 9	RMT	surface	Standard-RMT/Treibbeisfelder/Keine Eisberge im 3 sm-Bereich
PS65/669-1	20.04.04	03:40	68° 19,94' S	0° 0,22' W	0,0	SW 9	RMT	heave	GE52.2 402m ausgesteckt
PS65/669-1	20.04.04	04:06	68° 20,61' S	0° 2,45' W	3761,2	WSW 9	RMT	on deck	
PS65/669-2	20.04.04	04:18	68° 20,63' S	0° 2,69' W	3618,4	WSW 9	CTD/RO	surface	
PS65/669-2	20.04.04	04:40	68° 20,44' S	0° 2,61' W	3634,0	SW 9	CTD/RO	at depth	994m
PS65/669-2	20.04.04	05:08	68° 20,28' S	0° 2,65' W	3868,8	SW 9	CTD/RO	on deck	
PS65/670-1	20.04.04	07:29	68° 0,48' S	0° 0,11' W	0,0	SW 9	RMT	surface	Eisbedeckung: 3/10, Keine Eisberge
PS65/670-1	20.04.04	07:43	67° 59,87' S	0° 0,41' W	0,0	SW 8	RMT	heave	403m ausgesteckt
PS65/670-1	20.04.04	08:07	67° 58,82' S	0° 0,53' W	3670,0	SW 8	RMT	on deck	
PS65/670-2	20.04.04	08:25	67° 58,77' S	0° 0,71' W	0,0	WSW 7	MN	surface	
PS65/670-2	20.04.04	08:59	67° 58,90' S	0° 0,79' W	0,0	WSW 7	MN	at depth	auf 1066m
PS65/670-2	20.04.04	09:32	67° 58,97' S	0° 0,53' W	3526,4	WSW 8	MN	on deck	
PS65/670-3	20.04.04	09:50	67° 59,75' S	0° 1,64' W	3828,0	WSW 8	CTD/RO	surface	
PS65/670-3	20.04.04	11:19	68° 0,02' S	0° 0,75' W	4516,4	SW 10	CTD/RO	at depth	auf 4502m
PS65/670-3	20.04.04	12:45	67° 59,75' S	0° 1,27' E	4520,8	WSW 9	CTD/RO	on deck	
PS65/670-4	20.04.04	13:01	67° 59,21' S	0° 1,10' E	4524,8	SW 8	AFLOAT	surface	
									Standard-RMT/Kein Eis/Keine Eisberge im 3 sm-Bereich
PS65/671-1	20.04.04	15:18	67° 39,61' S	0° 0,85' E	0,0	SW 7	RMT	surface	Standard-RMT/Kein Eis/Keine Eisberge im 3 sm-Bereich
PS65/671-1	20.04.04	15:33	67° 40,17' S	0° 0,03' E	0,0	SW 5	RMT	heave	GE52.2 403m ausgesteckt
PS65/671-1	20.04.04	15:55	67° 40,95' S	0° 1,10' W	1,0	SW 4	RMT	on deck	
PS65/672-1	20.04.04	18:28	67° 19,93' S	0° 0,77' E	0,0	W 4	RMT	surface	Kein Eis/Eisberge
PS65/672-1	20.04.04	18:42	67° 20,16' S	0° 0,36' W	0,0	W 4	RMT	heave	auf 402m ausgesteckt
PS65/672-1	20.04.04	19:08	67° 20,62' S	0° 2,69' W	5000,0	SSW 6	RMT	on deck	
PS65/672-2	20.04.04	19:16	67° 20,56' S	0° 2,93' W	0,0	SSW 4	RMT	surface	
PS65/672-2	20.04.04	19:31	67° 20,11' S	0° 2,66' W	0,0	SW 4	RMT	heave	auf 400m ausgesteckt
PS65/672-2	20.04.04	19:55	67° 19,69' S	0° 0,63' W	5000,0	WSW 7	RMT	on deck	
PS65/673-1	20.04.04	22:15	67° 0,06' S	0° 0,08' E	0,0	WSW 3	SUIT	surface	
PS65/673-1	20.04.04	22:55	66° 58,07' S	0° 0,54' E	4650,0	WNW 6	SUIT	on deck	Kein Eis bzw. Eisberge
PS65/673-2	20.04.04	23:14	66° 58,02' S	0° 0,75' E	0,0	NW 6	MN	surface	
PS65/673-2	20.04.04	23:45	66° 57,97' S	0° 0,69' E	0,0	WNW 6	MN	at depth	auf 1071m
PS65/673-2	21.04.04	00:22	66° 57,90' S	0° 0,71' E	1,0	W 6	MN	on deck	

PS65/673-3	21.04.04	00:47	66° 59,91' S	0° 1,36' E	0,0	W 6	RMT	surface	Standard-RMT
PS65/673-3	21.04.04	01:01	66° 59,89' S	0° 0,04' W	0,0	W 6	RMT	heave	GE52.2 402m ausgesteckt
PS65/673-3	21.04.04	01:25	66° 59,93' S	0° 2,14' W	1,0	W 5	RMT	on deck	
PS65/673-4	21.04.04	01:33	66° 59,92' S	0° 2,17' W	0,0	W 6	RMT	surface	Standard-RMT
PS65/673-4	21.04.04	01:44	66° 59,97' S	0° 3,35' W	0,0	W 4	RMT	heave	GE52.2 303m ausgesteckt
PS65/673-4	21.04.04	02:18	67° 0,09' S	0° 6,64' W	1,0	W 6	RMT	on deck	
PS65/673-5	21.04.04	02:48	66° 59,93' S	0° 0,27' W	4711,2	W 6	CTD/RO	surface	
PS65/673-5	21.04.04	04:15	66° 59,83' S	0° 1,12' W	4712,0	W 5	CTD/RO	at depth	4681m
PS65/673-5	21.04.04	05:51	66° 59,90' S	0° 1,79' W	4714,8	NNW 6	CTD/RO	on deck	
PS65/673-5	21.04.04	05:56	66° 59,92' S	0° 1,89' W	4714,0	NNW 6	AFLOAT	surface	
PS65/674-1	21.04.04	08:15	66° 40,55' S	0° 0,04' W	0,0	NW 5	RMT	surface	kein Eis/ Eisberge
PS65/674-1	21.04.04	08:30	66° 40,04' S	0° 0,03' E	0,0	NW 6	RMT	heave	
PS65/674-1	21.04.04	08:54	66° 39,13' S	0° 0,13' E	4650,0	NNW 5	RMT	on deck	
PS65/674-2	21.04.04	08:59	66° 39,08' S	0° 0,19' E	0,0	NNW 6	HN	surface	
PS65/674-2	21.04.04	09:24	66° 38,93' S	0° 0,46' E	4760,0	W 4	HN	on deck	
PS65/675-1	21.04.04	11:34	66° 20,41' S	0° 0,00' E	0,0	NW 4	RMT	surface	
PS65/675-1	21.04.04	11:50	66° 19,94' S	0° 0,08' E	0,0	NNW 6	RMT	heave	Kein Eis/ Eisberge
PS65/675-1	21.04.04	12:16	66° 19,01' S	0° 0,19' E	1,0	NNW 6	RMT	on deck	
PS65/675-2	21.04.04	12:17	66° 19,01' S	0° 0,21' E	0,0	NNW 7	HN	surface	
PS65/675-2	21.04.04	12:47	66° 19,08' S	0° 0,79' E	1,0	NNW 6	HN	on deck	Diverse Handnetze
PS65/676-1	21.04.04	15:00	66° 0,27' S	0° 0,10' E	0,0	N 7	RMT	surface	Standard-RMT/Kein Eis/Keine Eisberge im 3sm-Bereich
PS65/676-1	21.04.04	15:14	65° 59,67' S	0° 0,22' E	0,0	NNW 6	RMT	heave	GE52.2 402m ausgesteckt
PS65/676-1	21.04.04	15:38	65° 58,63' S	0° 0,31' E	1,0	N 6	RMT	on deck	
PS65/676-2	21.04.04	15:51	65° 58,53' S	0° 0,42' E	3510,8	NNW 6	CTD/RO	surface	
PS65/676-3	21.04.04	16:14	65° 58,58' S	0° 0,58' E	3502,8	NNW 10	HN	surface	
PS65/676-3	21.04.04	16:47	65° 58,50' S	0° 0,37' E	3512,0	NNW 8	HN	on deck	
PS65/676-2	21.04.04	16:55	65° 58,47' S	0° 0,27' E	3517,6	NNW 8	CTD/RO	at depth	3461m
PS65/676-2	21.04.04	18:05	65° 58,32' S	0° 0,27' W	3545,2	NNE 5	CTD/RO	on deck	
PS65/677-1	21.04.04	20:14	65° 40,47' S	0° 0,10' E	3791,6	NW 8	RMT	surface	
PS65/677-1	21.04.04	20:27	65° 39,83' S	0° 0,23' E	3743,2	N 9	RMT	heave	
PS65/677-1	21.04.04	20:49	65° 38,82' S	0° 0,34' E	3727,6	NW 8	RMT	on deck	Kein Eis/Eisberge
PS65/677-2	21.04.04	21:02	65° 38,71' S	0° 0,03' E	3755,2	NW 7	RMT	surface	

PS65/677-2	21.04.04	21:27	65° 39,61' S	0° 0,24' E	3731,2	NW 6	RMT	heave	
PS65/677-2	21.04.04	21:34	65° 39,81' S	0° 0,30' E	3738,0	NW 6	RMT	on deck	
PS65/677-3	21.04.04	21:50	65° 39,61' S	0° 0,49' W	3792,0	NNW 6	SUIT	surface	
PS65/677-3	21.04.04	22:30	65° 37,69' S	0° 2,55' W	3800,0	NNW 6	SUIT	on deck	
PS65/678-1	22.04.04	00:38	65° 20,40' S	0° 0,07' W	3808,4	N 8	RMT	surface	Standard-RMT/Kein Eis/Keine Eisberge im 3 sm-Bereich
PS65/678-1	22.04.04	00:53	65° 19,77' S	0° 0,32' W	0,0	N 7	RMT	heave	GE52.2 400m ausgesteckt
PS65/678-1	22.04.04	01:19	65° 18,77' S	0° 0,77' W	1,0	NNW 4	RMT	on deck	
PS65/678-2	22.04.04	01:35	65° 18,66' S	0° 0,93' W	0,0	NNE 7	RMT	surface	Standard-RMT
PS65/678-2	22.04.04	01:43	65° 18,32' S	0° 1,14' W	0,0	NNE 6	RMT	heave	GE52.2 202m ausgesteckt
PS65/678-2	22.04.04	02:06	65° 17,41' S	0° 1,48' W	1,0	N 6	RMT	on deck	
PS65/679-1	22.04.04	04:08	65° 0,42' S	0° 0,07' W	0,0	NW 6	RMT	surface	
PS65/679-1	22.04.04	04:25	64° 59,73' S	0° 0,04' E	0,0	NW 6	RMT	heave	auf 400m ausgesteckt
PS65/679-1	22.04.04	04:50	64° 58,79' S	0° 0,02' E	3719,6	NNW 4	RMT	on deck	
PS65/679-2	22.04.04	04:59	64° 58,79' S	0° 0,15' E	3717,6	NNW 5	RMT	surface	Kein Eis, Keine Eisberge
PS65/679-2	22.04.04	05:07	64° 58,50' S	0° 0,05' E	3716,8	NNW 4	RMT	heave	202m ausgesteckt
PS65/679-2	22.04.04	05:31	64° 57,67' S	0° 0,23' W	3718,4	NW 4	RMT	on deck	
PS65/679-3	22.04.04	05:56	64° 59,95' S	0° 0,03' W	3736,0	NW 4	CTD/RO	surface	
PS65/679-3	22.04.04	07:07	64° 59,99' S	0° 0,24' W	3741,2	NNW 4	CTD/RO	at depth	auf 3695m
PS65/679-3	22.04.04	08:22	64° 59,97' S	0° 0,40' W	3743,2	NNW 4	CTD/RO	on deck	
PS65/679-4	22.04.04	08:28	64° 59,86' S	0° 0,30' W	3737,6	NW 4	AFLOAT	surface	
PS65/680-1	22.04.04	10:47	64° 40,19' S	0° 0,01' W	0,0	N 5	RMT	surface	
PS65/680-1	22.04.04	11:03	64° 39,55' S	0° 0,18' E	0,0	N 4	RMT	heave	
PS65/680-1	22.04.04	11:27	64° 38,65' S	0° 0,27' E	4650,0	N 5	RMT	on deck	
PS65/680-2	22.04.04	11:49	64° 38,64' S	0° 0,47' E	0,0	N 4	HN	surface	
PS65/680-2	22.04.04	11:57	64° 38,68' S	0° 0,56' E	1,0	NNW 5	HN	on deck	
PS65/681-1	22.04.04	14:32	64° 20,55' S	0° 0,03' W	0,0	N 0	RMT	surface	Standard-RMT/Kein Eis/Keine Eisberge im 3 sm-Bereich
PS65/681-1	22.04.04	14:47	64° 19,99' S	0° 0,00' W	0,0	NE 3	RMT	heave	GE52.2 402m ausgesteckt
PS65/681-1	22.04.04	15:09	64° 19,05' S	0° 0,11' E	1,0	NE 4	RMT	on deck	
PS65/682-1	22.04.04	17:27	64° 0,55' S	0° 0,04' W	0,0	ENE 5	RMT	surface	Kein Eis / Keine Eisberge
PS65/682-1	22.04.04	17:41	64° 0,01' S	0° 0,23' W	0,0	ENE 6	RMT	heave	auf 400m ausgesteckt
PS65/682-1	22.04.04	18:06	63° 59,00' S	0° 0,27' W	5203,6	ENE 6	RMT	on deck	

260

PS65/682-2	22.04.04	18:24	63° 58,90' S	0° 0,44' W	5204,0	NE 6	CTD/RO	surface	
PS65/682-2	22.04.04	20:00	63° 59,02' S	0° 0,92' W	5204,8	NE 7	CTD/RO	at depth	5190m
PS65/682-2	22.04.04	21:40	63° 58,61' S	0° 0,77' W	5320,0	NE 6	CTD/RO	on deck	
PS65/682-2	22.04.04	21:47	63° 58,60' S	0° 0,72' W	0,0	NE 6	SUIT	surface	
PS65/682-2	22.04.04	22:41	63° 56,98' S	0° 0,87' E	5230,0	ENE 7	SUIT	on deck	
PS65/682-3	22.04.04	22:56	63° 56,92' S	0° 0,91' E	5320,0	ENE 5	AFLOAT	surface	
PS65/683-1	23.04.04	00:55	63° 40,33' S	0° 1,00' W	0,0	ENE 6	RMT	surface	Standard-RMT/Kein Eis/Keine Eisberge im 3 sm-Bereich
PS65/683-1	23.04.04	01:10	63° 40,02' S	0° 0,22' E	0,0	NE 6	RMT	heave	GE52,2 401m ausgesteckt
PS65/683-1	23.04.04	01:37	63° 39,65' S	0° 2,31' E	1,0	ENE 7	RMT	on deck	
PS65/683-2	23.04.04	01:44	63° 39,67' S	0° 2,34' E	0,0	ENE 7	RMT	surface	Standard-RMT
PS65/683-2	23.04.04	01:52	63° 39,54' S	0° 3,05' E	0,0	ENE 7	RMT	heave	GE52,2 202m ausgesteckt
PS65/683-2	23.04.04	02:15	63° 39,31' S	0° 4,73' E	1,0	ENE 8	RMT	on deck	
PS65/684-1	23.04.04	04:41	63° 20,44' S	0° 1,09' W	0,0	ENE 9	RMT	surface	Kein Eis/Eisberge
PS65/684-1	23.04.04	04:55	63° 20,09' S	0° 0,53' W	0,0	ENE 12	RMT	heave	auf 403m ausgesteckt
PS65/684-1	23.04.04	05:20	63° 19,56' S	0° 0,86' E	5300,0	E 9	RMT	on deck	
PS65/685-1	23.04.04	08:13	63° 0,04' S	0° 0,93' W	0,0	E 10	RMT	surface	
PS65/685-1	23.04.04	08:27	63° 0,05' S	0° 0,19' E	0,0	E 9	RMT	heave	Kein Eis/Eisberge
PS65/685-1	23.04.04	08:54	63° 0,06' S	0° 2,15' E	5311,2	E 12	RMT	on deck	
PS65/685-2	23.04.04	09:03	63° 0,14' S	0° 2,07' E	5310,8	E 12	CTD/RO	surface	
PS65/685-2	23.04.04	10:40	63° 0,43' S	0° 1,60' E	5310,8	ESE 10	CTD/RO	at depth	auf 5287m
PS65/685-2	23.04.04	12:20	63° 0,47' S	0° 1,39' E	5310,0	E 10	CTD/RO	on deck	
PS65/686-1	23.04.04	15:30	62° 40,00' S	0° 1,46' W	0,0	E 12	RMT	surface	Standard-RMT/Kein Eis/Keine Eisberge im 3 sm-Bereich
PS65/686-1	23.04.04	15:43	62° 40,05' S	0° 0,33' W	0,0	E 12	RMT	heave	GE52,2 401m ausgesteckt
PS65/686-1	23.04.04	16:09	62° 40,26' S	0° 1,78' E	5300,0	E 12	RMT	on deck	
PS65/687-1	23.04.04	19:20	62° 20,01' S	0° 0,73' W	0,0	ESE 12	RMT	surface	Kein Eis/Eisberge
PS65/687-1	23.04.04	19:35	62° 20,08' S	0° 0,41' E	0,0	ESE 13	RMT	heave	auf 401m ausgesteckt
PS65/687-1	23.04.04	20:00	62° 20,34' S	0° 1,83' E	5210,0	ESE 12	RMT	on deck	
PS65/688-1	23.04.04	23:03	61° 59,91' S	0° 0,31' W	0,0	ESE 11	SUIT	surface	Kein Eis/Eisberge
PS65/688-1	23.04.04	23:43	62° 0,71' S	0° 3,17' E	5308,8	E 10	SUIT	on deck	
PS65/688-2	24.04.04	00:04	62° 0,82' S	0° 2,47' E	5371,6	ESE 11	CTD/RO	surface	
PS65/688-2	24.04.04	01:43	62° 1,27' S	0° 3,35' E	5370,8	ESE 8	CTD/RO	at depth	EL31 5379m ausgesteckt

PS65/688-2	24.04.04	03:26	62° 1,40' S	0° 4,54' E	5368,0	E 7	CTD/RO	on deck	
PS65/688-3	24.04.04	04:03	62° 0,10' S	0° 0,68' W	0,0	ESE 8	RMT	surface	
PS65/688-3	24.04.04	04:16	62° 0,38' S	0° 0,24' E	0,0	ESE 8	RMT	heave	auf 399m ausgesteckt
PS65/688-3	24.04.04	04:41	62° 0,91' S	0° 2,10' E	5300,0	ESE 8	RMT	on deck	
PS65/689-1	24.04.04	07:29	61° 40,05' S	0° 0,46' W	0,0	E 9	RMT	surface	Kein Eis/Eisberge
PS65/689-1	24.04.04	07:43	61° 39,95' S	0° 0,72' E	0,0	ESE 7	RMT	heave	auf 402m ausgesteckt
PS65/689-1	24.04.04	08:06	61° 39,76' S	0° 2,43' E	5320,0	ESE 10	RMT	on deck	
PS65/690-1	24.04.04	10:32	61° 20,43' S	0° 0,02' W	0,0	SE 6	RMT	surface	kein Eis/Eisberge
PS65/690-1	24.04.04	10:46	61° 19,91' S	0° 0,35' E	0,0	ESE 5	RMT	heave	
PS65/690-1	24.04.04	11:11	61° 19,61' S	0° 1,50' E	5120,0	E 7	RMT	on deck	
PS65/691-1	24.04.04	13:46	61° 0,04' S	0° 1,30' W	0,0	E 8	RMT	surface	Standard-RMT/Kein Eis/Keine Eisberge im 3sm-Bereich
PS65/691-1	24.04.04	14:00	61° 0,19' S	0° 0,47' W	0,0	E 7	RMT	heave	GE52.2 402m ausgesteckt
PS65/691-1	24.04.04	14:24	61° 0,22' S	0° 1,05' E	1,0	E 5	RMT	on deck	
PS65/691-2	24.04.04	14:38	61° 0,29' S	0° 1,04' E	5391,6	E 6	CTD/RO	surface	
PS65/691-2	24.04.04	16:19	61° 0,55' S	0° 1,73' E	5388,0	ESE 4	CTD/RO	at depth	auf 5378m
PS65/691-2	24.04.04	18:04	61° 0,84' S	0° 1,86' E	5385,2	E 5	CTD/RO	on deck	
PS65/691-3	24.04.04	18:09	61° 0,85' S	0° 1,88' E	5383,6	ESE 5	SUIT	surface	
PS65/691-3	24.04.04	18:15	61° 0,77' S	0° 2,60' E	5382,4	ESE 6	SUIT	start trawl	
PS65/691-3	24.04.04	18:40	61° 0,33' S	0° 6,04' E	0,0	ESE 5	SUIT	stop trawl	
PS65/691-3	24.04.04	18:51	61° 0,30' S	0° 6,60' E	5400,0	ESE 5	SUIT	on deck	
PS65/692-1	25.04.04	00:45	61° 0,98' S	1° 59,88' W	0,0	W 4	SUIT	surface	
PS65/692-1	25.04.04	00:52	61° 0,70' S	2° 0,11' W	0,0	W 4	SUIT	start trawl	GE52.2 120m ausgesteckt
PS65/692-1	25.04.04	01:18	60° 58,97' S	2° 1,17' W	0,0	WNW 3	SUIT	stop trawl	Beginn Hieven
PS65/692-1	25.04.04	01:28	60° 58,67' S	2° 1,24' W	5365,2	WNW 3	SUIT	on deck	
PS65/692-2	25.04.04	01:49	60° 58,58' S	2° 1,72' W	5363,2	NW 3	CTD/RO	surface	
PS65/692-2	25.04.04	03:26	60° 58,22' S	2° 3,04' W	5360,8	SW 4	CTD/RO	at depth	EL31 5372m ausgesteckt
PS65/692-2	25.04.04	05:07	60° 57,95' S	2° 4,07' W	5356,4	SW 1	CTD/RO	on deck	
PS65/692-3	25.04.04	05:31	60° 59,59' S	2° 0,15' W	5030,8	SSW 3	RMT	surface	
PS65/692-3	25.04.04	05:46	61° 0,22' S	2° 0,03' W	0,0	SSW 6	RMT	heave	auf 400m ausgesteckt
PS65/692-3	25.04.04	06:09	61° 1,11' S	1° 59,69' W	5000,0	VSW 10	RMT	on deck	
PS65/693-1	25.04.04	08:34	61° 19,85' S	1° 58,83' W	0,0	VSW 7	RMT	surface	Kein Eis/Eisberg
PS65/693-1	25.04.04	08:52	61° 19,99' S	2° 0,11' W	0,0	VSW 7	RMT	heave	

PS65/693-1	25.04.04	09:27	61° 20,40' S	2° 2,81' W	5320,0	WSW 6	RMT	on deck	
PS65/694-1	25.04.04	11:51	61° 39,93' S	1° 59,11' W	0,0	WSW 5	RMT	surface	kein Eis/Eisberge
PS65/694-1	25.04.04	12:07	61° 40,04' S	2° 0,58' W	0,0	W 5	RMT	heave	GE52.2 402m ausgesteckt
PS65/694-1	25.04.04	12:33	61° 40,18' S	2° 2,94' W	1,0	WSW 5	RMT	on deck	
PS65/695-1	25.04.04	14:59	62° 0,13' S	1° 58,58' W	0,0	WNW 2	RMT	surface	Standard-RMT/Kein Eis/Keine Eisberge im 3 sm-Bereich
PS65/695-1	25.04.04	15:15	62° 0,40' S	2° 0,17' W	0,0	W 2	RMT	heave	GE52.2 400m ausgesteckt
PS65/695-1	25.04.04	15:43	62° 0,81' S	2° 2,51' W	1,0	SSW 2	RMT	on deck	
PS65/695-2	25.04.04	15:51	62° 0,87' S	2° 2,74' W	5353,2	S 2	CTD/RO	surface	
PS65/695-2	25.04.04	17:28	62° 1,25' S	2° 3,91' W	5349,2	SSW 2	CTD/RO	at depth	auf 5357m
PS65/695-2	25.04.04	19:10	62° 1,56' S	2° 4,29' W	5347,6	SSE 3	CTD/RO	on deck	
PS65/696-1	25.04.04	21:22	62° 19,81' S	2° 0,34' W	0,0	SSE 6	SUIT	surface	Kein Eis/Eisberge
PS65/696-1	25.04.04	21:57	62° 21,20' S	1° 58,29' W	5120,0	SE 7	SUIT	on deck	
PS65/696-2	25.04.04	22:31	62° 19,19' S	2° 1,00' W	0,0	SE 8	RMT	surface	
PS65/696-2	25.04.04	22:49	62° 19,79' S	2° 0,04' W	0,0	SSE 8	RMT	heave	
PS65/696-2	25.04.04	23:14	62° 20,63' S	1° 58,75' W	5230,0	SE 9	RMT	on deck	
PS65/697-1	26.04.04	01:33	62° 39,48' S	2° 1,34' W	0,0	SE 10	RMT	surface	Standard-RMT/Kein Eis/Keine Eisberge im 3 sm-Bereich
PS65/697-1	26.04.04	01:49	62° 39,90' S	2° 0,25' W	0,0	SSE 11	RMT	heave	GE52.2 400m ausgesteckt
PS65/697-1	26.04.04	02:13	62° 40,55' S	1° 58,77' W	1,0	SSE 10	RMT	on deck	
PS65/698-1	26.04.04	04:34	62° 59,56' S	1° 59,92' W	0,0	SE 8	RMT	surface	
PS65/698-1	26.04.04	04:49	63° 0,08' S	2° 0,15' W	0,0	ESE 8	RMT	heave	auf 400m ausgesteckt
PS65/698-1	26.04.04	05:14	63° 0,78' S	2° 0,22' W	5200,0	SE 12	RMT	on deck	
PS65/698-2	26.04.04	05:25	63° 0,74' S	2° 0,37' W	5285,2	SSE 11	CTD/RO	surface	Kein Eis/Eisberge
PS65/698-2	26.04.04	07:02	63° 0,56' S	2° 0,21' W	5285,2	SSE 12	CTD/RO	at depth	5266m
PS65/698-2	26.04.04	08:43	63° 0,09' S	2° 0,61' W	5286,4	SSE 14	CTD/RO	on deck	
PS65/699-1	26.04.04	11:23	63° 19,45' S	2° 0,18' W	0,0	S 16	RMT	surface	Kein Eis/Eisberge
PS65/699-1	26.04.04	11:37	63° 19,96' S	2° 0,45' W	0,0	SSE 14	RMT	heave	
PS65/699-1	26.04.04	12:01	63° 20,88' S	2° 0,56' W	1,0	S 16	RMT	on deck	
PS65/700-1	26.04.04	13:22	63° 10,45' S	1° 43,47' W	0,0	S 17	CPR	into water	
PS65/700-1	27.04.04	08:05	59° 59,41' S	3° 29,34' E	5511,7	SW 8	CPR	on deck	
PS65/701-1	27.04.04	08:19	59° 59,04' S	3° 30,26' E	5368,1	SW 9	LANDER	surface	
PS65/701-2	27.04.04	08:34	59° 59,22' S	3° 31,14' E	5367,8	SW 8	MUC	surface	

PS65/701-2	27.04.04	11:32	59° 58,99' S	3° 32,63' E	5504,8	WSW 6	MUC	on deck	
PS65/701-3	27.04.04	11:35	59° 58,98' S	3° 32,62' E	5289,7	WSW 5	BWS	surface	
PS65/701-3	27.04.04	13:21	59° 59,11' S	3° 32,66' E	5399,4	WSW 2	BWS	at sea bottom	SE32.1 5317m ausgesteckt
PS65/701-3	27.04.04	13:29	59° 59,09' S	3° 32,62' E	5300,5	WSW 1	BWS	off bottom	
PS65/701-3	27.04.04	15:09	59° 59,09' S	3° 32,10' E	5343,8	NNE 2	BWS	on deck	
PS65/701-1	27.04.04	15:23	59° 58,93' S	3° 30,31' E	5364,8	NNE 2	LANDER	released	
PS65/701-1	27.04.04	15:29	59° 58,92' S	3° 30,14' E	0,0	N 2	LANDER	Information	Hydrophon an Deck
PS65/701-1	27.04.04	17:18	59° 59,04' S	3° 30,74' E	5350,0	NNE 6	LANDER	on Deck	
PS65/702-1	27.04.04	17:38	59° 58,93' S	3° 30,21' E	0,0	NNE 7	CPR	into water	
PS65/702-1	29.04.04	06:07	52° 35,35' S	9° 0,12' E	5300,0	WNW 17	CPR	on deck	
PS65/703-1	29.04.04	06:15	52° 35,12' S	9° 0,19' E	0,0	WNW 16	LANDER	surface	
PS65/703-2	29.04.04	06:36	52° 34,85' S	8° 59,50' E	3312,8	NW 16	MUC	surface	
PS65/703-2	29.04.04	07:42	52° 34,86' S	8° 59,58' E	3314,0	NW 16	MUC	at sea bottom	GE 52.2 auf 3298m
PS65/703-2	29.04.04	08:56	52° 35,17' S	9° 0,06' E	3320,0	NW 16	MUC	on deck	
PS65/703-3	29.04.04	09:03	52° 35,13' S	9° 0,11' E	3319,8	NW 16	CTD/RO	surface	
PS65/703-3	29.04.04	10:09	52° 35,34' S	9° 0,64' E	3337,5	NW 16	CTD/RO	at depth	auf 3299m
PS65/703-3	29.04.04	11:17	52° 35,59' S	9° 0,98' E	3361,0	NW 17	CTD/RO	on deck	
PS65/703-1	29.04.04	12:00	52° 35,08' S	9° 0,37' E	3334,2	NW 16	LANDER	released	
PS65/703-1	29.04.04	13:22	52° 35,30' S	9° 1,36' E	3383,8	NW 15	LANDER	on Deck	
PS65/703-4	29.04.04	13:31	52° 35,39' S	9° 1,79' E	3480,7	NW 16	AFLOAT	surface	
PS65/704-1	29.04.04	13:36	0° 0,00' N	0° 0,00' E	0,0	N 0	CPR	into water	
PS65/704-1	30.04.04	10:34	49° 1,11' S	12° 14,28' E	4336,0	W 14	CPR	on deck	
PS65/705-1	30.04.04	10:55	49° 0,06' S	12° 15,32' E	4293,0	W 14	LANDER	surface	
PS65/705-2	30.04.04	11:08	49° 0,29' S	12° 14,78' E	4302,0	W 15	MUC	surface	
PS65/705-3	30.04.04	12:20	49° 0,81' S	12° 15,30' E	4336,0	W 16	HN	surface	
PS65/705-2	30.04.04	12:32	49° 0,82' S	12° 15,06' E	4317,0	W 15	MUC	at sea bottom	GE52.2 4301m ausgesteckt
PS65/705-3	30.04.04	12:35	49° 0,83' S	12° 15,07' E	4318,0	W 15	HN	on deck	div. Handnetze für Plankton-Proben
PS65/705-2	30.04.04	13:53	49° 0,79' S	12° 14,78' E	4320,0	WSW 14	MUC	on deck	
PS65/705-4	30.04.04	14:05	49° 0,88' S	12° 14,84' E	4320,0	W 14	CTD/RO	surface	
PS65/705-4	30.04.04	15:33	49° 0,97' S	12° 14,82' E	4326,0	WSW 14	CTD/RO	at depth	EL31 4258m ausgesteckt
PS65/705-4	30.04.04	17:02	49° 1,35' S	12° 15,36' E	4347,0	WSW 12	CTD/RO	on deck	
PS65/705-1	30.04.04	17:25	48° 59,98' S	12° 15,46' E	4297,0	WSW 15	LANDER	released	
PS65/705-1	30.04.04	18:49	49° 0,07' S	12° 16,20' E	4290,0	WSW 15	LANDER	on Deck	

PS65/705-5	30.04.04	19:16	48° 59,98' S	12° 16,54' E	4284,0	WSW 17	MUC	surface	
PS65/705-5	30.04.04	20:23	49° 0,40' S	12° 17,13' E	4311,0	WSW 16	MUC	at sea bottom	auf 4279m
PS65/705-5	30.04.04	21:49	49° 1,16' S	12° 18,12' E	4355,0	WSW 16	MUC	on deck	
PS65/705-6	30.04.04	21:59	49° 1,17' S	12° 18,17' E	4353,0	WSW 20	NFLOAT	surface	
PS65/706-1	30.04.04	22:02	49° 0,97' S	12° 18,05' E	4374,0	WSW 18	CPR	into water	
PS65/706-1	01.05.04	08:16	47° 11,59' S	12° 39,86' E	4350,0	W 16	CPR	on deck	
PS65/707-1	01.05.04	08:33	47° 10,06' S	12° 40,31' E	0,0	W 17	MUC	surface	
PS65/707-1	01.05.04	10:08	47° 10,86' S	12° 41,70' E	4874,9	W 17	MUC	at sea bottom	auf 4925m
PS65/707-1	01.05.04	11:38	47° 11,74' S	12° 42,70' E	4866,6	W 17	MUC	on deck	
PS65/708-1	01.05.04	11:44	47° 11,69' S	12° 42,75' E	4788,3	W 15	CPR	into water	
PS65/708-1	02.05.04	09:50	44° 20,57' S	13° 30,30' E	4837,2	WNW 16	CPR	on deck	
PS65/709-1	02.05.04	10:04	44° 20,13' S	13° 30,50' E	4619,6	WNW 20	MUC	surface	
PS65/709-1	02.05.04	11:22	44° 20,17' S	13° 31,48' E	4742,0	WNW 18	MUC	at sea bottom	auf 4795m
PS65/709-1	02.05.04	12:48	44° 20,11' S	13° 32,10' E	4742,5	WNW 16	MUC	on deck	
PS65/709-2	02.05.04	13:05	44° 20,12' S	13° 32,21' E	4830,4	WNW 19	CTD/RO	surface	
PS65/709-2	02.05.04	14:35	44° 20,17' S	13° 32,37' E	4638,1	WNW 18	CTD/RO	at depth	EL31 4707m ausgesteckt
PS65/709-2	02.05.04	16:06	44° 20,13' S	13° 32,66' E	0,0	WNW 16	CTD/RO	on deck	

19. SHIP'S CREW / SCHIFFSBESATZUNG ANT XXI/4

01. Pahl, Uwe	Master	German
02. Grundmann, Uwe	1.Offc.	German
03. Pluder, Andreas	Ch.Eng.	German
04. Grimm, Sebastian	2.Offc.	German
05. Jahn, Thomas	2.Offc.	German
06. Spielke, Stefan	2.Offc.	German
07. Beiersdorf, Hansheinrich	Doctor	German
08. Hecht,Andreas	R.Offc.	German
09. Erreth Monostori, G.	1.Eng.	German
10. Hoffmann, Bernd	2.Eng.	German
11. Simon, Wolfgang	2.Eng.	German
13. Dimmler, Werner	Fielax-Elo	German
12. Holtz, Hartmut	Electr.	German
14. Kahrs, Thomas	Fielax-Elo	German
15. Nasis, Ilias	Fielax-Elo	German
16. Verhoven, Roger	Fielax-Elo	German
17. Clasen, Burkhard	Boatsw.	German
18. Neisner,Winfried	Carpenter	German
19. Burzan, Gerd-Ekkeh	A.B.	German
20. Hartwig-Lab, Andreas	A.B.	German
21. Kreis, Reinhard	A.B.	German
22. Leisner, Bert	A.B.	German
23. Moser, Siegfried	A.B.	German
24. Schröder, Norbert	A.B.	German
25. Schultz, Ottomar	A.B.	German
26. Beth, Detlef	Storekeep.	German
27. Arias Iglesias,Enr.	Mot-man	Chile
28. Dinse, Horst	Mot-man	Austria
29. Fritz, Günter	Mot-man	German
30. Krösche, Eckard	Mot-man	German
31. Fischer, Matthias	Cook	German
32. Martens, Michael	Cooksmate	German
33. Tupy, Mario	Cooksmate	German
34. Dinse, Petra	1.Stwdess	German
35. Wöckener, Martina	Stwdss/KS	German
36. Deuß, Stefanie	2.Stwdess	German
37. Schmidt,Maria	2.Stwdess	German
38. Streit, Christina	2.Stwdess	German
39. Tu, Jian Min	2.Steward	China
40. Wu, Chi Lung	2.Steward	German
41. Yu, Chung Leung	Laundrym.	Hongk.
42. Niehusen, Arne	Trainee/D	German
43. Scholl, Christoph	Trainee/D	German

20. PARTICIPANTS / FAHRTTEILNEHMER ANT XXI/4

1) Asmus, Kelly Marie	IWC
2) Bathmann, Ulrich	AWI
3) Baumann, Ludmilla	AWI
4) Bergström, Bo	BfF
5) Brauner, Ralf	DWD
6) Brenner, Matthias	AWI
7) Cembella, Barbara	Optimare
8) Demmler, Petra	Journalistin
9) Dorssen, Michiel van	ALTERRA
10) Engeler, Alexander	AWI
11) Flores, Hauke	ALTERRA
12) Franeker, Jan van	ALTERRA
13) Fuentes, Veronica	AWI
14) Gensheimer, Michael	AWI
15) Graupner, Rainer	Optimare
16) Guerra, Citlali	AWI
17) Haraldsson, Matilda	BfF
18) Harling, Benedict von	IfU
19) Herrmann, Regine	AWI
20) Kitchener, John	AAD
21) Kruse, Svenja	AWI
22) Marx, Ulrike	AWI
23) McKay, Shannon	IWC
24) Meijboom, André	ALTERRA
25) Meyer, Bettina	AWI
26) Pakhomov, Evgeny	UBC
27) Putte, Anton van de	LAE
28) Rogenhagen, Johannes	FIELAX
29) Sachs, Oliver	AWI
30) Sauter, Eberhard	AWI
31) Schöling, Susanne	BfF
32) Siegel, Volker	BfF
33) Sonnabend, Hartmut	DWD
34) Spahic, Susanne	AWI
35) Teschke, Matthias	AWI
36) Vortkamp, Martina	BfF
37) Wegener, Jan	AWI
38) Witte, Timo	Optimare

ALTERRA Marine and Coastal Zone Research, Texel; NL

BfF Bundesamt für Fischerei, Hamburg

DWD Deutscher Wetterdienst, Hamburg

FIELAX Firma Bremerhaven

IfU Institut für Umwelphysik, Heidelberg

IWC International Whaling Comm., Australia

LAE - Laboratory of Aquatic Ecologie, Leuven, Belgien

Optimare Firma Bremerhaven

UBC University of British Columbia, Vancouver, Canada

21. PARTICIPATING INSTITUTES / TEILNEHMENDE INSTITUTE

ALTERRA	ALTERRA, Marine and Coastal Zone Research PO Box 167 1790 AD Den Burg (Texel) The Netherlands
AWI	Alfred-Wegener-Institut für Polar- und Meeresforschung Am Handelshafen 27568 Bremerhaven
BfF	Bundesforschungsanstalt für Fischerei, Institut für Seefischerei Palmaille 9 22767 Hamburg
DWD	Deutsche Wetterdienst, Geschäftsfeld Seeschifffahrt Bernhard Nocht-Str. 76 D 20359 Hamburg
FILAX	FIELAX, Gesellschaft für wissenschaftl. Datenverarbeitung mbH Schifferstraße 10 – 14 27568 Bremerhaven
IfU	Institut für Umwelphysik, Universität Heidelberg Im Neuenheimer Feld 29 69120 Heidelberg
IWC	International Whaling Comm., Deakin University, PO Box 423 Warrnambool, Victoria 3280 Australia
Journalistin	Petra Demmler Hermann-Reutter-Weg 6 80939 München
LAE	Laboratory of Aquatic Ecologie Deberiotstraat 32 B-3000 Leuven, Belgien
Optimare	OPTIMARE Sensorsysteme AG Am Luneort 15a 27572 Bremerhaven
UBC	University of British Columbia, Deptm. Earth and Ocean Sciences 6339 Stores Road Vancouver, B. C., Canada V6T 1Z4

FAHRTABSCHNITT ANT XXI/5 KAPSTADT – BREMERHAVEN

Fahrtleiterin / Chief Scientist: Elisabeth Helmke

INHALTSVERZEICHNIS/CONTENTS

1. Zusammenfassung und Fahrverlauf	269
2. Summary and Itinerary	272
3. The meteorological conditions	275
4. Structure and activity of bacterial deep-sea communities	277
5. Isomeric and enantiomeric organic pollutants	278
6. Large scale latitudinal patterns of marine birds and mammals from the Antarctic to the North Sea during Polarstern transits	294
7. ¹³ C-sampling program	297
8. DOAS-measurements	298
Annex 1: Participants	299
Annex 2: Participating Institutions	300
Annex 3: Crew list	301
Annex 4: Station list	302

1. ZUSAMMENFASSUNG UND FAHRTVERLAUF

E. Helmke (AWI)

Der letzte Fahrtabschnitt der 21. Polarstern-Reise in die Antarktis (ANTXXI/5) führte zurück nach Bremerhaven. Am 8. Mai 2004 um 20 Uhr verließ FS Polarstern die Pier von Kapstadt Richtung Heimathafen. An Bord war eine vergleichsweise kleine Anzahl von Wissenschaftlern, die sich mit 5 unterschiedlichen Projekten befaßte. Die Projekte waren von der Fragestellung und vom Fachgebiet sehr unterschiedlich, hatten aber gemein, daß sie einen Vergleich von Daten aus sehr unterschiedlichen Klimazonen bzw. hydrographischen Bereichen anstrebten. Die Überfahrten von Polarstern-Reisen bieten die günstige Gelegenheit innerhalb einer relativ kurzen Zeitspanne von knapp 4 Wochen an solch unterschiedliches Proben- und Messdatenmaterial zu kommen.

Die luftchemischen Untersuchungen mit Hilfe der „Differentiellen Optischen Absorptions Spektroskopie“ (DOAS) zur Bestimmung der Konzentrationsverteilung von Spurengasen in der Atmosphäre sowie die Probennahmen zur ^{13}C -Isotopie des gelösten anorganischen Kohlenstoffs (DIC) waren bereits unter dem Aspekt der saisonalen und interannuellen Varibilität auf dem ersten Fahrtabschnitt durchgeführt worden. Die Säugetier- und Vogelbeobachtungen waren eine Fortsetzung vom 4. Fahrtabschnitt und sollten die Verbreitung dieser Tiergruppen in den gemäßigten und tropischen Klimazonen erfassen, nachdem sie im Antarktischen Bereich sehr intensiv untersucht worden waren.

Spektroskopische Messungen und Tierbeobachtungen sind vom fahrenden Schiff aus möglich. Auch die Probennahmen von Oberflächenwasser sind mit Hilfe der Klauspumpe en route ohne extra Stationszeit durchführbar. Oberflächenwasser wurde für die Bestimmung des ^{13}C -DIC sowie für die Bestimmung der persistenten organischen Umweltstoffe (POPs) benötigt. Die Konzentrationsänderungen der POPs wurden nicht nur horizontal im Oberflächenwasser, sondern auch vertikal bis in den Tiefseebereich verfolgt. Dafür, sowie für das mikrobiologische Programm, wurden 6 Tiefseestationen bearbeitet, die sich in 6 unterschiedlichen Tiefseebecken mit unterschiedlicher Hydrographie bzw. Oberflächenproduktion befanden. Es wurde die Wassersäule sowie das Bodensediment beprobt, um über die Verteilung der POPs und über die Aktivität und Struktur der bakteriellen pelagischen und benthischen Gemeinschaften Aufschluß zu erhalten.

Um die unterschiedlichen Tiefseebecken beproben zu können, musste vom üblichen Kurs abgewichen werden. Insgesamt wurde eine von 7100sm zurückgelegte.

Bereits am 10. Mai war unsere erste Tiefseesation im Namibia-Becken erreicht. Mit Hilfe der CTD wurde zunächst das hydrographische Profil erfaßt und danach die Wassersäule mit Hilfe des Rosettenschöpfers beprobt. Um in einem Arbeitsgang Wasser- und Sedimentbeprobung durchzuführen, wurde unter der Rosette ein Minicorer installiert. Die Gerätekombination brachte das gewünschte Probenmaterial an Deck ebenso wie der anschließend eingesetzte Bodenwasserschöpfer. Das von der Geochemie des AWI entwickelt Gerät kann die Wassersäule 2 m über dem Boden sehr fein aufgelöst beproben.

Die gleiche Gerätekombination wurde auch am 13. Mai im Angola-Becken erfolgreich eingesetzt. Unterstützt durch den Südostpassat kamen wir gut voran, so dass wir einen Tag später eine zusätzliche kurze Station zur Oberflächenwasserprobe einschieben konnten. Das Wasser wurde als Referenzprobe zu dem von der Klauspumpe geförderten Oberflächenwasser benötigt.

Die nächste Tiefseestation erreichten wir am 18. Mai im Bereich der Romanche Fracture Zone. Der hier vorhandene sehr tiefe Einschnitt des atlantischen Rückens ermöglicht es dem schweren Antarktischen Bodenwasser sich auf seinem Weg nach Norden auch auf der östlichen Seite des Atlantischen Ozeans auszubreiten. Diese besondere hydrographische Situation und auch die extreme Tiefe von über 6000m, machten diese Station für die Spurenstoffchemiker sowie für die Mikrobiologen besonders interessant. Die Station dauerte knapp 5 Stunden, obgleich diesmal der Bodenwasserschöpfer, der nur für Tiefen bis 6000m ausgelegt ist, nicht eingesetzt werden konnte.

Am nächsten Tag passierten wir bereits die "Innertropische Konvergenz Zone" (ITCZ), die nur einen kurzen kräftigen Schauer brachte, der den Spurenstoffchemikern für ihre geplanten Niederschlagsanalysen ausreichte.

Am 21. Mai befanden wir uns bereits im Einflußbereich des Nordostpassates, welcher die Geschwindigkeit des Schiffes spürbar drosselte. Die 4. Tiefseestation im Kapverdischen Becken wurde dennoch planmäßig erreicht. Die Kombination von Rosette und Minicorer sowie der Bodenwasserschöpfer wurden wie bisher eingesetzt, zusätzlich wurde eine Beprobung der oberen Wasserschicht mit einem. Weiteren Einsatz des Rosettenschöpfers bis 500m durchgeführt. Dadurch konnten insgesamt 13 unterschiedliche Wassertiefen beprobt werden und die Wasservolumen aus den größeren Tiefen erhöht werden.

Bei anhaltend gutem Wetter absolvierten wir am 24.05. unsere 5. Tiefseestation im Kanarischen Becken. Der Geräteeinsatz entsprach dem auf der 4. Tiefseestation und war wiederum erfolgreich. Am 27.05. erreichten wir unserer letzte Station im Bereich des Mittelmeerausstromes. Um die chemischen und mikrobiologischen Besonderheiten dieses in ca. 1100m Tiefe liegenden Wasserausstromes genauer analysieren zu können wurde eine zusätzliche Rosetten-Wasserprobennahme bis 1500m durchgeführt. Auf der letzten Station wurde wie zuvor die Rosette plus Minicorer und danach der Bodenwasserschöpfer eingesetzt.

Parallel zu diesen Stationsarbeiten liefen die Oberflächenwasserbeobachtungen mit Hilfe der Klauspumpe. Auch hier gab es keine technischen Probleme. Oberflächenwasserproben wurden bis in den englischen Kanal für die ^{13}C -DIC Isotopie und bis in die Nordsee für die organische Spurenstoffchemie gewonnen. Die Tierbeobachtungen ebenso wie die DOAS-Messungen wurden erst kurz vor Bremerhaven eingestellt. Auch die DOAS-Messungen liefen störungsfrei und wurden zudem durch die geringe Bewölkung begünstigt, so daß mit aussagekräftigen Ergebnissen gerechnet wird.

Planmäßig am 2. Juli früh morgens machte FS POLARSTERN an der Pier in Bremerhaven fest. Aufgrund der sehr guten Wetterlage und der einwandfrei funktionierenden Mess- und Probenahmegeräte konnte das Programm wie geplant abgeschlossen werden.

2. SUMMARY AND ITINERARY

E. Helmke (AWI)

The fifth and last leg of the 21st Antarctic cruise led RV "Polarstern" back to Bremerhaven. The research vessel left the pier of Cape Town on the 8th of May 2004 at 8pm. A comparably small group of scientists was aboard. They were involved in 5 different scientific projects which covered rather different scientific fields. The focus of interest of all projects was the comparison of very different climatic zones and diverse hydrographical regions respectively. The meridional transits of RV "Polarstern" offer the possibility to get such data sets within 4 weeks.

Two projects were follow-up investigations of the first leg with the intention to find long-term trends and interannual variability. One project determined concentrations of trace gases in the atmosphere with "Differential Optical Absorption Spectroscopy". Since these measurements were running continuously they covered a broad latitudinal area. Particular interest however was taken in the tropical regions which were up till now hardly studied.

The second project concentrated on the $\delta^{13}\text{C}$ -DIC disequilibrium of the surface waters in the Atlantic Ocean. Surface water samples were taken with regular spacing along the entire track.

The third follow-up project focused on diversity and abundance of marine birds and mammals and was a continuation from the 4th leg. The extensive data set collected in the Southern Ocean was extended for the temperate and tropical waters of the Atlantic Ocean up to the northern hemisphere.

The DOAS-measurements as well as the predator observations could be performed from the moving ship. Also no extra station time was needed for water sampling or the $\delta^{13}\text{C}$ -DIC analyses. Surface water was delivered continuously by the Klaus pump. Water from the Klaus pump was used also for determinations of persistent organic pollutants (POPs). The distribution of POPs in general and in particular of hexachlorocyclohexane (HCH) was followed up horizontally and vertically. Sampling from the surface layer up to the deep-sea floor was performed at 6 different deep-sea stations in different basins of the Atlantic Ocean. The microbiological project concentrated also on these 6 deep-sea basins which differ in surface productivity as well as hydrographical conditions. The microbiological investigations focused on the question to which extent productivity and hydrographical conditions influence structure and activity of pelagic and benthic bacterial deep-sea communities of the Atlantic Ocean.

To enable sampling in the different deep-sea basins the course of RV "Polarstern" had to be extended to 7100sm.

On the first day after departure unpacking of the equipment and establishing of the laboratories was performed facilitated by calm weather conditions. DOAS measurements, predator watching and surface water sampling could be started during the same day.

The position of our first deep-sea station in the Namibia Basin (5100m) was reached in the afternoon of the next day (10.05.). Water samples were taken from 6 differen-

depths by means of a rosette water sampler. To save time sediment sampling was combined with water sampling by fixing a minicorer beneath the rosette. The combined gears worked well and provided us with water from different depths as well as deep-sea bottom sediment. Since biogeochemical processes directly above the sea floor are generally enhanced this water layer was studied in more detail with a bottom water sampler. This sampler developed by AWI-geochemists can take 6 different overlaying water samples in the range of 20 to 200cm above the sea floor.

Three days later (13.05.) the second deep-sea station in the Angola Basin was successfully processed. The next day surface water was taken with the rosette sampler for reference measurements versus surface water received with the Klaus pump.

Supported by good weather conditions and the south-easterly trade-wind we arrived the third deep-sea station on May 18th in the area of the Romanche Fracture Zone. Here at the deepest point of the Middle Atlantic Ridge the cold Antarctic Bottom Water can pass and extend to the north on the eastern site of the Atlantic Ocean also. Due to the specific hydrographical situation as well as the extreme depth this station was of special interest for chemical as well as microbiological studies. Water and sediment was sampled at 6300m. The station lasted nearly 5 hours, although the bottom water sampler could not be deployed due to technical reasons.

The next day "Polarstern" passed the "Innertropical Convergence Zone" (ITCZ). A short but heavy rainfall was used by the chemists for investigations on the distribution of organic pollutants in the atmosphere.

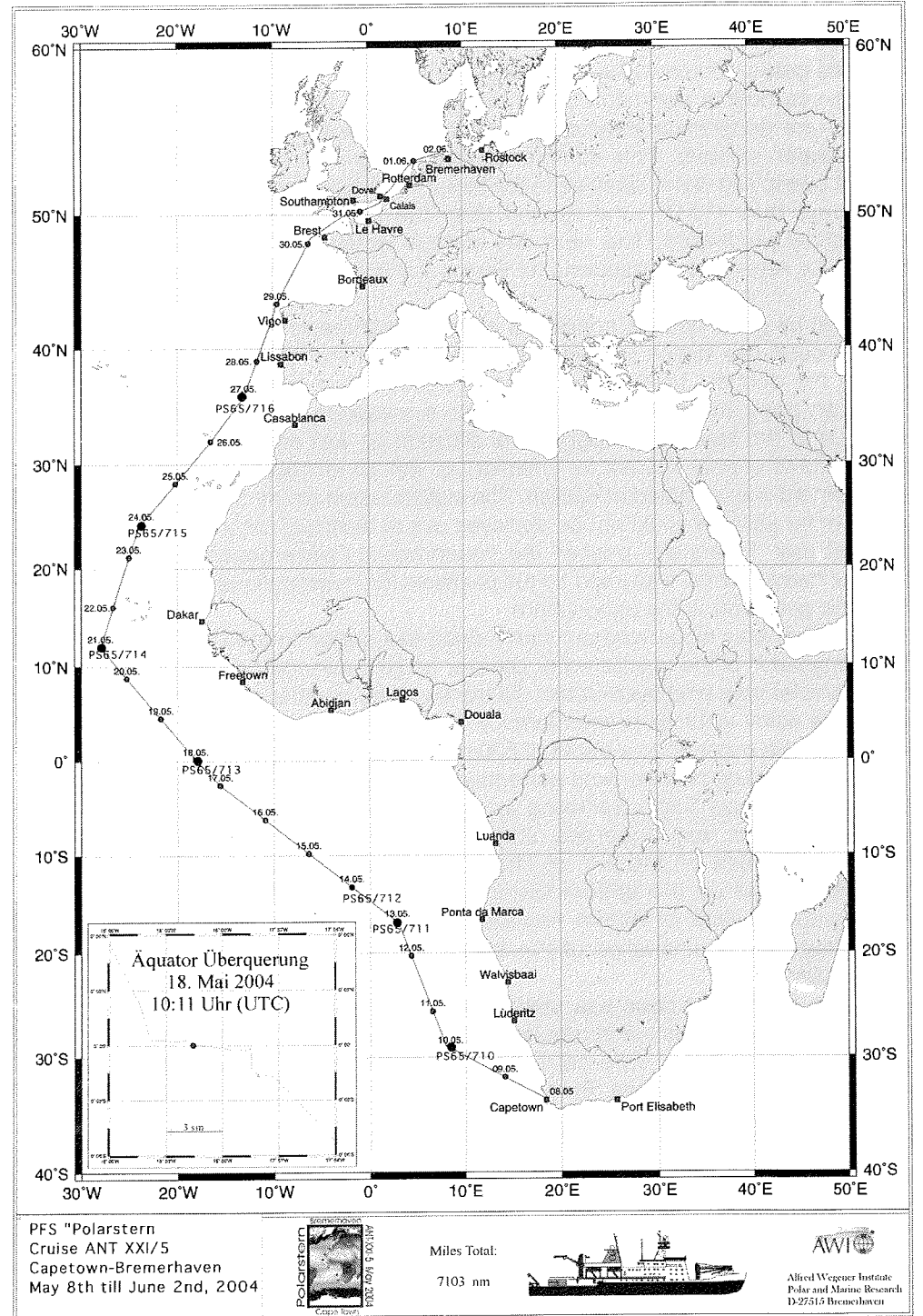
On the 21st of May we arrived our fourth deep-sea station in the Cape-Verde Basin. The combination of the rosette water sampler and the minicorer as well as the bottom water sampler was employed again. To increase the number of sampling depths as well as the water volumes preponderantly from greater depths a second rosette was used to sample water up to a depth of 500m.

The same sampling protocol was performed on the 24th of May at our fifth deep-sea station in the Canary Basin. Sampling was successful again.

We reached our last deep-sea station in the region of the outflow of the Mediterranean Sea on the 27th of May. The rosette sampler combined with the minicorer as well as the bottom water sampler were deployed as usual. Water sampling up to a depth of 1500m, however, was intensified to study the chemical and microbiological characteristics of the Mediterranean Outflow Water in a depth of about 1100m.

Beside the successful deep-sea station work the surface water sampling with the Klaus pump were carried out in regular spacing along the entire course. Sampling for ¹³C-DIC measurements were carried out up to the English Channel, for organic pollutants up to the North Sea. Predators were watched also up to the North Sea and the DOAS measurements run nearly up to Bremerhaven.

RV "Polarstern" arrived Bremerhaven in the early morning of the 2nd June as scheduled. Due to excellent weather conditions and perfectly working instruments and gears the program could be accomplished successfully giving rise to expect interesting results.



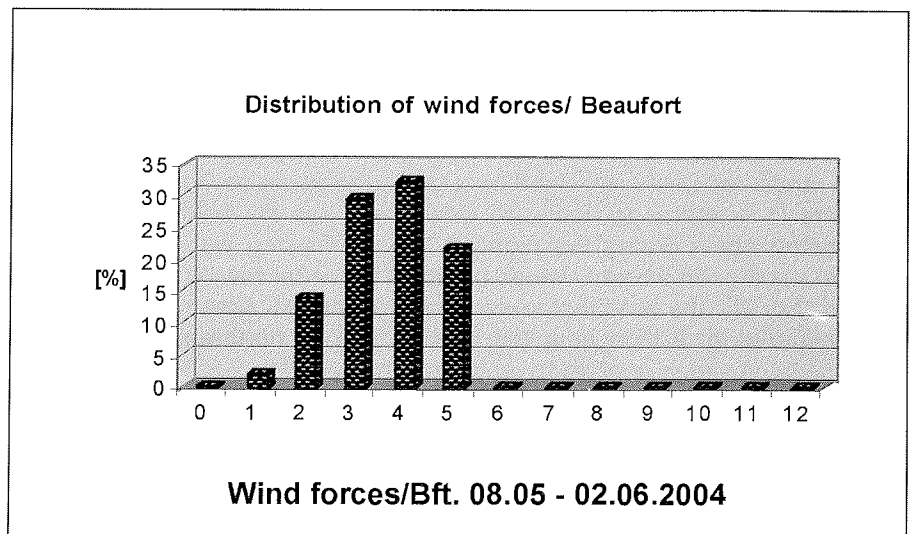
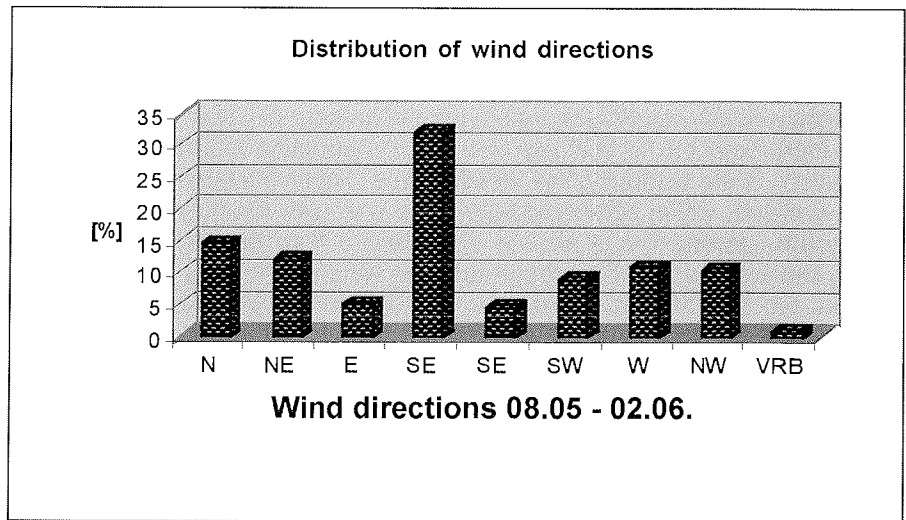
3. METEOROLOGICAL CONDITIONS DURING CRUISE ANT

XXIV/5

E. Knuth (DWD)

Under a lightly cloudy sky RV Polarstern left the harbour of Cape Town on May 8th at 8.15 pm local time on its last leg of the 21st Antarctica mission with destination Bremerhaven. In the beginning the weather was slightly influenced by southerly low pressure systems, which combined later on to a trough. On May 9th Polarstern was met by south-easterly winds around 4 Bft and a light thunderstorm. During the afternoon the cloud cover decreased and the wind changed to 5 Bft coming from north-west. On May 10th RV Polarstern was caught by light showers at times, but already on May 11th the W-WNW wind turned back to south-easterly winds with 4-5 Bft. Under a cloud cover changing between light and stronger cloudiness of cumulus and stratocumulus, Polarstern was headed towards the Equator within the influence of the south-easterly trade-wind. The work of the second scientific stop could easily be done under the conditions of the south-easterly trade-wind and a sea of 2m. Up until the fourth scientific stop at the Equator, weather, wind and sea were extraordinary moderate. Usually the south-easterly trade-wind tends to be much stronger in this area with a mostly spreaded cloud cover. After having crossed the equator, south-easterly winds were predominant for a short period before reaching the first stretches of the ITCZ with light showers in the early morning of May 19th. In this area mostly variable winds at 2 - 3 Bft. were prevailing. The late morning of the same day saw a strong rain shower, which also satisfied those scientists collecting precipitation. Even though Polarstern was still within the ITCZ, the following night as well as May 20th passed by under dry conditions without any precipitation. A broad almost cloudless part between two clusters ensured a mostly clear sky throughout the day. During that day a steady north-easterly trade-wind rose predominating the following days. On May 21st at 12°N the trade-wind reached its usual wind speed around 4-5 Bft, occasionally rising up to 6 Bft with little cloudiness. Up to that date, the visual range had been very good throughout the whole voyage, only south of the Cape Verde Is. it started to decrease slowly, yet was still better than 10nm. This became better again during the night of May 22nd along with a change in wind direction to north north-westerly winds around 2 Bft. After having passed the Canary Islands on May 25th the wind increased again to its usual speed of 4-5 Bft. On May 27th the influence of a high near the Azores with its north-easterly ridge of high pressure became strong enough to drop the wind speed to 2-3 Bft coming then from northerly directions. The last scientific stop on this leg took also place under very good weather conditions.

Under light south-westerly winds RV Polarstern passed Portugal and the Bay of Biscay. The continuing voyage to Bremerhaven was along the north side of the high near the Azores, which had increasing stretches also over southern Europe. Small depressions over the British Isles moved northwards and did therefore not influence the ship's cruise. RV Polarstern reached Bremerhaven on its scheduled time on June 2nd.



4. STRUCTURE AND ACTIVITY OF BACTERIAL DEEP-SEA COMMUNITIES

E. Helmke, K. Reuter, K. Berlitz, C. Heim (AWI)

Introduction

The deep sea is the largest habitat on earth nevertheless hardly studied. This is preponderantly due to time consuming sampling as well as to the high hydrostatic pressure conditions and the thereby caused technical problems to maintain *in situ* conditions during sampling and further processing. If deep-sea pressure and temperature conditions are not considered during working up with cultural methods or activity approaches results will be not so meaningful. Therefore, the additional use of non-cultural methods like the molecular biological techniques is recommended. In the last few years molecular biological methods advanced rapidly and they are nowadays excellent tools to get quite easily detailed information about the taxonomical structure of microbial communities without cultural approaches. They are predestined to be employed in combination with conventional cultural techniques as well as activity measurements to broaden our knowledge about the structures of pelagic and benthic deep-sea communities.

Our previous deep-sea studies focused on pelagic and benthic communities in the Southern as well as Arctic Ocean and on their adaptations to the extreme deep-sea conditions. Different cultural methods as well as activity measurements were used to differentiate active from inactive community members. It could be shown that in the deep pelagic realm very narrow deep-sea adapted bacteria exist beside numerically dominant inactive types. The benthic communities, however, were found to constitute preponderantly of piezophilic/psychrophilic bacteria. Since these results were obtained with decompressed sample material that however was further incubated under *in situ* like conditions it is important to corroborate these results by means of non-cultural methods also.

One aim of our studies during ANTXXI/5 was therefore to analyse the structure of the different deep-sea communities with cultural and non-cultural methods comparatively to examine previous results and deductions. Since molecular biological methods are powerful in analysing dynamics of community structures the question whether deep-sea communities are more influenced by vertical transport processes or lateral drifting will be tackled also. The water bodies of the polar oceans influence strongly the deep sea realm of the world's ocean even up to tropical regions it is of therefore of interest how far from their origin polar bacteria can be found. The transects of RV „Polarstern“ offer excellent opportunities to study all these questions.

Work at sea

On 6 deep-sea stations water samples were taken from the Niskin bottles of the rosette sampler. At least 6 different water depths were processed. Surface sediment as well as overlaying water was sampled from the multicorer at the same stations. Bottom water samples were taken at 5 deep-sea stations by means of a bottom

water sampler (Geochemistry AWI, E. Sauter) from depths of 40, 100, and 200cm above the sea floor.

Different sample preparations for subsequent processing as well as cultural and activity approaches were conducted with the samples in order to study the following parameters:

- total bacterial counts
- bacterial biomass
- viable bacterial counts,
- secondary production, by means of $^{3\text{H}}$ -thymidine.

Viable counts were determined by means of different cultural approaches applying various temperatures, pressures, substrate qualities, and substrate quantities. Cultures represent the basis for isolation work. Bacterial isolates are still a prerequisite to study adaptation mechanisms and function. The activity measurements were also conducted at different temperatures and hydrostatic pressures to get information about role and function of the various bacterial types.

Special emphasis was laid on the characterization of the structure of the bacterial communities by means of Denaturing Gradient Gel Electrophoresis (DGGE) and Fluorescence *in situ* Hybridisation (FISH). To perform these analyses in the home laboratory aboard high volumes of seawater had to be filtered to get sufficient amounts of DNA and RNA respectively. For FISH analyses smaller volumes were filtered and afterwards fixed, filtered and washed.

Preliminary results

The frozen samples, fixed material and the cultural approaches could be transferred to the home laboratory without disturbances. Most of the assays and experiments could not be performed aboard and had to be conducted or finished in the home laboratory. Only few results are available i.e. the growth activities of water samples measured so far corroborated previous results. To work up the entire set of samples it will take about one year.

5. ISOMERIC AND ENANTIOMERIC ORGANIC POLLUTANTS – TRANSPORT UND TURNOVER IN THE ATLANTIC OCEAN

K. Weber, W. Drebing, A. Müller (AWI)

Background

Only a small fraction of organic matter in the ocean surface is exported from production areas to adjacent ocean parts and the deep sea driven by advection and subduction of dissolved parts and net gravitational sinking of organic particles. Most primary metabolites and other marine natural products - either in the dissolved state

or in the suspended particle size - are completely degraded and resired within restricted areas on timescales of days to months. Only 2% is transferred to 1000 m and approximately 1% reaches deep sediments, quite independant of oceanic regions. This organic fallout is further degraded within decades finally leading to accumulation of inorganic nutrients in ancient water masses.

Similar turnover rates do not exist for persistent organic pollutants (POPs). POPs are mainly distributed by atmospheric transport in their early environmental history. Once introduced from the atmosphere into the ocean they remain there for longer periods of time allowing extensive horizontal and vertical distribution, accumulation in particulate matter as well as biomagnification in marine food chains. Changes in aggregation, interaction of dissolved, suspended and vertical moving particles promote distribution in all depths. Contrary to the atmosphere the ocean has a large capacity and has already become a major reservoir for many POPs. High levels are even reported to occur in endemic deep sea fish indicating fast vertical transport to the ocean bottom.

HCHs are presently the most common POPs in open marine waters exhibiting enhanced levels in high latitudes of the northern hemisphere. If not degraded in the sea surface they invade the mid and deep sea preferentially in convective zones. In the absence of light and at low temperatures degradation slows down and HCHs may spread to not yet charged areas decades after input. Though ocean currents are sluggish compared with atmospheric winds it has been increasingly recognized that they become dominant late in the history of HCHs. Distribution of persistent chemical tracers, like freons, has already been extensively used to reconstruct trajectories of transport and age of water masses in the world oceans.

Technical hexachlorocyclohexane (HCH) belongs to POPs of global concern. During the last 50 years it had been the most widely produced pesticide in the world with an estimated 10 million tons applied for seed, soil and plant protection. Application of technical HCH was stepwise restricted since the 1970s and is worldwide banned from ecotoxicological reasons since its last large scale usage in India and the former Soviet Union approximately ten years ago. However, the active insecticidal ingredient of the technical product, lindane, is still intensively applied in some countries, like Canada. Technical HCH is a mixture of stereoisomers mainly composed of α -HCH (60-70%), β -HCH (5-12%), γ -HCH (lindane, 10-12%) and δ -HCH (6-10%). The individual isomers differ only in the steric position of chlorine substituents, but exhibit distinct physical, chemical and toxicological properties. α -HCH exists in two enantiomeric forms in addition which may behave differently in biological processes. Though most HCHs have been degraded in zones of application few percents chemically survived and were globally distributed. Occurrence and composition of stereoisomeric and enantiomeric residues in the global environment depend on emissions, pathways of transport and compound properties. The latter significantly determine thermodynamic distribution between various compartments and chemical persistence.

Objectives

In a preceding work we described the time trend of α -HCH and γ -HCH levels in surface water of the Atlantic Ocean from 1987 to 1999 and characterized the air-sea equilibrium of both isomers in different climatic zones at the end of this period (Lakaschus *et al.* 2002). Now - 5 years later during the meridional transect ANT XXI/5 - we reinvestigate the spatial distribution of HCHs in the Atlantic to extend the time series in surface water for further 5 years. Sampling is now performed to resolve likewise deposition of HCHs from the atmosphere and removal by adsorption to sinking phytoplankton biomass. We also include persistent and bioaccumulative β -HCH, which has been recently shown to arrive in remote ocean environments. Since very few is known about the ultimate fate of the different HCH isomers investigations in the deep sea and near sediments are also performed paying special attention to enantiomeric (+)- α - and (-)- α -HCH. In addition to HCHs specific biomarkers will be analyzed along the transect to characterize the variability of eukaryotic phytoplankton and possible organic matter export to the ocean interior. We also plan to compare the biogeochemical fate of moderate persistent HCHs and moderate labile phytosterols.

The following questions concerning HCHs in the Atlantic Ocean will be particularly addressed. How fast is α -HCH disappearing in temperate and tropical surface water in comparison to slow losses in the Arctic ocean? Does enantioselective degradation of α -HCH in the surface ocean and deep sea differ in a predictable way? Is ongoing application of γ -HCH still reflected in its temporal and spatial distribution in the ocean? Where are the main sources for emerging β -HCH in the Atlantic Ocean? Is the equatorial surface ocean a preferred site of degradation and are decreasing HCHs replaced by more persistent degradation products. Is the deep ocean an intermediate storage place for HCHs lasting for decades to centuries or a destructive sink?

Work at Sea

Sampling

Water samples were obtained from the surface of the remote South and North Atlantic Ocean as well as from bathypelagic and bottom layers of East Atlantic basins. Locations of sampling are given in Table 1. In order to attain low detection levels ultra-clean sampling and specific analytical detection methods were used as far as technical possible. Therefore, particulate and dissolved fractions in water were not separated and internal standards not applied. All laboratory glassware was rinsed with acetone, n-hexane and seawater before use. Open analytic equipment was covered by aluminium foil except during handling. Organic solvents had been precleaned in the home laboratory and combined to one batch before use on board.

Table 5.1: Sampled material for GC/MS-analyses of hexachlorocyclohexane stereoisomers, enantiomers and natural trace organic compounds in surface, deep and bottom water

Date	Time	PS	Latitude, Longitude	Depth (m)	Description Area ¹	Operation ²	Amount (l)	Sample type ³ No.	GC/MS on board
04	(UTC)	Stat. No.							File No.
1.5.	15:54		S31°25',E13°11'	11	BCC	Klaus pump	20	W490	
1.5.	23:19		S30°36',E11°25'	11	BOC 1	Klaus pump	20	W491	433/434 FS 435/446/447 MID
1.5.	8:02		S29°37',E09°19'	11	BOC 2	Klaus pump	20	W492	
1.5.	13:38		S29°00',E08°01'	11	NB	Klaus pump	20	W493	
1.5.	17:16	710	S29°00',E07°59'	100/400	NB	Niskin	20	W494-1	
			901	NB	Niskin		20	W494-2	
			3003	NB	Niskin		20	W494-3	
			4000	NB	Niskin		20	W494-4	
			5153	NB	Niskin		20	W494-5	
			5173	NB	minicorer				
					supernatant	0.4	W495-1	458/459 FS	
					pore water	0.3	W495-2	461/462 FS	
					sediment	710g	S495		
			5173	NB	bw sampler				
					20,65,150cm	20	W496		
					Klaus pump	20	W497	464/465 FS 466 MID	
1.5.	8:00		S26°35',E06°57'	11	BOC 3				
1.5.	16:01		S24°46',E06°11'	11	BOC 4	Klaus pump	20	W499	
1.5.	0:00		S22°58',E05°26'	11	BOC 5	Klaus pump	20	W500	
1.5.	8:03		S21°09',E04°41'	11	BOC 6	Klaus pump	20	W501	
1.5.	16:24		S19°18',E03°56'	11	BOC 7	Klaus pump	20	W502	
1.5.	2:53		S17°00',E03°00'	11	AB 1	Klaus pump	20	W503	
1.5.	7:57	711	S17°00',E03°00'	100	AB	Niskin	20	W504-1	
			400	AB	Niskin	20	W504-2		
			900	AB	Niskin	20	W504-3		
			3000	AB	Niskin	20	W504-4		
			4000	AB	Niskin	20	W504-5		
			5500	AB	Niskin	20	W504-6	483 FS	
			5520	AB	minicorer				
					supernatant	1.6	W505-1	463/468 FS	
					pore water	0.3	W505-2	470/471 FS	
					sediment	960g	S505		
			5520	AB	bw sampler				
					20,65,150cm	14	W506	480 FS	
1.5.	16:18		S16°13',E01°58'	11	AB 2	Klaus pump	20	W507	
1.5.	0:01		S15°03',E00°26'	11	AB 3	Klaus pump	20	W508	478 FS 473/474 MID
1.5.	8:00		S13°52',W01°06'	11	ABFZ	Klaus pump	20	W509	
1.5.	12:58		S13°08',W02°04'	11	SEC 1	Klaus pump	20	W510	477 FS
1.5.	13:15	712	S13°08',W02°04'	15	SEC 1a	Niskin	20	W511	476 FS
1.5.	20:02		S12°09',W03°20'	11	SEC 2	Klaus pump	20	W512	
1.5.	23:55		S11°35',W04°05'	11	SEC 3	Klaus pump	20	W513	
1.5.	8:07		S10°22',W05°38'	11	SEC 4	Klaus pump	20	W514	481 FS/487 MID
1.5.	16:05		S09°11',W07°09'	11	SECC 1	Klaus pump	20	W515	
1.5.	23:55		S08°02',W08°38'	11	SECC 2	Klaus pump	20	W516	
1.5.	8:02		S06°50',W10°10'	11	SECC 3	Klaus pump	20	W517	
1.5.	16:18		S05°35',W11°46'	11	SEC 5	Klaus pump	20	W518	488 FS
1.5.	23:55		S04°26',W13°13'	11	SEC 6	Klaus pump	20	W519	
1.5.	8:03		S03°11',W14°48'	11	SEC 7	Klaus pump	20	W520	
1.5.	16:03		S01°51',W16°15'	11	SEC 8	Klaus pump	20	W521	
1.5.	20:07		S01°08',W16°56'	11	SEC 9	Klaus pump	20	W522	

Date 2004	Time (UTC)	PS 65/ Stat. No.	Latitude, Longitude	Depth (m)	Description Area ¹	Operation ²	Amount (l)	Sample type ³ No.	GC/MS File No.
18.5.	3:06	713	S00°02'W17°58'	30	RFZ	Niskin	20	W523-1	
				50	RFZ	Niskin	20	W523-2	
				100	RFZ	Niskin	20	W523-3	
				200	RFZ	Niskin	20	W523-4	
				300	RFZ	Niskin	20	W523-5	
				400	RFZ	Niskin	20	W523-6	
				500	RFZ	Niskin	20	W523-7	
				900	RFZ	Niskin	20	W524-1	
				2000	RFZ	Niskin	20	W524-2	
18.5.	6:40		S00°02'W17°58'	3000	RFZ	Niskin	20	W524-3	
				4000	RFZ	Niskin	20	W524-4	
				5000	RFZ	Niskin	20	W524-5	
				6277	RFZ	Niskin	20	W524-6	
				6297	RFZ	minicorer			
						supernatant	0.7	W525-1	497/9/50
						pore water	0.35	W525-2	490/491
18.5.	4:30		S00°02'W17°58'			sediment		S525	
						line fishing	710g	T524	
18.5.	12:42		N00°17'W18°13'	11	RFZ	Klaus pump	20	W526	
18.5.	18:39		N01°26'W19°10'	11	SEC 10	Klaus pump	20	W527	
18.5.	23:57		N02°22'W19°57'	11	SEC 11	Klaus pump	20	W528	
18.5.	8:04		N03°49'W21°09'	11	NECC1	Klaus pump	20	W529	493/503 496 MID
18.5.	11:15		N05°00'W22°08'	11	ITCZ	glass funnel	0.15	R530	502 FS
19.5.	16:08		N05°13'W22°18'	11	NECC 2	Klaus pump	20	W531	
19.5.	23:55		N06°35'W23°27'	11	NECC 3	Klaus pump	20	W532	
20.5.	8:07		N08°03'W24°40'	11	NEC1	Klaus pump	20	W533	
20.5.	16:02		N09°28'W25°52'	11	NEC 2	Klaus pump	20	W534	
20.5.	23:57		N10°54'W27°04'	11	NEC 3	Klaus pump	20	W535	
21.5.	7:08	714	N12°00'W28°00'	50	CVB	Niskin	20	W536-1	
				100	CVB	Niskin	20	W536-2	
				200	CVB	Niskin	20	W536-3	
				300	CVB	Niskin	20	W536-4	
				400	CVB	Niskin	20	W536-5	
				500	CVB	Niskin	20	W536-6	
21.5.	10:28		N12°00'W28°00'	900	CVB	Niskin	20	W537-1	
				2000	CVB	Niskin	20	W537-2	
				3000	CVB	Niskin	20	W537-3	
				4000	CVB	Niskin	20	W537-4	
				5000	CVB	Niskin	20	W537-5	
				5713	CVB	Niskin	20	W537-6	
				5733	CVB	minicorer			
21.5.	13:49		N12°00'W28°00'		supernatant	1.5	W538-1	506/505	
						pore water	0.35	W538-2	512 MID 507/508 513 MID
21.5.		5733	CVB		sediment bw sampler	1080g	S538		
						150cm	6	W539-1	
						20+65cm	12	W539-2	
						Klaus pump	20	W540	
						Klaus pump	20	W541	
						Klaus pump	20	W542	509 FS
						Klaus pump	20	W543	
						Klaus pump	20	W544	
						Klaus pump	20	W545	514/515 516 MID

Site	Time	PS 65/ 04	Latitude, Longitude	Depth (m)	Description Area ¹	Operation ²	Amount (l)	Sample type ³ No.	GC/MS on board
									File No.
3.5.	16:02		N21°58'W24°42'	11	CC 3	Klaus pump	20	W546	
3.5.	20:26		N22°53'W24°23'	11	CC 4	Klaus pump	20	W547	
4.5.	4:29	715	N24°00'W24°00'	900	CB	Niskin	20	W548-1	
				2000	CB	Niskin	20	W548-2	
				3000	CB	Niskin	20	W548-3	
				4000	CB	Niskin	20	W548-4	
				5000	CB	Niskin	20	W548-5	
				5150	CB	Niskin	20	W548-6	
				5170	CB	minicorer			
4.5.	7:23		N24°00'W24°00'	5170	CB	supernatant bw sampler	1.15	W549-1	
						150cm	5.6	W550-1	522 FS
						20+65cm	12	W550-2	523 FS
4.5.	9:37		N24°00'W24°00'	50	CB	Niskin	20	W551-1	
				100	CB	Niskin	20	W551-2	
				200	CB	Niskin	20	W551-3	
				300	CB	Niskin	20	W551-4	
				400	CB	Niskin	20	W551-5	
				500	CB	Niskin	20	W551-6	
4.5.	10:55		N24°11'W23°50'	11	CB	Klaus pump	20	W552	
4.5.	18:04		N25°20'W22°47'	11	CC 5	Klaus pump	20	W553	
4.5.	23:58		N26°17'W21°55'	11	CC 6	Klaus pump	20	W554	524 FS/525 MII
4.5.	8:01		N27°34'W20°44'	11	CC 7	Klaus pump	20	W555	
4.5.	16:00		N28°52'W19°31'	11	AC 1	Klaus pump	20	W556	
4.5.	23:50		N30°07'W18°20'	11	AC 2	Klaus pump	20	W557	534 FS/ 536 MII
4.6.	8:01		N31°26'W17°04'	11	AC 3	Klaus pump	20	W558	
4.6.	16:04		N32°46'W15°50'	11	AC 4	Klaus pump	20	W559	
4.5.	0:00		N34°06'W14°40'	11	AC 5	Klaus pump	20	W560	539 FS
4.5.	8:00		N35°28'W13°29'	11	AC 6	Klaus pump	20	W561	
4.5.	11:24	716	N36°00'W13°00'	300	above MOF	Niskin	20	W562-1	
				700	above MOF	Niskin	20	W562-2	
				900	MOF	Niskin	20	W562-3	
				1150	MOF	Niskin	20	W562-4	
				1300	below MOF	Niskin	20	W562-5	
				1600	below MOF	Niskin	20	W562-6	
4.5.	15:22			1000	MOF	Niskin	20	W563-1	
				2000	below MOF	Niskin	20	W563-2	
				2500	below MOF	Niskin	20	W563-3	
				3000	below MOF	Niskin	20	W563-4	
				4000	below MOF	Niskin	20	W563-5	
				4936	below MOF	Niskin	20	W563-6	
4.5.	18:28			4956	below MOF	bw sampler 200cm	5.4	W565-1	
						65+100cm	11	W565-2	
4.5.	20:27		N36°02'W12°59'	11	above MOF	Klaus pump	20	W566	
4.5.	7:00		N38°02'W12°05'	11	PC 1	Klaus pump	20	W567	

Date 2004	Time (UTC)	PS 65/ Stat. No.	Latitude, Longitude	Depth (m)	Description	Operation ²	Amount (l)	Sample type ³	GC/MS No.	File No.
28.5.	15:07		N39°33',W11°23'	11	Area ¹	Klaus pump	20		W568	
28.5.	22:53		N41°03',W10°40'	11	PC 2	Klaus pump	20		W569	
29.5.	6:01		N42°22',W10°02'	11	PC 3	Klaus pump	20		W570	
29.5.	14:01		N43°55',W09°16'	11	PC 4	Klaus pump	20		W571	
29.5.	22:00		N45°23',W08°12'	11	Biscaya 1	Klaus pump	20		W572	
30.5.	6:02		N46°53',W07°05'	11	Biscaya 2	Klaus pump	20		W573	
30.5.	14:00		N48°21',W05°58'	11	Cont. Slope	Klaus pump	20		W574	
30.5.	22:23		N49°23',W03°59'	11	Cont. Shelf	Klaus pump	20		W575	
31.5.	6:00		N50°00',W01°43'	11	Channel 1	Klaus pump	20		W576	
31.5.	14:05		N50°26',E00°48'	11	Channel 2	Klaus pump	20		W577	
31.5.	21:59		N51°37',E02°26'	11	Channel 3	Klaus pump	20		W578	
1.6.	5:01		N52°41',E04°01'	11	S NS1	Klaus pump	20		W579	

¹ BCC= Benguela Coastal Current , BOC = Benguela Oceanic Current, NB= Namibia Basin, AB= Angola Basin, ABFZ= Angola/Benguela Frontal Zone, SEO= South Equatorial Current, SECC= South Equatorial Counter Current, RFZ= Romanche Fracture Zone, ITCZ= Intertropical Convergence Zone, NECC= North Equatorial Counter Current, NEC = North Equatorial Current, CVB= Cape Verde Basin, CVFZ= Cape Verde Frontal Zone, CC= Canary Current, CB= Canary Basin, AC= Azore Current, MOF= Mediterranean Outflow, PC= Portugal Current, S NS= Southern North Sea
² supernatant = water 0-20cm above sediment, pore water = water 0-20cm below sediment, sediment = 0-20cm below surface
bw sampler= bottom water sampler

³ w = water, r = rainwater, s= sediment, t = squid

⁴ FS= Full Scan, MID= Multiple Ion Detection

Underway sampling of surface water

Surface water was sampled in the open ocean along the ship's track northbound from Cape Town to Bremerhaven including the equatorial ocean and the southern North Sea but otherwise keeping away from upwelling and shelf areas. Water was continuously collected underway during sailing with 10-15 mph. A magnetically driven rotary pump (Klaus pump) supplied a constant flow of 10 m³/h to the ship's V4A clean-water system. The sampling port in the ship's keel was located beyond the navigating bridge in 11 m depth. 20 l water samples were taken spotwise from this system in glass bottles approximately every 8 hours supported by high frequency shipboard measurements of conductivity and temperature (Polarstern data from both bow and keel sensors). During a short rainstorm within the Intertropical Convergence Zone (ITCZ) 150 ml of rainwater was sampled in glassware ca. 20 m above sea level sailing against prevailing winds.

Vertical sampling of deep water

Deep water was sampled during CTD casts from below the mixed surface layer down to 20 m above the bottom of East Atlantic basins, from the Equatorial Undercurrent down to the Romanche Fracture Zone as well as above, within and beyond the Mediterranean outflow into the Atlantic. Samples of 20 l were taken from two 12 l 'Niskin'- PVC bottles (General Oceanics) of a rosette sampler in 6 to 10 depths within the main Atlantic water masses and transferred to glass bottles via precleaned teflon tubing. Discrete sampling at each vertical station during up-casts was supported by CTD measurements during preceding down-casts.

Sampling of water near the bottom

5-10 l bottom water was taken by the 'Sauter bottom water sampler' (AWI patent) equipped with transparent 5 l 'flow through' PVC bottles operating 0.2 to 2 m above ground. 1-2 l supernatant water from loaded minicorer tubes were siphoned off by glass piston pipettes. Pore water and squeezed sediment were obtained by centrifuging the top 0.1 m aqueous sediment layer in 'Nalgene' polycarbonate bottles (Beckmann centrifuge type CL GS 6R, 3750 rpm, 1h, 5°C). All near bottom water samples were transferred to glass ware for subsequent work-up.

Chemical analyses

Briefly n-hexane was taken for enrichment of hydrophobic compounds from seawater by liquid/liquid extraction. Separation of extracted mixtures by gas chromatography (GC) followed including cold split injection of large volumes of concentrated extracts (CIS) and splitless evaporation of volatile parts. Mass spectrometry (MS) was applied for identification of individual compounds. For ultra-trace analyses of HCHs additional clean-up by two dimensional liquid chromatography was performed in advance of specific GC/MS methods. Procedural blanks and sensitivity checks were conducted each day. Analytical details are given below.

Chemical analyses was carried out during most of the transect, but had to be terminated slightly before the end due to a cascade of technical failures. Mainly non-repairable hardware damage of the injection system during port exchange and split adjustments prevented GC/MS work within the last 4 days of the transect.

Extraction

n-Hexane (p.a., Merck, Darmstadt) used for liquid/liquid extraction of hydrophobic compounds from seawater had been cleaned in advance both by adsorptive filtration on basic Al₂O₃ (super I, ICN) and fractionated by spinning-band distillation (8600 HP-SRS, B/R Instrument Corporation, U.S.A) in the home laboratory. Individual volumes of 100 ml originating from one common batch were supplied in sealed glass ampoules which were opened immediately before use. Each volume was applied for extraction of 20 l seawater within the sampling glass bottle. Extraction was accomplished by shaking for 20 minutes leaving 60 min time for phase separation at least. Finally organic extracts were removed from water by a special decantation device from glass to be attached to the sampling bottle. Recovery of the applied solvent yielded from 90% for extraction of deep water to 40% for extraction of continental shelf water. Loss of n-hexane through emulsification with natural seawater surfactants is considered by corrections based on volumetric measurements of extracts. For processing of rain and near bottom water, conventional separatory glass funnels and comparable volumes of water and extraction solvent were used.

Separation

Obtained organic extracts were either analyzed on board or sealed in glass ampoules and stored at -30°C for further processing in the home laboratory. For on board analyses half of the extract was concentrated by fractionating distillation in a

first step. Then calibration to a volume of 100 µl was achieved by solvent evaporation through a gentle stream of high purity helium. For separation of semivolatile, thermally stable compounds - corresponding to C₉ to C₄₀ n-alkanes – high resolution GC was used. Generally half of the concentrated extracts were injected containing trace organic compounds from 5 l seawater. Remaining volumes were sealed and stored as above.

GC conditions

Injection system: Gerstel CIS 3; 40°C, 50 µl n-hexanic extract/50 sec injection time, 1 min open split, purge gas 20 ml helium/min, stopped column flow during injection, splitless injection after 1 min by flash heating 10°C/sec from 40-325°C.

Chromatographic system: Bruker GC module; fused silica 30 m x 0.25 mm, film 0.25 µm, stationary phase DB-5, carrier gas helium, constant pressure with an average flow of 1.2 ml/min during separation, column temperature program 40-325°C with 6°C/min.

Detection and identification

Low resolution MS in full scan mode was applied for detection and identification of main compounds. NIST 98 was used as MS data base. Overall 39 samples and 27 standards were investigated on board. Gaschromatographic retention indices and rough quantifications of extracted compounds were calculated from external injection of authentic phytosterols and homologous series of n-alkanes respectively. Separation power did not yet allow independant identification of diastereoisomeric 24-alkylsterols.

MS conditions:

Bruker 640M mass spectrometer; ionization EI(+), 70 eV; nominal mass resolution; scan range 35-450 mu (TIC), scan cycle time 0.8 sec.

Data aquistion, processing and output:

PC Dolch Pac 586, operating system OS/2, software Bruker Labstar. PC Compaq Armada 3500, operating system Windows 95, software Bruker Data Analysis. HP Deskjet 895Cxi colour printer.

Additional clean-up for quantitative detection of HCH traces

Polar lipids were removed from 500 µl concentrated extracts by adsorption chromatography on 1 g neutral Al₂O₃ (ICN Biomedicals, Super I, deactivated with 10% preextracted water, preflushed with 5 ml n-hexane). Eluates obtained with 6 ml n-hexane were concentrated to 500 µl and subjected to gravity column chromatography on 2 g Florisil (Carl Roth GmbH, 60-100 mesh, adjusted with 0.55 % preextracted water, preflushed with 20 ml n-hexane) for the bulk isolation of HCH stereoisomers. Least polar compounds and HCHs were consecutively eluted with 14 ml n-hexane and 8 ml n-hexane/diethylether (1/1, v/v). Among HCH stereoisomers δ-HCH was not collected using the applied work-up procedures. Separation of α-, β-, γ-, δ- and ε-HCH isomers was achieved by high resolution GC. HCHs were quantified by recording MS fragment ions (MID) as intense and specific as possible depending on the chemical background of samples. GC/MS conditions were chosen

as described above, but applying reduced injection temperatures of 250°C. Authentic external HCH standards (Promochem GmbH) were taken for comparison. Detection limits of the complete analytical method amounted 10^{-14} to 10^{-15} g HCH isomer / g seawater. Trace analyses of HCHs on board were run in 13 samples and made sure against 25 standards.

Preliminary results and discussion

One rainwater, 66 surface and 60 deep water samples were collected between Cape Town and Bremerhaven and extracted to enrich trace organic compounds (Table 1). Most extracts were deep-frozen for investigations in the home laboratory, however, some extracts were analyzed immediately to improve sampling strategies and methods underway. From on board investigations preliminary results are reported.

Quality assurance of sampling and analytical methods

Continuous uptake of surface water underway turned out to be a procedure with low contamination risk though the sampling port was not up-current or near the bow of the ship. No man-made chemicals with higher levels than traces of phthalates (n-DBP and DEHP) were detected in extracts. However, during sampling in the deep sea contamination was severe and its extent independent from processed water amounts. Clean environments on board and near the ship could not be sufficiently guaranteed. Applied conventional techniques mainly derived from oceanographic investigations were only limited qualified for ultra-trace analyses of ubiquitous chemicals. Alternative use of specific equipment requiring extra ship-time was not feasible from logistic reasons during this cruise.

In addition to natural products plasticizers, antioxidants and various technical chemicals were identified in deep water samples in relative large amounts (see examples in Fig 1). Highest contaminant levels were found after minicorer sampling which required most work-up steps. Leaching of additives from plastic material and seals in samplers, dissolution of compounds from lubricants and grease used in seagoing equipment, diffuse emissions into the ship's environment after painting, fuel burning and other leakages belong to the main contaminant sources. Moreover, it can not be ruled out that xenobiotics taken up by sampler material in contaminated environments at any time redissolve after sampling of clean water and falsify results of ultra-trace analyses. Different pathways of contamination could not be investigated in detail within the time-schedule of analytical work on board.

Used solvents were free of detectable residues. Blanks of laboratory procedures - excluding natural matrixes - were repeatedly examined and proved also to be clean. Separation power and sensitivity were checked each day from comparison and spiking of standards. Service time of the GC/MS system could be generally extended to one week or more. However, chromatographic artefacts increased after analyzing extracts from coastal and upwelling areas. In those cases non-evaporating residues

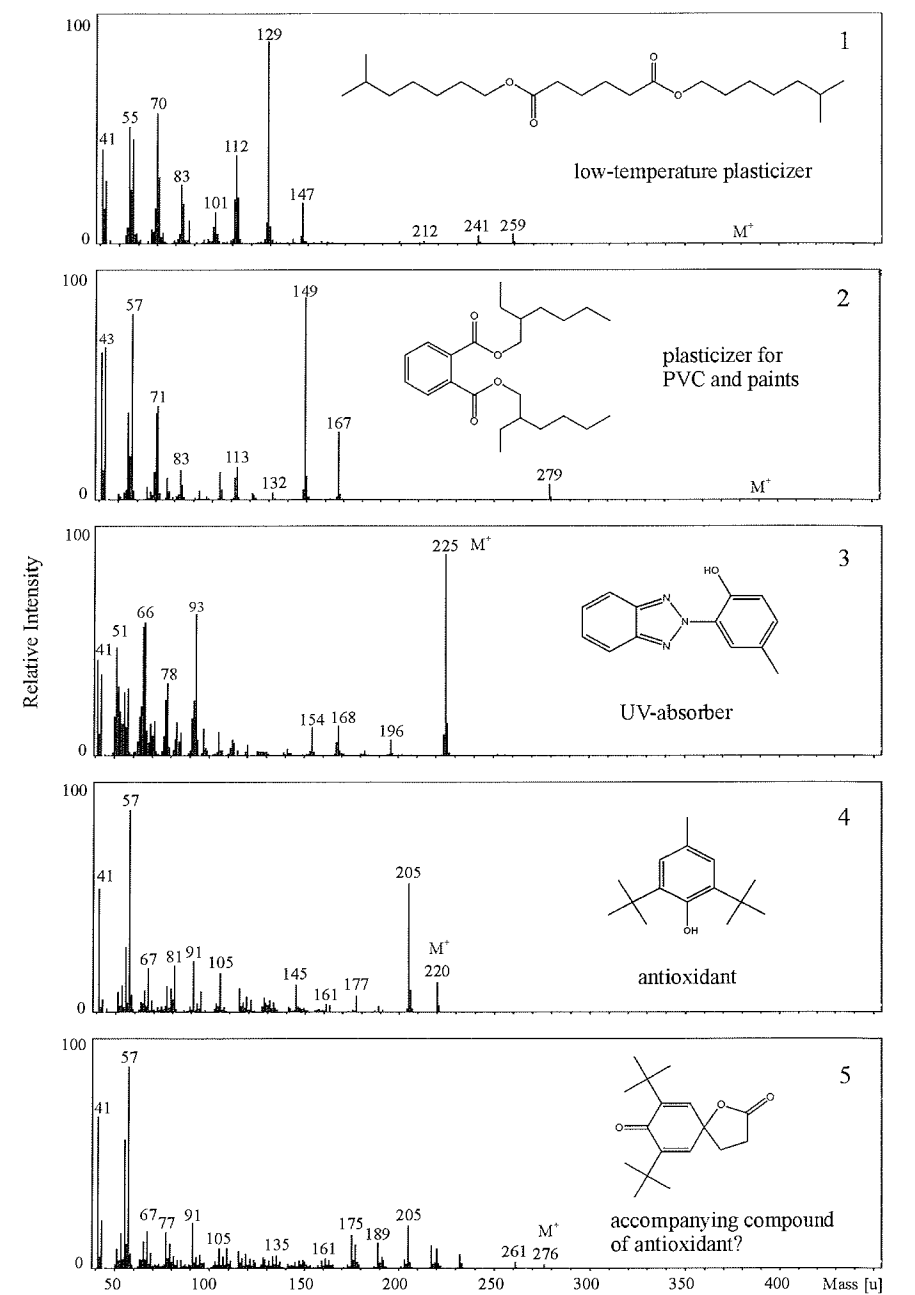


Fig.1: Mass spectra of preferred contaminants after sampling of rain water (1), deep water (2), bottom water (3), supernatant water (4) and pore water (5) (sampling methods see 'Work at Sea')

of extracts were successively accumulated in the injection port and separation column with subsequent occurrence of GC ghost peaks as well as changes in analytical selectivity and sensitivity. Since extensive clean-up of raw extracts could not be performed during the cruise exchange of the injection port and removal of the column inlet turned out to be the fastest way of repair. Readjustment of the split conditions was difficult to achieve after repair and made analyses of high volatile compounds (corresponding to C9 to C12 n-alkanes) time spending.

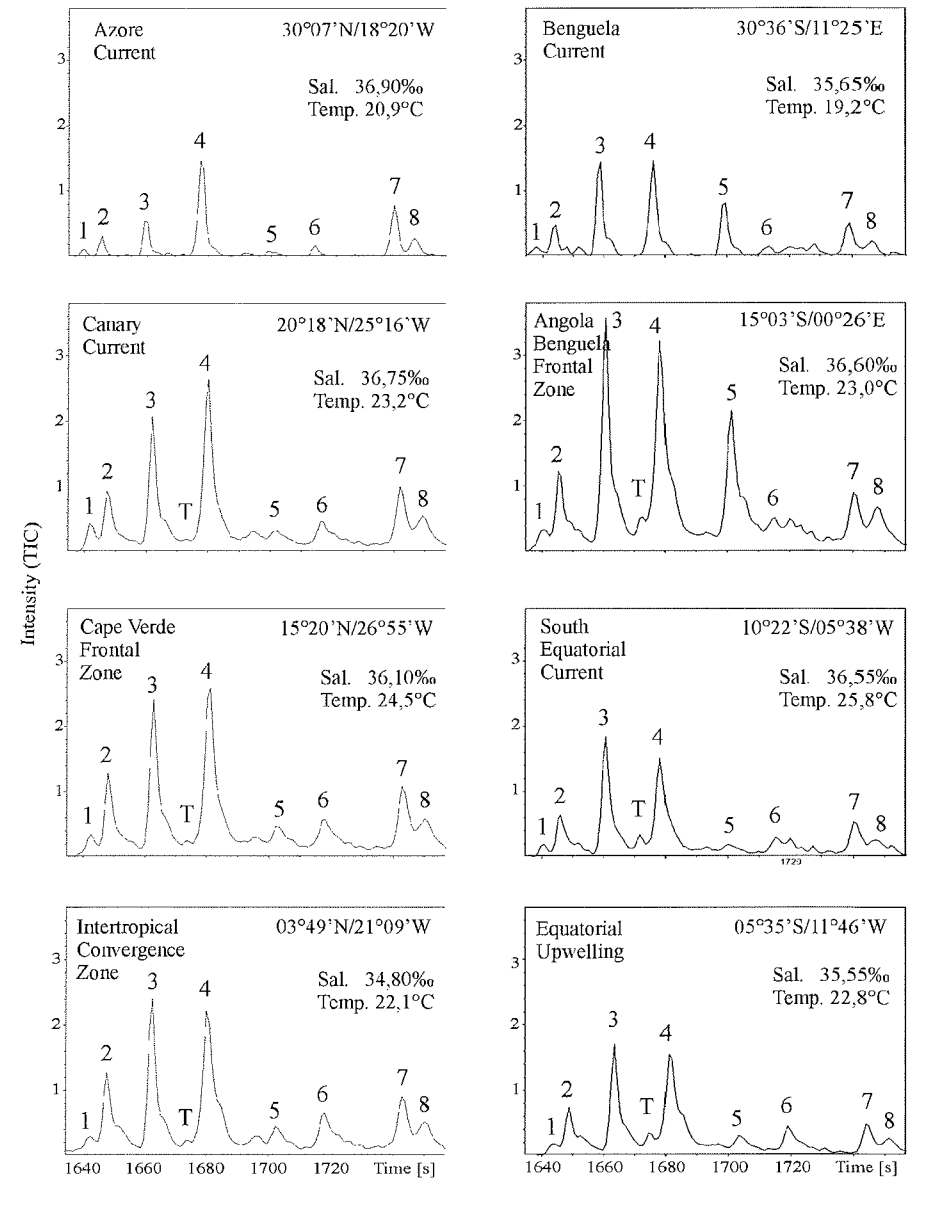
Phytosterols and biomass export

The main phytosterols - biomarkers for eukaryotic phytoplankton - and their distribution in surface water along the transect from 30°S to 30°N are shown in Fig. 2. Sampling positions and ocean areas as well as salinities and temperatures of the collected water are included. Only few qualitative and quantitative changes and no distinct seasonal effects were observed. Slightly higher levels of phytosterols were measured near frontal zones. Distinct impacts of individual phytoplankton groups on compound patterns were not indicated. Most differences turned out with 24-methylenecholesterol and cholesterol exhibiting highest levels in the Benguela Current. The diatom marker 24-norcholest-5,22E-dienol (with less GC retention than shown in Fig. 2) was only observed in traces in this sea area and even less elsewhere excluding the predominance of diatom species. Dinoflagellate sterols - like dinosterol (with higher GC retention than shown in Fig. 2) - could not be detected in surface water at all. Preferred depositions of dinosterols in basin sediments reported along the transect is hardly understood. Enhanced levels of C29-sterols in the northern hemisphere suggest continental input via the atmosphere with contributions from vascular plants. However, C29-sterols may also be synthesized by local phytoplankton which was recently shown from equal isotopic compositions of phytosterols and inorganic carbon compounds (DIC). We conclude from the qualitative and quantitative distribution of phytosterols between S 30° and N 30° that eukaryotic phytoplankton was not highly variable. Accordingly low and constant export of phytoplankton biomass and no gross pulses to the ocean interior had occurred. Irregular phytoplankton-induced depletion of HCHs may only occur during high settling fluxes of biomass following blooms in mid to high latitudes. Recent air-sea exchange had exclusive control for HCH levels during this transect.

HCH distribution

A few surface water extracts were analyzed for HCH isomers on board. Results for α -HCH and γ -HCH from S 30° to N 30° are shown in Fig. 3. For comparison data from 1989 and 1999 are included. The new facts fill gaps in knowledge of spatial distribution and temporal trends of both HCH isomers in the Atlantic Ocean.

α -HCH exhibits the highest vapor pressure of all isomers. It is readily distributed between the ocean surface and the atmosphere and accumulates in cold climate zones because of a strong dependency of its Henry's Law Constant on temperature. It is also relatively persistent in cold water because activation energy for chemical hydrolysis is high. Losses resulted mainly from microbial and chemical degradation as well as from transport to other ocean areas and the deep sea. In the Arctic a half-life of approximately 8 years was estimated for α -HCH between 1990 and 2000.



1 (22E)-27-Norcampesta/ergosta-dien-3 β -ol*
 2 (22E)-Cholesta-5,22-dien-3 β -ol
 3 Cholest-5-en-3 β -ol
 4 (22E)-Campesta/Ergosta-5,22-dien-3 β -ol*
 5 Ergosta-5,24(24')-dien-3 β -ol

6 (22E)-Stigmast/Poriferast-5-en-3 β -ol*
 7 Stigmast/Poriferast-5-en-3 β -ol*
 8 (24Z)-Stigmast-5,24(24')-dien-3 β -ol
 T 2R,4'R,8'R- α -Tocopherol
 * not separated

Fig.2: Meridional distribution of phytosterols in surface water of the Atlantic Ocean.
Total ion current (TIC) of GC/MS analyses.

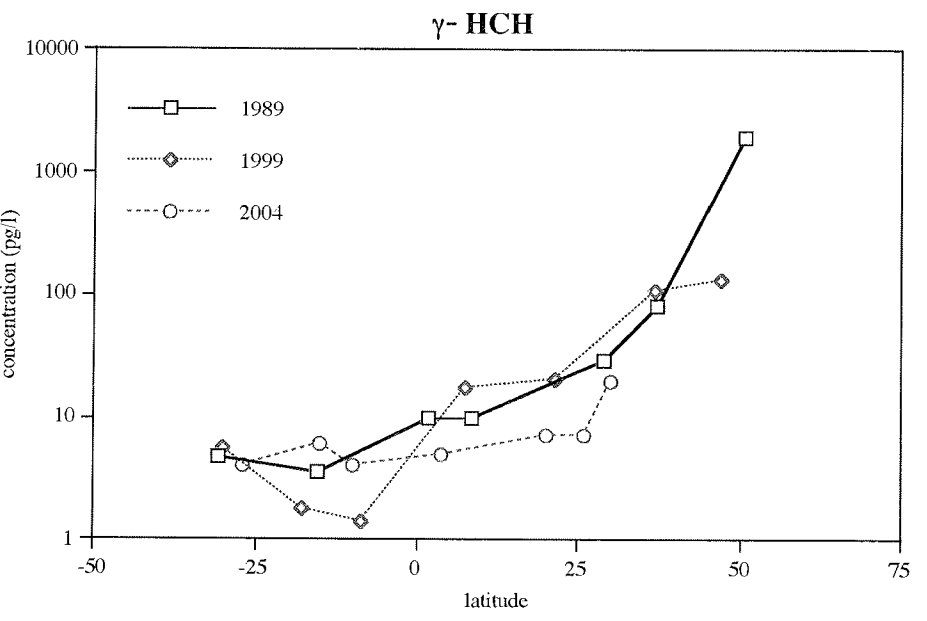
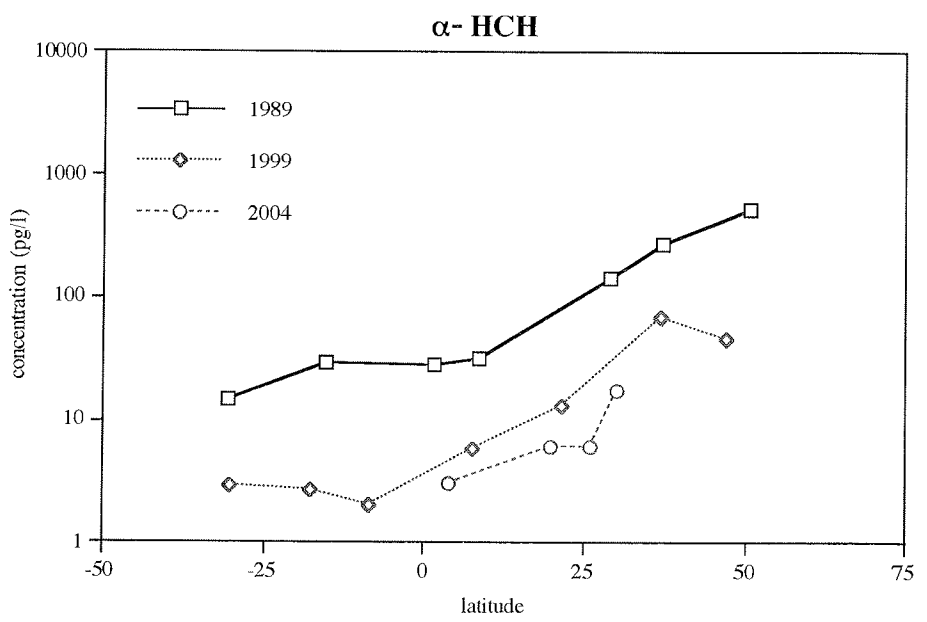


Fig. 3 : Meridional distribution of α -HCH and γ -HCH in surface water in the Atlantic Ocean

According to our results levels along the meridional Atlantic transect diminished faster than in the Arctic. A half-life of 2.5 years in open ocean surface water of the Atlantic Ocean could be concluded between 1989 and 2004. Our experimental data agree fairly well with results from zonally averaged multi-media models describing a global half-life of 2.0 years for α -HCH in northern subtropical zones. In spite of the overall reduction α -HCH levels still exhibit a distinct latitudinal gradient in North Atlantic surface water (Fig. 3) being probably preserved by different degradation rates at different environmental temperatures. South of the equator levels dropped beyond the detection limit of on board analyses and have to be completed by more sensitive investigations in the home laboratory.

γ -HCH is the most toxic and the most water soluble, but the least persistent of all isomers. Location and timing of its release into the environment is different from those of technical HCH. It is most easily distributed by long range transport in the atmosphere. Basic hydrolysis in tropical seas can be expected to be complete within few months. γ -HCH levels were found to be similar on both sites of the equator indicating application as insecticide in both hemispheres. Ongoing use of γ -HCH is shown by roughly unchanged levels in the open Atlantic between 1989 and 2004. Since 1999 it may have slightly decreased north and increased south of the equator (Fig. 3). Recently γ -HCH surpassed α -HCH levels first in South Atlantic and later in temperate North Atlantic surface water. Samples from higher latitudes during ANT XXI/5 still have to be analyzed for further evaluation.

β -HCH exhibits the lowest Henry's law constant and the highest chemical persistence. It is highly lipophilic, strongly sorbs to particulates and magnifies in biota. Alarming high levels of β -HCH in human milk are known since the late 1970s. Within the last decades β -HCH was seldom analyzed in water of the Atlantic Ocean and adjacent seas. During the 1990s it was reported to occur in the western Arctic ocean, where it accumulated after long-range tropospheric transport with Asian dust, wet deposition in the NE Pacific and oceanic transport through the Bering Strait. Though β -HCH has been increasing in the Arctic it is still an order of magnitude lower than α -HCH. However, in South East Asia it is currently the main soil residue after insecticide applications. In India technical HCH - including β -HCH - was used for mosquito control in the monsoon season up to the mid 1990s. During summer 2002 β -HCH was also remobilized from deposits in Eastern Germany by heavy precipitation and was later used as tracer for distribution of resulting flood water of the river Elbe in the North Sea. During ANT XXI/5 β -HCH was found to be approximately equal in surface water of the North and South Atlantic. Contrary to cruises in earlier years it clearly exceeded α - and γ -HCH in the South Atlantic.

Future Work and Perspectives

Currently we are working our way through the large number of spot samples available to us in the home laboratory as we aim to measure levels of HCHs in the Atlantic Ocean. Chiral cyclodextrines are used as stationary GC phases for separation of α -HCH enantiomers in addition to conventional phenylsilicones for

separation of stereoisomers. High resolution sector field mass spectrometry and MS/MS ion trap techniques are applied to improve the signal/noise ratio for detection of traces. Though vertical sampling was highly susceptible to contamination priority will be given to samples scheduled for analyses of HCHs from the surface down to the bottom of deep ocean basins. HCH distributions will be combined with gradients of conservative physical and traditional chemical properties as far as possible. Analyses of samples taken near the bottom will be especially considered. However, in future plastic material should be avoided for deep sea sampling and replaced by stainless steel to reduce risks of falsifications. Unavoidable seals and plugs used in samplers should be coated with teflon. To further improve analytical performance extended spot sampling in the ocean should be replaced by average sampling, guided by online measurements of conductivity, temperature, fluorescence and other significant variables. Calculation of backward trajectories for mass transport in the atmosphere and the ocean may also contribute for better evaluation of data.

Most work on the distribution of POPs has been done in the ocean/atmosphere boundary layer. α - and γ -HCH could be followed along pathways of transport under nonequilibrium conditions. Deposition of the stereoisomers into the upper ocean and evaporation into the lower atmosphere were shown to depend on time and investigated climatic zones. In future analyses of surface water for α - and γ -HCH should be continued to reveal shifting of distribution pathways due to global climate change. Recent feeding of β -HCH into the Atlantic Ocean should be explained and connected back to its sources. Analytical methods should also include δ -HCH which is currently lost during applied work-up procedures. Sampling and analyses in frontal zones, shelf areas and water above seamounts will help to better understand vertical mixing of HCHs in the ocean. Attending investigations of organic matter export into the deep sea should not only include the main phytosterols but also minor phytosterols possibly specific for sinking algal debris. Improvements in GC separation of C₂₄-alkylated diastereoisomeric sterols will facilitate source identifications. More time should also be given to assess the ultimate fate of individual HCH isomers. Analyses of bottom layers should be intensified to explore the impact of enhanced microbial activity near sediments. In low latitudes and oligotrophic gyres HCH loss will probably occur by photochemical and hydrolytic breakdown. However, respective degradation rates are only arbitrarily known and belong to the main knowledge gaps for modelling the global fate of HCHs. Intermediate degradation products should be looked for in the natural environment of the ocean surface and bottom layer in order to exhibit prevailing breakdown pathways of HCHs.

References

- Lakaschus, S.; Weber, K.; Wania, F.; Bruhn, R.; Schrems, O. (2002)
Environ. Sci. Technol. 36, 138-145.

6. LARGE SCALE LATITUDINAL PATTERNS OF MARINE BIRDS AND MAMMALS FROM THE ANTARCTIC TO THE NORTH SEA (POLARSTERN ANT-XXI-4 AND 5).

J. A. van Franeker, R. C. Fijn (Alterra)

Introduction

Alterra has participated in many Antarctic Polarstern cruises, studying top predators (marine birds and mammals) in relation to their Southern Ocean environment, in particular in the seasonal sea-ice zone. High densities and food requirements of top predator communities characterize the Antarctic sea-ice zone and various cold frontal areas in the Southern Ocean. A general perception is that the polar pelagic ecosystems are relatively rich in marine top predators as compared to those in the pelagic waters of the warmer climatic zones. However, top predator censuses using the same standardized observation methods throughout all different climatic zones are rare. Good comparable datasets are hardly available.

Therefore, following our participation in the ANT-XXI-4 SO-GLOBEC cruise (Van Franeker *et al.* this volume) continuation of the observations on Polarstern's home voyage ANT-XXI-5 to Bremerhaven, offered an excellent opportunity to build on a comparative dataset for top predator communities in a wide range of oceanic climate zones. Polarstern's trans-Atlantic track followed offshore deep waters like in most of our Antarctic observations. Comparative studies in different climatic zones will enhance understanding of the special features of Antarctic ecosystems in terms of animal abundance, biodiversity and processes involved.

Methods

Ship-based censuses of birds and mammals were made from an outdoor observation post installed on top of the bridge of Polarstern. Standard methods for censuses of marine birds and mammals were described in the ANT-XXI-4 report (Van Franeker *et al.*, this volume). Analyses in this paper are based on averages of all 10 minute counts per degree of latitude for both the Antarctic SO-GLOBEC study ANT-XXI-4 and the home voyage ANT-XXI-5. Results are expressed as food requirements of top predators ($\text{kg}/\text{km}^2/\text{day}$) because that is the most relevant parameter to combine strongly different sized animals into a single figure in terms of their relation to other components of the ecosystem.

Results and discussion

A total of 1719 quantitative 10-minute counts was conducted between 70°S and 51°N . The last day of obervations in the North Sea could not yet be included in the analysis. Counts were conducted in 84 of the 121 degrees of latitude because no observations are possible during night time. Per degree of latitude observed, the average number of 10 minute counts is over $20.5 \pm \text{sd } 13.1$ (min. 1; max 68). Total band-transect area surveyed was 1838 km^2 . Details of observations in the most southern part (south of 61°S) are given in Van Franeker *et al.*, this volume).

The best indicator of the range of climatic zones surveyed is the Sea Surface Temperature (SST). Averages for SST per degree of latitude, as measured by the

ship's keel sensor during the censuses of top predators, is shown in Fig.1. Water temperatures ranged from below minus 1.8°C in the far south to over 28°C in the tropics.

Food-requirements of the seabird community, averaged per degree of latitude, are shown in Fig.2. Bird densities in the Southern Ocean varied strongly, but were regularly high in the cold waters south of the Antarctic Polar Front (APF), which was situated around 40°S. It has to be noted that the peak values normally seen in sea ice areas (68°S to 70°S in this dataset) were not encountered during ANT-XXI-4, a phenomenon explained by the recent formation of sea-ice in that study. For clarity of the graph, one extreme value of bird food requirements at 65°S has been omitted from Fig.2. The high value (6.3 kg/km²/day) was caused by flocks of Antarctic Petrels north of the ice (see Fig.1 in Van Franeker *et al.*, this volume) with only a small number of counts (7) available in the 65°S block. North of the APF, bird abundance rapidly decreased, and except from some highly incidental situations, remained much reduced throughout the pelagic temperate and warm climatic zones. At the northern end of our transect more birds appeared, but these observations were made over the European continental shelf, not over deep water. The large scale pattern of seabird occurrence clearly shows their relative abundance in the Southern Ocean pelagic system. The overall pattern obscures much of the variability at smaller scales. Discrete patterns related to oceanographic features did occur in all zones, but simply do now show up at the overall scale.

Marine mammals followed a different pattern, as shown in Fig.3. Except for a single datapoint for ice seals in the far south, and some scattered Fur Seal occurrences in open water, the overall appearance of Fig.3 is determined by whales. Baleen whales, mainly Humpback whales, are responsible for elevated figures around 60°S. Toothed whales, including dolphins, account for most of the increased data values in the tropics and around 40°N. However, some of the highest values in the northern range were attributable to baleen whales (Fin Whale). The increased values to the north in Fig.3 might suggest an effect of enriched continental shelf waters, but the large majority of these observations were made over deep water, two to five km in depth.

Averaged over all our counts, the food requirements of marine mammals were calculated at 4.8 kg/km²/day, an order of magnitude above the 0.3 kg/km²/day that emerged as the average value for seabirds. Although elevated figures for the mammal group were generally associated with elevated figures for seabirds, proportional responses in different zones were very different, with seabird responses north of APF hardly visible in the scale of Fig.2. Experiences in the Southern Ocean do almost suggest that seabird concentrations will build up in any productive area, no matter of distance to breeding areas. At this stage, we can not explain why seabird concentrations did not build up to similar levels (in proportion to mammal responses) in clearly productive waters further north. To some extent seasonal aspects (northern hemisphere breeding season) could play a role. Further analyses will need to be conducted, with a closer look at different subareas, and distinction between various types of seabirds, baleen whales and toothed whales and their specific foraging systems and food preferences.

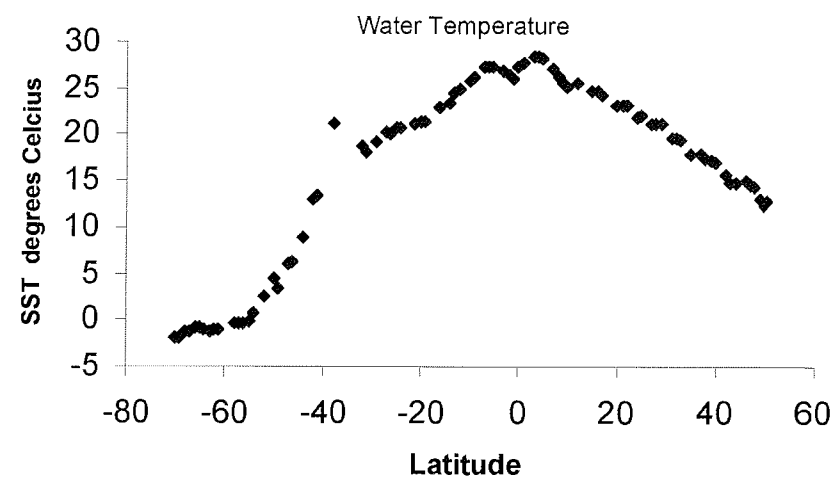


Fig. 1: Sea Surface Temperatures (SST; keel sensor) measured during 10-minute counts (n=1719) and averaged per degree of latitude for which observations were available (n=84).

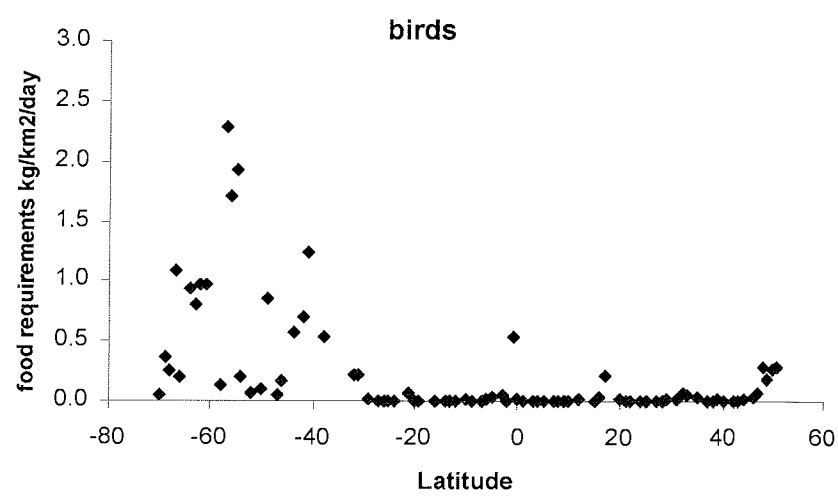


Figure 2: Average daily food requirements of marine birds per degree of latitude in between 70°S and 51°N. One extreme datapoint of 6.3 kg/km²/day at 65°S omitted. Virtually all observations, except those in the utmost south and north were conducted over deep ocean.

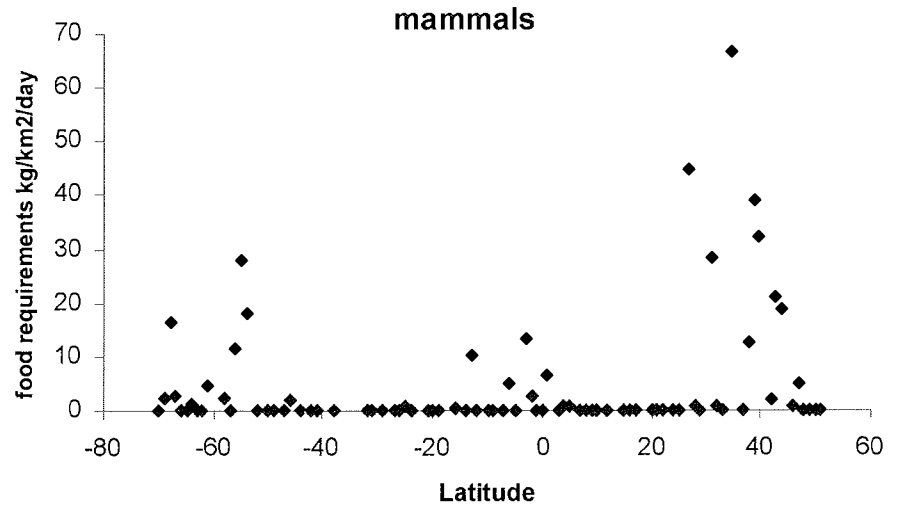


Figure 3: Average daily food requirements of marine mammals per degree of latitude in between 70°S and 51°N.

7. 13C- SAMPLING PROGRAM DURING POLARSTERN TRANSITS

S. Wriedt (Leibniz Kiel), A. Körtzinger

Objectives

The primary goal of the ^{13}C sampling program is to study the interannual variability and long-term trends in the air-sea $\delta^{13}\text{C}$ -DIC disequilibrium of surface waters in the Atlantic Ocean.

This is a joint project of Prof Dr. Paul Quay of the School of Oceanography, University of Washington, Seattle/WA, U.S.A and Prof. Dr. Arne Körtzinger of the Leibniz-Institut, Kiel.

Sampling and processing of samples

Surface samples for $\delta^{13}\text{C}$ -DIC are taken during the transect with regular spacing (8 hours) along the entire cruise track. These samples are going to be measured at Paul Quay's Stable Isotope Laboratory.

For this purpose, the CO_2 is extracted to $100 \pm 0.5\%$ using a helium stripping technique, and the $^{13}\text{C}/^{12}\text{C}$ ratio of the extracted CO_2 is measured later on a Finnigan MAT 251 isotope ratio mass spectrometer.

In order to enhance interpretation of the ^{13}C data parallel sampling for dissolved inorganic carbon (DIC) and total alkalinity (A_T) was carried out with a similar number of samples. The water samples were collected from the seawater pumping system at a depth of 11 m at the keel of the vessel. The system works with a "Klaus"-pump. Temperature- and salinity-data were measured by a thermostalinograph nearby the water in-flow. All samples are poisoned with $100 \mu\text{l}$ saturated HgCl_2 -solution.

Measurements of DIC and A_T will be carried out in Kiel using the following techniques:

DIC is measured by coulometric titration following extraction of the CO_2 with an automated system known as SOMMA [Johnson *et al.*, 1993]. A_T is determined by potentiometric titration in an open cell [Mintrop *et al.*, 2000 and references therein]. DIC and A_T analyses are checked every 10-15 samples by measuring a certified reference material provided by A. Dickson (Scripps Institution of Oceanography, La Jolla, CA, U.S.A.). The estimated accuracy is $1.5 \mu\text{mol kg}^{-1}$ for DIC and $2.5 \mu\text{mol kg}^{-1}$ for A_T .

Future aspects

This project is a long-term study which involves sampling during all POLARSTERN transits to and from the Southern Ocean.

References:

- Johnson, K.M., Wills, K.D., Butler, D.B., Johnson, W.K. and Wong, C.S., 1993. Coulometric total carbon dioxide analysis for marine studies: maximizing the performance of an automated gas extraction system and coulometric detector. Marine Chemistry 44, pp. 167-187.
Mintrop, L.; Perez, FF; Gonzalez Davila, M; Santana Casiano, JM; Koertzinger, A. 2000. Alkalinity determination by potentiometry: intercalibration using three different methods. Ciencias. Marinas Vol. 26., 23-37.

8. DOAS-MEASUREMENTS

B. Dix (IUPH)

Introduction

In the third year tropospheric and stratospheric trace gases like NO_2 , H_2O , HCHO , BrO and Ozone were determined by the method of the „Differential Optical Absorption Spectroscopy“ (DOAS) and by using a specifically developed instrument for measurements on „Polarstern“. The meridional transits of Polarstern offer the

opportunity to measure in very distinct marine regions and to study the dchemistry and physics of the atmosphere in relation to the latitudes.

Work on sea

The DOAS measurements on leg 5 run without problems delivering a complete data set from May 9th to June 1st. A preliminary analysis of the spectra determined in the UV-region corroborated a high quality of the data. The heavily polluted area in the region of the English Channel became obvious on the basis of increased NO₂ concentrations. A more detailed interpretation of the spectra is on the way and will be available in the next months.

ANNEX 1 PARTICIPANTS

1.	Albrecht	Sebastian	Fielax
2.	Berlitz	Katrin	AWI
3.	Dix	Barbara	IUP Heidelbg.
4.	Drebning	Wolfgang	AWI
5.	Feiertag	Thomas	Fielax
6.	Fijn	Ruben Chr.	Alterra
7.	Franecker, van	Jan Andries	Alterra
8.	Heim	Christine	AWI
9.	Helmke	Elisabeth	AWI
10.	Hoffmann	Mathias	Fielax
11.	Knuth	Edmund	DWD
12.	Müller	Annegret	AWI
13.	Reuter	Kristine	AWI
14.	Weber	Kurt	AWI
15.	Wriedt	Stefanie	Leibniz Kiel

Annex 2 Participating Institutes ANT-XXI/5

Acronym	Address
<u>Germany</u>	
AWI	Alfred-Wegener-Institut für Polar- und Meeresforschung Columbusstraße 27568 Bremerhaven
DWD	Deutscher Wetterdienst Geschäftsfeld Seeschifffahrt Jenfelder Allee 70 A 22043 Hamburg
Fielax	FIELAX Gesellschaft für wissenschaftliche Datenverarbeitung mbH Schifferstrasse 10-14 27568 Bremerhaven
Leibniz Kiel	Liebniz-Institut für Meereswissenschaften an der Universität Kiel Wischhofstr. 1-3 24148 Kiel
IUPH	Universität Heidelberg Institut für Umwelophysik Im Neuenheimer Feld 69120 Heidelberg
<u>Netherlands</u>	
ALTERRA	ALTERRA-Texel, Marine and Coastal Zone Research POB 167, 1790 AD Den Burg (Texel) Netherlands

ANNEX 3 Ship's crew ANTXXI/5

Name	Rang
Pahl, Uwe	Master
Schwarze, Stefan	1.Offc.
Schulz, Volker	Ch.Eng.
Grimm, Sebastian	2.Offc.
Spielke, Steffen	2.Offc
Kohlberg, Eberhard	Doctor
Hecht,Andreas	R.Offc.
Erreth, Gyula	1.Eng.
Hoffmann, Bernd	2.Eng.
Simon, Wolfgang	2.Eng.
Dimmler, Werner	Fielax-Elo
Gerchow, Peter	Fielax-Elo
Holtz, Hartmut	Elec.Tech..
Kahrs, Thomas	Fielax-Elo
Verhoeven, Roger	Fielax-Elo
Clasen, Burkhard	Boatsw.
Neisner, Winfried	Carpenter
Burzan, G.-Ekkehard	A.B.
Hartwig-Lab., Andreas	A.B.
Kreis, Reinhard	A.B.
Moser, Siegfried	A.B.
Pousada Martinez, S.	A.B.
Schröder, Norbert	A.B.
Schultz, Ottomar	A.B.
Beth, Detlef	Storekeep.
Arias Iglesias,Enr.	Mot-man
Dinse, Horst	Mot-man
Fritz, Günter	Mot-man
Krösche, Eckard	Mot-man
Fischer, Matthias	Cook
Martens, Michael	Cooksmate
Tupy,Mario	Cooksmate
Dinse, Petra	1.Stwdess
Wöckener, Martina	Stwdss/Kr
Deuß, Stefanie	2.Stwdess
Schmidt,Maria	2.Stwdess
Streit, Christina	2.Stwdess
Tu, Jian Min	2.Steward
Wu, Chi Lung	2.Steward
Yu, Kwok Yuen	Laundry.
Feiertag, Thomas	Trainee
Hoffmann, Mathias	Trainee
Niehusen, Arne	Trainee
Scholl, Christoph	Apprent.

ANNEX 4 Station list ANT XXI/5

Date	Station No.	Time (UTC)	Latitude	Longitude	Depth	Operation
PS65/710-1	10.05.04	13.55-17.16	28° 59,84' S	7° 59,17' E	5067	CTD/RO/MIC
PS65/710-2	10.05.04	17.17-21.06	29° 0,43' S	7° 58,74' E	5077	BWS
PS65/711-1	13.05.04	03.00-07.07	17° 0,08' S	3° 0,27' E	5467	CTD/RO/MIC
PS65/711-2	13.05.04	07.18-10.55	17° 0,01' S	3° 0,00' E	5467	BWS
PS65/712-1	14.05.04	13:03-13.18	13° 8,37' S	2° 4,16' W	4879	CTD/RO up to 50m
PS65/713-1	18.05.04	02.31-03.15	0° 1,65' S	17° 58,12' W	6294	CTD/RO up to 500m
PS65/713-2	18.05.04	03.52-08.13	0° 1,64' S	17° 58,05' W	6295	CTD/RO/MIC
PS65/714-1	21.05.04	06.18-07.17	12° 0,07' N	28° 0,05' W	5582	CTD/RO up to 500m
PS65/714-2	21.05.04	07.57-11.41	12° 0,26' N	28° 0,15' W	5583	CTD/RO/MIC
PS65/714-3	21.05.04	11.51-16.04	12° 0,27' N	27° 59,82' W	5577	BWS
PS65/715-1	24.05.04	01.55-05.27	24° 0,03' N	24° 0,01' W	5039	CTD/RO/MIC
PS65/715-2	24.05.04	05.40-09.02	24° 0,01' N	23° 59,99' W	5039	BWS
PS65/715-3	24.05.04	09.08-09.40	24° 0,01' N	24° 0,09' W	5039	CTD/RO up to 500m
PS65/716-1	27.05.04	11.18-12.28	35° 60,00' N	13° 0,04' W	4820	CTD/RO up to 1600m
PS65/716-2	27.05.04	13.19-16.37	36° 0,02' N	13° 0,07' W	4819	CTD/RO/MIC
PS65/716-3	27.05.04	16.45-20.30	36° 0,02' N	13° 0,19' W	4820	BWS

CTD/RO= Conductivity/Temperature/ Depth/Rosette

MIC= Minicorer

BWS=Bottom water sampler